OCS Study
MMS 2009-039

Northern Gulf of Mexico Continental Slope Habitats and Benthic Ecology Study

Final Report

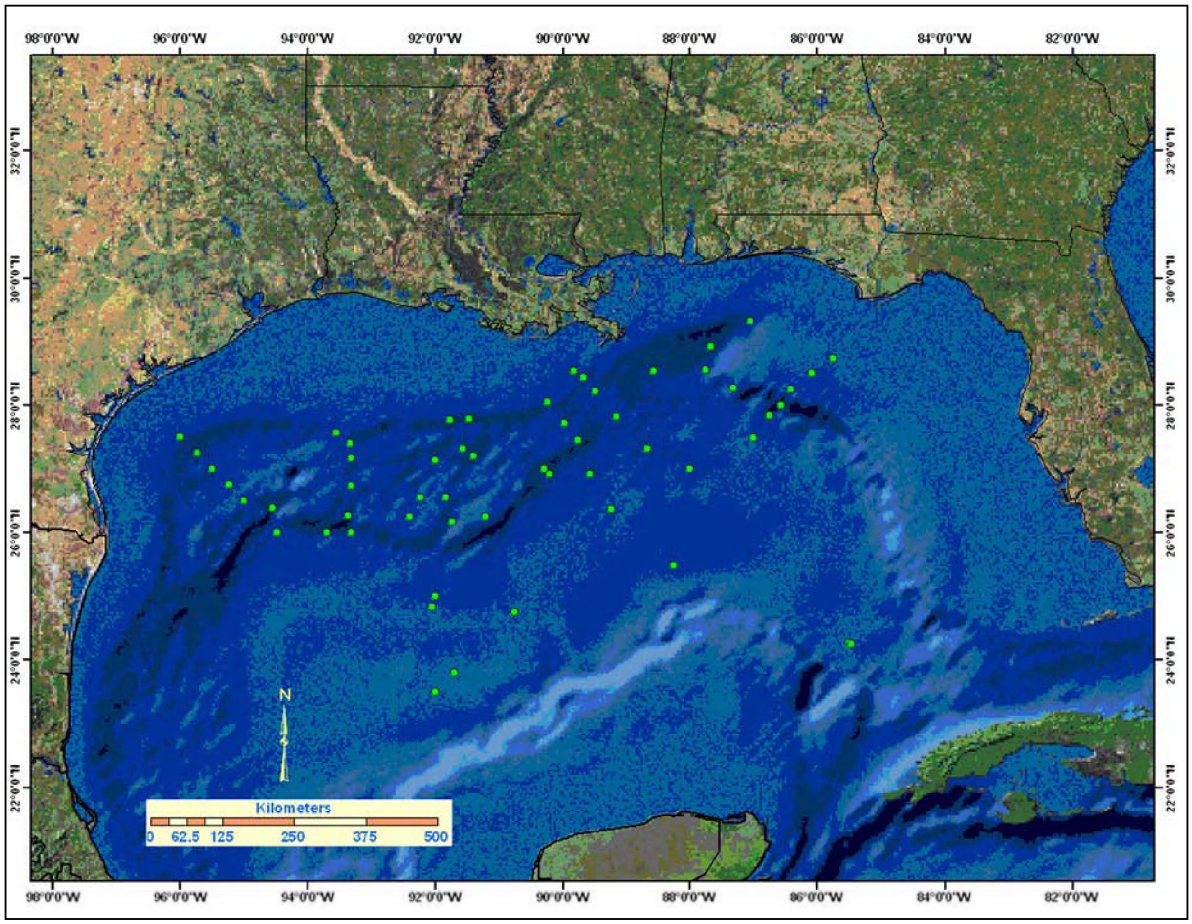

U.S. Department of the Interior
Minerals Management Service
Gulf of Mexico OCS Region

OCS Study
MMS 2009-039

Northern Gulf of Mexico Continental Slope Habitats and Benthic Ecology Study

Final Report

Authors

Gilbert T. Rowe
Mahlon C. Kennicutt II

Prepared under MMS Contract
1435-01-99-CT-30991 (M99PC00001)
by
Texas A&M University
Texas Engineering Experiment Station
College Station, Texas 77843

Published by

U.S. Department of the Interior
Minerals Management Service
Gulf of Mexico OCS Region

New Orleans
July 2009

DWH-AR0009352

DISCLAIMER

This report was prepared under contract between the Minerals Management Service (MMS) and the Texas A&M Engineering Extension Service. This report has been technically reviewed by the MMS, and it has been approved for publication. Approval does not signify that the contents necessarily reflect the views and policies of the MMS, nor does mention of trade names or commercial products constitute endorsement or recommendation for use. It is, however, exempt from review and compliance with the MMS editorial standards.

REPORT AVAILABILITY

Extra copies of this report may be obtained from the Public Information Office (Mail Stop 5034) at the following address:

U.S. Department of the Interior
Minerals Management Service
Gulf of Mexico OCS Region
Public Information Office (MS 5034)
1201 Elmwood Park Boulevard
New Orleans, Louisiana 70123-2394
Telephone (504) 736-2519 or
1-800-200-GULF

CITATION

Rowe, G.T. and M.C. Kennicutt II, eds. 2009. Northern Gulf of Mexico continental slope habitats and benthic ecology study: Final report. U.S. Dept. of the Interior, Minerals Management. Service, Gulf of Mexico OCS Region, New Orleans, LA. OCS Study MMS 2009-039. 456 pp.

ABOUT THE COVER

Sites sampled during the Deep Gulf of Mexico Benthos (DGoMB) project.

ACKNOWLEDGMENTS

The group of investigators who participated in the Deep Gulf of Mexico Benthos (DGoMB) for the Minerals Management Service (MMS) wish first of all to thank Mr. Gregory Boland and Dr. Thomas Ahlfeld of MMS for their support and assistance throughout the project. The Texas Engineering Experiment Station of the Texas A&M University System deserves appreciation for their support of cost-shared equipment and graduate student support during the initial stages of the project. A total of 57 undergraduate and graduate students participated in sample collection and analysis over the entire course of the project, many as volunteers, and they have been appreciated. The R/V GYRE, its crew and officers, in particular Capt. Dana O. Dyer, provided service that was competent and professional, for which we are exceedingly grateful. The Department of Oceanography (OCNG), the Department of Biology (BIOL), the Department of Wildlife and Fisheries Sciences (WFSC), the Department of Marine Science (MARS) and the Geochemical and Environmental Research Group, all of Texas A&M University, provided space, staff and financial support throughout various phases of the project, for which we are grateful. Other institutions whose contributions should be acknowledged are the University of Texas (UT), the University of Washington (UW), the University of South Carolina (USC), the Woods Hole Oceanographic Institution (WHOI), the University of Southern Mississippi (USM), the *Universidad Autonoma de Mexico (UNAM)*, and the Australian Museum of Natural History.

The Scientific Review Board was composed of Drs. Will Schroeder, K. L. Smith, Jr., and Michael Rex. Their advice throughout the project consistently improved each stage of the program. The time and effort they devoted were appreciated by all participants.

Two close colleagues, whose dedication to the deep Gulf of Mexico should not go unacknowledged, were lost during the course of the study. Dr. Robert Avent at MMS nurtured the idea of and need for the study within MMS long before it was even initiated. Following its inception, he kept close tabs on all activities, even participating on one trip on the GYRE. It is unfortunate that he has not been able to see what has been generated out of his dedication. Dr. Guin Fain Hubbard passed away in 2006, just as the final report was being prepared. Fain had immeasurable influence on the cadre of graduate students tasked to sort and identify the macrofauna from the box cores. He probably had more direct influence on their education as biologists than any other single individual.

EXECUTIVE SUMMARY

The Deep Gulf of Mexico Benthos (DGoMB) project was initiated for the Minerals Management Service of the U.S. Department of the Interior in 1999 to investigate the structure and function of the biota associated with the sea floor in the deep water of the northern Gulf of Mexico. The purpose of the study has been to determine how living resources inhabiting deep-water habitats might be impacted by oil and gas exploration and exploitation. The strategy of the field work was to survey a broad region during an initial stage from which community structure could be determined, accompanied by extensive sampling of physico-chemical variables within both the water column and the sediments of the sea floor. Eight hypotheses were tested on the basis of this survey, all related to how the environmental variables control or affect community biomass, standing stocks, diversity and recurrent assemblages of species. The variables tested were depth, location within small (5 to 15 km diameter) basins, canyons, geographic location in the east vs. western half of the northern gulf basin, location below steep escarpments, proximity to high vs. low surface water productivity, and association with or next to methane seeps. The components of the seafloor community sampled included sediment bacteria, small protists and metazoans (meiofauna, >63 micrometer mesh sieves), small metazoan invertebrates (macrofauna, >300 mesh sieves), large bottom-dwelling invertebrates (megafauna, > ca. 1 cm diameter), and demersal fishes. Sampling devices utilized to capture these organisms were a 0.2 m^2 box corer (along with subsampling from within the cores); 40 foot otter trawl, with 2.5 cm stretch mesh net; and sea floor photography. Profiles of water column variables were determined using a Conductivity-Temperature-Depth profiling sensors (CTD), and a rosette of sampling bottles for measurement of standard water-column chemical variables (temperature, salinity, oxygen, suspended organic matter, inorganic nutrients and plant pigments). The sampling crossed the continental margin from depths of 200 m on the upper continental slope out to 3,750 m on the Sigsbee Abyssal Plain and extended geographically from the Mexican border on the west over to north Florida (Figures 5-1 to 5-3).

A subset of six locations was chosen from the data generated by the survey to conduct more intensive sampling from which diagnostic properties of sea floor community function could be measured. The strategy was to compare community function at sites with extremes in high and low standing stocks. At these locations, an autonomous benthic lander was used to set incubation chambers on the sea floor to measure sediment community oxygen consumption (respiration) (SCOC). Subcores taken from box cores were incubated in the ship's laboratory. Microelectrodes made profiles of oxygen concentration in the pore water of the surface sediments in subsamples from cores to determine oxygen penetration depth and consumption. A suite of radionuclides was used to estimate sediment mixing rates, burial and consumption of organic carbon within the sediments.

The biota, in terms of standing stocks, biodiversity and species composition, was shown to be related to water depth, location in the Mississippi and De Soto canyons, co-location with methane seeps, sediment organic matter content, association with high surface water primary production and an east-west geographic location. Data do not indicate that the biota was affected by location in small basins, sediment grain size, oxygen concentration, temperature, salinity or chemical contaminants within the sediments. The data base generated at the species level by taxonomists associated with the project allows extensive detailed maps to be drawn of a broad suite of biological characteristics.

Stock size and sediment community oxygen consumption (SCOC) decreased exponentially with depth, and this is inferred to be controlled by decreasing food supplies from the surface

water or exported offshore to deeper water from the upper depths of the continental slope. Groups of recurrent species occurred in four primary depth zones that lined the basin between isobaths. These zones appear to be related to specific levels of food supply in the form of sedimenting particulate organic matter. Diversity among most groups reached a maximum on the upper continental slope between 1.2 and 1.6 km depth, from which it declined to the abyssal plain. While alpha diversity was lower in the Mississippi Canyon within individual sampling sites, the total number of species was higher in the canyon compared to adjacent transects, due, it is thought, to the canyon's higher physical complexity.

The SCOC declined rapidly as depth increased. It was approximately three to ten times lower on the upper slope (500 to 2,000-m depth) than on the adjacent continental shelf (10 to 200 m depth), but the upper slope was approximately ten times higher than out on the abyssal plain (2 to 7 mg C m^{-2} d^{-1}). The turnover time of the living carbon pool (the total standing stock of the biota), calculated by dividing the total biomass by the SCOC, was on the order of days to months, whereas the detrital organic carbon turnover time was in years.

The standing stock information from each group has been assembled into a set of food web budgets for each of the six sites where community function was measured. Rates of respiration, growth and predation have been estimated in terms of carbon cycling (mg C m^{-2} d^{-1}) at presumed steady state for each stock. These data illustrate that the importance of large animals (the megafauna, the fishes and the macrofauna) decreases more rapidly with depth than the small size groups (meiofauna and bacteria). The detrital carbon is the largest pool in all sediments, but its relative importance increases with depth, suggesting that much of it is unreactive. All the metazoan stocks declined with water depth in a statistically significant pattern, but the bacteria did not, suggesting that the role of the bacteria in community function is increasing as the organic matter becomes less reactive.

The completion of DGoMB was accomplished through cooperation of ten different institutions in three countries. Fiftyseven students at the undergraduate and graduate level participated in either the field work, sample processing or data analysis. All the data generated have been deposited in the archives of the National Oceanographic Data Center (NODC) and the faunal listings are included in the Ocean Biological Information System (OBIS). Individual species lists and the environmental data are available from the MMS, the Program Manager or the individuals who generated the separate data by category, with appropriate restrictions.

It can be concluded that potential interactions between the biotic communities and O&G industry activities, including potentially delaterious faunal alterations of the resident biotic communities, could be substantially greater on the upper continental slope (down to 2,000-m depth) simply because the standing stocks are so much higher on the upper slope. On the other hand, the "upper slope" biota may be better adapted to respond to and thus survive alterations in available substrate and organic loading, because of the greater variability at those depths than in deeper water. Alternatively, the carbon-based food web models suggest that the introduction of biodegradable organics, whatever the source, could stimulate biomass production at all locations in the deep GoM where the biota is food limited. The general principle has emerged that the biota, in the rather quiescent and benign environment of the deep ocean, is controlled by various sources of organic nourishment, including those introduced by mankind's activities. This might cause a shift in the location or depths of the biotic zones described by enhancing concentrations of organic material in association with exploration or production at a well head. It remains to be seen if and when such a hypothetical model prediction might be valid.

TABLE OF CONTENTS

LIST OF FIGURES

LIST OF TABLES

1. INTRODUCTION

The topography, geology, geophysics, currents, hydrography, chemistry and biota of the continental slope are much less well known than those of the continental shelf. The earliest information on the deep-sea biota of the Gulf of Mexico comes from studies that used benthic trawling and photography (TerEco 1976, 1983). The largest study, The Northern Gulf of Mexico Continental Slope Study (NGoMCSS), concentrated on knowledge of geologic features, water circulation, chemistry, and biological communities (LGL and TAMU 1988). New scientific findings in the area, including chemosynthetic communities and a better understanding of the geological complexity of the region, have significantly altered our view of the northern GoM deep-sea (MacDonald 1998; MacDonald et al. 1996). Rapid expansion of energy industry activities into the deep-sea has occurred over the past decade. It is expected that this trend will continue and that deep-sea regions of the northern GoM will be the site of energy exploration and development activities for decades to come.

An MMS workshop report on the deepwater GoM concluded that there was a need for additional information on the composition and structure of benthic communities, the associated biogeochemical processes, habitat heterogeneity and physiography, trophic interactions, and the biological "health" of the region (Carney 1998). The deep-sea is a setting within which benthic communities survive and propagate in the northern GoM. The deep-sea is characterized by total darkness, low temperature, nearly featureless mud, sparse food resources, predictable biomass patterns, unusual diversity patterns, and poorly defined couplings to topography, biogeochemistry, and currents.

The present program, referred to as Deep Gulf of Mexico Benthos or DGoMB, was designed to provide a better understanding of:

1) the present condition of biological communities in the study area,
2) the distribution patterns of deep-sea biota,
3) the biological and physical processes that control the environmental setting, and
4) the effects that these processes have on the character of benthic and benthopelagic communities.

The program has emphasized understanding the make-up and variability of soft-bottom biological communities with a secondary effort to characterize the important biological and abiotic processes that sustain or change the observed patterns. The study has included:

1) the composition and structure of slope biological communities,
2) inferred the relationship between these communities and local conditions and forcing factors,
3) characterized the "health" and functioning of deep-sea communities, and
4) compared and contrasted the GoM region with similar oceanic basins.

The DGoMB program design was developed based on historical knowledge of deep-sea communities in the GoM. The interdisciplinary nature of the scientific objectives was recognized and the study design balances the benthic survey aspects of the program with experimental (or "process") oriented studies needed to understand the deep-sea community's structure and

function. A careful analysis of previous information was used to focus the study on the most relevant areas and those areas most likely to provide the greatest likelihood of establishing generalities about the structure and function of deep-sea benthic communities. The results now provide a predictive capability for areas not directly sampled or observed. This predictive capability is a framework for ascertaining the potential for, and the most likely impact from, fossil fuel exploration and exploitation in the deep-sea.

Each work element is nested in an integrated design that links data collection to a coherent framework that provides maximum complementary information based on a detailed foodweb model of the interacting biological components of the system. Survey station results were used to choose experimental stations. Experimental stations chosen were a subset of reoccupied survey stations tightly linking all observations and data in space and time. Each measurement was taken to provide quantitative estimates of unknown elements of the model, to improve the quantitative accuracy of the elements of the models, and/or to test and refine the underlying assumptions of the model.

A review of previous studies, particularly the NGoMCSS slope study, provided valuable insights for designing the new study (LGL and TAMU 1988). The program design incorporated the following strategies:

1) An equal sampling effort was concentrated at different water depths to determine if "zones" exist. Site selection emphasized equally spaced depth intervals and replication at the treatment level (sites that are mostly similar except for depth) recognizing that gradients in ecosystem properties are more likely than "zones."

2) Depth dependence in community structure and composition was evaluated in the context of other recently recognized confounding factors such as seafloor topography, and currents.

3) Sampling sites were chosen based on characteristics believed to be important in establishing biological patterns such as detrital flux to the seafloor as influenced by near surface patterns of primary productivity.

4) Proximity to the Mississippi River and Fan was an important spatial consideration.

5) Benthic communities were nestled in different topographic and sedimentologic settings that are influenced by slope failure and varying inputs of terrigenous materials.

6) Sampling sites were selected to compare benthic communities associated with known physical features such as the thermohalocline, the oxygen minimum, and high current regimes.

7) The program was designed to provide flexibility by revising and rethinking the underlying strategy and design on a regular basis in response to collection of new data and re-evaluation of historical data.

8) Temporal variations in community structure and composition may be important and were considered by reoccupying historical sites and visiting a subset of sites during each of the three planned field programs.

9) An improved understanding of community structure and composition required better and more thorough measurements of biomass for input into the conceptual model.

10) Improved estimates of the megafaunal role in the ecosystem are important and included a three pronged approach to surveys: trawling (with improved quantitative methodologies), photosurveys, and baited traps.

11) The number of sites sampled, the overall geographic area and the intensity of sampling were all increased over previous studies.

12) Replication and the size of the sample were increased over the previous studies to ensure that the total number of animals collected adequately represented the diversity of the communities being studied.

13) The data have been managed meticulously so that they are readily available for future reassessment as our understanding of the deep-sea evolves.

The methods and approaches adopted for this program are the same, or compatible with, the methods of other corollary programs, thus allowing for seamless integration of new results with the results of other programs in the final synthesis. This will result in a holistic evaluation of the GoM deep-sea benthos and the linkages between abiotic and biotic processes that control the complex ecological patterns of the deep-sea benthos.

1.1 Program Objectives

The structure and function of deep-sea benthic communities is the end-result of complex interactions between and among the biota and the topography, geology, currents, hydrography, chemistry, and physical setting. The NGoMCSS study was an attempt to describe the geology, water circulation, chemistry, and biologic communities on the vast northern GoM continental slope region (LGL and TAMU 1988). The current project is intended to build on, improve, and supplement this pioneering study (Table 1-1). A reassessment of continental slope ecosystems, in the context of intensive oil and gas exploration and exploitation in the region, is considered essential for the management and protection of biological resources in the deep-sea.

The overarching goals of DGoMB were to:

- determine in greater detail the composition and structure of slope bottom biological communities and to infer relationships between biological patterns and major controlling processes and;
- characterize the area as to its present "health" and function and compare and contrast the region with similar oceanic regions.

Table 1-1

Program Team—Key Personnel*

Name	Discipline	Role	Institution
Gilbert T. Rowe	Deep-sea Benthic Ecology	Project Manager, Principal Scientist, Chief Scientist, Group Leader-Deep-sea Ecology	Texas A&M University Galveston
Mahlon C. Kennicutt II	Environmental Chemist	Deputy Program Manager, Contaminant Chemist	Texas A&M University
Gary A. Wolff	Data Management	Data Manager	Texas A&M University
Jody Deming	Microbiology	Co-PI Ecology	University of Washington
Paul Montagna	Benthic Ecologist	Co-PI Ecology, Study Design	University of Texas
Richard Haedrich	Bottom Fishes	Co-PI Ecology	Memorial University
	Megafauna	Data Analysis	
Richard Heard	Macrofauna Taxonomy	Co-PI Ecology	University of Southern Mississippi
John Morse	Inorganic	Geochemistry	Texas A&M University
	Geochemist	Group Leader	
William Bryant	Geological	Geology	Texas A&M University
	Oceanographer	Group Leader	
Worth Nowlin	Physical	Oceanography	Texas A&M University
	Oceanography	Group Leader	
Joan Bernhardt	Foraminifera		University of South Carolina
Norman Guinasso	Physical Oceanography Field Program		Texas A&M University
Bob J. Presley	Metal Contaminants		Texas A&M University
Terry L. Wade	Organic Contaminants		Texas A&M University
Steven DiMarco	Physical Oceanography		Texas A&M University
Michael Rex	Community Structure	Science Review Board	University of Massachusetts - Boston
Kenneth L. Smith, Jr.	Community Dynamics	Science Review Board	Scripps Institution of Oceanography
William W. Schroeder	Gulf of Mexico Ecology	Science Review Board	Dauphin Island Marine Laboratory, University of Alabama

*Does not include taxonomists.

Specific DGoMB objectives were to:

- improve the conceptual model that serves as the guide for the design and overall conduct of the study and to test specific hypotheses related to the models;

- compile and synthesize data from existing databases and on-going programs to interpret new results;
- conduct field collections to describe the distribution and structure of benthic communities on the continental slope of the GoM and to elucidate the functional interactions among them in known environmental settings;
- characterize the hydrographic structure and measure the dissolved and particulate water column nutrient concentrations, primary productivity, and chlorophyll *a* at the study sites;
- characterize the sediments at the study sites including grain size and hydrocarbon, metal, carbonate, and organic carbon concentrations;
- characterize the basic attributes of the benthic microbiota and biomass at the study sites;
- characterize the soft-bottom macro- and megafauna at the study sites;
- relate variations in benthic biota patterns to sedimentary processes and to the chemical and physical setting;
- define basic levels of animal and bacterial activity and production and describe interactions between and among benthic biota, the several ecological/biological compartments, and the abiotic environment; and
- compare and contrast the GoM benthic marine environment and communities with those in other basins of similar depth ranges and oceanic settings.

The program was conducted over a 65-month period of performance. Three major oceanographic cruises were conducted, one in each of the first three years of the program. The fourth year of the program was dedicated to completing sample analyses begun in the first three years; the next year was devoted to work by taxonomists on organisms taken in the field program; the 5th year has been dedicated to data management and interpretation, model refinement, and production of the Synthesis Report.

1.2 The Program

The program consisted of four tasks:

TASK 1—Re-examination of Existing Data and Field Study Design

All available scientific records and databases have been identified, collected, and re-examined. Previous studies of particular importance are the TerEco Corporation synthesis (1976 and 1983), the MMS NGoMCSS (LGL and TAMU 1988), and chemosynthetic ecosystem studies (MacDonald 1998 and MacDonald et al. 1996). Industry data, MMS leasing history and production data, U.S. Geological Survey (USGS) Gloria data, National Oceanographic Data Center (NODC) data, governmental holdings of results of various MMS physical oceanography programs (Texas-Louisiana Shelf circulation and Transport Process Study [LATEX], NEGOM Deepwater), and other information has been integrated into the new findings. These data formed the basis for final recommendation of study sites to the Contracting Officer Technical Representative (COTR) and the Scientific Review Board (SRB). This information was used to describe the study sites, how each site contributed to the overall program design and verification of important features of the conceptual model.

TASK 2—Field Sampling

The *R/V Gyre* was used to conduct all three cruises. Conventional sampling methodologies were used for the community structure survey and innovative experimental approaches were used for process studies. Year II and III cruises occupied those sites selected on the basis of information produced in Year I and II, respectively. The goal of the sampling program was to describe the benthic communities in distinct and identifiable settings in the study area in time and space. A phased-in approach concentrated the benthic survey portion of the work in Year I allowing ample time to process samples and analyze data. Year II and III were a mix of infilling of survey stations based on programmatic results. Experimental stations were added to address key questions related to processes and forcing factors during cruises in years two and three. The experimental stations were a subset of survey stations providing for a close integration of all data collected.

TASK 3—Sample and Data Processing and Analysis

All samples and data were processed as specified in Sections 7 and 8. The quality of data and samples was ensured by a comprehensive data management plan (i.e., the Program Management Plan). Chain-of-custody and sample tracking activities guaranteed the integrity and quality of the samples and data from shipboard collection to final synthesis. All parameters that can be reasonably measured onboard the ship (nutrients, salinity, oxygen, etc.) were measured using standard protocols, unless otherwise noted in the Results.

TASK 4—Data Interpretation, Synthesis and Reporting

This Final Report contains an assessment of historic information, the data collected, descriptions of methods and analyses, interpretations of the analyzed information, and the results and discussions of the findings. Models have been revised in light of new information. This report presents charts, maps, or schematics that portray faunal and habitat variability and the major forcing factors related to community structure and function in the deep-sea GoM, based on the new data available. In addition to this final report, publications in the open peer-refereed literature are being written, a special issue of Deep-Sea Research II is in the planning stage, and a growing set of graduate student theses and dissertations are being based on the results accrued by the study at the collaborating research and graduate educational institutions.

2. PRESENT STATE OF KNOWLEDGE

A comprehensive review of deep-sea biology is beyond the scope of this report. However, a brief review of the salient features of deep-sea ecology in general, with a focus on the GoM, provides a context for the DGoMB program. References to more detailed discussions are provided.

2.1 General Deep-Sea Ecology

The biota of the deep-sea has been sampled for almost two centuries. An age of exploration, utilizing mostly rather simple qualitative gear (trawls and dredges), continued up until the middle of the 20th century. Quantitative sampling developed for fisheries research in shallow waters began finding wide use in the deep-sea shortly after World War II. Many of the early qualitative and quantitative studies resulted in global generalizations about the "community structure" of the deep benthos (Menzies et al. 1973). Benthic metazoans have been subdivided into meiofauna, macrofauna, and megafauna, and these categories are further defined on the basis of size or major taxa. Near-bottom or demersal fishes are often lumped with the megafauna. Microbiota include heterotrophic protists such as ciliates, flagellates and forams and a suite of functional groups of bacteria. All the size groups listed, decline markedly in biomass and abundance as water depth increases although some decline at faster rates than others. A similar decline in abundance was correlated with distance from shore and surface seawater productivity (Rowe 1971). Most species, it was concluded, exhibit "zonation" with depth (Rowe and Menzies 1969) although this is more accentuated in some groups than others. A number of authors have generated elaborate schemes of "zones" based on the occurrence of faunal groups. Although the deepest parts of the ocean are thought of as "deserts," in terms of biomass, the diversity of the fauna is high compared to shallow water depth (Hessler and Sanders 1967). Many genera appear to be cosmopolitan, but in fact, a great many species are endemic to specific oceanic basins or subsets of basins. In general, Menzies et al. (1973) supported the argument that the "oldest" forms, on geologic time scales, are found at intermediate depth (slope depths) rather than at the greatest depths. The deeper living forms tend to be more specialized and hence "younger" in a geologic sense.

The summary of Menzies et al. (1973) marked a significant turning point in deep-sea biology from studies of community structure to a recognition and inclusion of studies of the dynamic aspects of the biota. These studies have been summarized in a number of articles over the years. A decade after Menzies et al. (1973), a series of papers on deep-sea community structure and function was published (Rowe 1983). Gage and Tyler (1991) review community structure, including an extensive natural history of the different functional, taxonomic and size groups of organisms. The latter work is most lucid in its description of animal growth rates. It is pointed out that many animals spawn in a seasonal manner, most likely in response to seasonal inputs of particulate organic carbon. The deep-sea is the ultimate sink for detrital particulate carbon (Rowe and Pariente 1991).

Recent investigations of "community function" were made possible by new observational capabilities such as deep submersibles, the most important being the *Deep Submergence Vessel (DSV) Alvin*, and moorings and landers that operate remotely on the sea floor without attachments to a mother ship. Reviews have documented measurements of sediment community respiration (Smith and Teal 1973); time series studies of the rapid destruction of wood by deep-sea boring organisms (Turner 1973); baited traps to attract large scavengers that rapidly consume

carcasses (Hessler et al. 1978); measurement of the slow rain of particulate matter to the deep ocean and its seasonality (Deuser and Ross 1980); and the seemingly slow deterioration of organic matter enclosed in *DSV Alvin* when it unintentionally was lost for a brief period on the sea floor. The reviews imply that low biomass, low rates of metabolic processes, and low growth rates (Gage and Tyler 1991) are a result of the minimal input of photic-zone organic carbon (Rowe and Gardner 1978). However, some taxonomically narrow groups of organisms can rapidly consume allocthonous organic matter (scavengers and wood borers, for example).

The decade of the 70's ended with a pivotal biological discovery in the deep-sea: extensive biological communities supported by reduced inorganic chemicals at hydrothermal vents (Hessler 1981). The spreading centers between the plates of the earth's crust are often characterized by fluids rich in sulfides. Symbiotic bacteria, living in the tissues of large invertebrates, oxidize the sulfide and the energy gained is used to synthesize organic matter for both the symbionts and the host. Numerous vents around the world are now known to support a wide variety of unusual but locally abundant organisms (Tunnicliffe et al. 1998). The latter review also notes that similar faunas occur near dead whales and petroleum seeps, including those in the GoM (Kennicutt et al. 1985). MMS has sponsored two programs to study GoM seep communities (MacDonald 1998; MacDonald et al. 1996) and a third study is planned in the near future. In this report, no further discussion of seeps or vents is provided, except related to the potential effects of seeps on non-seep communities.

Contemporary studies of deep-sea benthic communities continue to address a series of long-standing questions. To a large degree, these studies are designed to explore the relationships between the structure and function of deep-sea communities. The consensus appears to be that biomass and animal abundance decline at log-normal rates with increasing water depth in many of the ocean's basins. However, meiofauna and bacteria decline less rapidly than macrofauna, creating an increase in the relative importance of these taxa as depth increases (Rowe et al. 1991). This has been assumed to reflect a decline in the reactivity of detrital organic matter that requires a bacterial recycling loop at the base of the food web (Richardson and Young 1987). The Joint Global Ocean Flux (JGOFS) program has included benthic components in the Indian Ocean, the east Atlantic off NW Africa, upwelling ecosystems, polar or subpolar environments and the equatorial Pacific, all of which demonstrate the direct response of biomass, sediment mixing rate, organism growth and respiration to input of particulate organic matter (POC) from the water column. Most of the larger studies have been summarized in dedicated issues of marine science journals.

The reasons for variations in diversity remain elusive. Most new ideas are variations on Sander's original stability-time hypothesis (reviewed in Gage and Tyler 1991). Rex (1983) has pointed out that a monotonic increase in diversity does not exist in the deep-sea. To the contrary, Rex found that diversity indices peak between 2 to 3 km. Further work by others recently confirmed this pattern exists in many oceanic basins (Levin and Gage 1998). The idea that "a temporal and spatial mosaic" of physical and chemical variability enhances or preserves diversity has been tested by emplacement of sediment trays on the sea floor followed by harvesting of organisms after various deployment times. Snelgrove et al. (1996), for example, suggest that aged patches of *Sargassum* promote high diversity by providing fauna with a series of micro-habitats in time and space. However, the numbers of "expected species" in such experiments are lowest in the trays with added organic matter, leading to the possibility that competitive exclusion occurs in response to enrichment.

Some progress has been made in allocating food resources to various size or functional groups (stocks) in the deep-sea. It has been suggested for example that among the suite of organisms living within the sediments, the bacteria consume approximately 30% of the available organic matter at some locations (Rowe and Deming 1985). In the benthic boundary layer above the sea floor, organic detritus is parceled among a wide variety of epibenthic holothuroids, benthopelagic crustacea and migrating fishes, but most of the total organic matter flux, according to Smith's carbon budget, is consumed by sedimentary organisms (Smith 1992). Another consensus is that the rain of pelagic detrital organic carbon is tightly coupled to water column processes. Although it has been proposed that the lateral transport of detrital organic carbon is important, in the deep Pacific there appears to be a long-term imbalance between the input of organic matter and its remineralization (Jahnke et al. 1990; Smith and Kaufman 1999).

A growing body of information suggests that the flux of organic matter to the seabottom has considerable control over both the structure and the dynamics of benthic communities. The basic structure of the living components of the near-bottom ecosystem have been identified in terms of functional groups (Rowe 1981). Information is mounting on the relative importance of some taxa in carbon cycling and energy flow (Rowe 1983; Smith 1986a; Deming and Baross 1993; Smith 1992). Using biomass spectra to estimate production, Haedrich and Merrett (1991) suggested that a number of characteristics of community energy or carbon flow among the fishes can be inferred. While fish densities drop markedly over the slope, biomass is relatively constant to depths of almost 2,600 m, suggesting that mean size per fish increases with depth over the slope. Hence, it is inferred that the relative importance of fishes increases compared to other size and functional groups with increasing water depth to 2,600 m. At greater water depths, fish biomass precipitously declines.

Sediment-dwelling organisms appear to respond directly to fresh inputs of organic matter (Linke 1992; Deming and Baross 1993). Working at 200 to 500 m depths in the sub-Arctic Atlantic Ocean, were able to construct a budget that balances carbon input into sediment traps with total community respiration and sediment burial. A model of the functional components responsible for the cycling of carbon was then constructed. Evidence that little of the carbon was channeled through the bacteria supports the suggestion of others, that bacteria are less important at high latitudes. The dependence of the cycling of energy and carbon on input rates has also been demonstrated in comparisons of deep sub-oxic environments with oxic counterparts (Eldridge and Jackson 1991). Deep-sea sediment biomass, in general, appears to be enhanced by the fresh input of organic matter (Rowe 1971; Rowe 1983). The latter work modified and simplified the conceptual benthic boundary layer model of Smith (1992), and conducted numerical simulations to determine how biomass and respiration were redistributed within a "fertilized" system. This model, validated independently by work at Deepwater Dump site #106 in the northwest Atlantic, implies that it might be possible to predict "bioenhancement" (of biomass) in response to new carbon. This does not mean that diversity would increase. To the contrary, some models suggest that diversity would actually decrease initially due to competitive exclusion, in agreement with data presented in Snelgrove et al. (1996). The rates at which new "steady states" are reached might be much slower than in shallow water at higher temperatures. The relationship between POC input and bathymetric zonation also remains speculative.

The deep-sea is seemingly benign, rather than stressful. However some exceptions should be noted. Low oxygen zones occur in isolated basins, near large rivers and in eastern tropical areas affected by upwelling. Stress from low oxygen in the eastern Pacific for example causes a decrease in macrofauna and megafauna (Menzies et al. 1973; Rowe and Deming 1985) and

diminished diversity and tight zonation perpendicular to the oxygen gradient (Levin and Gage 1998). Likewise, hydrocarbon seeps are now known to occur widely around the world on continental margins. Some have unique communities that utilize petroleum as a source of carbon and energy, but the effects of the communities to either enhance or degrade the surrounding benthos is unclear (Montagna et al. 1989). Another natural potential "stress" studied in the deep-sea is high current velocities (Thistle et al. 1991). Referred to as the high engery benthic boundary lager experiment (HEBBLE) project, studies in high current velocities appear to harbor unique species. Recent observations have confirmed the occurrence of episodic strong currents at the base of the Sigsbee escarpment (Bryant and Nowlin, pers. comm.). An asphalt-like pavement on the abyssal plain of the Bay of Campeche is characterized by seep-like organisms, suggesting that short-chained hydrocarbons can support unique assemblages, even at abyssal plain depths.

In summary, three characteristics of community structure are recognized as important, quantifiable features of deep-ocean communities, regardless of size category:

1) variations in biomass and density per unit area,
2) variations in diversity and
3) zonation of species and recurrent groups of species with depth or parallel to bottom topography.

The general radical decline in density and biomass with depth is presumed to be related to a decline in the input of organic matter from the water column; the parabolic variation of diversity as a function of depth, with a mid-depth maximum, recurs persistently, but an explanation for it is speculative; and while species and groups of species are known to be replaced rapidly as a function of depth, the precise causes of species turnover with depth is speculative. Likewise, the continuity of the zones along depth intervals is unknown because most studies do not cover an appropriate geographic area. All three structural qualities are presumed to be related to food supply, but mechanistic explanations of the cause and effect relationships remain obscure.

2.2 Deep-Sea GoM—Geologic Setting

The GoM Basin is a study in physiographic contrasts. The simple topography of the West Florida and Campeche continental slope, the Mississippi and Bryant submarine fans and the extremely flat Sigsbee Abyssal Plain give way to the complex slump structure of the East Mexican Slope and the extremely complex topography of the Texas/Louisiana continental slope. The continental slope off Texas, Louisiana, and portions of Mississippi is geologically and physiographically the most complex in the world. Over ninety basins and seven submarine canyons dissect the continental margin of the northwestern GoM. The halokinesis of allochthonous salt is the main mechanism of interslope interlobal and interslope superlobal basin creation in mid- to lower-slope areas. Most slope basins are filled with turbidites and debris flow deposits overlain by a Holocene hemipelagic sediment cover that varies from 2 to 10 meters thick except in areas of active slumping such as the Beaumont Basin. The supralobal basins of the lower slope are probably formed by the downbuilding of salt withdrawal under the influence of turbidite sands. The termination of the slope, the Sigsbee Escarpment, is the southern most extent of a salt nappe that extends from the mid- to lower-slope. The salt nappe can prevent the migration of thermogenic gas and oil into overlying sediments. Major portions of the middle and lower slope appear to be devoid of gas seeps; thus, gas hydrate and chemosynthetic communities are not expected to be present except at the edge of the nappe (Sigsbee Escarpment) and in salt-

free basins. In contrast, the upper slope contains numerous salt diapiric structures such as mud and gas mounds, fluid expulsion features, hard-grounds, erosional gullies, and numerous gas seeps and gas hydrate deposits.

Superimposed, and eroded into the complex topography of the Texas/Louisiana slope, are four major canyon systems: the Mississippi, Keathley, Bryant, and Alaminos Canyon. The Mississippi Canyon is a Pleistocene feature resulting from slumping processes, debris flows, and turbidity current flows that were most active during the Wisconsinian. Alaminos, Keathley, and Bryant Canyon were created by a combination of coalescing salt canopies and turbidity current and debris flow erosional events. Three smaller canyons, Farnella, Green, and Cortez breach the escarpment and were formed by mass flow events. Smaller upper- and mid-slope canyons that do not extend to the escarpment are common features related to mass flow processes.

Since the late Pleistocene; Alaminos, Bryant, and Keathley Canyon have undergone extensive alteration due to infilling of the canyons by the upward migration of salt. As much as 800 meters of infill has taken place within the Bryant Canyon system over the last 12000 years. This equates to an average vertical salt movement of 6 cm/year. It is unknown if the upward motion of salt is continuous or episiodic. Recent seafloor faulting indicates that salt migration is ongoing today.

An unusual form of density flow resulting in extensive bedforms on the seafloor was recently found associated with Vaca Basin, a supralobal basin due east of Bryant Canyon. The salt infill of Bryant Canyon has resulted in brine eroding vast fields of gullies on the slopes of Vaca Basin and adjacent areas. Recent studies indicate that other large bed forms, seafloor furrows, occupy an area 15 km wide southward of the base of the Sigsbee Escarpment. These furrows are current induced structures and extensive erosion is taking place at the present time.

The geologic setting in the northern GoM is diverse, heterogeneous on several spatial scales, and actively changing within timeframes that might be expected to effect biological communities living in and on the sediments. This temporal and spatial heterogeneity of substrate in the deep-sea GoM has been fully appreciated only in recent years. This realization has lead to a new perspective on how biological communities might be interacting with geological processes.

2.3 Geochemistry of Deep-Sea Sediments

The two variables generally considered most important to the geochemistry of deep-sea sediments overlain by oxic seawater are the rate of sediment accumulation and the relative proportion of biogenic material to detrital minerals (e.g., Berner 1980). Both factors are closely related to the extent to which biologically driven reactions occur. Sediment accumulation rate controls the speed with which material is buried away from the sediment-water interface increasingly insulated from the overlying oxic waters. Consequently, the degree to which metabolizable organic matter is decomposed, at or very near the sediment-water interface, depends on sediment accumulation rate. If accumulation rates are low, little metabolizable organic matter is buried and the sediments may only reach suboxic conditions, whereas at higher accumulation rates sulfidic conditions can be reached. Related to these conditions is the second major variable, the relative input rate of the particulate organic carbon. Sediments on continental margins and beneath highly productive open-ocean waters can have a much higher rate of carbon input than those beneath oligotrophic waters. Both of these factors combine to control how far down the redox "ladder" (e.g., Stumm and Morgan 1996) reactions will progress for electron acceptors associated with organic matter remineralization and the depth spacing between the various "rungs" on the redox ladder.

An important overall general concept that is basic to this program is that physical, chemical and biologic processes are intimately intertwined. It is also particularly germane that it is the availability of metabolizable organic matter that will largely control benthic biogeochemistry and community structure. This is not simply related to the total organic matter content of sediments (e.g., Morse and Emeis 1990, 1992; Boudreau 1996). It is, therefore, necessary to look at the consumption of electron acceptors (e.g., oxygen, nitrate, manganese and iron oxides, sulfate) and the production of reaction products (e.g., carbon dioxide, ammonium, hydrogen sulfide) to understand the rates and extents to which heterotrophic activity is occurring on and beneath the seafloor.

Although there are of course many complicating factors leading to exceptions, the very general rule is that sediments tend to have lower accumulation rates and hence become less reducing with increasing water depth. This also reflects decreasing biologic activity with increasing water depth. The geochemistry of GoM sediments has been investigated over much of the study area and adjacent regions (e.g., Lin and Morse 1991; Rowe et al. 1990; Morse and Rowe 1999) to a water depth of ~2,000 m. A primary indicator of biologic activity is the integrated rate of sulfate reduction. This generally decreases with increasing water depth. However the rates are about three times higher at a given depth on the slope near the Mississippi River than at GoM slope far from the river. A distinct secondary maximum in sulfate reduction rate has been observed at ~500 m water depth. These results suggest that deep-sea biological community structure in the GoM is not simply related to depth, but may be influenced by factors such as down slope transport of sediments and organic matter. Further confounding simple relationships between structure and geochemical forcing factors, is the presence of hydrocarbon seeps. The MMS chemosynthetic community studies on the Louisiana slope, have documented integrated sulfate rates near seeps that exceed those in surrounding sediments by over a factor of fifty (Morse, unpublished data).

2.4 Physical Oceanography of the GoM

The GoM is a semi-closed basin with both broad and narrow continental shelves surrounding a deep abyss reaching 3,600 m. At the boundary in the southwestern GoM, the energetic Loop Current intrudes northward into the GoM and exits east through the Straits of Florida. The Loop Current is a permanent feature of the circulation and virtually dominates the circulation in the eastern GoM and its influence is felt throughout the GoM as anticylonic rings and topographic Rossby waves spawned by the Loop Current translate west and south. GoM tides are modest. The world's third largest river, the Mississippi River, and dozens of lessor rivers discharge tremendous volumes of fresh water into the GoM affecting stratification over large areas and enhancing wind-driven coastal jets along frontal boundaries. Wind driven upwelling occurs with regularity along the western and northeastern GoM and along the Yucatan Peninsula. Winter cyclones and summer hurricanes are not uncommon events.

The open waters of the GoM can be divided into two regimes: the eastern GoM with the anticyclonic Loop Current and the western GoM with the anticyclonic Loop Current eddies and associated cyclones. Approximately every nine months (on average, but with considerable variability), it sheds anticyclonic, mesoscale current eddies with average lifetimes longer than one year (Elliott 1982). These eddies typically migrate to the western GoM, often decaying away in the northwest corner of the GoM. The eddies can spawn cyclonic rings during interaction with one another or the continental slope. The Loop Current eddies have characteristic diameters of 200-400 km when newly detached, decreasing by 45% within 150 days and 70% within 300 days

(Vukovich and Crissman 1986). The eddies translate westward with an average speed of about 5 $km \cdot d^{-1}$ and a range of 1-14 $km \cdot d^{-1}$. Currents associated with the Loop Current and its eddies extend to depths near slightly greater than the sill depth of The Florida Straits (800 m). The currents may have surface speeds of 150-200 $cm \cdot s^{-1}$ or more; speeds of 10 $cm \cdot s^{-1}$ are not uncommon at 500 m (Cooper et al. 1990). Because of their longevity, the effects of the Loop Current eddies can persist at one location for weeks or even months.

Anticyclonic Loop Current eddies interact with one another and with the continental slope resulting in their decay. In the process of the interactions, and of the interaction of the Loop Current with topography, many cyclonic eddies are generated within the GoM. Some evidence exists that anticyclonic eddies may also be formed by ring-ring interactions, but they would not have the high salinity core characteristic of Loop Current eddies. Below 1,000 m, strong current events have been observed (e.g., Science Applications International Corporation [SAIC] 1989). The Loop Current and Loop Current eddies may influence the dynamics to the deepest portions of the GoM (~3,500 m; Smith 1986b; Hamilton 1990) through the generation of phenomena such as barotrophic Rossby Waves. Likewise strong, episodic atmospheric events (e.g., hurricanes or cyclones) can generate currents that extend to depths of 1,000 m or more. Speeds up to 50 $cm \cdot s^{-1}$ have been observed associated with these classes of deep currents. Deep currents are the main interest of the MMS-sponsored inventory and synthesis of physical oceanographic data in the deepwater GoM.

Characteristic relationships of physical and chemical water properties (e.g., temperature, salinity, dissolved oxygen, and nutrients) can be used to identify water masses and their sources. Surface waters of the GoM are greatly modified by heat and freshwater exchanges through the surface, river discharges, and wind mixing, but no subsurface water of consequence is thought to be locally formed. Waters from the global ocean enter the GoM only through the Yucatan Channel from the Yucatan Basin of the Caribbean Sea. Seawater properties can be used to identify the five water masses that enter the GoM (Table 2-1). Source regions for these waters are discussed in Morrison and Nowlin (1982). Morrison and Nowlin (1977) described the water masses found in the Loop Current of the eastern GoM, and Morrison et al. (1983) described the water masses and properties found offshore in the western GoM. As the waters of the Loop Current enter the GoM, those along its western boundary are vertically mixed by the interaction of the current with bathymetry, resulting in an averaging of properties (Nowlin 1972). Moreover, after separation, Loop Current eddies eventually spin down in the GoM. That process entails mixing, which likewise lessens property extrema. Below the Yucatan Channel sill depth of about 2,000 m, the potential temperature, salinity, and dissolved oxygen concentrations show no measurable horizontal variation throughout the GoM (Nowlin 1972).

Table 2-1

GoM Water Masses with Associated Property Extrema and Potential Densities

Water Mass	~ Depth Range (m)	Identifying Feature(s)	Sigma-theta ($mg\ cm^{-3}$)
Subtropical Underwater	50-250	salinity maximum	25.40
18°C Sargasso Sea Water	150-250	oxygen maximum (weak in west)	26.50
Tropical Atlantic Central Water	250-500	oxygen minimum	27.15
Antarctic Intermediate Water	500-1000	salinity minimum; nitrate, phosphate, and silicate maxima	27.30-27.50
Upper North Atlantic Deep Water	> 1000	silicate maximum	≥ 27.70

The earliest attempt at a comprehensive synthesis of the physical oceanography of the GoM is found in Capurro and Reid (1970). Since then, and particularly in the last 15 years, the study of the physical oceanography of the GoM has greatly accelerated. Much, if not most, of this increased study has been funded by the MMS acting in response to intense energy exploration and production activities on the shelf, slope, and rise. The first such study, initiated in 1982, was a five-year program implemented as a series of regional studies. These studies included field work in the west, central, and eastern portions of the northern GoM. The results, detailed in a final report, emphasize eddy variability. MMS also sponsored a synthesis of GoM meteorology and climatology data during this same period (Florida A&M University 1988). A major MMS-funded physical oceanography study was the LATEX program which surveyed and maintained current moorings between 1992-1994 along the Texas-Louisiana shelf from the 10-m isobath to the shelf break from Brownsville to 90.5°W. The LATEX program was a joint effort accomplished by TAMU, Louisiana State University (LSU), and Science Applications International Corporation (SAIC). Other study units sponsored by MMS, but not strictly part of LATEX, generated significant amounts of related collateral data during the same time period. Taken collectively, this study was the largest and most comprehensive shelf study ever conducted. Following LATEX, a new series of programs similar in scope to LATEX but organized differently, were initiated in the northeastern GoM. The most significant circulation studies include a large (>350 drifters) program conducted by Peter Niiler of Scripps Institute of Oceanography and Walter Johnson of MMS between February 1996 and February 1997, a moored array and hydrography program conducted by SAIC in DeSoto Canyon from March 1997 to March 1999, and an ongoing hydrography and water chemistry program over the shelf and slope between the Mississippi River and Tampa, Florida from November 1997 to August 2000. In 1998, a data synthesis study of the physical oceanography of the deep water GoM was begun by TAMU under MMS sponsorship. The results of this study, it will include a complete database of all available information and the design for a deep mooring array.

2.5 Deep-Sea Ecology of the GoM

The earliest studies of the deep GoM biota were by Alexander Agassiz (1888) but his voyages never penetrated the western Gulf. The National Marine Fisheries Service has long maintained an exploratory fishing fleet in Pascagoula, MS and information is available from extensive trawling on the continental slopes of the GoM and the Caribbean. In the mid-1960s studies on the biota of the deep GoM were initiated (Pequegnat et al. 1990). A wide range of investigations of the deep water ensued, including the first quantitative samples with a Campbell grab coupled with a camera (Rowe 1966). Several bottom contact and automatic cameras were used and camera lowerings were dispersed more or less evenly around the GoM margin, including the Gulf of Campeche near Veracruz, Mexico. A benthic "skimmer" was built to catch larger forms and it was outfitted with an odometer to determine bottom distance traveled. These samplings included the Caribbean, as well as the GoM. Faunal groups studied from the deep GoM included squids, crustaceans (Firth 1971; Pequegnat 1970), echinoderms (Carney 1971), molluscs, and fishes (Bright 1968) among others. Assemblages of both the megafauna and the macrofauna were also studied. Fish feeding habits were intended to link the two. Photographs of an "iron stone bottom" north of the Yucatan Strait suggested deep bottom currents sweep some areas free of sediments (Pequegnat 1972). Some taxa displayed remarkable "zonation" by species, such as the bivalve molluscs (James 1972) and the asteroid echinoderms. The macrofauna appeared to be grouped into assemblages, based on measures of similarity, that were

distributed within "zones" down the slope and onto the abyssal plain, but no justification was found for separating deep-living fauna into zoogeographic provinces by latitude or longitude (Kennedy 1976).

In 1968, semi-quantitative samples were taken across the Sigsbee Abyssal Plain and then in 1972, quantitative samples were obtained from the lower slope up onto the continental shelf on two transects seaward of Galveston and Pascagoula. These quantitative data suggested that the deep fauna of the GoM was depauperate in numbers and biomass, and that the mean size of the macrofauna was in general smaller than that in the Atlantic at similar depths (Rowe 1971, Rowe and Menzel 1971, Rowe et al. 1974). Later studies, such as the NGoMCSS, used the conversion factors from numbers and size to estimate biomass. The log-normal relationship between biomass and depth has now been confirmed for numerous ocean basins (Rowe 1983), but the slope of the line for the GoM is steeper than that in most basins. It has been suggested that this is due to the low primary production in the GoM.

The most extensive sampling of the sediment biota of the northern GoM was the NGoMCSS study supported by the MMS in the 1980's. This consisted of paired GoMEX (not to be confused with GoMEX) boxcores (Boland and Rowe 1991), bottom survey camera lowerings and trawl samples. The stations studied included three transects down the slope in the western, the central and the eastern GoM with a line along the upper slope connecting the west and central transects along isobaths. Several reports were written describing the work but the most concise summary is a paper by Pequegnat et al. (1990). In the descriptions of the characteristics of the three dominant size classes (the meiofauna, the macrofauna and the megafauna) the meiofauna appeared to dominate the biomass, a feature that would be odd for shallow water but a relationship that is becoming increasingly apparent at deep-sea stations when size groups are compared (Rowe et al. 1991). It was also suggested that the fauna were distributed in "zones" along isobaths on the upper slope, but less so on the lower slope. As is true for most deep ocean basins, the meiofauna were dominated by nematodes, the macrofauna by polychaetes and the megafauna by echinoderms. Lesser numbers in each size category were also quite predictably encountered in taxa such as the molluscs and crustaceans. Similarity indices suggested that the eastern GoM, east of the DeSoto Canyon, was not similar to that in the northwestern GoM at similar depths. "Zonation" with some groups was modest, at best. This was true of the polychaete annelids. Within this group, no species was encountered below the sill depth of about 2 km that was not encountered at lesser depths as well.

An important discovery made during earlier slope studies were communities of large organisms associated with petroleum hydrocarbon seeps (MacDonald et al. 1996). Such communities, bearing a resemblance in both taxa and function to those associated with hydrothermal vents, have now been documented at numerous locations on the continental slope of the northwestern GoM in areas where fossil hydrocarbons make their way to the sediment surface. Bubbling or seeping gas appears as "wipeout zones" in acoustic surveys of the bottom. These communities are the subject of ongoing studies supported by MMS and other agencies and will not be described in detail here (MacDonald 1998). Cold seeps supported by hydrogen sulfide in "ground water" appears to support communities of large invertebrates, again being somewhat similar to those at hydrothermal vents, on the lower reaches of the Florida Escarpment (Paull et al. 1984).

The Instituto Ciencias del Mar y Limnologia of the Universidad Nationale Autonoma de Mexico (UNAM) has conducted extensive studies in the southern GoM. Early studies of megafauna on the shelf were expanded down slope into the "salt diapir zone" just west of the

Campeche Bank. These studies were extended into the Sigsbee Abyssal Plain close to the exclusive economic zone (EEZ) between the U.S. and Mexico (26°N. Lat.) as well. Pathways of carbon and nitrogen in the benthic foodweb were inferred by stable isotopic analysis (Soto and Escobar 1995). In deep water studies across the *Cordilleras Mexicanas* or "Mexican Ridges" of the upper continental rise out onto the Sigsbee Abyssal Plain regions that contain enhanced biomass have been identified under water masses that have high rates of primary production (Escobar-Briones et al. 1999). Polychaetes dominated the infauna and a mid-slope maximum in abundance similar to that encountered in the northern GoM has been documented (Pequegnat et al. 1990). The fauna could be partitioned into three groups within depth intervals of >3 km, between 1.5 and 3 km, and <1.5 km. This contrasts with the view of Pequegnat et al. (1990) that five faunal groups can be divided into recurrent "zones."

Several studies currently being conducted in the GoM are also important. Studies in the Bay of Campeche in the northwestern GoM are producing important findings (TAMU/UNAM). In 1997, at a station in 3.6 km water depth (25°15' N. Lat. x 93°26' W. Long.) on the northern Sigsbee Abyssal Plain, the first sediment oxygen consumption measurements in the deep western GoM were made. The sediment oxygen consumption was equivalent to 3.8 mg carbon/m^2-day. Quantitative analysis of samples of the benthic community on the Sigsbee Abyssal Plain confirm that benthic biota are extremely sparse. Baited bottom traps in the area attracted deep-sea scavenging amphipods. The diversity of polychaetes was not appreciably different from that measured in the NGoMCSS study (LGL and TAMU 1988).

Another important investigation is a study of mollusc shell "taphonomy" which measures preferential preservation of material in the fossil record. Ongoing, *in situ* experiments at about a dozen long-term sites within the MMS study area have been established. The strategy is to set out shell material and assess diagenetic changes over time frames of years. Bottom chamber measures of sediment oxygen consumption and quantitative faunal samples at each site have also been collected. The hypothesis being tested is that the chemical dissolution of carbonate is accentuated in areas of high oxygen consumption. These sites stretch from the brine pool at the Flower Gardens down to ~1,000 m depth. Oxygen consumption measurements have been taken at a number of locations in the study area.

3. A CONCEPTUAL MODEL OF THE DEEP-SEA

A conceptual model of the deep-sea, it's living and non-living components, has been constructed to represent the interacting stocks of organisms that make-up a typical benthic boundary layer community (Figure 3-1). A biological boundary layer is defined as approximately 1 m deep into the sediments, extending up through the mixed layer of the water column to approximately 100 m above bottom. This biological boundary layer thus conforms to that previously used to describe the principal interacting components of a deep-sea benthic community (Smith 1992). This conceptual model has been drawn in software called STELLA II. The software allows flexibility in reformulating the structure and internal relationships within the system. The formulation presented is a modification of the model used by Smith (1992) and represents a deep-sea food chain. The modifications consist of defining every stock variable, living or non-living, as a "box" and every process, such as predation or respiration, as an "arrow." Thus all interactions between the biota and the sources and sinks of organic matter are explicit either as "boxes" or "arrows." On the other hand, "physical" processes are not explicitly represented. These implicit factors affect the "arrows" between the "boxes." Each "box" has a "size" in terms of concentration, biomass or abundance that is the sum of the "arrows" entering the "box" minus the "arrows" leaving the "box." At steady-state, each "box" does not change with time, and thus the inputs equal the outputs or losses. An important process, respiration, has been omitted in this conceptual food chain. Each stock can be taken separately in a submodel (Figure 3-2). Macrofaunal biomass, for example, is a function of what it consumes, what consumes it, respiration, and feces production.

The contents of each stock can be expressed as a differential equation. The set of differential equations of all the stocks can be used to simulate the behavior of the entire food chain over time. The problem with doing this in the deep-sea is that data to quantify the stocks and processes are sparse at best. While considerable information exists on the stocks in a few locations and a few data exist on the rates of processes in others, the locations where both stocks and fluxes are known, even in the most minimal sense, are quite limited. One exception is a study of the central North Pacific, but even this study treated the sediment dwelling biota as one functional group due to a lack of detailed information on the foodweb (Smith 1992; Smith and Kaufmann 1999).

An advantage of this model is that with adequate data it can be used to simulate how the ecosystem will function under different conditions. Previously this approach has been used in an oligotrophic upper continental slope environment off eastern Greenland (Rowe et al. 1997). Boxcore standing stocks of the components represented were coupled with measures of community respiration (using a bottom lander with benthic chambers) and laboratory measures of bacterial activity to simulate the variations in biomass over time in response to a single seasonal pulse of organic matter related to a short ice-free period. In a purely hypothetical situation, the bioenhancement of infauna due to the disposal of organic rich material, such as sewage sludge or dredge spoils, was modeled, based on a simplified rendition of the Smith (1992) model (Rowe 1998). By adding organic matter in a pulse, the community "shifted up" to higher biomass and higher respiration and the alteration predicted by the model was validated by actual data at Deepwater Dumpsite 106 on the continental rise in the northwest Atlantic Ocean. This feature of "shifting" up or down in response to different input terms will be an important tool for interpreting the response of community structure and function in the deep-sea GoM in reaction to inputs from oil and gas exploration and production activities. The two most relevant

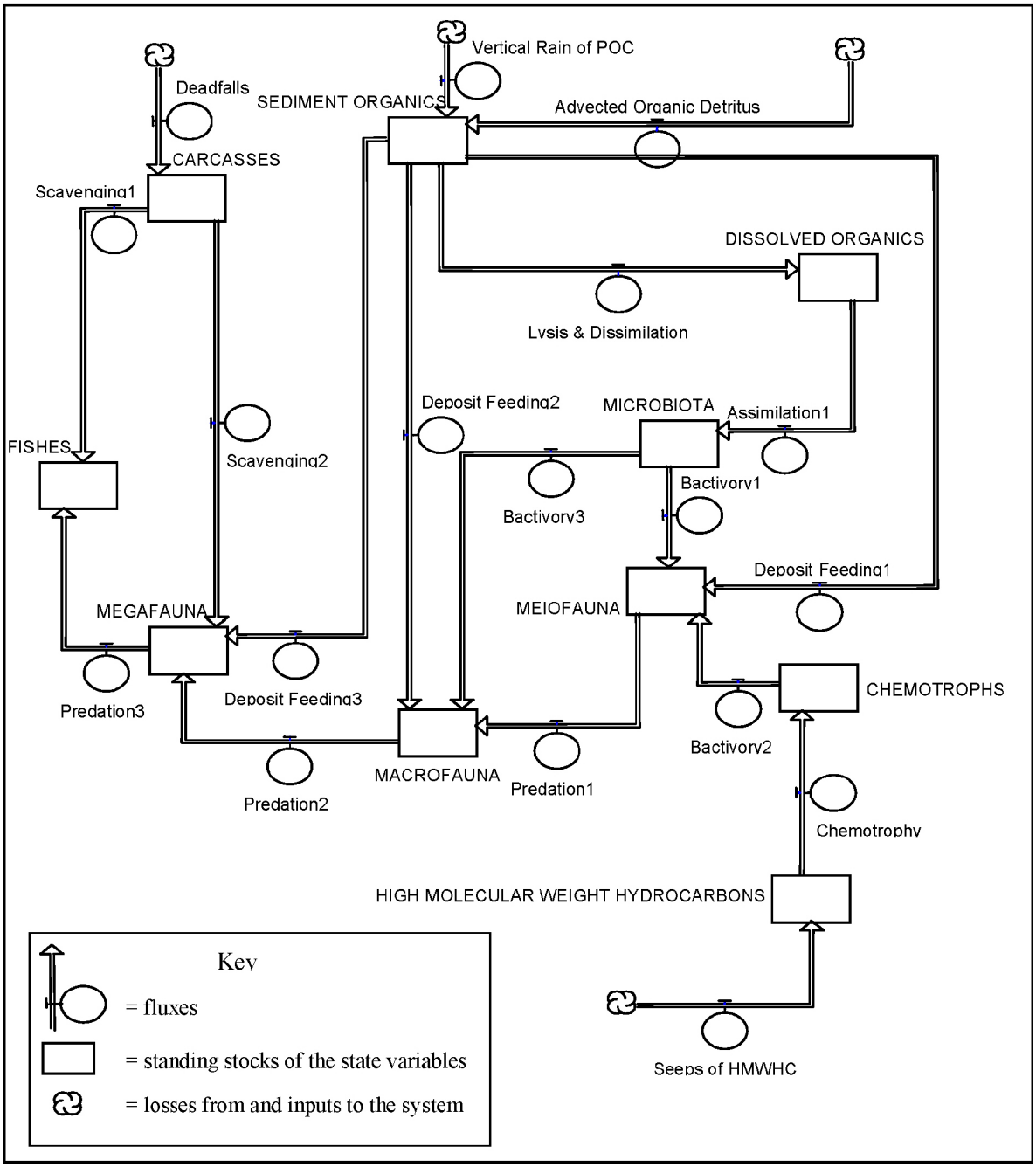

Figure 3-1. Preliminary conceptual model of the deep-sea Gulf of Mexico.

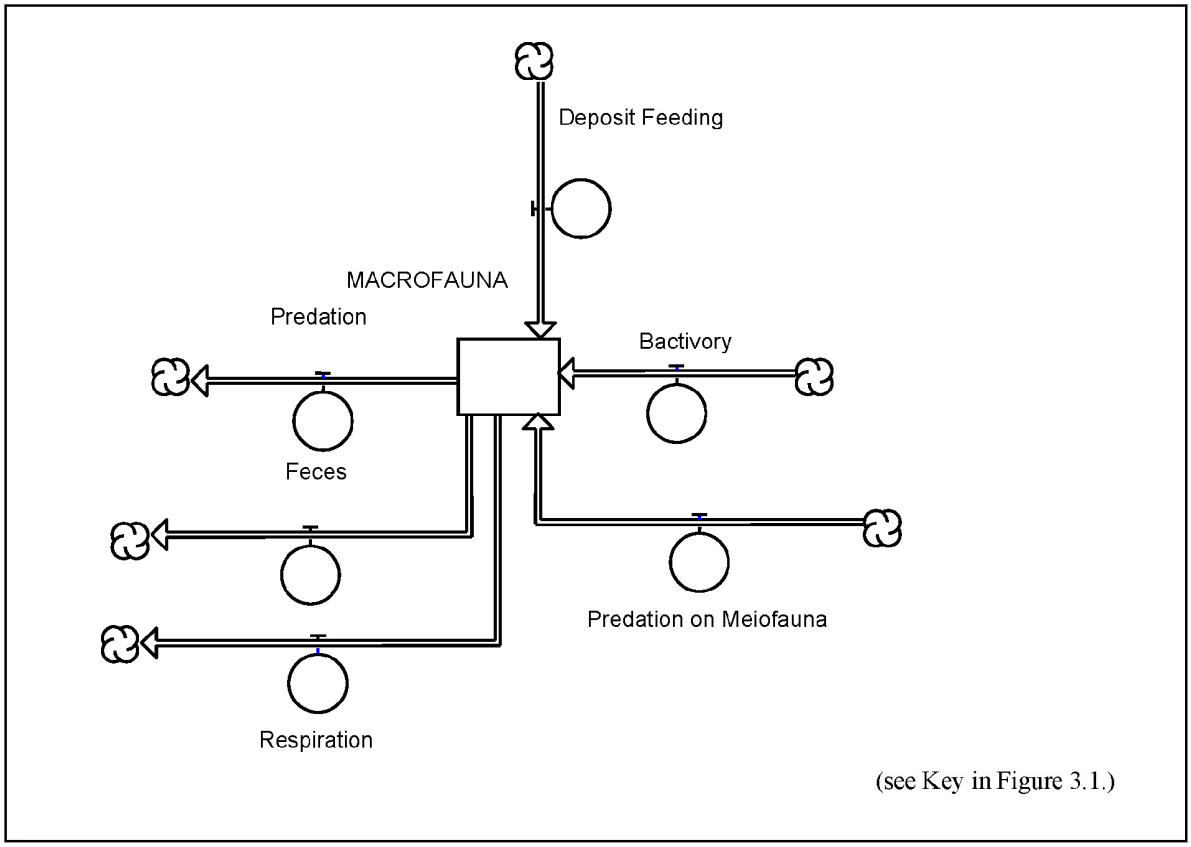

Figure 3-2. Macrofauna submodel of system carbon food chain model.

inputs at platforms are organic enrichment due to a "reef" effect and the introduction of contaminants.

3.1 Biotic Variables

The details of the conceptual model can be described as a number of biotic and abiotic variables (living and non-living). In addition, the model is described in terms of various derived variables related to community structure and function. In-the-end, an understanding of the model components and their interactions are used to select the set of variables to be quantified that best describe the functioning of the system being studied. These inferences are then ground-truthed by in-the-field observations and the model is revised as needed. The biotic variables include the microbiota, meiofauna, macrofauna, megafauna, and fishes. These groups of biota make up the overall stocks of the system which are estimated through conventional quantitative sampling as described in Sections 6.0 and 7.0.

Microbiota. The microbiota are the "bottom" of the food chain. Microbiota are represented by the bacteria and protists, including benthic foraminifera. Their principal food source is thought to be dissolved organic matter, although particulate material can be directly utilized if the biota can produce exoenzymes to mobilize particles. The protists can engulf and assimilate particulate material as well. The bacteria generally have a density of about 10^9 per mL of wet sediment, measure about a micrometer in size, and can have very short turnover rates in the presence of reactive organic substrates. The protists can be much larger and occur in far fewer numbers than the bacteria. Protists are thought to be important components of ecosystems in

areas of reduced oxygen. With the exception of the forams, microbiota have rarely been evaluated in the deep-sea.

Bacteria that are specially adapted to utilizing methane and sulfide are common in areas characterized by petroleum seeps (MacDonald et al. 1996; MacDonald 1998). Many of these are symbiotic, living in the tissues of large invertebrates. While these specialized associations are explicit in this model, they are presumed to be confined to "seep" areas.

Foraminifera are large shelled protozoans, often the size of metazoan meiofauna. Few studies have compared foraminiferal biomass to other benthos in the deep-sea, but biomass can exceed the meiofauna (Coull et al. 1977) and abundances commonly exceed the meiofauna plus the macrofauna (Snider et al. 1984; Gooday 1986). Although little is known regarding foraminiferal energetics, it has been shown that foraminiferal metabolism is markedly increased by organic enrichment (Linke 1992). Therefore, accurate deep-sea carbon and energy budgets should include the foraminifera.

Meiofauna. In this model, meiofauna are defined as metazoans that are retained on a 63 micron sieve. Meiofauna include nematode worms, harpacticoid copepods, and several other taxa. In some studies benthic forams are also included, but in this model, forams are considered part of the microbiota because they are single-celled organisms, rather than metazoans. Most meiofauna feed on small particles consisting of detritus, bacteria, other meiofauna, and small protozoa such as ciliates and flagellates. Turnover rates for meiofauna can be as short as a few days when temperatures are high and food is plentiful. No reliable generalizations can be made about their turnover times or growth rates in the deep-sea, but it is assumed that both are substantially slower than in shallow water due to food limitation and cold water temperatures. In shallow waters meiofauna biomass is less than that of the macrofauna, but in the deep-sea this appears to be reversed.

The finding that meiofauna biomass is higher than macrofauna biomass in the northern GoM (Pequegnat et al. 1990) indicates that meiofauna may be responsible for much of the organic matter metabolism in deep-sea sediments. Therefore, a survey of meiofauna community density and biomass is needed to characterize this energetically important group. In shallow coastal systems, meiofauna remove bacteria at a rate that equals sediment bacterial production (Montagna 1995). This indicates meiofauna are most likely responsible for maintaining bacterial populations in log-phase growth cycles and are therefore indirectly responsible for maintaining rates of nutrient recycling. Despite the apparent importance of meiofauna in deep-sea energetics, there is no knowledge of the rates at which these processes occur. Therefore, process studies are needed to assess meiofaunal consumption rates. Techniques to measure meiofaunal bacterial feeding rates on bacteria have only been used in shallow water (Montagna 1995).

Macrofauna. Macrofauna, in this model, are the invertebrates retained on a 300 micron sieve. The principal organisms are polychaete worms (≈50%), bivalve molluscs, and crustaceans in the groups Isopoda, Amphipoda, and Tanaidacea. The production to biomass ratio of the macrofauna in shallow water communities is often assumed to be unity, but this can vary widely. In the deep-sea, it is assumed the ratio is much lower but there is little evidence for this one way or the other. Biomass and densities decline sharply with depth in most ocean basins. Macrofauna consume microbiota, meiofauna and organic detritus. Macrofauna are preyed upon by megafauna and fishes.

Megafauna. The megafauna are organisms that are routinely sampled by trawls with 2.5 cm stretch mesh or organisms that can be seen easily in bottom photographs, usually about 1 cm or so in diameter. They are composed for the most part of decapod crustaceans and echinoderms.

Cnidaria, such as sea pens, soft corals and anemones, are also common in the megafauna. Megafauna can be suspension feeders, predators, scavengers or deposit feeders. For the purpose of the model, the swimming scavengers that consume carcasses, such as the large amphipod *Eurythenes grillus*, are included in this group. Megafauna have been extensively observed with photographic techniques.

Fishes. Demersal fishes are defined as those species that live on or near the bottom. Fishes are both predators and feed on dead falls, megafauna and macrofauna.

3.2 Community Structure

Community structure, in the context of this model, has two interpretations. It is represented explicitly in the conceptual model as the standing stocks of the living components of the ecosystem as discussed above, and as such it represents the relative and absolute importance of the stocks in terms of biomass and rates of processes in the model. Secondly, community structure refers to the parameters that quantify the living stocks, as described below.

Biomass. A measure of the standing stock in some currency of mass per unit area of seabottom is biomass. Wet weight is a common measure. It can also be measured as dry weight, ash-free dry weight or carbon. The model currency is carbon, so the ideal measure is in terms of carbon. Biomass tends to be inversely related to depth, in a log-normal fashion. Within the entire community, the highest biomasses are found in the total bacterial counts, both in shallow and deep water. All the size fractions in the deep-sea have biomass values that are somewhat lower that 1 g C/m^2. In shallow water, each fraction can have biomasses of 10's of g C/m^2 in unusually fertile conditions. This is not expected in the deep-sea.

Abundances. A surrogate for biomass, that is often measured in ecosystem studies, is animal abundance or density. However, mean sizes can vary. In the GoM, mean size seems to decrease with depth. Common abundances for the organismal groups in the model are bacteria, 10^9/mL wet sed.; meiofauna, 0.25 to 1.5 x $10^6/m^2$; macrofauna, 10^2 to $10^4/m^2$; megafauna and fishes, several hundred to a thousand per hectare. The abundances of each group are hypothesized to be a function of the input of carbon and energy to the stock. If the relationship of numbers to biomass is known, these abundances can be used in the model. The NGoMCSS studies used conversion factors from the studies of Rowe (1971) to calculate biomass from densities.

Diversity. Measurements of the numbers of different species are expressed as diversity values. Diversity has been assessed on macrofauna, megafauna, and fishes. Diversity indices attempt to lessen the effects of sample size, to aid comparisons between regions of differing animal densities. Common indices of diversity are Sanders Rarefaction, Hurlburt's expected species number E(s) and the information function H'(s). The GoM appears to be somewhat different from large ocean basins in that maximum diversity is not found on the deep slope or upper rise, but rather on the upper slope or outer shelf. Thus it is similar to other isolated "mediterranean" basins where diversity declines with depth down the slope. It is expected that intense inputs of organic matter will decrease diversity due to competitive exclusion. Diversity is not calculated by the model.

Zonation. The degree to which individual species and groups of species are isolated across isobaths (zonation), between geographic regions, or any other physico-chemical gradient is referred to as zonation. Zonation by groups of species as a function of depth has been measured by "rates of species change" across depth intervals or measures of percent similarity between depths. These can be measured on meiofauna, macrofauna, megafauna, and fishes. Groups of species appear to occur in zones, but considerable overlap has been observed as well, with few

distinct, immutable boundaries. On the other hand, some individual species of megafauna tend to have a shallow water boundary that is sharp and severe and a deeper water boundary that is a slow decline in numbers with depth. Zonation down slope is hypothesized to be a function of competition along a gradient of declining food supplies. Zonation is not calculated by the model but can be addressed through hypothesis testing.

3.3 Community Function

The processes, or arrows, in the model encompass a wide range of interactions amongst the model's components.

Microbial Activity. The respiration and the assimilation of organic substrates by the microbiota are dependent on inputs of organic matter and temperature. In the model this can be either sedimenting POC or hydrocarbons. The sedimenting POC can be derived from several sources, as indicated above. A basic assumption is that, in general, smaller organisms are consumed by larger organisms because it is more energy efficient. If the organic matter is reactive, the food web will compete for the organic matter. If the organic matter is highly refractory then it is assumed that a food chain will dominate in which the bacteria remobilize the organics in order to make it available to metazoans. Predation is represented as arrows between the living components of the model as indicated. It is assumed that large organisms will preferentially take large prey rather than small prey because it is more energy efficient. Macrofauna are assumed to be deposit feeders. Heterotrophic bacteria are assumed to consume sediment organic matter. Scavengers consume carcasses and are included in the megafauna. Fishes consume megafauna and carcasses. Respiration is one of the most important measures for each organismal group because it dominates the carbon cycle. However, respiration is not explicit in the conceptual model. Most carbon that is consumed (50 to 90%) is recycled to metabolic carbon dioxide. Respiration is estimated from animal size and temperature for the larger organisms based on literature values.

Growth, Reproduction and Recruitment. The rates of growth, reproduction, and recruitment are poorly known in deep-sea organisms. The model can calculate growth by fundamental or size group. Reproduction and recruitment are not well known. It is assumed that growth, reproduction and recruitment can be seasonal in some species but this kind of information for the GoM slope is inferential at best. It should be noted that in the NGoMCSS study's central transect, it did appear that there were about 1.5 times as many macrofauna individuals on the upper slope in the spring than in other sampling periods, suggesting that some type of growth, reproduction, and/or recruitment had occurred, but the mechanism that gave rise to this observation is unclear.

3.4 Sediment Properties

Non-living model variables include the "fuel" for the system and those processes that supply carbon and energy to the ecosystem. Inputs of carbon are critical to the functioning of the ecosystem, and is often present in limiting amounts in the deep-sea. On the GoM slope, labile organic matter is transported to the communities from primary productivity (either directly settling to the site or being laterally advected), fossil sources of carbon (oil and gas to support chemosynthesis), and potentially from large animal carcasses and sinking *Sargassum*.

Sedimentary organic matter includes a suite of natural organic compounds found in deep-sea sediments. Organic matter is derived mostly from the slow rain of particulate organic matter (POM) originating from dead cells, crustacean molts, and fecal pellets produced by plankton in the overlying photic zone. Some POM sinks very slowly but aggregates and pellets can rapidly

reach the seafloor. The composition of organic matter that reaches the sediment is largely unreactive and poorly characterized. POM is extensively reworked in the water column either being remineralized or transformed to dissolved organic matter (DOM). The amount of POM that reaches the sediment, its ultimate repository, is affected by many factors but, in particular, the water depth. POM concentrations in the sediments of the deep-sea are low. Relatively refractory terrigenous-sourced organic matter is an increased percentage of the POM close to shore and river discharge points. POM is usually inversely proportional to grain size, but does not correlate well with the biomass of the living components. In spite of its meager reactivity, it is assumed to be the basis of the deep-sea food chain except at hydrocarbon seep sites.

Three sources of sediment organic matter are possible in the deep-sea and two are explicit in the model: vertical transport from the photic zone and lateral export from the continental margin. The third source is slumping of material from organic matter-rich areas up-slope and its importance is unknown.

The discovery of chemosynthetic communities with large megafaunal communities dependent, through their symbionts, on methane and sulfide derived from natural seeps has highlighted a non-photosynthetic source of carbon and energy for deep-sea GoM organisms. Hydrocarbons migrate to near-surface sediments from deep subsurface reservoirs of oil and gas. The megafauna communities of note utilize the hydrocarbons but are living within the larger organisms, not in the sediments or within the hydrocarbons. "Seeps" support high biomass but their influence on biota outside of the immediate vicinity of the seeps is largely unknown. Recent chemical evidence indicates that the biogeochemical influences of seeps in sediments tend to be localized (John Morse, pers. comm.). The oil and gas is often degraded by bacteria inducing anoxic conditions in the adjacent sediments producing sulfidic environments.

A poorly quantified input of organics to the deep-sea are falls of carcasses that die or are killed in the water column, usually near the surface. Carcasses can range in size from a few centimeters to a whale of several tons. The relative importance of this source of organic matter is not well established. It is known that scavengers exist that can take advantage of such sources, if and when they are available. Similarly, *Sargassum, Thallasia,* wood, etc. has been observed on the bottom as well.

There is a range of abiotic variables that has been shown to influence biotic patterns in marine environments. One type are those related to the physical texture of the sediment and including properties such as grain size, permeability, porosity, and organic and inorganic carbon content. As the substrate that supports the benthos, variations in these physical properties are important in understanding biotic patterns. In addition, it is known that influxes of organic matter and contaminants can cause changes in community structure and abundance. Introductions of labile carbon will cause opportunistic animals to flourish and others to do less well. Organic matter enhancement also leads to anoxic conditions that produce a range of toxic chemicals such as sulfides. Organisms are also known to be selectively sensitive to chemical contamination from hydrocarbons and trace metals. Some animals can tolerate exposure better than others causing shifts in populations when communities are exposed to pollution. In addition, hydrocarbons, particularly aliphatics can be metabolized by microbes and may actually enhance sedimentary microbial populations rather than exert a toxic effect, though as mentioned above, oxygen and sulfate consumption can produce toxic chemicals.

Explicit in the model is microbial biomass but functional groups of bacteria are not defined. All of the bacteria and protists are assumed to be heterotrophs, as opposed to possible chemoautotrophs in the "chemotrophs" stock. However, the terminal electron acceptors

(oxidants) of heterotrophs can differ. In the oligotrophic central gyre areas of the deep-sea where sediments are oxic, all the bacteria are assumed to be aerobes. In sediments on continental margins, this is probably not true. Below the sediment-seawater interface the functional bacterial groups are defined by the terminal electron acceptor (TEA) they use (Figure 3-3). Few comparisons of the importance of the different TEA's (oxidants) have been made, but in rapidly accumulating sediments near the Mississippi delta, oxygen and sulfate were of equal importance. However, as oxygen declined and became limiting, sulfate reduction dominated heterotrophic metabolism. These processes are measured by examination of the porewater chemistry with depth in the sediment. These processes are important in situations where organic loading depletes oxygen in significant relative to oxygen consumption. Oxidized metals can also be used as oxidants. Comparisons with other oxidants are limited but in some situations this process is thought to be important. In sediments containing even modest amounts of reactive organic compounds, sulfate reduction can become the dominant respiratory process, even greater than oxygen. This is because sulfate is the fourth most abundant ion in seawater, having a concentration that is 140 times that of oxygen at saturation. Lin and Morse (1991) have made a series of cross slope transects around the GoM in which they derived integrated sulfate reduction rates down core. Highest rates were near the Mississippi River. Lowest rates were in oligotrophic areas of the southern GoM. Methane can be produced as a breakdown product of metabolism of large carbon compounds and it can be formed when carbon dioxide is used as the oxidant. Methane can then be used as an energy source by bacteria. This methanotrophy occurs in methane seeps near hydrocarbon seeps. Therefore, characterization of the geochemical properties at a location is important for ascertaining the basic metabolic processes that are important to the base of the food chain. Significant alteration of the inputs to the system, in particular carbon, can result in large shifts in bacterial populations and metabolic strategies. In addition, the rate of sediment accumulation and the intensity of bioturbation (mixing) are important in establishing the sediment redox conditions and provide insight into the reactivity of sedimentary organic matter.

3.5 Water Column Properties

The currents in the overlying water column are important when considering biotic patterns. Near-bottom currents are in part responsible for establishing the sediment properties by transport to the site and also winnowing/erosion of sediments. The water column is also the medium through which the overlying primary productivity is transported to the sediment. The currents serve as a mechanism for transport of larvae and juveniles throughout the system. So any model of the deep-sea must take into account the dynamic nature of the physical oceanography, and the hydrography of the water masses that overlie and interface with seabottom habitats.

3.6 Community "Health"

While widely discussed, the concept of ecosystem "health" remains elusive. Due to the complex nature of natural ecosystems an overall assessment of health is difficult to define. Specific portions of an ecosystem can be characterized by parasite infestation, pathologies, reproductive success, demographics (age distribution), and the presence of measurable responses to stress (such as stress proteins and the inducement of P450 detoxification enzymes) to name just a few potential indicators of "health." However, a mechanism or approach to provide an overall integrated assessment of the community "health" has yet to be agreed to. For example, in

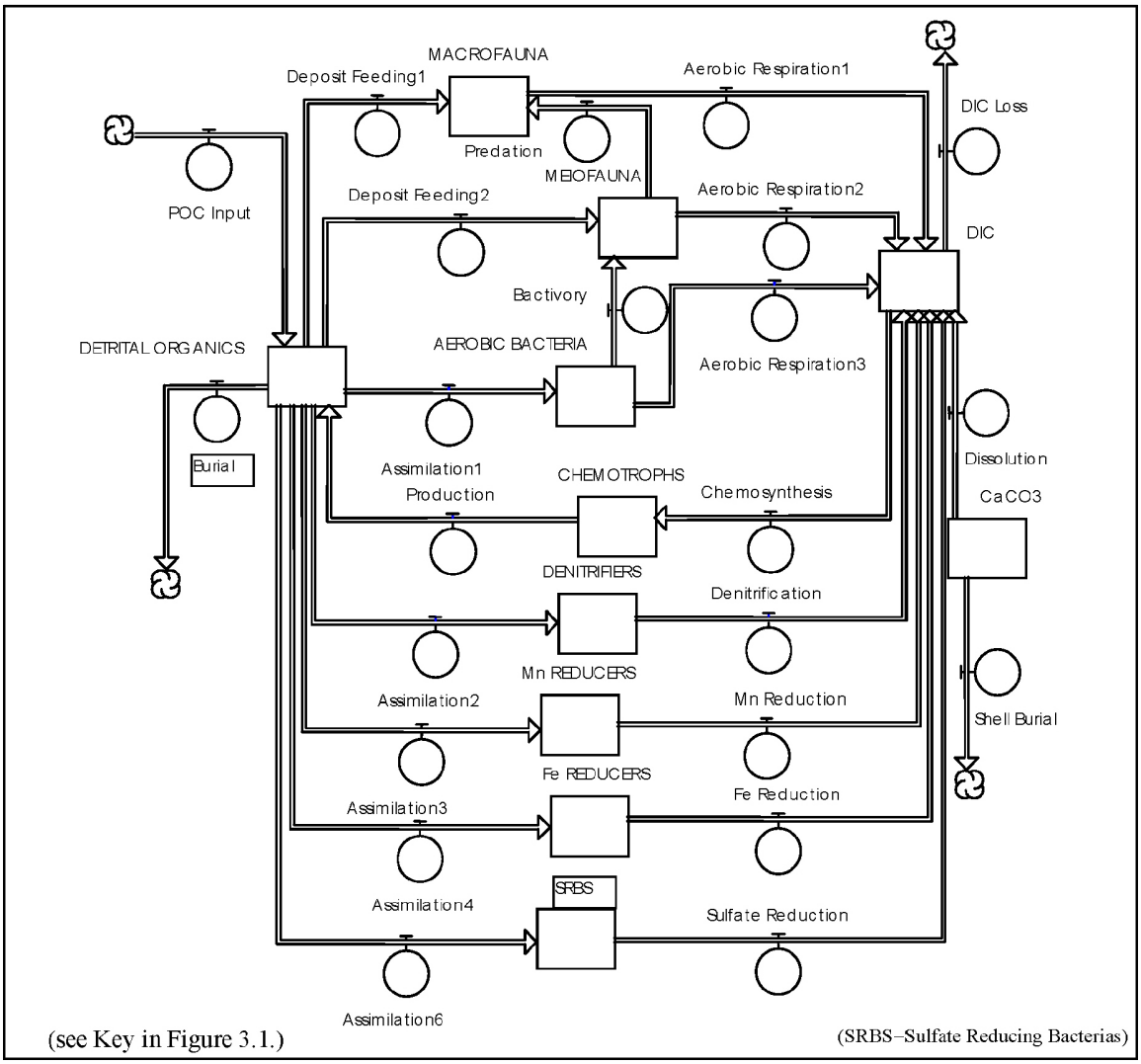

Figure 3-3. Sediment submodel of functional bacterial groups as defined by utilization of different terminal electron acceptors.

the past it was thought that simple increases in biomass were positive for a group of organisms, but now it is recognized that these biomass increases can be accompanied by significant changes in community structure. Is this positive or negative for the community and is the community "healthy"? Acute deterioration of a community, such as massive mortalities or disappearance of species, is easily recognizable, but over longer time frames it has become clear that some of the more intractable issues related to sublethal effects are often difficult to quantify or even recognize in the early stages of change. For example, loss of biodiversity is seen as a deterioration in ecosystem health, but the natural processes that also effect biodiversity are not well understood.

Ecosystem "health" may be measured by such things as community structure, e.g., the classic view that a healthy benthic community is one of high diversity and high productivity. Therefore, unhealthy ecosystems share a number of properties—lessened productivity, declining biodiversity, dominance by lower trophic levels and others. It has also been suggested that systems degraded beyond a certain point cannot recover (Rapport and Whitford 1999; Rapport et. al. 1998; Rowe and Haedrich 1979; Haedrich et al. 1980; Haedrich and Maunder 1985; Snelgrove and Haedrich 1985; Haedrich and Merrett 1988; Merrett and Haedrich 1997). Therefore "health" can be inferred from community composition, abundances, and size frequencies. "Health" will be assessed by comparisons of the structure of similar ecosystems world-wide that have been subjected to varying degrees and types of disturbance.

At the individual level, "health" has been inferred from physiological responses such as disease incidence, size and condition, and reproductive state. Parasites, and the diseases they cause, are often important determinants of population health. Measurable effects include mortality, decreased reproductive effort, decreased condition, and reduced or aberrant growth. The outgrowth of these effects are increased morbidity, decreased fecundity and even effects on predator/prey relationships.

From another point of view, "health" may be a measure of response to the stresses a population experiences due to anthropogenic disturbances. As a first order indication of this exposure, inventories of chemicals in sediments and biological tissues are measured. While this is at least an indication that the potential for impact is present, simply documenting the presence of contaminants is not sufficient to infer biological effect in most instances. However, a range of biological effects criteria for sedimentary concentrations of contaminants have been used to infer the possibility of effects. Once the potential for exposure has been verified, first-order biological responses to contaminant exposure are often important variables to monitor. These include a range of responses including production of contaminant metabolites, the induction of detoxification enzyme systems, and molecular level indications of genetic damage, to name a few indicators of sublethal biological response to contaminant exposure.

4. SAMPLING DESIGN

4.1 General Design Considerations

Several general principles guided the development of the overall sampling plan. First, treatments, or in this case similar stations, were chosen that would falsify the null hypotheses. Due to resource limitations and the large geographic area to be studied, it was impossible to measure everything, everywhere. However, it was important to measure what were judged to be the most important variables at the most important sites.

Second, pseudoreplication was avoided, i.e., replication was at the treatment level. A treatment was a factor level, or combination of factor levels, applied to a sampling unit. Sampling units were stations or replicate samples within stations where all other variables but the variable to be tested were as similar as possible. The generic form of all null hypotheses was that the treatment level effect equaled zero, i.e., the stations themselves were not fundamentally different by other than the variable being tested. For example, if each treatment was only represented by a single station, then one would only know that the stations were different, not why the stations were different.

Third, station locations were optimized to test more than one hypothesis. This was a cost reduction technique. For example, stations along a transect to test for depth differences were paired with stations in specific habitats to test a second hypothesis.

Fourth, confounding factors were minimized. A common problem was that more than one variable could be changing at a given station. For example, two stations could differ by water depth, distance from shore, and distance from the Mississippi River. In the end, it is not known which variable (or if an interaction of the variables) is causing the observed differences and thus generalities are difficult, if not impossible, to discern. Therefore, stations were chosen where comparisons could be based on differences in a single or related set of variables.

Fifth, balanced sampling designs were used. An uneven distribution of sampling effort can cause distortion of sample means when there is a difference in the number of observations between the datasets being contrasted.

Sixth, a design of appropriate power was used. Power is the ability to detect change. The first five design considerations primarily protect at the α level against Type I errors (rejecting the null hypothesis when it is true). But Type II errors protected at the β level were also considered (accepting the null hypothesis when it is false). Replication had to be sufficient to detect the amount of change that is expected, given variations in the variable of interest. A large multi-factorial design with little replication has many interaction terms that are often significant, thus limiting the interpretation and robustness of tests for the most important effects. In this case, previous studies suggest that a minimum of five replicate boxcores were needed at each site to adequately sample within-station heterogeneity.

Finally, a meta-analysis (or synthesis) has been created (Section 9). Assembled in its entirety, this meta-data set contains information that does not exist within the individual analyses. In the end, all of the stations and replicates are only surrogates for the environmental factors that regulate biological processes leading to the observed patterns of faunal composition. Therefore, measurements have been made synoptically at locations, or subsamples (replicates) have been taken within a location, so that the meta-data set could be created for the synthesis and integration of the overall study results (Section 9).

4.2 Working Hypotheses and Station Selection

The sampling design was developed from a series of testable null hypotheses derived from the conceptual model. The set of hypotheses was then used to select sampling sites so that power was sufficient to detect differences in the dependent variables being measured (i.e., abundance, biomass, diversity, analyte concentrations, etc.). The null hypotheses were based on the current understanding of deep-sea benthic community structure and function and prior knowledge of the range of habitats that occur in the GoM.

The following characteristics were utilized to choose sampling sites in order to maximize hypothesis testing power:

1) water depth (multiple transects perpendicular to isobaths);
2) geographic location—juxtaposition to the Mississippi River (east-west transects); distance from shore;
3) physiographic position – in or out of a mesoscale halokinetic basin; in a canyon; below an escarpment;
4) influx of organic carbon—primary productivity derived carbon, petroleum seep and chemosynthetic derived carbon; and
5) temporal change -time series sampling; location of historical sampling sites.

The sampling design was NOT simply conducting the traditional geographic survey with closely spaced stations. This hypothesis-testing approach was adopted to establish generalities about communities in the study area because the area is so large that sampling everywhere was cost prohibitive. The hypothesis-testing was adopted because it allows a prediction of when and where particular types of communities, both in terms of structure and function, will or will not be encountered. Hypothesis testing provides a powerful tool for either increasing or limiting sampling intensity in time and space as new data are collected and historical data are jointly re-interpreted. Each hypothesis, as described below, explores mechanisms believed to explain much of the variation in community structure and function in the deep GoM.

Based on the above considerations the following kinds of contrasting environments or habitats were sampled for comparisons:

- Depth.
- Water depth is probably the single most important gradient in determining faunal compositions and forcing factors in the study area (Hypothesis H_{O1}). Comparisons were made along a series of transects.

Stations: RW1-RW6, W1-W6, C1-C12, MT1-MT6, S35-S44 (Figures 4-1 to 4-3)

- Nutrients (organics)
- The input of organic nutrients from Mississippi River discharge causes an east to west gradient in faunal compositions and forcing factors (Hypothesis HO2). Comparisons were made along isobaths at similar distances from shore at varying distances from the Mississippi River.

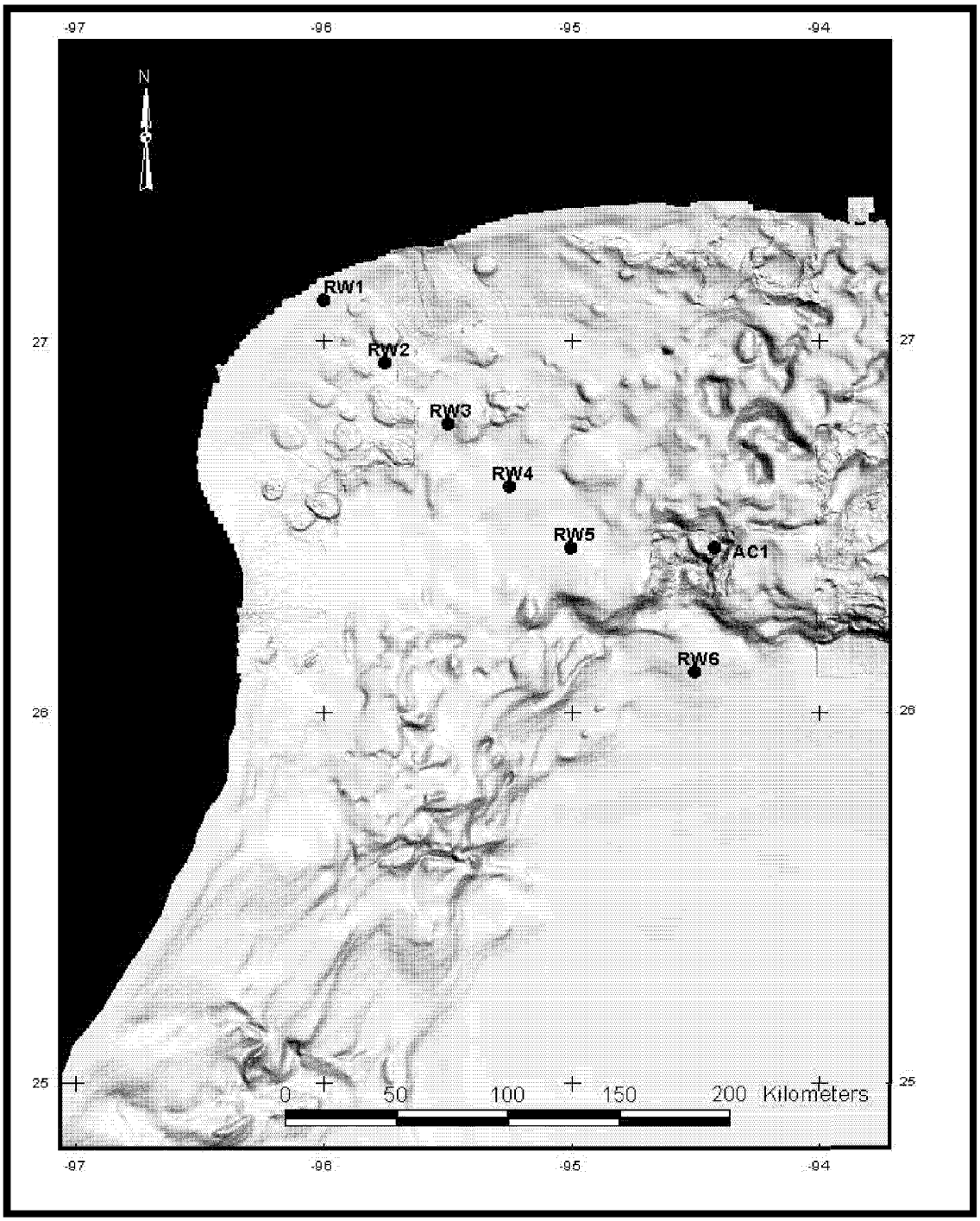

Figure 4-1. Benthic survey stations in the far northwest GoM.

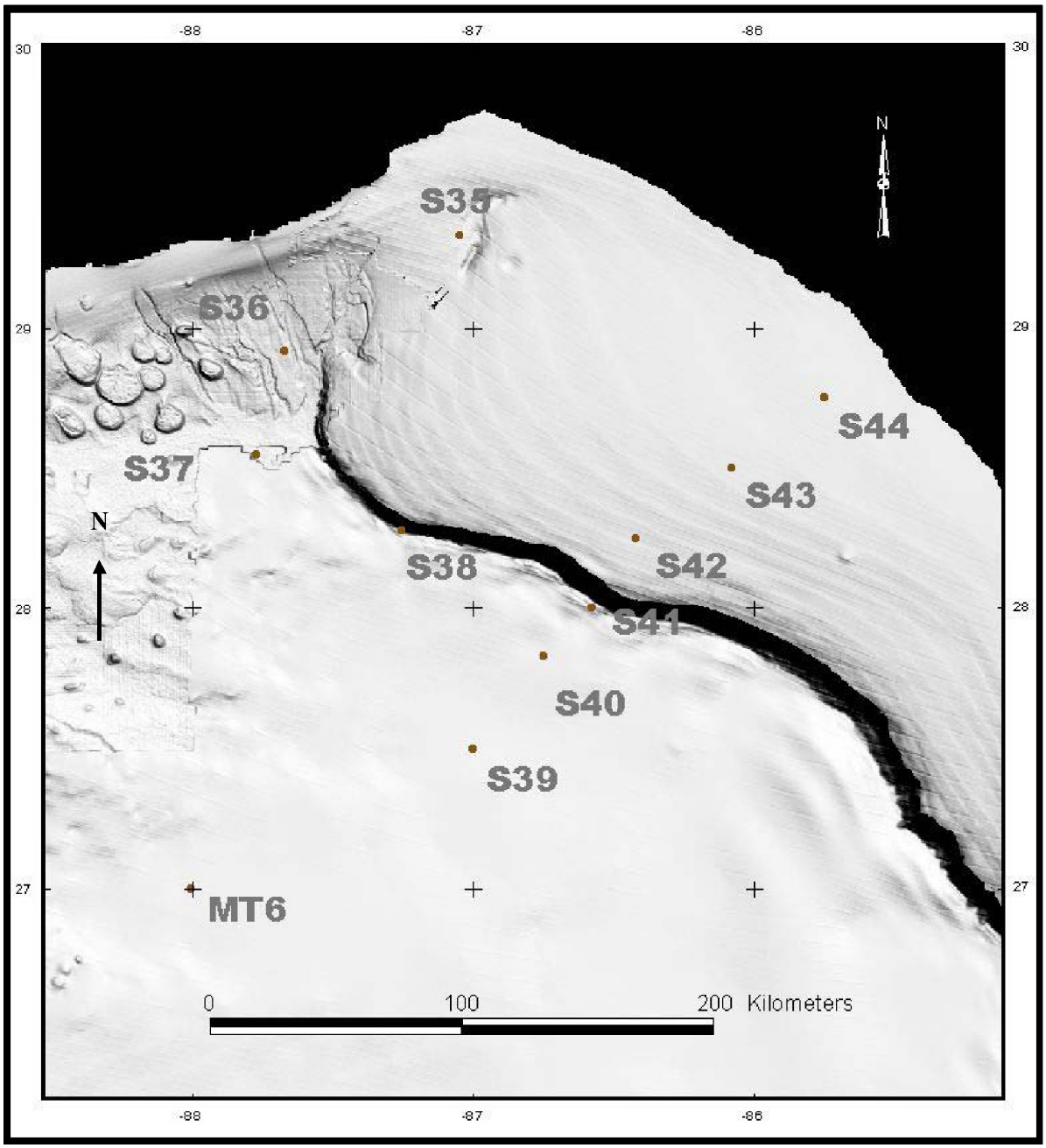

Figure 4-2. Benthic survey stations across the Florida Escarpment (for regional context see Figure 5-1).

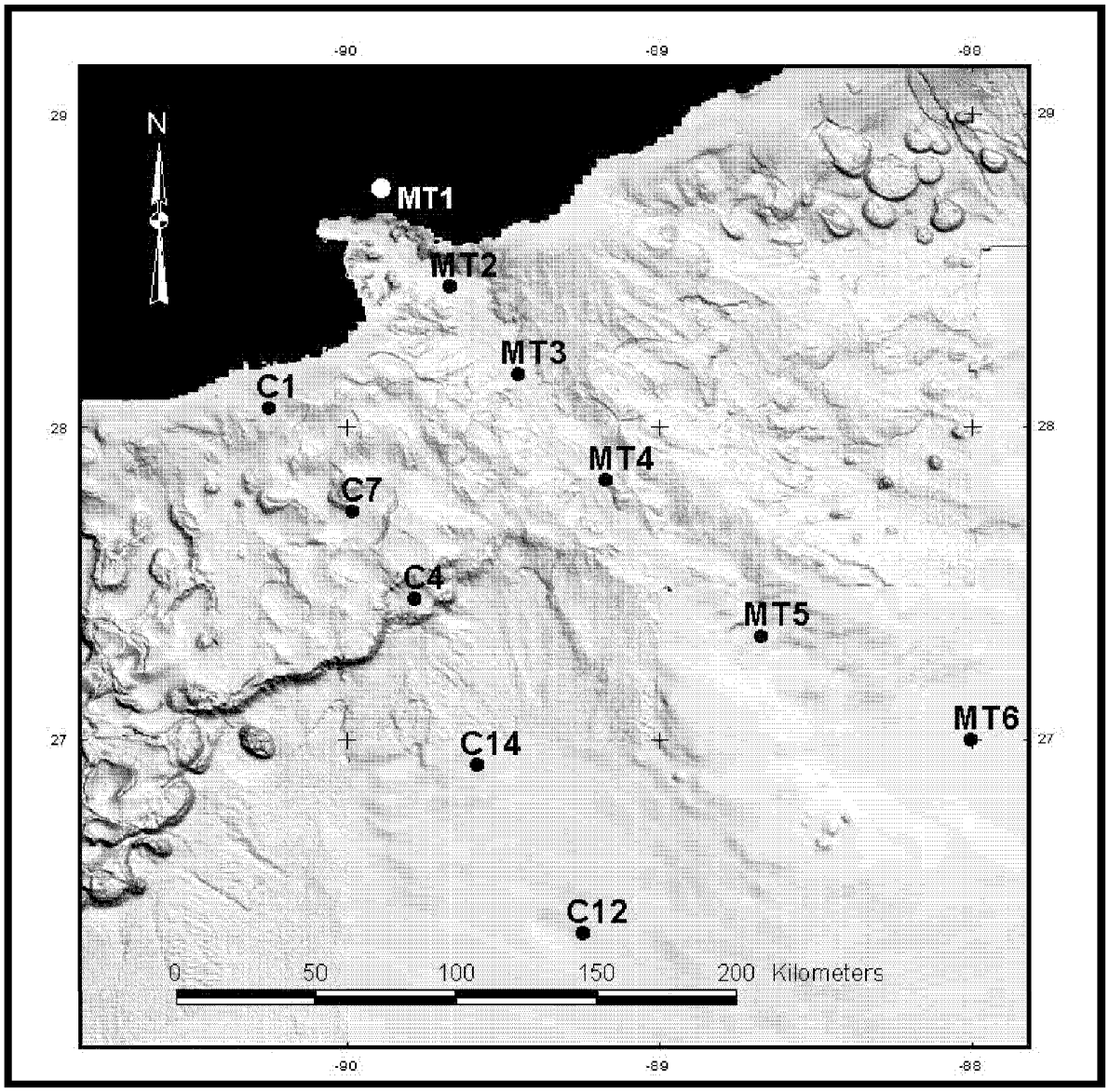

Figure 4-3. Sampling sites along the Mississippi Trough (MT1-MT6). Historical sites from the NGoMCSS study were also included (C1-C14; for regional context see Figure 5-1).

Stations: RW1-RW6, C1-C12, S37-S42 (Figures 4-1 to 4-3)

- Basins.
- The common mesoscale basins found on the slope, unless influenced by seeps, have the same faunal compositions and forcing factors as the "normal" slope because the entire slope is draped in a similar Holocene "blanket" of silt and clay within which the biological communities live (Hypothesis H_{O3}). Comparisons were made within and outside of basins at comparable water depths and distances from the Mississippi River and shore.

Stations: WC12, B1-B3, NB2-NB5 (Figure 4-4)

- Canyons.
- Faunal compositions and forcing factors are the same in or out of submarine canyons (Hypothesis H_{O4}). Comparisons were made between stations within and outside of canyons at comparable depths and distances from the Mississippi River and shore.

Stations: MT1-MT6, W5, W6, RW6 (Figures 4-1, 4-3, and 4-4)

- Steep Escarpments.
- Faunal composition and community structure parameters are the same on the "normal" slope as they are at the base of the Sigsbee Escarpment (Hypothesis H_{O5}). Comparisons were made between sites on the slope and at the base of the Sigsbee escarpment at similar water depths.

Stations: S39-S42 (Figure 4-2)

- Productivity.
- Cyclonic and anticyclonic features in the surface waters consistently alter surface primary productivity and this results in differing seafloor fauna composition and community structure (Hypothesis H_{O6}). Comparisons were made between stations that underlie areas of historically documented differences in sea surface primary productivity, holding other variables as constant as possible.

Stations: RW1-RW6, S35-S36, DeSoto Canyon [HIPRO] (Figures 4-1 and 4-2)

- Hydrocarbon Seeps.
- Hydrocarbon seeps affect energy and carbon supplies contributing to different faunal composition and structure (Hypothesis H_{O7}). This is tacitly true since chemosynthetic fauna are restricted to seep sites. Rather than a direct test, stable isotopes were used to assess inputs of chemosynthetic carbon to the foodweb. Data produced from the chemosynthetic community studies was compared with equivalent non-seep data. Explicit testing by paired stations was not attempted. Questions of "how close is close" are still difficult to resolve even in studies concentrated at seep sites. The decision to address this question in a limited way recognizes the fact that other studies are already being conducted at seep sites and that the primary focus of this program was non-seep environments.

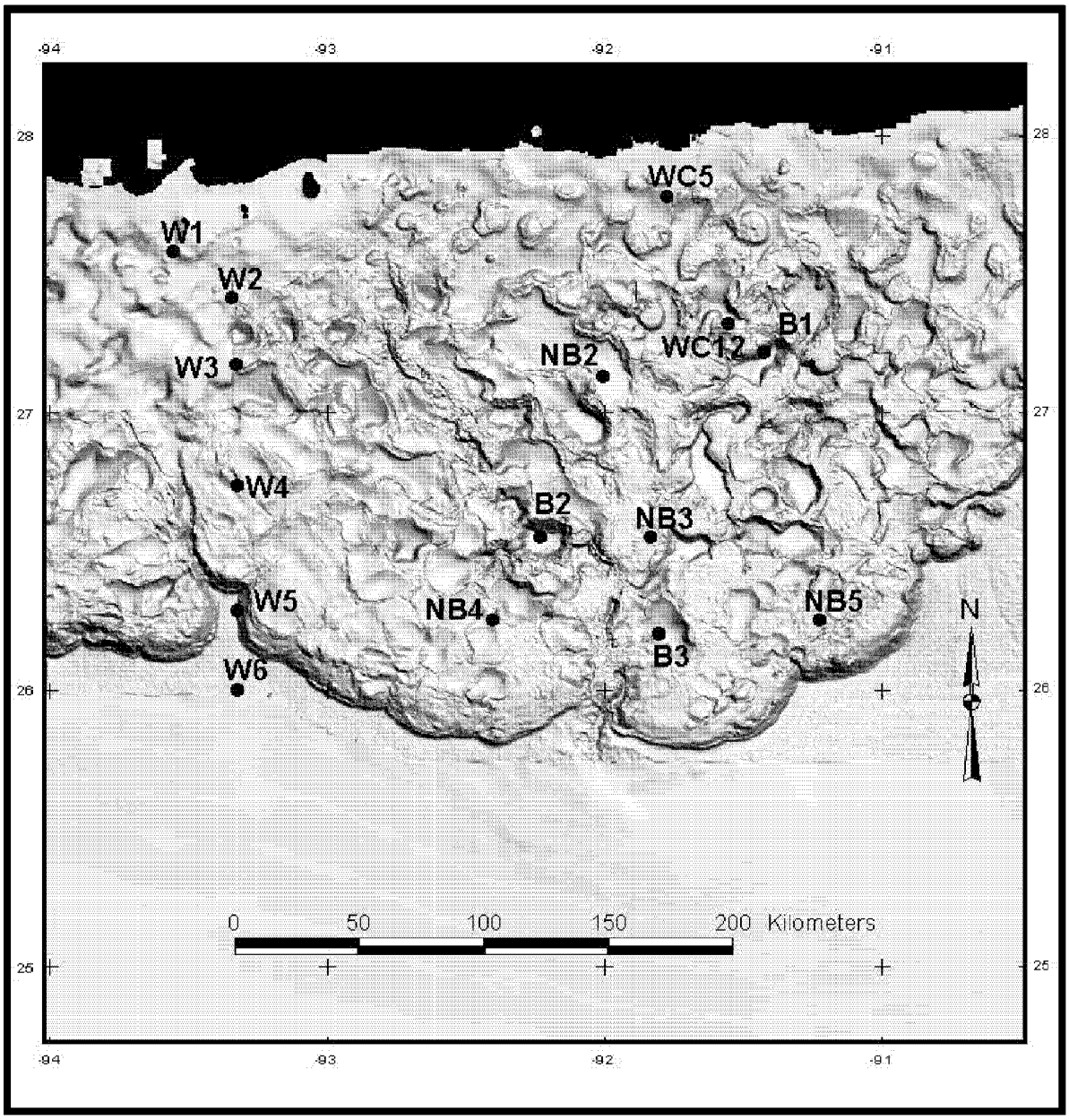

Figure 4-4. Physiographic comparisons within (B) and outside (NB) mesoscale basins in the Central GoM. Historical stations from the NGoMCSS study are also included (W1-W6, WC-5, and WC-12; for regional context see Figure 5-1).

- Temporal Changes.
- Faunal composition and community structure of benthic fauna vary with time (Hypothesis H_{O8}). Comparisons were made at a subset of survey stations sampled during each of the three planned cruise activities. In addition, to provide a longer timeframe for comparisons, historically sampled sites were reoccupied. The evaluation of data between studies was explicitly addressed to ensure that inter- program comparisons were valid.

Stations: W1-W6, WC6, C1-C12 (Figures 4-3 and 4-4)

- The above comparisons have been translated into testable null hypotheses (Table 4-1). A critically important part of program design was selection of the most appropriate locations to test the hypotheses. This was especially true for this program because the area to be characterized is large, the area contains a wide range of habitats and there are several important forcing factors that tend to confound delineation of cause and effect relationships. As summarized in the introductory materials, the northern GoM represents one of the most complex geological and oceanographic settings in the world. The challenge was to determine if peculiar subregions, as listed in the hypotheses, harbor faunas with peculiar quantifiable properties. Additional factors explicitly considered during the selection of proposed sampling sites include the location of historical sampling (to extend timeseries observations), the current and future trends in energy resource exploration and exploitation, and possible anthropogenic effects related to proximity to existing production facilities (primarily accommodated by screening all locations for contaminants). The study sites, to the degree possible, were explicitly tied to the hypothesis testing as listed.

Survey stations initially were chosen to sample at depths between 300 m and 3,000 m within the EEZ boundary with Mexico. The site selection spanned the range of known conditions providing the best tests of the hypotheses posed. Thus, the first year of sampling occurred along a transect just north of the Mexican border (RW1-RW6) over to one transect across the Florida escarpment (S37-S42; see Figures 4-2 and 4-3). This inclusive range of conditions enabled us to gain an understanding of the whole northern GoM deep-sea benthos, rather than isolated parts. The smooth upper slope of the northern Florida slope is contrasted with the heterogeneous topography off Texas. A transect down the Mississippi Trough (MT1-MT6) provided an evaluation of the effect of particulate and nutrient input from a large river (Figure 4-4). The basins on the upper slope were included as a test of how such basins might trap shelf-derived organic detritus and resultant effects on the biota (WC12, B1-B3, NB2-NB5; see Figure 4-4). Two locations at the upper end of the DeSoto Canyon (S36, S35) were chosen because one is frequented by whales and the other is characterized by high nitrate concentrations semi-permanently in the euphotic zone (see Figure 4-2). In 2001, HIPRO was added to reinforce the relationship between high benthic densities in all size groups and the high primary productivity along this strip of the upper continental margin.

Table 4-1

Summary of Benthic Survey Experimental Design:
Null Hypotheses, Station Selection Criteria, Number (No.) of Stations (Sta.), and Number Samples
(The number of samples is based on five replicates per station.)

Null Hypotheses	Design Criteria	No. Stations	No. Samples
H_{O1}: There is no variation in benthic fauna explained by depth	3 Replicate transects over 7 depths; occupy historical stations and others	21	105
H_{O2}: Faunas do not exhibit an East to West gradient	Additional transect to H_{O1}; remove confounding geological effects and water mass effects	7	35
H_{O3}: Basin faunas are not different from non-basin faunas	3 salt bottom and 3 salt surrounded basins	6	30
H_{O4}: Canyon fauna is not different from slope fauna	4 Canyons to be compared to non-canyon and non-basin biota from H_{O1}-H_{O3}	8	40
H_{O5}: Fauna below escarpments is not different from slope	Add sta. below escarpment in addition to H_{O1}- H_{O4} in area of furrows	7	35
H_{O6}: Surface primary production does not explain faunal differences	Add sta. to (H_{O1}-H_{O2}) in "hot spot" defined by historical water column data	7	35
H_{O7}: Proximity to organic input causes no bioenhancement	Add sta. in proximity to "geochemical anomalies" (hydrates, brine pools, methane seeps)	8	40
H_{O8}: There is no variation in benthic fauna over time.	6 stations (or other elements of the design, H_{O1} -H_{O7}) over 2 years	12	60

Experimental, or "process" stations were chosen to reflect the greatest range in community dynamics, as inferred from the benthic survey data conducted in 2000. The survey site selection was based on inferences about where the greatest variations in community structure might be observed based previous studies world-wide. The next step, conducted in late 2000 and early 2001 after a substantial representative portion of the samples had been processed, was to identify the experimental or 'process' stations at those survey sites where the greatest ranges in community structure were actually observed in the 2000 survey.

The first interim meeting in February 2001 was used to up-date the hypotheses based on Survey Cruise data, select sites to be repeated, add new sites to strengthen comparisons and identify sites for process studies. Following considerable open discussion among the investigators, the team decided on the following four locations for process studies: MT3, S36, S42, and MT6. This initial choice provided the following combination of biotic conditions: high densities at modest depth (MT3); high densities at mid depth (S36); modest densities at shallow depths (S42); and low densities at great depth (MT6).

New sites added were the giant sediment furrows below Green Knoll (GKF), on the top of Green Knoll (GK), a site between the Mississippi Trough (MT) and the DeSoto Canyon (HIPRO), and near (ca. 1 km) the Bush Hill seep (BH). See Section 5.3 for a discussion of the new sites.

4.3 Dependent and Independent Variables

Based on the various hypotheses described in the previous section, a set of dependent and independent variables was chosen that would provide the set of observations at each station to

test the validity of the null hypotheses (Tables 4-2 to 4-4). These variables also provide the stocks and processes for initial input to the model.

4.4 Statistical Analyses

Statistical analyses to test for differences among treatment means were performed using parametric, general linear models. Prior to analysis, data were transformed, generally by natural logarithm, to achieve homogeneity of error variance, normality of residual errors, and additivity of effects. A data set of residual errors was created for each model and tested for normality. Both untransformed and transformed residuals were computed, and the datasets that were normally distributed with means of zero were used for analyses.

The models that follow describe the relationships among the independent design variables only. The measured dependent variables are described in the methods sections. The notation used follows conventions described by Kirk (1982).

Table 4-2

Independent Variables Fixed by the Sampling Plan Design

Physiographic Characteristics	Water Masses
Water Depth Basins underlain by salt Basins surrounded by salt Basins subjected to slumping/erosion Basins overlain by an undisturbed drape of Holocene silt and clay Canyons Escarpments Proximity to seeps Basin slope angle	Loop Current Consistently "cool" water between eddies Warm eddies
	Geographic Location
	East vs West Distance from shore
	Time
	Months Years

Table 4-3

Dependent Variables To Be Measured

Community Structure	
Bacterial density	Macrofaunal species composition
Bacterial biomass	Megafaunal density
Foraminiferal biomass	Megafaunal biomass
Meiofaunal density	Megafaunal diversity
Meiofaunal biomass	Megafaunal species composition
Meiofaunal composition to major group	Fish density
Macrofaunal density	Fish biomass
Macrofaunal biomass	Fish diversity
Macrofaunal diversity	Fish species composition
Community Function	
Bacteria growth rates	Fish respiration[1]
Bacteria respiration	Fish predation on megafauna[2]
Bacteria response to different substrates	Fish scavenging on carcasses[2]
Foraminiferal respiration[1]	Nutrient Regeneration
Foraminiferal feeding rates[1]	Denitrification rate
Meiofaunal feeding rates on bacteria	Sediment accumulation rate[2]
Macrofaunal respiration[1]	Sedimentary community oxygen consumption
Community Function	
Macrofauna growth rates[2]	Sulfate reduction rate
Macrofauna predation rates[2]	Foodweb studies
Macrofauna predation rates on meiofauna, bacteria, and organic matter	
Megafaunal respiration rates[2]	
Megafaunal predation rate on megafauna, meiofauna, bacteria, and organic matter[2]	
Megafaunal scavenging on carcasses[2]	

[1]-calculated based on size and temperature, [2]-estimated from sub-model.

Table 4-4

Ancillary Variables To Be Measured at Survey and Experimental Stations

Water Column Profiles	Sediment Properties
• Depth • Temperature • Salinity • Oxygen • Nitrate and Nitrite • Ammonium • Silicate • Phosphate • Particulate Matter (PM) • Particulate Organic Carbon (POC) • Light • Currents Water Column Profile • Photosynthetic Pigments • Primary Production ical Contaminants • Hydrocarbons • Metals	• Grain Size • Porosity • Elemental composition (organic carbon, nitrogen, sulfur) • Percent inorganic carbon (TIC) • Permeability • Shear Strength • Bulk Density Geochemistry[1] • Nutrients • Dissolved Organic Carbon (DOC) • SO4=/Cl- • Dissolved Inorganic Carbon (DIC) • δ13C DIC • Sulfate Reduction Rate • pH • H2S • O2 • Reactive Fe • Reactive Mn • Acid Volatile Sulfide

[1] Composite sample at survey station, profiles for fluxes at experimental station.

4.4.1 Univariate Analyses

Univariate analyses were used to test each hypothesis based on the following models. The stations used to test each hypothesis are summarized in Table 4-2.

The first two hypotheses are as follows:

H_{O1}: There is no variation in benthic fauna with depth, and
H_{O2}: There is no difference in fauna along an east to west gradient.

The effect of depth was tested with sites along transects. Multiple transects were necessary to replicate at the treatment level. The effect of longitude was tested with sites on an east - west gradient along isobaths, so this design tested two major hypotheses. This was a two-way completely random factorial analysis of variance (ANOVA) that is described by the following model:

$$Y_{ijk} = \mu + \alpha_j + \beta_k + \alpha\beta_{jk} + \in_{i(jk)}$$

where Y_{ijk} is the measurement for each individual replicate, μ is the overall sample mean, α_j is the main effect for transects and j=1-4, β_k is the main effect for depths and k=1-7 (300, 750,

1,200, 1,650, 2,100, 2,550, and 3,000 m), $\alpha\beta_{jk}$, is an interaction term, and $\in_{i(jk)}$ is the random error for each replicate measurement and i=1-5.

The third hypothesis is:

H_{O3}: There is no difference between basin fauna and non-basin fauna.

Geological complexity exists in the northern GoM. One expression of this complexity are the multiple, mesoscale (5 to 15 km diameter) basins formed by salt halokinesis. Such features may alter currents or act as receptacles that concentrate a rain of detrital material. Such detrital POC could originate in the overlying water or be exported from the continental shelf. This could affect benthos. One site within a basin was paired with two nearby locations already sampled for H_{O1} and H_{O2} above to test for basin effects. Station pairing was necessary to control for distance from shore and depth. The entire experiment was replicated at 6 different sites, so each location was a blocking effect. The experiment was a two-way completely random factorial ANOVA that is described by the following model:

$$Y_{ijk} = \mu + \alpha_j + \beta_k + \alpha\beta_{jk} + \in_{i(jk)}$$

where Y_{ijk} is the measurement for each individual replicate, μ is the overall sample mean, α_j is the main effect for replicate sites and j=1-6, β_k is the main effect for treatments and k=1-3 (basin, non-basin same distance from shore, and non-basin same depth), $\alpha\beta_{jk}$, is an interaction term, and $\in_{i(jk)}$ is the random error for each replicate measurement and i=1-5. Differences between sites were not of interest because they replicate the basin effect, so it doesn't matter if that test is significant. The main test of interest is a multiple comparison tests among treatment levels if there is a significant difference among treatments.

The fourth hypothesis is:

H_{O4}: There is no difference between canyon fauna and non-canyon fauna.

Another form of geological complexity in the GoM is canyons. Often sediment slumping occurs in canyons in addition to alteration in near-bottom current patterns. One station within a canyon will be paired with nearby stations at similar depths that are not in a canyon. The entire experiment is replicated at three (3) different features: Alaminos Canyon, Mississippi Trough and DeSoto Canyon, each with distinctive features. The experiment is a two-way completely random factorial ANOVA that is described by the following model:

$$Y_{ijk} = \mu + \alpha_j + \beta_k + \alpha\beta_{jk} + \in_{i(jk)}$$

where Y_{ijk} is the measurement for each individual replicate, μ is the overall sample mean, α_j is the main effect for replicate sites and j=1-4, β_k is the main effect for treatments and k=1-2 (canyon and non-canyon), $\alpha\beta_{jk}$, is an interaction term, and $\in_{i(jk)}$ is the random error for each replicate measurement and i=1-5.

The fifth hypothesis is:

H_{O5}: There is no difference between the fauna located immediately below an escarpment and that at sites that are not adjacent to an escarpment.

Another form of geological complexity in the GoM is escarpments. The fauna on the steep walls may be different from more gently sloping areas, but this was not sampled because conventional (surface ship) approaches cannot sample the hard and complex surface of steep slopes adequately. This experiment was intended to determine if detrital buildup at the base of an escarpment affects the fauna there, a condition that has been observed in shallow water as well as the deep ocean (Sokolova ref.). One sampling site adjacent to the base of an escarpment was paired with nearby locations at a similar depth that were not adjacent to an escarpment. The entire experiment was replicated at 7 different sites. The sites were chosen based on pairing stations with samples already taken to test H_{O1}-H_{O5}. The experiment is a two-way completely random factorial ANOVA that is described by the following model:

$$Y_{ijk} = \mu + \alpha_j + \beta_k + \alpha\beta_{jk} + \in_{i(jk)}$$

where Y_{ijk} is the measurement for each individual replicate, μ is the overall sample mean, α_j is the main effect for replicate sites and j=1-7, β_k is the main effect for treatments and k=1-2 (escarpment and non-escarpment), $\alpha\beta_{jk}$, is an interaction term, and $\in_{i(jk)}$ is the random error for each replicate measurement and i=1-5.

The sixth hypothesis is:

> H_{O6}: There are no differences in benthos in areas with different amounts of water column primary production.

The sites were chosen based on pairing stations with samples already taken to test H_{O1}-H_{O5}. The design is nested as a completely random hierarchical design described by the model:

$$Y_{ijk}= \mu + \alpha_j + \beta_{k(j)} + \in_{i(jk)},$$

where μ = overall sample mean, α_j = main effect of treatments and j=1-3 (high, medium, and low productivity), $\alpha_{k(j)}$ = nested effect for replicate stations and k =1-7, and $\in_{i(jk)}$ is the random error for each replicate measurement and i=1-5. The F-test used the mean square error for stations as the denominator. A second approach was analysis of covariance, where actual values indicating primary production (e.g., measured values or chlorophyll standing stock) were used as covariates.

The seventh hypothesis is:

> H_{O7}: There is no difference in benthic fauna near and far from seeps.

Another form of geological complexity in the GoM is organic and inorganic inputs in geochemically anomalous environments, e.g., hydrocarbon or brine seeps. Eight (8) stations are added to pair with existing non-seep stations. The station pairs will be in 4 site regions. The sites will be chosen based on pairing stations with samples already taken to test hypotheses H_{O1}-H_{O6}. The experiment is a two-way completely random factorial ANOVA that is described by the following model:

$$Y_{ijk} = \mu + \alpha_j + \beta_k + \alpha\beta_{jk} + \in_{i(jk)}$$

where Y_{ijk} is the measurement for each individual replicate, μ is the overall sample mean, α_j is the main effect for replicate sites and j=1-4, α_k is the main effect for treatments and k=1-4 (brine seep, hydrocarbon seep, control for distance from shore, control for depth), $\alpha\beta_{jk}$, is an interaction term, and $\in_{i(jk)}$ is the random error for each replicate measurement and i=1-5. Differences between sites are not of interest because they are replicating seep effects, so it doesn't matter if that test is significant. The main test of interest is a multiple comparison test among treatment levels if there is a significant difference among treatments.

The eighth hypothesis is:

> H_{O8}: There are no differences in benthic fauna among different sampling dates.

Six of the stations sampled for H_{O1}-H_{O7} were chosen for reoccupation in years 2 and 3 so that there will be a time series for at least 3 years. In addition, site C7 was occupied in a previous study and thus extended the time series to 5 sampling periods for that site. The experiment is a three-way completely random factorial ANOVA that can be described by the following model:

$$Y_{ijkl} = \mu + \alpha_j + \beta_k + \alpha\beta_{jk} + \gamma_l + \alpha\gamma_{jl} + \beta\gamma_{kl} + \alpha\beta\gamma_{jkl} + \in_{i(jkl)}$$

where Y_{ijkl} is the measurement for each individual replicate, μ is the overall sample mean, α_j is the main effect for sampling periods and j=1-3, β_k is the main effect for sites and k=1-2, γ_l is the main effect term for depths and l=1-3 (shallow, mid-depth, deep), $\alpha\beta_{jk}$, $\alpha\gamma_{jl}$, $\beta\gamma_{kl}$, and $\alpha\beta\gamma_{jkl}$ are interaction terms, and $\in_{i(jkl)}$ is the random error for each replicate measurement and i=1-5.

4.4.2 Power Analysis

Power analysis was performed to determine the detectable change in the population at a given power ($1-\beta$) and sample size (n). Power is calculated by:

$$\Delta = \frac{(t_\alpha + t_\beta) x SD x \sqrt{\frac{2}{n}}}{\overline{X}}$$

where Δ is the percent change in the population, SD is the pooled standard deviation, t_α and t_β are tabled values for a two-tailed test assuming a pooled estimate of variance from a large sample size, and $\overline{X}$ is the sample mean. Values of α=0.05, and powers of 0.95, 0.80, 0.50 were used in the analysis.

4.4.3 Multivariate Analyses

A meta-analysis (or synthesis) was performed at the end of the study. The goal of the synthesis was to merge all data sets of response variables to create one large data set. All the ANOVA's listed above were analyzed in multivariate mode (MANOVA) to test the null hypothesis that the vector of population means equals zero. That is, we determined if all measured variables respond to the dependent variables in the design in a similar fashion. The advantage of MANOVA is that multivariate error is controlled. That is, error rates are controlled at α across all response variables.

As stated previously, all stations and replicates are simply surrogates for the environmental factors that regulate biological processes at different scales. These scales vary greatly from small- (replicate boxcores), meso- (across transects, basins, or nearby stations) to large- (across the entire GoM). In addition, there is a temporal scale to the variation in all measurements. Multivariate analysis has allowed us to test the meta-data set for correlation or covariation among the independent variables that are measured. Two multivariate techniques were employed: a parametric method (principal components analysis, PCA), and a non-parametric methods (multidimensional scaling, MDS).

Multidimensional scaling is a non-parametric multivariate technique that was utilized for examining similarity or dissimilarity between stations, replicates, or other dependent variables in the experimental design. First, a similarity or dissimilarity index was computed for elements of the design (e.g., stations) and then a plot of the distance among points was created. The plot enabled us to identify unknown variables that affect the similarity or dissimilarity between sampling locations. Its utility, and thus its popularity, derives from its use of non-parametric tests.

Principal components analysis (PCA) is a parametric variable-reducing technique that makes a new set of uncorrelated variables in order of decreasing variance. Analysis of abiotic variables was used to summarize the co-varying environmental influences on different levels of replications, i.e., different spatial and temporal scales. Factor loading scores were generated for abiotic summaries of observations (rows), which were then used in other analyses.

5. THE FIELD PROGRAM

The Field Program was designed to initiate benthic community structure descriptions before community function and biogeochemical process investigations, thus allowing the choice of process study sites to be based on observed community structure. To accomplish this, the first year (2000) consisted of an extensive survey of the standing stocks of all size categories under investigation. This allowed the selection of the limited number of process sites (four sites initially) to be chosen for years two and three based on extremes in organism abundances. The Field Program included seven weeks at sea in 2000 for the extensive survey, three weeks at sea in June, 2001, for the initial study of processes, followed by two repeated legs of two weeks each in June and August, 2002, in the third year onto the Sigsbee Deep in Mexican waters.

The first cruise concentrated on accumulating samples to test the eight hypotheses based on community structure, followed by two years in which there was a mixture of survey and experimental activities. The survey field effort (Cruise I) included boxcoring, trawling, photosurveys, and hydrocasts. Experimental stations (Cruises II and III) included a variety of specialized sampling efforts designed to identify important processes and forcing factors at four sites selected from the survey sites. The four sites were to be repeated in year three, but the plan was changed when it was decided to venture onto the greatest depths of the abyssal plain in Mexican waters. Ultimately, six full-fledged process sites were investigated, with two additional locations where a limited number of process measurements were made.

In brief, the cruises and their objectives are as follows:

Cruise I: Ship—*R/V Gyre*; Chief Scientist—Dr. Gil Rowe; Conducted May 3 to June 21, 2000.

Cruise II: Ship—*R/V Gyre*; Chief Scientist—Dr. Gil Rowe; Schedule—June, 2001; Duration 20 days; Activities—12 survey stations (60 boxcores, 12 trawls, 12 CTD/hydrocasts, 12 photosurveys) and 4 experimental stations (20 boxcores, 4 trawls, 4 CTD/hydrocasts, 4 photosurveys, 4 ADCP casts, microbiological process studies, 4 benthic lander deployments, 4 pore water and solids geochemical studies, 4 stable isotope food web collections, and 4 specialized biological/ecological studies), Staffing—23 scientists, students and observers.

Cruise III: Legs one and two: Ship – R/V Gyre, Chief Scientist – Dr. Gil Rowe: leg one – June 1-15, 2002; process studies on the abyssal plain at two sites, community structure sampling at five sites (including the two above); leg two – August 1-14, 2002, trawling and box coring to fill in sites that need re-sampling

The details of the field and laboratory methods are provided in Sections 6 and 7.

5.1 The Ship—R/V GYRE

R/V Gyre was owned by Texas A&M University and operated by the Department of Oceanography of Texas A&M University. As the homeport of the *Gyre* was Galveston, all field work originated and ended in Galveston. The *Gyre* is a general-purpose, open-ocean research

vessel. The deck plans and diagrams of the ship can be accessed at the ships URL: http://www.ocean.tamu.edu/Cruise/plns.html

The *Gyre*, now property of TDI-Brooks Intl., was being retired as of 31 August 2005. Inquiries should be directed to Dr. Wilford Gardner, Department of Oceanography, Texas A&M, College Station, TX, 77843, wgardner@ocean.tamu.edu.

5.2 Cruise I—Survey (Figure 5-1; Table 5-1)

Cruise 1 was devoted to a survey of deep-sea communities of the northern GoM. Each standard survey station consisted of the following activities:

A. One (1) CTD: The CTD was deployed with the starboard hydrowinch using conductor cable (the CTD remained attached to the conducting cable for the entire cruise, unless problems were encountered);
B. Five (5) Boxcores: The boxcore was deployed with the hydraulic winch on the non-conducting cable. A pinger was attached to the wire above the boxcore at depths of 1 km and greater. Otherwise wire out and tension was adequate to determine bottom contact.
C. One (1) Camera Lowering: The camera system was deployed with the non-conducting cable on the starboard hydrowinch. A pinger was attached to the frame to determine bottom contact and distance to the bottom. The camera takes up to 50 exposures.
D. One (1) Bottom Trawl: The otter trawl was deployed with the heavy-duty winch on the fantail.

The shipboard scientific crew operated on watches of 12 hours on and 12 hours off. Between stations, the trawl samples were sorted to species and fixed in jars by those assigned to trawling. The five sediment sievers on watch fixed and bottled the box core material and then assisted with the trawl sorting to species, displacement volume measurements (for biomass), preservation and labeling. Shipboard marine technicians analyzed samples for oxygen, nutrients, and salinities between stations.

Each watch was assigned a "watch chief" (Clif Nunnally and Chris Gudeman) who had the duty of keeping records, notifying the Chief Scientist when problems arose, notifying the watch when the ship was on station, waking the new watch at the appropriate hour, and notifying the bridge when station activities were completed. The watch chief maintained a log in the main laboratory on the main deck that documented each activity in chronological order. Comments on the success or failure of the activity and inventory of all samples taken were kept. The watch chief and assistant ensured that the station logs on the bridge agreed with those in the laboratory. Each "watch chief" reported directly to the Chief Scientist. The "watch chief" communicated between the bridge and scientists on the deck.

5.3 Cruise II—Processes (Figure 5-2)

Plans for the first processes cruise were made during the first interim meeting in February 2001. The plans were made on the basis of findings to date. Extremes of high and low densities in bacteria, meio- and macrofauna were used for selection criteria. The sites chosen were MT3, S36, S42, and MT6. High densities characterized MT3 and S36 at 1,000 and 1,850 m depth in

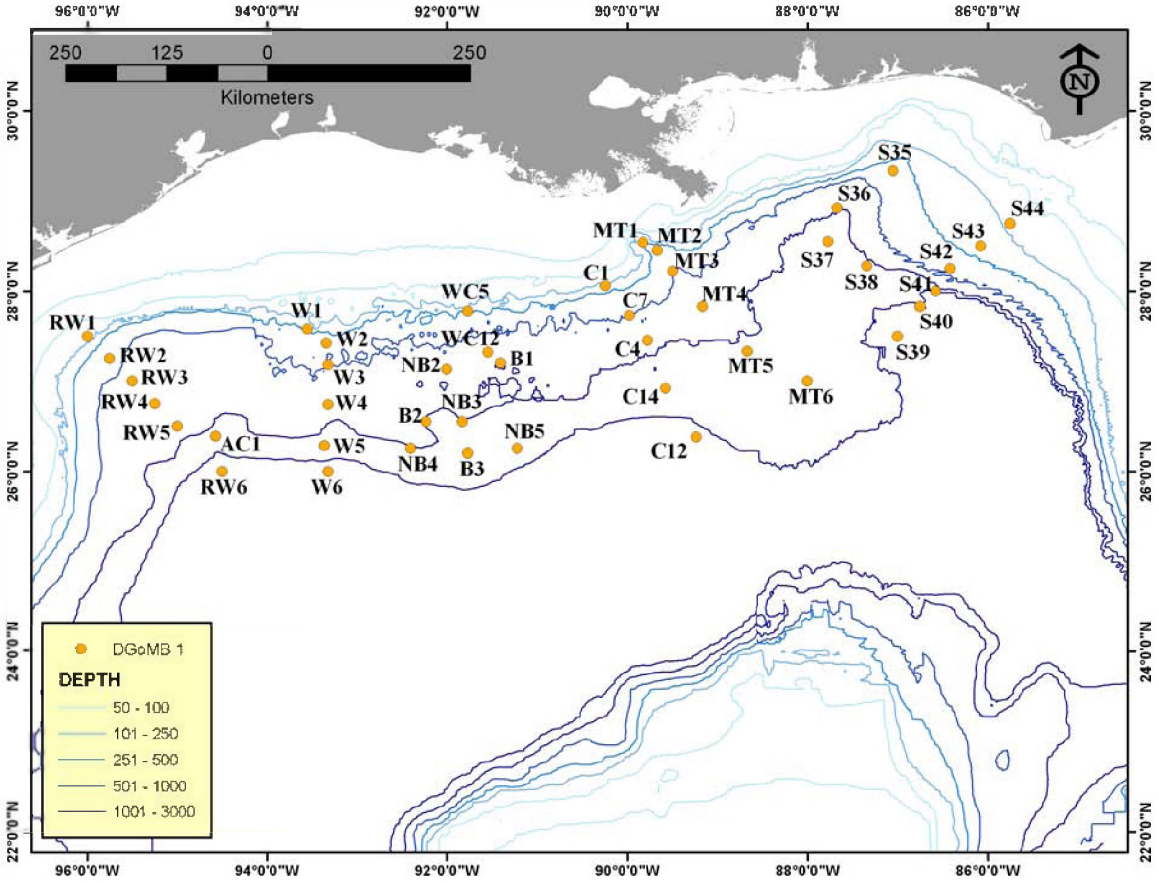

Figure 5-1. Benthic survey stations for Cruise I, May and June 2000.

Table 5-1

Summary of Sampling Conducted During Cruise I

Station	Trawl	Boxcore	Camera	CTD
RW1	1	5	1	1
RW2	1	5	1	1
RW3	0	5	1	1
RW4	0	5	1	1
RW5	0	5	1	1
RW6	1	5	0	1
AC1	0	5	1	2
W6	1	5	1	1
W5	0	5	1	1
W4	0	5	0	1
W3	1	5	1	1
W2	0	5	1	1
W1	1	5	1	1
WC5	1	5	1	1
WC12	0	5	1	1
B1	1	5	1	1
NB2	1	5	1	1
NB3	1	5	1	1
B2	3	5	1	1
NB4	1	5	0	2
B3	1	5	1	0
NB5	1	5	1	1
C12	1	4	1	1
C14	1	5	1	1
C4	1	5	1	1
C7	1	5	1	1
C1	1	5	1	1
S36	1	5	1	1
S37	1	5	1	1
S38	1	5	1	1
S35	1	5	1	1
S44	1	5	1	1
S43	1	5	1	1
S42	1	5	1	1
S41	1	5	1	1
S40	1	5	1	1
S39	1	5	1	1
MT6	1	5	1	1
MT5	1	5	1	1
MT4	1	5	1	1
MT3	1	5	1	1
MT2	1	5	1	1
MT1	1	5	1	1

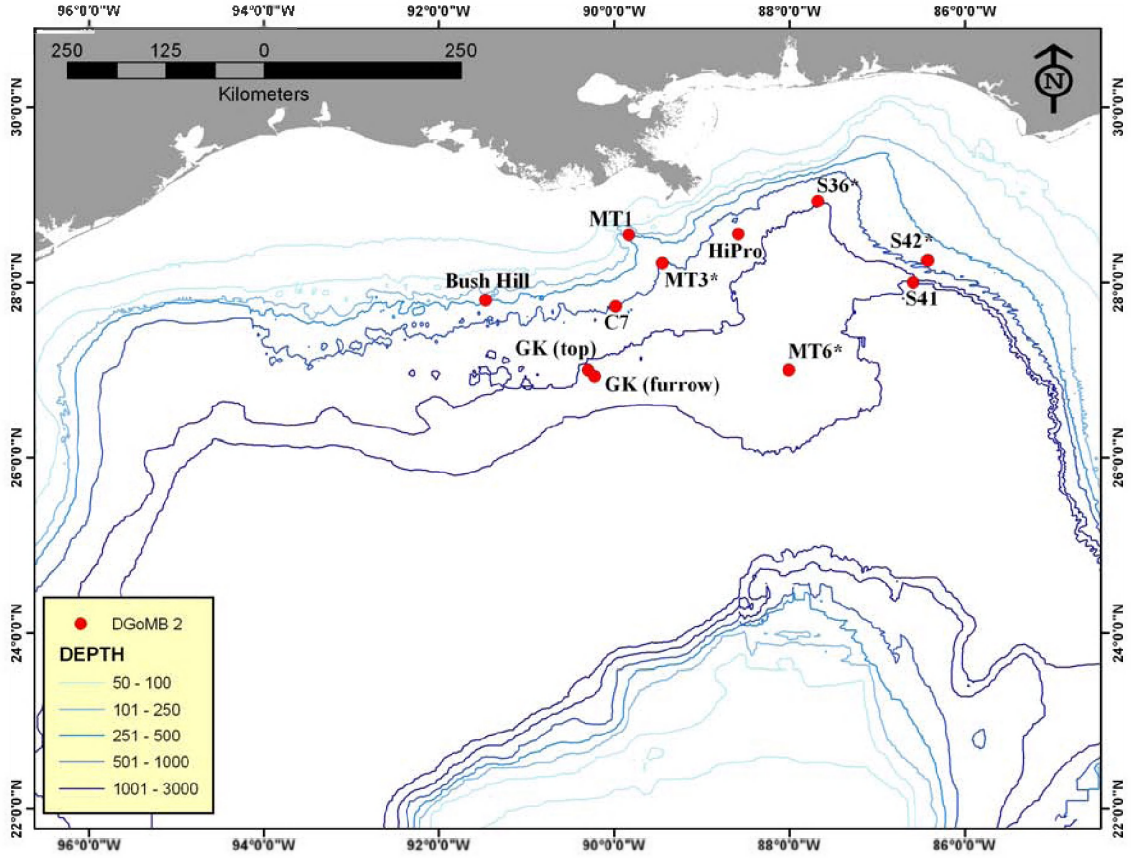

Figure 5-2. Sampling sites during Cruise II, the first "processes" cruise, June 1-19, 2001. Sites MT3, S36, S42, and MT6 were designated as experimental sites.

the Mississippi and DeSoto Caynons, whereas low densities were found at S42 and MT6 at 750 and 2,750 m depth.

Other sites chosen for repeating were MT1 (to test Ho4-effects of canyons), C7 (to test Ho8-time), and S41 (to test Ho5-escarpments). New sites added were "HIPRO" (to test Ho6-surface productivity), "furrows" (effects of furrows or furrow-causing currents), "Green Knoll," "Bush Hill" (Ho7-seeps), and "Fe Stone" (effects of iron crust).

Eleven sites were occupied during Cruise 2 (Processes; Figure 5-2). The lander was used successfully at S42 and MT3, providing estimates of total community respiration rates measured *in situ*. Shipboard incubations were made of total community oxygen uptake, sulfate reduction, thymidine incorporation into bacteria and bacteria grazing by meiofauna at four sites: MT3, S36, S42, and MT6.

5.4 Third-Year Field Activities

The original plan called for a single cruise of 20 days in June 2002. The revised plan utilized two trips of two weeks each in June and August 2002. These concentrated on the Sigsbee Deep abyssal plain at depths of 3,400 to 3,650 m within the Mexican EEZ. The locations were chosen to provide broad geographic coverage (Figure 5-3). The head of the Mississippi Trough (MT1) was added as a 'process' site because of its peculiarly soft clay sediments and tremendous

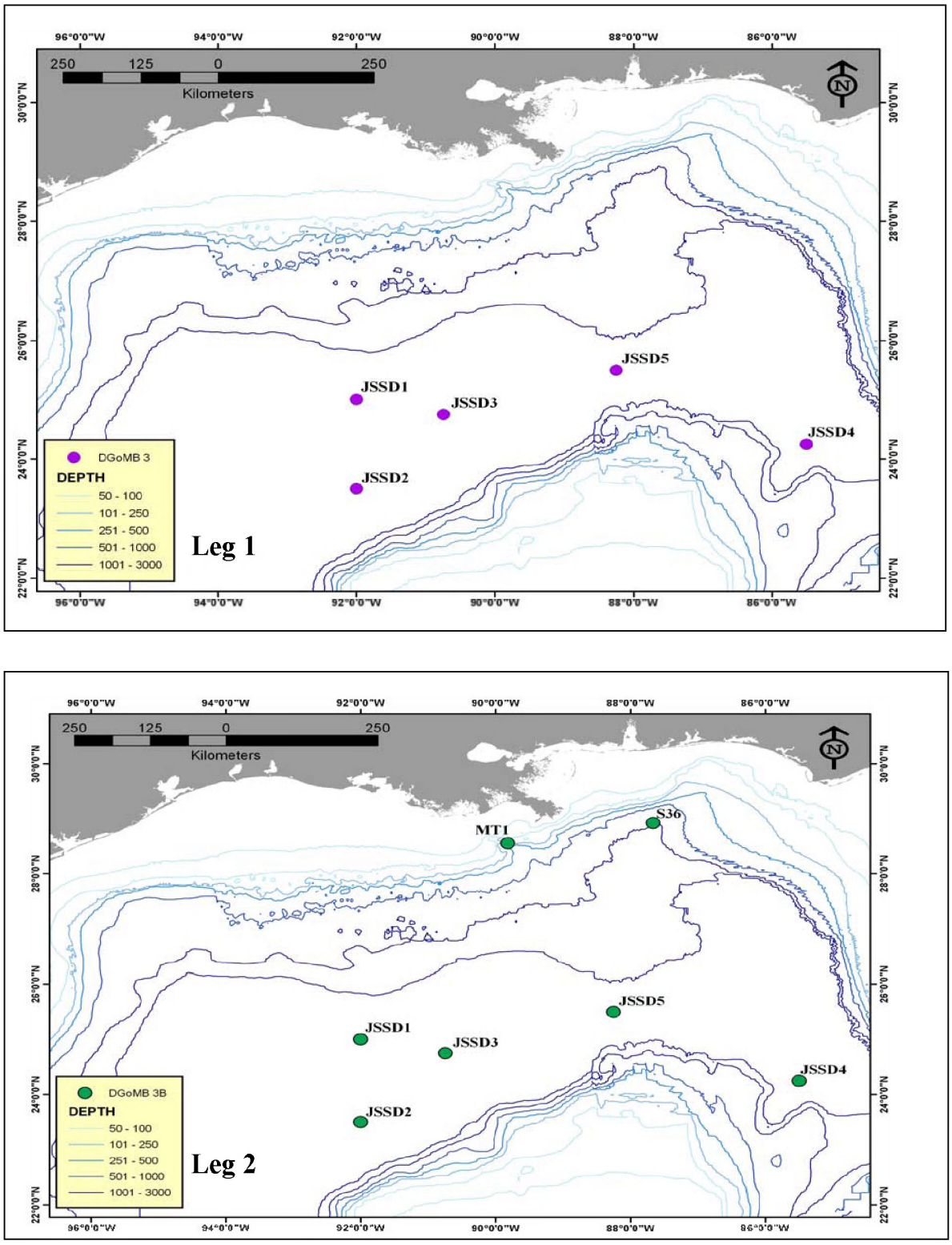

Figure 5-3. Sampling sites on Leg 1 and 2, DGoMB cruise 3. Note repeated sampling at S36 in the DeSoto Canyon on second leg.

densities of a single species of amphipod crustacean. In retrospect, it was realized that this should have been a key station initially, but progress on sample processing had not progressed adequately to realize this at the time that the four process sites were identified by the group.

The first of the two emphasized processes with use of the lander, acoustic doppler current profilers (ADCP) mooring, and baited trap array. The usual survey site sampling was conducted to supplement and fill in the sampling, the survey activities were emphasized on the August trip, including trawling. Likewise, some repeat sampling at previous survey and process sites was inserted into the latter field program. The principal reason for the two legs was to accommodate all of the different components and the specialties, including the additional Mexican (UNAM) participants. The standard sampling included CTD cast, camera lowering, box cores (with sub-sampling) and a trawl. All routine sampling was attempted on leg 1, with the exception of the trawls, which were done on Leg 2. At the two process sites (S1 and S4) additional sampling included as many as three or four additional box cores devoted to biogeochemical process measurements and living foram biomass estimates; the benthic lander deployment; and the ADCP mooring deployment. The Mexican participants requested 3 additional box cores at each site for preservation of the macrofauna in ethyl alcohol for molecular genetics characterization. Baited bottom-moored traps were deployed during trawling operations.

Given the additions of the two Sigsbee sites and MT1, the total number of process sites was seven (7). This provided maximal depth coverage with the most extreme biotic parameters, in terms of biomass and abundance, but unfortunately not all the initially planned process analyses could be completed on all seven sites.

6. FIELD METHODS

The Field Program was designed to collect a range of observations at survey and experimental stations. Survey stations were characterized by measuring a set of biological, chemical, sedimentological, hydrographic, and oceanographic variables. Samples were collected from the sediments, at the sediment-water interface, and in the overlying water column. At experimental sites, all standard survey variables were measured but in addition, sediment oxygen fluxes were measured to provide information on rates of total sediment community metabolism.

6.1 Standard Sampling Techniques

6.1.1 Boxcoring

A 0.2 m^2 GOMEX or Gray-O'Hara boxcore (Boland and Rowe 1991) was used for the sampling on the Survey Cruise. The boxcore was equipped with a cross bar onto which core liners of various diameters and lengths were attached with hose clamps. Routinely the boxcoring team attached six (6) such subcores to the cross member. On return to the surface, caps were placed on the tops of the core liners to prevent contamination. Surface water overlying the sediments but outside the core liners was siphoned off through a 300 micron sieve. Then the surface 15 cm of sediment was removed for sieving for macrofauna. Once this surficial 15 cm was removed, the individual subcores were capped on the bottom, the hose clamps were opened, and the core liners were removed. Excess mud on the liners was washed through the 300 micron sieves to prevent loss of macrofauna.

The six subcores were used for meiofauna, bacteria, geology, geochemistry, and contaminants. All six subcores were taken on all five boxcore replicates at each station. The original plan called for mixing these into a single sample for analysis of each of the variables. It was decided not to mix the samples but to initially analyze a single replicate and to archive the other cores. In that way, if odd or interesting values were observed in the single replicate, the whole suite of replicates from the other cores at each site would be available for further measurements (Figure 6-1). Having these archived samples available has been especially valuable for validating or rejecting questionable analyses.

6.1.2 Trawling

Megafaunal invertebrates and fishes were sampled with bottom trawling and bottom photography. Trawling was conducted using a 40' otter trawl with 2.5" stretch mesh. These types of trawls have been extensively employed during similar studies (Haedrich and Rowe 1977; Haedrich et al. 1975, 1980). Steel doors or conventional 7' x 14' wooden doors were used on a single warp (shrimp trawlers use a double warp or two wires). The trawl was lowered at a rate of 25 m of wire/minute. When the trawl was on the bottom, the vessel increased speed parallel to the isobaths (or into the wind or surface current, if this is required to control the vessel's position relative to the wire and its angle with the surface) up to a speed of approximately three to four knots.

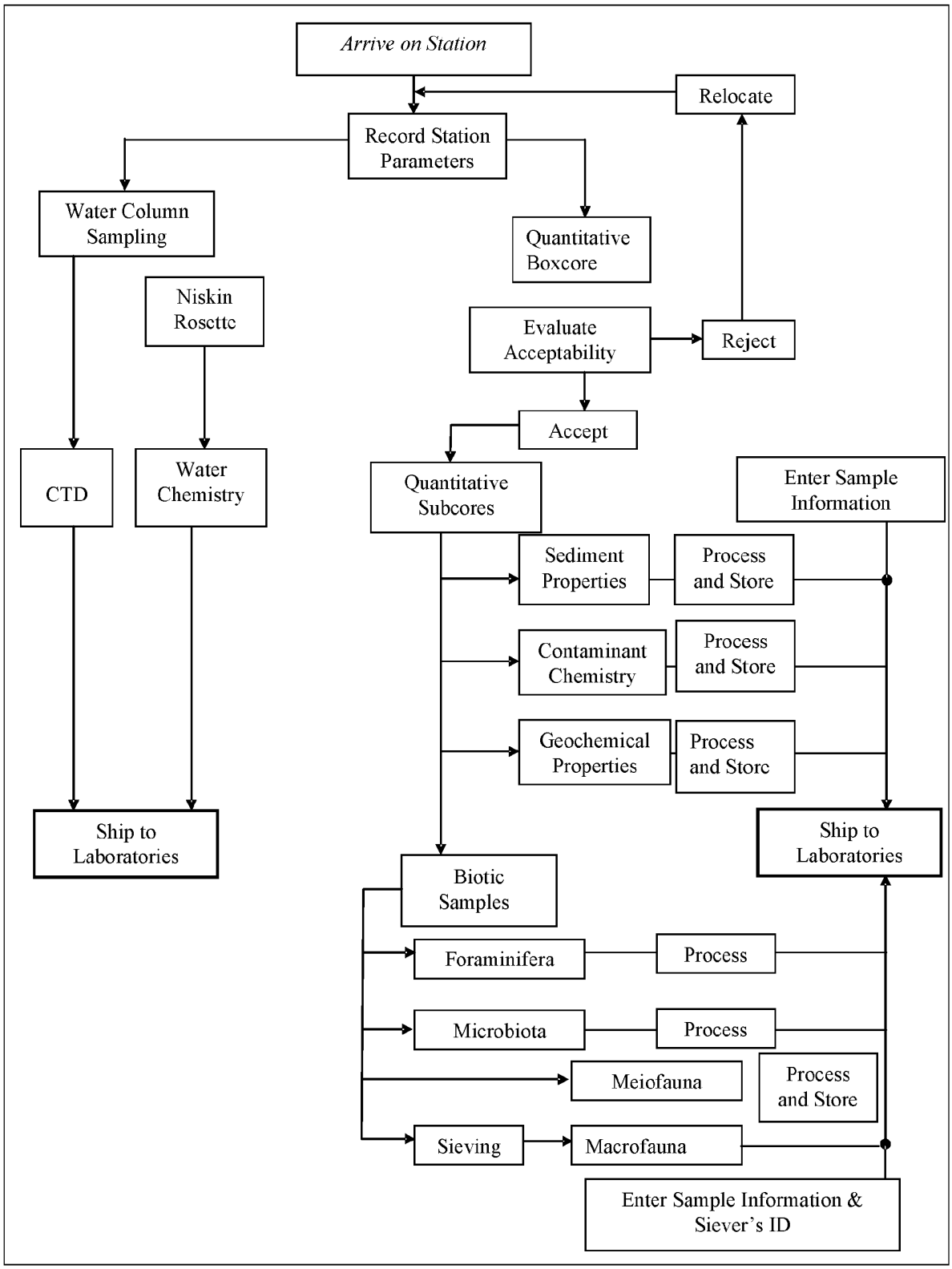

Figure 6-1. Schematic of quantitative boxcore station activities and sampling protocols.

A DGPS fix was made at this point. As the trawl was pulled, the wire was gradually paid out until the "wire out" was approximately 1.5 to 2 times the water depth. Steaming continued until the total bottom time was equal to 30 minutes per 1,000 m of water depth. That is, at 3,000 m the bottom time would be 1.5 hours. At the end of the bottom time, another DGPS fix was taken to give over-ground distance traveled by the trawl. The trawl was then retrieved at speeds less than 50 m/minute. Samples retrieved by trawling were processed at sea for distribution to taxonomic specialists or archiving (Figure 6-2).

6.1.3 Photo-Apparatus

A Benthos digital camera, with a strobe, was utilized to take up to 50 photographs of the seafloor. The camera was actuated by a bottom contact switch in order to assure that the same area of sea bottom was photographed with each exposure at each site (Rowe and Menzies 1969). Bottom contact was determined by placing a 12 kHz pinger 25 m above the camera and monitoring its position in relation to the sea floor on the strip chart recorder of the Precision Depth Recorder (PDR). The trigger weight distance from the bottom to the camera determined the area covered by each shot – approximately 2.0 m^2. The bottom-contact approach has the advantage that the area covered by each shot was consist throughout each lowering and between lowerings, as opposed to taking automatic, timed exposures during which the distance to bottom is monitored using the pinger and PDR (Hecker 1990). In the earlier NGoMSCSS study at many of the same sites, an automatic film camera was coupled with a calibrated pair of laser spots directed at the bottom in each exposure to determine area of each exposure. The advantage of the digital camera was that the sea floor could be observed immediately after retrieval of the camera back aboard ship. The disadvantage was that far fewer pictures were taken (ca. 40 as opposed to several hundred).

6.1.4 Water Column Profiles

CTD/rosette casts were taken at all survey and all experimental stations (Figures 6-1 and 6-2). All sampling was conducted to the same standards and using the same types of equipment and personnel as employed on the MMS-sponsored programs LATEX-A and NEGoM. A SeaBird Model 911plus CTD and a General Oceanics rosette with Niskin bottles were the equipment of choice. An altimeter allowed safe lowering of the package to within a few meters of the bottom. *In vivo* fluorescence was measured by a submersible fluorometer. Light penetration was measured as downwelling irradiance with a Biospherical Instruments, Inc. Model QSP-200L irradiance profiling sensor. Light transmission was measured with a SeaTech 25 cm transmissometer. Additionally a D&A Instruments and Engineering optical backscatter sensor provided continuous profiles of particle scattering.

In addition, a downward-looking ADCP was deployed to the seabottom at the beginning of each experimental station. The ADCP recorded bottom currents for the duration of each experimental station. The equipment of choice is a 300 kHzWorkhorse ADCP from RDI, model 300S Sentinal rated to 6000 m. The ADCP measures horizontal currents at 0.5 to 2.0 m intervals in the lower 50-90 m of the water column to define short-term variability in bottom currents. The instrument was equipped with a syntactic foam collar for floatation, weighted with expendable anchor material, and released using two Benthos acoustic releases. The backscatter data from the bottom-mounted ADCP was used to quantify the temporal variability of the bottom nepheloid layer during experimental stations.

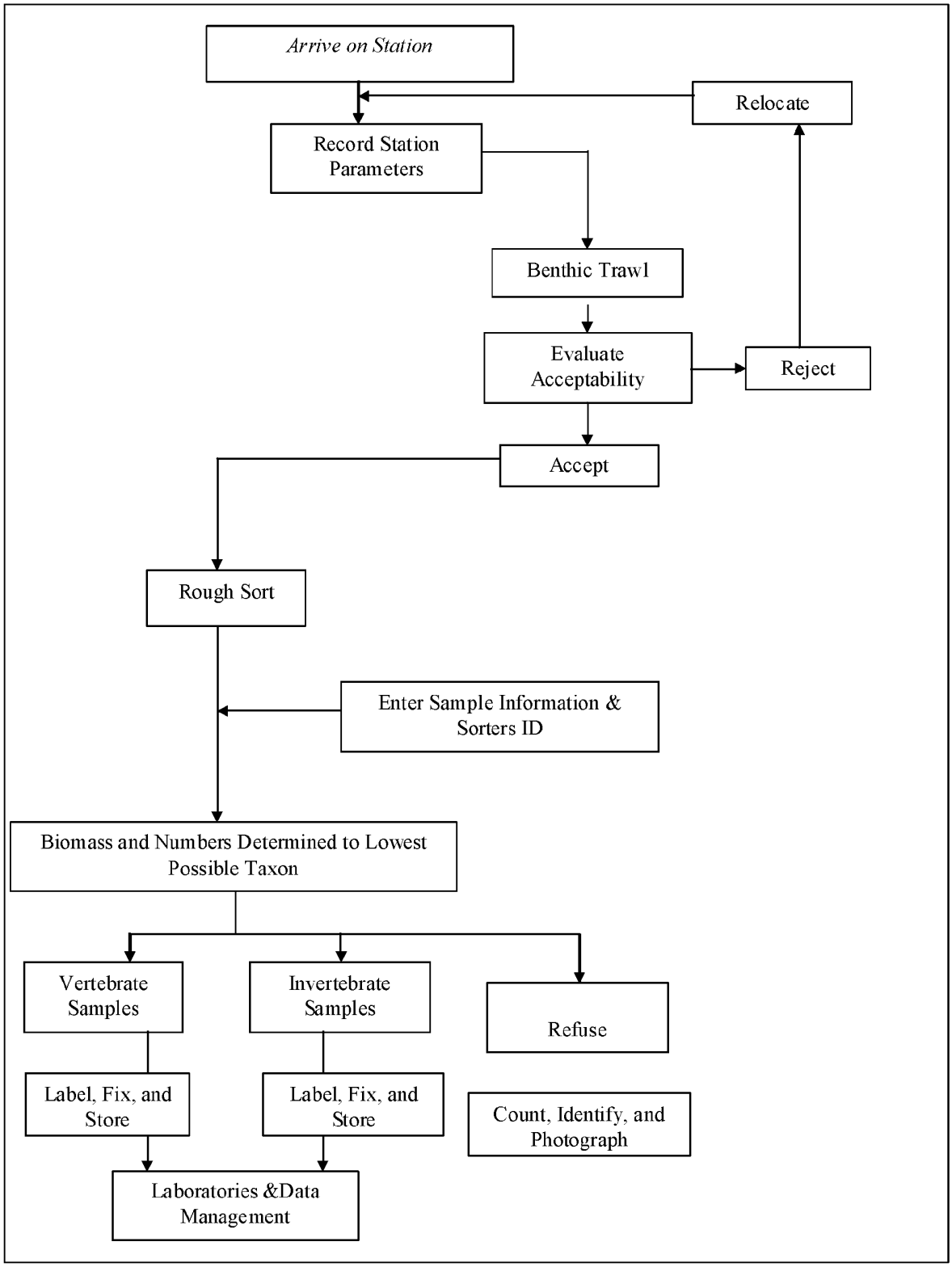

Figure 6-2. Schematic of trawl station activities and sampling protocols.

6.1.5 On-site Sampling Mapping

The specialized navigation program (GERGNav) was utilized throughout all sampling operations to determine precisely where each type of sample was taken in relation to all the other sampling. This includes drifting during all operations while sampling is being conducted or while an instrument is on the way to the bottom or back to the surface. This detailed mapping allows investigators to determine the spatial relationships between samples at scales of meters. This is important when sampling the complex topography such as mesoscale basins, canyons or escarpments in the GoM. It was especially useful for determining the distance over which the trawl was on bottom, the extent of a camera transect, and the location of box cores relative to each other. Maps were generated while on station showing the location of all the samples taken relative to one another on scales of 10's of meters.

6.2 Community Structure

Community structure measurements were made at all the survey and experimental stations (Table 4-2) In order to provide quantitative information for the conceptual model, all important taxa were sampled including the microbiota, meiofauna, macrofauna, megafauna, and fishes. Each type of assemblage was sampled by different techniques that provide the best chance to quantitative sampling of the community. In some cases, multiple techniques were employed as a cross-check (e.g., trawling, photosurveys and trap baiting for megafauna) and to provide complementary data from the same community. Each type of sample had specific field collection and processing techniques that are widely used and accepted as standard protocols. These protocols are described below.

6.2.1 Bacteria

Immediately upon boxcore retrieval shipboard, the temperature of the overlying seawater and the sediments was determined with a metal thermometer inserted in the sediment. Determining the temperature is important in evaluating the integrity and utility of the recovered sediment for measuring microbial activity under simulated *in situ* conditions.

For bacterial counts, the sediment subcores were extruded and sliced, using aseptic techniques, at predetermined depth intervals. The subsamples were fixed in a final concentration of 2% formaldehyde, prepared in a sterile, particle-free (0.2 um filtered) solution of artificial seawater (ASW) and stored (and shipped) in the dark at 4°C for shore-based analysis.

6.2.2 Protozoa (Foraminifera)

Five replicate subcores were obtained from the boxcorer at each experimental station to measure foraminifera biomass. The cores were vertically sectioned at 0-1 cm, 5-6 cm, and 10-11 cm for analysis. Foraminifera densities at depths greater than ~10 cm were low and thereby precluded analysis in deeper sections. When feasible, individual organisms were sorted on ship-board, so the samples did not need to be preserved.

6.2.3 Meiofauna

Two core samples were taken from each boxcore sample, and stored for meiofaunal community analysis. Meiofauna were collected by a core tube (5.1 cm i.d.) that was mounted inside the boxcore. A mounted corer within a box ensured that meiofauna were collected from an undisturbed surface. [Insertion of a core tube after the sample has already been sloshed around the deck of the ship is known to create artifacts including loss of organisms. Surface disturbance can occur when the boxcore is placed on the ship's deck. Taking the sample from an inner subcore reduces edge effects (Eckman and Thistle 1988).] The bow waves of sampling devices in deep water can have an impact on estimates of surface dwelling meiofauna (Hulings and Gray 1971).

The two critical sampling issues for meiofauna were core size and sampling depth. A 1.9 cm diameter core tube (2.8 cm^2) was used during previous MMS projects, e.g., Santa Barbara seeps (Montagna et al. 1989), CAMP (Montagna 1991), and GoMEX (Montagna and Harper 1996) sampling programs. A 3.5 cm i.d. core was used to collect meiofauna in the NGoMCSS study (Pequegnat et al. 1990). Densities in the deep-sea Gulf of Mexico are low (Table 6-1), so a large core must be used. About 80% of the meiofauna were in the top 4 cm of sediment. A sampling depth between 2 and 6 cm was used in seven of nine deep-sea studies reviewed by Thistle et al. (1991). The NGoMCSS study (Pequegnat et al. 1990) sampled to a depth of 5 cm. To resolve these two issues, a study was performed during the shakedown cruise (16-18 February 2000) to determine the most appropriate core size and vertical sampling depth for meiofauna in the current study area. To compare sizes, four cores ranging from 2.2 to 6.7 cm inner diameter (i.d.) were used to collect the top 1 cm of sediment, and five replicates were taken. To exam the vertical distribution of meiofauna, a 5.1 cm core tube was used. Samples were taken at 1 cm intervals down to 20 cm, and five replicates were taken. All samples were taken at station W-2 in water depths of about 661 m.

More organisms were found in progressively larger cores (Table 6-1). But, there was no statistically significant differences for abundances of total meiofauna, nematodes, harpacticoids and other taxa among different core sizes. Although total abundance in the smallest core was about half that found in the three larger cores, it was not statistically different. Because each core yielded the same abundance estimate, total counts per core were used to choose the appropriate core size. For statistical purposes, it is imperative to obtain > 30 organisms in a taxon per sample. Therefore, the 5.1 cm core was chosen for the benthic survey.

There were no meiofauna found below 13 cm sediment depth, so just the top 13 cm are plotted (Figure 6-3). Most organisms were found in the top 3 cm. A total of 87% of total meiofauna were in the top 3 cm, and 97% of the harpacticoids. In addition, 77% of the harpacticoids were found in the top 1 cm. Because the distribution is so skewed to the surface, it was decided to sample the top 3 cm only during the benthic community survey cruise. Because harpacticoids were so restricted to the top 1 cm, the core was split into 2 sections: 0-1 cm and 1-3 cm.

After the sections were collected, the meiofauna were relaxed in 7% $MgCl_2$ and preserved in an equal volume of 10% buffered formalin (yielding a final concentration of 5% formalin) (Hulings and Gray 1971). The buffered formalin was made up with seawater that was filtered through a 0.042 mm mesh to exclude plankton. Rose bengal was added to the preservative to distinguish cytoplasm-containing foraminifera from empty foraminiferal tests (shells).

Table 6-1

Effect of Core Tubes Size (Inner Diameter)
on Meiofauna Counts and Average Density
(Based on Five Replicates Taken at Station W-2. Abundance Is Detransformed
From ln, So Taxa Averages Do Not Sum to the Total Average.)

	Counts (*n*/core)				Abundance (*n*/10 cm^2)			
Core Size (cm i.d.)	2.2	3.1	5.1	6.7	2.2	3.1	5.1	6.7
Taxa								
Nematodes	20.2	64.8	161.0	219.0	31.3	59.4	50.5	54.3
Harpacticoids	5.4	30.8	74.2	99.4	2.3	26.1	20.8	24.4
Nauplii	7.2	38.6	72.2	85.6	0.2	29.2	22.9	19.0
Others	12.2	14.0	27.8	45.8	3.6	14.5	8.5	10.6
Total	45.0	148.2	335.2	449.8	54.0	135.7	111.3	112.2

6.2.4 Macrofauna

Macrofauna were sampled from five (5) replicate boxcores per station. Sieve size was 300 microns. Sieving, a critical stage in macrofauna analysis, was conducted using the gentle floatation method developed by Howard Sanders of the Woods Hole Oceanographic Institution (WHOI). A set of five (5) sieving stations was constructed, one for each replicate boxcore sample. Sievers were limited to experienced biologists. One was assigned to each core. The top 15 cm of each boxcore surface was copped out and deposited into a 50 gallon plastic trash can. Sea water, filtered with an in-line water filter to remove surface water organisms and particulate matter, was allowed to flow by hose into the bottom of the can with the sample. The trash cans were mounted in an adjustable frame, referred to as the "tipper" constructed of marine-grade plywood. The water flowed into the trash can, through the sample at the bottom of the can, and out a 20 cm long, 3 cm diameter spout 20 cm from the top of the can. On exiting the spout, the sample goes immediately into a sieve, which was held in place by an adjustable sieve holder also constructed of marine grade plywood. This process floated the animals out of the sediments and onto the sieve with the least possible trauma. This was a critical step because severe losses of animals can occur. Each siever signed the boxcoring deck log and entered comments in the margin on sample quality at the end of the sieving process. The samples were fixed in 10% formalin with sea water that was filtered as above. Rose Bengal was added to aid in rough sorting in the laboratory. On return to the laboratory, the formalin-Rose Bengal solution was changed to a 70% EtOH solution. At this point, the samples were more or less permanently preserved.

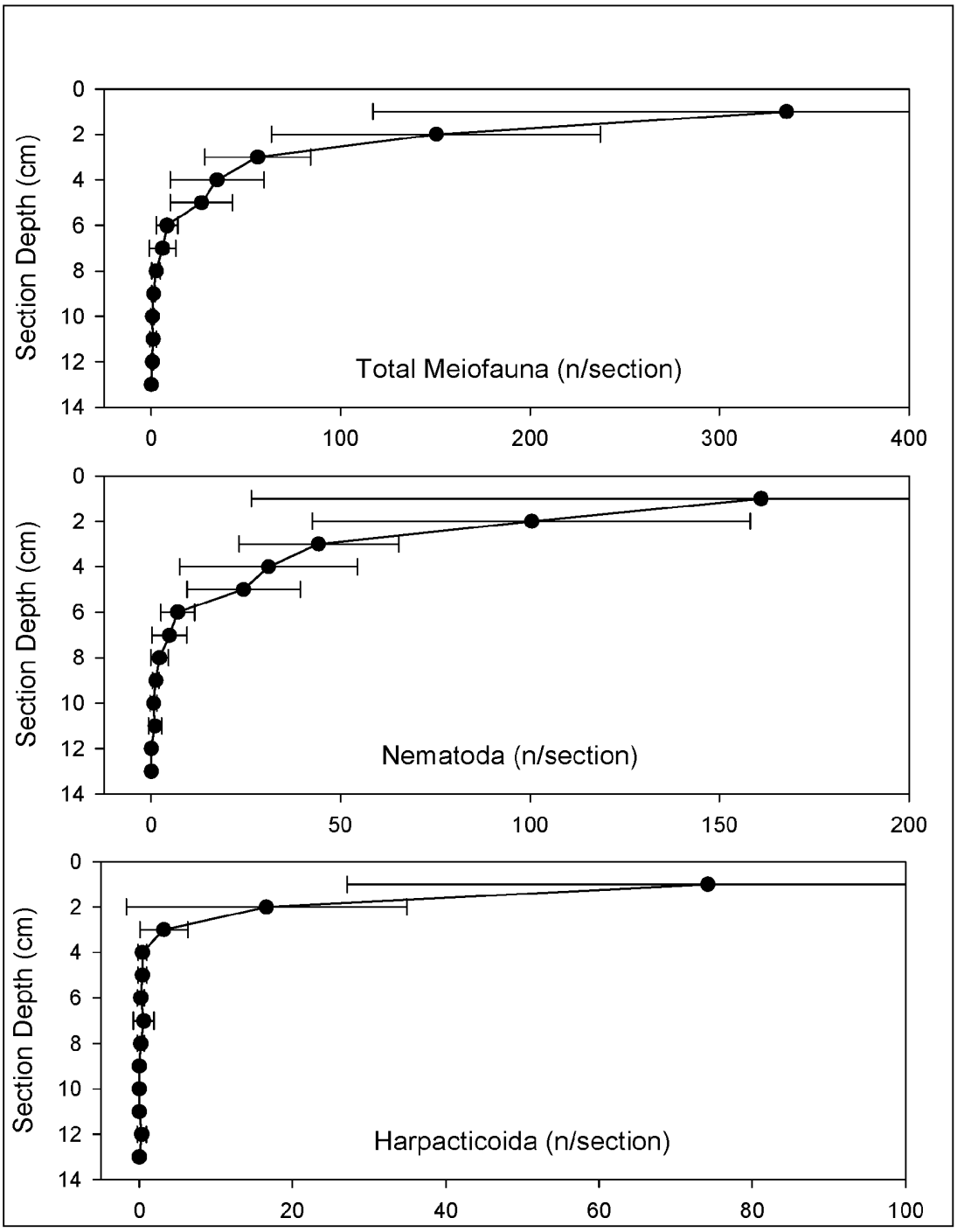

Figure 6-3. Vertical distribution of meiofauna taxa for Cruise I. Average of 5 replicates.

6.2.5 Megafauna and Fishes

6.2.5.1 Trawl Samples

Once onboard, the trawl sample was removed from the net and placed in large plastic tubs (Figure 6-2). Organisms were then sorted to species to the best of sorters' abilities. Each species was counted, its displacement volume determined, and each individual's length was measured and recorded. The samples, sorted by species, were placed in ziplock bags or small plastic jars, labeled with indelible solvent proof labels, and preserved in 10% formalin and seawater solution. All species were stored together in five gallon plastic containers covered with tight plastic lids. For fishes, the body cavity of the larger individuals were opened to enhance fixation. Trash was separated out and stored in separate five gallon plastic containers. Larger items were photographed and discarded or saved for disposal on land.

6.2.5.2 Photosurveys

The purpose of the camera lowerings was to quantify the megafauna. This is important because the megafauna are an explicit component of the conceptual model of the ecosystem. If the biota are abundant then good estimates can be made with few exposures. For example, it has been demonstrated that from the upper slope down to the lower slope, on the order of 30 or so exposures, each covering an area of six square meters, is adequate to quantify the dominant megafauna (Rowe and Menzies, 1969; Grassle et al. 1975). At lower densities, more exposures are required. During the NGoMCSS study, approximately 48,000 photographs were taken, but only 25% of them were ultimately analyzed. A digital camera was used so that the images could be easily scanned upon system retrieval. The images are also easily electronically transmitted and archived on CD ROMs.

6.3 Community Function

In addition to the standard set of analyses performed at all survey and experimental stations, a series of specialized studies was conducted at experimental stations to develop a better understanding of rates of biological processes at the process sites. These studies will be conducted on samples provided by the standard set of techniques and equipment, specialized sampling protocols, and gear. These methods have been used during Cruises 2 and 3a and 3b.

6.3.1 Microbial Metabolism

For microbial activity measurements, subsamples from three sediment depths per boxcore (per station) were diluted in artificial seawater to prepare sediment slurries for homogeneous amendment with the desired radiolabeled substrates. Separate aliquots, in duplicate, were then incubated and sacrificed at each of five time intervals to develop rate measurements of substrate respiration and incorporation into biomass. Such sediment slurries provide an upper bound on microbial activity due to the oxygenation and disruption of microniches caused by sample retrieval. Cross-site comparisons will be important.

6.3.2 Sediment Community Oxygen Demand

A key component of the experimental studies was the measurement of total sediment community oxygen consumption (SCOC) using the benthic lander and *in situ* chambers (Figure

6-4). The GoMEX (for Gulf of Mexico) lander was designed to estimate fluxes of oxygen and metabolites into or out of the sediments by incubating the bottom water and sediment surface in enclosed, stirred chambers. Thorough descriptions of the GoMEX lander have been published in Pomeroy et al. (1991), Rowe et al. (1994), and Miller-Way et al. (1994).

Figure 6-4. Benthic lander.

The GoMEX lander, as used in this study, consists of a square aluminum-pipe frame measuring 2 m on a side. This frame holds 1) two acrylic incubation chambers, 2) a multi-function electronic timed release system, with "burn wire" release mechanisms, 3) a deep-sea multishot camera and strobe system, 4) two disposable anchor weights, and 5) glass floatation balls. The two chambers each contain an oxygen sensor and thermistor, a submersible pump, an

additional stirring motor, and three 60 cc hypodermic syringes. Each chamber encloses a sediment surface area of 906 cm^2 under a volume of seven liters of bottom water. A stirring bar inside the chamber is driven by a magnet attached to an electric motor in an oil-filled water-tight case outside the chamber. The camera and strobe are attached to the frame opposite the chambers to monitor proper contact with the sediments and syringes. Two disposable anchors (totaling 200 lbs) composed of cylinders of lead are dropped under the control of the electronic timed release, with corrosive links of variable duration as a backup. Relocation on the surface is aided by a flag, two radio direction finders and a strobe flasher. The chambers remain on the bottom for periods of 8 to 36 hours.

The sequence of events for this "free vehicle" involves floating to the bottom and then undergoing a series of programmed mechanical operations that are controlled by an electronic timer that burns release wires on command. The chambers incubate bottom water from which metabolic substrates are consumed and into which metabolic by-products are produced. The fluxes are calculated as:

$$Flux = \frac{(Change\ in\ Conc.)\ x\ Vol.}{area\ x\ time}$$

6.3.3 Foodweb Studies—Stable Isotopes

Organism tissues were selected for stable isotope analysis for foodweb studies. The tissue was excised or the whole organism was frozen whole at -4°C. Isotope analyses were conducted on selected whole sediment, Sargassum recovered in trawls and floating at the surface, selected large invertebrates and amphipods collected in deep baited traps.

6.4 Sediment Properties

Subcores for sediment properties were taken from each of the five replicate boxcores. These were not pooled but were stored separately. The top two centimeters were sampled using a spatula or scoop. Shear strength was measured in the shore-based laboratory.

6.5 Chemical Contaminants

Subcores for trace metals and hydrocarbons were taken from each of the five replicate boxcores. The subcores were extruded and the upper 2 cm of the sediment was sectioned with a teflon-coated spatula. Total organic and inorganic carbon were measured on the hydrocarbon sample. Hydrocarbon subsamples were immediately placed into precleaned (combusted at 425°C) ½-pint glass jars with teflon-lined lids (~150 g). Trace metal samples were immediately placed into pre-cleaned plastic jars (~150 g). All sediment samples for contaminant chemistry werestored frozen (-20°C).

6.6 Geochemistry

At each survey site, near surface (about 0 to 2 cm) samples from each of the five (5) replicate samples were frozen but analytical work was completed at shore-based laboratories on only one sample. The other five have been archived frozen.

7. LABORATORY METHODS

Once samples and data were collected on the various cruises, extensive shore-based laboratory analyses were performed. The samples were uniquely labeled and preserved for storage onboard the ship to ensure their integrity during transport to the various PI's laboratories. The methods employed standard techniques widely used for similar programs, ensuring that comparisons with historical studies are valid. This data compatibility is important to provide the greatest value in the final synthesis. The laboratory methods are described in detail below.

7.1 Taxonomy

Taxonomy is a vital component of the GoM deepwater study. Many of the hypotheses will be tested at the species level. A team of taxonomists was selected was selected to assist with the identifications (Table 7-1). The first step was getting good samples but the next step was accurate and thorough sorting of the samples to major group. This was accomplished by graduate students who were supervised by experienced professional invertebrate zoologists.

Rose Bengal-stained invertebrates were separated from sediment samples, after sieving and preservation, and sorted to major taxonomic group: polychaetes, oligochaetes, mollusks, crustaceans, and others. Sorting efficiency was tested by re-sorting the "waste" sediment materials prior to storage. All materials collected during the program were stored until the program was complete so that it can be reviewed as needed. Poorly sorted samples discovered during resorting were sorted again. The initial sorter was identified and retrained to increase sorting efficiency.

The major groups were sent to the appropriate lead taxonomist. The polychaete taxonomist was Dr. Guinn Fain Hubbard (TAMU), who also supervised the macrofauna sorting laboratory. The taxonomists then sorted the major group to species, identifying those that had been described and giving species designations to those that either could not be identified or had not yet been described. Mis-sorts (organisms placed in the wrong major group by the sorting lab) were returned to Dr. Hubbard in the sorting lab for redistribution to the proper taxonomist. The taxonomists then sent a species list and the identified specimens back to TAMU, retaining those specimens on which further work was warranted. The species list was then entered into the data base by Dr. Wolff.

The mollusk identifications were made by Mr. Roe Davenport, with assistance from graduate student Min Chen and Prof. Mary Wicksten. Dr. Richard Heard (University of Southern Mississippi) was the crustacean taxonomist. Dr. George Wilson (Australian National Museum) identified the isopods. While most of the adult echini were taken in the trawl samples, juveniles were sometimes encountered in the boxcores.

Each lead taxonomist was responsible for identifications to the species level. Any misidentifications by the sorters that were encountered were returned to the sorting laboratory for redirection.

Table 7-1

Taxonomists Involved in the Analysis of the Macrofauna and Corresponding Taxonomists Working on UNAM Mexican National Collections

Taxon	DGoMB	UNAM	Other
Fishes	John McEachran (TAMU)/R. Haedrich(MUN)	Luis Zambrano	
Amphipoda	Richard Heard (USM)/John Foster/Yousra Soliman(TAMU)	Fernando Alvarez	
Aplacophora	Amely Scheltema (WHOI)		
Ascidiacea			
Asteroidea	Archie Ammons (TAMU)	Alfredo Laguarda, Francisco Solis	
Bivalvia	Min Chen/R.Davenport/ M.Wicksten		
Brachiopoda	Mary Wicksten (TAMU)		
Bryozoa			Nielsen
Cumacea	Heard/Chihlin Wei/L. Petrescu	Alvarez	
Decapoda	Wicksten	Alvarez	
Echinoidea	Wicksten, Ammons	Laguarda, F. Solis	
Echiura			Eibye-Jacobsen
Gastropoda	Rex/Davenport	Garcia Cuba(*Conus* & *Terebra)*	
Harpacticoida	H. Lee (Montagna)	Alvarez	
Holothuroidea	Wicksten, Ammons	Laguarda, F. Solis	
Hydrozoa			
Isopoda	Geo. Wilson(Aust. Nat. Mus.)	Alvarez	
Kinorhyncha		Rhinehard Kristensen (Danish Mus.)	
Mysidacea	Heard	Alvarez	
Nematoda	N.A.		
Nemertini	Jon Norenburg(USNM)		
Oligochaeta			
Ophiuroidea	Wicksten, Ammons	Laguarda, F. Solis	
Ostracoda		Gío Argaez	
Polychaeta	G. Fain Hubbard	Vivien Solis	
Porifera		Patricia Gomez	
Priapulida			
Pycnogonida	Allen Child		
Scaphopoda			
Scyphozoa			
Sipunculida			
Tanaidacea	Heard/Kim Larsen	Alvarez	
Turbellaria			
Anthozoa	Daphne Fautin (U.Kansas)		
Copepoda	Lee (Montagna)		
Chaetognatha	Gerald McLellan (USM)		
Halacaridae		Anna Hoffman-Mendizabel	
Crinoidea		Laguarda, F. Solis	
Cladocera			

7.2 Community Structure

Community structure refers to the standing stocks, biomass and species composition of any assemblage of organisms. It has been used to test the eight hypotheses in this study. For some groups only standing stocks was measured. For others, complete identification down to the species level was possible. The standing stocks in all size groups were utilized in the carbon budget that integrates all the process measurements.

7.2.1 Bacteria

Bacterial abundance in sediments was determined using a dual staining technique (acridine orange and DAPI stains) and standard epifluorescence microscopy for marine sediments (Relexans et al. 1996 and Schmidt et al. 1998). This procedure does not attempt to remove bacteria from the sediment grains prior to counting. Separating the bacteria from the sediment inevitably results in an underestimate of abundance, since bacteria tightly bound to the sediments are left behind. Instead, the method of choice views the bacteria directly in the presence of the grains after treatment with Triton-X detergent and sonication (to loosen the attached or aggregated cells). For each sediment core, a down-core profile of bacterial abundance was determined at ten (10) closely spaced sampling intervals from 0-15 cm with spot checks to a depth of 30 cm. Sediment bacterial abundances were rarely examined at depths greater than 15 cm. The deeper samples (done to 30 cm) are important in understanding bacterial distributions in deep-sea sediments. The potentially unique nature of some of the targeted slope sediments suggests that significant variations from typical pelagic marine sediment downcore profiles known may be observed (Schmidt et al. 1998). Since ultimately abundance was integrated over depth in the sediment to provide benthic bacterial mass estimates at each station for modeling and hypothesis testing purposes, unusual abundance profiles in the deeper layers of sediment would have been important, if encountered.

Bacteria were also sized in selected samples by measuring the length and width of photographed cells stained with acridine orange and projected onto a flat white surface (Lee and Fuhrman 1987) to convert bacterial abundance to biomass. This method was a significant improvement in the accuracy of benthic bacterial biomass estimates.

7.2.2 Foraminifera

Biomass of foraminifera is difficult to measure because foraminiferal assemblages include a combination of live specimens and empty shells. Measurement of only the organic fractions was appropriately done by measuring ATP content at the experimental stations. From each sample, 50 specimens were individually measured for length and subsequently extracted for ATP following the procedure of Bernhard (1989).

7.2.3 Meiofauna

Meiofauna were extracted from sediment using the Ludox centrifugation technique (deJonge and Bouwman 1977). Extraction efficiency has been shown to be 95%–99% of organisms over all sediment grain sizes. Samples were then sieved and counted to major metazoan taxonomic category. Protozoan, primarily Foraminifera and Ciliata, were enumerated when stained as well and reported

The term "meiobenthos" was first coined by Mare (1942) to describe benthic organisms of intermediate size. These are metazoans that are smaller than macrofauna but generally larger than the single-celled microbenthos (e.g., bacteria, microalgae, and protozoans). By convention, the definition of meiofauna is those animals that pass through a 500 micron sieve but are retained on a 63 micron sieve (Hulings and Gray 1971; Coull and Bell 1979; Giere 1993). Because deep-sea organisms are small, most meiofaunal ecologists use 42 micron sieves to retain meiofauna (eight of nine papers reviewed in Thistle et al. 1991). To conform with other studies of deep-sea meiofauna, a 45 micron sieve was used to retain meiofauna.

Meiofauna were identified to the major taxon level. Meiofaunal communities are composed of two groups. Temporary meiofauna are those juveniles of the macrofauna that will eventually grow into larger organisms. Permanent meiofauna are those groups where adults are less than 300 microns, e.g., Nematoda, Copepoda, Gastrotricha, Turbellaria, Acarina, Gnathostomulida, Kinoryncha, Tardigrada, Ostracoda, and some Rhyncocoela, Oligochaeta, and Polychaeta. In 1971, Thiel suggested that the grouping of benthic organisms according to size differences had little taxonomic or ecological justification, except convenience of sample processing (quoted from Thiel 1975). However, ecological literature since 1971 has shown that meiofauna are different from macrofauna and have different roles in marine ecosystems (for reviews see: Coull and Bell 1979, Coull and Palmer 1984, Giere 1993). Even where meiofauna share ecological properties with macrofauna, the processes operate on much smaller spatial and shorter temporal scales for the meiofauna (Bell 1980).

Meiofauna biomass was measured or calculated (Montagna 1984; Montagna and Li 1997) for all samples. There is an extensive literature on biomass techniques. Robinson (1984) compared five methods for nematode biomass and recommends calculating volume based on a cylinder the length of the nematode and the diameter of the nematode's area/length ratio. Pearre (1980) compared five methods for copepod biomass and recommends calculating volume based on a cylinder. Techniques and formulas for other meiofauna are given in Duplisea and Hargrave (1996). Volume estimates were converted to wet biomass with the assumption that organic matter has a specific gravity of 1.2 It is well known that biomass is underestimated by 30%–40% in formalin preserved samples, so biomass was adjusted for this loss (Frithsen et al. 1986). For small organisms (e.g., meiofauna) biomass was calculated based on volume measurements and conversion factors in the above references. Conversion factors specific to the deep-sea GoM do not exist, so they will be empirically determined in 10% of the samples by direct measurements using a CHN analyzer and electrobalance (Montagna 1984). There is also an extensive literature on how best to calculate the volume of meiofauna based on length and width measurements.

7.2.4 Macrofauna

The macrofauna samples were stained with Rose Bengal, buffered and fixed in a 10% seawater and formalin solution aboard ship. On return to the laboratory, the samples sieved again with fresh water if considerable fine sediment has been retained in the sample. After this additional sieving, the stained macrofauna were sorted under dissecting microscopes to major taxonomic groups and preserved in 70% ethanol. Sorting efficiency was estimated on all sorted samples. All residues continue to be properly preserved and have been retained for the duration of the project for review as needed.

Taxa that are routinely considered meiofauna but were retained on the 300 micron sieve were also separated and quantified. The numbers and biomass of these larger animals were included in the total biomass and density calculations of the macrofauna, but were not included in the

zonation or diversity estimates. Most of these taxa were nematodes, harpacticoid copepods, and forams.

Determination of biomass as wet weight was accomplished on a subset of representative organisms at the group level prior to distribution to the taxonomists. For larger organisms, this was done by weighing the organisms in their alcohol preservative as a group (Rowe 1983). For smaller organisms, this was done by measuring them with a calibrated ocular micrometer, calculating their displacement volumes, and assuming a density of 1.2 g/cc. Organic carbon weight, which is the unit used in the food web budgets (See Section 9), was estimated from the conversion factors for each major group (Rowe 1983).

7.2.5 Megafauna and Fishes

In the field, the fishes and megafauna recovered by trawl were processed as followed: 1) sorting of fishes and megafauna to "tentative" species (along with volume, measurements, counts, and length by species; 2) selecting specimens for tissue samples for stable isotopic and deoxyribonucleic acid (DNA) analyses; 3) processing, labeling, and storing tissue for shore-based analysis; 4) fixation in 10% neutral buffered formalin, and 5) recording any unusual occurrences in the trawl performance that might effect the catch. Upon return to the laboratory, tissues for stable isotopic analysis were delivered to the appropriate PI. The fish subsamples were soaked in water to remove all traces of formalin and then transferred to 70% ethanol. The megafauna and fish identifications were verified and transferred to a single jar per species per station. These samples were distributed to the taxonomists listed above (Table 7-1).

The material from 2002 studies within the Mexican EEZ were transported to the collections of the Institute of Zoology at the National University of Mexico (UNAM) in Mexico City immediately after the GYRE returned to Galveston. The fishes were identified by Richard Haedrich and Jessica Bangma, on a visit to UNAM the following year, in cooperation with graduate students at that institution. The data are entered now into both UNAM and DGoMB data bases. These specimens have acquisition numbers in the UNAM collections and are available for taxonomic study on request, either at Institute or on a loan basis, in accord with traditional international museum protocols.

7.3 Community Function (Process Studies)

At each experimental station a specialized set of process studies provided important information to support those data obtained at the standard survey stations during. These studies were performed using techniques and methodologies specific to each programmatic component.

7.3.1 Bacterial Metabolism

Bacterial productivity was estimated in sediment samples from the process stations using the tritiated thymidine approach, as applied by Alongi (1990) to other deep-sea sediments. For comparative purposes, we tested for activity in undiluted and diluted surface sediments and in samples incubated at atmospheric pressure and in situ pressures, all at in situ temperature. We ran endpoint, time-course and variable substrate concentration experiments to assess isotope dilution and other procedural issues. Incubations were terminated shipboard using 80% ethanol. Returned samples were processed further to assess thymidine incorporation into DNA, again following procedures of Alongi (1990).

7.3.2 Meiofaunal Feeding Rates

Meiofaunal feeding rates on benthic bacteria were measured by incubating sediment cores with radiolabeled thymidine (3HTdr; Montagna 1984, 1993). Initially, 2 uCi of 3HTdr is injected and incubated for 8 h, after which formalin is injected into the cores to stop label uptake. A one ml subsample was then withdrawn from the core. This subsample was filtered onto a 0.2 micron Millipore filter and rinsed three times with seawater to estimate uptake of 3HTdr by bacteria. The subsample was dispersed and suspended in five mL of distilled water and 15 mL insta-Gel for dual label liquid scintillation counting. Meiofauna were separated from sediments by diluting samples with 2% formalin, swirling to suspend animals, and decanting them and the supernate onto 63 micron Nitex screen filters. Meiofauna were then rinsed into jars and kept refrigerated in 2% formalin until sorting at a shore-based facility.

The labeled meiofauna collected were sorted under a dissecting microscope. The individual taxa were placed in one mL of water in a scintillation vial. The meiofauna were then dried at 60°C and solubilized in 100 mL Soluene tissue solubilizer for 24 h. Samples were ultimately counted by dual-label scintillation spectrophotometry in 15 mL of Insta-gel.

7.3.3 Sediment Community Respiration

The changes in the chemical concentrations of oxygen, dissolved inorganic carbon (DIC), ammonia, nitrate, nitrite, manganese, iron, silicate, and phosphate in the benthic chambers were used to estimate total community respiration by organisms living within the sediments in benthic chamber incubations. The oxygen concentrations was determined from a continuously recording polarographic oxygen electrode, backed-up by a miniaturized Winkler method (uses 25 mL samples). The other chemicals were measured in syringe samples from the beginning, middle, and end of the incubations. Conventional wet chemistry was employed as described in the geochemistry section.

7.3.4 Foodweb Analyses—Stable Isotopes

Selected organismal tissues were sampled and preserved for stable isotope analysis. The tissues were analyzed for carbon and nitrogen stable isotopic compositions. Most samples were measured with a Finnigan MAT Delta S Elemental Analyzer-Isotope Ratio Mass Spectrometer (EA-IRMS). If, for any reason, samples cannot be processed by EA-IRMS, they will be measured by standard tube combustion methods similar to those described in Cifuentes et al. (1988). Finally, the stable carbon isotope ratio of bacteria in sediments were determined by proxy, in phospholipid fatty acids, a biomarker of bacterial biomass (Salata 1999).

7.4 Sediment Properties

Sediments retrieved from the boxcores were preserved and returned to shore-based laboratories for analysis (see below).

7.4.1 Grain Size

Grain size was determined by the standard Folk settling method. Fifteen to twenty grams of sediment were treated with hydrogen peroxide for twelve hours to remove organic matter. After washing with distilled water, the sediment was dispersed with hexametaphosphate solution and poured over the appropriate screen. The material that passes through the screen was then subjected to a series of prescribed settling techniques that were based on removing materials at

set times. The individual fractions that were collected were dried and weighed to provide quantitative values for each size fraction as a percent of the total weight of sediment. Per cent gravel, sand, silt, and clay were calculated. Duplicates were analyzed with every batch of twenty samples to estimate precision.

7.4.2 Geotechnical Properties

All boxcore samples were examined and sampled for shear strength, bulk density, water content, and grain size. Selected samples were tested for permeability. Shear strength was determined by hand held vane shear devices and was used to determine the cohesion of the sediment at several depths and locations in a non-contaminating and non-disturbing manner within each boxcore. Bulk density and water content was determined by standard geotechnical techniques. Porosity was determined from the bulk density measurements. Permeability was the capacity of the sediment to transmit fluids without impairment of the structure of the medium. Permeability regulates the rate of flow of interstitial waters resulting from the compaction process and was important in the transport of fluids and gases within sediments. Permeability was determined on selected samples by pressure permeameters and a constant gradient consolidometer. Of the above sediment physical properties, grain size is the only one for which a large number of correlations have been made with benthic communities. It was reasonable to presume however that they may correlate or co-correlate with animal distributions.

7.4.3 Total Organic and Inorganic Carbon

Total organic and inorganic carbon was determined by standard LECO combustion techniques or by Carlo Erba element analyzer. A freeze-dried and homogenized sample is burned in the presence of oxygen and accelerator to CO_2 which is swept from the combustion chamber into a detector. The detector is calibrated with rings of known carbon content and the sample carbon content is calculated from the detector response. Inorganic carbon is determined as the difference in carbon content between an untreated and acid-treated sediment sample.

7.5 Chemical Contaminants

Each survey and experimental site were screened for the presence of chemical contaminants. Hydrocarbon and relevant metals were measured at each site.

7.5.1 Hydrocarbons

Sediment samples were analyzed for polynuclear aromatic hydrocarbons (PAHs) using NOAA National Status and Trends Methods (Denoux et al. 1998; Qian et al. 1998). The proficiency and validity of this method has been established by 14 years of laboratory intercomparisons. Briefly, deuterated PAH are added before the extraction and are used to calculate analyte concentrations. Sediment samples are mixed with anhydrous sodium sulfate and are extracted with methylene chloride/acetone in an Automated Solvent Extractor (ASE). The extracts are separated from possible interfering compounds by silica/alumina columns. The purified extracts are analyzed on a HP 5890/5970 gas chromatograph with a mass selective detector (GC/MS) using a selected ion detection technique. The GC/MS is calibrated with known concentrations of analytes at five different concentration levels and the average response factors of the analytes are used for PAH concentration determination. Concentrations of PAHs are reported as nanogram/gram (ng/g) on dry weight basis for sediment samples. Both non-alkylated

(parent PAHs) and alkylated PAHs are reported. Each sample batch of 20 samples or less includes a procedural blank, a matrix spike, a matrix spike duplicate and a standard reference material. These quality assurance samples ensured that the analytical results for each batch are valid and of acceptable accuracy and precision.

7.5.2 Trace Metals

Sediment samples were analyzed for Ba, Cd, Cr, Fe, Hg, Pb, and Zn. These have been shown to correlate with drilling and production in previous studies (e.g., Kennicutt, et al. 1996a,b) and/or are known to be toxic to organisms. The analyses followed the well-established National Status and Trends methods. Methods included atomic absorption spectroscopy (AAS), instrumental neutron activation analysis (INAA) and/or inductively coupled plasma spectrometry (ICP), depending on the metal and the concentration (e.g., Taylor and Presley 1998). INAA was used to determine Ba, Cr and Fe. The precision and accuracy for these elements by INAA is excellent regardless of the matrix, including pure drilling mud. A more sensitive method was used when needed for other metals to insure accurate and precise values.

Sample preparation begins with freeze-drying a representative sediment aliquot and grinding it to a fine powder. No further treatment is needed for INAA, providing a check on the sample dissolution techniques needed for AAS/ICP analysis. For INAA, 0.5 g aliquots of the powdered samples is weighed directly into plastic vials and heat sealed. The samples are irradiated for 12 hours in the 1 megawatt TRIGA reactor. After a 10 day cooling period to allow Na, Cl, and other interfering isotopes to decay to low levels, the samples are counted using a hyper-pure germanium detector coupled to a Nuclear Data Corp. model 9900 multichannel analyzer integrated with a Digital VAX II/GPX graphics workstation. Concentrations were obtained by comparing counts for each sample with those for sediment and rock reference materials of accurately known elemental composition. Details of this method are given in Boothe and James (1985), including information on counting geometry, reference materials, spikes, blanks and other aspects of QA/QC.

The National Status and Trends Program methods (Lauenstein and Cantillo 1998) were used in for AAS/ICP analysis. The method for Hg is the standard Environmental Protection Agency (EPA) sulfuric acid-permanganate digestion of a dry powdered sample followed by stannous chloride reduction to Hg metal and detection by cold vapor AA. For other metals, 200 mg aliquots of the powdered sediment samples are weighed into teflon "bombs" and completely dissolved in a mixture of nitric, hydrofluoric and boric acids by prolonged exposure of the closed bombs to a temperature of 130°C. Various dilutions were made on the clear digests to bring them into the working range of the AAS or ICP.

A Perkin-Elmer Corp. model 3300DV (dual view) ICP was used when element concentrations permitted. When concentrations were too low for this instrument, a Perkin-Elmer 3030Z AA equipped with an HGA-600 graphite furnace and an auto sampler were used. Details of furnace programs, matrix modifiers, blanks, spikes, reference materials and other QA/QC information can be found in the reference given above. The methods utilized ensured that matrix spike recovery for all elements was greater than 90% and that recoveries of certified values for reference materials from the National Research Council of Canada were 90% or better as well.

7.6 Geochemical Properties

The geochemistry component measured a range of relevant sedimentary properties at both survey and experimental sites. Single replicate samples were analyzed at the survey sites and

detailed profiles were determined at experimental sites to determine important flux rates. Various geochemical properties were measured on pore waters and solid phases. Analyses that are best performed immediately after sample retrieval were conducted onboard, whereas other analyses which require more time consuming methods can only be performed at shore-based facilities (Tables 7-2 and 7-3). Pore water was separated from the solid phase by centrifugation or pressure filtering.

Table 7-2

Summary of Parameters To Be Analyzed and the Methods To Be Used

Type of Component	Component	Analytical Method
Pore water	O_2, H_2S, Fe and Mn	Microelectrodes
	Total CO_2 (DIC)	Coulimetric titration
	Sulfate and chloride	Ion chromatograph
	pH	Electrodes
	Nutrients	Auto analyzer
	Dissolved organic C (DOC)	DOC analyzer
Sediment Solids	C stable isotopes	Extract/mass spectrometer
	Porosity	Wt. change on drying
	CHNS	Carla Erba analyzer
	Reactive Fe and Mn	CD extraction, FAAS
	Carbonate carbon	Leco C analyzer
	Metals	NS&T Methods
	Hydrocarbons	NS&T Methods
Biologic	Radioisotopes	Counting
	SO_4^{2-} reduction rate	^{35}S tracer method

Table 7-3

Chemical Parameters To Be Analyzed

Parameter	Survey Station	Experimental Station
Sediment Properties		
CHNS	L	L
Carbonate content	L	L
Contaminants		
Metals	L	L
Hydrocarbons	L	L
Indicators of Biologic Activity		
Nutrients	L	L
DOC	L	L
SO^4/Cl	L	L
DIC		L
δC^{13} DIC		L
Radioisotopes		L
Reactive Fe and Mn		L
Sulfate reduction rate		F
pH		F
H_2S		F
O_2		F
Dissolved Fe		F
Dissolved Mn		F

The geochemistry studies at experimental stations included detailed depth profiles of biogeochemically important parameters, measurement of sulfate reduction rates, and benthic flux measurements using incubation chambers, in addition to survey variables. Isotopic studies were also carried out at selected stations. In addition to the shore-based analyses described for the survey stations, near interfacial profiles of O_2, H_2S, Fe and Mn were acquired by the microelectrode method of Luther et al. (1998). Sulfate reduction rates were determined using the $^{35}SO_4^{2-}$ tracer technique in order to measure the approximate rate of hydrogen sulfide generation within the sediment (Lin and Morse 1991). Pore waters were extracted from sectioned cores to produce depth profiles of nutrients, pH, DIC, dissolved organic carbon (DOC), and sulfate/chloride ratios. All of these were analyzed on shore. Carbon stable isotopes were determined on the DIC samples. Total dissolved inorganic carbon in pore waters was determined by Coulometric titration. Pore water nutrients (nitrate, nitrite, ammonia, urea, phosphate, and silicate) were determined by standard auto-analyzer techniques much like those for water column nutrients. Dissolved organic carbon in pore waters was determined with a high temperature combustion DOC analyzer. Selected measurements of the stable carbon isotope ratio of porewater dissolved inorganic carbon will be performed according to Salata et al. (1996).

The following table lists the chemical parameters analyzed and categorizes them by station type: survey or process, and whether the analyses were made in the field (F) or laboratory (L). Note that at the survey sites only the surficial sediments were analyzed, whereas at experimental stations depth profiles were determined for most parameters.

Analysis of selected radionuclides has been used to determine sediment accumulation and mixing (bioturbation) rates at experimental stations. Samples along a depth profile were gamma counted and analyzed for ^{210}Pb and $^{239,240}Pu$ by wet chemistry followed by alpha counting. Gamma counting of samples was carried out on a high purity Germanium (HPGe) Well Detector for ^{210}Pb (46 keV), ^{234}TH (63 keV), ^{226}Ra (351 keV), ^{7}Be (575 keV), and ^{137}Cs (661 keV).

The radionuclide analyses were designed to:

- measure the natural ^{7}Be and ^{234}Th activity concentrations in the surface sediments by gamma counting to determine short-term, near-surface mixing (bioturbation) rates.
- measure the natural $^{210}Pb_{xs}$ (^{210}Pb-^{226}Ra) activity concentrations in sediments from boxcores to determine the steady-state sediment accumulation rates and ^{210}Pb inventories for the assessment of radionuclide and sediment focusing effects.
- measure the bomb fallout nuclide ^{137}Cs and $^{239,240}Pu$ activity concentrations in sediments to determine sediment accumulation rates from the 1963 bomb fallout peak. [It is necessary to determine both nuclides, because ^{137}Cs can show substantial post-depositional mobility in marine sediments.]

For analysis, core material was dried and homogenized. Sediment samples of about 10 g size were used for non-destructive gamma counting in a low-background, high-efficiency high purity Germanium (HPGe) well detector followed by wet chemical extraction procedures and alpha counting for individual radionuclides. Procedures are given in Santschi et al. 1999 and references therein.

For ^{210}Pb determinations, samples of approximately 1 g each were used for by alpha counting for complete digestion and chemical separation. Gamma counted samples provided a less precise ^{210}Pb value used as a cross-check. For ^{226}Ra, ^{234}Th, ^{137}Cs, ^{7}Be, and ^{137}Cs, samples of 10 g each

were analyzed by non-destructive gamma counting. For $^{239,240}Pu$, samples of 10 g each were analyzed by wet chemistry and alpha counting.

7.7 Water Column Profiles

As summarized in Section 6.1.4, most water column properties are measured at sea by standard techniques: autoanalyzer for nutrients, Winkler titration for oxygen, and salinometer for salinity. In addition, total suspended particulate matter is determined by gravimetric analysis of filters. Particulate organic carbon is determined by total combustion of an acidified filter sample followed by detection of CO_2. Phytoplankton pigments are determined by a high performance chromatography (HPLC) method with quantitative UV detection. The pigment analysis quantitatively determines chlorophylls and carotenoids used to assess the relative importance of the various phytoplankton groups. The methods employed duplicate other recent MMS projects in the GoM (Jochens and Nowlin 1998).

Continuous monitoring sensors produce detailed profiles at each of the stations during the hydrocasts (see Section 6.1.4). A "quick look" at the data was performed at-sea to uncover potential problems in the data at the earliest possible opportunity. A quick-look also provides the opportunity to scan for features and to revise sampling plans to more appropriately sample any observed features. Data are further validated on return to shore by checking all of the metadata (e.g., times of sampling, depths, positions, or calibration checks) against the cruise logs and the data file format. For CTD data, pressure versus time is examined to remove ship motions. All out-of-range, unrealistic outliers, gaps and discontinuities in the dataset are manually checked. The continuous data is then discretized at 0.5 m intervals and written into computer files as space delimited columns of plain ASCII text. Characteristic plots are prepared for each station.

The water column chemical measurements were done aboard with discrete water samples collected on the upcast of the rosette sampler. A Guideline Model 8400B salinometer was used for salinity analyses. The microWinkler technique was used for measurement of dissolved oxygen. Nutrients (nitrate, nitrite, ammonia, urea, phosphate, and silicate are analyzed using a Technicon Autoanalyzer and standard colorimetrc techniques. At-sea analysis ensures high precision and accurate measurements as opposed to preservation, storage, and shipment to shore-based laboratories. In addition, water is sampled for various particulate matter parameters. Two-liter water samples were vacuum filtered through pore-weighed filters for total suspended particulate matter (PM) analysis. Another liter of water was filtered through 25-μm precombusted glass fiber filters (GFF) for determination of POC. Another liter of water was filtered through 0.45 micron Millipore filters for analysis of the major phytoplankton pigments. All filters were carefully placed in combusted aluminum foil or plastic bags and properly stored for transport to shore-based laboratories for analysis.

7.8 Archival of Specimens

All the biological material in this study that has been identified to species by taxonomists has been retained for the duration of the project by the taxonomists, at the sorting lab in the Oceanography Department at TAMU, at the sorting lab at the Ft. Crockett facility at the Galveston campus, or at the Deep-Sea Systematics Collections of the Texas Cooperative Wildlife Collections (TCWC) maintained by the Department of Wildlife and Fisheries Sciences (WFSC) in the College of Agriculture and Life Sciences (COALS) at Texas A&M in College Station, Mary Wicksten, Deep-sea Invertebrates Curator (Prof., Dept. of Biology, TAMU). At the end of this project, invertebrate voucher specimens were archived at the U.S. National

Museum of the Smithsonian Institution as directed by MMS. These include the megafauna and macrofauna but not the meiofauna and bacteria. In addition to the voucher specimens given to the Smithsonian, regional working systematic reference collections will also be encouraged to access, curate and catalogue voucher specimens for future research and education when such specimens are available. This will include the TCWC Deep-Sea Invertebrate Collections and The Australian National Museum of Natural History. It does not include the collections of the Institute of Biology of UNAM in Mexico City, but material can be studied there or be requested on loan following international protocols accepted widely within the taxonomic community. All fish and megafauna sampled at S1 through S5 (JSSD1 to JSSD5) within the EEZ of Mexico were deposited in the taxonomic collections of the Institute of Biology at UNAM in Mexico City. Inquiries should be made directly to the Director of that institute.

7.9 Statistical Analyses

The discrete values of abiotic environmental information and the individual faunal groups were treated with a comprehensive set of numerical and statistical analyses. The purpose of these treatments, along with maps of the data, were carried out in order to put the diverse and complex data into forms that were more readily comprehensible. The statistical tests concentrated on accepting or rejecting the eight hypotheses on which the study was based.

7.9.1 Bathymetric Zonation of Recurrent Groups of Related Organisms

- Cluster analysis: Bray-Curtis similarity and group average linkage clustering was used on numbers of individuals of each species at each site to find the natural faunal groupings.
- Non-metric Multidimensional Scaling (MDS): Inter-point distance representing the dissimilarity between samples served as a surrogate for the cluster analysis.
- Analysis of Similarity (ANOSIM): Statistical validity of zones was established by performing ANOSIM tests to the hypothetical zones.
- Mapping the faunal zones (statistically significant recurrent groups) across the entire sampling area illustrate the geographic relationships between the groups of organisms.

7.9.2 Uni-variate Analysis

- Analysis of variance (ANOVA): One-way ANOVA was used to test the null hypothesis that there were no differences between the faunal zones defined by previous cluster analysis.
- The dependent variables that were tested included biotic and abiotic parameters. The factor levels in the tests were the different faunal zones.
- Biotic parameters: density, biomass, species number, Shannon-Weiners index, and expected number of species
- Abiotic parameters: Depth, temperature, POC, % Organic carbon, % Nitrogen, and Grain size
- Multiple Comparisons were performed to determine the effects of each variable on each factor level.

7.9.3 Multivariate Analysis

- Principle Component Analysis (PCA) was used for reduction (consolidation) of environmental variables.
- Analysis of Similarity (ANOSIM): ANOSIM was used again to test effects of environmental data, based on the hypotheses supported by tests of the faunal species-level or density data.
- Testing Matched Similarity Matrices (RELATE): RELATE was used to test the null hypothesis that there were no relationships between biotic information and abiotic patterns.
- Biota and Environment Matching (BIOENV): BIOENV routine was used to match the biotic abundance data to environmental patterns to get a combination of best-matched environmental variables and correlation coefficients.
- Similarity Percentage-species contributions (SIMPER): SIMPER was used to breakdown the average similarity within group and the dissimilarity between groups to determine how individual species contributed to the similarity values.

7.9.4 Depth-Related Changes in Species Composition and Organism Densities

Species Recruitment Curve: The addition and loss of species along the depth gradient was plotted graphically and the rate of change calculated. The species turnover (the relationship between 'new' or added versus 'lost' species down the gradient) was used to determine the boundaries between zones (defined a levels of maximum change or turnover) (adapted from Menzies et al. 1973).

Rate of faunal composition change: The Bray-Curtis similarity was used to compute rates of change (or levels of difference) from reference stations within each zone, versus all sites, to examine the zonal interaction and estimate the rate of faunal composition change along the depth gradient.

Regression analyses: quantitative biotic (organism density and biomass per unit area) and abiotic (concentrations or percents in terms of grams of sediment or volume of sediment pore water) data were used in linear and non-linear regression analyses by transect, grouped by geographic areas (canyon vs non canyon, basin vs non-basin, east vs west, etc.), and composite (all transects together) to determine effects of depth and depth-correlated variables on distributions. Where appropriate, these regressions were conducted as an aid to hypothesis tests and served as one approach to separating out depth-related controls from variables that might be independent of depth. These regressions were conducted on all size groups of organisms, from the bacteria up through the fishes. They were also conducted on a number of the abiotic variables (%OC, %N, grain size parameters, contaminants, radionuclide accumulation and mixing, and oxygen sediment penetration depth).

7.9.5 Statistical Packages Used

- SPSS 12.0 (SPSS Inc., 2003)
- Primer 5.0 (Primer-E, 2000)

8. PROGRAMMATIC RESULTS AND DISCUSSION

Results for each work element are summarized in this Section, including tests of the eight hypotheses. The different components of the abiotic environment are considered first, followed by subsections on each biological size group, starting with the bacteria and ending with the fishes. Each subsection starts with a summary of the basic data which are available in the data base. This is followed in each subsection by hypothesis tests using various one-way and multiple ANOVAs, regression analysis, or, in some cases, non-parametric tests. Principal Components Analysis and Multidimensional Scaling have also been utilized in some instances. In almost all subsections, the variables, whether abiotic or a part of the biotic community, are mapped quantitatively across the entire northern GoM.

Following the basic presentation of the data, the statistical tests and the maps are then used in each subsection for discussions of how and why the geographic or physico-chemical variables control the distributions of the variables in question. These discussions are limited in scope for the most part to each section; cross-discipline synthesis is provided in Section 9.

8.1 Physical Oceanography

8.1.1 Physical Oceanographic Forcings

The physical oceanographic data provide information about the physical environment above each benthic station. The water column influences primary production and carbon flux to the underlying sediments. The major physical forcings responsible for current fields, such as sea surface topography, winds and freshwater, are considered in this section. The features discussed here include energetic, upper-layer current features observed in sea surface height fields – the Loop Current, anticyclonic eddies and cyclones. Focus is on the northern GoM, with no discussion of the Bay of Campeche, which was outside the DGoMB study area. Wind stress is a forcing function for the upper waters. The climatological wind fields for summertime were examined, as well as the energetic wind events during the DGoMB summers. Upper currents, forced mainly by a combination of winds and eddies, were measured during each cruise. Buoyancy forcing from Mississippi River was expected to be relatively minimal because such discharge is concentrated largely over the shelf.

8.1.1.1 Sea Surface Height Fields

Sea surface height (SSH) fields were prepared under the direction of Dr. Robert Leben of the Colorado Center for Astrodynamic Research (CCAR) at the University of Colorado and posted to the publicly available web page, "CCAR Gulf of Mexico Near Real-Time Sea Surface Height Data Viewer," at http://www-ccar.colorado.edu/~realtime/gsfc_gom-real-time_ssh/ Satellite altimeter data from TOPEX/POSEIDON, ERS-2, and other available sources were blended together using a procedure developed at CCAR (Leben et al. 2002; Sturges and Leben 2000; Lillibridge et al. 1997). Daily maps of SSH were created using an objective analysis procedure with spatial and temporal decorrelation scales of approximately 100 km and 12 d, respectively. The CCAR Gulf of Mexico SSH Data Viewer is a tool that allows the user to obtain a custom SSH plot of selected GoM regions and dates. All SSH fields included here were generated by this tool, denoted by the CCAR logo in the lower left corner of each plot. DGoMB tracks then were overlain on the SSH fields. Because of the temporal decorrelation scale, one plot per cruise is adequate to gain an understanding of the forcing by eddies during those cruises. Figures 8-1 through 8.5 present the SSH fields from the mid-date of each cruise, with the ADCP cruise track and CTD and moored ADCP stations shown.

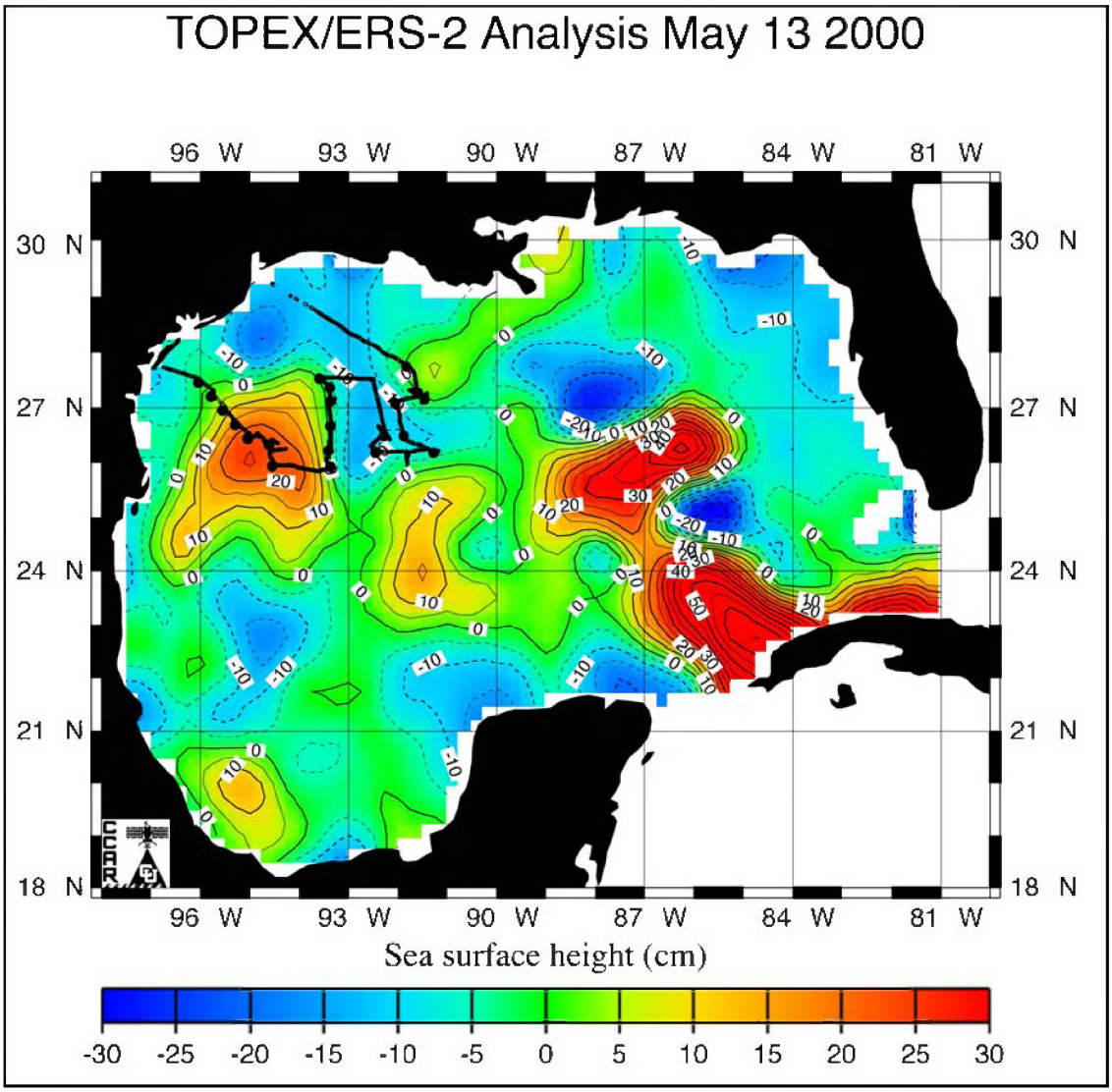

Figure 8-1. Sea surface height field for 13 May 2000 with ADCP cruise track and CTD stations for Leg 1 of DGoMB cruise 1 overlain. [SSH field courtesy of Dr. Robert Leben, CCAR].

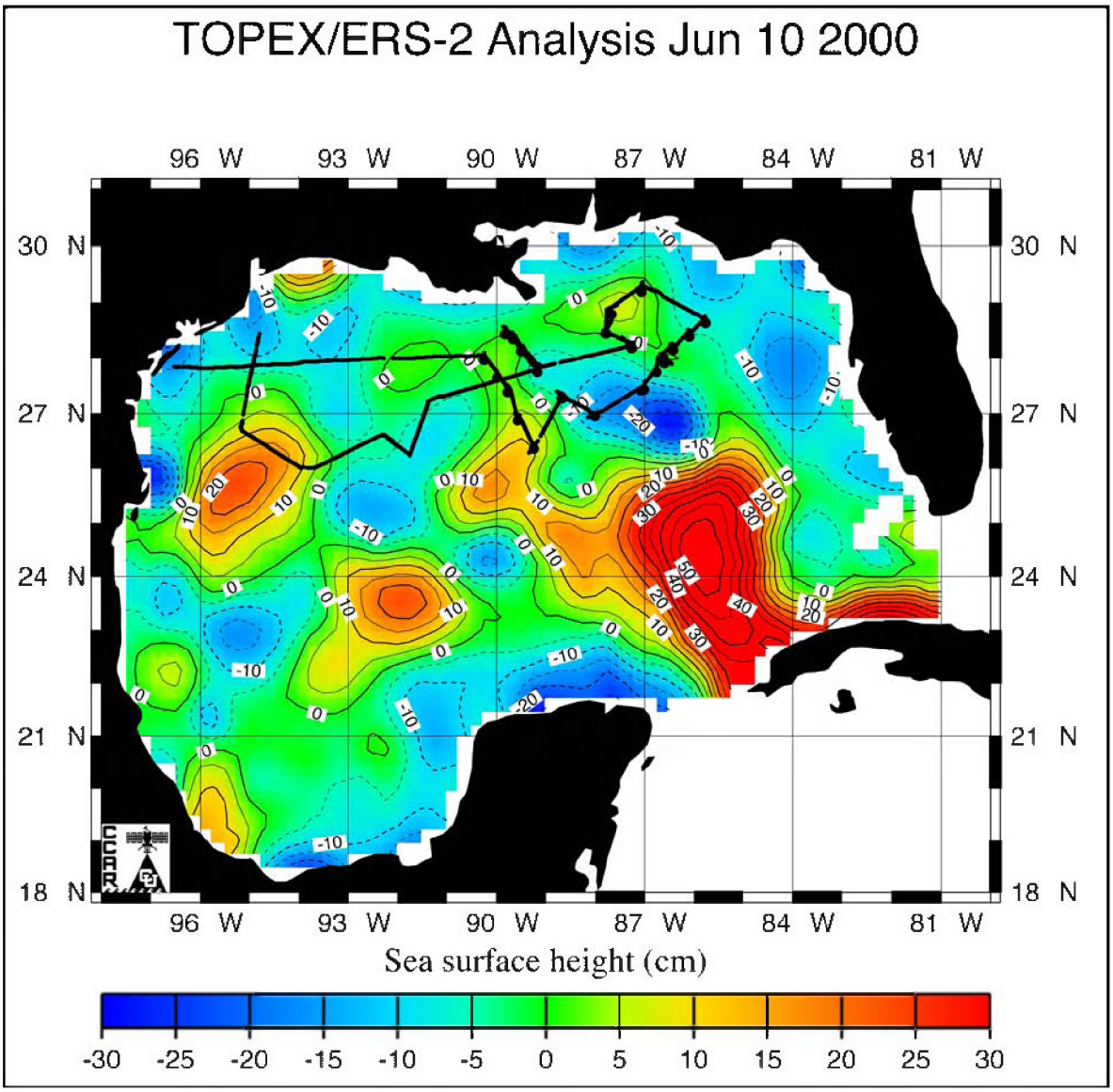

Figure 8-2. Sea surface height field for 10 June 2000 with ADCP cruise track and CTD stations for Leg 2 of DGoMB cruise 1 overlain. [SSH field courtesy of Dr. Robert Leben, CCAR].

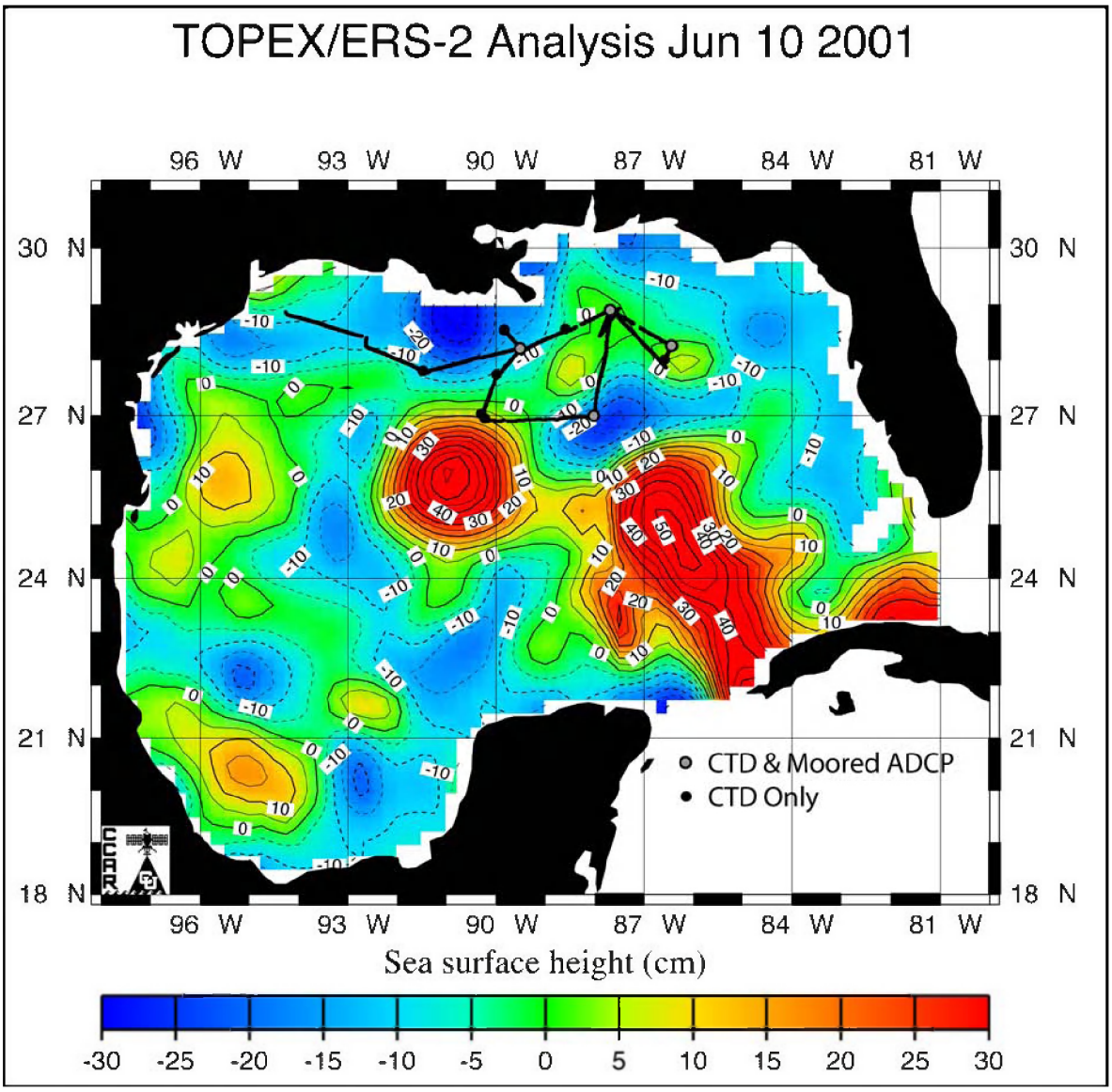

Figure 8-3. Sea surface height field for 10 June 2001 with ADCP cruise track, CTD stations, and moored ADCP locations for the DGoMB cruise 1 overlain. [SSH field courtesy of Dr. Robert Leben, CCAR].

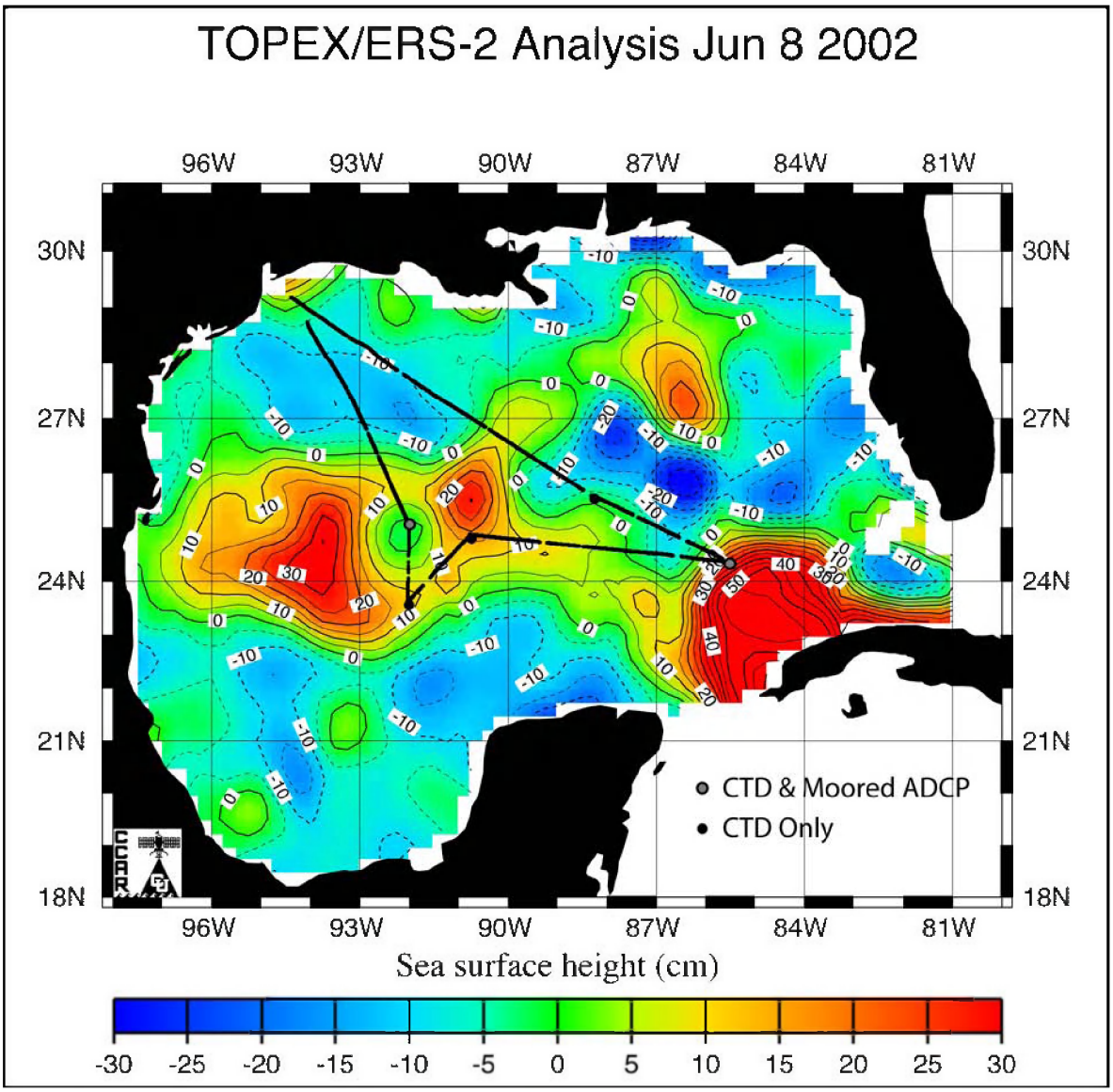

Figure 8-4. Sea surface height field for 8 June 2002 with ADCP cruise track, CTD stations, and moored ADCP locations for DGoMB cruise 1 overlain. [SSH field courtesy of Dr. Robert Leben, CCAR].

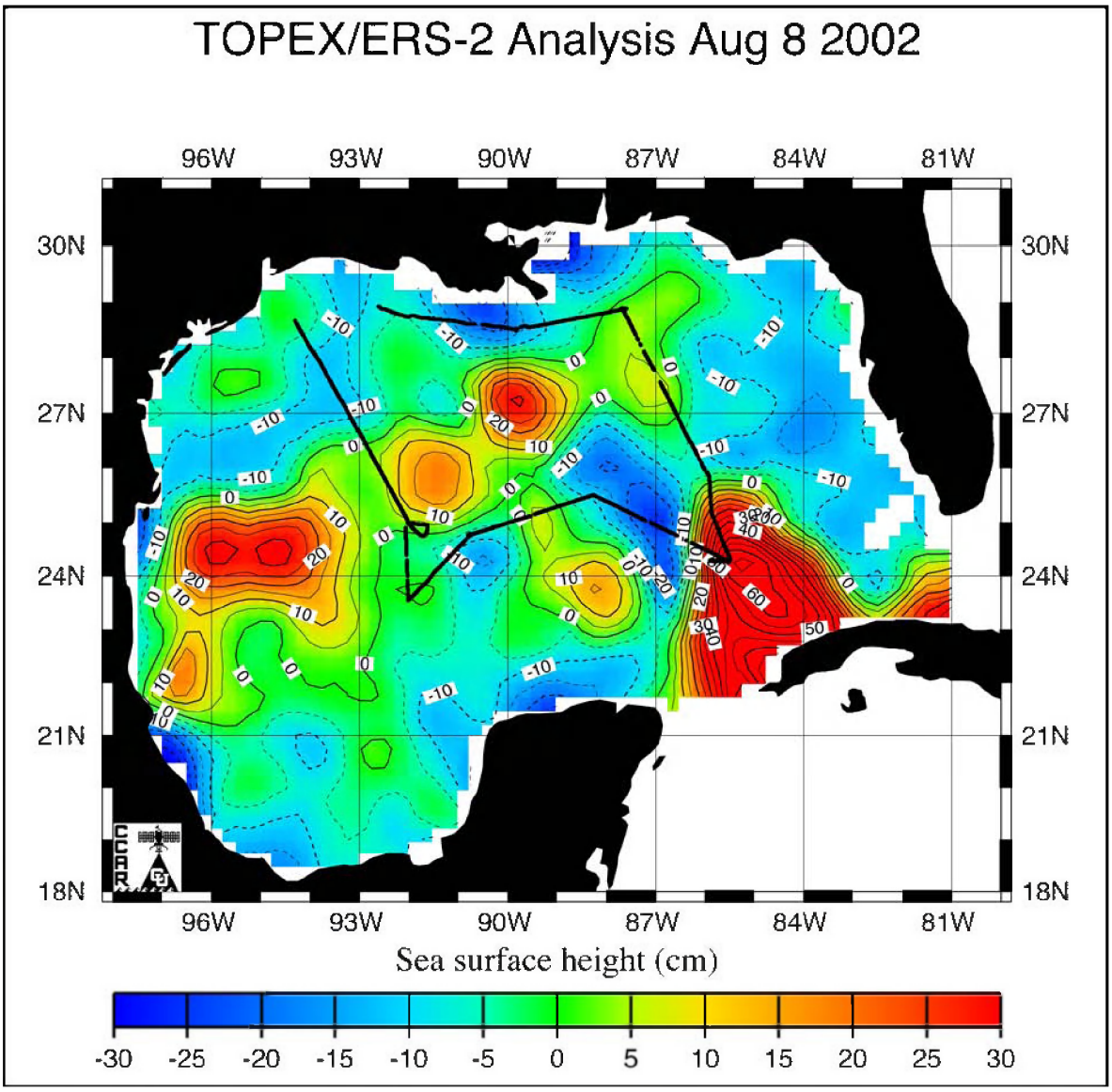

Figure 8-5. Sea surface height field for 8 August 2002 with the ADCP cruise track for DGoMB cruise 1 overlain. [SSH field courtesy of Dr. Robert Leben, CCAR.]

Examination of Figures 8-1 through 8-5 reveals a number of characteristics that were common in SSH fields of the GoM. The Loop Current was a permanent feature present in all years. However, the extent of penetration of its northern boundary into the GoM was variable (e.g., Vukovich 1988). This is seen in the five figures, which show the Loop Current as the region of high SSH (intense red with maximum > 50 cm) that enters the GoM through the Yucatan Channel between Cuba and the Yucatan Peninsula of Mexico and exits through the Florida Straits between Cuba and Florida. The variability of the extension of the Loop Current into the GoM is seen by comparison of the location of the northern boundary. This boundary extended farther into the GoM in summer 2000 and 2001 than in summer 2002. Physical oceanographic DGoMB data in the region of the Loop Current consist mainly of ADCP data collected only during the summer 2002 cruises, so there is little direct data within this feature. Historical data show that nutrients are low in the photic zone (approximately the upper 60-100 m) of the Loop Current (Morrison and Nowlin 1977).

The extension of the Loop Current far into the GoM is a precursor to the separation of a Loop Current Eddy (LCE; e.g., Vukovich 1988; Sturges and Leben 2000). An LCE is an anticyclonic (clockwise) circulation feature, with diameters often of ~200-400 km when newly shed from the Loop Current. After separation, the LCEs moved into the western GoM and decay or split into smaller anticyclones. Like the Loop Current itself, these eddies tend to be low in nutrients in the photic zone (see Section 8.2.2 for additional discussion). Figures 8-1 through 8-5 show anticyclonic eddies (closed contours of SSH highs, note particularly the features in yellow and orange). In May 2000, a decaying anticyclone, which was a combined remnant of LCEs Indigo and Juggernaut, was centered near 26°N 95°W (Figure 8-1). It moved eastward as May and June progressed (Figure 8-2). A smaller anticyclone, which was a remnant of LCE Juggernaut that had split off in April, was centered near 23.5°N 92°W. In June, it intensified, as indicated by the increase in the maximum SSH and the horizontal SSH gradient (compare Figures 8-1 and 8-2). This combination of LCE remnants, splitting of eddies into parts, and intensification of eddies in the presence of other eddies is typical of the dynamics of LCEs in the GoM. The larger anticyclone was sampled with ADCP measurements during the two legs of the 2000 DGoMB cruise and with CTD/nutrient/oxygen data on Leg 1. Another common feature in the GoM are smaller anticyclones in the slope region. For example, there was a small anticyclone in the western DeSoto Canyon region, centered about 29°N 87.5°W (Figure 8-2).

In June 2001, LCE Millennium had nearly separated from the Loop Current (Figure 8-3). It was an intense feature with SSH of ~50 cm centered near 26°N 91°W. The DGoMB cruise did not sample in this feature. However, it did circumnavigate the small slope anticyclone, called Eddy Nansen, off the Mississippi River Delta (centered about 28°N 88.5°W), and ADCP data measured the currents between the LCE Millennium and the small slope eddy (see Section 8.2.2). There was also a warm-core, anticyclonic remnant centered near 26°N 95°W.

During summer 2002, an LCE moved into the western GoM, elongated east-west along about 24°N, and began to separate into two parts (Figures 8-4 and 8-5). The June DGoMB cruise sampled through the region where this eddy was separating, and the August cruise repeated sampling through that area, although the eddy had split in two (Quick Eddy to the west and QE2 to the east).

Of great interest to issues of productivity are the presence of anticyclones near the shelf edge and the presence of cyclonic eddies that often spin up in association with the anticyclones. The cyclonic (counter-clockwise rotating) eddies are seen as the closed circulation regions of low SSH (blues). Note that the region near DeSoto Canyon (e.g., near 29°N 87.5°) had cyclones or

anticyclones near the shelf edge in all of the summers with DGoMB sampling. Similar conditions existed in the northwest GoM, where many of the anticyclonic LCEs decay near the shelf edge and spin up adjacent cyclonic eddies. Examination of a monthly time series of SSH fields throughout the years indicates these small slope eddies (cyclonic or anticyclonic) are typical of the slope area. Time scales of these features can be on the order of months, persistent enough to have biological impacts. Cyclones also spin up in association with the Loop Current or LCEs in deep water (e.g., see the cyclone in Figures 8-4 and 8-5 centered near 25°N 87°W northwest of and adjacent to the Loop Current). Off DeSoto Canyon, these features can move low salinity, biologically productive Mississippi river discharge off the shelf into deeper water (Figure 8-6), with consequent influence on the productivity of the deep water benthos (Jochens et al. 2002). These features also can bring nutrient-rich deep water up into the photic zone when anticyclones interact with the topography or cyclones. The centers of cyclones are also regions of upwelling. This can increase productivity in the surface waters, with, it is presumed, consequent increase in delivery of organic matter to the benthos.

8.1.2 Gulf of Mexico Winds During Summer

Wind stress produces currents in the upper waters of the ocean that transport nutrients, sediments, phytoplankton, and other biologically important matter from regions of generation or discharge, as in the case of river-borne material, to other regions in the GoM. Long-term patterns generated by wind stress include an anticyclonic circulation in the western GoM with a westward intensified boundary current (Sturges 1993) and a persistent cyclonic circulation in the Bay of Campeche (Vázquez de al Cerda et al. 2005; Vázquez de la Cerda 1993). The DGoMB study was not designed to identify the biological effects of these long-term wind-induced circulation patterns.

To consider the possible effects of wind-forcing during the DGoMB cruises, the climatological wind fields were examined to determine whether there was a dominant pattern in summer. Then the details of the May through August winds for the years 2000 through 2002 were examined.

Jochens et al. (2002) examined the climatological winds using the COADSPACS Enhanced 1960-1997 data (Figure 8-7). The Comprehensive Ocean-Atmosphere Data Set (COADS) is an extensive collection of monthly summaries of surface marine data on a 1-degree latitude by 1-degree longitude grid. COADSPACS Enhanced data are provided by the NOAA-CIRES Climate Diagnostics Center, Boulder, Colorado, from their Web site at http://www.cdc.noaa.gov (see Woodruff et al. 1987). To determine the monthly mean wind climatology for the GoM, the average mean wind velocity components were computed for each month based on the total values available at each grid location. The mean vector was then assembled from the mean u and v components. Winds at grid locations with less than 6 years of data are not shown. Also shown are ellipses of the principal axes of variance of monthly means for that month.

Figure 8-8 shows the time periods when tropical cyclones (hurricanes, tropical storms, and tropical depressions) were located in the GoM. There were no hurricanes during May through August of 2000-2002. Of the five cyclones shown in Figure 8-8, Tropical Storm Barry in 2001 passed the closest to the two NDBC buoys. It formed near 26.3°N 84.8°W, moved westward to 26.7°N 87.9°W, and then moved northward where it made landfall at the western end of the Florida Panhandle. The Tropical Storms (TS) and Tropical Depressions (TD) during these

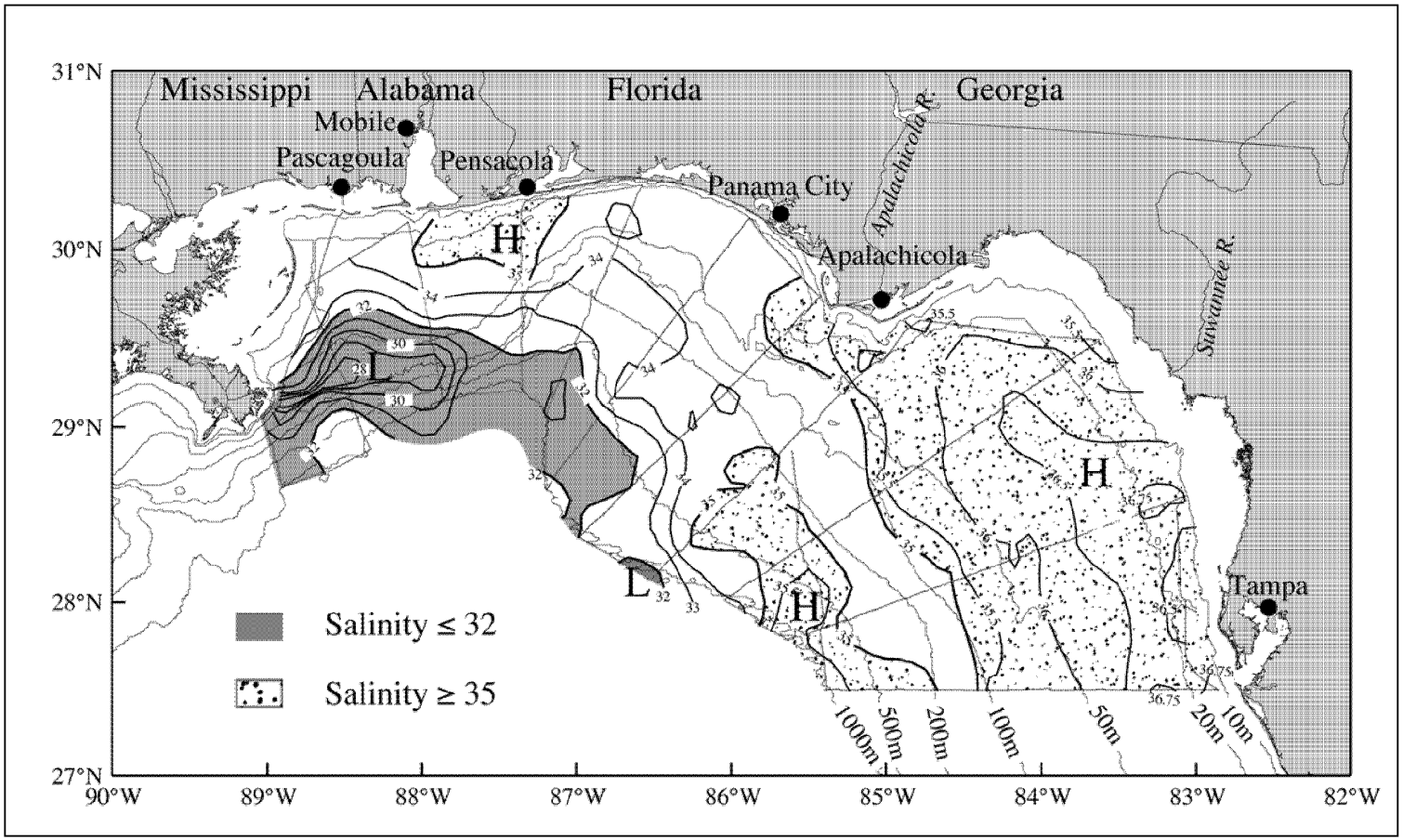

Figure 8-6. Salinity at approximately 3.5-m depth from thermosalinograph observations on NEGoM cruise N9 in July-August 2000. Dots show sample locations and give the track lines. Note that salinity *increases* from the shelf edge toward the coast, resulting from the movement of Mississippi River water off shelf by a slope eddy.

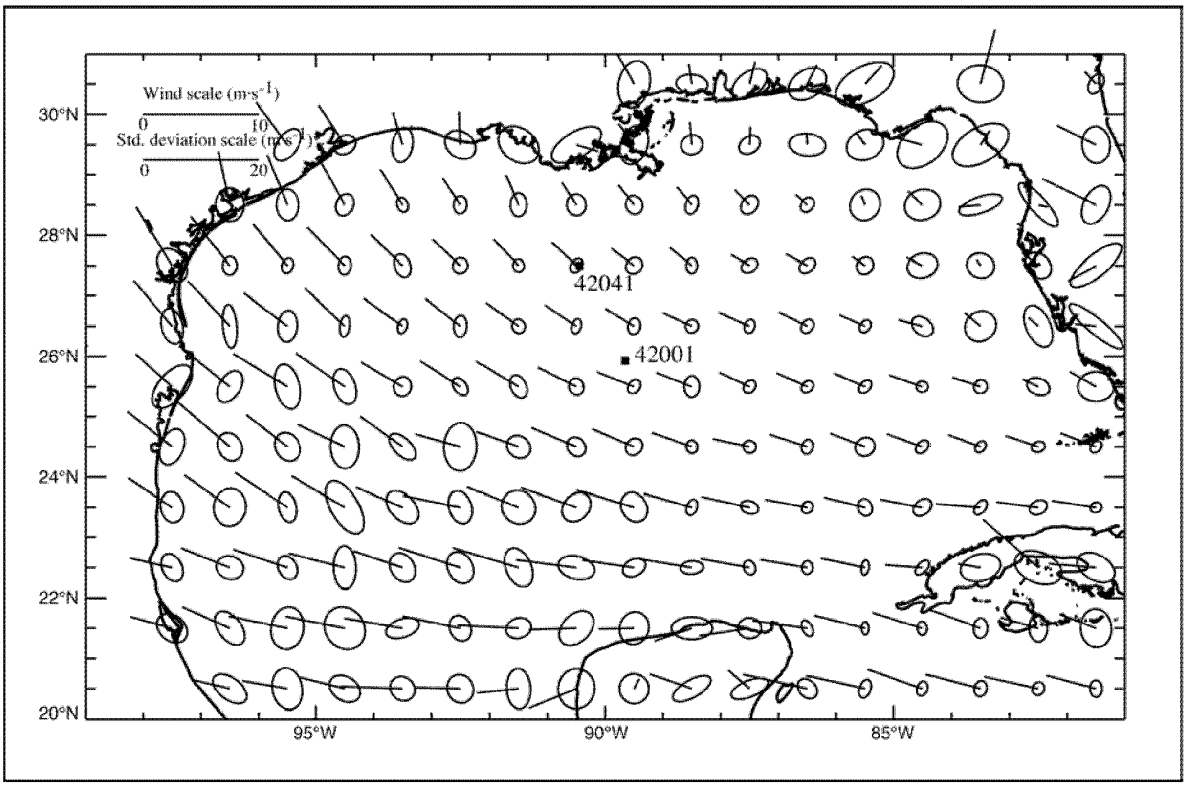

Figure 8-7. COADS enhanced mean wind field and principal component ellipses for June. Data were averaged over the period 1960-1997. NDBC meteorological buoys 42041 and 42001 are denoted by the squares.

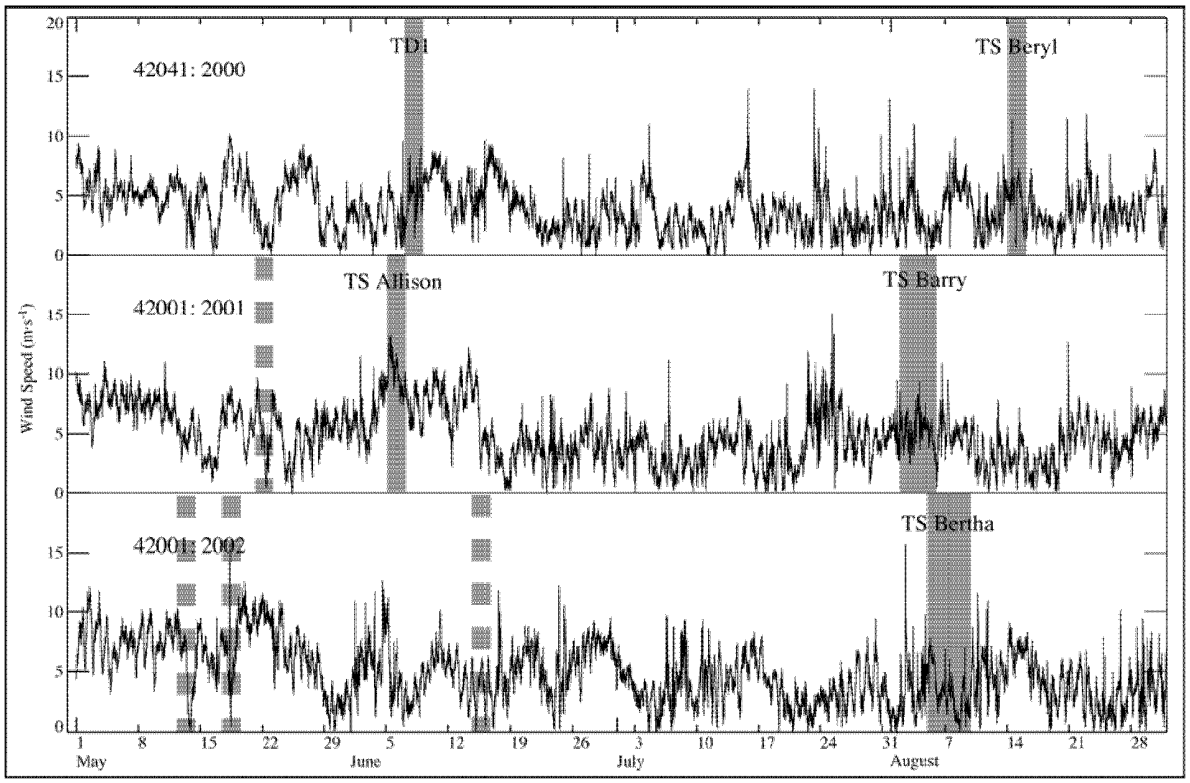

Figure 8-8. Wind speed from National Data Buoy Center meteorological buoys 42041 (2000) and 42001 (2001 and 2002) for May through August during the DGoMB field program. Periods with tropical cyclones in the Gulf are shown by vertical lines (TD is Tropical Depression; TS is Tropical Storm).

summers had no observable effect on the winds at the buoys, likely because neither buoy was in the direct path of the cyclones. This is consistent with the findings of Nowlin et al. (2001) who compared deepwater current meter data with the tracks of tropical cyclones for the period 1977-2000. They also found the effects of tropical cyclones on oceanic currents were intense but localized and short-lived with diminishing effects observable about 7-10 days after passage (see also Nowlin et al. 2000 for discussion of literature).

The NCDC *Daily Weather Maps* for May through August in 2000 and 2001 and the 3-hourly Surface Analysis of the Hurricane Prediction Center for May through August 2002 were examined for the occurrence of the passage of cold fronts through the GoM. In all three years, there were weak fronts that skirted the northern GoM coastline while moving eastward, with occasional extension into the northeast GoM. Such events occurred mainly in May and June. There were no frontal passages crossing the deepwater GoM during these months in 2000. In 2001, one cold front passed through the GoM on 22-23 May. The time of this event is indicated by the dashed vertical line in Figure 8-8. The front passed by the buoy locations, but seems to have had no pronounced effect on the winds or, by inference, on the oceanic currents and transport of materials thereby. In 2002, there were three fronts that passed near the buoys: two in May (13-15 and 18-20) and one in June (15-16) as shown on Figure 8-8. The paucity of frontal passages in summertime has been noted by DiMego et al. (1976), Henry (1979), Nowlin et al. (1998), and Jochens et al. (2002). The strongest frontal passages are those that evolve into extratropical cyclones during the non-summer months, particularly in winter. Nowlin et al.

(2001) compared the deepwater current meter data with the occurrence of extratropical cyclones and found that most of these cyclones had no effect on the currents. In summary, the frontal passages and extratropical cyclones had little or no effect on deepwater currents and hence on transport of materials, and when there was any effect, it was localized in time and space.

8.1.3 Influence of River Discharge

The Mississippi River discharges on the order of 1,000 million $m^3 \cdot d^{-1}$. The 72-year mean daily discharge from the Mississippi River, measured at Tarbert Landing, Louisiana, is shown in Figure 8-9 (repeated in each of the three years 2000-2002). The mean daily discharge peaks in May and is at a minimum in October. The standard deviation, also shown, is largest in spring and smallest in fall. The major influence of this discharge is over the shelves adjacent to the points of discharge. However, eddy processes can move riverine water off-shelf into deep water. There may be areas, such as the slope east of the Mississippi River Delta and associated with the western DeSoto Canyon, where such movement is frequent enough to have potential influence on the near-surface biology with possible consequent impacts to the benthic biology (e.g., see discussion of high faunal densities near DeSoto Canyon, 8.5). DGoMB physical oceanographic sampling was insufficient to determine how extensive and consistent this might be from year to year.

The daily discharges for each of the three years of DGoMB field work also are shown in Figure 8-9. During 2000, the spring discharge was below average. For the DGoMB cruise in May-June 2000, the two stations off the Mississippi River Delta in DeSoto Canyon (S35 and S36) have near-surface salinities that are slightly lower (< 34) than adjacent stations (>35), suggesting some limited mixing of Mississippi River water with oceanic waters. Note the peak discharge in the July time period. This discharge occurred several weeks prior to the cruise for which the near-surface salinity, with its clear indication of mixing of Mississippi River water with oceanic water, is shown in Figure 8-9. The peak discharge in spring 2001 occurred approximately two months prior to the DGoMB cruise; the stations nearest the Mississippi River (S36 and HiPro) show no influence from the river water. During spring 2002, the daily river discharge was above average, with two peaks exceeding one standard deviation above the mean. During the June-July 2002 period immediately after the June DGoMB cruise, low salinity water over the slope west of DeSoto Canyon was observed (Jochens, personal communication), indicating mixing of riverine with oceanic waters. The DGoMB cruise did not sample in this region. The August 2002 DGoMB work did not collect CTD data. However, a cruise for another program in August-September 2002 that started shortly after the DGoMB cruise sampled near surface salinity along the upper slope around the Mississippi River Delta and DeSoto Canyon. Near-surface salinities along the 1,000-m isobath to the southeast and southwest of the Mississippi River Delta on that cruise were low, with some values < 30, but the values along the slope of De Soto Canyon were not unusually low (Jochens and Biggs 2003). The evidence suggests that riverine influences extend to the upper slope between approximately –89.5°W and –87°W frequently enough to possibly enhance the productivity in this area. The DGoMB cruises, however, were not designed to test this or to determine whether there might be other areas susceptible to such export of fresh water from the shelf.

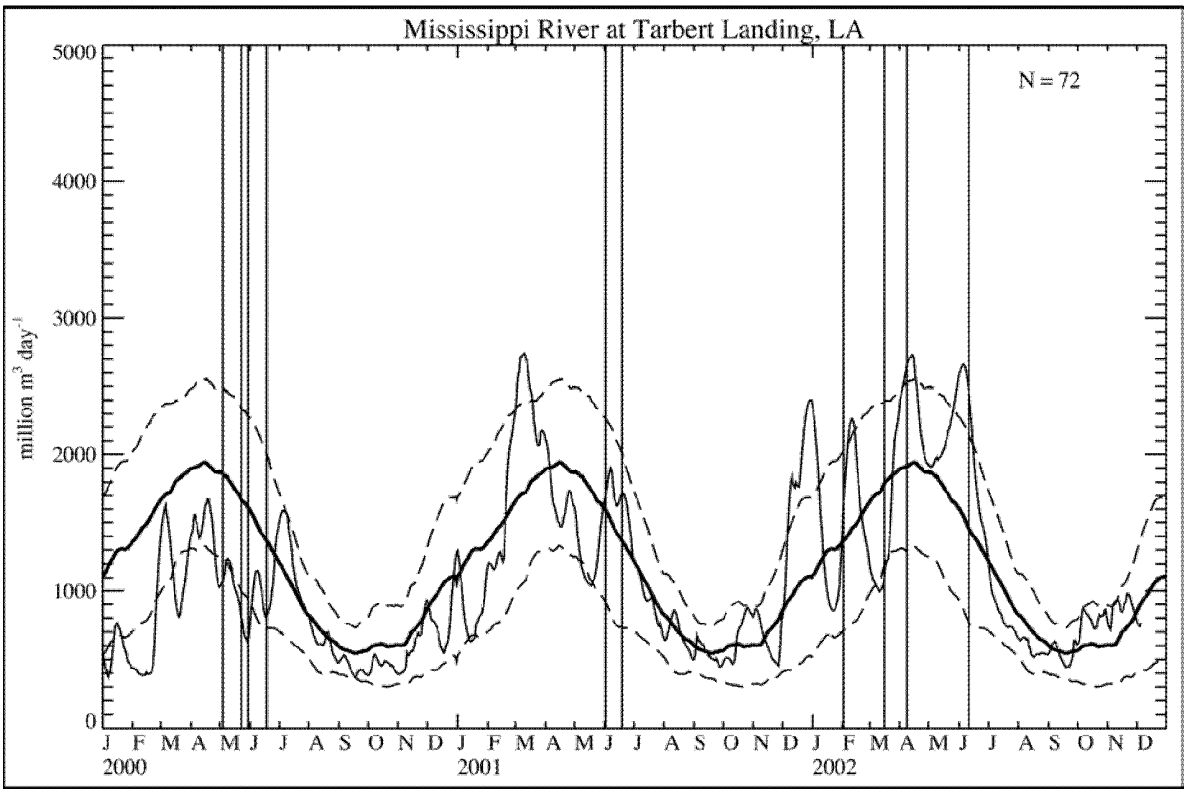

Figure 8-9. Daily discharge for 2000-2002 from the Mississippi River, measured at the Tarbert Landing, Louisiana, gauge. The daily discharges for 2000 through 2002 are shown as the thin line. The mean daily discharge (thick line) for a 72-year record is repeated in each of the three years. The dashed lines show ± one standard deviation from the mean. DGoMB cruises occurred between pairs of vertical lines.

8.2 Physical Oceanography

8.2.1 Water Property Patterns

Temperature and salinity measurements were made on the DGoMB cruises in May/June 2000, June 2001, and June 2002. Measurements of nitrate, phosphate, silicate, and dissolved oxygen concentrations were made on the cruises in 2000 and 2001. The vertical patterns of these properties were analyzed. The station spacing did not allow detailed or meaningful examination of horizontal patterns. The vertical patterns were related to features in the circulation field shown by the sea surface height fields (see Section 8.1.1). The measurements were compared to historical data sets. This section describes the results of these analyses.

Patterns observed in water properties during DGoMB cruises: Vertical profiles in depth and density for salinity and potential temperature are shown for seven DGoMB CTD stations (Figures 8-10 and 8-11). Station locations are shown in Figure 8-12. These stations were selected to represent the variety of differing conditions in the GoM. They show the typical range of values that were measured at the DGoMB CTD stations. The full range from all the stations is slightly broader in the upper 500 m than shown by the selected stations; profiles below 500 m are within the bounds shown in the figures. The selected stations are: S4 (blue) located in the Loop

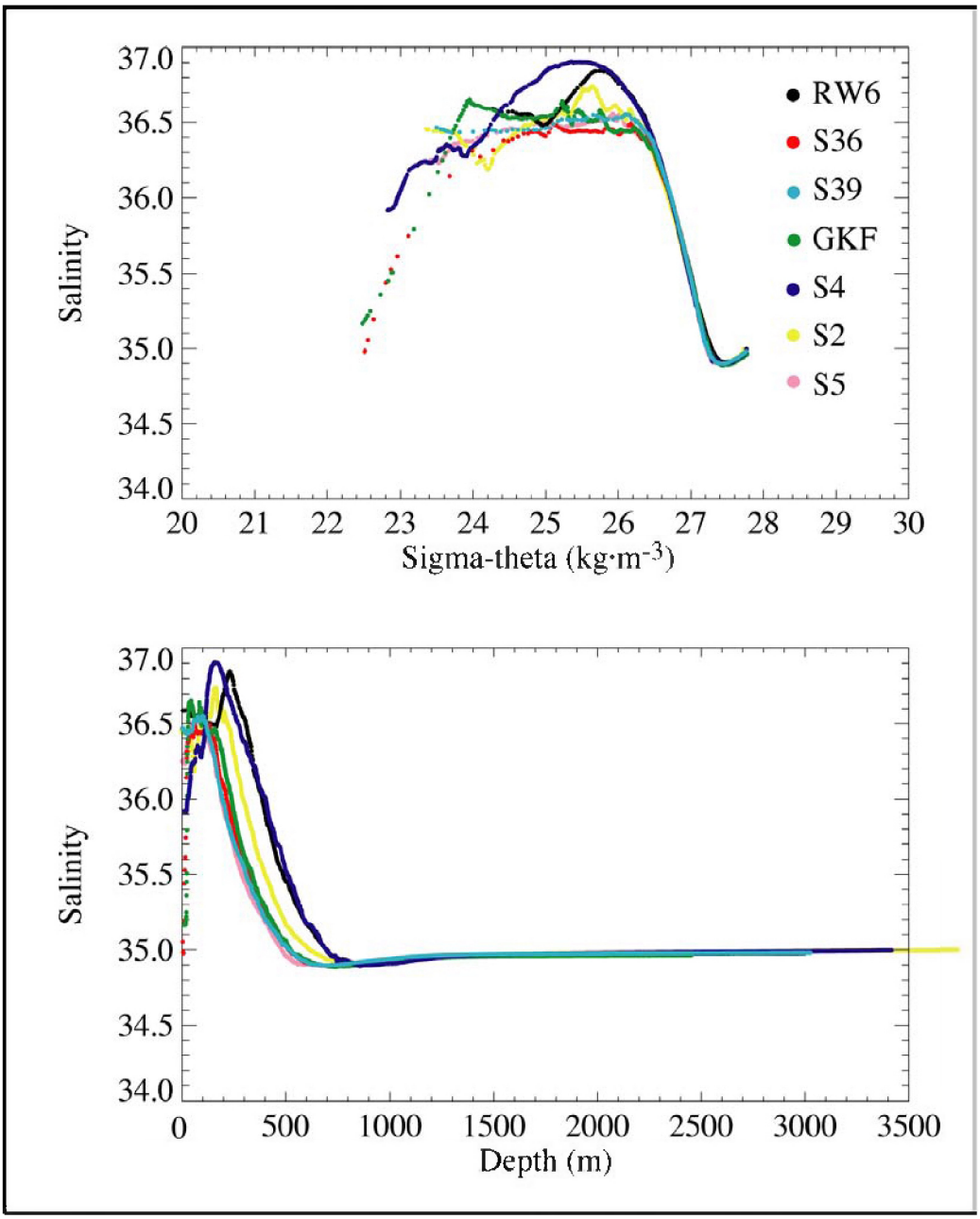

Figure 8-10. Selected station data showing salinity versus density (top) and depth (bottom). Shown are stations RW6 (2000) in a Loop Current Eddy in the western GoM, S39 (2000) in a cyclonic eddy in the northeastern GoM, GK-Furrows (2001) at the edge of a Loop Current Eddy in the north-central GoM, S4 in the Loop Current, S2 at the edge of a Loop Current Eddy in the south central GoM, and S5 at the edge of a cyclone in the eastern GoM. Station locations are shown in Figure 8-12.

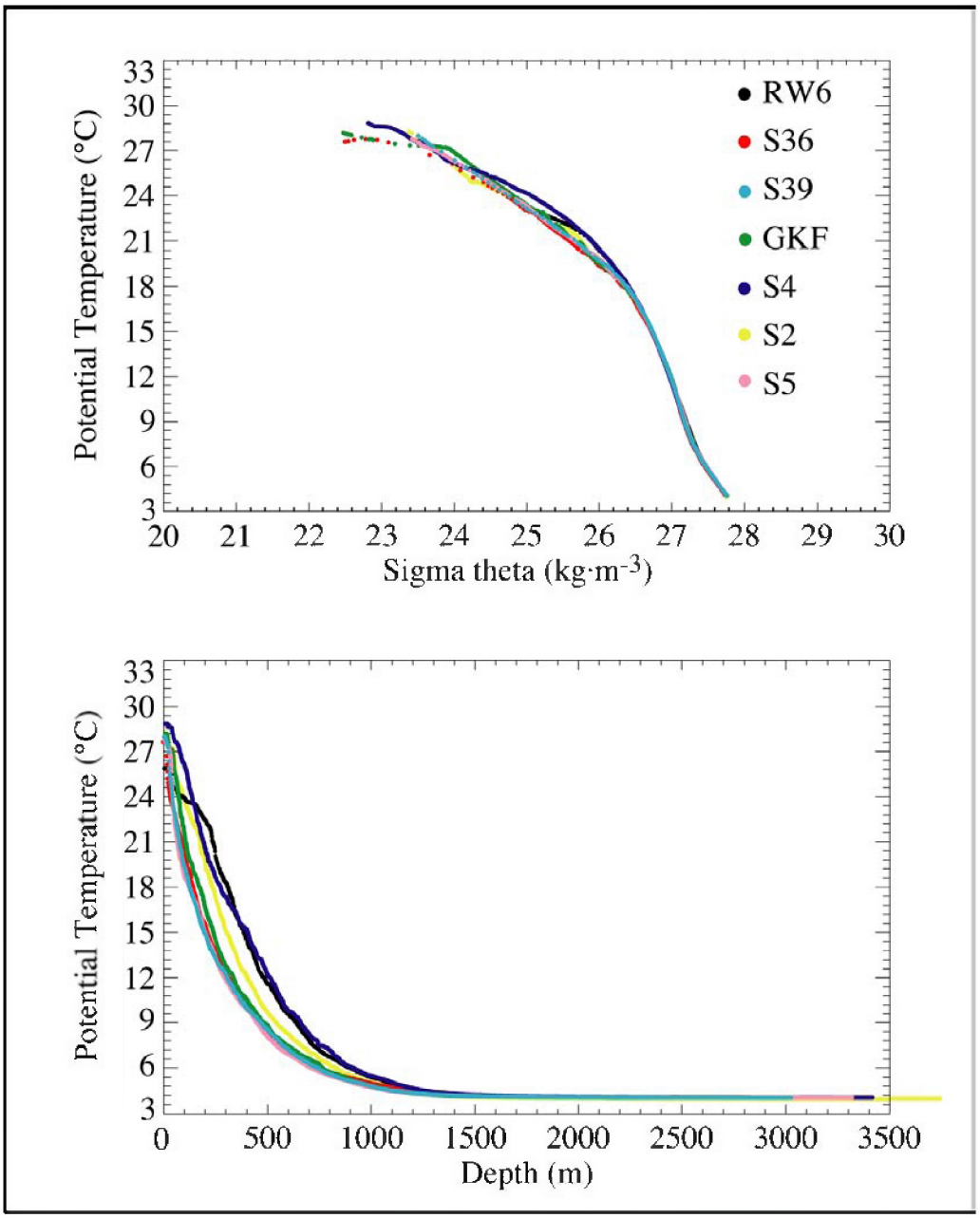

Figure 8-11. Selected station data showing potential temperature versus density (top) and depth (bottom). Shown are stations RW6 (2000) in a Loop Current Eddy in the western GoM, S36 (2000) in a slope anticyclonic eddy in the northeastern GoM, S39 (2000) in a cyclonic eddy in the eastern GoM, GK-Furrows (2001) at the edge of a Loop Current Eddy in the north central GoM, S4 in the Loop Current, S2 at the edge of a Loop Current Eddy in the south central GoM, and S5 at the edge of a cyclone in the eastern GoM. Station locations are shown in Figure 8-12.

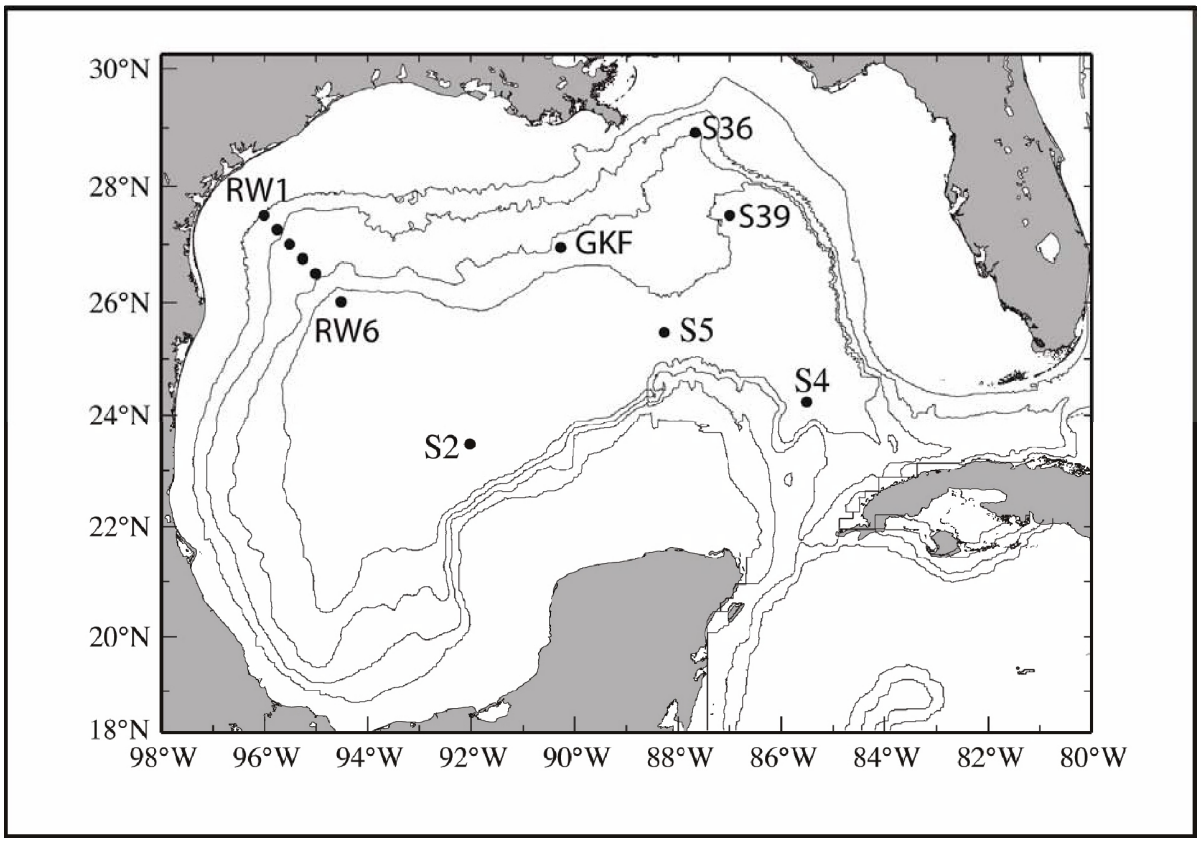

Figure 8-12. Locations of selected CTD/bottle stations on the DGoMB cruises in summers 2000-2002. Bathymetric contours shown are 200, 1,000, 2,000, and 3,000 m.

Current in the southeastern GoM (see Figure 8-4), RW6 (black) located in a Loop Current Eddy (LCE) in the northwest GoM (see Figure 8-1), S36 (red) located in a slope anticyclonic eddy in the northeastern GoM (Figure 8-2), S39 (light blue) located in a cyclonic eddy in the northeastern GoM (Figure 8-2), GK-Furrows (green) located at the edge of an LCE in the north central GoM (Figure 8-3), S2 (yellow) located in a splitting LCE in the deep basin of the central GoM (Figure 8-4), and S5 (pink) located at the edge of a cyclonic eddy in the deep basin of the eastern GoM (Figure 8-4).

The Loop Current is the source water for the deep basin of the GoM. One CTD station, S4 in June 2002, was taken in the Loop Current at approximately 24.25°N 85.5°W (Figure 8-4). The vertical profile of salinity at this station is characterized by a salinity maximum of > 36.6 at a depth of approximately 150 m and a density surface of 25.4 $kg \cdot m^{-3}$ σ_θ (Figure 8-10, blue). The waters with this property are part of the Subtropical Underwater water mass that enters the GoM with the Loop Current. The profile of potential temperature for this station (Figure 8-11, blue) is characterized by warmer water deeper in the water column compared to other stations in the GoM. This is a typical characteristic of anticyclonically circulating features including the Loop Current.

The general salinity pattern for all stations consists of four major characteristics. Most notable is lack of horizontal variability in salinity below depths of approximately 1,000 m. This is present in all station CTD data. Second is a salinity maximum. This maximum is found to be reduced with increasing distance from the source waters. However, this is not only a function of

distance from the Loop Current. For example, station S36 (2000) was located in the northeastern GoM in DeSoto Canyon near 29°N 87.5°W (Figure 8-2). Thus, it was geographically closer to the Loop Current than was station RW6 (2000), which was located in the western GoM near 26°N 95°W (Figure 8-1). Yet, station S36 has a very reduced salinity maximum (Figure 8-2, red), whereas station RW6 has a predominant salinity maximum pattern comparable to that of the Loop Current station S4 (Figure 8-10, black compared to blue). Station S36 sampled in a small slope anticyclone, where waters were subject to mixing due to eddy and bathymetric effects and to entraining of shelf waters, all contributing to the consequence erosion of the salinity maximum. Station RW6 sampled near the middle of an anticyclonic LCE, which had carried Loop Current water into the western GoM. Evidence of erosion of the salinity maximum is present in RW6 as the sharp reduction in salinity at σ_θ of less than 25.6 $kg \cdot m^{-3}$.

The third characteristic of the salinity profiles is the salinity minimum at about 600-800 m or σ_θ of 27.3-27.5 $kg \cdot m^{-3}$. This is associated with the Antarctic Intermediate Water that is brought into the GoM by the Loop Current. The depth at which this minimum occurs is variable. It appears to be related to the type of eddy feature the station sampled or the proximity to the bathymetric effect of the slope. For example, the depths of the minima for S4 in the Loop Current and RW6 in a LCE in the western GoM are comparable, whereas those for S36 in a weak anticyclone over the northeastern GoM slope and S39 in a cyclone are approximately 200 m higher in the water column. Distance westward may also be a factor as suggested by comparison of stations S2 in the deep western GoM basin and S4 in the eastern GoM. Both were relatively distant from bathymetry and both were in anticyclonic features. Yet, the minima at S2 is located about 100 m higher than that at S4.

The fourth characteristic is the variability in the near-surface salinity values. Considered are the salinities in the upper 50-100 m. These upper waters have lower salinity concentrations than at depth. Part of this, of course, is related to the presence of the salinity maximum. However, part of the variability is due to the mixing of low salinity water from the Mississippi River with the near-surface oceanic waters. Of the selected stations shown in Figure 8-10, the lowest near-surface salinity values occur at S36, which is located southeast of the Mississippi River. Other stations west as well as east of the Mississippi River mouth exhibit low salinity. In the cases examined, there were circulation features adjacent to the Mississippi River mouth that likely transported shelf water, which had been diluted by mixing with river water, to the slope regions adjacent to the river. This situation has been observed in other programs (Belabbassi et al. 2004).

In addition to the lack of horizontal variability in potential temperature below depths of approximately 1,000 m, the temperature profiles in Figure 8-11 show generally cooler water from the surface through the main thermocline to about 1,000 m. In the main thermocline, the depth at which a particular potential temperature value occurs is related to the circulation feature present at the time of sampling. The anticyclonic eddies tend to depress isotherms, whereas isotherms in cyclones tend to dome upward. For example, station RW6 is in a strong LCE so its isotherms are lower in the water column than those of the other stations except S4, which is in the Loop Current. In contrast, station S39 is located in a cyclone and its isotherms are higher in the water column.

Vertical sections of properties were examined where the station locations allowed. Spacing of stations was large, being generally 35 km or greater. This spacing allows consideration of large-scale features only. In general, the few transects showed similar results. Transects taken across strong anticyclonic eddies showed the characteristic pattern of depressed isolines near the eddy center. Examples are discussed below. There were no transects with reasonably spaced

stations taken across strong cyclonic eddies. However, the transects that crossed weak parts of cyclones showed a tendency for doming isolines. No examples are presented here.

The transect selected for discussion here was the western-most line on the first DGoMB cruise in May-June 2000. It extended from the shelf edge at about 27.5°N 96°W to approximately the middle of an anticyclonic LCE at about 26°N 94.5°W (see Figure 8-12 for locations). Figure 8-13 shows the contours of density anomaly (σ_θ) along this transect. The station taken at the shelf edge was RW1 at the left side of the figure, while the station taken near the middle of the LCE was RW6 at the right side. With the exception of near-surface waters, isopycnals show the stability of the water column by their monotonic increase with depth. The isopycnals in the upper 500 m or so tend to slope downward from the shelf edge to station RW6. The isopycnals below about 500 m, however, tend to be more bowl-shaped, with the center of the bowl being near station RW5. This suggests that the LCE was tilted in the water column, which is not unusual as the LCE is approaching the shelf edge and so is interacting with bottom topography. The vertical pattern of potential temperature (not shown) is similar, although the temperature monotonically decreases with depth.

Salinity contours, shown in Figure 8-14, follow a similar downward trend in the upper 500 m from the shelf edge station and bowl-shaped pattern below as seen in density. There is a salinity maximum between 100-200 m depth, which is near the 25.4 $kg \cdot m^{-3}$ σ_θ line (shown as a dashed line), that corresponds to the signature of the Subtropical Underwater mass that the LCE has transported into the western GoM from the Loop Current. The Antarctic Intermediate Water mass, with its salinity minimum, is evident in water depths of about 900 m and σ_θ of 27.5 $kg \cdot m^{-3}$ (also shown as a dashed line). This water mass also was transported to the western GoM by the LCE.

Vertical contours of nitrate and dissolved oxygen along the transect are shown in Figures 8-15 and 8-16, respectively. Both exhibit the downward trend in isolines indicative of an anticyclonic circulation feature. The nitrate concentrations are below detection limits in the upper 100-150 m. The phosphate and silicate (not shown) are also very low, being < 0.5 µM and < 1 µM, respectively, in the upper water column. This reflects the consumption of the nutrients by phytoplankton in the presence of sunlight. The complete utilization of nitrate, with some phosphate and silicate still being detectable, indicates the biological system is nitrate limited. All three nutrients increase with depth, reflecting nutrient regeneration as detritus falls through the water column transport of nutrient-rich deep waters into the GoM. The Antarctic Intermediate Water mass is evident in the nitrate maximum at about 900 m and σ_θ of 27.5 $kg \cdot m^{-3}$ (shown as a dashed line). The oxygen section shows the presence of the Tropical Atlantic Central Water, which is characterized by the oxygen minimum located at about 600 m depth and σ_θ of 27.15 $kg \cdot m^{-3}$ (shown as a dashed line). The effects of atmospheric exchanges with the surface are seen in the high values of oxygen (> 4.5 $mL \cdot L^{-1}$) in the upper 100 m. The deep waters below about 1,000 m also are relatively high in oxygen; the sources of this oxygen are the highly oxygenated deep water masses entering into the GoM through the Yucatan Channel.

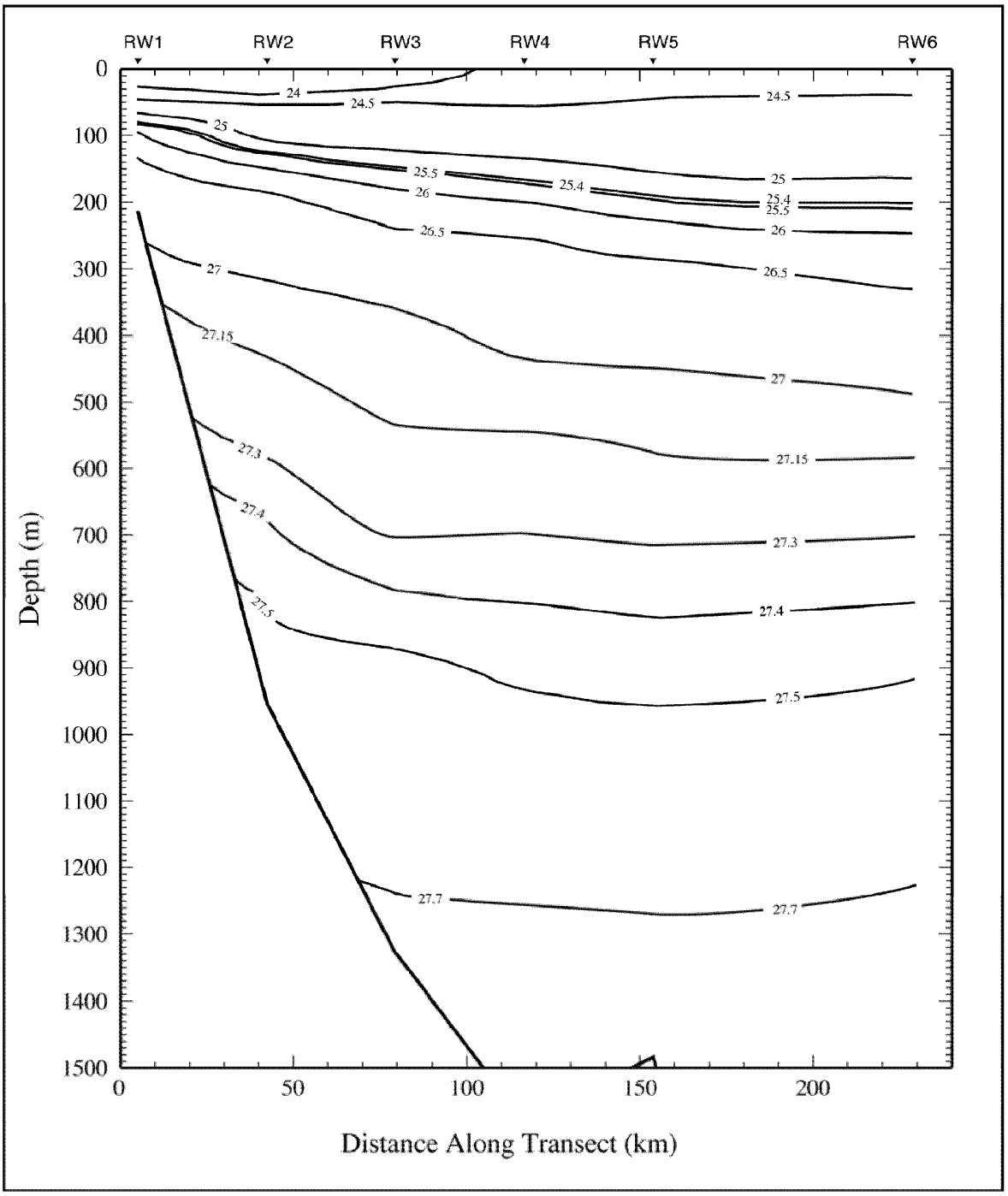

Figure 8-13. Density anomaly (σ_θ in kg·m^{-3}) on western-most transect of DGoMB cruise 1, 4 May-17 June 2000. CTD data were spaced every 0.5 m.

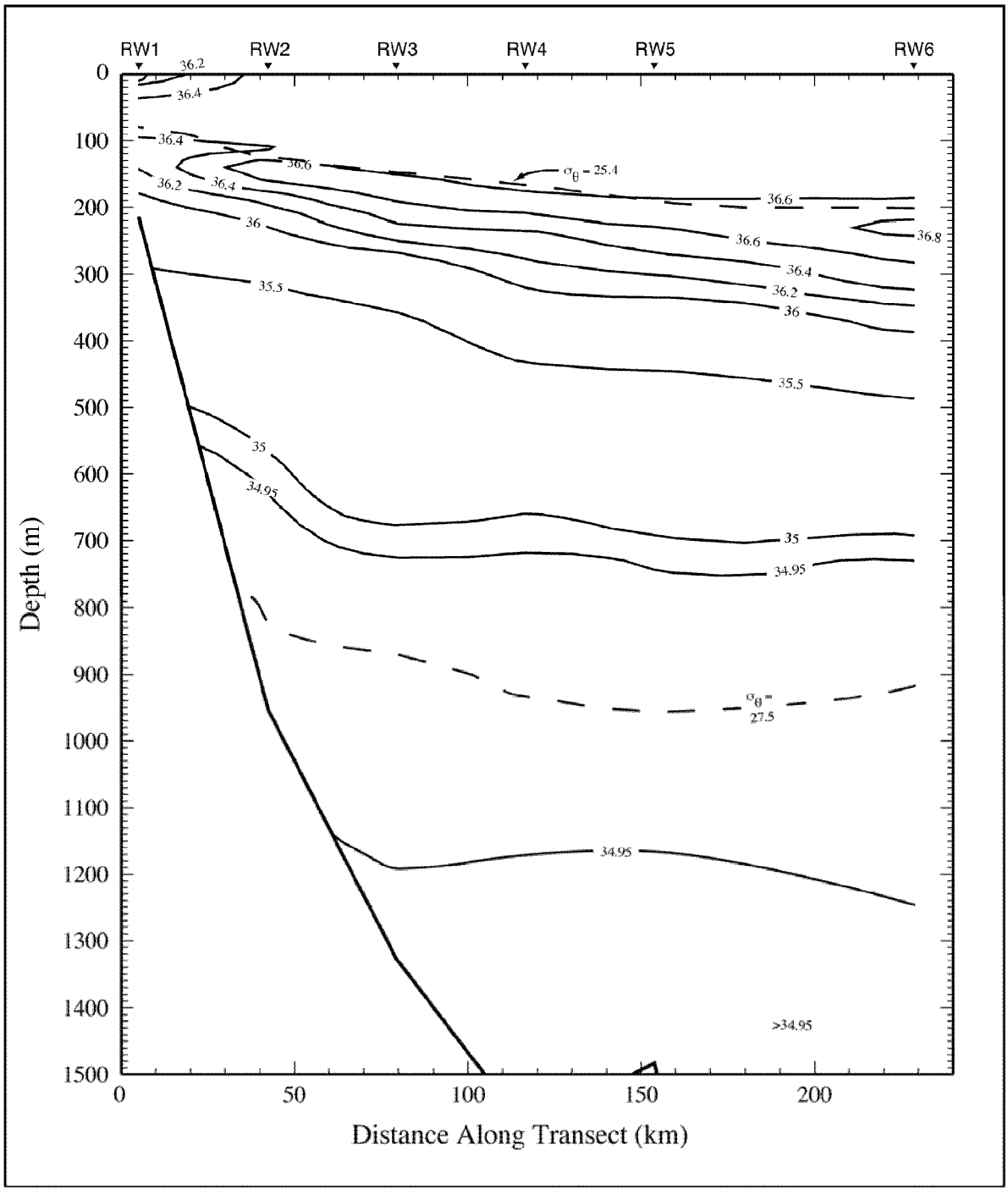

Figure 8-14. Salinity from the CTD on western-most transect of DGoMB cruise 1, 4 May-17 June 2000. Dashed lines show sigma-theta density surfaces of the Subtropical Underwater and the Antarctic Intermediate Water. Salinity data were spaced every 0.5 m.

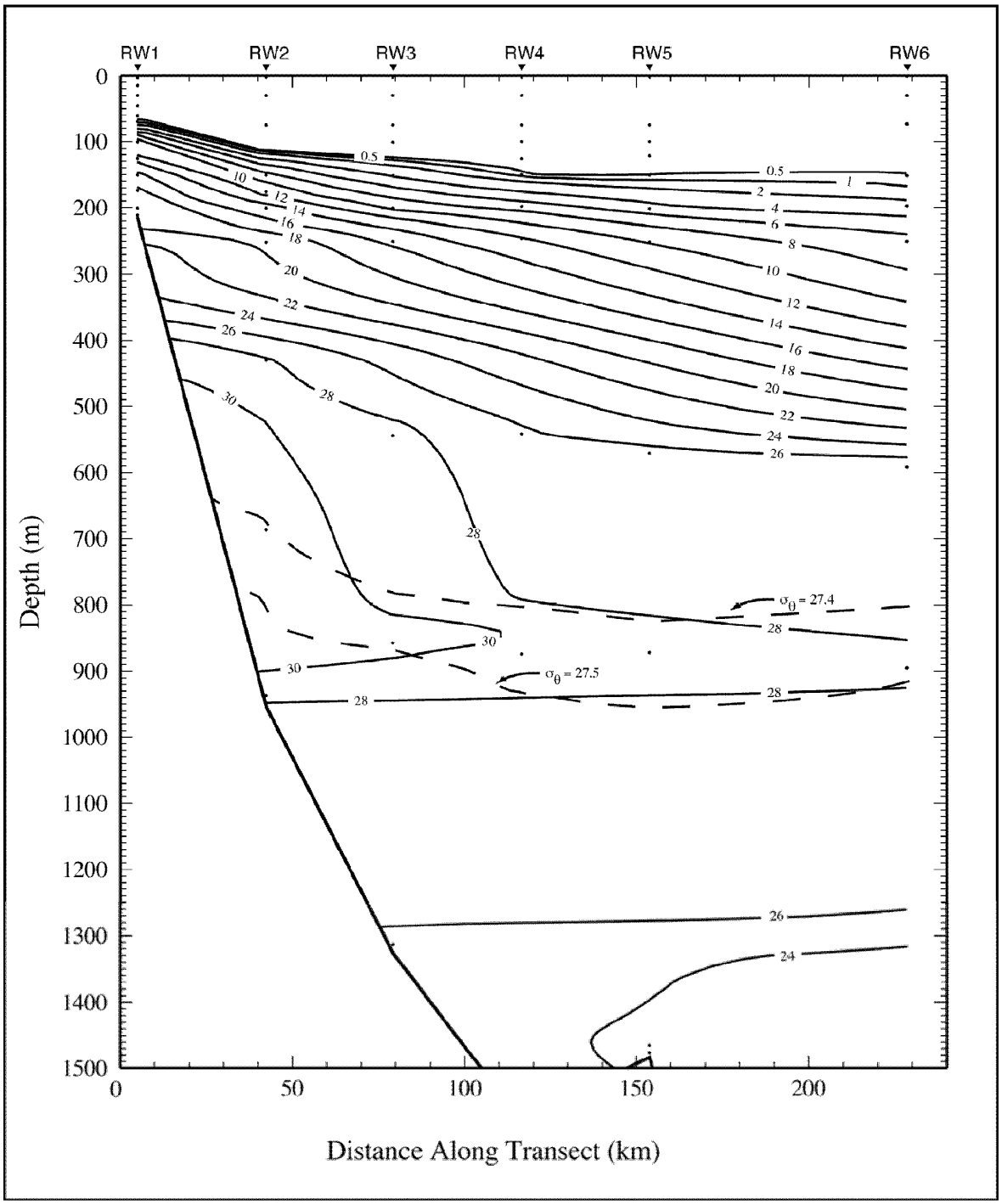

Figure 8-15. Nitrate (μM) on the western-most transect of DGoMB cruise 1, 4 May-17 June 2000. Dashed lines show two of the sigma-theta density surfaces associated with the Antarctic Intermediate Water. Dots show sampling locations.

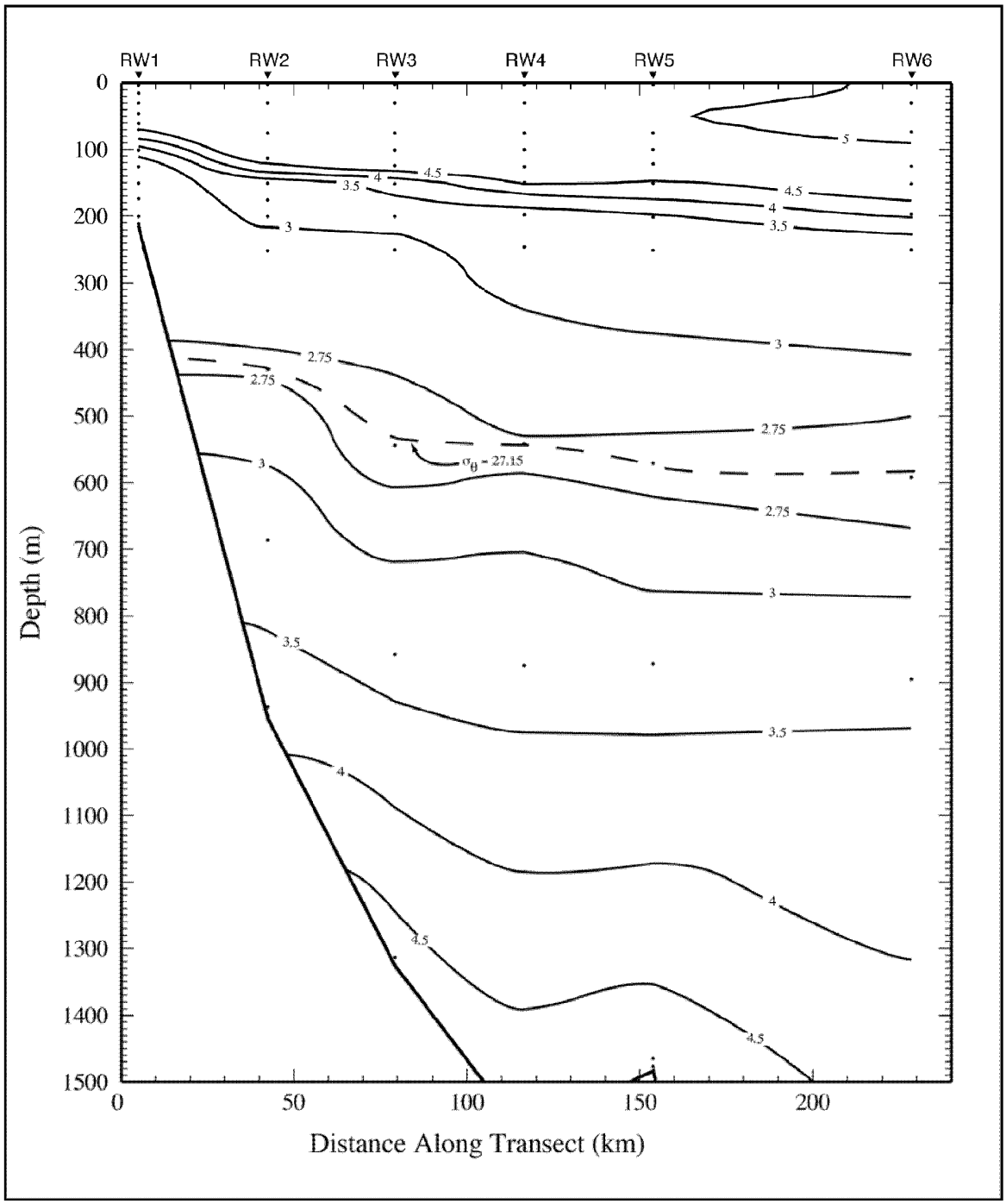

Figure 8-16. Dissolved oxygen (mL/L) on the western-most transect of DGoMB cruise 1, 4 May-17 June 2000. Dashed line shows the sigma-theta density surface of the Tropical Atlantic Central Water. Dots show sampling locations.

Figures 8-17 and 8-18 show profiles versus depth and density, respectively, of dissolved oxygen, nitrate, phosphate, and silicate from all DGoMB 2000 and 2001 data. The profiles distinguish between data taken in the eastern GoM (pluses) and those taken in the western GoM (dots). Here west is taken to be west of 90°W. Overall patterns are the same in the east and west. The differences in distributions in the upper 100-200 m of the water column are likely to be related to differences in the number and types of features and the bathymetric regions sampled, as well as differences caused by surface processes, such as localized photosynthesis and respiration, winds and associated mixing, heating and cooling, and precipitation and evaporation, that impact rates of oxygen input and consumption.

The oxygen profiles (Figures 8-17a and 8-18a) show high concentrations in the upper water column, reflecting photosynthesis and exchanges with the atmosphere. Values decrease with depth in the upper 500 m, as expected from the vertical oxygen distribution of the source waters, particularly the Tropical Atlantic Central Water. Local consumption of oxygen in the near-surface waters during the decay of detritus falling through the water column also contributes to this structure. Below about 500 m, the oxygen concentration then increases with depth. Compare the high variability of oxygen concentrations in the upper water column with the small variability in the deep water column. This is most clearly seen in the density plots, with the small horizontal variability seen for $\sigma_\theta > 27.15$ kg·m^{-3}. This difference reflects the variability in processes that input or consume oxygen.

The nutrient profiles (Figures 8-17b-d and 8-18b-d) also reflect the processes that increase or decrease the concentrations. The upper water column, where the nutrients have largely been consumed by phytoplankton, has low concentrations. Concentrations then increase with depth to a maximum near the depth or density surface of the Antarctic Intermediate Water mass (indicated by the line). This reflects the distribution of the nutrients in the source water masses, although the local decay of detritus regenerates the nutrients and contributes to this distribution. Deeper in the water column the concentrations decrease or remain fairly constant, again due mainly to the distributions found in the source waters.

Comparison of DGoMB with historical water property patterns: The DGoMB water properties were compared to published historical data sets from the eastern and western GoM basins. Morrison and Nowlin (1977) published results from a May 1972 cruise of the *R/V Alaminos* conducted in the eastern GoM with emphasis on the region occupied by the Loop Current. Morrison et al. (1983) published results from an April 1978 cruise of the *R/V Gyre* in the western GoM. The historical data from the 1972 cruise were available; so plots show actual data. The historical data from the 1978 cruise are not available from any identifiable source; so plots show estimates based on scanned figures from the Morrison et al. (1983) paper.

The dissolved oxygen, nitrate, phosphate, and silicate data from the DGoMB cruises (black pluses) are shown with the data from the 1972 and 1978 cruises (red dots) for the eastern (Figure 8-19) and western (Figure 8-20) GoM. Examination of these figures shows that the basic patterns seen in the DGoMB data described above were present in the historical data. There is less variability (both deep and shallow) in the DGoBM data than in the historical data. In general, this likely is due to improvements in sampling and analysis techniques and skills, rather than a climatic change in the patterns. The extreme example for nitrate near $\sigma_\theta = 27.4$ in the eastern GoM is most likely due to sampling problems reported for these historical nitrate data.

The oxygen pattern in the east (Figure 8-19a) suggests that the oxygen concentrations for $\sigma_\theta \leq 26$ kg·m^{-3} might be greater in the 1972 data than in the DGoMB data. This reflects the sampling

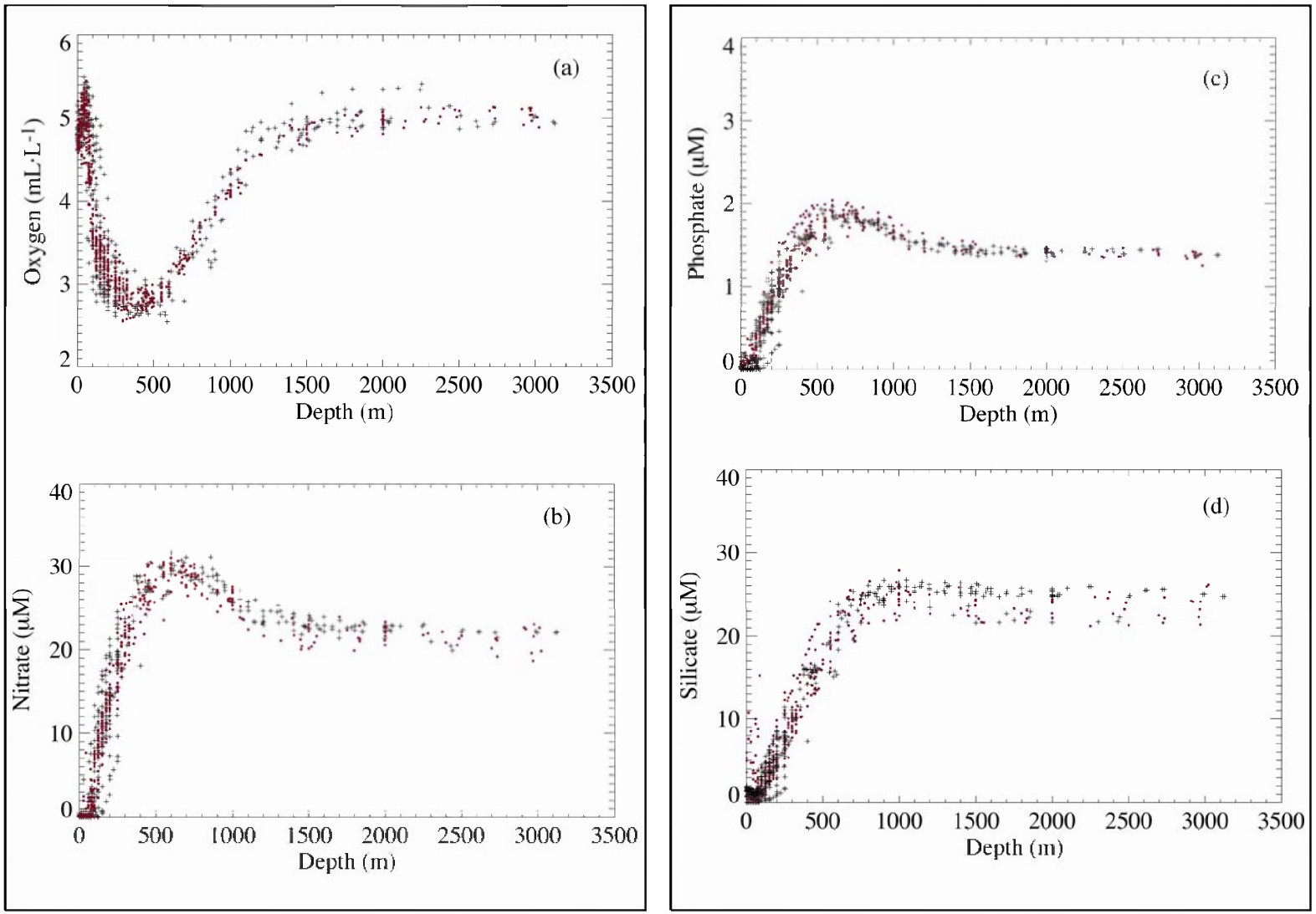

Figure 8-17. Water properties versus depth for DGoMB cruises in 2000 and 2001. Shown are (a) dissolved oxygen, (b) nitrate, (c) phosphate, and (d) silicate. Pluses denote data collected west of -90°W; dots from -90°W and east.

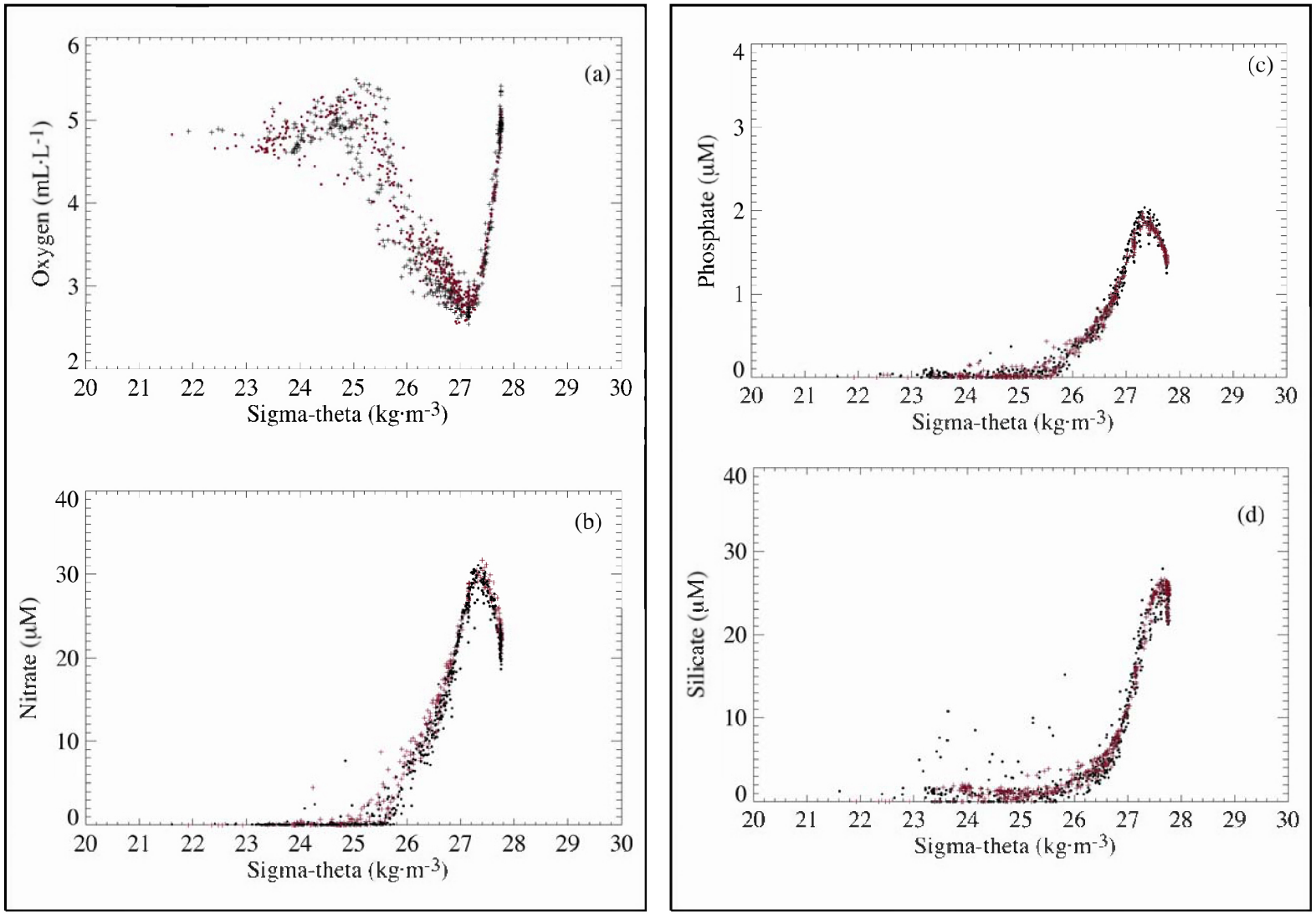

Figure 8-18. Water properties versus density for DGoMB cruises in 2000 and 2001. Shown are (a) dissolved oxygen, (b) nitrate, (c) phosphate, and (d) silicate. Pluses denote data collected west of -90°W; dots from -90°W and east.

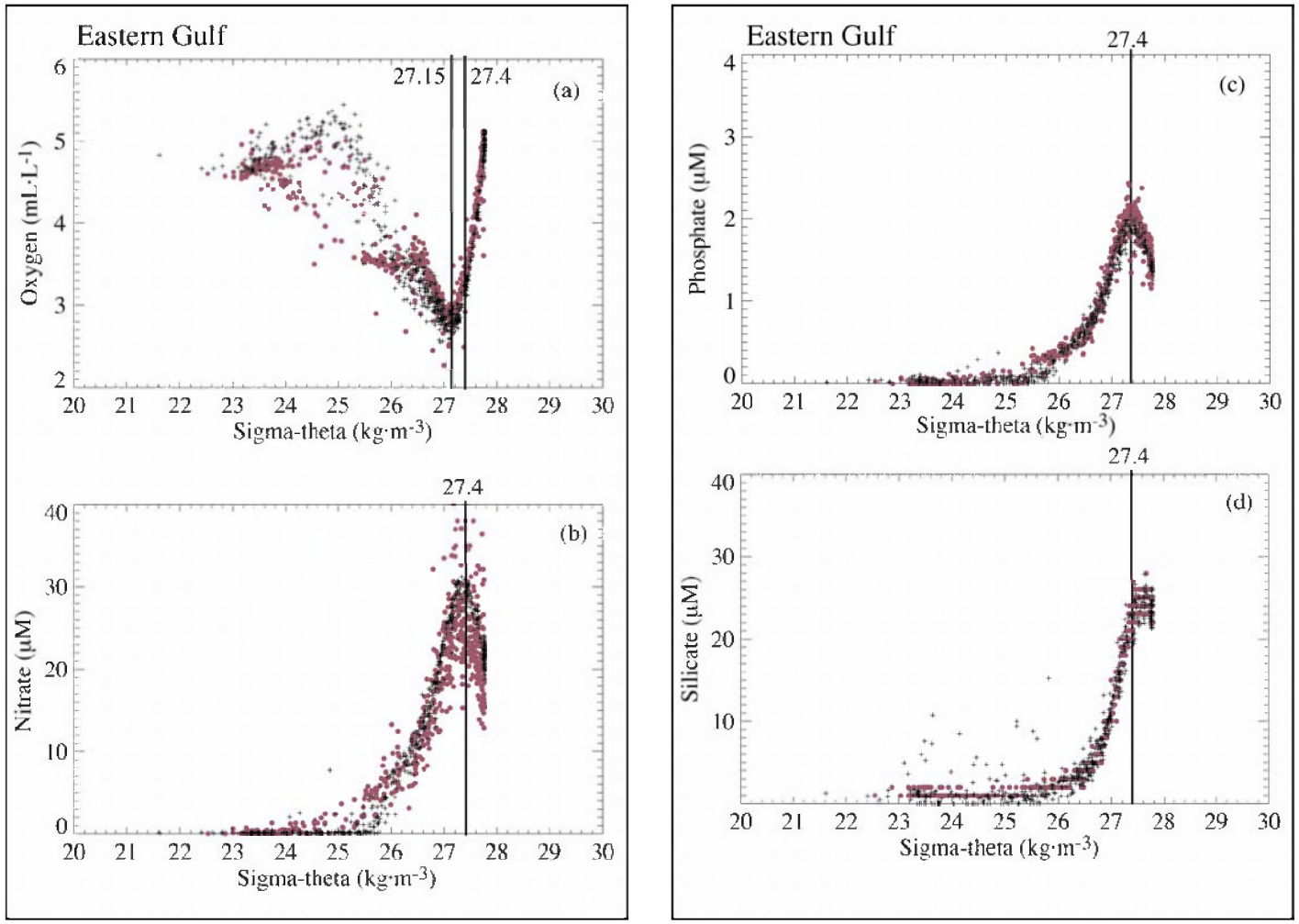

Figure 8-19. Water properties versus density for the eastern GoM. Shown are (a) dissolved oxygen, (b) nitrate, (c) phosphate, and (d) silicate. Pluses are from DGoMB cruises in May/June 2000 and June 2001; dots are from the *Alaminos* 72A09 cruise in May 1972. A line is drawn at 27.4 sigma-theta, which is one of the isopycnals associated with the Antarctic Intermediate Water. The line at 27.15 sigma-theta is associated with the 18°C Sargasso Sea Water.

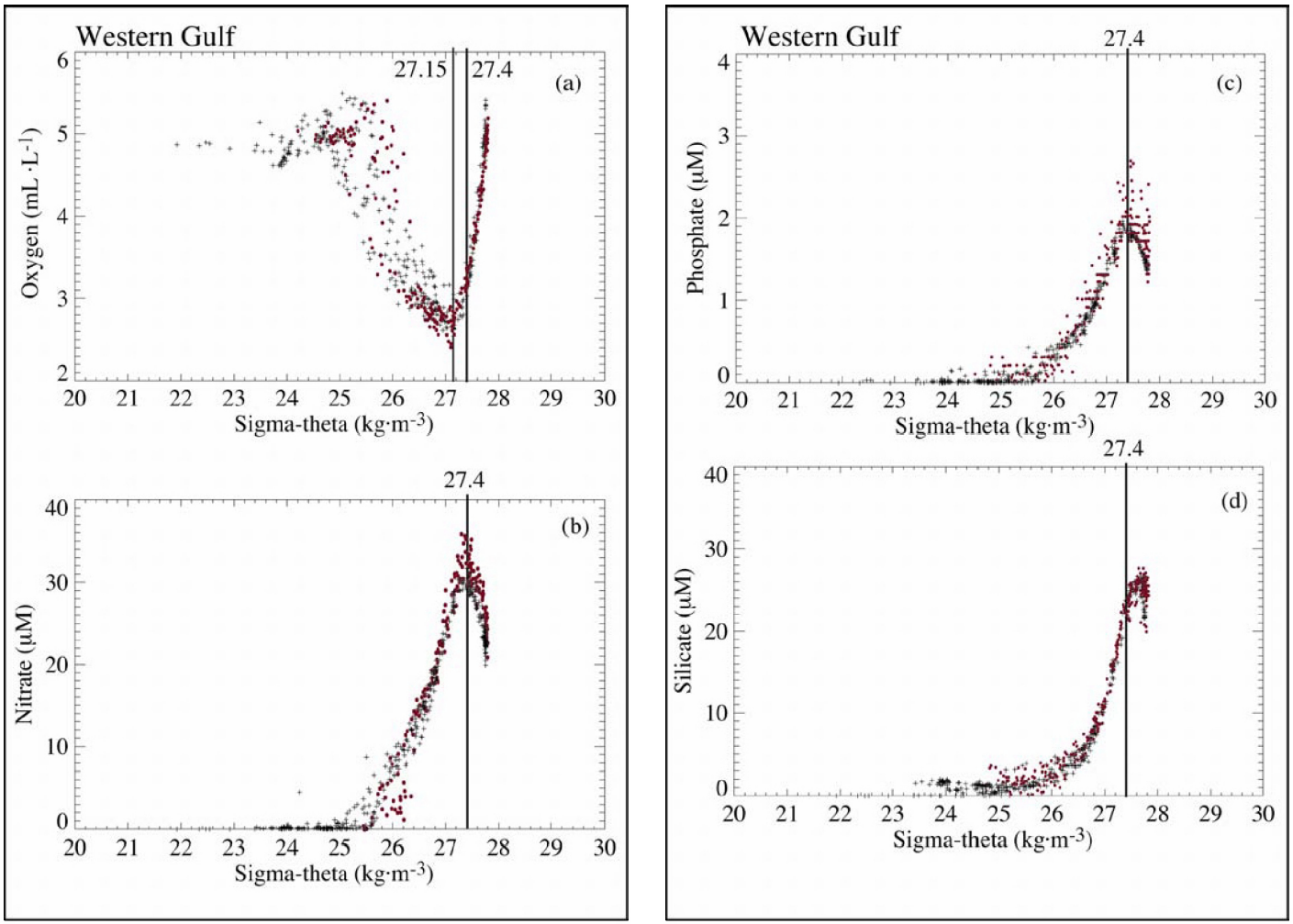

Figure 8-20. Water properties versus density for the western GoM. Shown are (a) dissolved oxygen, (b) nitrate, (c) phosphate, and (d) silicate. Pluses are from DGoMB cruises in May/June 2000 and June 2001; dots are estimated from Morrison et al. (1983) Figure 3 showing data from 78G03 cruise in April 1978. A line is drawn at 27.4 sigma-theta, which is one of the isopycnals associated with the Antarctic Intermediate Water. The line at 27.15 sigma-theta is associated with the 18°C Sargasso Sea Water.

on the earlier cruise was mainly in the region of the Loop Current, while the DGoMB sampling was throughout the eastern GoM. The older data also sampled in the area where the oxygen maximum associated with the 18°C Sargasso Sea Water is present, whereas many DGoMB stations were located in regions where this water mass had eroded away. Thus, this difference in DGoMB versus 1972 oxygen concentrations does not reflect a climatic change, but rather the fact that the 1972 sampling occurred directly in the source waters for oxygen in the eastern basin and so have not been diluted by mixing from other processes that modify oxygen content.

8.2.2 Circulation Patterns from ADCP Measurements

8.2.2.1 Moored ADCP Measurements

Summer 2001: During the 2001 summer cruise, a 300-kHz ADCP was deployed at each of four process stations (MT3, S42, S36, and MT6). The instrument was placed 35 m above the bottom in a downward-looking configuration. The deployments were short, ranging from 20-60 hours. Because of the short deployment period, these observations should be considered as a representative snapshot of the physical conditions that existed while each process station was occupied. The current observations should not be considered as the climatology of currents possible at each location. To determine the current climatology, a much longer current meter record would be required.

The near-bottom currents at the four process stations during summer of 2001 were generally weak with record-length mean speeds of 2.5, 7.5, 2.5, and 5 cm/s at stations, MT3, S42, S36, and MT6, respectively (Figure 8-21). Mean directions were generally aligned along local bathymetry. Vertically, current speeds decreased slightly with closeness to the bottom. Standard deviations of speed were nearly uniform for all four deployments at 1-2 cm/s. The sea temperature at the ADCP transducer head was nearly constant throughout each deployment with values near 5.0°, 6.0°, 4.1°, and 4.2°C. Vertical and error velocities (an indicator of the amount of horizontal inhomogeneity of currents in the water column) were small (1-2 cm/s) for all deployments.

For three of four deployments, the bottom boundary layer appeared to be just less than 30 m thick. At S42, there was more vertical structure as the record-length mean cross-slope velocity changed sign at about 20 m above bottom, down-slope below 20 m, and upslope above 20 m. The record-length mean along-slope component was nearly zero from 30 m above bottom to the bottom. Examination of the time series of both velocity components showed a clear near-diurnal oscillation with amplitude of about 7 cm/s and about 6 hours out of phase. Because of the short deployment it is not possible to determine whether this oscillation is due to tidal forcing, which is believed to be small in the deep GoM, or is of inertial origin. Diurnal oscillations were also present at stations MT3, S36, and MT6, although significantly weaker than at S42, i.e., amplitudes of 2-3 cm/s

Summer 2002: The 300-kHz ADCP was deployed twice during summer 2002 at process stations in the Sigsbee Basin (station 1) and beneath the Loop Current (station 4). Both of these stations were in ultra-deep water (depths greater than 3,000 m). Deployment lengths were 36 and 48 hours. Data quality was a concern for these deployments as quality generally decreased with distance from the instrument, such that data more than 20 m from the instrument, i.e., 40 m above bottom, were considered useless. We attribute the data loss to a lack of acoustic scatterers. Record-length mean currents were much stronger than the previous year's observations increasing from 20 to 40 cm/s between 55 and 40 m above bottom (Figure 8-22). The standard deviation of current also increased considerably in this range from 10 to 30 cm/s as the number

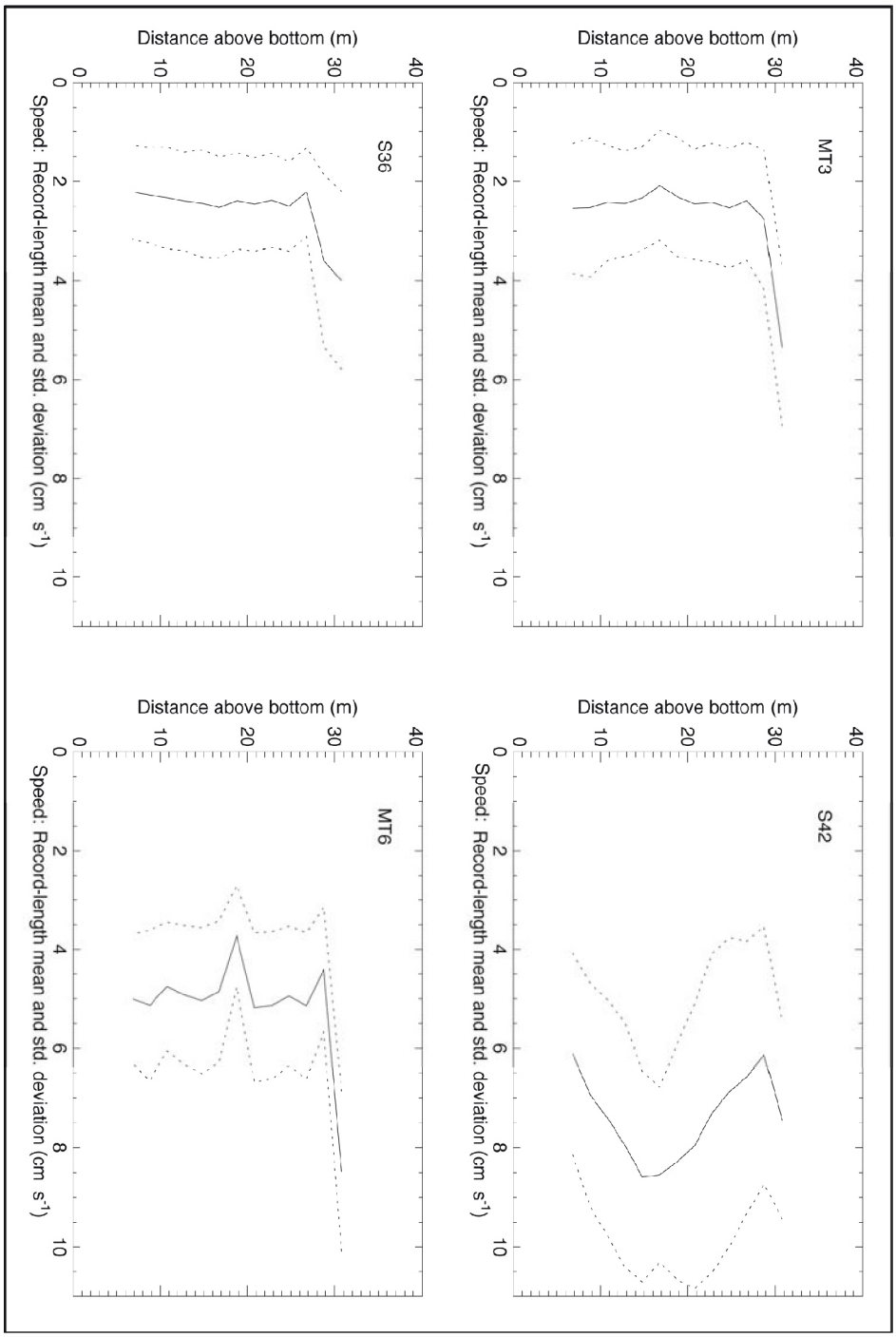

Figure 8-21. Record-length mean speed (solid) and plus and minus one standard deviation (dashed) of currents measured using a bottom-moored downward-looking 300-kHz ADCP during four deployments of Cruise 3 in 2001. Instrument was 35 m above bottom. Deployments sites are: MT3 (top left), S42 (top right), S36 (bottom left), and MT6 (bottom right).

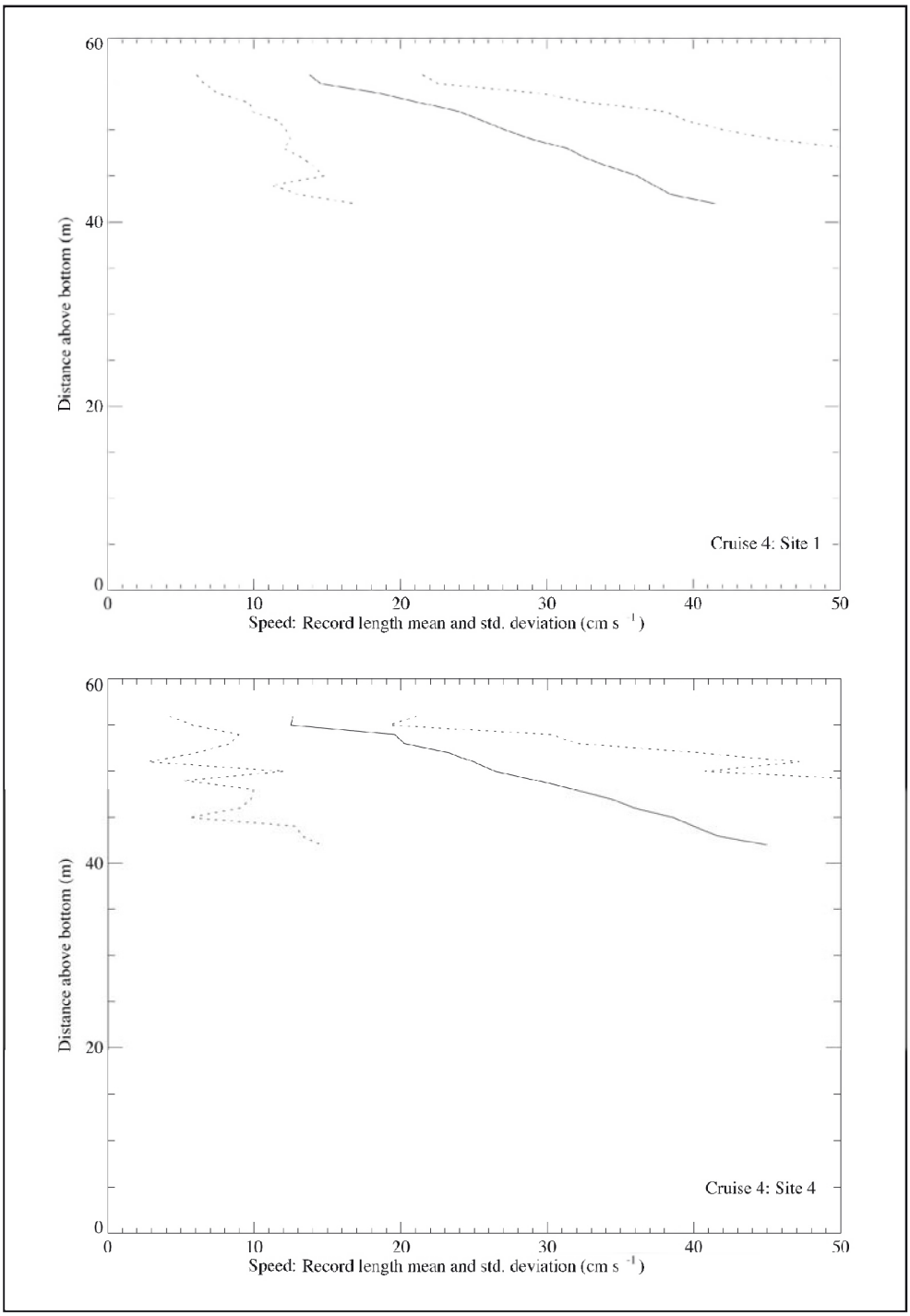

Figure 8-22. Record-length mean speed (solid) and plus and minus one standard deviation (dashed) of currents measured using a bottom-moored downward-looking 300-kHz ADCP during two deployments during Cruise 4 in 2002. Deployment sites are: Site 1 (top) and Site 4 (bottom).

of usable data decreased. The increase in speed with depth may likely be an artifact of the decrease in data quality with depth. The record-length mean of individual velocity components show a mean southwest direction at both stations. Neither deployment shows a detectable tidal signal. Mean temperatures are about 4.3°C. Vertical and error velocity components are disturbingly large (at times greater than 10 cm/s).

8.2.3 Shipboard ADCP Measurements

Shipboard ADCP observations of near-surface currents along the cruise track of each cruise were obtained using 150 kHz and 38 kHz ADCPs. The instrumentation and settings used during each cruise are detailed in Sections 1.2.2 and 1.3.3. The following paragraphs present summaries and interpretations of the observations.

Summer 2000: The physical oceanography of the GoM during the spring and summer of 2000 was dominated by the Loop Current in the eastern GoM (east of 90°W) and by the presence and interaction of Eddies Indigo and Juggernaut in the western GoM (Section 8.1.1). Eddy Indigo was centered near 26.25°N, 94.75°W as evidenced by satellite altimeter observations. Figure 8-23 shows the sea surface height field of the northwestern GoM on 13 May 2000. Superimposed on the SSH field are near-surface (14-m) current velocity vectors showing the magnitude and direction of currents along the cruise track. The cruise track of Cruise 1 passed through several mesoscale circulation features during this cruise. Observations were made along the eastern edge of Eddy Indigo during a north-south transect near 93.5°W before passing west near the eddy center and northwest toward the Texas coast. The ship also passed through a cyclonic feature centered near 26.25°N, 92°W. Currents were strongest in Eddy Indigo, particularly along the eastern limb of the eddy and in the region between the northwestern edge of the eddy and the continental shelf. Maximum near-surface speed exceeded 100 cm/s at both the eastern and northwestern edge of the eddy. Vertically, the speed core of Eddy Indigo extended to roughly 200 m depth, as indicated by the 60 cm/s isotachs (Figure 8-24).

The mean currents for the length of the record for the entire cruise show surface intensification and exponential decay with depth, in agreement with previous studies (Nowlin et al. 2001) of moored current meter records of the deep GoM. For the May 2000 cruise, the record-length mean surface currents exceeded 30 cm/s in the upper 100 m and decayed to less than 15 cm/s at 250 m depth. Below 250 m mean currents smoothly decayed from 15 cm/s to 9 cm/s at 750 m. The standard deviation of currents shows a similar decay pattern with depth with values of 25 cm/s in the upper 100 m and about 7 cm/s below 600 m. This pattern has been identified as the first baroclinic dynamic mode (Charney and Flierl 1981) based on hydrographic data of the deep GoM (Nowlin et al. 2001).

In June 2000, the position of Eddy Indigo changed little, but it weakened slightly. The position of the cyclone moved southward to about 25°N. The near-surface current velocity vectors observed along the cruise track of Cruise 1, leg 2, are shown in Figure 8-23. The cruise track passed through the center of Eddy Indigo and north of the cyclone. The cruise spent considerable time south and southeast of the Mississippi River Delta in the north-central GoM. Current speeds there were variable and weak as a result of the lack of strong circulation features. As during May, the strongest currents were in the northwestern GoM and associated with Eddy Indigo. The eddy may have pushed closer to the continental shelf and intensified currents along its northwestern limb. Currents exceeded 120 cm/s near surface and 60 cm/s above 200 m. Owning to the longer time spent in the quiescent central GoM, mean speeds for the cruise

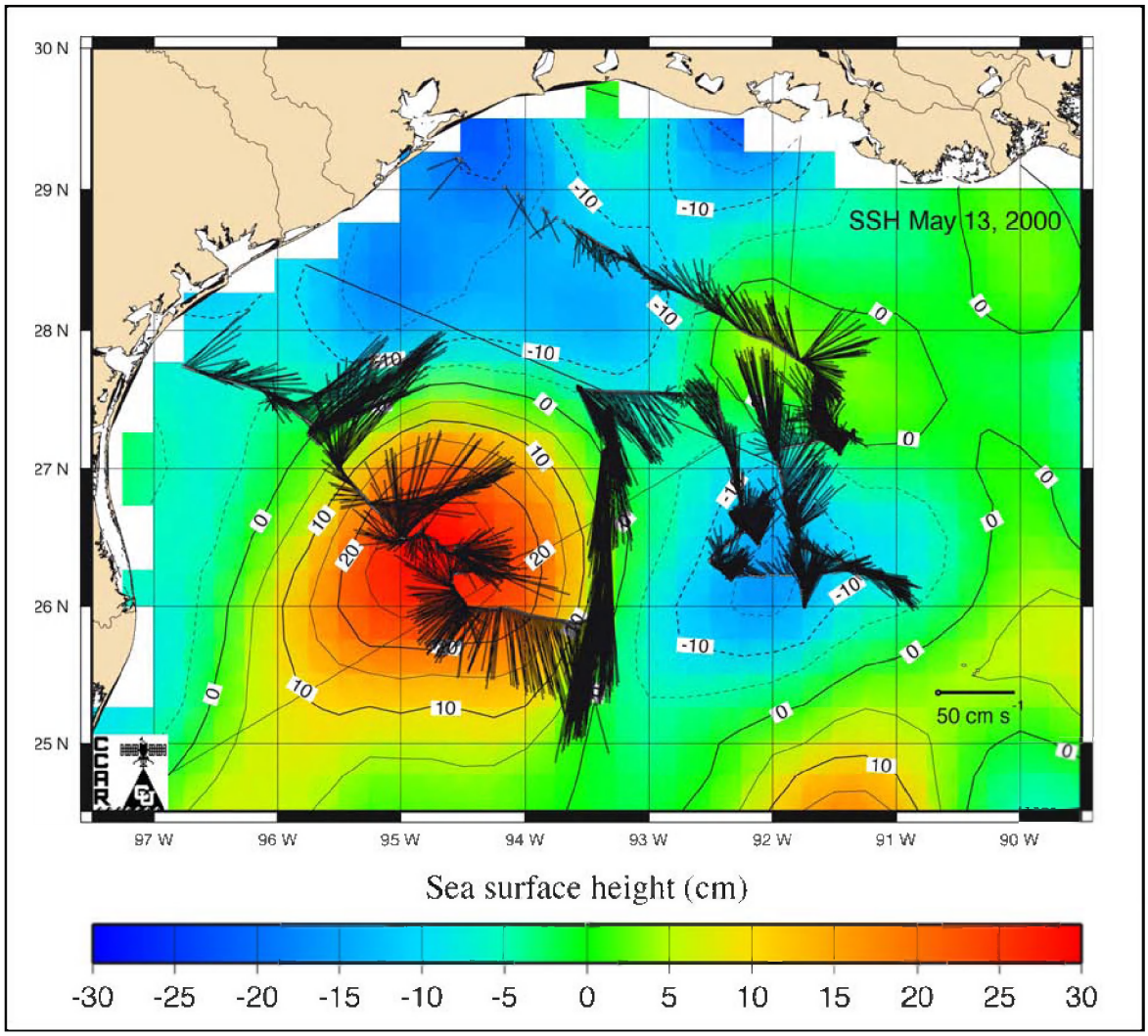

Figure 8-23. Contours of sea-surface height from satellite altimeter data and near-surface velocity vectors from shipboard ADCP during Cruise 1, leg 1. SSH data are from 13 May 2000 and are courtesy of R. Leben (CU).

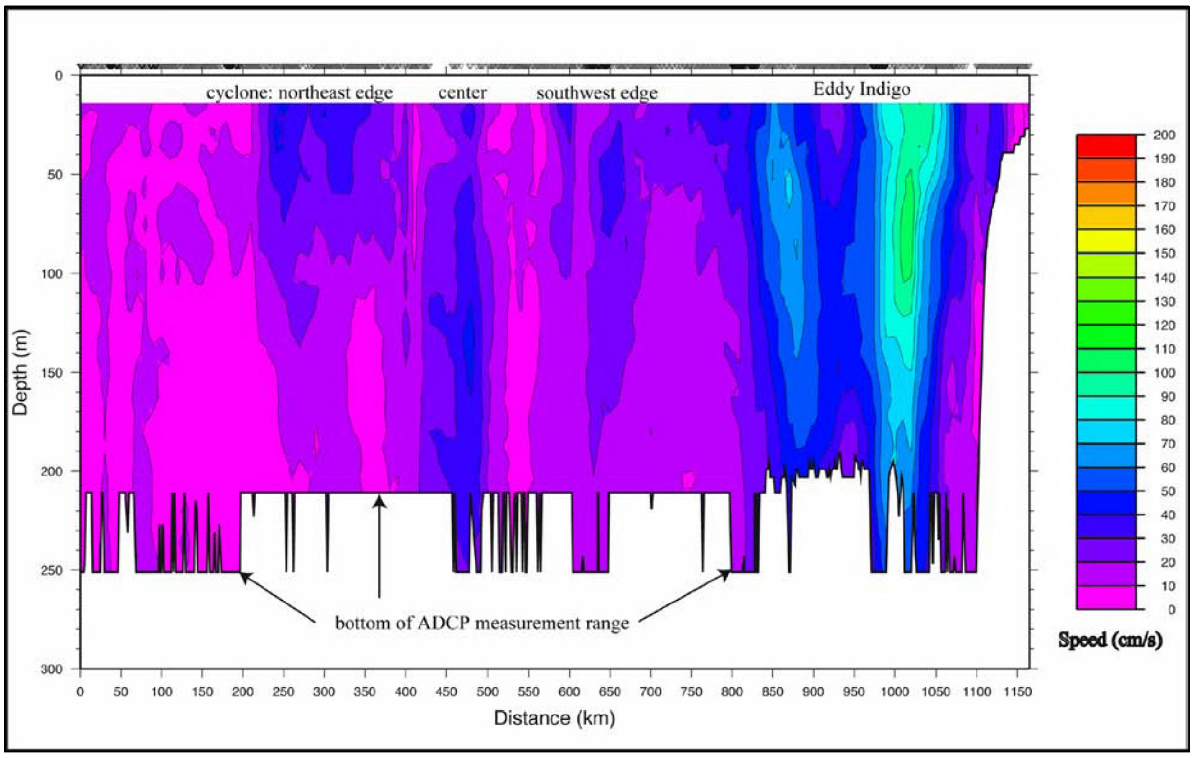

Figure 8-24. Vertical section of current speed based on shipboard 150-kHz ADCP data collected along a section in the western GoM during Cruise 1, leg 1, in June 2000. Positions of circulation features are indicated above the controus. See Figure 8-23 for section location.

decayed from only 23 cm/s near surface and were roughly 10 cm/s from 250 m to 750 m depth. The vertical structure of currents during this cruise, however, was similar to the structure of the first dynamic mode for the GoM as seen on the previous month's cruise.

Summer 2001 (Cruise 2): By the summer of 2001, a weak anticyclone, likely the remnant of Eddies Indigo and Juggernaut, dominated the western GoM. The central GoM was dominated by the presence of a newly detached Loop Current Eddy centered at 25.5°, 91°W and the Loop Current in the east GoM was confined south of 27°N. The track for Cruise 2 was limited to the north-central GoM, south of the Mississippi River Delta. The track circumscribed a weak slope anticyclone centered at 28°N, 88.5°W (Figure 8-25). Observed surface currents were generally weak during this cruise with notable exceptions on the west side of the weak anticyclone and in the region of interaction between the anticclone and the cyclonic feature centered at 27°N, 87.5°W (Figure 8-26). There was an indication of intensified currents in this region, as currents exceeded 80 cm/s. Further, the currents were strongest about 50 m below the surface, perhaps due to the influence of the cyclone, whose phenomenon class is typically intensified below the surface.

Summer 2002 (Cruise 3a and 3b): During the summer of 2002, the tracks of both legs extended from the northern GoM to the Loop Current. During Cruise 3a in June 2002, the track passed through or near several energetic circulation features, including the Loop Current, a detached Loop Current Eddy (24°N, 94°W), a strong cyclone northwest of the Loop Current, and other weaker features (Figure 8-27). In general, currents were aligned with altimeter contours of sea surface height. The strongest observed currents during this cruise were associated with the

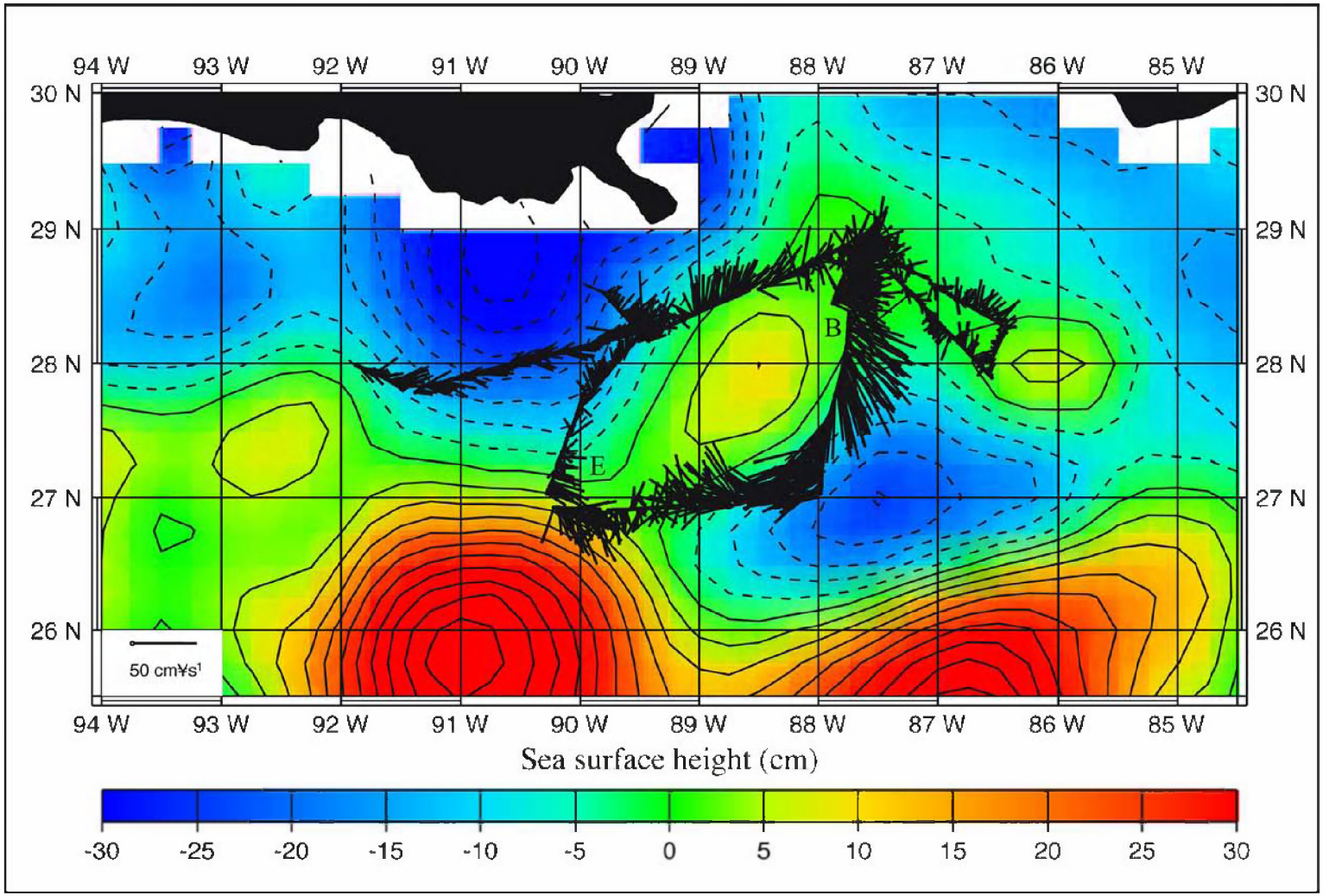

Figure 8-25. Contours of sea-surface height from satellite altimeter data and near-surface velocity vectors from shipboard ADCP during Cruise 2. SSH data are from 15 June 2001 and are courtesy of R. Leben (CU).

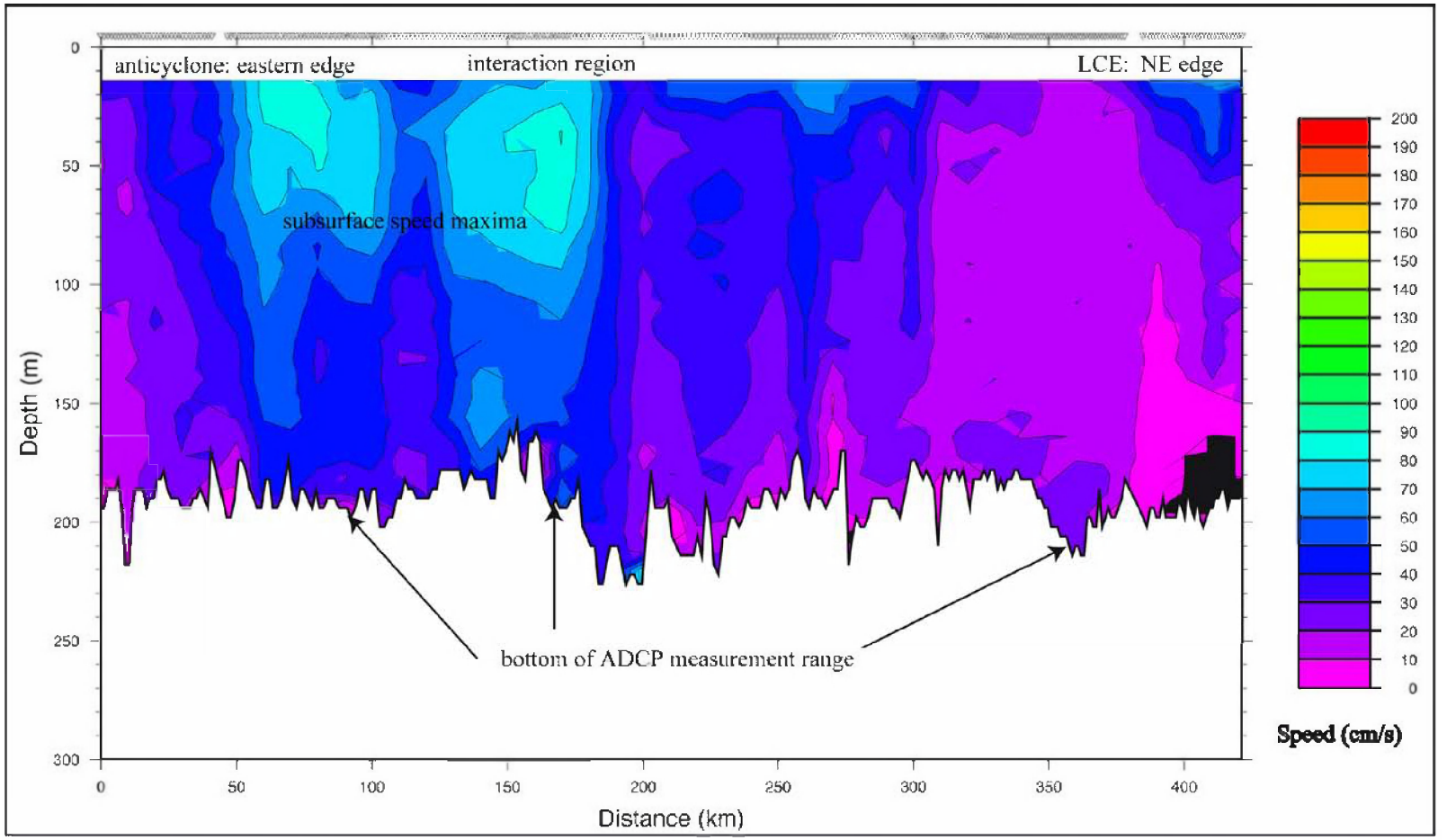

Figure 8-26. Vertical section of current speed based on shipboard ADCP data collected along a section in the north-central GoM during Cruise 2 in June 2001. Positions of circulation features are indicated above the contours. See Figure 8-25 for section location.

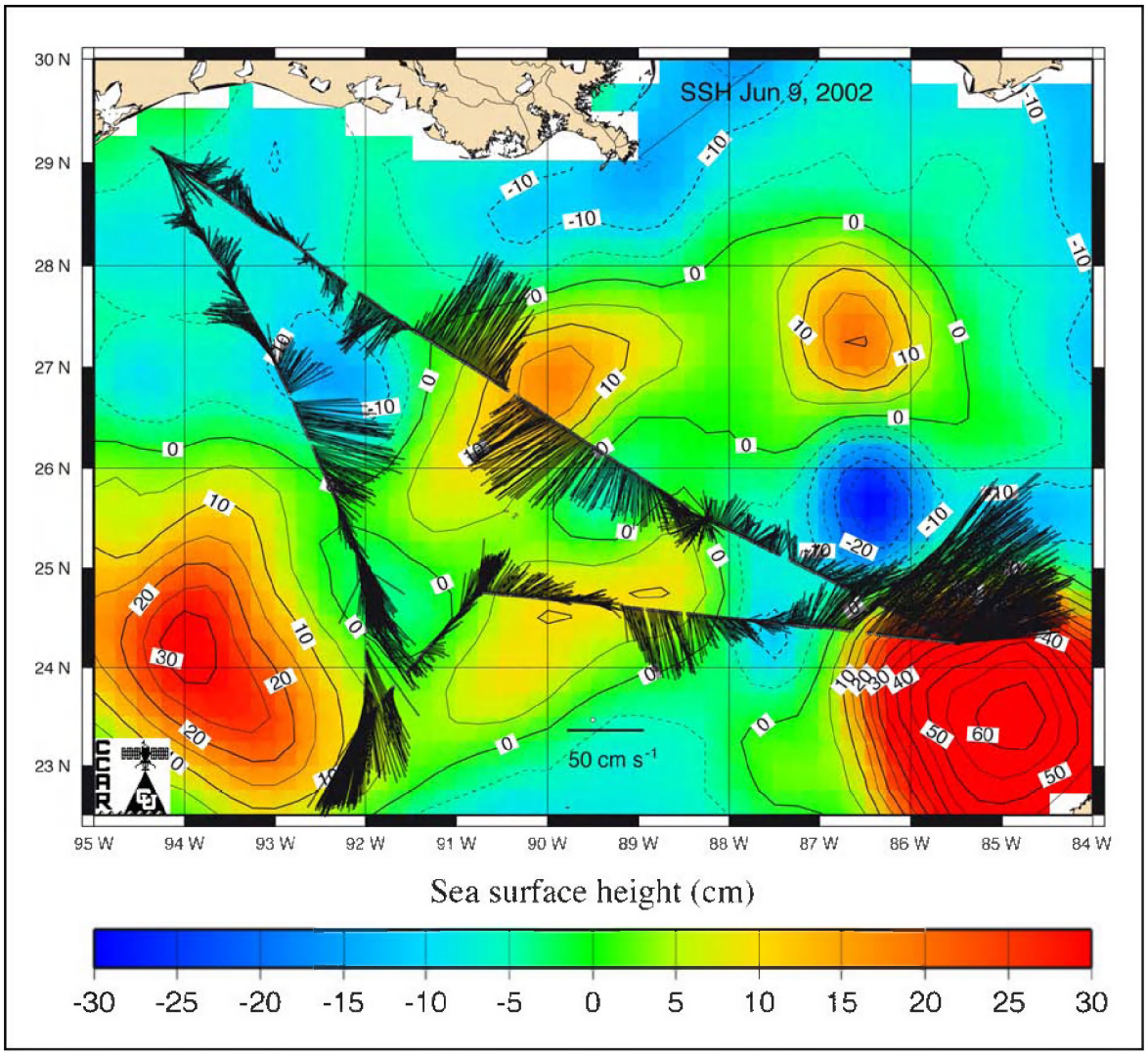

Figure 8-27. Contours of sea-surface height from satellite altimeter data and near-surface velocity vectors from shipboard ADCP during Cruise 3a. SSH data are from 9 June 2002 and are courtesy of R. Leben (CU).

Loop Current and the currents associated with anticyclonic features. In the Loop Current, currents exceeded 135 cm/s in the upper 100 m and 100 cm/s in the upper 150 m. Useful observations were limited to the upper 200 m because of the operation frequency (150-kHz) of the ADCP used (the 38-kHz ADCP failed to produce useful data).

Currents in the weak anticyclone near 27°N, 90°W peaked above 60 cm/s and averaged greater than 30 cm/s in the upper 200 m. Similar values were found on the eastern limb of the Loop Current Eddy. Mean currents in the upper 200 m of the water column ranged from 38 cm/s at 10 m depth to 13 cm/s at 200 m. The standard deviation similarly ranged from 25 cm/s at 10 m to 10 cm/s at 200 m.

During Cruise 3b, August 2002, the central GoM was nearly devoid of energetic circulation features, as evidenced by a nearly flat SSH field (Figure 8-28). The dominant feature was the

Loop Current, which extended slightly further northward than in June 2002. Currents in the Loop Current exceed 180 cm/s to 50 m depth and 120 cm/s to 150 m (Figure 8-29). The standard deviation of currents while in the Loop Current was nearly constant with depth at about 13 cm/s. Record-length mean currents by depth level for this cruise decay from about 30 cm/s at the surface to about 10 cm/s at 200 m.

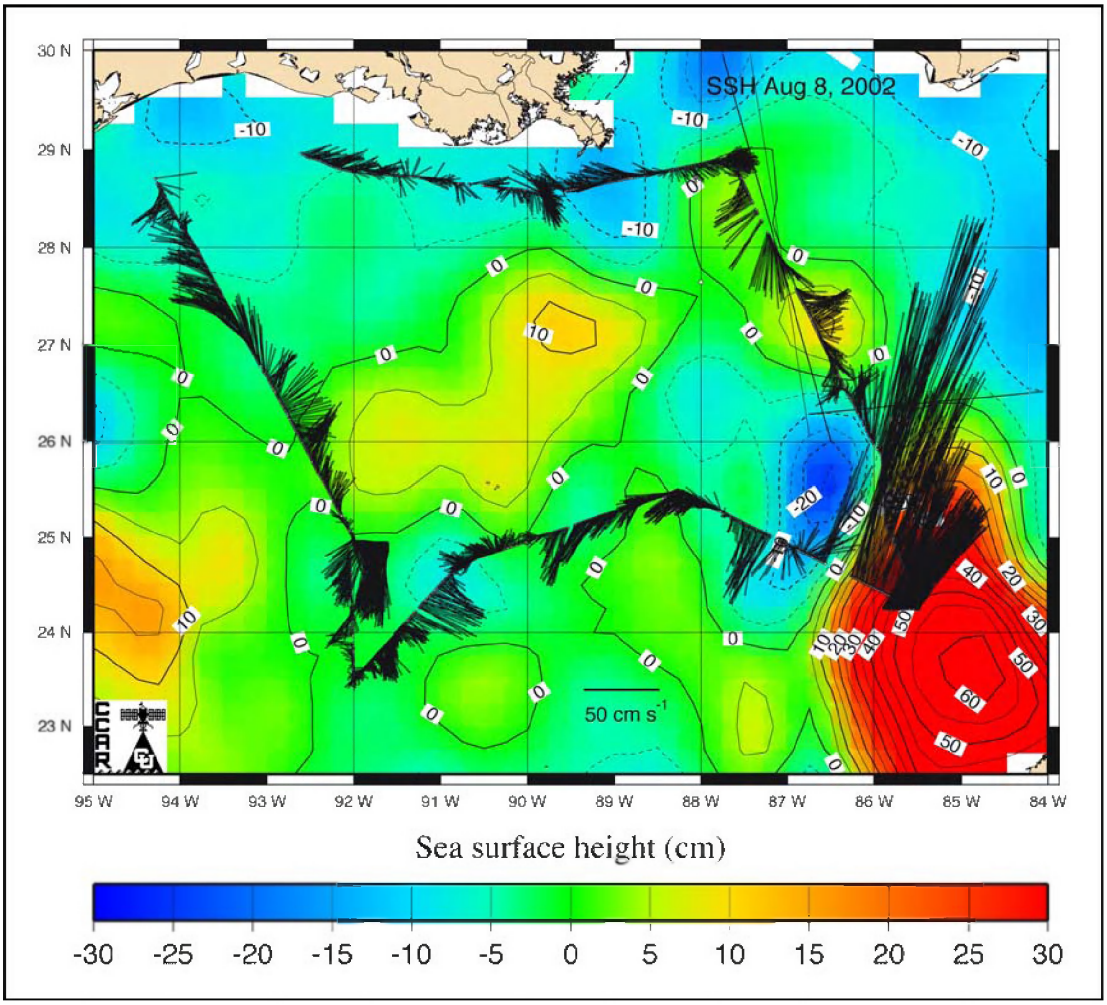

Figure 8-28. Contours of sea-surface height from satellite altimeter data and near-surface velocity vectors from shipboard ADCP during Cruise 3b. SSH data are from 8 August 2002 and are courtesy of R. Leben (CU).

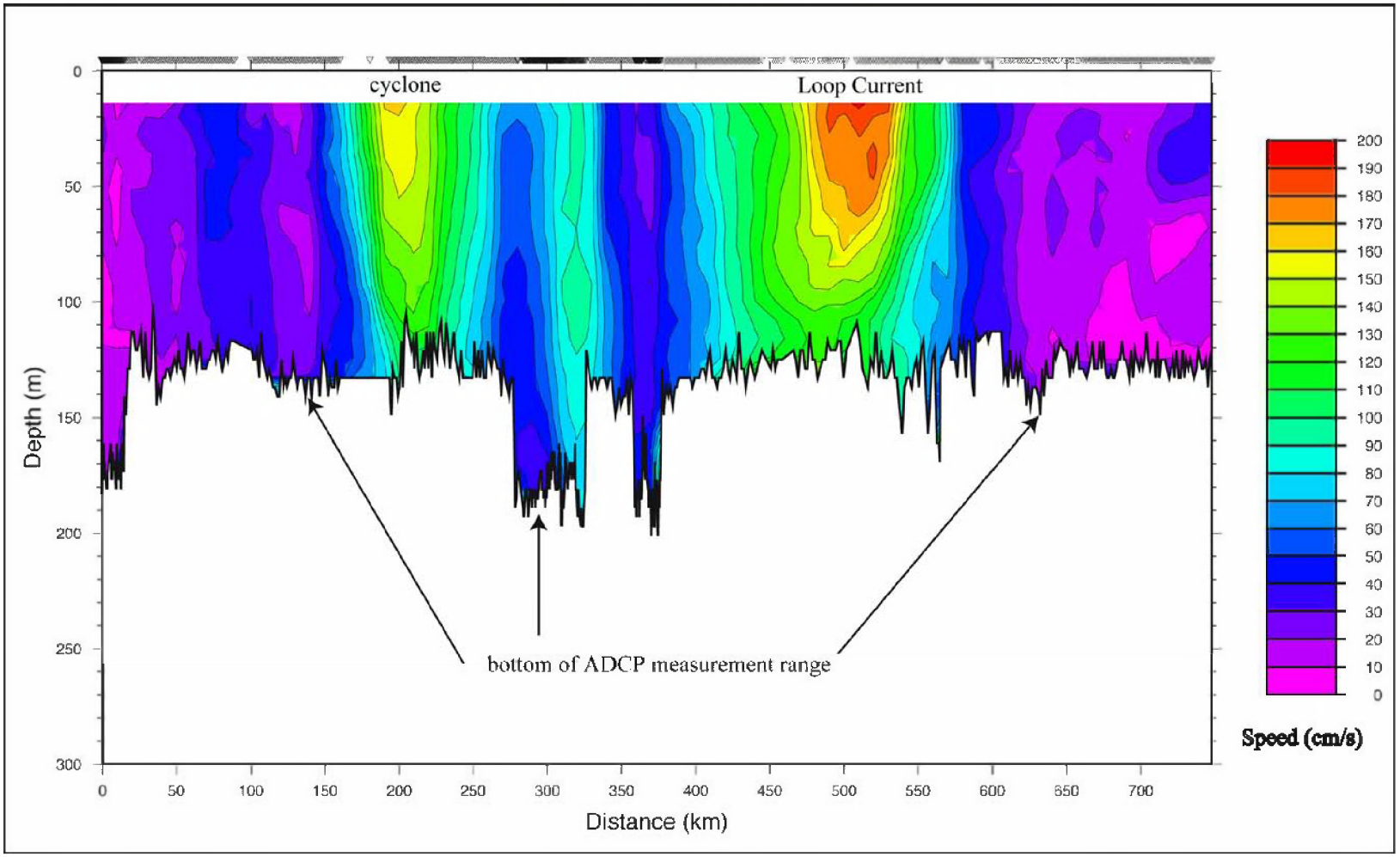

Figure 8-29. Vertical section of current speed based on shipboard ADCP data collected along a section in the southeastern GoM during Cruise 3b in August 2002. This section was roughly taken as the cruise track passed through the Loop Current (see Figure 8-29)

8.3 Ocean Color Climatology

Phytoplankton pigment concentration in the first optical depth in the deepwater GoM undergoes a well-defined seasonal cycle which is generally synchronous off the shelf, where the bottom is deeper than 200 m. Müller-Karger et al. (1991) reviewed monthly climatologies of near-surface phytoplankton pigment concentration from multiyear series of coastal zone color scanner (CZCS) images for the period 1978-1985. They reported that highest near-surface pigment concentration (dominated by chlorophyll concentration, CHL) occurs in offshore waters between December and February and lowest values occur between May and July. They also reported there is only about a 3-fold variation between the lowest (~0.06 mg m^{-3}) and highest (0.2 mg m^{-3}) deepwater near-surface pigment concentration. Model simulations show that the single most important factor controlling the seasonal cycle in near-surface CHL concentration is the depth of the mixed layer (Walsh et al. 1989). Müller-Karger et al. (1991) concluded that because of this dependence, annual cycles of algal biomass are one or more months out of phase relative to the seasonal cycle of sea surface temperature.

Müller-Karger et al. (1991) extracted two multi-year time series of regional mean monthly variability in pigment concentration from the CZCS data for a western and an eastern deepwater GoM location. Each was averaged for a 200 km x 200 km area. Their western GoM location was centered at 25°N, 93°W in water depth > 3 km. Their eastern GoM location was also in deep water, centered just north of the Yucatan Channel at 24°N, 86°W and in the path of the Loop Current inflow. Because CZCS was an experimental sensor that was only turned on as prearranged, for at most a few minutes a day, and this led to sparse coverage in space and time, the CZCS time series available to Müller-Karger et al. was discontinuous for the some of the 7 year period. Nevertheless, the means for any month at both western and eastern areas were clearly similar in amplitude and phase. Highest values (to 0.4 mg m^{-3}) occurred in December-January and lowest values (to 0.05 mg m^{-3}) occurred in summer months. Subsequent study of CZCS imagery by Melo-Gonzalez et al. (2000), who compiled three-month averages from additional deepwater regions of the GoM and northern Caribbean Sea, reinforced the idea that seaward of the continental shelf, deepwater surface pigment concentration is lowest in spring-summer (Julian Days 60-300) and highest November-Februrary.

As we will show from analysis of the 1998-2000 ocean color data collected during the follow-on Sea viewing Wide-Field Sensor (SeaWiFS) mission, the 22 DGoMB stations over the continental slope in the northwestern GoM (north of 26°N and west of 91°W) show essentially the same annual cycle in magnitude and phase of CHL that was reported from the predecessor CZCS mission (Figure 8-30). However, at the 22 DGoMB stations over the continental slope in the northeastern GoM (north of 26°N and east of 91°W), there are often large biweekly variations in both magnitude and phase of the mean CHL concentration. We will show that these variations are correlated with the presence of mesoscale eddies that occur in the northeastern GoM, and we will cite results from the Northeastern Gulf of Mexico Chemical Oceanography and Hydrography companion MMS-funded program (NEGoM) as well as from Hu et al. (2003) that document this is because such eddies can entrain low salinity, high CHL Mississippi River water and transport this green water off shelf and into the deepwater of the eastern GoM.

Table 8-1 summarizes the annual mean CHL at DGoMB stations for the period 1998-2000. This summary has been compiled three different ways: a) with quick-look (4-km resolution) data for 1998+1999; b) with 1-km resolution data for 1998-1999; and, c) with 1-km resolution data

Table 8-1

Summary of Mean CHL at DGoMB Stations for Biweekly Time Series of 2 Years Versus 3 Years

DGoMB Station	1998+1999 4 km pixels 5x5 pix mean	1998+1999 4 km pixels 5x5 pix stdev	stdev/mean ratio column 3 to column 2	1998+1999 1 km pixels 5x5 pix mean	1998+1999 1 km pixels 5x5 pix stdev	stdev/mean ratio column 6 to column 5	4 km v 1 km ratio column 5 to column 2	1998-2000 1 km pixels 5x5 pix mean	1998-2000 1 km pixels 5x5 pix stdev	stdev/mean ratio column 11 to column 10	3 yrs v 2 yrs ratio column 10 to column 5
Western GoM											
RW1	0.33	0.21	0.64	0.34	0.23	0.70	1.03	0.31	0.20	0.65	0.92
RW2	0.23	0.09	0.41	0.24	0.12	0.49	1.05	0.24	0.11	0.48	1.01
RW3	0.20	0.07	0.34	0.22	0.09	0.44	1.09	0.21	0.10	0.49	0.98
RW4	0.21	0.10	0.47	0.22	0.12	0.57	1.04	0.19	0.11	0.59	0.89
RW5	0.18	0.05	0.28	0.19	0.07	0.37	1.04	0.18	0.08	0.44	0.94
RW6	0.18	0.06	0.36	0.18	0.07	0.38	1.01	0.17	0.07	0.43	0.96
AC1	0.18	0.07	0.38	0.18	0.07	0.40	0.97	0.17	0.08	0.44	0.97
W6	0.17	0.06	0.33	0.17	0.05	0.30	0.98	0.17	0.05	0.29	0.99
W5	0.17	0.05	0.28	0.17	0.05	0.27	1.01	0.17	0.05	0.27	0.99
W4	0.19	0.06	0.31	0.18	0.06	0.32	0.96	0.18	0.06	0.31	0.98
W3	0.19	0.06	0.32	0.19	0.07	0.35	0.99	0.19	0.07	0.35	0.98
W2	0.21	0.07	0.35	0.21	0.08	0.38	0.99	0.20	0.08	0.39	0.97
W1	0.23	0.09	0.38	0.24	0.10	0.42	1.06	0.23	0.10	0.43	0.96
WC5	0.23	0.09	0.39	0.23	0.10	0.42	1.00	0.22	0.10	0.44	0.96
WC12	0.20	0.07	0.34	0.20	0.08	0.42	1.00	0.19	0.08	0.42	0.96
B1	0.19	0.07	0.35	0.19	0.08	0.44	0.99	0.19	0.08	0.45	0.98
NB2	0.18	0.06	0.34	0.19	0.07	0.38	1.01	0.18	0.07	0.38	0.97
NB3	0.18	0.06	0.33	0.18	0.07	0.37	1.00	0.17	0.06	0.36	0.96
B2	0.18	0.05	0.31	0.17	0.06	0.32	0.96	0.17	0.06	0.33	1.00
NB4	0.17	0.04	0.25	0.17	0.05	0.31	1.00	0.17	0.05	0.29	0.99
B3	0.18	0.06	0.33	0.17	0.06	0.36	0.97	0.17	0.06	0.34	0.99
NB5	0.18	0.06	0.33	0.18	0.06	0.36	1.00	0.18	0.07	0.41	0.99
mean for W	0.20	0.07	0.35	0.20	0.08	0.41	1.01	0.19	0.08	0.42	0.97

Table 8-1 Summary of Mean CHL at DGoMB Stations for Biweekly Time Series of 2 Years Versus 3 Years (continued)

DGoMB Station	1998+1999 4 km pixels 5x5 pix mean	1998+1999 4 km pixels 5x5 pix stdev	stdev/mean ratio column 3 to column 2	1998+1999 1 km pixels 5x5 pix mean	1998+1999 1 km pixels 5x5 pix stdev	stdev/mean ratio column 6 to column 5	4 km v 1 km ratio column 5 to column 2	1998-2000 1 km pixels 5x5 pix mean	1998-2000 1 km pixels 5x5 pix stdev	stdev/mean ratio column 11 to column 10	3 yrs v 2 yrs ratio column 10 to column 5
Eastern GoM											
C12	0.18	0.06	0.36	0.19	0.15	0.79	1.07	0.20	0.15	0.75	1.05
C14	0.20	0.09	0.45	0.20	0.11	0.53	1.02	0.19	0.10	0.51	0.95
C4	0.24	0.16	0.65	0.23	0.11	0.47	0.95	0.22	0.11	0.48	0.95
C7	0.34	0.47	1.39	0.30	0.34	1.11	0.89	0.28	0.29	1.03	0.93
C1	0.94	1.95	2.08	0.63	1.08	1.71	0.67	0.50	0.90	1.79	0.80
S36	0.87	1.37	1.58	0.65	0.73	1.12	0.75	0.56	0.63	1.12	0.87
S37	0.43	0.42	0.96	0.47	0.49	1.04	1.09	0.42	0.45	1.08	0.88
S38	0.24	0.10	0.44	0.24	0.12	0.52	1.01	0.25	0.14	0.56	1.04
S35	0.60	0.70	1.17	0.64	0.76	1.18	1.08	0.57	0.64	1.14	0.88
S44	0.37	0.28	0.75	0.52	0.58	1.10	1.42	0.46	0.53	1.15	0.88
S43	0.39	0.44	1.13	0.36	0.39	1.08	0.92	0.32	0.33	1.03	0.89
S42	0.28	0.25	0.88	0.29	0.25	0.88	1.01	0.28	0.25	0.89	0.98
S41	0.24	0.15	0.63	0.26	0.22	0.85	1.08	0.30	0.44	1.47	1.14
S40	0.22	0.08	0.39	0.22	0.10	0.44	1.01	0.22	0.12	0.54	1.02
S39	0.21	0.07	0.33	0.21	0.11	0.52	0.99	0.21	0.10	0.47	0.99
MT6	0.19	0.06	0.31	0.18	0.07	0.36	0.99	0.19	0.08	0.42	1.04
MT5	0.25	0.19	0.78	0.26	0.23	0.88	1.04	0.24	0.20	0.80	0.94
MT4	0.62	1.45	2.34	0.44	0.62	1.41	0.71	0.41	0.54	1.31	0.94
MT3	1.42	2.58	1.82	0.84	1.13	1.34	0.59	0.75	1.03	1.38	0.89
MT2	3.68	5.42	1.47	2.60	3.29	1.27	0.71	2.13	3.00	1.41	0.82
MT1	4.91	6.58	1.34	2.80	3.58	1.28	0.57	2.47	3.57	1.45	0.88
HiPro	0.85	1.41	1.66	0.76	1.10	1.44	0.89	0.66	1.02	1.54	0.87
mean for E	0.80	1.10	1.04	0.60	0.71	1.18	0.75	0.54	0.66	1.09	0.90

for 1998-2000. Several patterns are evident: (1) means are quite similar for 4-km resolution data and for 1 km resolution data; (2) means are quite similar whether the record length is 2 years (1998+1999) or 3 years (1998+1999+2000); (3) means are higher at DGoMB stations east of 91°W than at stations in the western GoM.

Specifically, note that (1) Column 8 of Table 8-1 (the ratio of means for 2 years of 1 km resolution data divided by 2 years of 4 km resolution data) averages close to 1.0, especially for stations in the western GoM (range just 0.96-1.09); (2) the last column of Table 8-1 (the ratio of means for 3 years of 1 km resolution data divided by 2 years of 1 km resolution data) also averages close to 1.0, especially for stations in the western GoM (range just 0.89-1.01); (3) mean CHL at the 22 stations north of 26°N and west of 91°W in the western GoM averaged 0.19 mg m^{-3}, but mean CHL averaged 0.54 at the 22 stations north of 26°N and east of 91°W in the eastern GoM. After review of the summary results in Table 8-1, we stopped averaging after just 3 years of data from DGoMB stations in the western GoM in order to compute the annual mean CHL. But we continued to average additional data (Oct 1997 – Feb 2001) for stations in the eastern GoM, and also to produce composite monthly average ocean color scenes, to better describe the inter-annual variability at DGoMB stations there.

The coefficient of variation (CV) statistics that are summarized in Columns 4, 7, and 12 of Table 8-1 present the ratio of standard deviation to mean CHL for the 2-year or 3-year time series constructed from biweekly means, in contrast to the CV statistics for 5x5 or 9x9 pixel averages that are given in Table 8-2. Note that CV statistics are generally low (usually <50%) for stations in the western GOM but that for stations in the eastern GoM these average two-fold higher (about 1.0). In other words, variance is rather evenly distributed about the mean (CV << 1.0) in the western GoM, but variance is more randomly distributed about the mean (CV ~ 1.0) in the eastern GoM.

Additional details of the seasonal cycle of CHL in western and eastern GoM are summarized as Figures 8-30 to 37. Figure 8-30 shows the seasonal cycle of CHL at the nine deepest of the "Deepwater Stations" in the western GoM (RW6, AC1, W5, W6, NB5, B1, NB4, B2, and B3). Water depth at each of these nine stations was greater than 2 km. The top panel in Figure 8-31 shows the average biweekly CHL at each of the nine stations for the three years 1998-2000, while the bottom panel graphs the average biweekly concentration (averaged for the three years). In the top panel, the 3-year time series were fit station-by-station using spline fits. In the bottom panel, the annual cycle has been summarized by a quadratic fit to the averages of 3 years of biweekly data at the westernmost deepwater station, RW6. Both of these visualizations show the pattern previously reported from analysis of the CZCS archives by Muller-Karger et al. (1991) and by Melo-Gonzalez et al. (2000): deepwater CHL is lowest in spring-summer (Julian Days 60-300) and highest November-February.

Figures 8-32 to 8-34 summarize the annual cycle of CHL at the Far Western stations (RW1-RW6), Western Stations (W1-W6), and Louisiana Slope Stations. Apart from an occasional biweekly higher CHL at the two shallowest stations on RW and W transects, the annual cycle was the same as that shown in Figure 8-31: deepwater CHL was lowest in spring-summer (Julian Days 60-300) and highest Nov-Feb. From Table 8-1, note the annual grand mean average CHL was about 0.2 mg m^{-3} at the 4 deepest stations on the RW transect (range 0.17-0.21), and at the 4 deepest stations on the W transect (range 0.17-0.19), and at AC1 and the nine Louisiana Slope Stations (range 0.17-0.22). From Figures 8-32 and 8-33, note that periods when biweekly CHL locally exceeds 0.4 mg m^{-3} at RW1, RW2, W1, and W2 do not occur only in November-February, but vary from year to year.

Table 8-2

Variability of StdDev/Mean Ratios for Time Series of Biweekly Mean CHL with Different Pixel Resolution and Grid Areas

	4 km resolution 5x5 grids (287 km^2) 1998+1999	1 km resolution 5x5 grids (18 km^2) 1998+1999+2000	1 km resolution 9x9 grids (57 km^2) 1998+1999+2000
22 stations west of 91W			
RW1	0.238	0.086	0.129
RW2	0.147	0.094	0.108
RW3	0.143	0.085	0.099
RW4	0.162	0.086	0.123
RW5	0.161	0.089	0.143
RW6	0.158	0.095	0.104
AC1	0.157	0.108	0.134
W6	0.192	0.084	0.096
W5	0.146	0.082	0.093
W4	0.142	0.089	0.155
W3	0.145	0.078	0.095
W2	0.194	0.070	0.094
W1	0.186	0.093	0.104
WC5	0.149	0.084	0.090
WC12	0.157	0.092	0.103
B1	0.150	0.090	0.101
NB2	0.142	0.084	0.093
NB3	0.137	0.082	0.090
B2	0.157	0.090	0.097
NB4	0.172	0.083	0.092
B3	0.186	0.079	0.087
NB5	0.152	0.084	0.095
grand mean CV in W	0.162	0.087	0.106
22 stations east of 91W			
C12	0.170	0.134	0.173
C14	0.181	0.093	0.113
C4	0.515	0.098	0.136
C7	0.445	0.116	0.169
C1	0.512	0.174	0.315
S36	0.569	0.224	0.221
S37	0.344	0.202	0.294
S38	0.197	0.129	0.137
S35	0.355	0.267	0.267
S44	0.190	0.274	0.313
S43	0.463	0.129	0.170
S42	0.274	0.177	0.402
S41	0.161	0.303	0.294
S40	0.177	0.148	0.166
S39	0.198	0.130	0.234
MT6	0.168	0.095	0.136
MT5	0.242	0.244	0.207
MT4	1.004	0.259	0.294
MT3	0.753	0.204	0.343
MT2	0.502	0.206	0.279
MT1	0.534	0.137	0.243
Hi-Pro	0.500	0.319	0.253
grand mean CV in E	0.379	0.185	0.235

East of 91°W, the "typical" deepwater annual cycle in CHL was often swamped by unusually high CHL, especially during summertime. Figures 8-35, 8-36, and 8-37 show that high surface CHL in summertime was evident at the 3 stations along the Eastern Transect (S44, S43, S42), at 5 of the 6 stations on the Mississippi Trough Transect (MT1-MT5), and at the 3 stations farthest upslope along the Central Transect (C1, C7, C4). High summertime CHL is evident, as well, at 3 of the stations farthest upslope along the DeSoto Canyon Transect (S35, S36, S37). Because of this, the annual mean CHL concentration at these eastern GoM stations averaged 0.54 rather than 0.19 mg m^{-3} (Table 8-1).

The annual cycle of CHL at DGoMB stations in the western GoM and at the deepest stations (water depth > 2 km) in the eastern GoM shows the high-in-winter, low-in-summer pattern previously reported from analysis of the CZCS ocean color data archives by Müller-Karger et al. (1991). At DGoMB stations in water depths of 300-1,800 m east of 91°W, though, the typical "deepwater" annual cycle in CHL is swamped by unusually high summertime CHL. A combination of remote sensing altimetry data and hydrographic data collected from R/V *Gyre* in support of the Northeastern GoM Chemical Oceanography and Hydrography program (NEGoM) has provided the explanation why this occurs. The altimetry data show that in summers 1998, 1999, and 2000, warm slope eddies (WSEs) were centered over the deepwater of the DeSoto Canyon (Figure 8-38). In general, anticyclonic eddies with SSH > 25 cm are considered to be strong WSEs, while those with SSH of just 10-20 cm are considered to be weaker WSEs. A strong WSE that was centered south of 28°N in summer 1999, as well as less strong WSEs located farther north on the slope in summers 1998 and 2000, all acted to entrain low salinity, high CHL "green water" from the Mississippi River and transport this green water plume seaward into deepwater. As a result, high surface CHL in summertime was evident at most of the DGoMB stations on the Mississippi Trough Transect (MT1-MT5), and at the three stations farthest upslope along the Central Transect (C1, C7, C4), and at the three stations farthest upslope along the DeSoto Canyon Transect (S35, S36, S37). High summertime CHL was evident, as well, at three of the stations along the Eastern Transect (S44, S43, S42).

That WSEs in deepwater of the eastern GoM do indeed entrain low salinity Mississippi River water and transport it off-margin has been verified by Hu et al. (2003) and by Belabbassi et al (in review), from analysis of near-surface salinity data collected during R/V *Gyre* NEGoM cruises in summers 1998, 1999, and 2000. By carrying out high performance liquid chromatography (HPLC) analyses of the phytoplankton pigments collected from R/V *Gyre* in these low salinity plumes during these same cruises, Qian et al. (2003) verified this low salinity water had locally high CHL standing stocks.

We caution, though, that the results (CHL climatology, seasonal variations, etc.) presented here should be viewed in a relative way only, especially the statistics (standard deviations, CVs), for several reasons. First, although the accuracy in the SeaWiFS determined CHL (SeaDAS version 2) is relatively high and acceptable (Hu et al. 2003) for deep stations without river plume interference, CHL tends to be overestimated in shallow water coastal areas (depth < 30 m) due to the presence of terrestrial runoff (particles + dissolved matter) under river influence. Second, the statistics were performed on the composite data over periods of two-weeks to one month, not on the original daily data, which often experienced significant cloud cover. For example, for a pixel with 14 valid data values from the 2-week period, only the average value was used in the composite data and its weight in the statistics would be the same as another pixel with only 1 valid data value from the 2-week period.

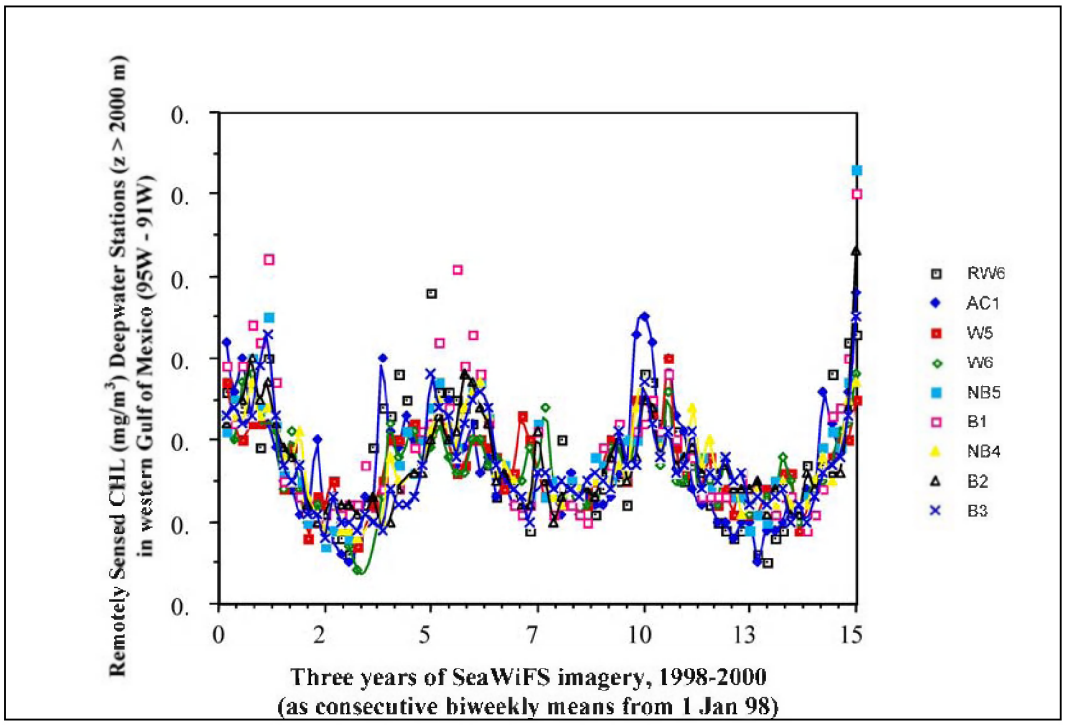

Figure 8-30. Three-year climatology of biweekly averaged SeaWiFS ocean color data 1998-2000 at the nine DGoMB stations in water depth > 2,000 m in the western GoM.

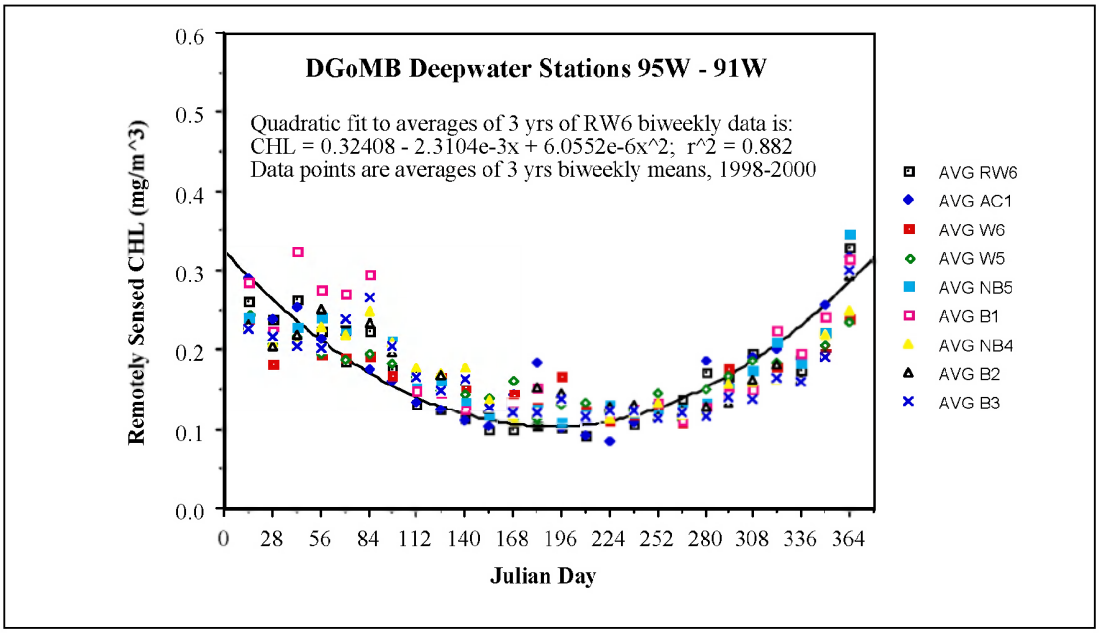

Figure 8-31. Average annual cycle of chlorophyll at these deepwater stations in the western GoM, illustrating the typical annual range from summertime lows of about 0.1 mg m^{-3} to November-February highs of about 0.3 mg m^{-3}.

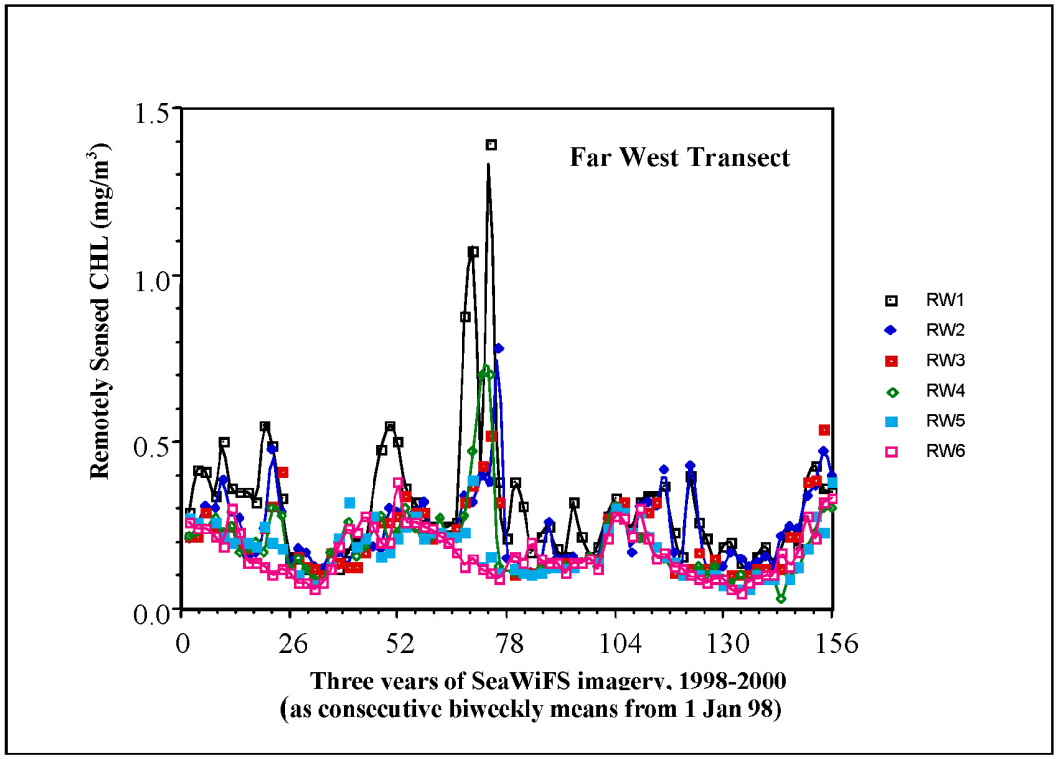

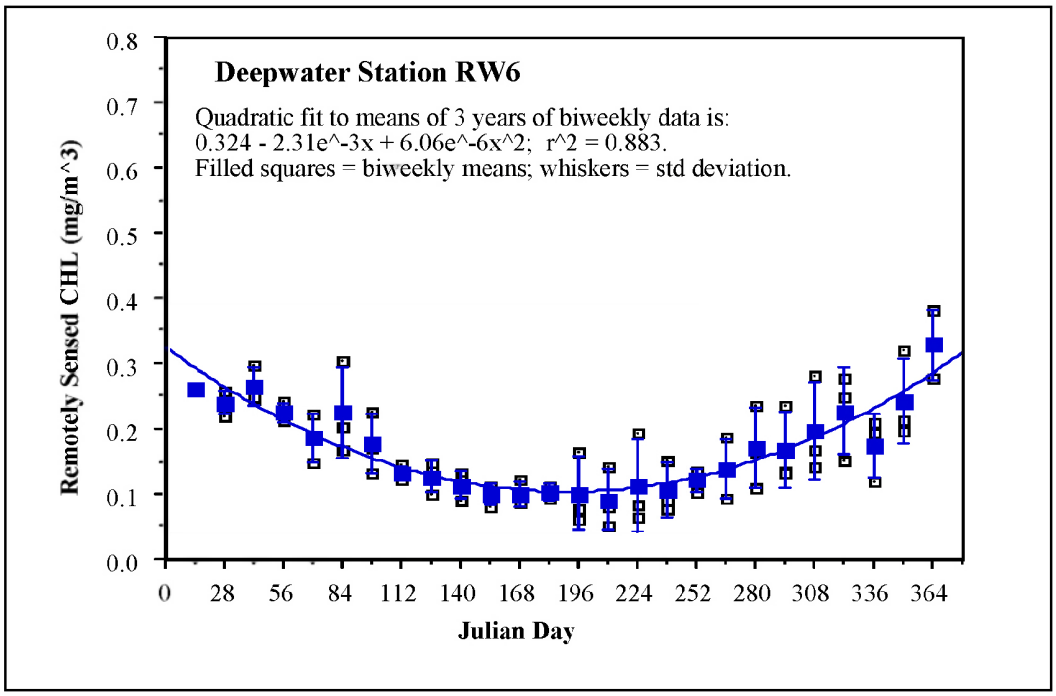

Figure 8-32. Top panel: Three-year climatology of biweekly averaged SeaWiFS ocean color data 1998-2000 at the six DGoMB stations along the Far West (RW) transect in the western GoM. Bottom panel: The annual cycle of chlorophyll at RW-6, the deepest of the six Far West stations.

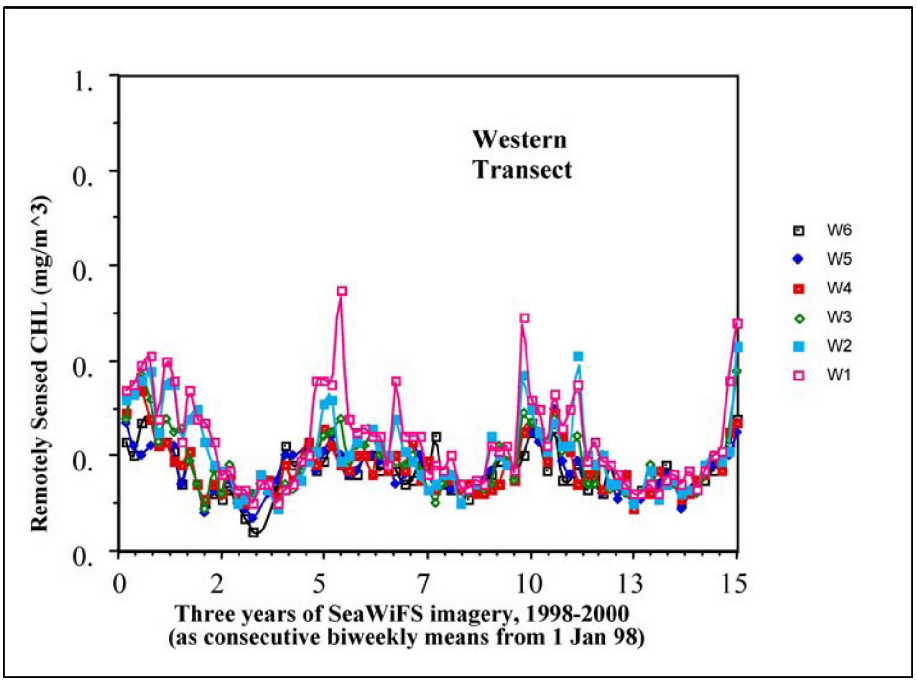

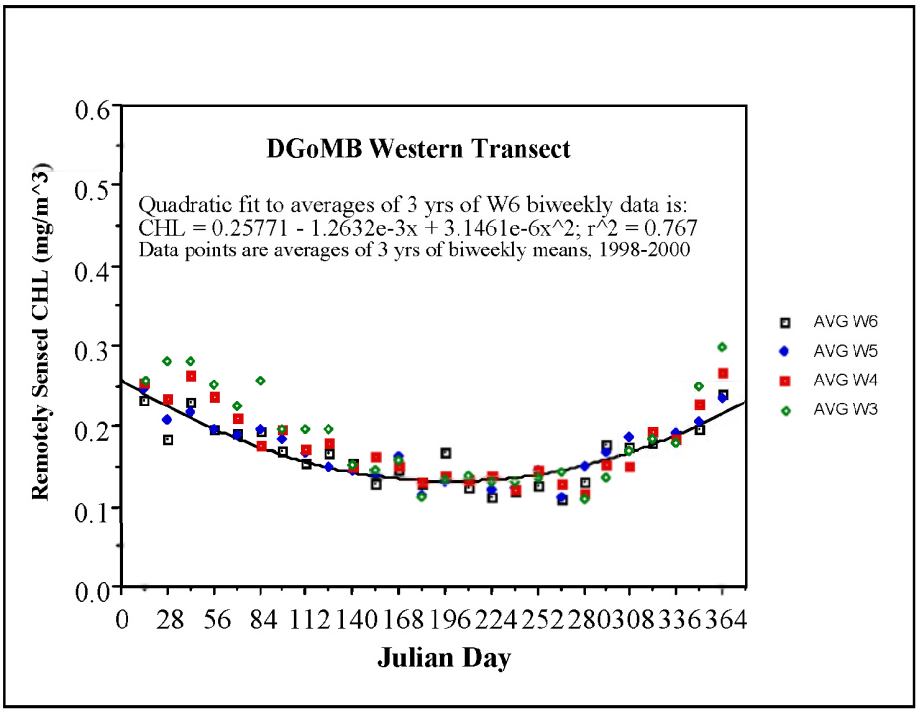

Figure 8-33. Top panel: Three-year climatology of biweekly averaged SeaWiFS ocean color data 1998-2000 at the six DGoMB stations along the Western (W) transect in the GoM. Bottom panel: The average annual cycle of chlorophyll at four of the Western stations.

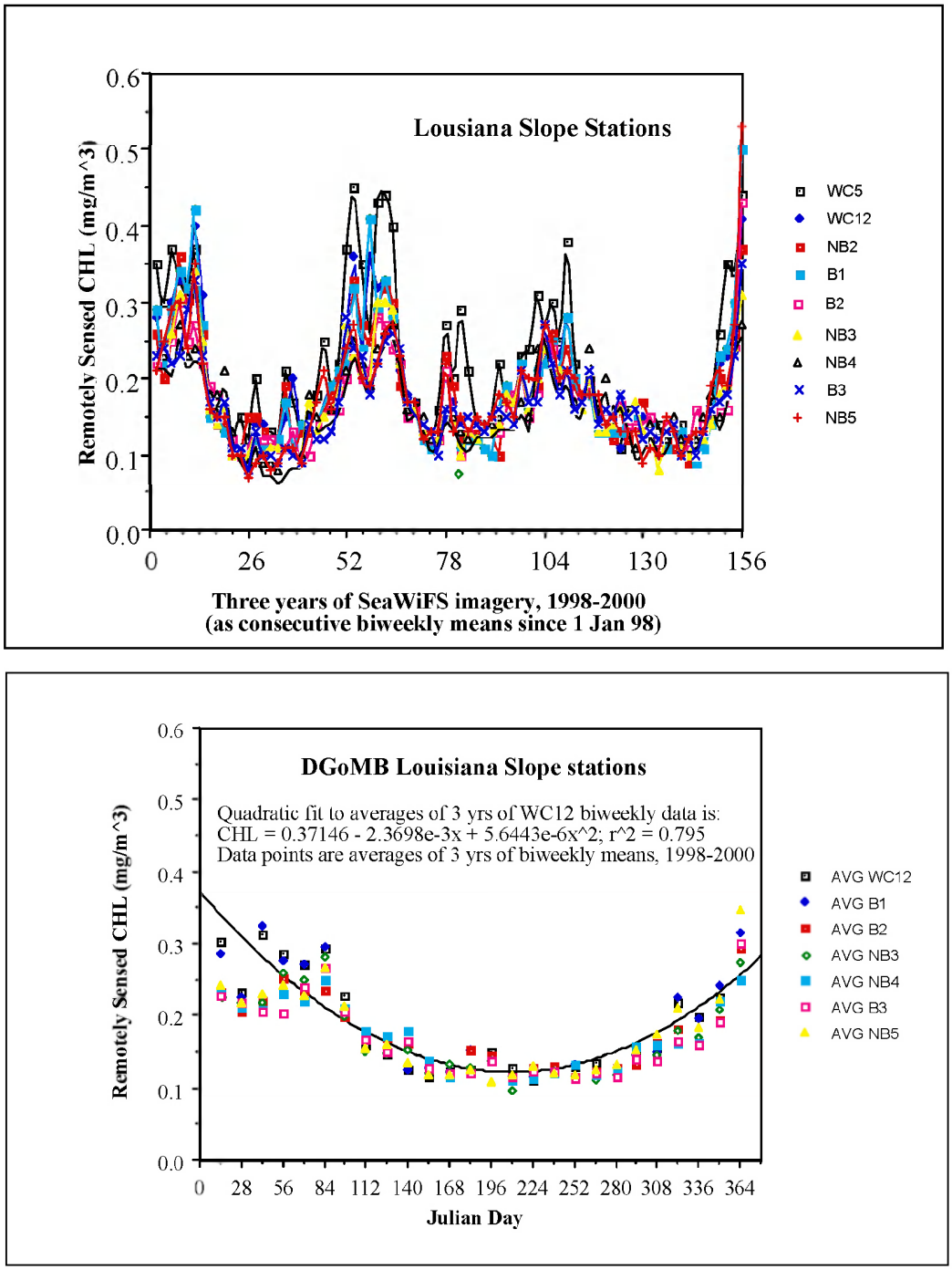

Figure 8-34. Top panel: Three-year climatology of biweekly averaged SeaWiFS ocean color data 1998-2000 at the nine WC, NB, and B DGoMB stations located between 93W and 91W over the Louisiana continental slope in the western GoM. Bottom panel: The average annual cycle of chlorophyll at the seven deepest of these Louisiana slope stations.

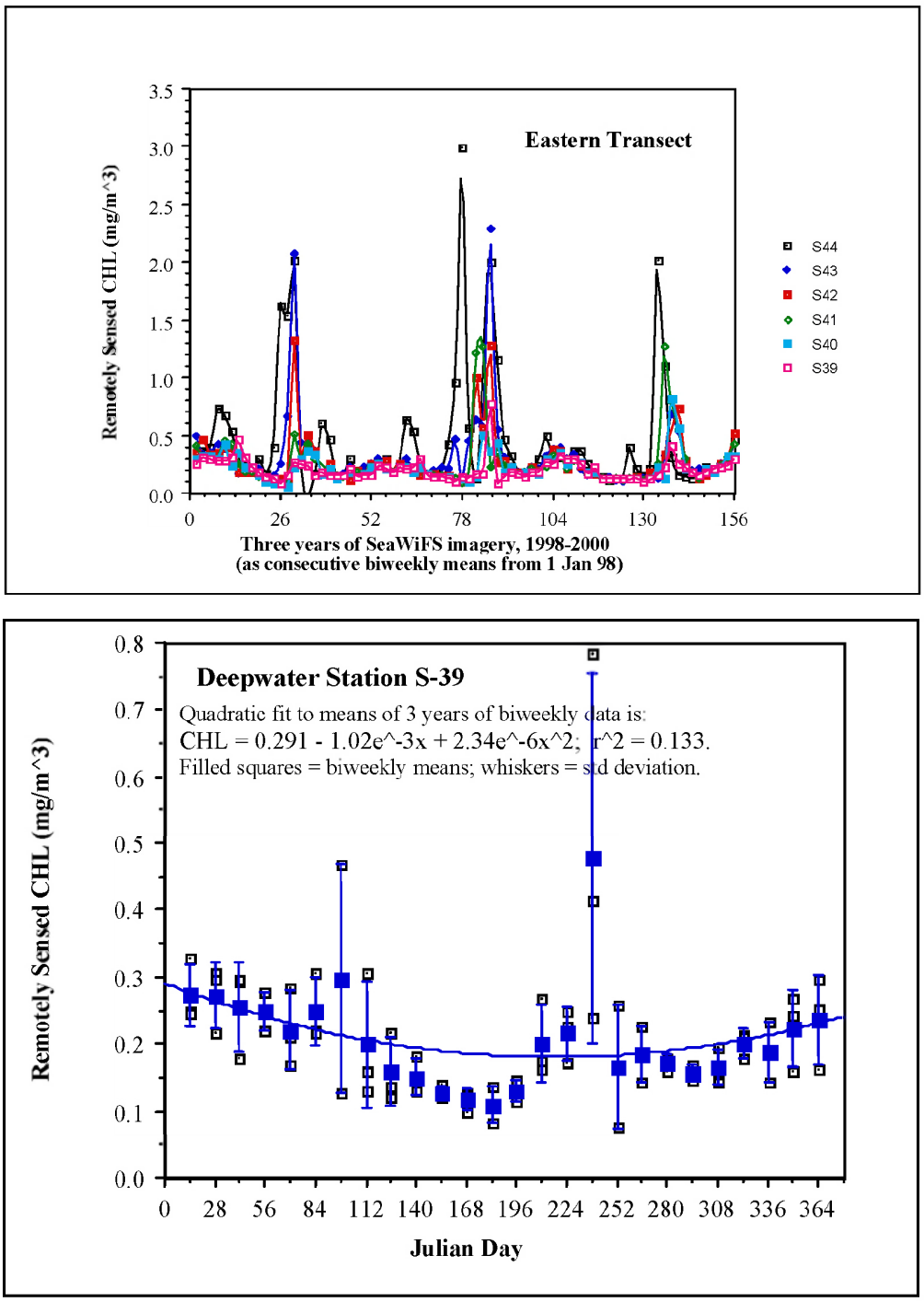

Figure 8-35. Top panel: Three-year climatology of biweekly averaged SeaWiFS ocean color data 1998-2000 at the six DGoMB stations along the Easternmost (S) transect in the eastern GoM. Bottom panel: The annual cycle of chlorophyll at S39, the deepest of the Eastern transect stations.

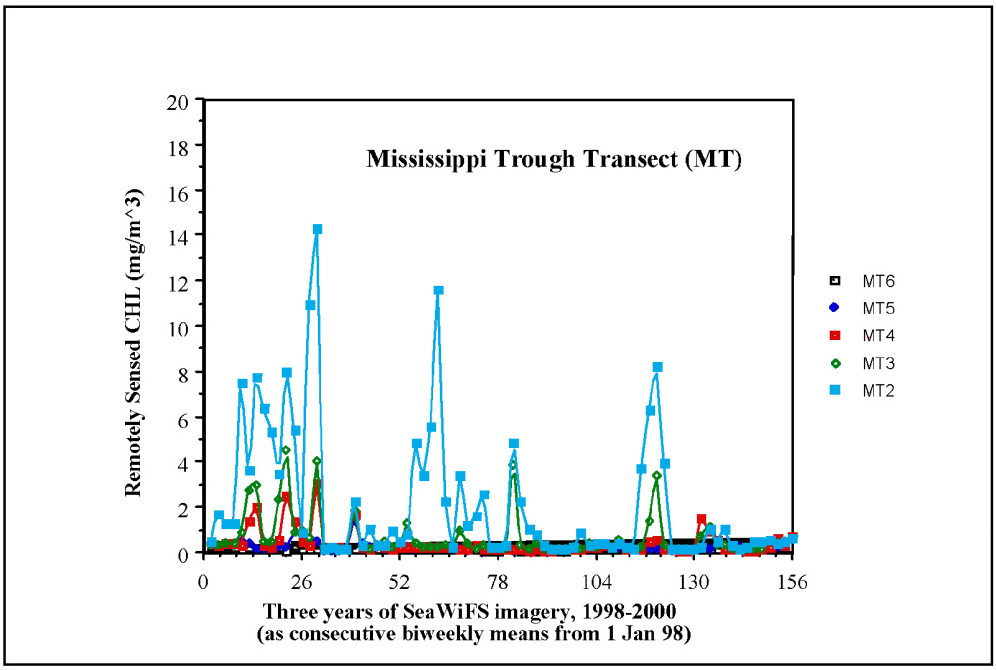

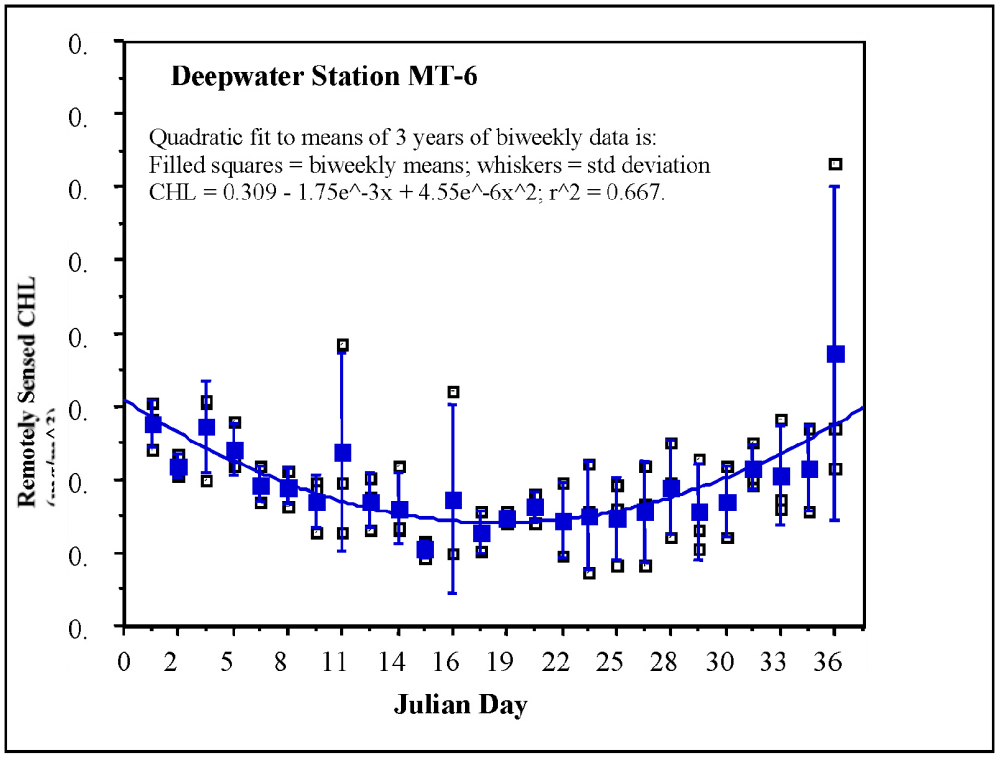

Figure 8-36. Top panel: Three-year climatology of biweekly averaged SeaWiFS ocean color data 1998-2000 at five DGoMB stations along the Mississippi Trough (MT) transect in the eastern GoM. Bottom panel: The annual cycle of chlorophyll at MT6, the deepest of these Mississippi Trough transect stations.

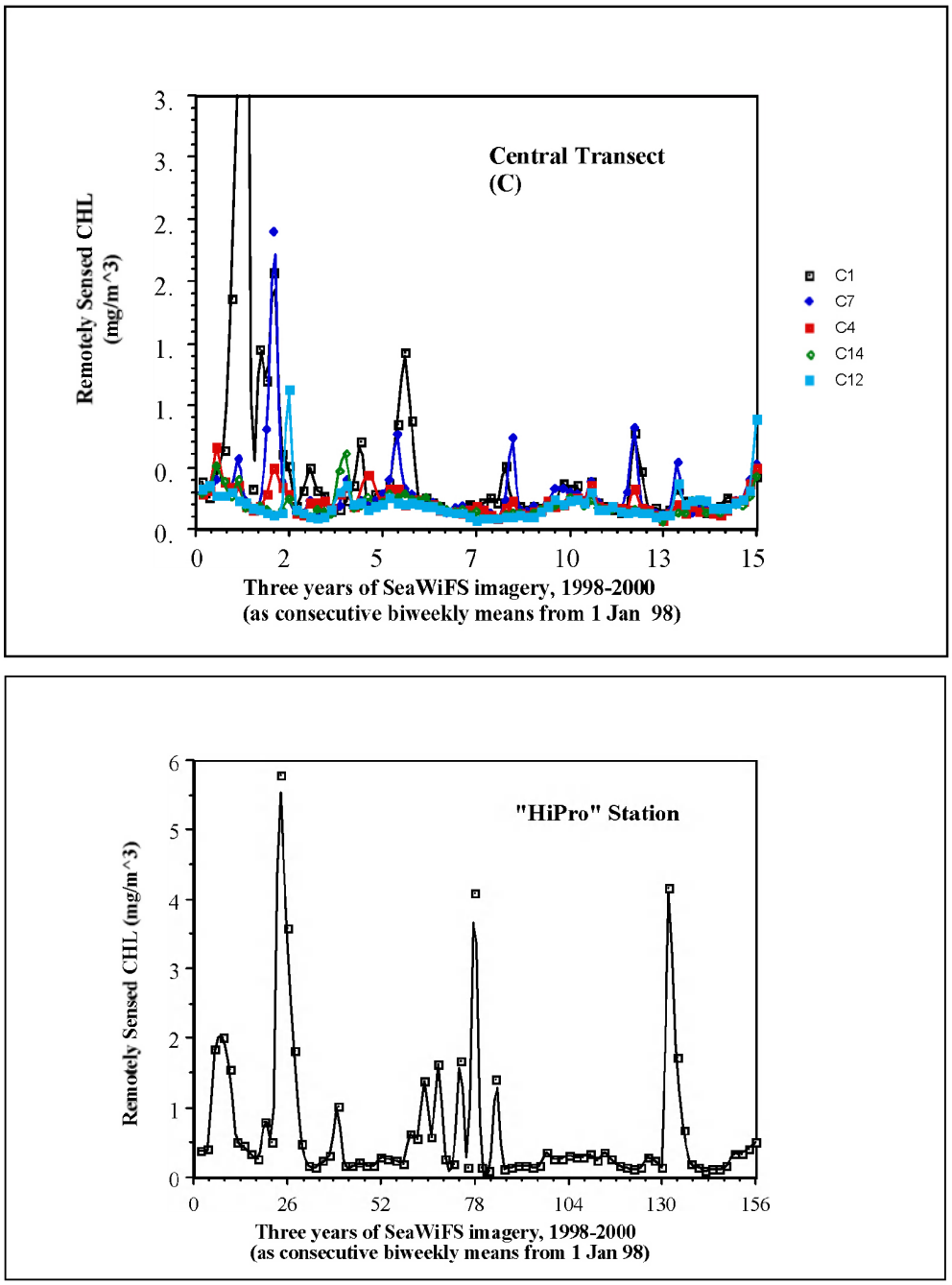

Figure 8-37. Top panel: Three-year climatology of biweekly averaged SeaWiFS ocean color data 1998-2000 at the five DGoMB stations along the central (C) transect in the eastern GoM. Bottom panel: Three-year climatology of biweekly averaged SeaWiFS ocean color data 1998-2000 at the high productivity (Hi-Pro) station in the eastern GoM.

Colored dissolved organic matter (CDOM) fluorescence and light absorption coefficient were also measured along with surface salinity and chlorophyll during the R/V *Gyre* NEGoM cruises conducted in 1998-2000. Strong correlations between the CDOM absorption coefficient (a_{g443}) and CDOM fluorescence (330 nm excitation and 450 nm emission filters) were consistently observed (Hu et al. 2003; Nababan et al. in review). Relatively high a_{g443} (≥ 0.1 m^{-1}) was generally observed inshore (inner shelf) near the major river mouths, but this a_{g443} decreased rapidly with distance from shore except when riverine waters were entrained and transported offshore by WSEs. Because CDOM as well as CHL contributes to the ocean color signal measured by SeaWiFS, we likely over-estimated CHL at some of the shallowest DGoMB stations (Hu et al. 2003). Specifically, the CHL spikes > 4 mg m^{-3} shown in Figure 8-36 for stations MT1 and MT2 close off the Mississippi River Delta may be overestimated by perhaps 50-100%. However, the relative synoptic patterns as well as the relative temporal variation patterns should remain valid.

8.4 Geology

Two hundred and forty-five cores, 30 to 35 cm in length, were recovered from 43 stations during the survey in 2000. Each core was analyzed at 1 cm intervals for bulk density, porosity, water content, p-wave velocity, void ratio, and impedance. That analysis resulted in 48,500 individual measurements of geotechnical properties available in the database. All cores were split and photographed and shear strength measurements were attempted but the surficial sediments have shear strengths lower than our instruments could measure. Grain size was determined from the subsample at the sediment-water interface.

8.4.1 Sediment Texture—Grain Size Distributions

The sediments of the deep northern GoM were found to be composed primarily of silt and clay, with variable fractions of sand (Figure 8-39 and Figure 8-40), in general agreement with previous studies (Balsam and Beeson, 2003). The sand fraction is derived almost entirely of planktonic foram tests from the overlying water column and ranges from 0.5 up to 63% by weight. The percent sand is reduced in the sediments of the upper continental slope nearshore in the western GoM because of the high loading of Mississippi River-derived material. The lowest value was at MT1 in the Mississippi Canyon head that is notched into the continental shelf just off the river's debouchment into the Gulf's open waters. The percent sand was also somewhat lower at the abyssal plain sites because of carbonate dissolution due to cold and pressure. The highest sand fractions were at intermediate depths (1 km to 3 km) of the continental slope, at sites in the eastern GoM (S sites, 29.8%, σ=16.1, n=7), whereas generally low values were measured along the entire RW transect in the extreme west of the study area (4.9%, σ=2, n=5). The sediments west of DeSoto Canyon can be considered terrigenous lutite with some carbonate sand, whereas the sediments east of the axis of DeSoto Canyon can be considered primarily foram-derived carbonate composed of more or less equal fractions of sand, silt and clay. This east-west pattern agrees with the "weight % carbonate" distribute map of Balsam and and Beeson (2003). The central GoM is dominated by the Mississippi Fan or Cone of sediments that extends seaward and downslope from the delta region. The four shallow sites sampled along the axis all had some of the lowest sand fractions (1.48%, σ=0.95, n=5), but the two deepest were some of the highest values (23.4%, σ=17, n=4). The "basins" on the "Texas Louisiana Slope" had less sand than non-basin sites (3.1 vs. 9.5%), but, as will be seen in later sections (8.8 on "benthic biology" in particular), there was no biological evidence that basins were different from

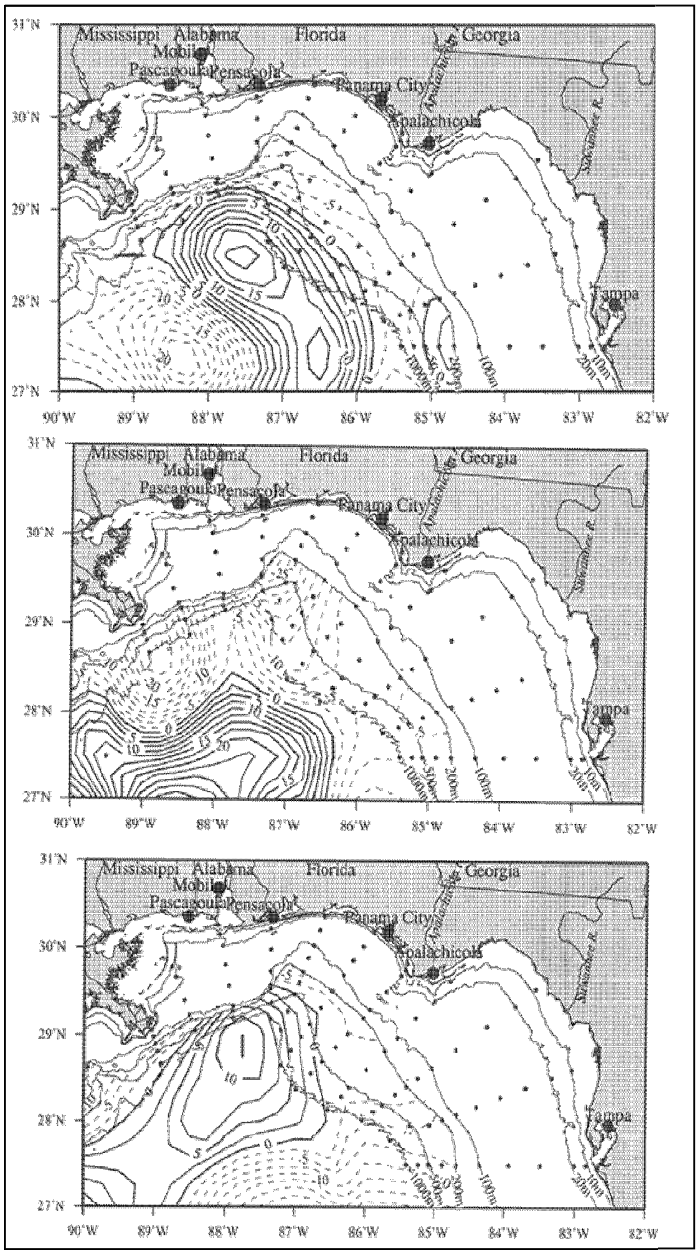

Figure 8-38. Sea-surface height (SSH) maps compiled by the University of Colorado, showing the location of warm slope eddies (positive SSH anomalies) in the eastern GoM in summers 1998-2000. Dots mark the location of hydrographic stations occupied on each of three summertime NEGoM cruises. Top panel: Cruise N3 (25 Jul-9 Aug 1998); Middle panel: Cruise N6 (15-28 Aug 1999); Bottom panel: Cruise N9 (29 Jul-8 Aug 2000). All from Belabbassi et al (in review).

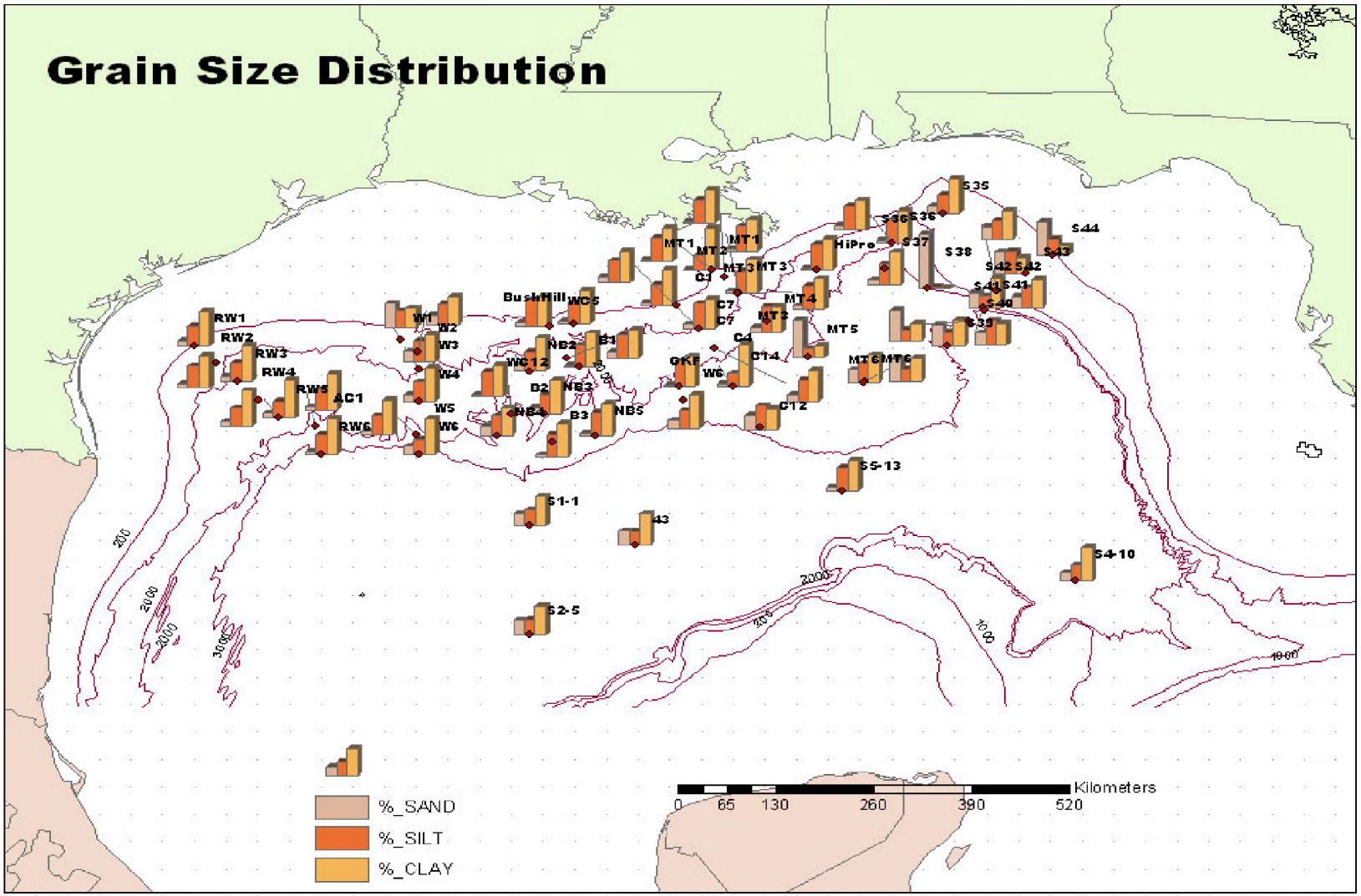

Figure 8-39. Percent sand, silt and clay at each site.

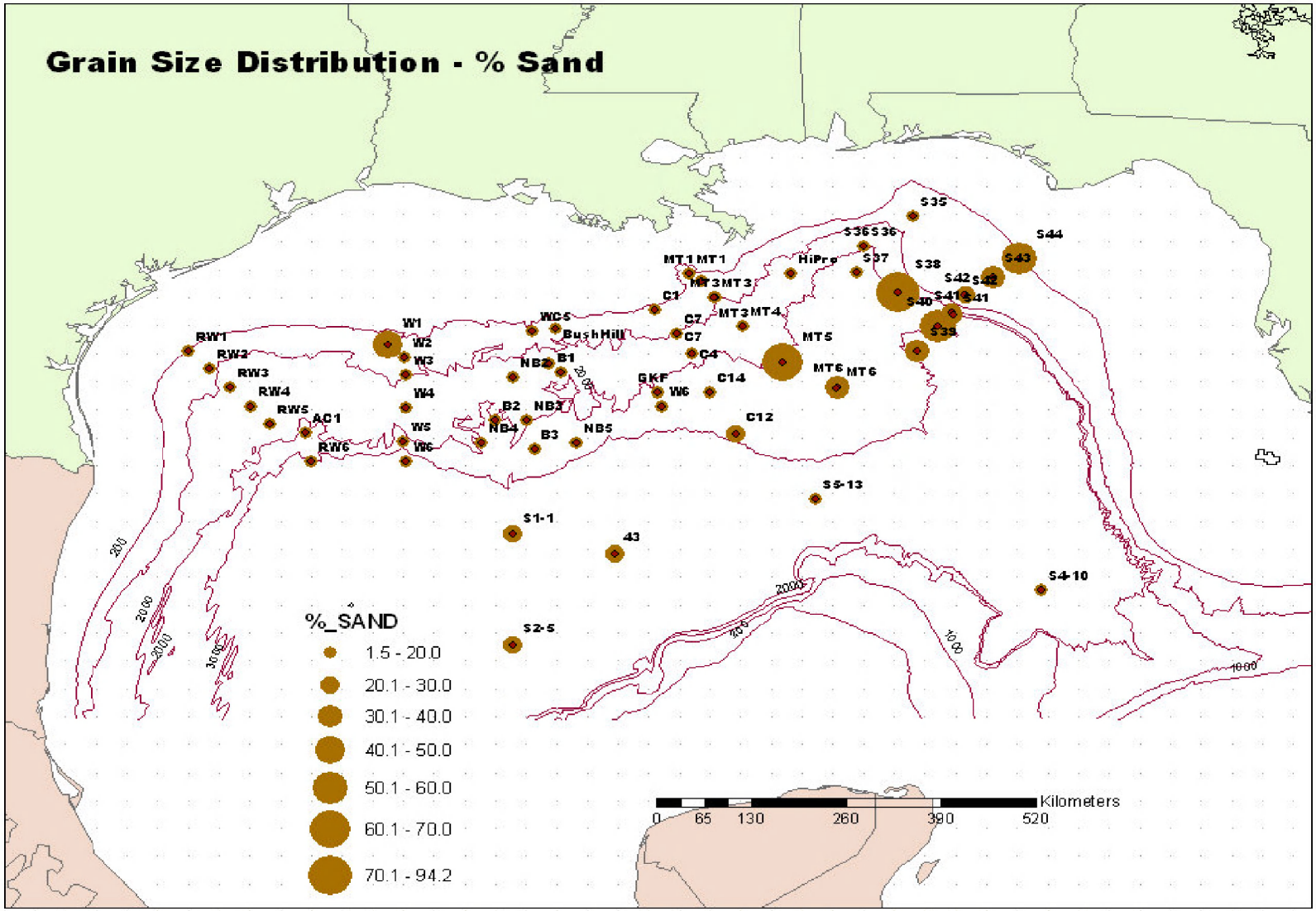

Figure 8-40. Relative amounts of percent sand at each site.

adjacent non-basin habitats. The lone area where material larger than sand-sized was encountered was in the "iron stone" region of the mid-to-lower Mississippi Fan (MT 5 and 6), where cobble-sized reddish-colored sedimentary rocks were common features in box cores, bottom photographs and trawls.

8.4.2 Sediment Physical Properties

An example of the physical properties is illustrated in Figure 8-41. All five cores at Location NB3 had very similar measurements between the geotechnical properties and depth within the cores. In contrast to that uniformity at NB3, the cores recovered at C7 display a wide variation in properties with depth within each core (Figure 8-42). The location of sites that have large variations in geotechnical properties between cores taken at the same location are shown in Figure 8-43. The uniformity in shear strength, porosity and composition suggest that deposition has been uniform and continuous with little alteration by exogenous processes. On the other hand the wide spread in such properties indicates that deposit over time has been altered or interrupted by biological or physical processes over time. Resuspension and redeposition are a possibility as is biological reworking, as noted below.

8.4.3 Indications of Bioturbation

All cores were examined for the degree of bioturbation that the sediments had experienced. Figure 8-44 is a photograph of a split core taken at W4, where the sediment had undergone very little to no bioturbation. In contrast, the core from MT5 (Figure 8-45) illustrates a high degree of bioturbation. A core from Location RW5 (Figure 8-46) illustrates sediment that has undergone slight to moderate bioturbation. Figure 8-47 illustrates the bioturbation encountered at all locations in cores from the year 2000 survey. There was a very distinct and significant boundary between sediments consisting of slight to no bioturbation and those that were highly bioturbated.

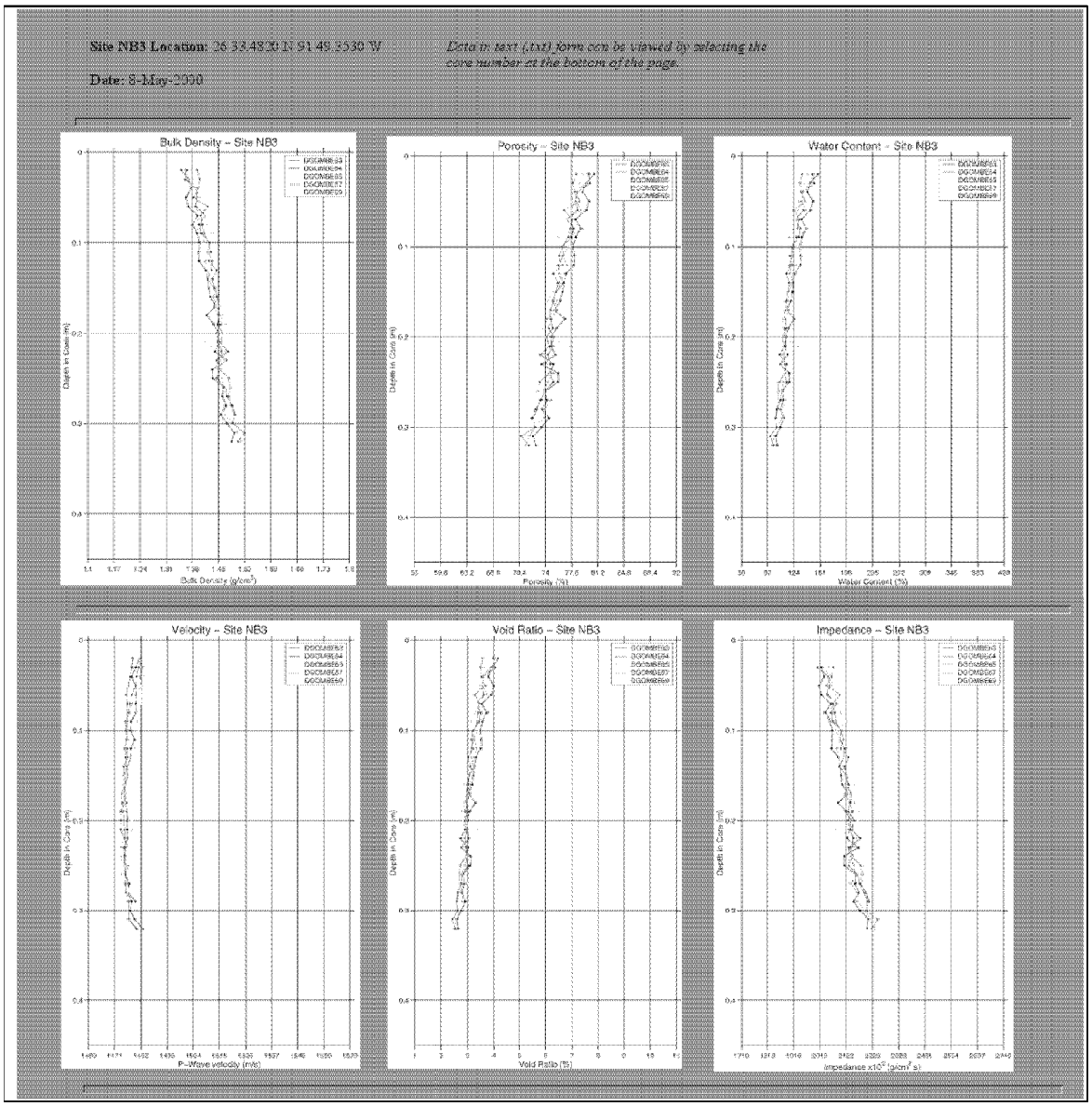

Figure 8-41. The sediment geotechnical properties of cores (5 replicates) taken at the NB3 location. Note the compact arrangement of the various properties with depth in the core that indicate uniform physical properties.

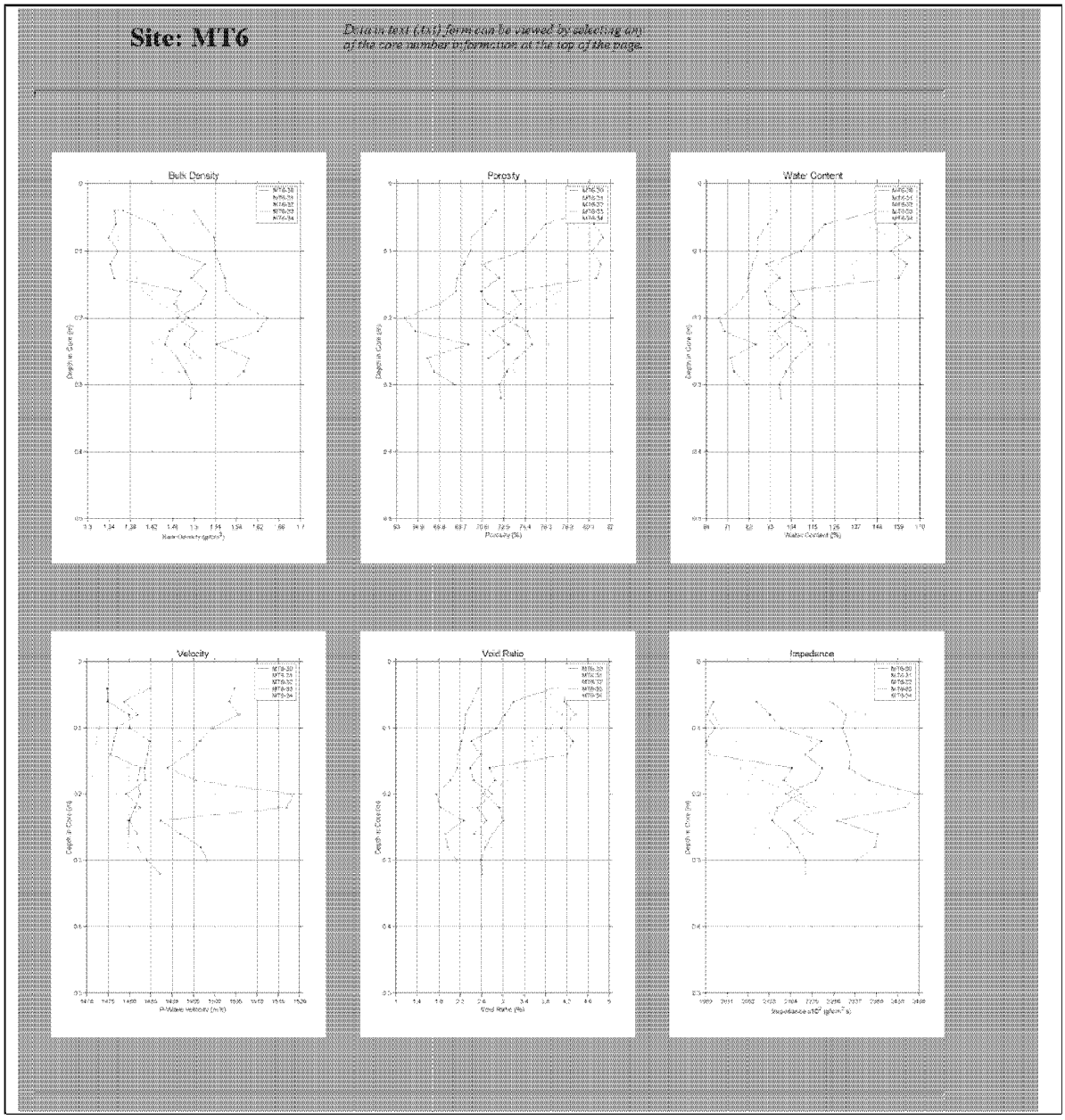

Figure 8-42. The sediment geotechnical properties of cores (5 replicates) taken at the MT6 location. Note the dispersed properties with depth that indicate a wide variety of sediment types at location MT6.

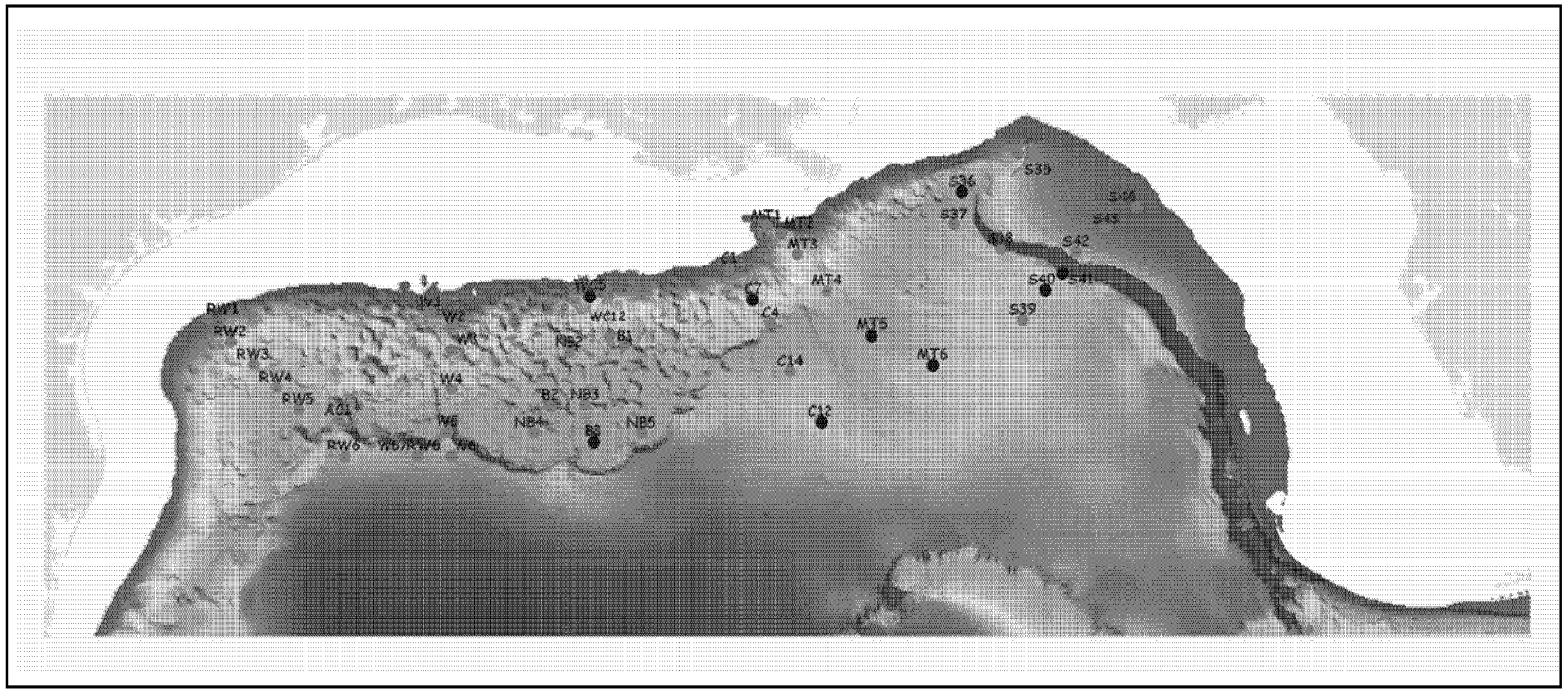

Figure 8-43. Map showing the locations of the stations that have highly variable geotechnical properties.

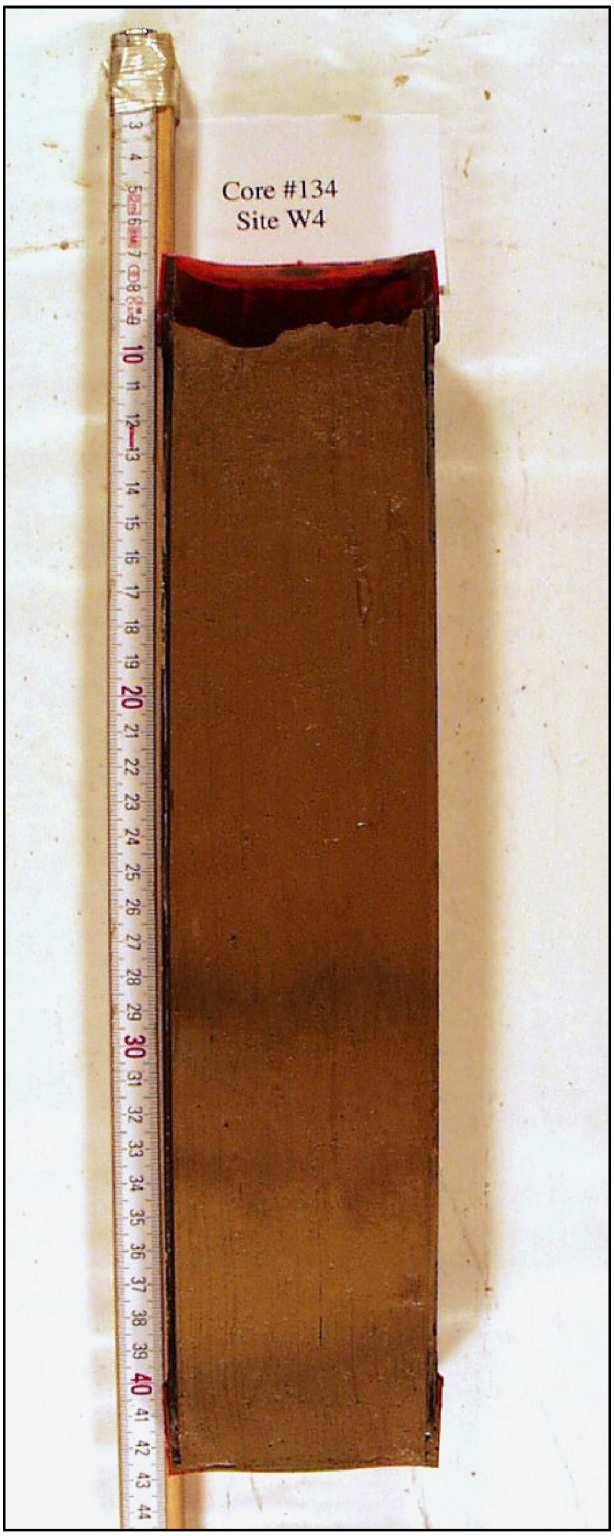

Figure 8-44. Boxcore 134 at station W4 illustrating sediment that has almost no sediment bioturbation.

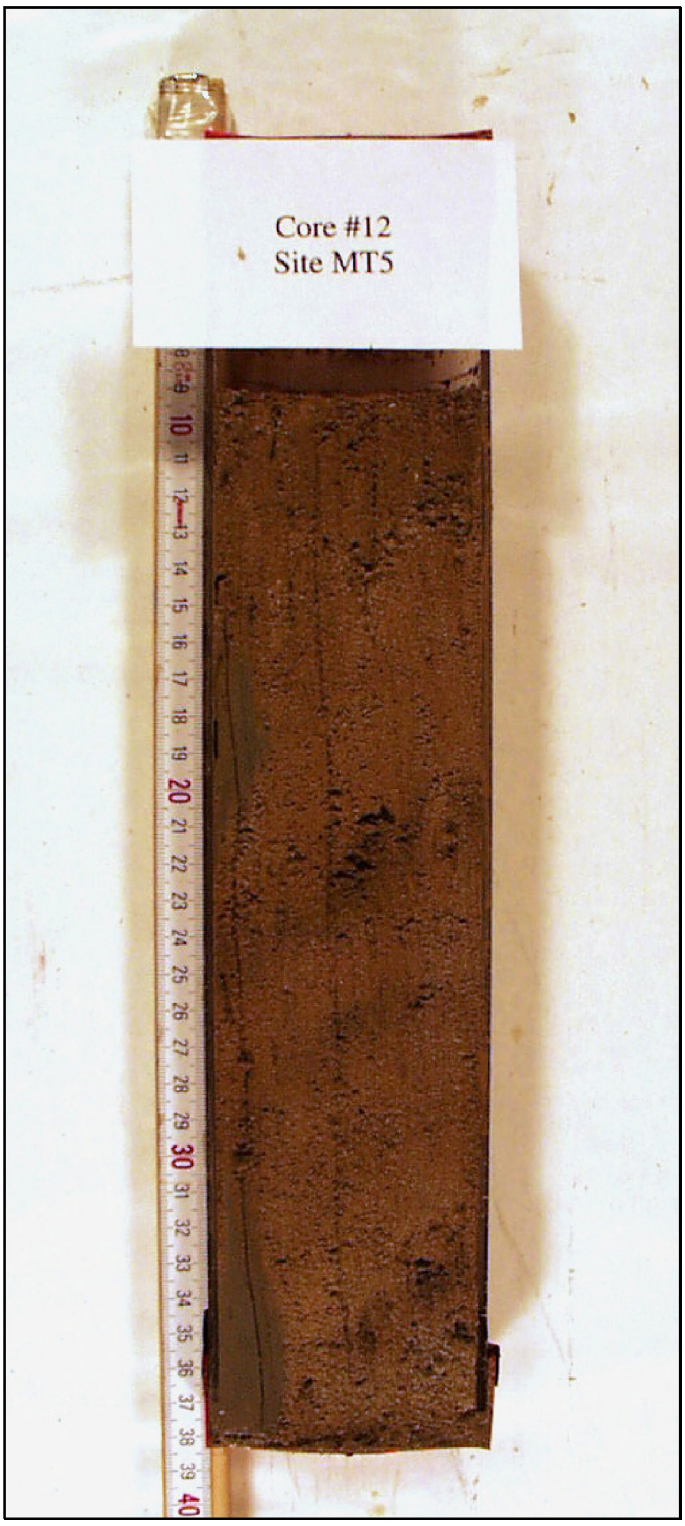

Figure 8-45. Boxcore 12 at station MT5 illustrating sediment that has undergone a high degee of bioturbation.

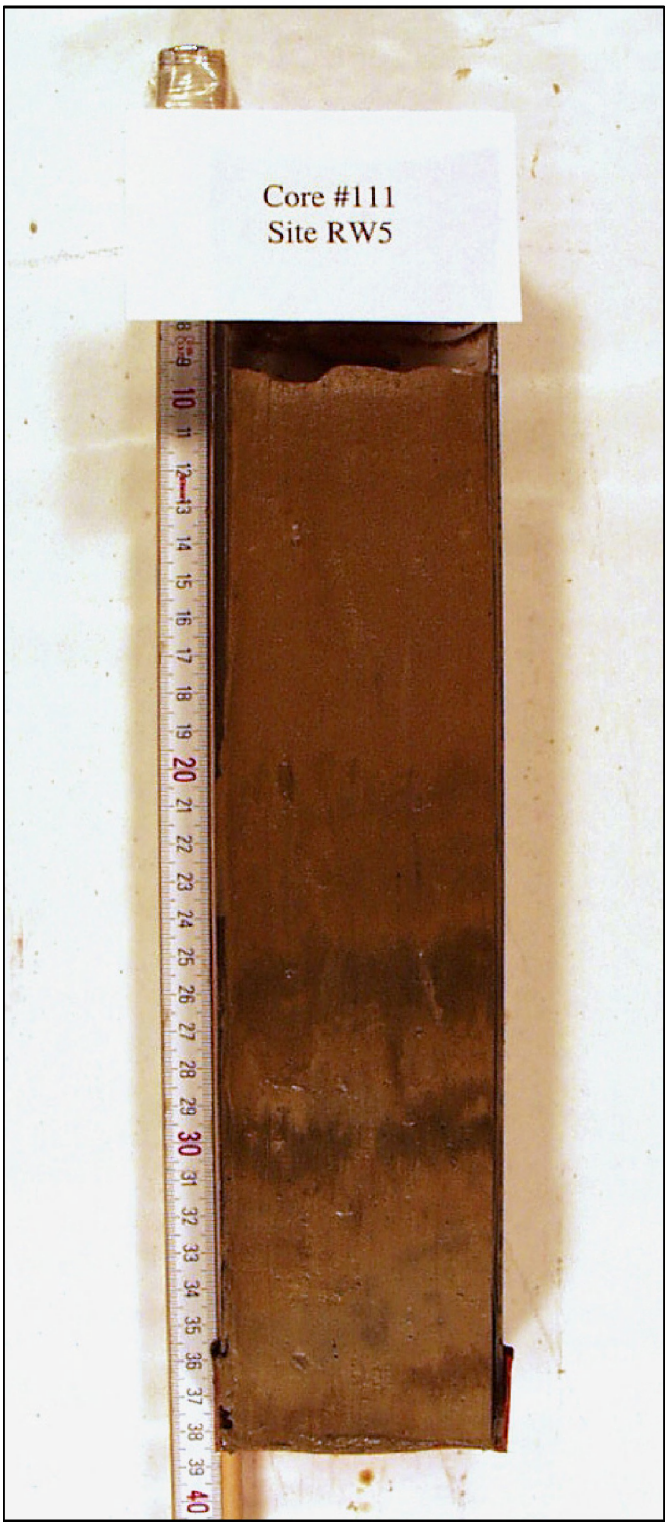

Figure 8-46. Boxcore 111 at station RW5 illustrating a low degree of bioturbation.

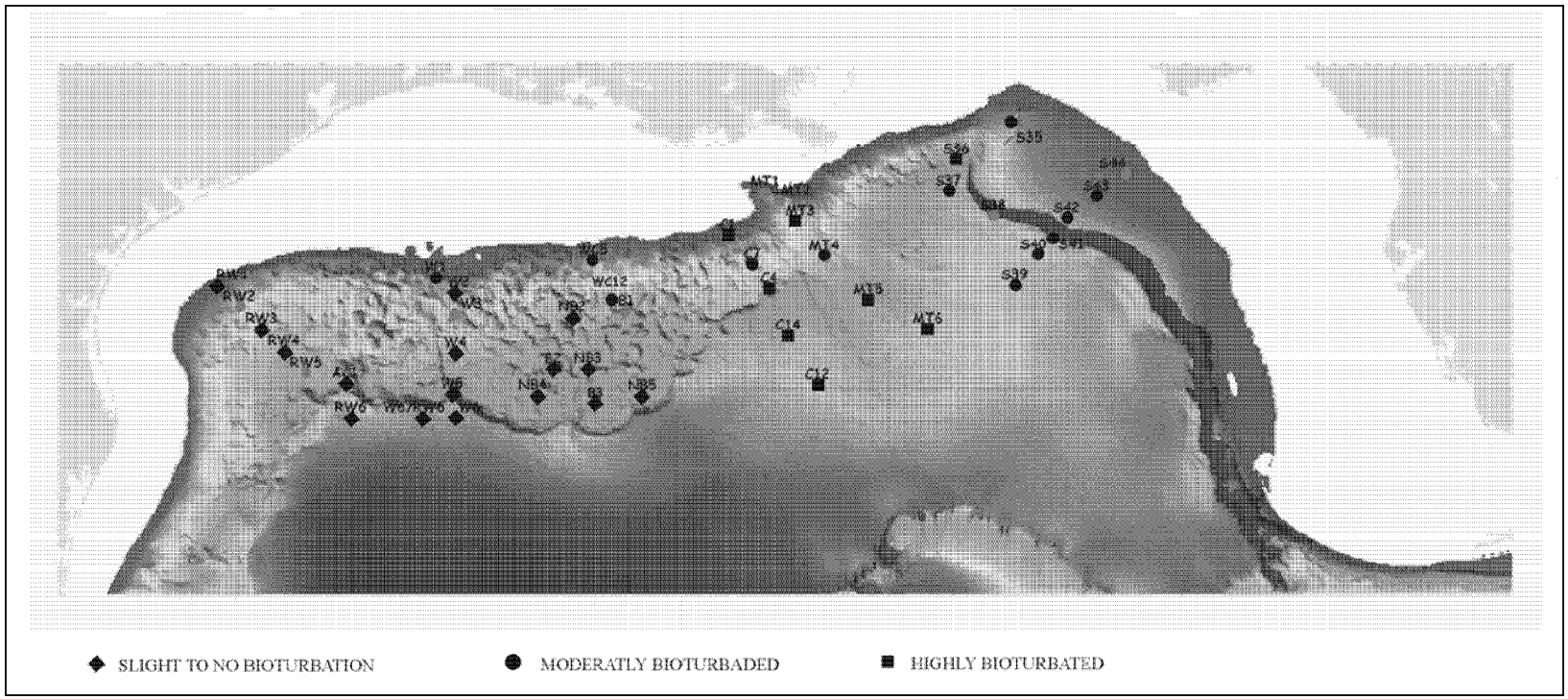

Figure 8-47. Map showing the degree of sediment bioturbation present at the survey sites.

8.5 Biogeochemistry

The geochemistry component measured a range of relevant sedimentary parameters at both survey and experimental sites. Surface sediments were analyzed at the survey sites and detailed profiles were measured at experimental sites. Various geochemical properties were measured on pore waters and solid phases. Analyses that were best performed immediately after sample retrieval were conducted onboard, whereas other analyses, which require more time consuming methods, were performed at shore-based facilities.

8.5.1 Bulk Sediment Organic Carbon and Nitrogen

The percent organic carbon data for survey stations are shown in Figure 8-48. The highest values were measured on the Florida slope region, but there were no obvious trends with either water depth or across an east-west gradient. Values were in the range reported for oceanic sediments in non-upwelling regions. Similarly, the C:N data, which ranged from <7 to 10 (Figure 8-49), did not display uniform geographical trends. The values measured, however, were in the range reported for northern Gulf of Mexico shelf sediments (Bianchi et al., 2002; Gordon and Goni, 2003) and suggestive of predominantly marine organic matter. The isotopic data discussed for stations MT1, MT2 and MT3 support this observation.

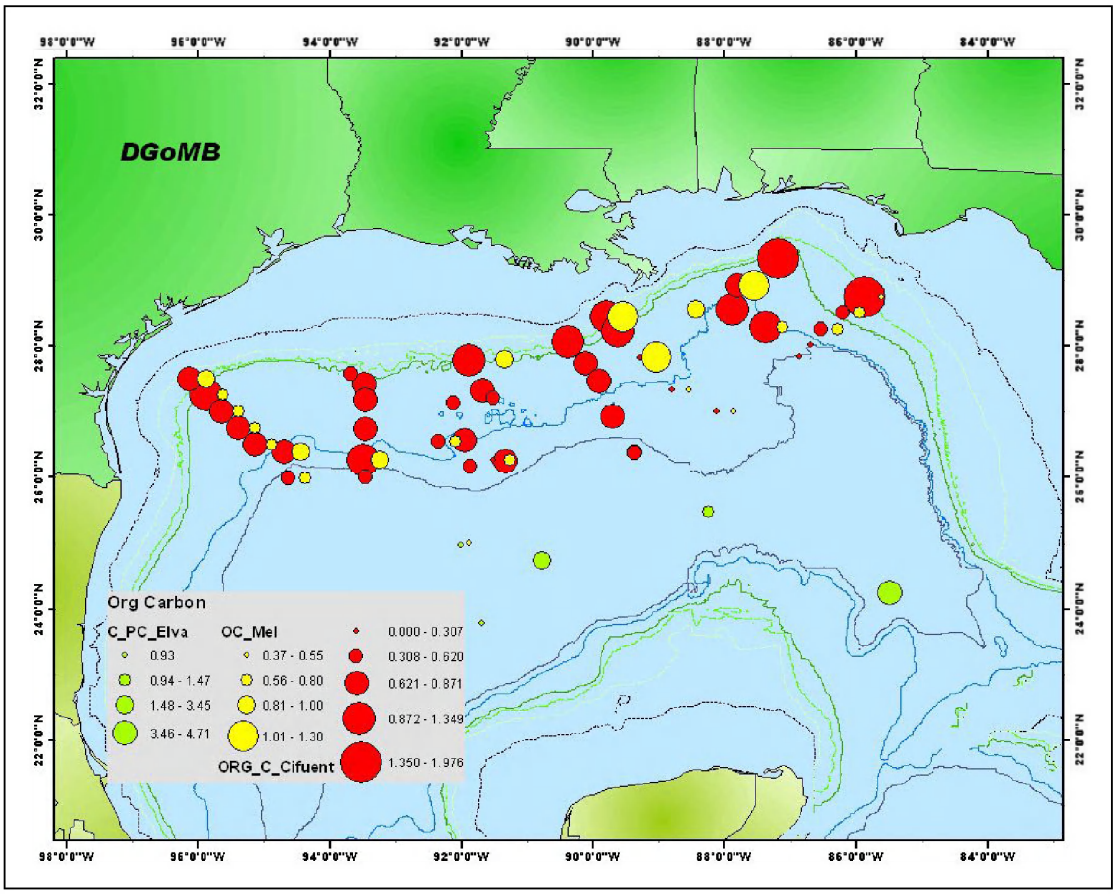

Figure 8-48. Percent organic carbon data for survey stations.

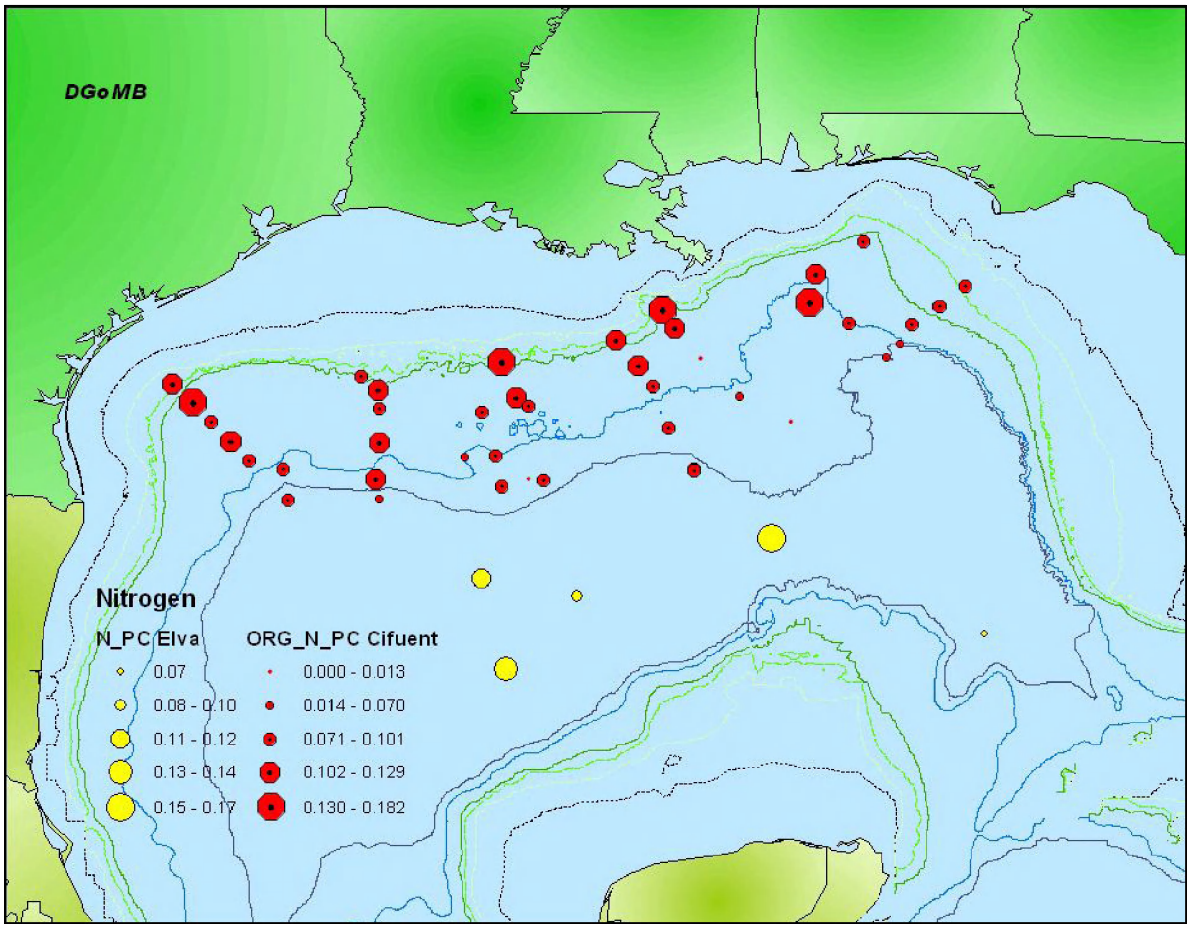

Figure 8-49. Sediment organic carbon and nitrogen. Top: three sets of organic carbon data from, UNAM (abyssal plain) and TAMU (continental margin); bottom: two sets of total sedimentary nitrogen data, analyzed at UNAM (yellow) and TAMU (red).

8.5.2 Sediment Profiles of Organic Carbon

Profiles of organic carbon were generated for the process sites (Yaeger et al. 2004), as provided in (Figures 8-50 to 8-55). They illustrate that maximum values of approximately 1.5% were consistently encountered in the Mississippi Canyon (MT3, 1,000 m depth) surface sediments, which declined to ca. 1% at about 10 to 15 cm depth into the sediments. In the DeSoto Canyon, in somewhat deeper water (1,850 m), the values were slightly less in the top layers (0.8 to1.2%). These too declined with depth into the sediments down to ca. 0.6 to 0.8%. The deep aspects of the Mississippi Canyon line (MT6, 2,750 m) presented no vertical pattern, with values ranging from 0.4 to 0.6%, and one deep outlier of 1.4%. [Recall in Section 8.4 that the deep half of the MT had highly variable physical properties, suggesting physical mixing, variable deposition and/or intense bioturbation.] On the abyssal plain at the western most process station (JSSD1 or S1) the values ranged from 0.1 up to 0.8%, but all the points together on average illustrate a decline from ca. 6% at the surface down to ca. 0.2 to 0.3% at a depth of 15 cm. At the eastern and southern-most site (JSSD4, S4), the values had much the same range (1.5 to 5%), but the values did not follow a consistent decline with depth. The maximum of 5% was

encountered at about 5 cm down into the sediment, with what appeared to consistent declines both above and below that. The last panel from the upper Florida slope (S42, 740 m depth) indicates a sharp decline from 8% at the surface down to 4.5% at less than 4 cm into the sediment, followed by no decline over the next 10 to 15 cm.

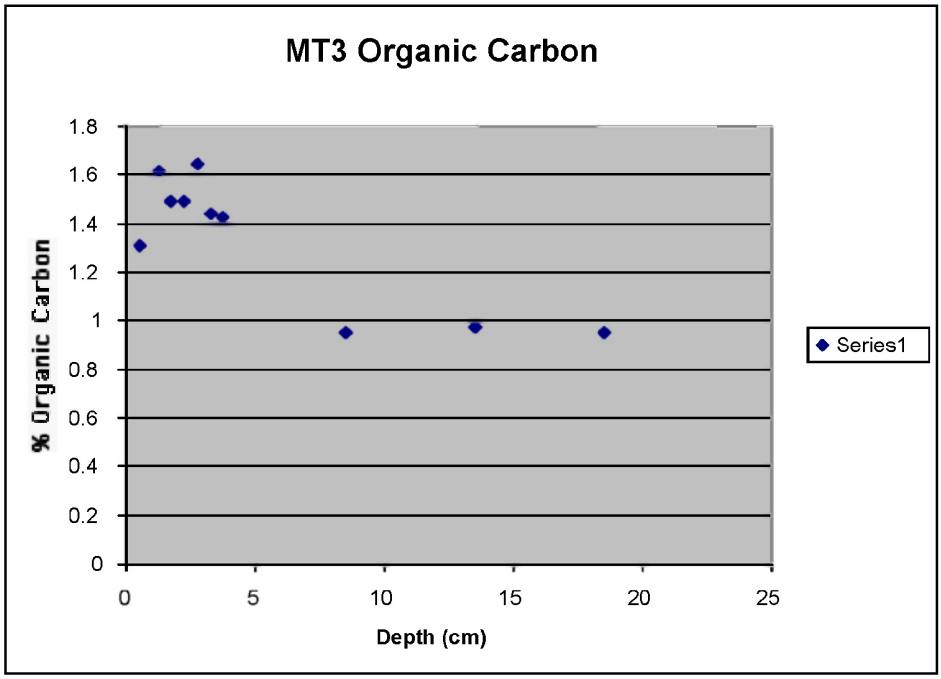

Figure 8-50. Profiles of organic carbon.

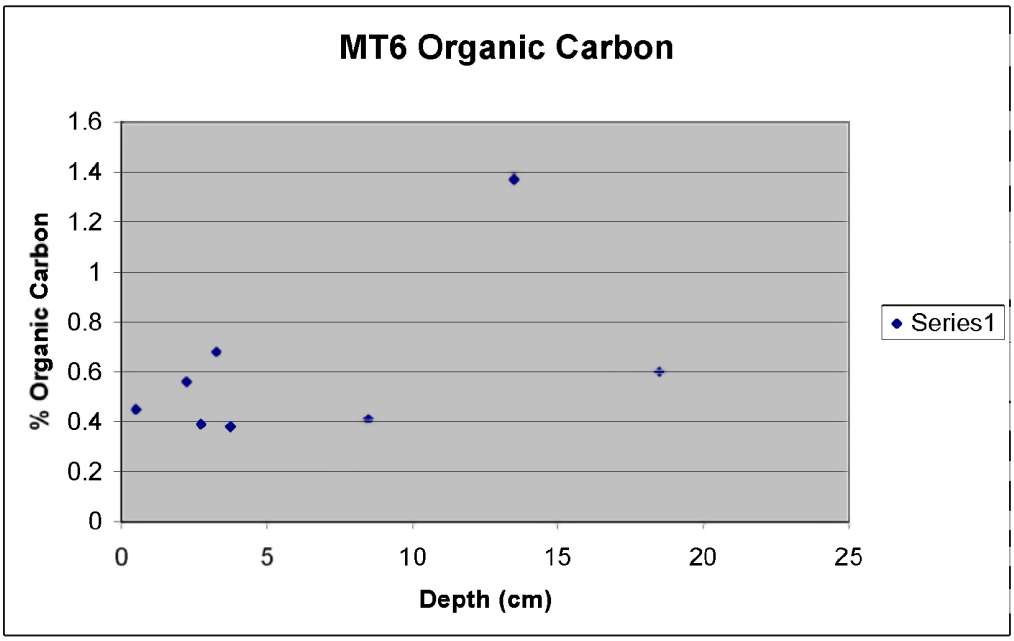

Figure 8-51. Profiles of organic carbon MT6.

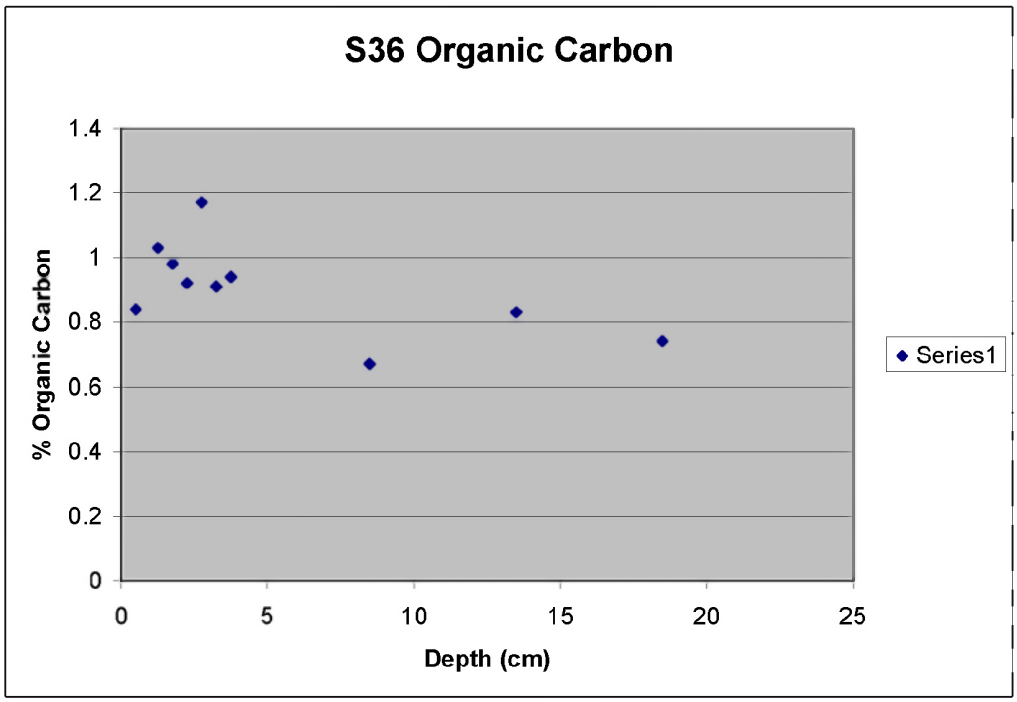

Figure 8-52. Profiles of organic carbon S36.

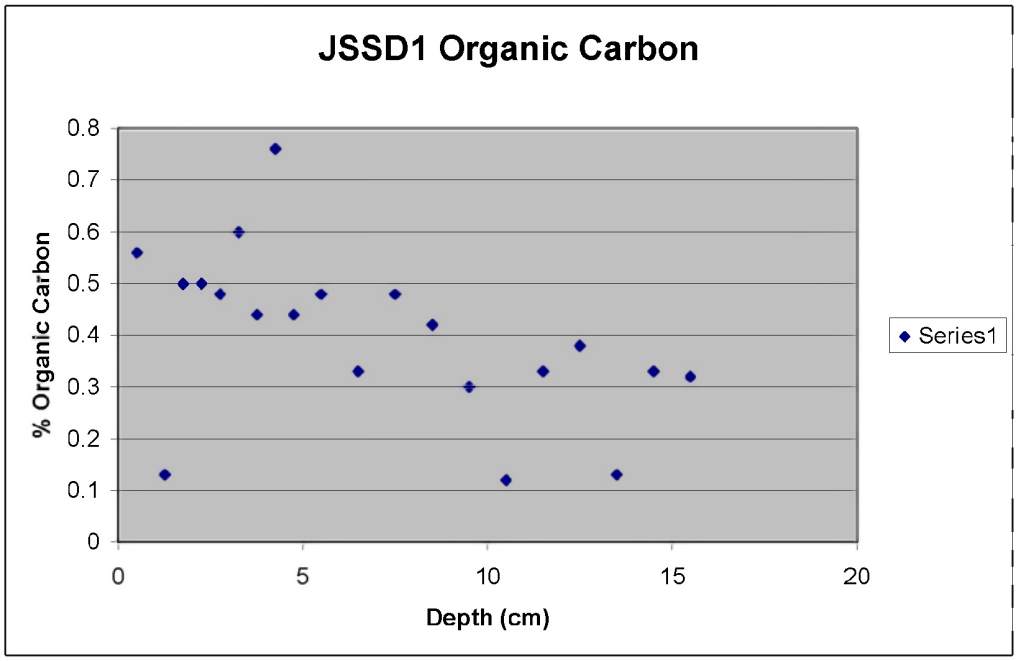

Figure 8-53. Profiles of organic carbon JSSD1.

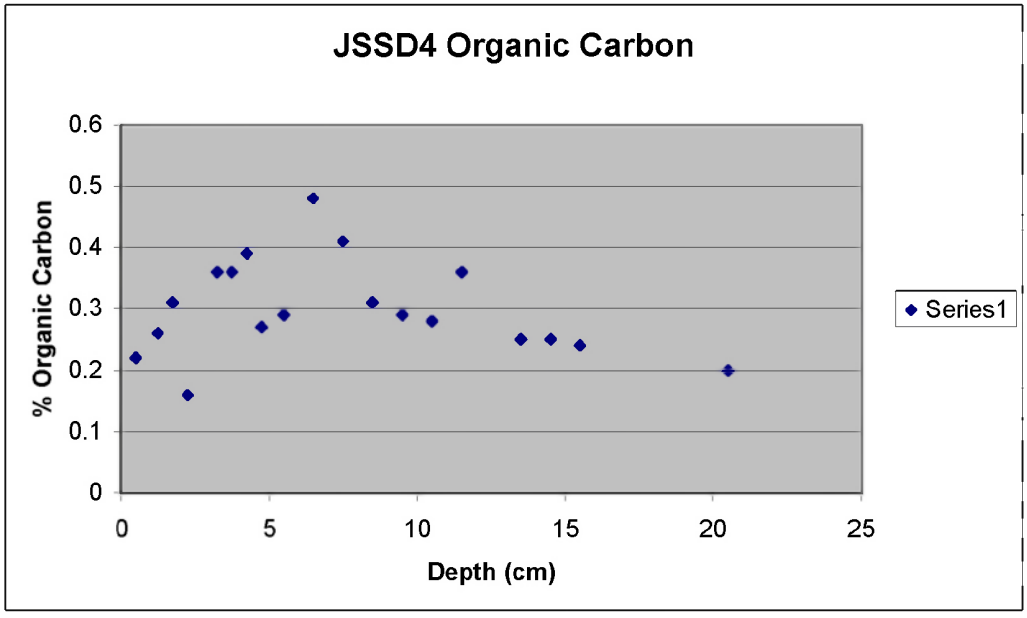

Figure 8-54. Profiles of organic carbon JSSD4.

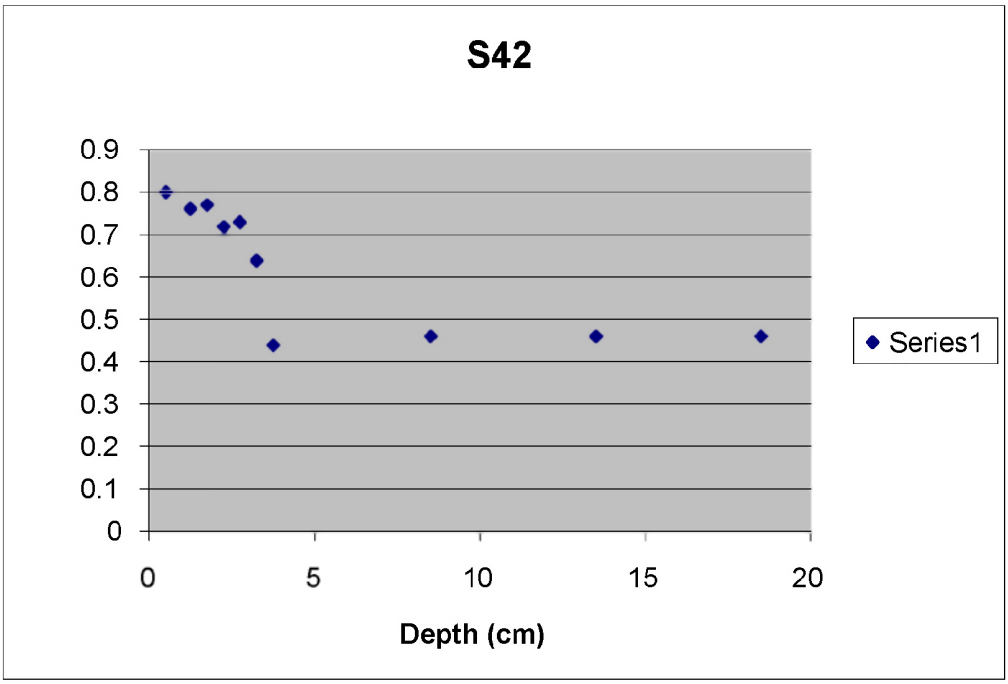

Figure 8-55. Profiles of organic carbon S42.

8.5.3 Dissolved Organic Carbon (DOC)

Dissolved organic carbon (DOC) data for centrifuged samples from 10 sites are shown in Figure 8-56. Mean values ranged from 5 to 20 mgC L^{-1}, and were well within the range reported for porewater concentrations at similar depths in North Carolina continental slope sediments by Alperin et al. (1999). The mean DOC concentrations were quite variable among these stations, as were the standard deviations. Values appeared to be lower at stations GKF and MT6, which were two of the deepest stations. There was, however, no obvious trend with water depth.

The DOC data for six experimental stations are also shown in Figure 8-56. It must be noted that the concentrations measured in surface sediments by whole squeezing at stations MT3, MT6, S36, S42 were consistently higher than those measured for centrifuged samples (Figure 8-56). Alperin et al. (1999) noted higher values for centrifuged samples compared with data acquired by sippers. Both comparisons suggest sample handling alters the DOC concentrations as has been reported previously (e.g., Martin and McCorkle 1993). Depth profiles for DOC (Figure 8-56) showed an increase with depth at all sites. The concentrations measured and trends observed with core depth were consistent with those reported for North Carolina continental slope sediments by Alperin et al. (1999).

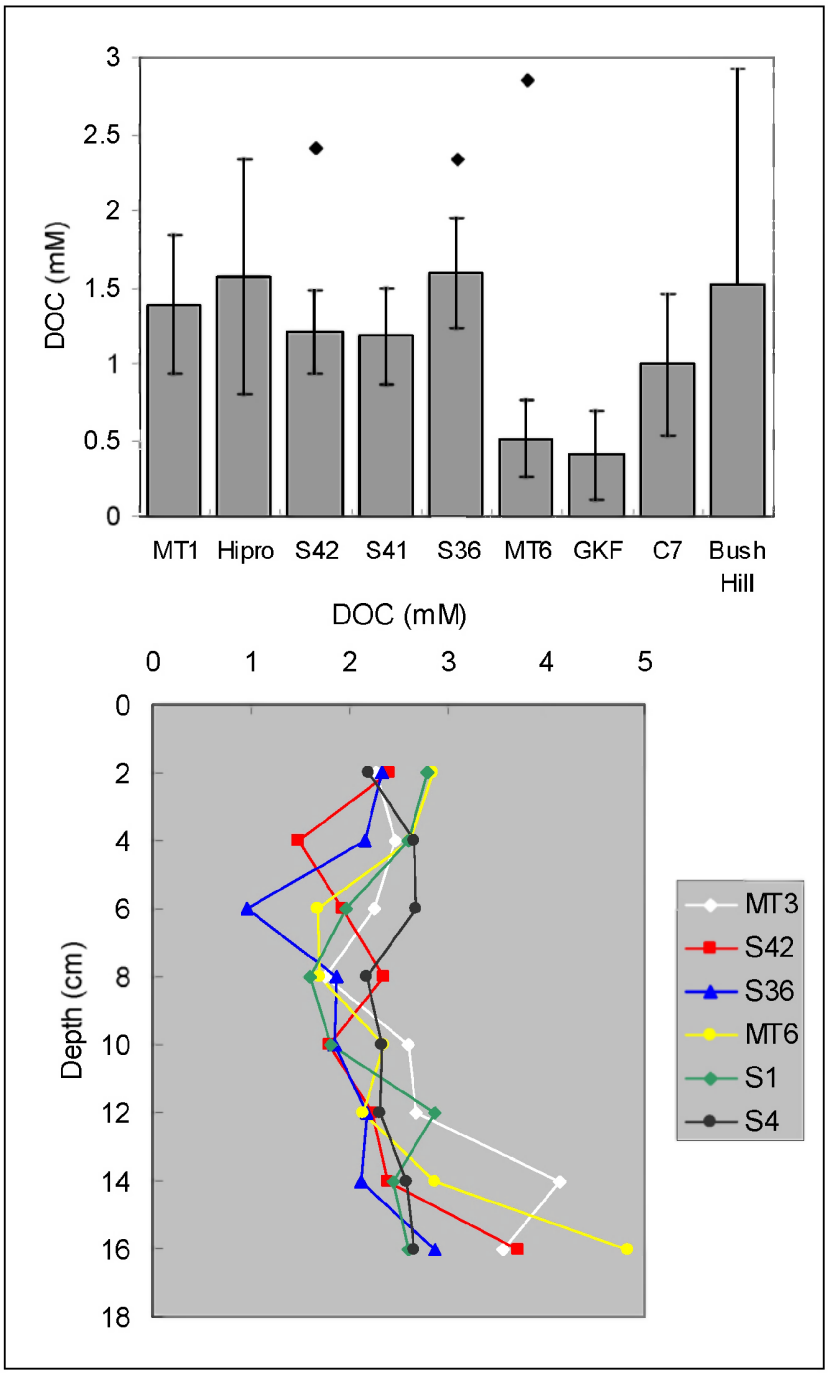

Figure 8-56. Top: Site means and standard deviations (2σ) for dissolved organic carbon (DOC) in the top 5 cm of sediment. The filled circles are the concentration measured for the top 2 cm of a sectioned core taken at the same location. Bottom: Pore water depth variations for DOC from experimental stations.

8.5.4 Dissolved Inorganic Carbon (including $\delta^{13}C$)

Dissolved inorganic carbon (DIC) concentration and stable isotope ratios of DIC ($\delta^{13}C$-DIC) for centrifuged samples from 10 sites are shown in Figure 8-57 (middle and bottom), respectively. DIC concentrations were similar across stations and close to the 2.2 mM value expected for seawater. Close inspection suggests a decrease in DIC concentration with depth in the water column, but the standard deviations were too large to confirm this trend (Figure 8-58). With the exception of station MT1, the $\delta^{13}C$-DIC was in the range of 1‰ with no obvious trend with water depth. This value is close to what would be expected in the overlying water column. In contrast to the DOC data, only one station, MT3, had significant differences between centrifuged and whole squeezed samples. The same was observed for $\delta^{13}C$-DIC. It is possible that variability between cores at station MT3 were not due to porewater sampling technique.

Consistent with what Alperin et al. (1999) reported for North Carolina slope sediments, DIC concentrations increased slightly with depth at all stations, excepting MT3. At this station, the depth profile was more complex. As DIC is a product of organic matter diagenesis, the trend of higher DIC concentration was expected as decomposition is taking place in the sediments. Further evidence for remineralization of organic matter was provided by the $\delta^{13}C$ -DIC (Figure 8-59 bottom; the value at station S42 may be an outlier.). Values became ^{13}C-depleted with depth in the core as the organic matter (about –21‰) was remineralized. The isotopic data suggest the greatest amount of organic matter decomposition occurred at station MT3.

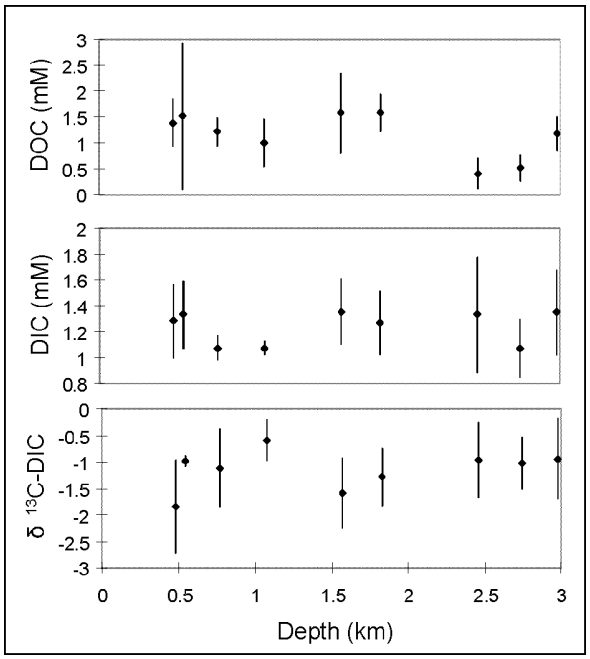

Figure 8-57. Site means and standard deviations (2σ) versus station water depth for dissolved organic carbon (DOC; top), dissolved inorganic carbon (DIC; middle) and stable carbon isotope ratio of DIC ($\delta^{13}C$-DIC bottom) in the top 5 cm of sediment.

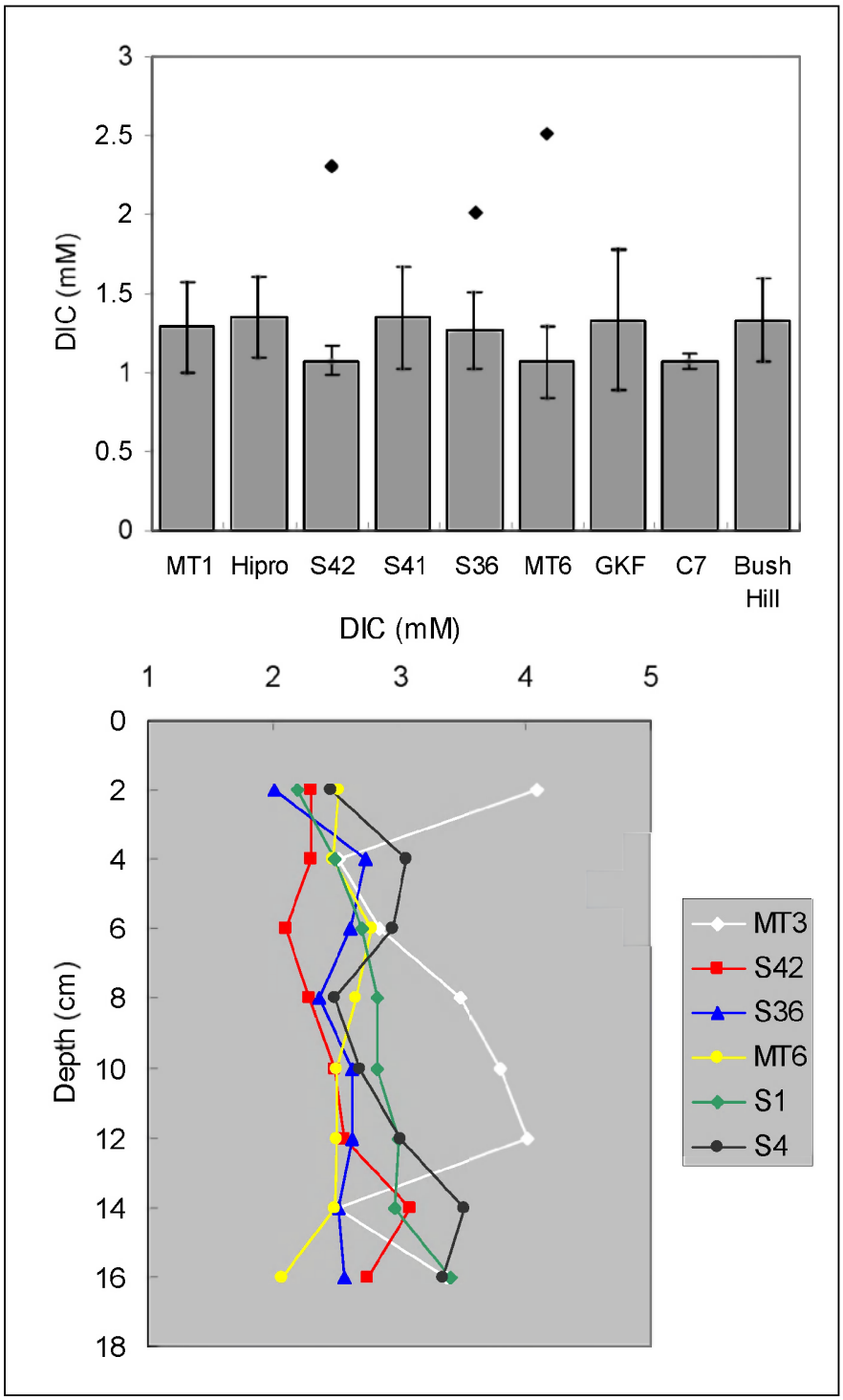

Figure 8-58. Top: Site means and standard deviations (2σ) for dissolved inorganic carbon (DIC) in the top 5 cm of sediment. The filled circles are the concentration measured for the top 2 cm of a sectioned core taken at the same location. Bottom: Pore water depth variations for DIC from experimental stations.

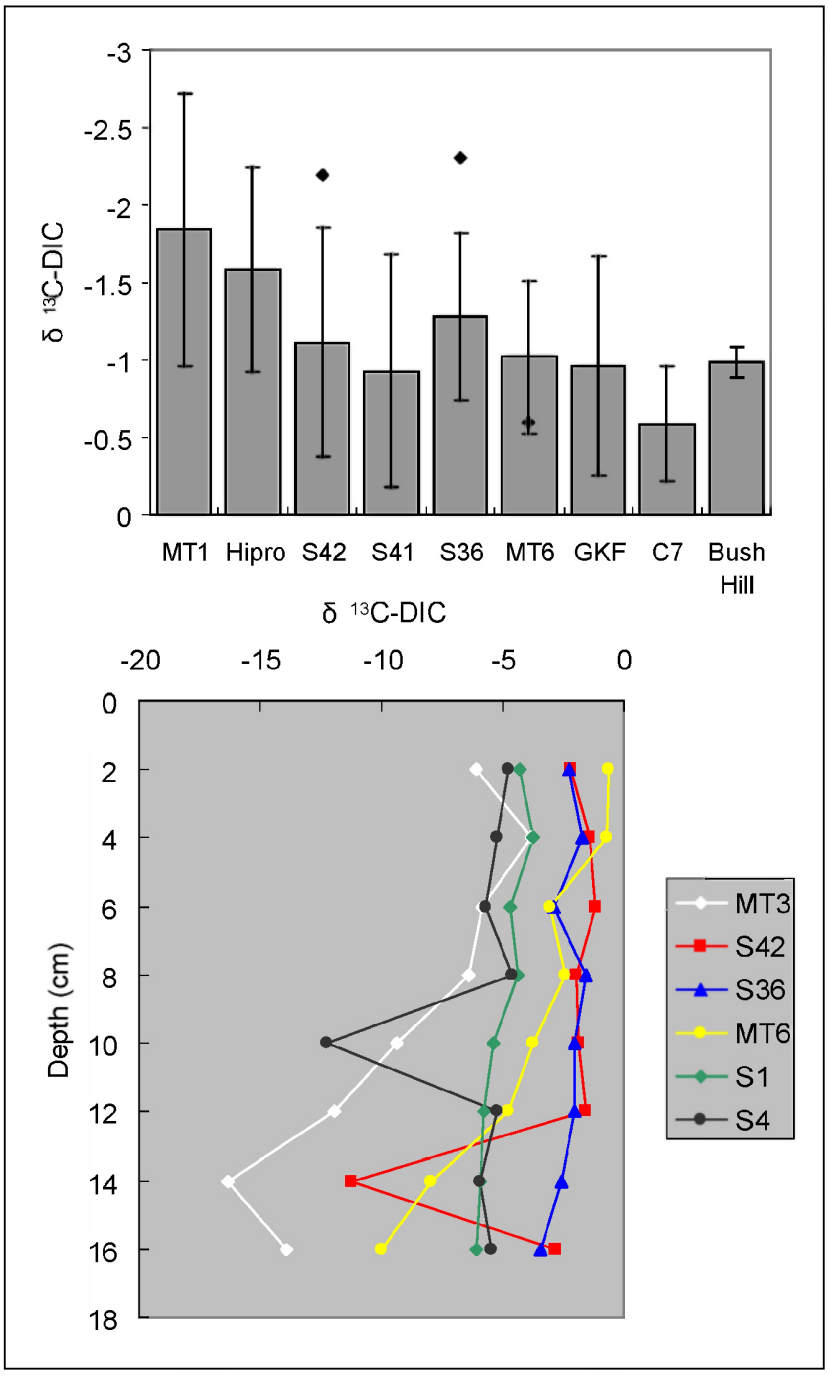

Figure 8-59. Top: Site means and standard deviations (2σ) for stable carbon isotope ratios of dissolved inorganic carbon (δ^{13}C-DIC) in the top 5 cm of sediment. The filled circles are the concentration measured for the top 2 cm of a sectioned core taken at the same location. Bottom: Pore water depth variations for δ^{13}C-DIC from experimental stations.

8.5.5 Stable Isotope Ratios from Sediment-dwelling Bacteria

Gas chromatography/combustion/isotope ratio mass spectrometry analysis of phospholipid fatty acids (PLFAs) was used at stations MT1, MT2 and MT3 to link organic matter (OM) sources with sedimentary bacteria (Boschker et al. 1999; Jones et al. 2003). Previously, it was reported that isotope ratios of PLFA i&a15:0 could be used as biomarker of bacterial isotopic ratios, while isotope ratios of PLFA 16:0 were more indicative of all living or recently senescent sources of organic matter (e.g., Jones et al. 2003). Correspondence between isotope ratios of sedimentary OM and PLFA 16:0 indicate living or recently senescent organic matter are the main sources of OM in sediments. In turn, correspondence between isotope ratios of sedimentary PLFA 16:0 and PLFA i&a15:0 suggest living or recently senescent organic matter was predominantly bacterial or both were using similar sources of organic matter. Finally, isotopic correspondence between PLFA i&a15:0 with that of sedimentary OM imply close coupling between these two pools.

The stable carbon isotope ratio ($\delta^{13}C$) of sedimentary OM (Figure 8-60) was remarkably constant both among stations and down-core. Values were close to –21‰, which is similar to values reported for northern Gulf of Mexico shelf sediments (Bianchi et al. 2002; Gordon and Goni 2003). In contrast, the $\delta^{13}C$ of PLFA 16:0 were more variable, which is partly indicative of the lower precision of the measurement, and significantly enriched in ^{13}C. Moreover, the values were more ^{13}C-enriched at the deeper stations. The source of organic matter with that level of ^{13}C-enrichment is not obvious; however, Ishihi et al. (2001) reported similar $\delta^{13}C$ for a species of *Sargassum*. Admittedly, Ishihi et al. analyzed attached *Sargassum* and not the pelagic species that has been observed in deep Gulf of Mexico trawl samples and photographs.

The trend for the $\delta^{13}C$ of PLFA i&a15:0, the biomarker of bacterial biomass, was similar at all three MT stations. At the surface values were equivalent to that of PLFA 16:0 at station MT1, and in between those of PLFA 16:0 and sedimentary OM at stations MT2 and MT3. With depth the isotopic value of PLFA i&a15:0 approached that of sedimentary OM. This change with depth implies different food sources to the bacterial community along the sediment depth gradient. Until the source and behavior of the biomass contributing to the PLFA 16:0 in these sediments is identified, it is difficult to speculate on the behavior of the $\delta^{13}C$ of the bacterial biomarker.

8.5.6 Dissolved Oxygen

Depth profiles for dissolved oxygen in pore waters were made using anodic stripping voltammetry microelectrodes. The primary objectives were to determine the oxygen gradient and "penetration" depth (OPD). The stations studied were MT3, MT6, S36, S42, and deep water stations S1, S2, S4 and S5. At the deep-water sites, heavy ship vibration during measurements made the microelectrode analyses very difficult and consequently the data should be viewed with caution.

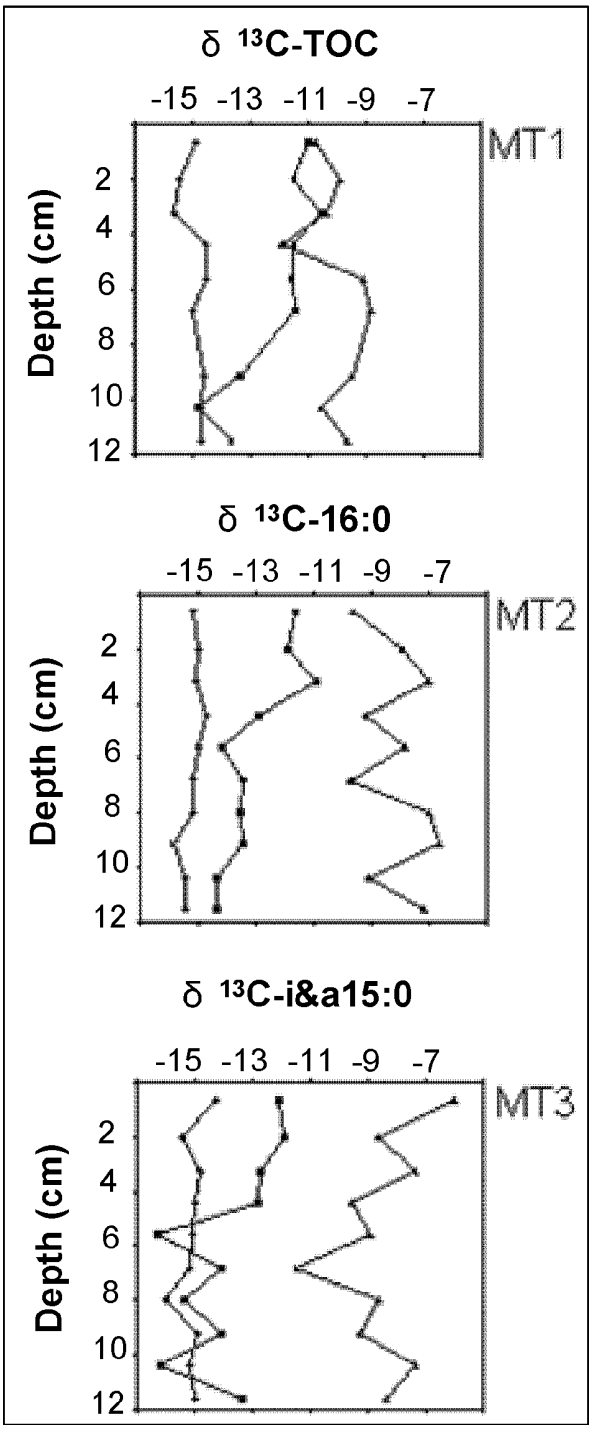

Figure 8-60. Stable carbon isotope ratio ($\delta^{13}C$) of sedimentary organic matter, phospholipid fatty acid (PLFA) 16:0 and i&a15:0 at stations MT1, MT2, and MT3.

Oxygen depth profiles for stations MT3, MT6, S36 and S42, are illustrated in Figure 8-61. At station MT3 the OPD was close to 0 mm. This is reasonable, given that dissolved manganese was observed to occur to within 1 mm of the sediment-water interface (see next section). The S36 and 42 stations had close to same OPD: 45 and 40 mm, respectively. Deep stations S1 and S2 had OPDs greater than the intervals measured (100 and 130 mm, respectively), whereas deep stations S4 and S5 had relatively shallow OPDs of roughly 30 and 12 mm, respectively.

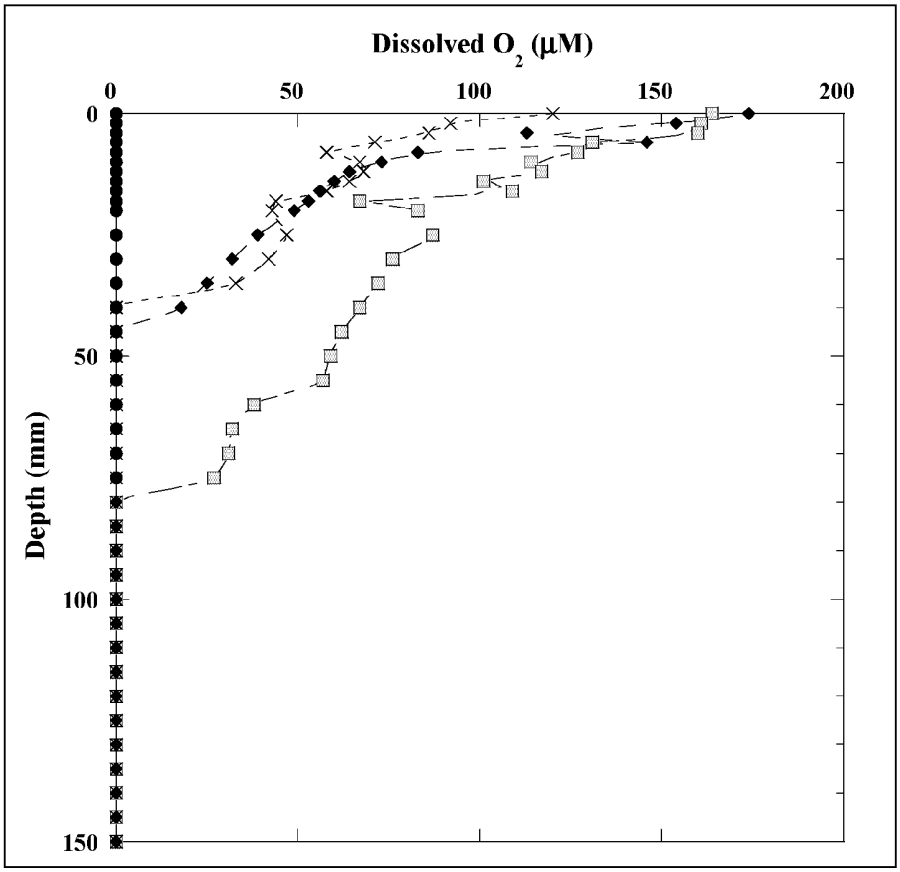

Figure 8-61. Dissolved oxygen distribution with depth in stations MT3 (solid circle; note all values below detection limit), MT6 (open square), S36 (solid diamond), and S42 (X).

8.5.7 Dissolved Manganese and Sulfate

Dissolved iron and sulfide were not detectable at any of the experimental stations, nor were any changes in the dissolved sulfate to chloride ratios observed.

Dissolved Mn^{2+} was observed only at station MT3 (Figure 8-62). At this station dissolved manganese exhibited a classic (e.g., Berner 1980) broad subsurface maximum from about 30 to 80 cm, which averaged about 210 µM. This is the zone of major manganese reduction. Above this zone diffusive transport of manganese is the primary process and below this zone manganese is precipitated primarily as the carbonate mineral pseudokuntnahorite ($MnCa(CO_3)_2$; Mucci 1988) These results indicate that, with the exception of station MT3, only oxygen and nitrate

were important electron acceptors for organic matter oxidation in the DGoMB study experimental sites. (Note data do not exist for station MT1, which is likely to have been at least as reducing as station MT3.)

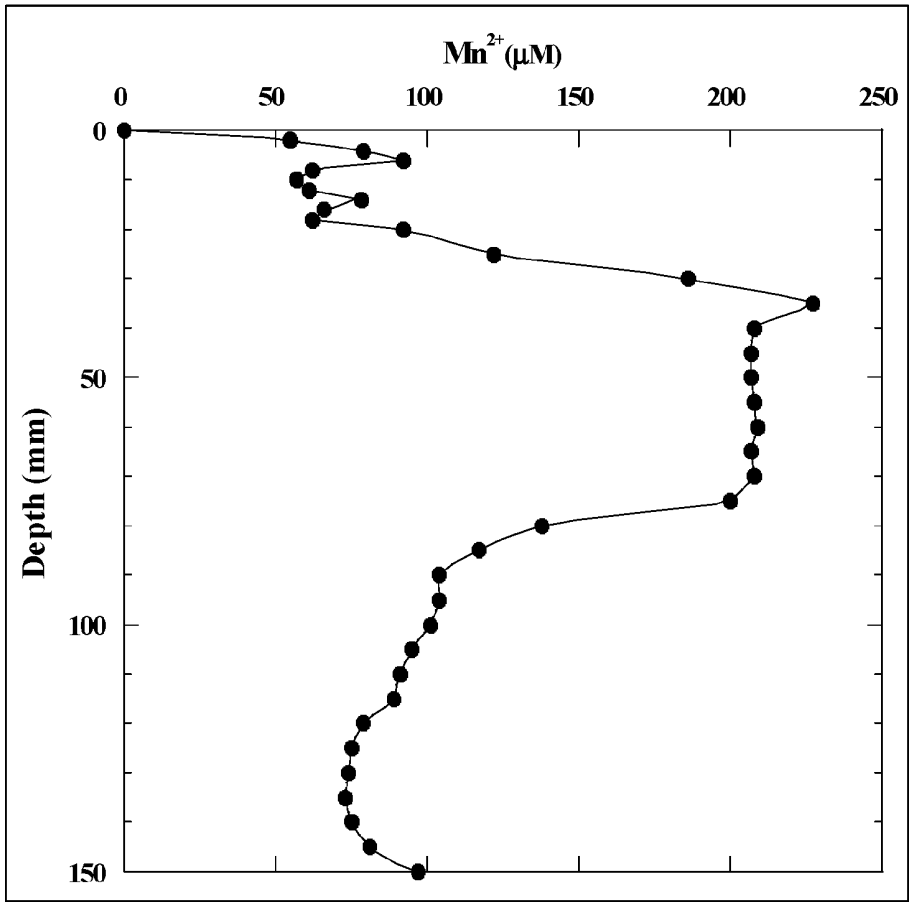

Figure 8-62. Dissolved Mn^{2+} at station MT3. Note the maximum from about 3 to 8 cm depth and that dissolved manganese was detected to within ~2 mm of the sediment-water interface.

8.5.8 Sulfate Reduction Rates

Sulfate reduction rates were below detection limits. This is consistent with the finding of no detectable decrease in dissolved sulfate at any stations during the 2000 fieldwork. Sulfate reduction was not measured at deep abyssal sites in 2002, based on the negative results at shallower stations in 2000 and 2001. The deep oxygen penetration depths at these sites indicate sulfate reduction is not likely to occur.

It should be noted that although no detectable sulfate reduction was observed, it could be occurring at deeper sediment depths than those sampled (~20 cm). Lin and Morse (1991) observed reduced sulfur species on the GoM continental slope, but substantially deeper in the sediments.

8.5.9 Sediment Community Oxygen Consumption (SCOC)

Sediment community oxygen consumption (SCOC) is generally accepted as the most resilient method of determining the total heterotrophic metabolism of the complete sediment-dwelling community. It is considered to be a reasonable estimate of gross input of reactive organic matter to any given site in the deep ocean (Jahnke, 1990). Two methods were employed in this project to estimate SCOC: in situ incubations in which benthic chambers were implanted with a remote lander and laboratory incubations aboard ship of small chambers retrieved from the box cores.

Data from 11 measurements have been included, with two earlier studies added, for a total of 13 SCOC values. The rates have been transformed from oxygen uptake per square meter per hour into units of mg C produced m^{-2} day^{-1} to agree with units in the food web carbon budget. This transformation assumes that the Respiratory Quotient is 0.85. [Thus, to transform the rates given back into O_2 demand, divide by 0.85 moles CO_2/moles O_2 and multiply by 12 mg C/millimole CO_2.]

The mean rate at the 13 sites was 34.7 mg C m^{-2} d^{-1} (range of 4 to 91) at a mean depth of 1.7 km (range of 500 to 3,650 m). The mean rate of the in situ measurements was less than that from the laboratory studies (21.9 vs. 49.7), partly because the in situ rates were from deeper sites than those incubated in the laboratory aboard ship. However, some of the difference in rates may be attributable to decompression of the laboratory cores, or some other unidentifiable variable altered by sample retrieval or incubation conditions. While rates using both approaches at S36 were within the generally expected range of variation, the ship-board incubations were approximately two times the in situ rates at the two other sites where both approaches were used (S42 and MT3).

All 13 rates have been plotted as a function of depth (Figures 8-63 and 8-64). The decline with depth is evident; an exponential rate was observed.

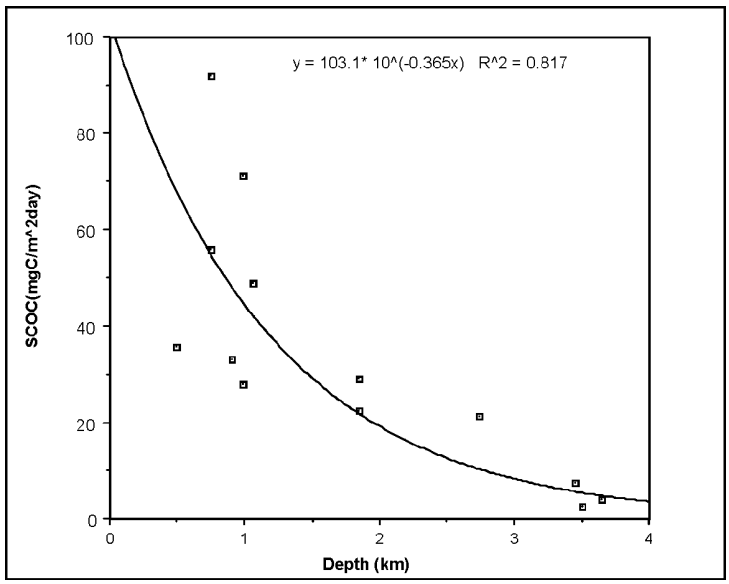

Figure 8-63. Sediment Community Oxygen Consumption (SCOC) expressed as carbon (see text for conversion details), plotted as a function of water depth.

The rates on the continental slope had a wide range of values, whereas those out on the abyssal plain were all in a narrow cluster. This reflects the wide range of community heterotrophic metabolism at the shallow sites versus the narrow clustering of very low rates out at the greatest depths far from coastlines where the input of organic matter is limited. The regression line allows us now to predict the mean rate at any depth, but this prediction is far more accurate at the deep sites than at those on the upper slope, using all the data. The precision can be improved by eliminating the shipboard incubations at all but the shallowest site, and a straight line provides a more reasonable estimate of variations in SCOC as a function of depth (Figure 8-64). The linear regression of the constrained data has an origin that is similar in magnitude to high rates on the continental shelf and in estuaries, suggesting that this regression is a better overall estimate of rates than the line generated from all the data. The regression lines and the rates at the individual sites can be used now to constrain the rates in the carbon budget and be compared with other methods used in this study to estimate carbon cycling at the process sites.

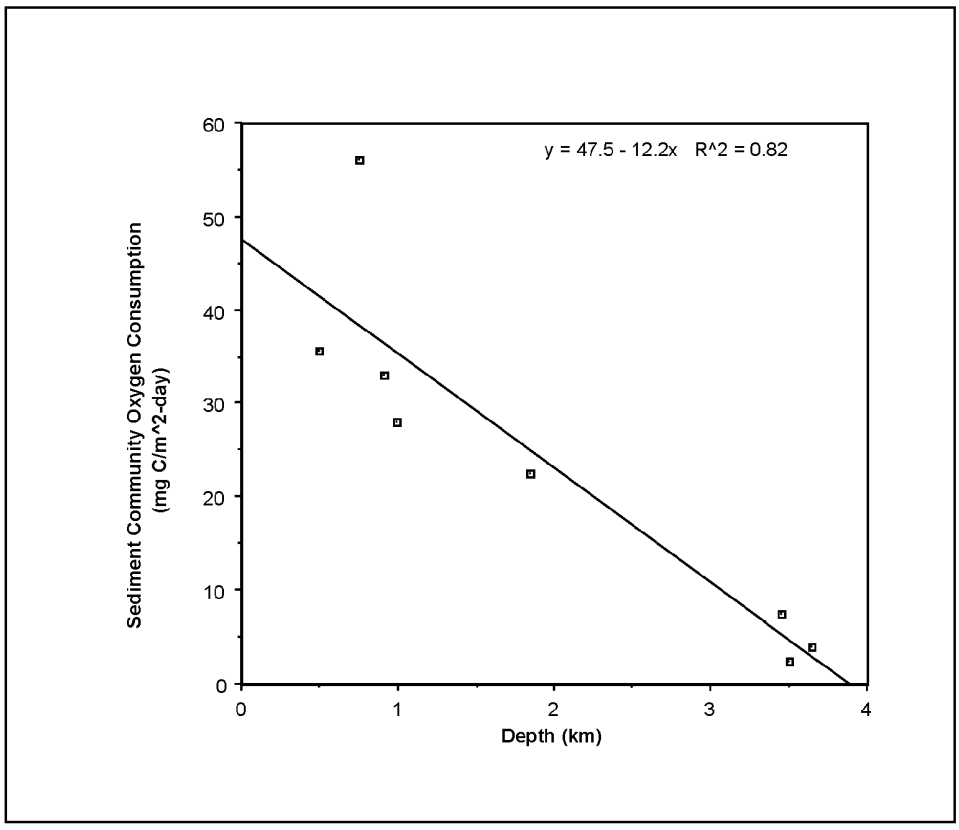

Figure 8-64. Sediment Community Oxygen Consumption (SCOC) as a function of depth. Respiration of oxygen expressed as carbon dioxide-carbon; see text for conversion details.All data from in situ incubations, with the exception of the shallowest site (MT1 at 500m).

8.5.10 Radiochemistry of the Sediments

General: Primary data for all stations, including total ^{210}Pb, ^{226}Ra, $^{210}Pb_{xs}$, $^{234}Th_{xs}$, ^{238}U, $^{239,240}Pu$, %POC and porosity are given in the data report. $^{234}Th_{xs}$ data from station S36 are not available, as samples were counted too long after collection ($t_{1/2}$ = 24 days). These data are used to calculate particle reworking (bioturbation), sedimentation and accumulation rates, discussed in detail below. The fallout radionuclides ^{137}Cs and ^{7}Be were not resolved at sufficient activities in any core to be useful.

Bioturbation rates: Bioturbation rates can be quantitatively derived from $^{234}Th_{xs}$ profiles as described by Santschi *et al.* (1980, 1999) and from the analysis of peak shapes of different tracer concentration profiles. $^{234}Th_{xs}$ profiles, which are calculated as the difference between ^{234}Th (total) and supported ^{234}Th ($^{234}Th_{supp}$ = ^{238}U), were used to determine particle reworking (bioturbation) rate coefficients, D_b, shown in Figure 8-65 and listed in Table 8-3 along with mixing depths, inventories, macrofaunal densities and other station data. Assuming steady state conditions, D_b is calculated as follows:

$$[^{234}Th_{xs}(z)] = [^{234}Th_{xs}(0)]\exp(-(\lambda/D_b)^{1/2}z) \quad (1)$$

where λ = decay constant of ^{234Th} (0.0288 day $^{-1}$), and z = depth. Numerical mixing and sedimentation models discussed in Santschi *et al.* (2001) illustrate that the constant D_b model is conservative in that it tends to over predict mixing rates at depth.

$^{234}Th_{xs}$ penetration depths are between 0.5 and 4 cm, and bioturbation coefficient values, D_b, range from approximately 2 – 30 cm^2/yr. Because particle re-working or bioturbation rates are expected to decrease exponentially with depth, coincident with the depth distribution of benthic infauna (Stull *et al.* 1996), it is not likely that the depth of more intensively mixed sediment is much higher than that observed by $^{234}Th_{xs}$. The longer "memory" of the fallout radionuclides $^{210}Pb_{xs}$ and $^{239,240}Pu$ do indicate deeper penetration depths than $^{234}Th_{xs}$ as summarized in Table 8-3 for all but the deepest stations. This is not surprising. While active mixing is certainly confined to the upper few centimeters, as reflected by $^{234}Th_{xs}$ data, the relatively long-lived radionuclides $^{210}Pb_{xs}$ and $^{239,240}Pu$ ($t_{1/2}$ = 22, 24 x 10^3 and 6540 yr., respectively) combined with low sedimentation and accumulation rates and non-local episodic mixing events, results in penetration depths for these isotopes which are often considerably deeper. In deep water, such as for stations JSSD1 and JSSD4 (3,520, 3,560 m, respectively) there was very little $^{239,240}Pu$ and the penetration depths for $^{234}Th_{xs}$ and $^{210}Pb_{xs}$ are essentially the same.

Sedimentation and accumulation rates: According to the constant initial concentration (CIC) model, sedimentation rates can be calculated assuming steady state conditions and at relatively constant porosity, using:

$$[^{210}Pb_{xs}(z)] = [^{210}Pb_{xs}(0)]\exp(-\alpha z) \quad (2^a)$$

$$\alpha = (\lambda/S) \quad (2b)$$

where $[^{210}Pb_{xs}(z)]$ and $[^{210}Pb_{xs}(0)]$ represent excess ^{210}Pb concentration at depth z and at the sediment interface, respectively; S = sedimentation rate (cm/yr.); λ = decay constant of ^{210}Pb (0.031 $year^{-1}$). As sediment porosity was nearly constant over the depth intervals modeled for S, sediment accumulation rates were also determined using:

$$SA = S\,[(1-\phi)(\rho)] \quad (3)$$

Table 8-3

Summary Data and Modeling Results for All Stations
(n/d or nd = no data, D_b values determined using $^{234Th}_{xs}$ data. An upper and lower limit for S are listed for this station due to a high error, resulting from few points available below the ^{239,240}Pu penetration depth at this station.)

Station	Depth (m)	$^{210}Pb_{xs}$ inventory (Bq/cm^2)	^{239,240}Pu inventory (mBq/cm^2)	POC inventory (upper 5cm) (mg/cm^2)	Bioturbation coefficient (D_b) ($cm^2/yr.$)	Bioturbation Depth (cm) $^{234Th}_{xs}/^{210}Pb_{xs}$	Sedimentation rate (cm/yr.)	Accumulation rate ($g\ cm^{-2}\ yr.^{-1}$)
S42	767	0.96 ± 0.07	1.66 ± 0.33	14.3 ± 0.5	6.6 ± 0.3	1.75/2	0.44 (0.26 – 1.55)*	0.36 – 0.76*
MT3	985	3.48 ± 0.07	6.83 ± 0.82	21.5 ± 0.2	29.3 ± 8.2	3.25/15	0.07 ± 0.06	0.03 ± 0.02
S36	1849	1.81 ± 0.12	5.53 ± 1.1	20.2 ± 0.6	n/d	nd/15.50	0.09 ± 0.05	0.05 ± 0.03
MT6	2737	0.35 ± 0.01	1.89 ± 0.45	11.8 ± 0.2	30.1 ± 33.7	3.25/12.50	0.10 ± 0.03	0.05 ± 0.01
JSSD1	3520	0.97 ± 0.28	0.07 ± 0.02	14.5 ± 1.2	2.7 ± 0.8	1.75/2	0.04 ± 0.01	0.02 ± 0.01
JSSD4	3560	0.69 ± 0.21	0.02 ± 0.01	11.2 ± 0.5	32.8 ± 6.2	1.75/2	0.08 ± 0.03	0.04 ± 0.02

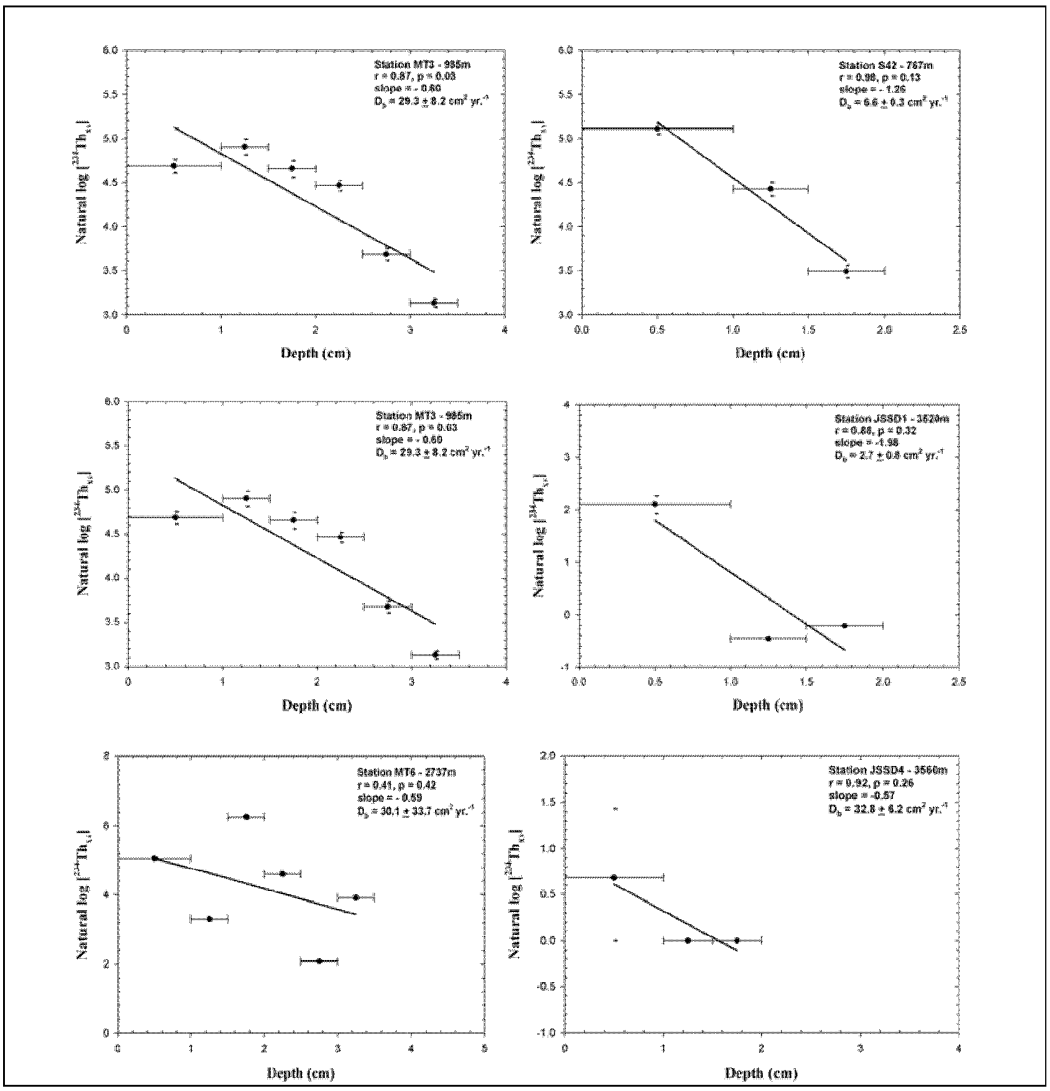

Figure 8-65. $^{234}Th_{xs}$ ([^{234}Th(total)] – [^{238}U]) penetration into surface sediments at each station, allowing determination of particle reworking (bioturbation) rate (D_b) and depth (z_m), units are mBq/g. D_b was calculated from the slope of $\ln[^{234}Th_{xs}(z)] = \ln[^{234}Th_{xs}(0)] - (\lambda/D_b)^{1/2}z$. Errors in ln $^{234}Th_{xs}$ data are plotted for each point, but are often less than the size of the data symbol.

where SA = sediment accumulation rate (g cm^{-2} yr.$^{-1}$), ϕ = porosity, i.e., sediment percent pore space and ρ = sediment bulk density (2.5 g cm^{-3}).

The CIC method also assumes that particle re-working rates are not significant over the depth interval of the ^{210}Pb profile, and that fluxes of both sediments and ^{210}Pb have been constant. $^{234}Th_{xs}$ data were also used to determine the upper depth limit for particle mixing. All $^{210}Pb_{xs}$ data below this depth were then plotted in semi-log format (Figure 8-66); then only those $^{210}Pb_{xs}$ data below the lower limit mixing depth, as defined by the depth where significant ^{239,240}Pu activities cease, were used to determine an upper limit for both sedimentation rates (S) and sediment accumulation rates (SA). While ^{239,240}Pu data were not of sufficient resolution to accurately mark discrete temporal stratifications within the sediment profiles based on known high fallout years,

they were sufficient to illustrate depth intervals within the sediment profiles where local or non-local mixing was suspected (worm burrows, etc.). Inventories, mixing depths and modeled parameters are summarized for each station in Table 8-3.

The ranges of apparent sedimentation and accumulation rates determined by this approach for these stations are 0.04 – 0.44 cm $yr.^{-1}$ and 0.02 – 0.56 g cm^{-2} yr^{-1}, respectively, showing that after approximately 1,000 m water depth, sedimentation and accumulation rates become essentially constant at approximately 0.08 cm/yr., and 0.04 g cm^{-2} $yr.^{-1}$, respectively, within the error. Apparent sedimentation and accumulation rates could not be corroborated here through use of a second tracer radionuclide (^{137}Cs or $^{239,240}Pu$). $^{239,240}Pu$ profiles were of insufficient resolution at all stations to allow for identification of discrete peaks corresponding to high fallout years. In addition, the 1963 peak for either ^{137}Cs or $^{239,240}Pu$ would likely have been obliterated, as these apparent sedimentation and accumulation rates combined with the mixing depths evident at these stations would have placed those peaks in the strongly bioturbated upper few centimeters. No other data exist on sedimentation or accumulation rates at these GoM stations, either as part of this research effort or in the literature. In fact, reliable, published sedimentation rates for the GoM outside the immediate area of the Mississippi River Delta region are essentially non-existent in the literature. The estimates of sedimentation rates and sediment accumulation rates presented here do fall in line with rates from similar continental margin marine settings, including the northwestern Mediterranean Sea (0.01 – 0.60 cm $yr.^{-1}$, Zuo *et al.* 1997), the eastern Arabian Sea (0.06 – 0.66 cm $yr.^{-1}$, Somayajulu et al. 1999), the Bay of Biscay, northeastern Atlantic (0.06 – 0.4 cm $yr.^{-1}$) and the middle Atlantic Bight (0.03 -0.04 cm yr.-1, 0.02 – 0.05 g cm^{-2} $yr.^{-1}$ Anderson et al. 1994).

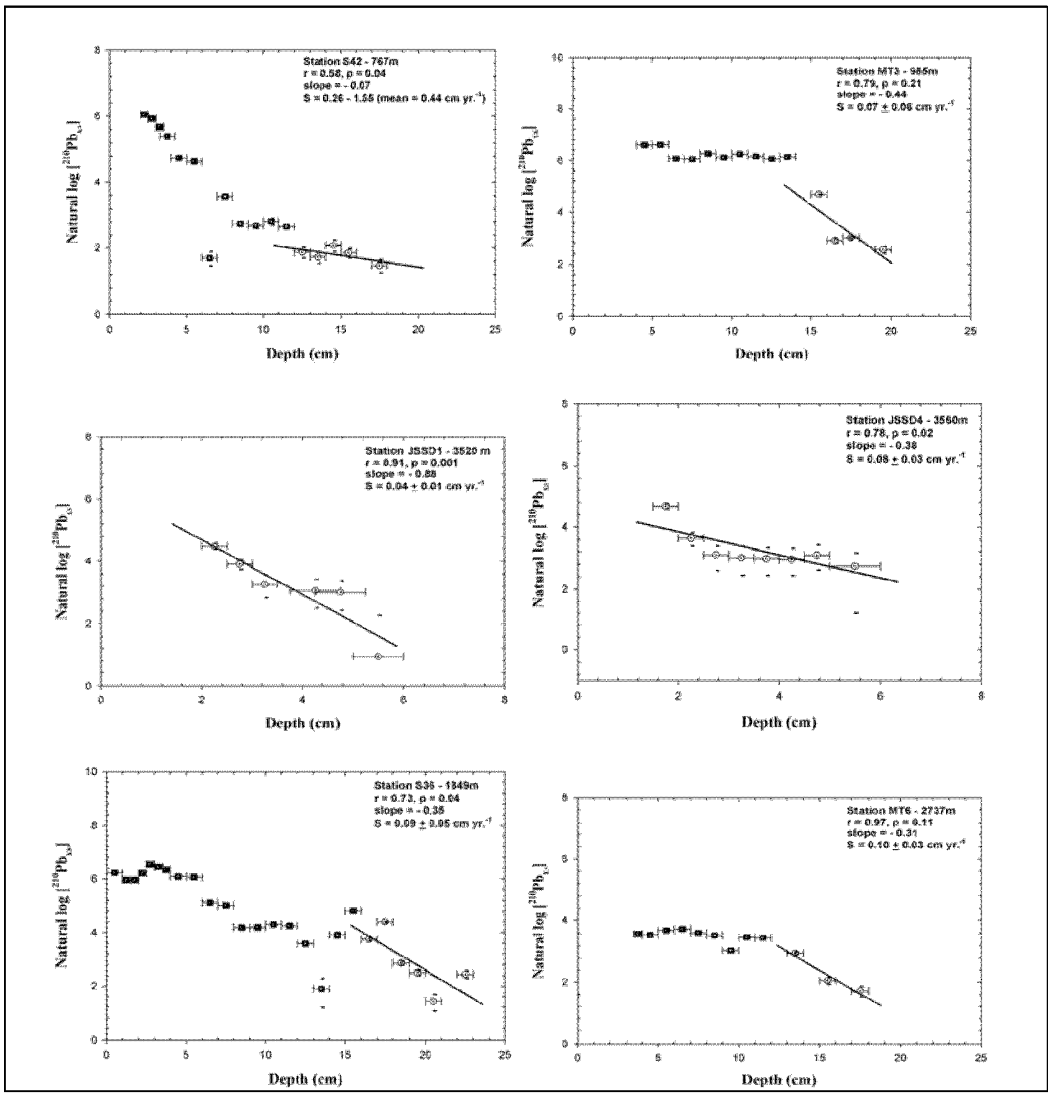

Figure 8-66. $^{210}Pb_{xs}$ ([210Pb (total)] – [^{210}Pb (supported) = ^{226}Ra]) profiles for all stations, all $^{210}Pb_{xs}$ data below the $^{234}Th_{xs}$ penetration depth is plotted. Sedimentation rates (S) were determined from the slope of $\ln[^{210}Pb_{xs}(z)] = \ln[^{210}Pb_{xs}(0)] - (\lambda/S)z$, using only those points below significant ^{239,240}Pu activity (open circles). Errors in ln $^{210}Pb_{xs}$ data are plotted for each point, but are often less than the size of the data symbol.

8.6 Contaminant Chemistry

8.6.1 Metals

Location maps show that some of the sampling sites are within areas with numerous offshore drilling and production platforms. This includes areas around sampling sites C1, MT1, 2, 3 and WC5. On the other hand, many of the sampling sites were many kilometers from present-day intensive petroleum development. It has been previously shown (Boothe and Presley 1989) that significant metal contamination of sediments by off-shore drilling and production is restricted to within a few hundreds of meters of platforms. Therefore, it was not expected that sediments would be contaminated at the DGoMB stations.

For this study, elements known to be major constituents of drilling fluids (barium [Ba], chromium [Cr]), as well as some of environmental concern, were determined. Metals were measured to assess potential effects on the benthos. In addition, aluminum, calcium, iron, and silicon were determined to facilitate recognition of sediment trace metal variations caused by natural (non-anthropogenic) differences in sediment texture and mineralogy. A total of 20 elements were determined in all sediment samples.

The data sets for all sampling periods agree well, in almost all cases, with only a few differences of more that 10% between individual data points. This, along with the good spike recoveries and good results for analysis of standard reference materials, gives confidence in the analytical results. Many of the trace elements were in low concentration in these samples, but all elements in almost all samples were above the detection limits of the methods used. Both Al and Fe were used to normalize trace metal concentrations, as they exhibited a strong covariance. Trace metal concentrations that fall above a best fit line through the data are of interest, assuming that most of the data are background values.

Average concentrations of potential pollutant metals; Ag, Cd, Cu, Hg, Pb, and Zn; in the study area samples were similar to average crustal abundances and to average values for areas of the northern GoM thought to be low in pollutant metals. Average values may not, however, be the best way to evaluate this data because of the relatively small number of samples and the considerable variability in the data, some of which is due to the variable $CaCO_3$ content of the samples. A better comparison is the slope of a best fit line through the data for each element on an element versus Al or Fe scatter plot to that expected for Mississippi River Delta material. The Mississippi River is the most likely source of most of the silicate fraction of the sediments at the study sites.

When concentrations of several elements are plotted against Al (Figures 8-67 and 8-68), most data points not only lie near a best fit line but the line has almost the same slope as one drawn through data for Mississippi River Delta sediment. This is true for Be, Co, Cr, Fe, Si, Tl, V, and Zn (plus K and Mg not reported here) which have positive slopes on the metal versus Al plots and for Ca and Sr (not reported here) which have negative slopes. Thus, for these metals there is no indication of additions from human activity. Rather, the metal concentrations in a particular sample are determined by the relative amounts of Mississippi River derived silicate material and plankton-derived carbonate in the sediment. The picture is less clear for the other elements. Ni, Pb, Cd, As, and especially Cu concentrations, show more scatter on the metal versus Al plots than do the elements discussed above. Furthermore, the slopes suggest a general enrichment in these elements of 25 to 50% over Mississippi River derived material.

A few points on each of the metal vs Al plots are also far enough off the general trend line to suggest possible human influence. On the other hand, Mn concentrations are more variable and

much more elevated over Mississippi Delta material than are those of any of the other elements. It is very unlikely that this Mn enrichment is due to human influence. Rather, it is due to remobilization of Mn from buried reduced sediment. The Mn then diffuses up through the sediment column and redeposits in near-surface sediment under oxidizing conditions. This phenomenon has been well documented for northern GoM sediments by Trefry and Presley (1982) and others. As noted above in the geochemistry section (8.5.7), the profile of Mn in the pore water suggests that MnO_2 can be a quantitatively significant terminal electron acceptor in the remineralization of organic matter just below the sediment – water interface. At this point it is not possible to attach a rate to that process however.

Other metals have been shown to undergo the same diagenetic remobilization process that affects Mn (e.g., Presley et al. 1992) and it seems likely that this process is at work in the DGoMB area. The fact that there is not a good correlation between Ni, Pb, Cd, and Cu concentrations and Mn does not mean that all have been unaffected by similar diagenetic processes. The situation is complicated by the intensity of reducing conditions, the relative amounts of available sulfide which would precipitate metals, and variable metal sulfide solubilities. In short, it seems likely that the somewhat anomalous Ni, Pb, Cd, and Cu concentrations in the DGoMB area are due to natural diagenetic and transport processes rather than to human activity. In any case, all of the concentrations are well below levels that would be expected to have harmful effects on organisms.

In contrast to the elements discussed above, Barium (Ba) shows a few values that are higher than those of average crustal material and average clay-rich sediments but are typical of near-platform sediments from the northern GoM. In the case of Ba, it seems likely that the enrichments, which are up to almost a factor of ten, are due to disposal of oil well drilling mud. Up to 90% of the dry weight of drilling muds can be Ba (Boothe and Presley 1985), so small amounts of mud could account for the Ba enrichments seen in the sediments. The Ba-enriched samples are from the three shallowest sites in the Mississippi Trough (sites MT1, 2 and 3) and from site C1 and WC5 just to the west of these. All are in an area of intense petroleum exploration and development. Previous studies have found even greater enrichments of Ba near some drilling platforms in the northern GoM. Barium concentrations of tens of thousands of ppm have been found in many samples (e.g., Boothe and Presley 1989). Even at the most Ba-enriched sites in the present study, the concentration is well below that thought to adversely affect organisms (e.g., Neff et al. 1989)

In summary, the samples analyzed for this project were a mixture of carbonate and terrigenous silicate materials and thus varied considerably in aluminum, calcium, and iron concentrations. Trace metal concentrations also varied considerably, as would be expected with a varied mineralogy. Concentrations of the elements Al, Ca, Sr, Na, K, Mg, Be, Co, Hg, Cr, Ti, V, and Zn were within the ranges expected for coastal GoM sediments with equivalent Fe concentration. Copper, As, Cd, Pb, Ni, and especially Mn concentrations were found to be somewhat higher than those in Mississippi Delta and shallow GoM samples but were not unexpectedly high considering the deeper water from which the present samples came. The enrichments are almost certainly due to complex natural transport and diagenetic processes, not to human activity. The strong Ba enrichments of up to almost a factor of ten in a few samples are suspected to be due to the presence of residues of oil well drilling muds discharged from the many drilling platforms in the area. Based on literature data, none of the metal concentrations in the study area sediments is high enough to adversely affect marine organisms.

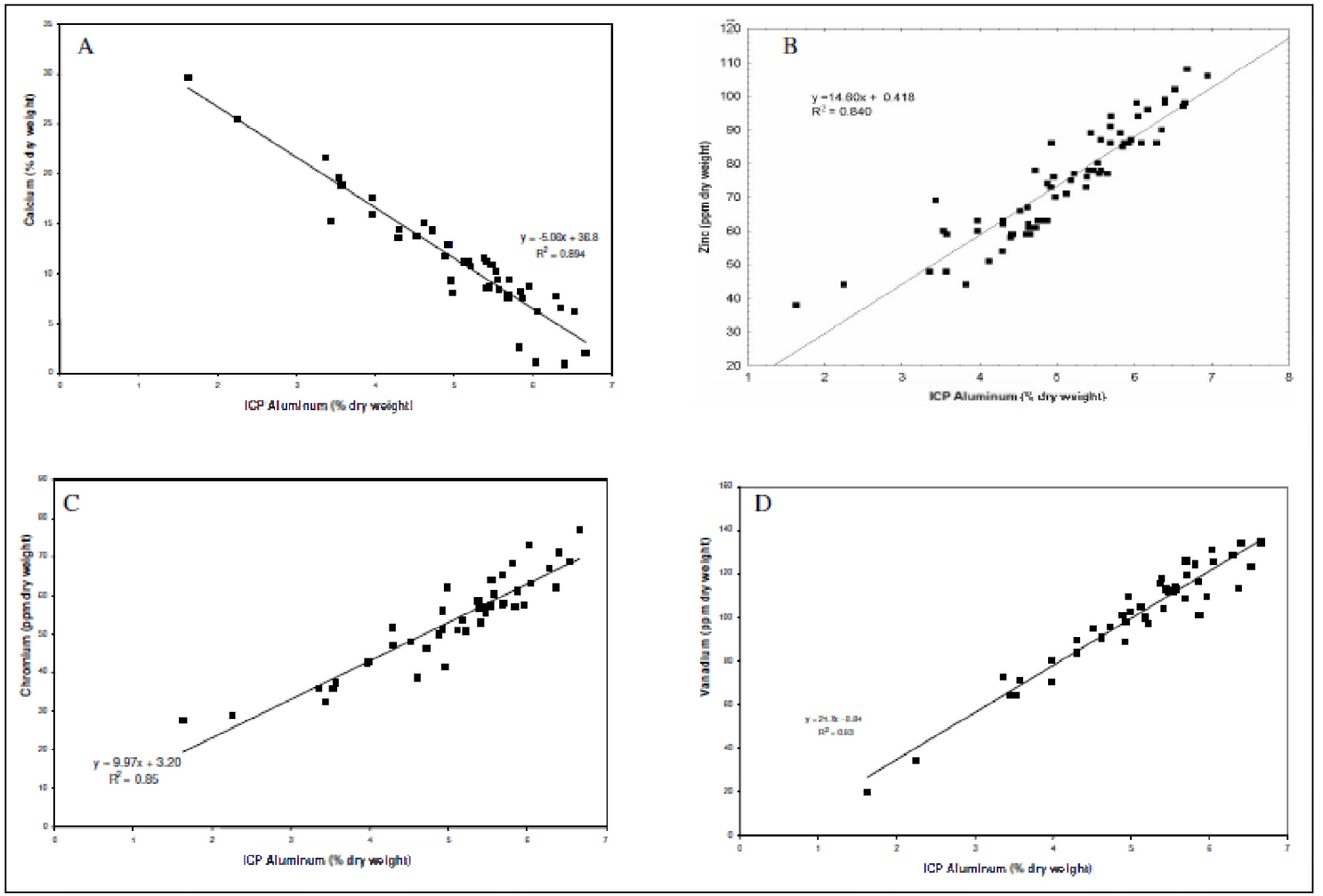

Figure 8-67. Variations in total sediment calcium (A), chromium (B), zinc (C), and vanadium (D) concentrations as a function of changes in sediment mineralogy (as indicated by sediment aluminum levels) measured by inductively coupled plasma spectrometer (ICP).

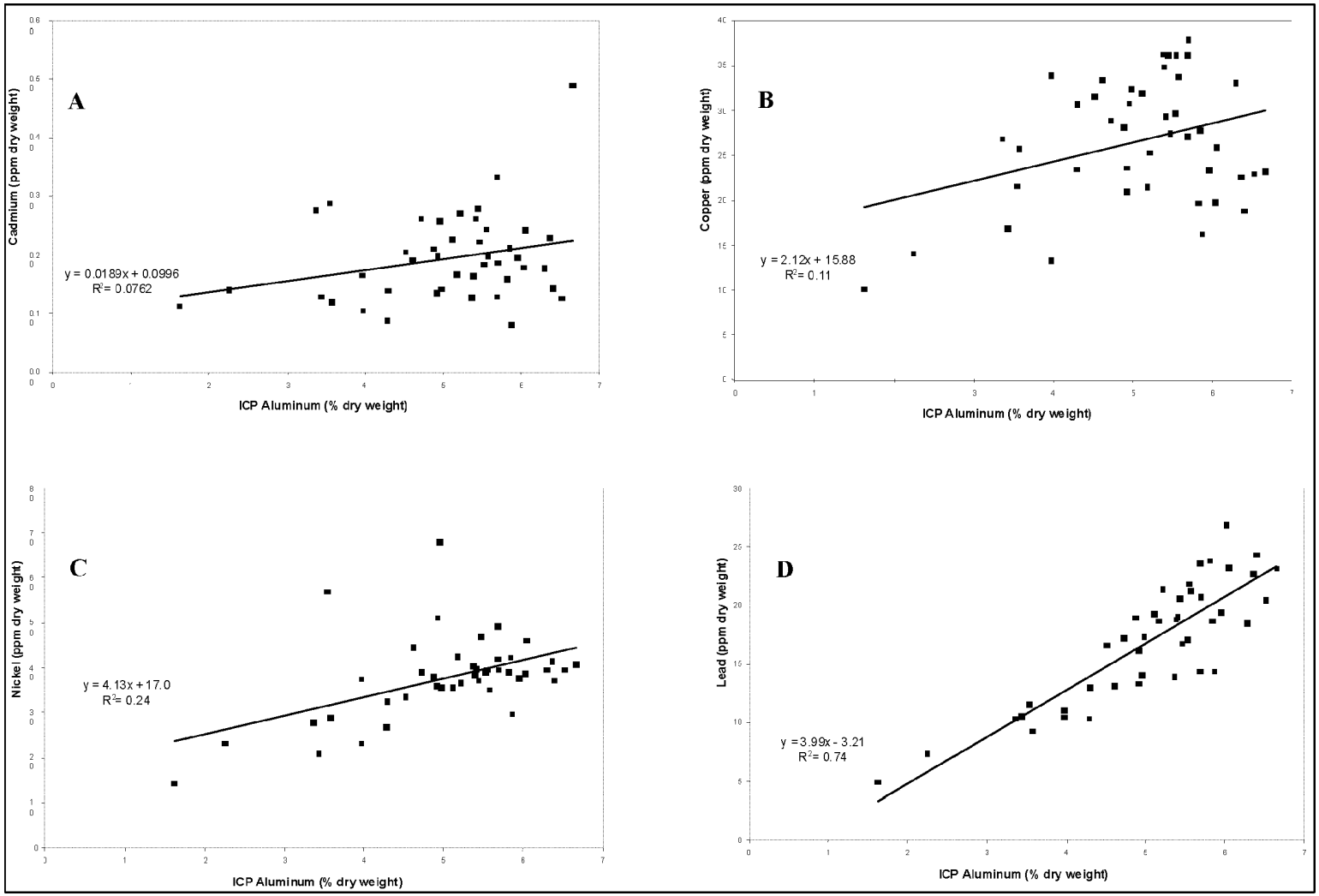

Figure 8-68. Variations in total sediment cadmium (A), copper (B), nickel (C), and lead (D) concentrations as a function of changes in sediment mineralogy (as indicated by sediment aluminum levels).

8.6.2 Contaminant Organic Compounds

Polynuclear aromatic hydrocarbons (PAH) are a major toxic component of petroleum. The sources of PAH in offshore sediments include natural petroleum seepage, offshore production platform operations, spills, sediment transport and atmospheric deposition. Previous studies around production platforms showed that sediments close to platforms (<500 m) contained discharged drilling muds and cuttings. Hydrocarbons, including PAH and trace metals (Ag, Ba, Cd, Hg, Pb, and Zn) contaminants, were associated with these coarse-grained sediments (Kennicutt et al. 1996b). However, contaminant concentrations including PAHs close to platforms were below concentrations thought to induce negative biological responses.

Sediment samples collected on the shakedown cruise were analyzed for PAH. A total of five sediment samples were collected, four with the GoMEX boxcorer and one with an USNEL spade corer. The total PAH concentrations ranged from 47 to 159 ng/g with a mean of 113 ng/g and a relative standard deviation of 37%. These total PAH concentrations are low. The PAH concentration in samples collected with the USNEL spade corer was 108 ng/g and was close to the mean, indicating the sampler type does not bias PAH results. The relative standard deviation of 37% is expected for the combined effects of analytical uncertainty (~10%) and the natural inhomogeneity of sediments. These samples were collected about 23.5 km (14.5 miles) southwest of Station W1 and 35.5 km (22 miles) west of Site W2. Samples collected at Site W2 and W3 had total PAH concentrations of 53 ng/g and 41 ng/g, respectively, which is within or slightly below the lower end of the range of total PAH concentrations from the shakedown cruise.

A total of 67 sediment samples were analyzed for PAH from DGoMB Cruises 1, 2, 3a, and 3b. These samples represent 50 stations. Concentrations for total PAH ranged from not detected (ND) to 1033 ng/g with a mean of 140 ng/g and a median of 92 ng/g. Replicate samples were collected from selected sites and analyzed as replicates on the Survey Cruise (2000). Some sites were sampled during the next consecutive years (2001 and 2002). The data for these replicate analyses are reported in Table 8-4. There were nine (9) sites where samples were analyzed as replicates from one cruise, analyzed from two cruises, or both. The mean, standard deviation (SD), and relative percent standard deviation (RPSD) are reported for within cruise duplicates and between cruise duplicates. Three sites (MT1, B4, and JSSD3) had at least three (3) replicates from the same cruise. The RPSD for these sites were 25%, 38%, and 45% (Table 8-4) with a mean of 36%.

These results are similar to the RPSD of 27% found from the shakedown cruise. These results indicate that the RPSD for within-cruise replicates are less than 45%. The RPSD for the seven (7) sites where two or more samples were analyzed from two cruises ranged from 34 to 109%, with a mean of 61% (Table 8-4). The between-cruise RPSD, as expected, is generally higher than the within-cruise RPSD. The mean concentration for sites with replicates was used for the geographical display of the data.

Table 8-4

DGoMB Replicate Total PAHs (ng/g)

Site	Cruise 1	Cruise 2	Cruise 3	Site Mean	Site SD	Site RPSD
C 7	37.7	292.0		165.0	180.0	109%
MT 1 A	733.0	221.0		446.0	230.0	52%
MT 1 B		306.0				
MT 1 C		524.0				
MT 1 Mean	733.0	350.0				
MT 1 SD		156.0				
MT 1 PRSD		45%				
MT 3 A	1033.0	191.0		543.0	438.0	81%
MT 3 B	404.0					
MT 3 Mean	719.0	191.0				
MT 6	59.2	96.5		77.9	26.4	34%
S 36	80.1	147.0		114.0	47.3	42%
S 41 A	97.4	76.6		109.0	39.5	36%
S 41 B		153.0				
S 41 Mean	97.4	115.0				
S 42	35.1	110.0		72.6	53.0	73%
BH A		357.0				
BH B		157.0				
BH C		282.0				
BH Mean		265.0				
BH SD		101.0				
BH RPSD		38%				
JSSD3 A			105.0			
JSSD3 B			123.0			
JSSD3 C			97.8			
JSSD3 D			98.8			
JSSD3 E			56.3			
JSSD3 Mean			96.2			
JSSD3 SD			24.5			
JSSD3 RPSD			25%			

The concentration of perylene from all cruises is depicted for the sampling sites in Figure 8-69. Perylene is a PAH produced by biological processes as well as by combustion. Perylene is often detected as the major PAH in sediments from relatively pristine areas. In the sediment samples analyzed for this study, the percentage of perylene of total PAH ranged from 0 to 63%. Perylene concentrations ranged from ND (<1 ng/g) to 110 ng/g with a mean of 17 ng/g. Perylene

is also produced from combustion or processing of fossil fuels (e.g., perylene is present in creosote made from the heating of coal). Due to its anthropogenic as well as biogenic origins, the total PAH data for this report is discussed both with and without perylene. Other PAH are predominantly from anthropogenic sources. The geographic pattern of perylene concentrations (Figure 8-69) is complex but it does not co-vary with the total PAH distribution. The six (6) highest perylene concentrations are at sites S26, MT1, C1, B2, NB4, and RW6. These sites are found through the sample area with no discernable geographic pattern.

The concentration of total PAH without perylene is depicted in Figure 8-70. Sites with relatively high concentrations include MT1, MT3, and C1. These sites, based on their PAH distribution, can be divided into two types: sites with PAH predominantly from oil and those with PAH predominantly from combustion sources. For sites MT1 and MT3, oil appears to be the major source of PAH. For C1, combustion sources predominate. Combustion PAH in the sampling area may be discharged from ships or platforms (e.g., bilge pumping) or come from atmospheric deposition of PAH from onshore industrial areas or sediments transported from coastal areas. The ship/platform operations are the most likely sources, as atmospheric deposition and would be expected to produce similar PAH concentrations over large regions. The geographic distribution of PAH indicates a possible input from PAH in the plume of sediments from the Mississippi River, but that cannot be confirmed from the present data.

The total PAH concentration without perylene is plotted versus barium concentration in Figure 8-71. Most of the sites lie near the origin because they have both low PAH and low barium concentrations. Some sites have high barium and PAH concentrations (MT1, MT3, and C1). Barium is a tracer of drilling muds from platform operations. The elevated barium and PAH at the MT1, MT3, and C1 sites are likely due to inputs from platform operations in the vicinity of these sites.

A frequency distribution for total PAH and total PAH without perylene concentrations are plotted as cumulative percentages (Figure 8-72). The concentrations, plotted on a log scale, have similar "S" shaped distributions. The addition of perylene causes a slight increase in concentrations over the entire range. The median concentration for total PAH is 92 ng/g and for total PAH without perylene is 76 ng/g. This indicates the relative importance of perylene, especially at low concentrations. Similar frequency distributions for total PAH were reported for the GoMEX program (Kennicutt et al. 1996a) and the cumulative curves had similar shapes. The concentrations of PAH found in close proximity to production platforms ranged from 10 to 6400 ng/g, with the highest concentrations close to the platforms. However, most concentrations were less than 1000 ng/g (Kennicutt et al. 1996a). The frequency distribution for total PAH for the GoMEX study (Kennicutt et al. 1996a, b) is similar to the distribution found here, except that only one value exceeded 1000 ng/g in this study. When the frequency distributions found in this study are compared to those for other nearshore studies (NOAA NS&T and EPA-EMAP-NC), the median PAH concentration for this study is lower by about a factor of four. Total sediment PAH concentrations greater than 4000 ng/g are expected to elicit a biological effect 10% of the time (Long and Morgan 1990). The highest total PAH concentration found in sediments from this study (1033 ng/g) is four times less than the "biological effects" level.

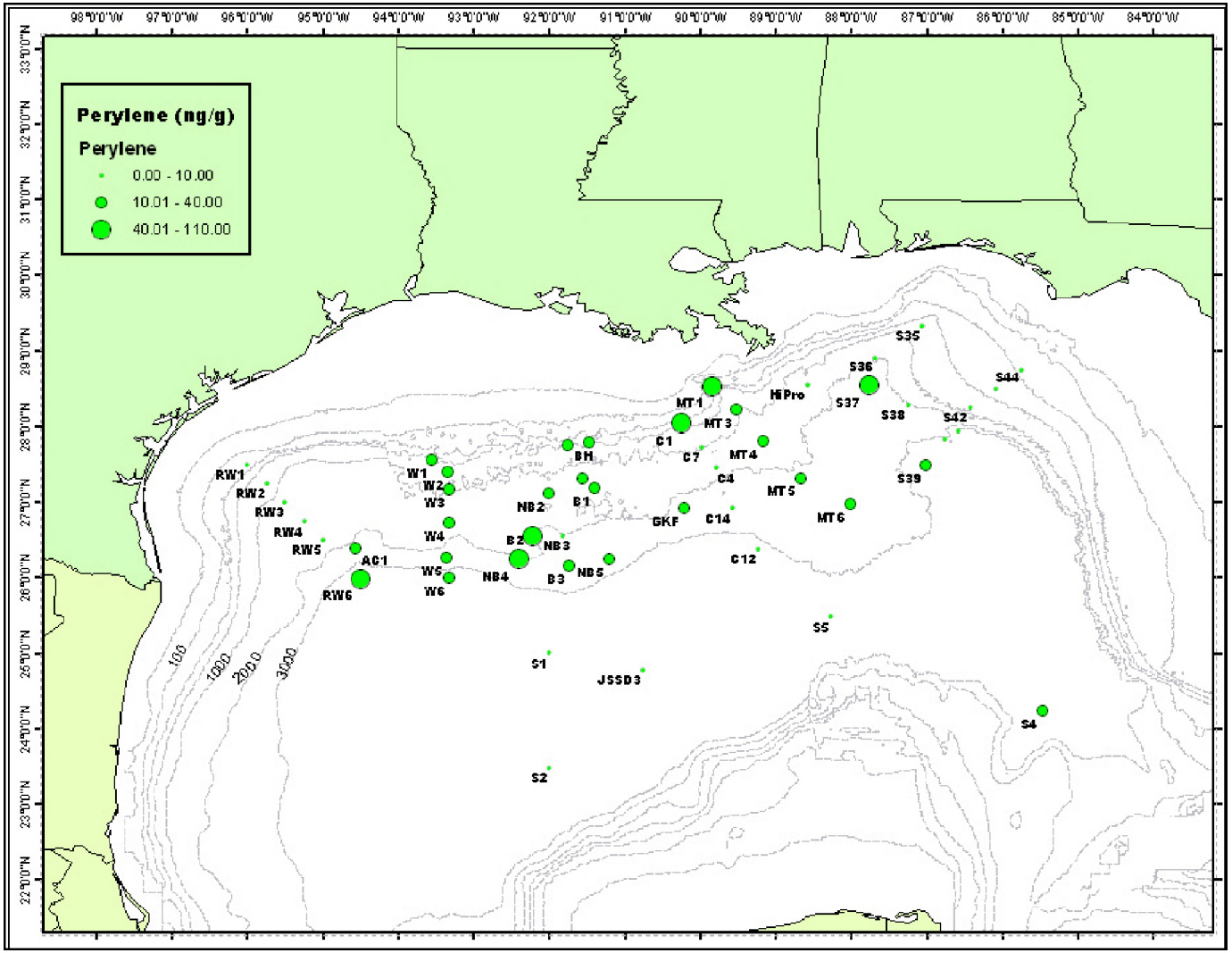

Figure 8-69. The concentration of perylene in sediments.

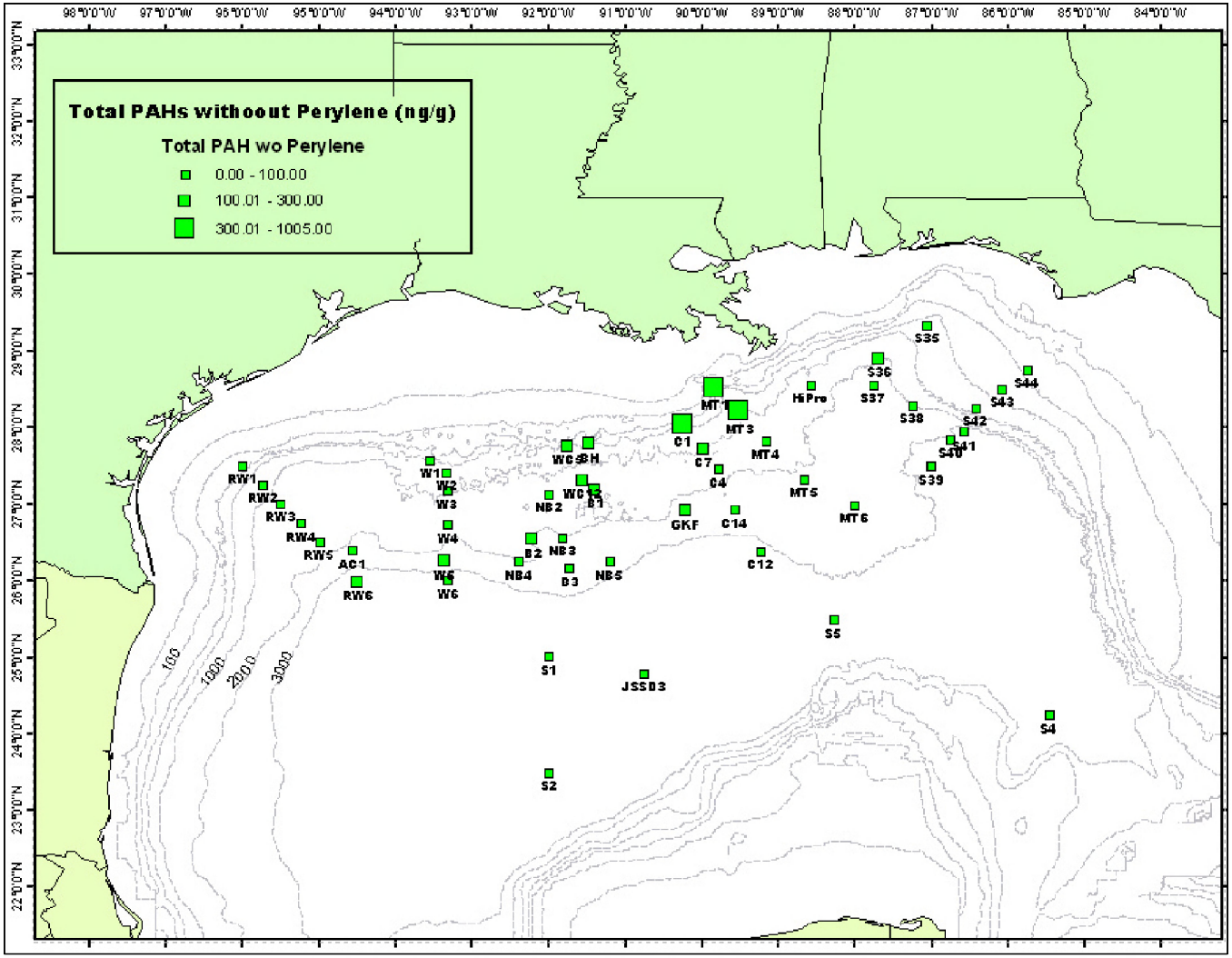

Figure 8-70. The concentration of total polycyclic aromatic hydrocarbons (PAH) without perylene in sediments.

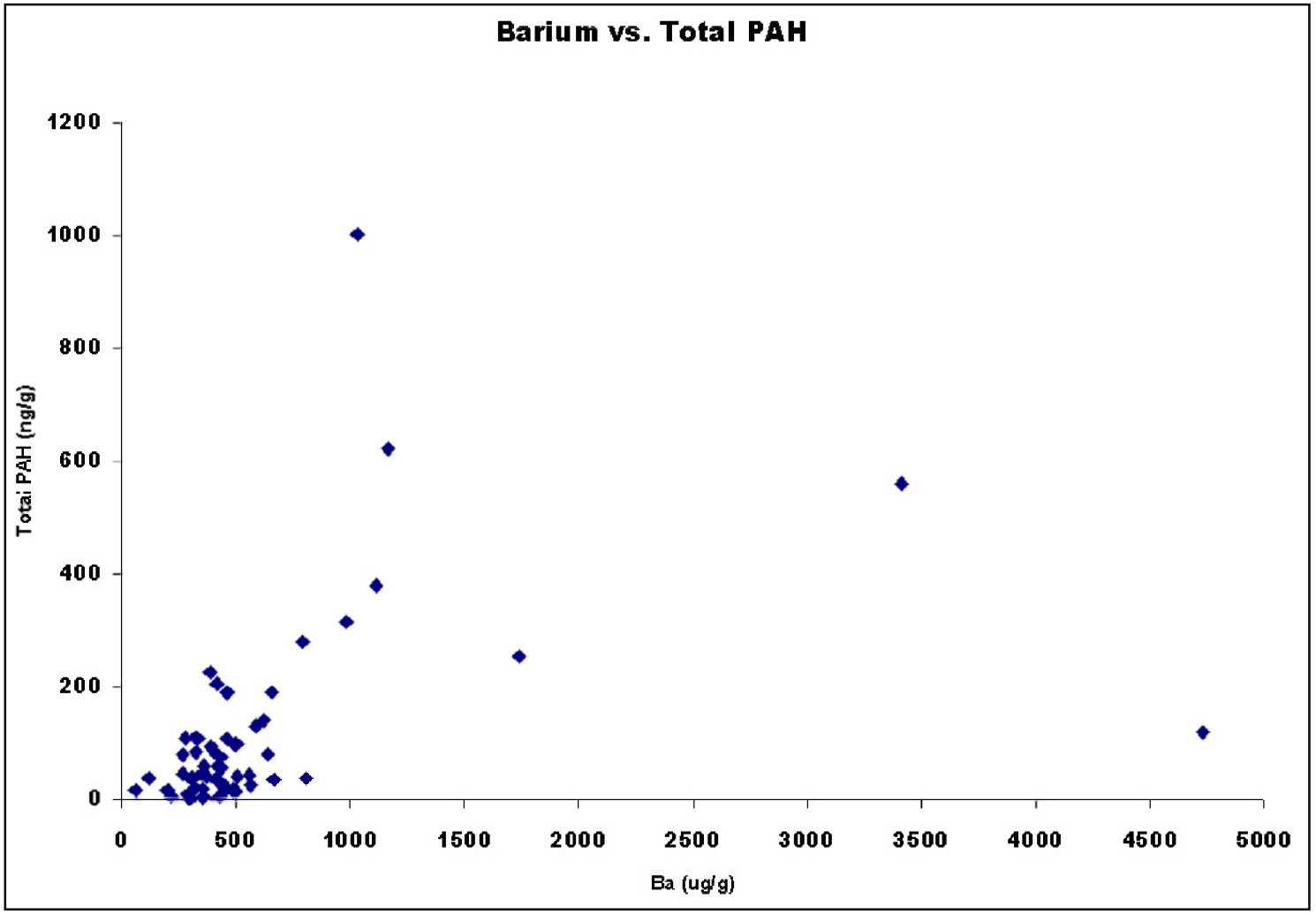

Figure 8-71. The total PAH concentration without perylene versus barium concentration.

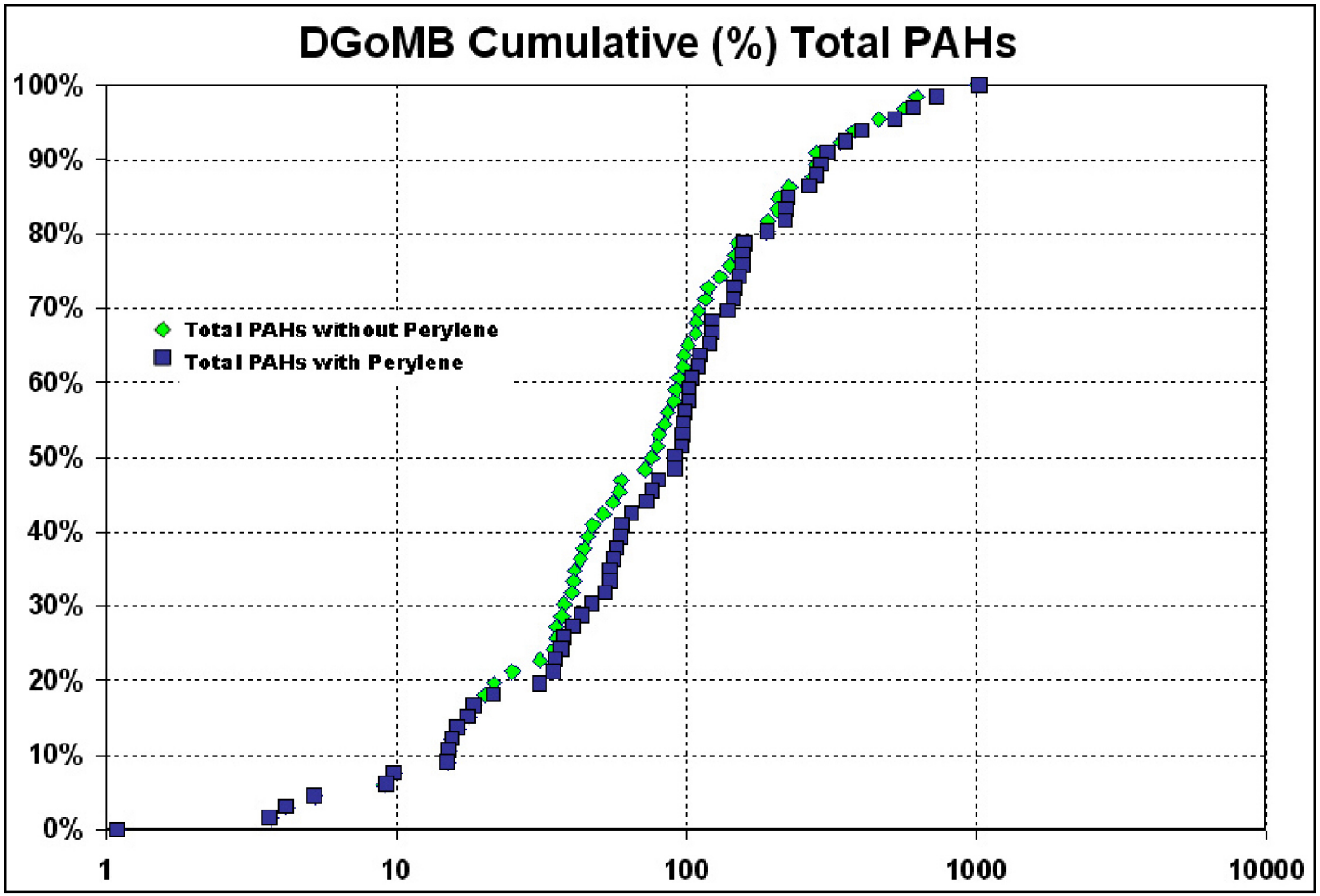

Figure 8-72. Frequency distribution of total PAH and total PAH without perylene concentrations versus cumulative percentage.

In summary, concentrations of PAH measured for the DGoMB project from offshore GoM sites were low, as expected. Perylene, a PAH with a biogenic source, was the major PAH detected at many locations, indicating a biological origin. Sites that had high PAH concentrations (MT3, MT1 and C1) also had high barium concentrations. This indicates that drilling operations in the vicinity of these sites was a likely source of PAH. Total sediment PAH concentrations at all sites were less than 1033 ng/g. It is unlikely that the PAH concentrations found at any of these sites would have an adverse effect on the biota living in these sediments. It is notable too that the three sites with the highest PAH levels were in or near the Mississippi Canyon, and thus the Mississippi River effluent itself cannot be ruled out as a source of contaminants.

8.7 Large Plant Detritus and Human-Generated Refuse

Large fragments of plant detritus, such as *Sargassum, Thalassia and Zostera (LPD)*, and human-generated refuse (HGR) have occasionally been observed and documented in the deep-sea. This component of the present survey was not included in the original sampling plan because it was not expected to be of much significance. As the trawl samples were consistently characterized by such material, the categories of "large plant detritus" (LPD) and "human generated refuse" (HGR) were added.

Scraps of wood, bark, macrophytes and fruit that serve as both habitat and nourishment to marine organisms (Rowe and Staresinic 1979; Turner 1973; Heezen and Hollister 1971), and wood construction material have been anecdotally documented in deep-sea trawl samples off and on for at least 3 decades (Wolff 1979; Pawson 1982). No definitive quantitative documentation, however, yet allows generalizations to be made about LPD or HGR in deep-sea environments. In this study, trawls were recovered from 34 stations spread all across the northern GoM. The closed dots in Figure 8-73 represent sites where HGR was retrieved, whereas open dots indicate samples without HGR. Closed triangles represent poor or failed trawls.

Samples were initially categorized into HGR and LPD. HGR was further separated into the following categories: wood, aluminum cans, ceramics, clinkers, cotton cloth, discarded fishing gear, glass, metal, paint utensils, paper products, plastics, rope, rubber, tar, and miscellaneous items.

Natural LPD had a wide and fairly even geographical distribution within the study area (Figure 8-74). Approximately one-half of the sites contained *Sargassum* sp,, which was inhabited in many instances by mollusks, crustaceans and covered with epiphytes. *Thalassia testudinum* was recovered from water depths up to 3,000 m.

Trawls from twenty-five of the thirty-four sites (74%) contained HGR (Figure 8-73) which was dominated by plastics, aluminum cans, wood, and fishing gear. Unlike the natural refuse, the majority of the HGR was concentrated in the area of the Mississippi River Trough (Figure 8-73). Petroleum, metal containers, plastics and paint supplies were found at approximately 70% of the sites. Each slowly degrade and remain persistent in the environment.

The concentration of HGR and in particular Sargassum within and adjacent to the Mississippi River Trough suggests that the Mississippi River serves as a point source delivery system that may contribute to the localization of refuse in this area. Highly erosive deep-sea storms serve as significant transportation of sediments loads along with fauna (Aller 1989). It is reasonable to assume that these storms may also transport refuse to depressional areas, which may serve as *debris traps*. As sediment moves downslope, it forms debris flows and turbidity currents (Nardin et al. 1979), which may serve as an additional transport mechanism.

At two of the sites that appear as closed triangles in Figure 8-73, the trawl was either dislodged from the bridal, or in one instance, from the main cable. The amount of force required for such a feat is quite strikingly large and indicative of a rather large object such as a sunken ship. It is possible that these areas may serve as hard substrates for epifaunal communities in an otherwise soft sediment environment.

Notably, more than 80% of the aluminum cans originally contained beer. Furthermore, greater than 60% of the glass was beer bottles. Other unique items included a fully intact sidewinder missile (Figure 8-75) that was recovered along the Florida Escarpment at a water depth of approximately 217 m. A 50-caliber shot casing was recovered seaward of the Mississippi River Trough in about 2,400 m water depth. Monofilament fishing line was recovered in over 22% of the trawls (Figure 8-76). In one instance, within the Mississippi River Trough at approximately 500 m water depth, a 2 meter-by-3 meter mass of longliner monofilament was reclaimed (Figure 8-75). The hooks were removed, indicating that it was discarded as a tangled mass on purpose and not simply lost while in use fishing.

The amount of HGR in the deep-sea is poorly known. It may be possible that organic substrates are absorbed onto HGR which sink to the deep-sea floor and are incorporated into the benthic food chain (Gage and Tyler 1991). Observations made through this survey provide evidence that HGR accumulates preferentially in certain areas which can be referred to as *debris traps*.

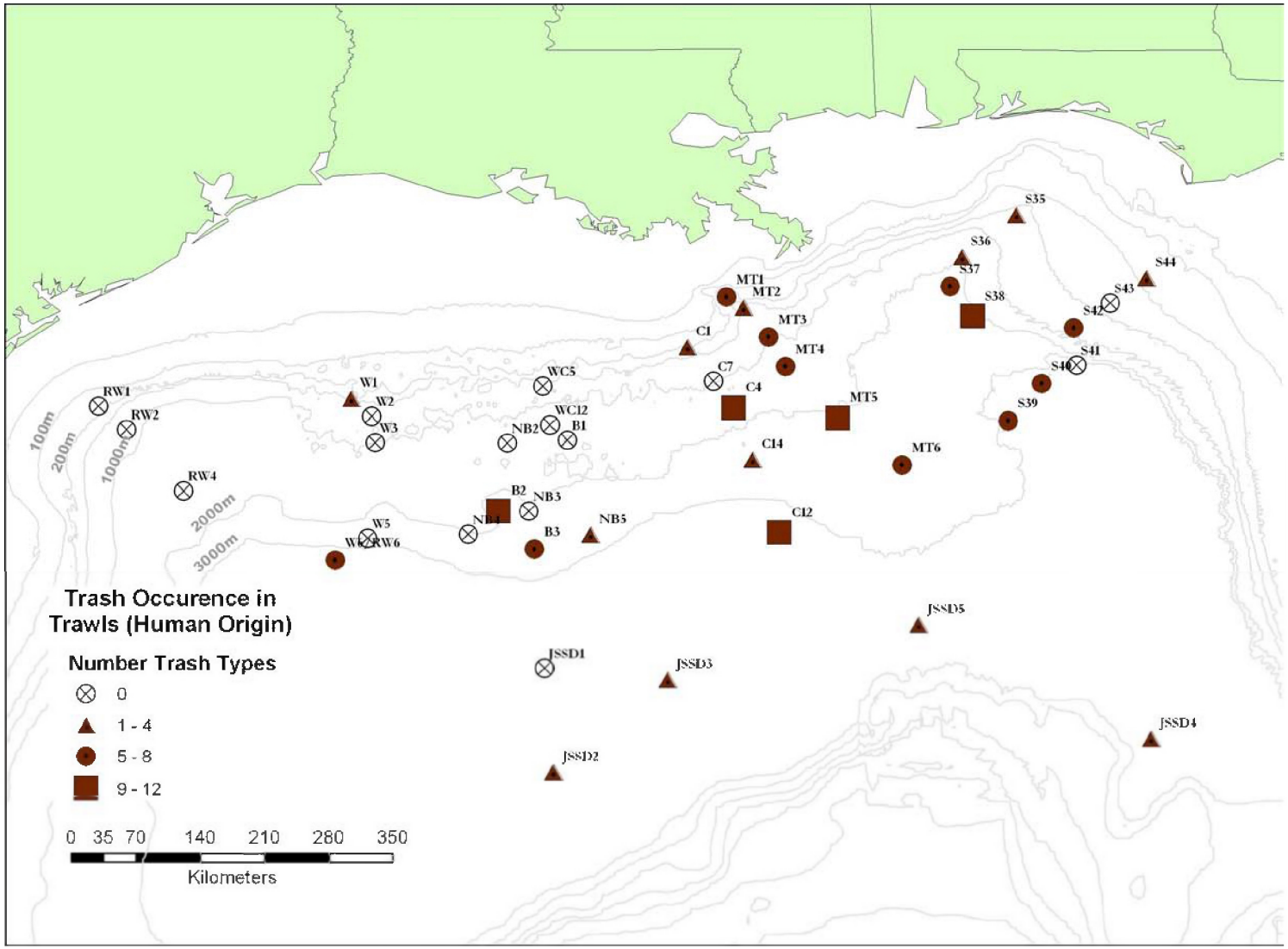

Figure 8-73. Trash occurrence in trawls.

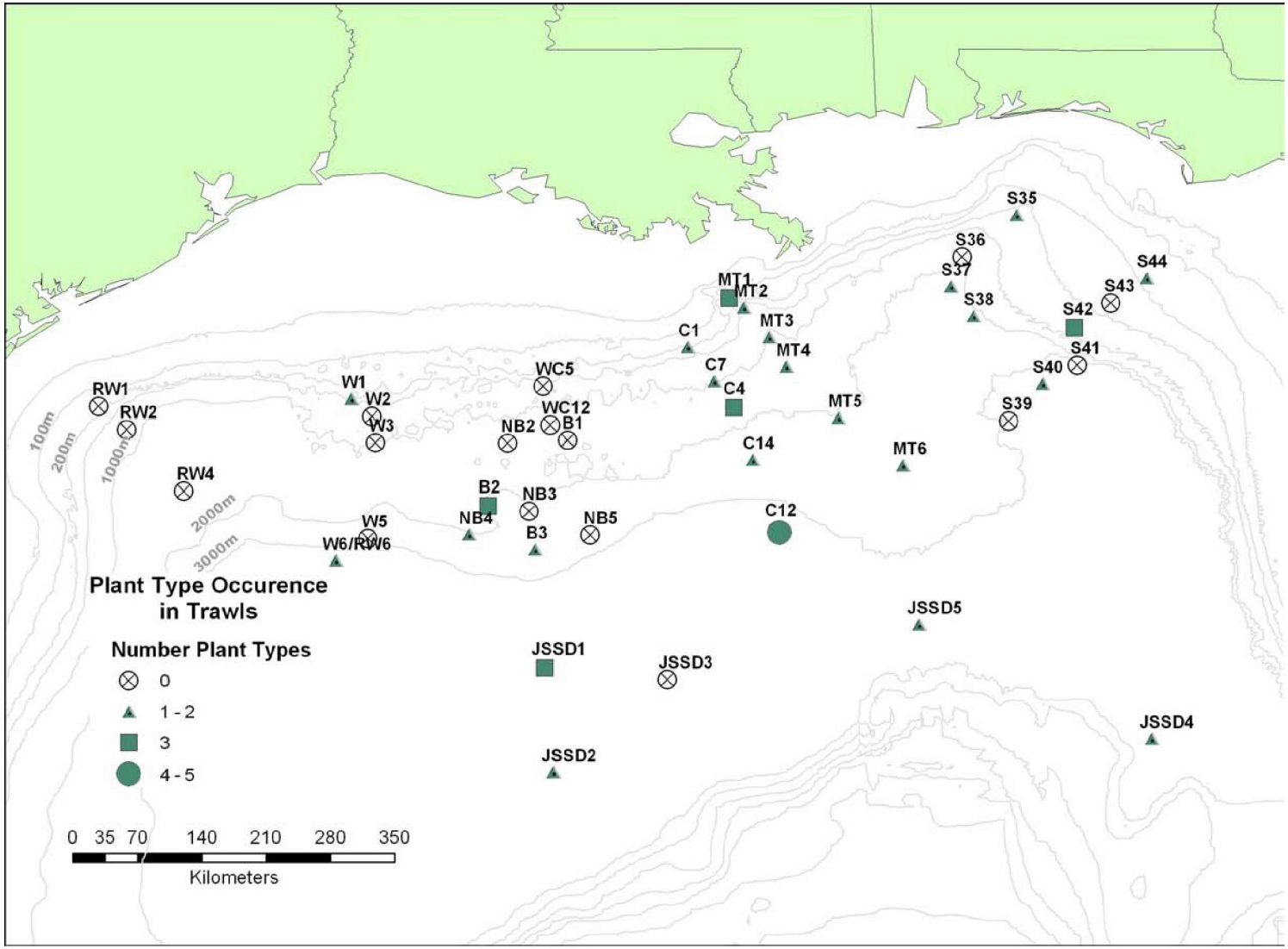

Figure 8-74. Plant type occurrence in trawls.

Figure 8-75. Sidwinder missle recovered on the Florida slope.

Figure 8-76. Longline fishing line, hooks removed, measuring ca. 1 m by 3 m.

8.8 Benthic Biology

All size categories of the sediment-associated biota were sampled on Cruises 1 and 2. These included 1) microbiota, 2) meiofauna, 3) macrofauna, 4) megafauna, and 5) demersal fishes. Each fraction was fixed and labeled aboard ship as described above and distributed to respective PI's immediately at the end of the cruise. These resulted in species lists for each category at each site sampled, all of which are now available in the database. In addition, biomass (total) for each group at each site was measured. For some groups, average biomass of the individuals have been measured. Both biomass and size data can be found in the database as well. The results are all presented below in this subsection in order of increasing organism size, with special kinds of analyses concluding the section.

8.8.1 Microbiota

8.8.1.1 Benthic Bacterial Abundance and Biomass

The microbiota component of the overall project included collection of an unprecidented set of data ($n > 1000$) on bacterial abundance in the sediments. Abundance was measured at four depth horizons (0–1, 4–5, 9–10, 14–15 cm) in triplicate cores at each of 59 survey and process stations, ranging in depth from 19 to 3,732 m, during three cruises (DGoMB 2000, 2001, and 2002). Because the station at 19 m was anomalous for its shallow depth (all others stations were at 213 m or much deeper), nearly anoxic state and high bacterial abundance (always plotting off-scale), the data obtained there (and provided in the database) have been excluded from all subsequent ranges and analyses. With that caveat in mind, the horizon-specific measurements ranged over more than an order of magnitude, from 1.00×10^8 to 1.80×10^9 bacteria cc^{-1} sediment. This range falls within that reported previously by the same methods for surface sediments from similar station depths elsewhere in the ocean (Alongi 1990; Deming and Baross 1993). Subsurface DGoMB sediments were often inhabited by numbers of bacteria equivalent to, and on occasion higher than (e.g., at stations NB5 and S35), those observed in surface sediments (see database for individual measurements), implying bioturbation. The general pattern of bacterial abundance decreasing only moderately if at all with depth into the seabed also implies that our depth-integrated estimates of bacterial abundance (or biomass), though reflective of conditions to 15 cm, underestimate the total carrying capacity of the seabed (to depths below 15 cm).

The size (biovolume) of benthic bacteria was also measured at four depths in triplicate cores for selected stations (see Table 8-5) in order to convert seabed abundance estimates to biomass in a DGoMB-specific manner, rather than relying solely on previously published conversion values. Mean bacterial volume in a given sediment horizon ranged from 0.027 (± 0.008; at 5 cm, station MT6) to 0.072 (± 0.033; at 15 cm, station MT3) μm^3. This range falls near the middle of size-class ranges considered for marine bacterioplankton (Norland 1993) and largely below that reported for intertidal sediments (0.07 to 0.22 μm^3; Kuwae and Hosokawa 1999). That downcore profiles of bacterial biovolume were essentially constant (overlapping error bars between horizons) may also suggest bioturbation.

Ultimately, we developed station-based estimates of benthic bacterial abundance and biomass by integrating results over the sampled depth interval of 0–15 cm and calculating the mean value for triplicate cores. The resulting estimates scaled to square meter of seafloor are the focus of remaining analyses in this section. These mean values for benthic bacterial abundance

ranged from 4.40 x 10^{13} to 1.75 x 10^{14} bacteria m^{-2} across station depths of 213–3,732 m. Before evaluating these data and biomass estimates developed from them, we revisit two methodological issues.

Table 8-5

Benthic Bacterial Biomass at Selected DGoMB Stations[1] and from the Literature

Cruise or reference	Station or location	Station depth (m)	Bacterial biomass (g C m^{-2}, 0–15 cm)	
			Based on biovolume, abundance[2], and 390 fg C um^{-3}	Based on abundance[2] and 10 fg C $cell^{-1}$
DGoMB 2000	S42	767	1.18 (1.30)	0.66 (0.73)
	MT3	987	2.32 (2.55)	1.25 (1.38)
	S36	1828	1.68 (1.85)	1.10 (1.21)
	MT6	2700	0.92 (1.01)	0.68 (0.75)
DGoMB 2002	S4	3410	N.D.[2]	1.48
	S1	3535	N.D.	1.40
Rowe and Deming, 1985	Bay of Biscay	4100	N.D.	0.10
	Demerara Basin	4500	N.D.	0.21
		4800	N.D.	0.12
Relexans et al., 1996	Mesotrophic site off West Africa	3100	N.D.	0.64
	Oligotrophic site off West Africa	4500	N.D.	0.18

[1] Where bacterial biovolume measurements were made.
[2] Parenthetic values adjusted upwards 10% (see text).
* N.D. = not determined (no bacterial biovolume measurements made).

First, procedures for determining bacterial abundance and biomass relied upon established methods in epifluorescence microscopy to obtain an internally consistent data set. Nevertheless, the laboratory dilution scheme used to prepare microscopic slides of shelf and slope sediments (DGoMB 2000 and 2001) differed from that used for the abyssal sediments (DGoMB 2002). The different schemes were necessary to obtain countable slides, but in comparative dilution studies, we determined that the shelf-slope samples may have been underestimated by 10% as a result (see Section 7.2.1). Others using our data as provided in the database may wish to increase the reported shelf/slopes values by 10%, as we have done in selected analyses, specified below. This slight adjustment may be important to evaluations of the data in an absolute sense (e.g., in carbon-based partition models of the benthos) or when comparing the entire bacterial data set (shelf-slope plus abyssal stations) against another entire data set (e.g., other variables measured in parallel sediment cores).

Second, in order to apply the biovolume measurements made for a subset of stations to the global data set, we developed an interpolation scheme as follows. Bacterial biomass was calculated from the measured biovolume and abundance measurements using the conversion factor of 390 fg C μm^{-3} (Bjornsen and Kuparinen 1991). Biomass was also calculated more

simply from abundance measurements using the deep-sea conversion factor of 10 fg C per bacterium, as in previous studies (e.g., Rowe and Deming 1985; Alongi 1990; Relexans et al. 1996). The biovolume-based estimates, which should represent improved estimates, were always higher than their counterparts by a factor of 1.4–1.9 (Table 8-5). The factor difference between the two approaches (y), when plotted against station depth in meters (x), yielded the linear regression equation: $y = 2.040 - 0.0002598\ x$. The negative slope, and thus convergence towards unity of the two methods as station depth increases, implies that the calculation of benthic biomass directly from abundance (using the deep-sea conversion factor of 10 fg C $cell^{-1}$) may well be an adequate approach to estimating bacterial biomass in abyssal sediments. Unknown but different and likely depth-specific conversion factors are needed for shallower shelf-slope depths; otherwise, acquiring biovolume measurements is recommended.

Using the equation described above, we then calculated the biomass for all remaining stations. No comparable biovolume-based biomass estimates exist for other sediments, but a comparison of the simpler abundance-based estimates can be made to similarly determined estimates in the literature (from depths of 3100–4800 m in the Atlantic Ocean). That comparison reveals that bacterial biomass in DGoMB sediments is higher (Table 8-5). The comparison is most relevant between abyssal sediments, where the simpler estimates may also be considered as accurate as biovolume-based values (and no 10% adjustment issue pertains). The available abyssal data sets for this comparison are small and depth ranges do not overlap precisely. Nevertheless, the abyssal GoM sediments (at 3,410–3,732 m) appear to support more bacterial biomass, by a factor of six, than abyssal sediments elsewhere (mean of 1.48 g C m^{-2}, S.D. = 0.17, n = 5, versus mean of 0.25 g C m^{-2}, S.D. = 0.22, n = 5).

Graphical examination of the global DGoMB data set on benthic bacterial abundance (Figure 8-77) and on biovolume-based biomass (Figure 8-78) reveals the importance of considering the latter estimates and thus of obtaining biovolume measurements, rarely done for sediment bacteria, given the technical difficulties (Kuwae and Hosokawa 1999). For example, when bacterial abundance is considered as a function of station depth, no relationship is detectable by linear regression analysis, with or without the 10% adjustment to the shelf-slope stations (without, $R^2 = 0.000$, n = 58; Figure 8-77; with, $R^2 = 0.005$, n = 58, Table 8-6). Although earlier studies with limited data sets (reviewed by Deming and Yager, 1992; Deming and Baross 1993) suggested weak depth-dependencies, the study closest to ours in size (ten stations) and depth range (695–4350 m) also failed to detect a significant decrease in benthic bacterial abundance with depth (Alongi 1990). Alongi attributed the absence of a depth-dependent relationship to densities of potential grazers and geological differences among the sites. Deming and Yager (1992) found the supply of new resources or POC flux to the seafloor to be a stronger determinant of benthic bacterial abundance than ocean depth or measures of organic carbon (TOC) already present in the sediment. The latter finding reflects the relatively rapid responses of bacteria to pulses of organic carbon, even under abyssal conditions (Deming 1985; Lochte and Turley 1988). Each of these explanations will also pertain to the absence of a bacterial depth-dependency in the DGoMB study, but we offer an additional interpretation: biovolume-based biomass and not abundance may be the more relevant bacterial variable to consider. Even given the vast and varied environments sampled in this study, a detectable (albeit weak) relationship emerges when the global set of biovolume-based bacterial biomass estimates is regressed against station depth ($R^2 = 0.300$, n = 58; Figure 8-78; with the 10% adjustment to shelf-slope data, $R^2 = 0.350$, n = 58, Table 8-6).

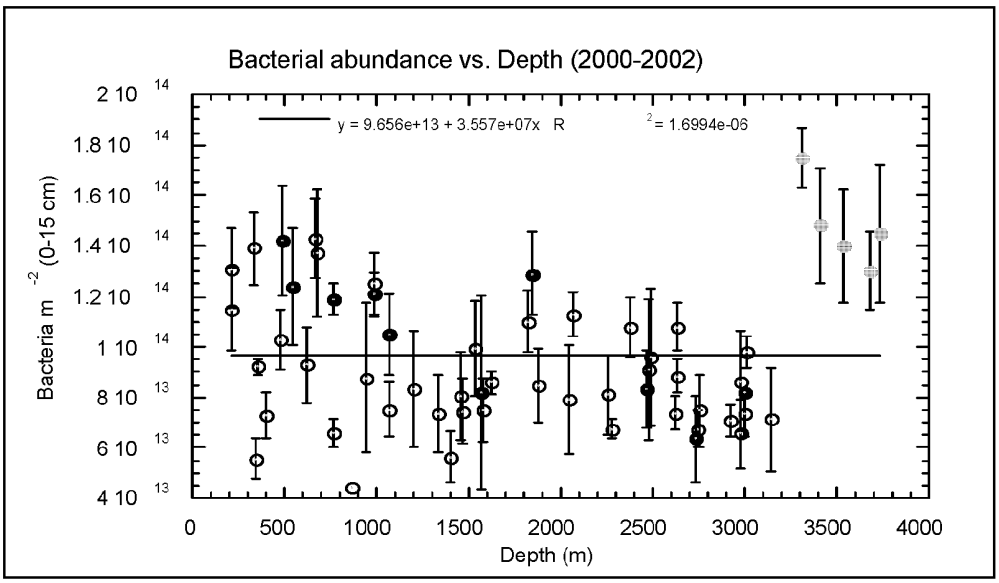

Figure 8-77. Global data set for depth-integrated, benthic bacterial abundance versus station depth (without 10% adjustment to shelf-slope stations). Open symbols indicate data from DGoMB 2000; solid black symbols, from DGoMB 2001, gray symbols, from DGoMB 2002. Error bars indicate standard deviation of the mean from triplicate cores. Note that lowest data point at 863-m depth (station W3) was not replicated (has no error bar).

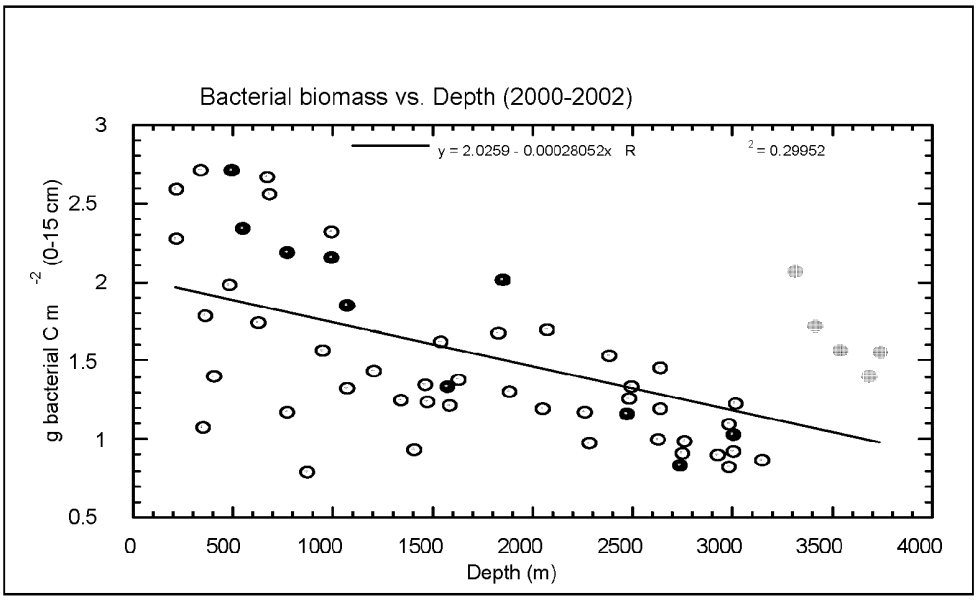

Figure 8-78. Global data set for depth-integrated, biovolume-based, benthic bacterial biomass versus station depth (without 10% adjustment to shelf-slope stations). Open symbols indicate data from DGoMB 2000; solid black symbols, from DGoMB 2001, gray symbols, from DGoMB 2002.

Table 8-6

R^2 Values From Linear Regression Analyses of Benthic Bacterial Data on Abundance and Biovolume-Based Biomass as a Function of Station Depth

Cruises included	Stations included[1]	Number of stations	Abundance	Biomass
DGoMB 2000, 2001 and 2002	All (no 10% adjustments)	58	0.000	0.300
	All	58	0.005	0.350
	All but S5[2]	57	0.006	0.390
	All but W3[3]	57	0.012	0.394
	All but S5 and W3	56	0.344	0.437
DGoMB 2000 and 2001	All	53	0.158	0.479
	Only transects (C, RW, MT)	40	0.217	0.525
	Only transects, no W3	39	0.280	0.591
	MT transect only	9	0.656	0.768

[1] Data from Hypox station at 19-m depth always excluded; data from 2000 and 2001 adjusted upwards by 10% (see text) except in the first case above (see also Figure 8-56).
[2] Station with highest abundance; anomalous abyssal station for signs of oxygen limitation.
[3] Station with lowest abundance; anomalous for lack of triplication (single-core analysis).

A minor paring, however, of both the abundance and biomass data sets not only improves the biomass depth-dependency, but also reveals a weak one for abundance, as summarized in Table 8-6. Excluding two of the 58 data points – the lowest and the highest for abundance – improves the R^2 value for biomass versus depth from 0.350 to 0.437 and for abundance, from 0.005 to 0.344. These data exclusions are not based solely on their endmember status. The lowest estimate came from the only station (W3) where we lacked triplicate cores (see absence of error bar on the lowest point, a depth-integrated value from a single core, at 860-m depth on Figure 8-77). The highest came from the abyssal station (S5) already anomalous for its signs of anoxia.

If we consider only the slope data, and subsets thereof, to ask whether or not benthic bacterial variables are depth-dependent, then stronger depth-dependencies become evident (Table 8-6). For example, if the data from stations located in basins or other specific slope features are excluded and only transect data (from the C, RW, and MT stations) are analyzed, the R^2 value for a biomass depth-dependency is 0.525 (n = 40, Figure 8-77). It improves to 0.591 if station W3 (where we lacked replication) is also excluded (n = 39, Table 8-6). The highest R^2 value obtained from any of our depth-related analyses is 0.768, derived from the regression analysis of the MT transect data against depth. When only these MT transect data are considered, a relatively strong depth-dependency with bacterial abundance emerges for the first time (R^2 = 0.656, n = 9; Table 8-6). The more narrowly defined the sampling region, the more likely a depth-dependency, as has also occurred in previous and far less extensive studies of benthic bacterial abundance.

When the benthic bacterial abundance and biovolume-based biomass data were used to test hypotheses associated with what influences the quantity and composition of life in the deep ocean (Section 4), the issue of depth dependency in the Sigsbee region reflected the general results described above (Figures 8-78 and 8-79). Specifically, no significant difference was detected between slope and abyssal sites in terms of bacterial abundance (P = 0.151), but the

difference was significant in terms of biomass (P = 0.020, Table 8-7). Support for other hypotheses that we could test with our data set – that benthic bacterial abundance is determined by east versus west location in the study region or by high versus low overlying productivity – was not obtained, nor did considering biomass instead of abundance change the test result (Table 8-7). A final hypothesis that we could test with our data alone concerned annual variability in seabed measurements at seven stations across the shelf and slope that were sampled in both 2000 and 2001. A possible trend towards higher benthic biomass in 2001 on the upper slope, seen graphically in Figure 8-80 (note solid symbols and their positions above the regression line primarily at shallower depths) could not be verified as significant (P = 0.322).

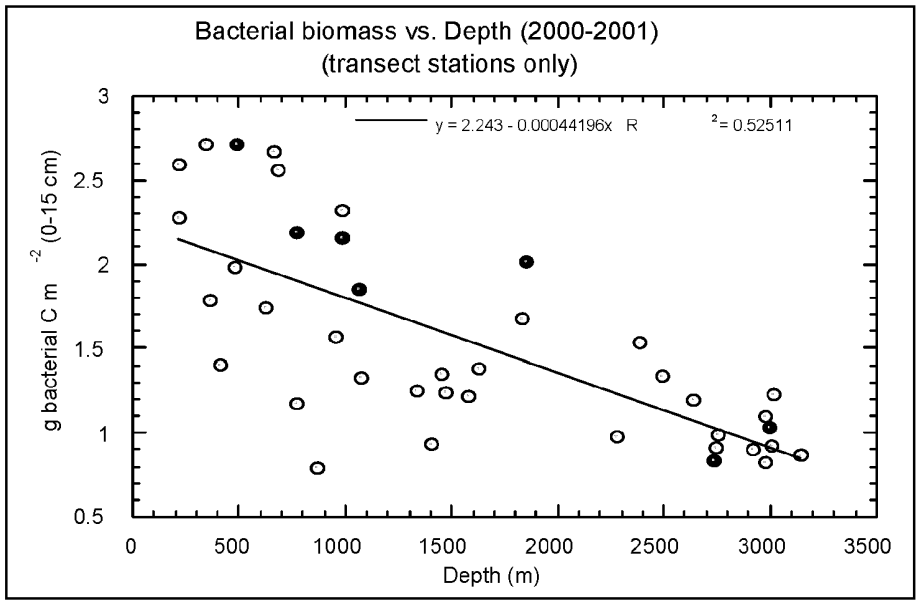

Figure 8-79. Depth-integrated, biovolume-based, benthic bacterial biomass versus station depth for transect stations only. Open symbols indicate data from DGoMB 2000; solid symbols, from DGoMB 2001.

Table 8-7

Hypothesis Testing (Single Factor ANOVA, $\alpha = 0.05$) for Factors that May Determine Benthic Bacterial Abundance or Biomass on the Shelf-Slope Regions of the Study Area

Factor examined	Number of stations	P-values		Interpretation
		for abundance	for biomass	
Shallow versus deep station depth (in Sigsbee region)	8	0.151	0.020	No effect on abundance, negative effect on biomass
East versus West location (3 tests: east–mid, mid–west, east–west)	10	0.633 0.229 0.501	0.233 0.264 0.845	No effect on abundance or biomass
Low versus high primary production	10	0.075	0.191	No effect on abundance or biomass

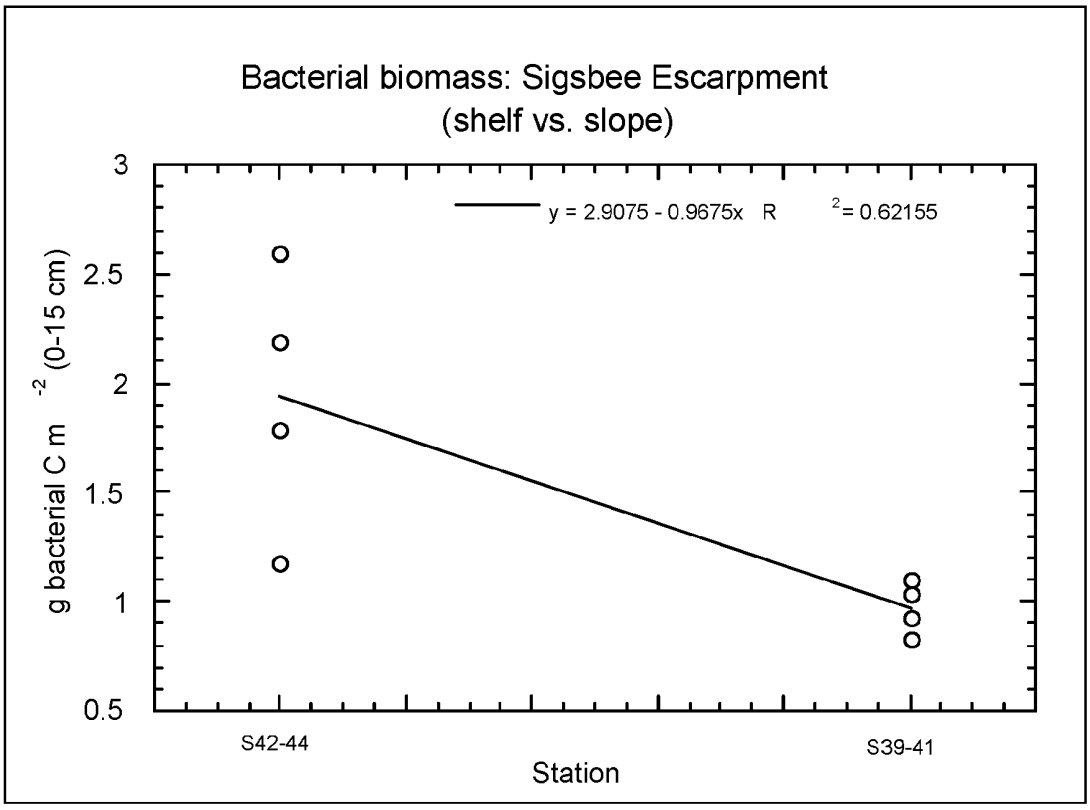

Figure 8-80. Significant difference (P = 0.020; Table 8-7) between biovolume-based, benthic bacterial biomass on upper slope (S42-44) versus lower slope/rise stations (S39-41) of the Sigsbee Escarpment.

8.8.1.2 Benthic Bacterial Production and Respiration

In addition to the extensive survey of benthic bacterial abundance and biomass described above, the microbiota component of the overall project included experiments to measure rates of bacterial activity in sediments from selected stations. Rates of bacterial production were determined from sediment incubation experiments at *in situ* temperature (except at station S4 where refrigeration problems prevented incubation below ~10°C), with and without in situ pressure applied shipboard, using ^{3}H-thymidine as a tracer for DNA production (see Section 7.3.1). Only surface sediments (0-1 cm) were examined by this method, since the uptake of ^{3}H-thymidine by anaerobic bacteria at subsurface depths is unlikely. The method yielded detectable rates of bacterial production at all six stations examined, covering a depth range of 767–3,535 m (Table 8-8). Application of *in situ* pressure resulted in higher rates (barophilic responses) only for sediments from depths ≥ 2,700 m, including the temperature-compromised station at 3,410 m (though not abyssal station S1).

Our estimated *in situ* bacterial production rates (range of 5–75 µg C m^{-2} d^{-1}), however, are low when compared to the other published rates obtained by similar methods from similar depths (pressures) and temperatures. Alongi (1990) reported rates of 34–7010 µg C m^{-2} d^{-1} in sediments with bacterial abundances similar to ours over a depth range of 695–4350 m in the Solomon and Coral Seas near Australia (Table 8-9). The only methodological differences we can identify

Table 8-8

Samples from Which Benthic Foraminifera Were Extracted for ATP

Station	Depth Interval (cm)	Number Extracted
	Cruise 2	
	Process Stations	
MT3, replicate 1	0-1	53
	1-3	50
	14-15	50
MT3, replicate 2	0-1	50
	1-3	50
	9-10	50
S42	0-1	50
	1-3	50
	9-10	50
S36	0-1	75
	1-3	50
	14-15	50
	“tree” foraminifers from other S36 boxcores	6
MT6	0-1	50
	1-3	50
	9-10	50
	Non-Process Stations	
C7	0-1	50
	1-2	50
Bush Hill	0-1	50
	1-2	50
Total for DGoMB Cruise 2		984
	Cruise 3a	
JSSD1BC5	0-1	50
	1-3	50
	7-8	50
JSSD4BC27	0-2	75
	2-3	50
	9-10	25
JSSD4BC31 (replicate)	0-1	57
	Non-Process Stations	
JSSD2BC13	0-1	50
	1-2	60
JSSD5BC38	0-1	50
	1-2	57
Total for DGoMB Cruise 3a		574

Table 8-8 Samples from which benthic foraminifera were extracted for ATP (continued)

Station	Depth Interval (cm)	Number Extracted
	Atlantis Cruise (October 2000)	
Farnella Canyon (*Alvin* Dive 3628	0-1	130
Green Knoll (*Alvin* Dive 3629)		
Core 66	0-1	28
Core 67	0-1	40
Florida Escarpment (Dive 3634)	0-1	100
	2-3	26
Total for *Atlantic* Cruise		324
TOTAL All Cruises		1,882

Table 8-9

Bacterial Production Rates in Surface Sediments (0–1 cm),
Based on 3H-Thymidine Incubations at in Situ Temperature and Both in Situ Pressure and 1 Atm

Cruise or reference	Station	Depth (m)	Bacterial production (µg C m^{-2} d^{-1})		Rate ratio[1] (in situ atm/ 1 atm)
			in situ atm	1 atm	
DGoMB 2001	S42	767	4.6	33.0	0.14
	MT3	987	6.3	35.7	0.18
	S36	1828	14.8	33.6	0.44
	MT6	2700	52.0	26.6	1.95
DGoMB 2002	S4	3410	44.6[2]	19.5[2]	2.29[2]
	S1	3535	75.1	109.1	0.69
Alongi, 1990 (Solomon and Coral Seas)[3]	PNGS1	695	4680	N.A.[4]	(> 1)[4]
	CSP9	1454	7010	N.A.	(> 1)
	QT5	2256	776	N.A.	(> 1)
	WB5	2395	475	N.A.	(> 1)
	PNGS2	2426	1740	N.A.	(> 1)
	WB6	2775	911	N.A.	(> 1)
	WB7	2800	733	N.A.	(> 1)
	PNGS3	3264	968	N.A.	(> 1)
	CSB13	4008	34	N.A.	(> 1)
	CSB4	4350	141	N.A.	(> 1)

[1] Ratios greater than one indicate barophily.
[2] Incubation temperature (~10°C) was ~5°C warmer than in situ temperature.
[3] Samples were incubated within 1–2°C of in situ temperature (range of 1.8–7.6°C).
[4] N.A. = not available, but text reports that pressurized rates were higher than 1-atm rates.

between these two studies are our sampling of a thicker sediment horizon (0–1 cm versus 0–0.5 cm) and use of a lower ratio, by a factor of seven, of amount of thymidine injected to sediment volume.

Even if we were to adjust our rates upwards by that factor (requiring more assumptions than some would find reasonable), they would still be lower overall. Although the comparative data sets are small, DGoMB slope/abyss sediments thus appear to support lower rates of bacterial production than the slope sediments of the Solomon and Coral Seas near Australia. At abyssal depths, rates from the two studies appear to converge. A cross-disciplinary examination of the two study areas would be required to derive possible explanations for the shallow discrepancies and abyssal convergence. A cross-disciplinary examination of DGoMB data may help to explain the non-intuitive finding that our estimates of bacterial production rates under *in situ* pressures tended to increase with station depth.

In addition to bacterial production rates using the ^{3}H-thymidine approach, we also measured rates of respiration (conversion to CO_2), with and without in situ pressure applied shipboard, of ^{14}C-labeled amino acids substrates at four depth horizons in sediments from the two abyssal stations, S4 and S1. From the resulting downcore profiles (Figure 8-81), depth-integrated estimates of bacterial respiration in the seabed were obtained and compared to the few literature values obtained using the same methods and mixture of amino-acid substrates (Table 8-10). Our rates are considerably higher, by 1–2 orders of magnitude, than those obtained for two abyssal sites off West Africa (Relexans et al. 1996). Part of this difference may be attributable to the different incubation temperatures used: 5 or 10°C for the DGoMB samples; 1–2°C, for the West Africa samples (Relexans et al. 1996). Even considering a maximal 10°C difference (between our unavoidably warmed samples from station S4 and the West African samples), however, could only account theoretically for a doubling of the rate. Another consideration is the relative constancy of activity with depth in the DGoMB sediments (Figure 8-81) compared to the West African core profiles. In the latter cases, activity often approached undetectable levels at 15-cm depth (Relexans et al. 1996), as also observed in other abyssal Atlantic sediments, albeit when ^{14}C-glumatic acid was used as substrate (Rowe and Deming 1985). Subsurface bacterial activity may thus be more important to overall benthic carbon cycling in the GoM than usually considered. Although the comparative data sets are very small, the abyssal seabed of the GoM appears to support depth-integrated rates of bacterial respiration that are considerably higher than observed elsewhere.

In the meantime, the kinetics of ^{14}C-amino acid respiration, as measured under simulated in situ conditions in surface sediments (Figure 8-82), also suggest substantial rates of organic carbon remineralization by benthic bacteria in the abyssal GoM. Although the data from temperature-compromised station S4 did not fit Michaelis-Menten kinetics, those from station S1 yielded an in situ amino-acid turnover time (respiration only) of one day (see y-intercept on figure). The modest slope of the regression line for increasing concentration of added amino acids suggests that the bacterial community may have been respiring the naturally available mixture of amino acids at near-maximal capacity. The results of incubating diluted sediments for the purpose of determining the cellular fate of the added ^{14}C-amino acids indicated that the bulk of the carbon was being respired, with only 9.3–23% incorporated into biomass. The arrival of new organic substrates could thus be expected to shift the community from a largely respiratory (cellular maintenance) mode into a more rapid growth phase, incorporating a greater fraction of the carbon into new biomass. Measured growth rates (bacterial production rates) in surface sediments were relatively low (see above), suggesting the potential for stimulation. In summary,

the abundant bacteria present in the abyssal sediments of the GoM at the time of our sampling appeared to be reproducing at lower rates but respiring carbon more rapidly than in other regions examined using comparable methods.

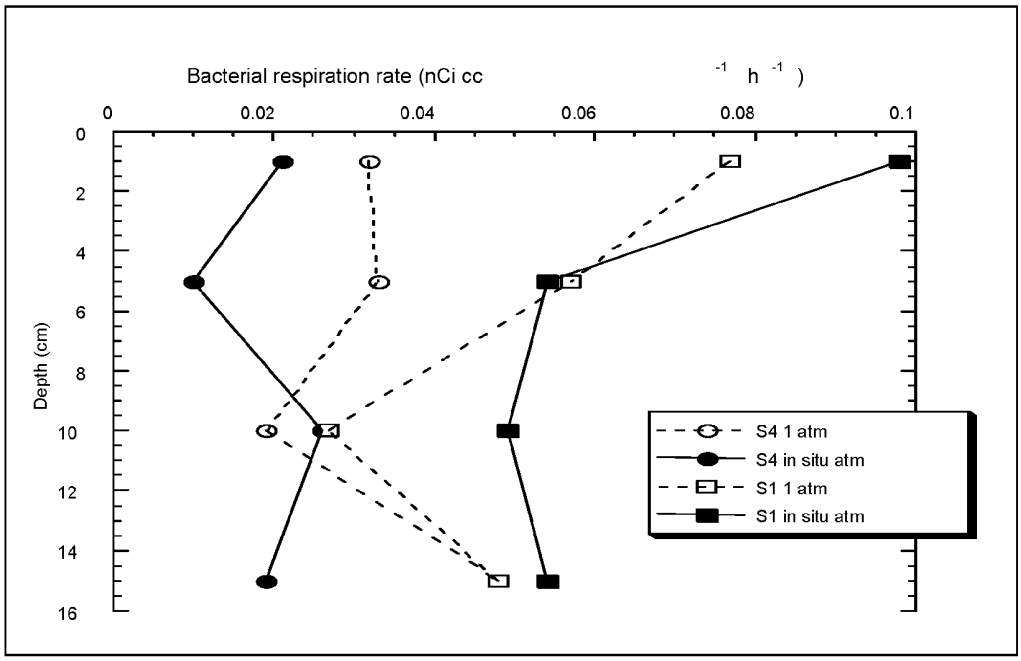

Figure 8-81. Downcore profiles of ^{14}C-amino acid-based, benthic bacterial respiration.

Table 8-10

Depth-Integrated (0–15 cm) Benthic Bacterial Respiration Rates
Based on ^{14}C-Amino Acid Incubations at in Situ Temperature and Both in Situ Pressure and 1 Atm

Cruise or Reference	Station	Depth (m)	Bacterial respiration (µg C m^{-2} d^{-1})		Rate ratio[1] (in situ atm/ 1 atm)
			in situ atm	1 atm	
DGoMB 2002	S4	3410	75.9[2]	105[2]	0.72[2]
	S1	3535	242	198	1.22
Relexans et al., 1996[3]	Mesotrophic site off West Africa	3100	5.7	N.A.[4]	(> 1.0)[4]
	Oligotrophic site off West Africa	4500	1.8	N.A.[4]	(> 1.0)[4]

[1] Ratios greater than one indicate barophily.
[2] Incubation temperature (~10°C) was ~5°C warmer than in situ temperature.
[3] Samples were incubated at 1–2°C; rates were integrated to 10-cm depth (from 10–15 cm they approached zero); substrate incorporation into biomass at the mesotrophic and oligotrophic sites was 45–65% and 0–5%, respectively.
[4] N.A. = not available in text, but pressurized rates were higher than 1-atm rates (J. Deming, unpublished).

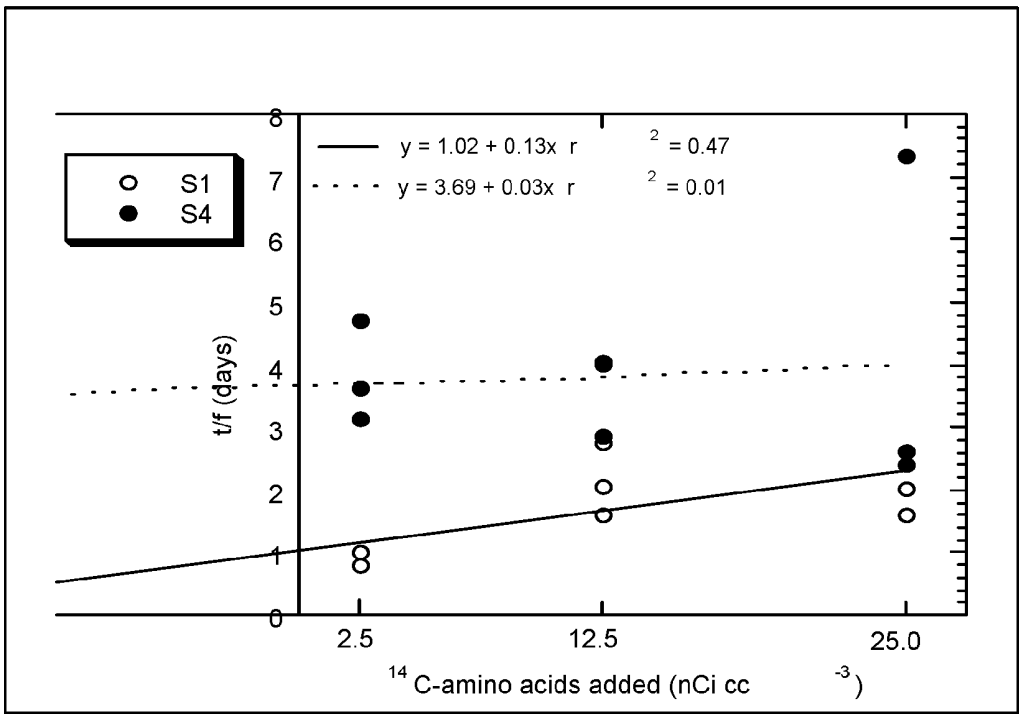

Figure 8-82. Kinetics of ^{14}C-amino acid-based, benthic bacterial respiration under in situ pressure and temperature, except for station S4 where the incubation temperature was ~10°C.

8.8.2 Benthic Foraminifera

A total of 1882 foraminifera were extracted for ATP, and thus biomass determinations (Table 8-10). Samples were taken at all process stations as well as at an additional two stations during DGoMB cruise 2 (C-7 and Bush Hill), two more stations on DGoMB cruise 3a (JSSD2, JSSD5), and three other sites sampled by the submersible *Alvin* (Farnella Canyon, Green Knoll, Florida Escarpment during an October 2000 *Atlantis* cruise, Ian MacDonald, Chief Scientist). Only the top one or two cm was processed for the survey site cores and auxiliary cores. At site S36 there was an abundant community of arborescent foraminifera (up to 5 cm in height), six of which were analyzed for ATP although none occurred in the foraminiferal biomass core.

Results from cores collected by *Alvin* were far lower in comparison to other data (Table 8-11). Because these samples were exposed to long periods of warm temperatures during submersible ascent and recovery, their results are omitted from analyses and interpretations.

When *Alvin* results are omitted, benthic foraminiferal abundances ranged over an order of magnitude (~3,600-44,500 individuals m^{-2}; Table 8-12) and foraminiferal biomass ranged from ~2-53 mg C m^{-2}.

Numerous large (up to 5 cm long) "tree-like" agglutinated foraminifers occurred at site S36 (1,848 m), with densities up to ~130 m^{-2}. These are tentatively identified as *Pelosina* sp. (Figure 8-83). Although no specimens were in the subcore for foraminiferal biomass quantification, they were observed in most boxcores collected from this site. *Pelosina* sp. biomass, determined from ATP analysis, ranged from ~2.8-13 µg C individual^{-1}, thus comprising a monospecific biomass

Table 8-11

Benthic Foraminiferal Biomass Data (mgATP/m^2), Abundance (#live/m^2) and Average Foraminiferal Volume (avg Vol) for Pushcores Collected by *Alvin* in October 2000 (n = number of foraminifers extracted (individually))

Station	Date	Water Depth (m)	Latitude	Longitude	Water Depth (cm)	ngATP/cm^3	mgC/m^2	#live/m^2	Avg Vol (mm^3) (+/-std dev)
Farnella Cyn (dive 3628)	21 Oct	2884	26-26.75N	90-46.50W	0 to 1	0.07	0.2	2407	0.014 (0.007)
Green Knoll (dive 3629)	22 Oct								
c66		2463	25-55.43N	90-12.87W	0 to 1	0.02	0.1	1070	NA
c67		2457	25-55.43N	90-12.87W	0 to 1	0.04	0.1	535	0.424(0.301)
Florida Esc. (dive 3634)	27 Oct	~2876	28-02.41N	86-33.05W	0 to 1	0.29	0.9	3477	0.028(0.014)
					2 to 3	0	0	0	0

Table 8-12

Benthic Foraminiferal Abundances (#/m^2) and Biomass (mgC/m^2) for the Surface cm (0-1 cm) and Integrated over the Top 3 cm (0-3 cm)

Site	Water Depth (m)	Latitude °N	Longitude °W	0-1 cm		0-3 cm	
				Density (# m^{-2})	Biomass (mgC m^{-2})	Density (# m^{-2})	Biomass (mgC m^{-2})
Bush Hill	548	27°47.8	91°28.2	45,455	47.1	81,819	98.1
S42 2001	768	28°15.3	86°25.6	3,636	2.9	7,272	6.0
MT3 2001	985	28°13.3	89°30.6	12,727	8.8	23,636	18.9
C7 2001	1076	27°43.7	89°58.7	25,455	53.4	41,819	74.9
S36 2001	1848	28°55.4	87°39.0	29,091	52.5	44,546	62.1
MT6 2001	2742	27°00.2	88°00.9	4,545	1.8	9,090	3.4
JSSD5	3316	25°29.5	88°16.2	10,909	20.9	27,273	23.8
JSSD4	3410	24°14.5	85°29.1	44,545	8.4	50,000	9.8
JSSD1	3520	25°00.6	92°00.7	27,273	3.7	30,909	6.4
JSSD2	3732	23°30.0	92°00.2	34,545	8.0	74,545	11.9

of up to ~1.7 mg C m^{-2}. A few additional *Pelosina* sp. specimens were also observed at site C7 (1,076 m).

Foraminiferal abundances were roughly comparable to typical deep-sea foraminiferal standing stocks. Abundances did not consistently vary with water depth, latitude or longitude. Foraminiferal biomass did vary somewhat with depth but this correlation was not significant ($p>.05$ for both 0-1 cm and 0-3 cm). For example, in the surface centimeter at one ~1,000-m site (Site MT3; 985 m), foraminiferal biomass was relatively low (~9 mg C m^{-2}) while another ~1,000-m site (Site C7; 1,076 m) had the highest foraminiferal biomass (~53 mg C m^{-2}). These sites were geographically separated by only ~75 km (Figure 8-83). The sites with the two highest estimates of foraminiferal biomass (Bush Hill, C7) are near hydrocarbon seeps. The site with the third highest biomass (S36) may be situated beneath a gyre that provides high rates of organic carbon input. The site with the lowest foraminiferal biomass is on the Mississippi Fan (MT6; 2,742 m), where sedimentation rate may negatively affect standing stocks. Although most samples from Sigsbee Plain (>3,000 m) had low foraminiferal biomass, one Sigsbee sample had >20 mg foraminiferal C m^{-2} (JSSD5). Down-core (i.e., 1-3 cm) maxima in foraminiferal biomass occurred at the three shallowest sites, suggesting that residual organic matter is also utilized by these benthic communities.

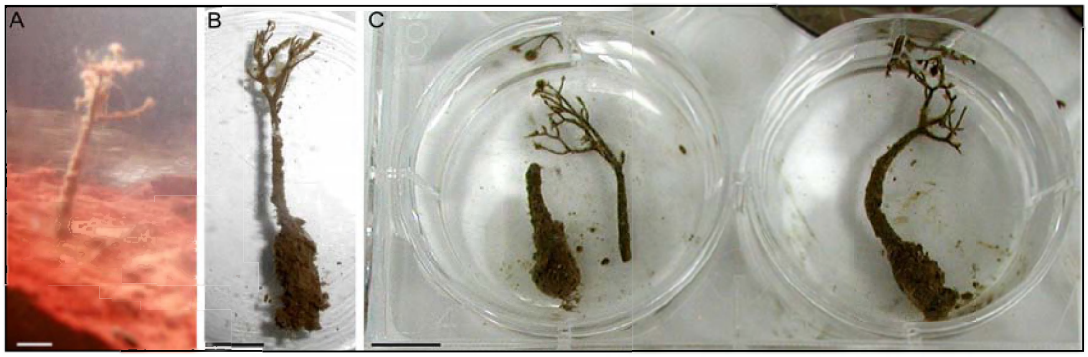

Figure 8-83. *Pelosina* sp., large agglutinated arborescent foraminifer. A. Specimen *in situ*. B. Specimen removed from sediment to show sub-surface "root" structure. C. Two additional specimens, one broken. Approximate location of the sediment-water interface is indicated by the arrows. All scale bars ~1 cm.

Foraminiferal density never exceeded metazoan meiofaunal density (Tables 8-13 and 8-14; Figures 8-84 and 8-85). Foraminiferal biomass did, however, exceed the pooled biomass of nematodes + copepods at half the sites (Tables 8-14 and 8-15; Figures 8-86 and 8-87). Because foraminiferal biomass exceeded that of the most common metazoan meiofauna (nematodes, copepods), foraminifers comprise a major component of deep-water meiofaunal biomass and are, thus, a major component of bathyal and abyssal communities.

Table 8-13

Comparison between Foraminiferal and Metazoan Meiofaunal Density (#/m^2) and Biomass (mgC/m^2) for the Surface Centimeter
(Note that metazoans biomass is exclusively copepods and nematodes. Shaded cells with bold text denote samples where foraminiferal biomass exceeded the pooled biomass of copepods and nematodes.)

Site	Water Depth (m)	0-1 cm			
		Density (# m^{-2})		Biomass (mgC m^{-2})	
		Metazoa	Foraminifera	Nematode & Copepod	Foraminifera
Bush Hill	548	232,841	45,455	22.2	47.1
S42 2001	768	123,745	3,636	6.9	2.9
MT3 2001	985	22,981	12,727	1.6	8.8
C7 2001	1076	140,581	25,455	11.3	53.4
S36 2001	1848	64,566	29,091	3.9	52.5
MT6 2001	2742	67,512	4,545	5.0	1.8
JSSD5	3316	178,883	10,909	16.8	20.9
JSSD4	3410	268,745	44,545	20.4	8.4
JSSD1	3520	34,724	27,273	3.0	3.7
JSSD2	3732	303,637	34,545	20.4	8.0

Table 8-14

Comparison between Foraminiferal and Metazoan Meiofaunal Density (#/M^2) and Biomass (Mgc/M^2) for the Top 3 Centimeters
(Note that metazoans biomass is exclusively copepods and nematodes. Shaded cells with bold text denote samples where foraminiferal biomass exceeded the pooled biomass of copepods and nematodes)

Site	Water Depth (m)	0-3 cm			
		Density (# m^{-2})		Biomass (mgC m^{-2})	
		Metazoa	Foraminifera	Nematode & Copepod	Foraminifera
Bush Hill	548	407,851	81,819	36.8	98.1
S42 2001	768	276,279	7,272	18.5	6.0
MT3 2001	985	78,961	23,636	5.7	18.9
C7 2001	1076	242,355	41,819	18.4	74.9
S36 2001	1848	192,435	44,546	13.7	62.1
MT6 2001	2742	122,145	9,090	9.3	3.4
JSSD5	3316	398,424	27,273	31.9	23.8
JSSD4	3410	493,716	50,000	33.8	9.8
JSSD1	3520	55,664	30,909	4.4	6.4
JSSD2	3732	459,959	74,545	29.3	11.9

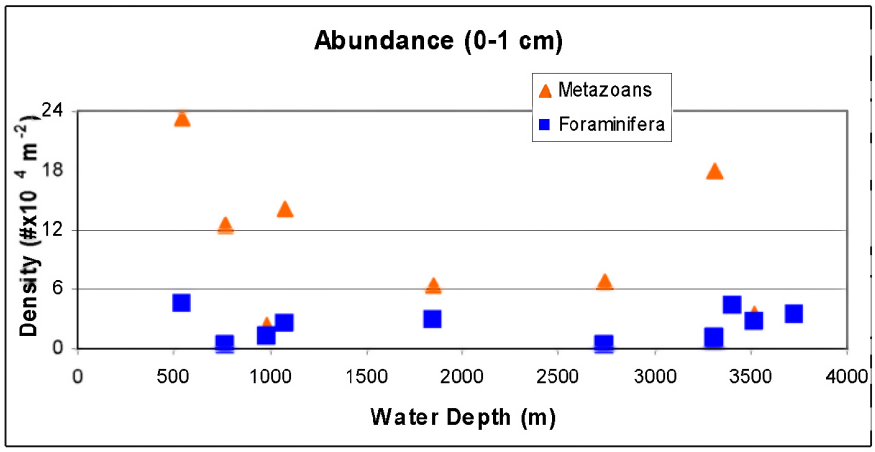

Figure 8-84. Scatter plot comparing foraminiferal abundance in the surface 1 cm to that of meiofaunal metazoans.

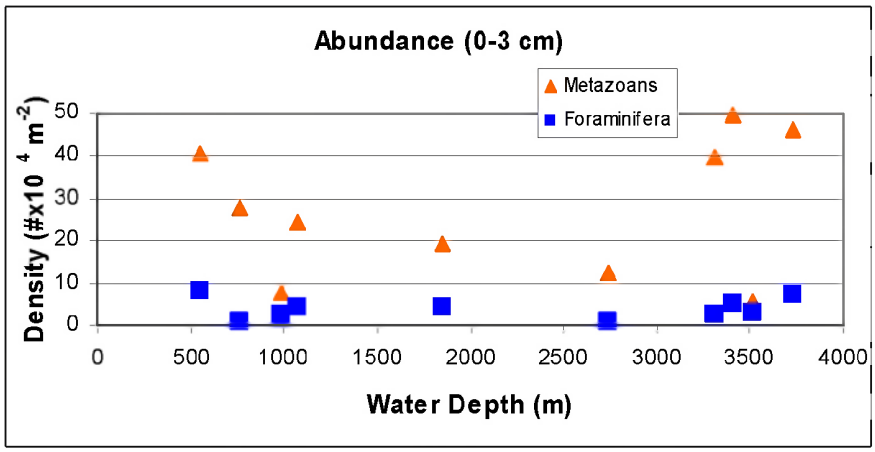

Figure 8-85. Scatter plot comparing foraminiferal abundance in the top 3 cm to that of meiofaunal metazoans.

Table 8-15

Effect of Core Tubes Size (Inner Diameter) on Meiofauna Counts and Average Density
(Based on five replicates taken at station W-2. Abundance is detransformed from natural log (ln), so taxa averages do not sum to the total average.)

	Counts (n/core)				Abundance (n/10 cm^2)			
Core Size (cm i.d.)	2.2	3.1	5.5	6.7	2.2	3.1	5.5	6.7
Taxa								
Nematodes	20.2	64.8	161.0	219.0	31.3	59.4	50.5	54.3
Harpacticoids	5.4	30.8	74.2	99.4	2.3	26.1	20.8	24.4
Nauplii	7.2	38.6	72.2	85.6	0.2	29.2	22.9	19.0
Others	12.2	14.0	27.8	45.8	3.6	14.5	8.5	10.6
Total	45.0	148.2	335.2	449.8	54.0	135.7	111.3	112.2

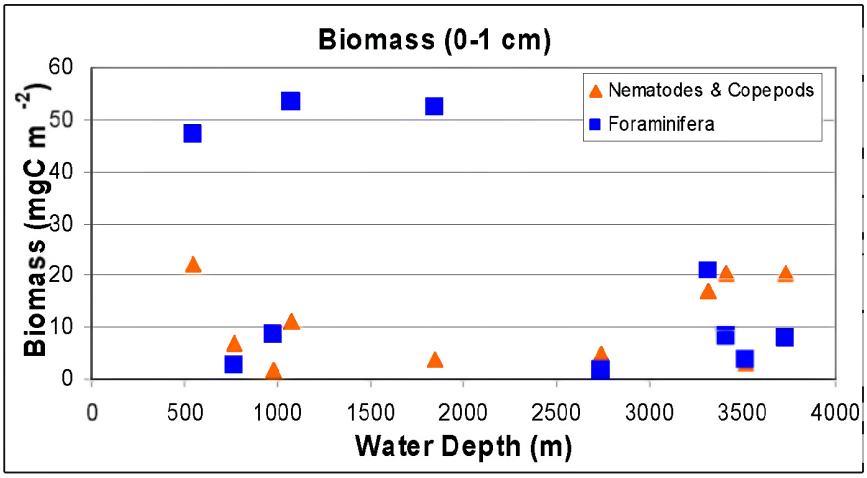

Figure 8-86. Scatter plot comparing foraminiferal biomass in the surface 1 cm to that of meiofaunal copepods and nematodes combined.

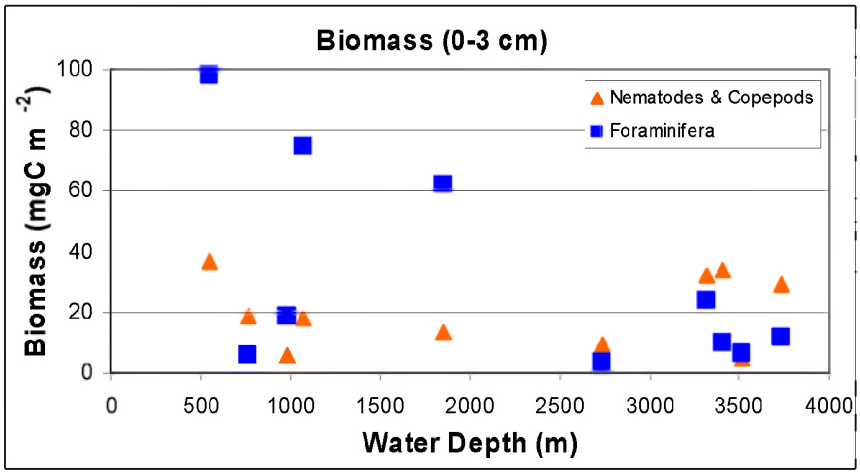

Figure 8-87. Scatter plot comparing foraminiferal biomass in the top 3 cm to that of meiofaunal copepods and nematodes combined.

8.8.3 Meiofauna

8.8.3.1 Quantitative Distribution of Meiofauna

8.8.3.1.1 Core Size Comparison, Sediment Sampling Depth, and Box Core Comparison

More organisms were found in progressively larger cores (Table 8-15). But, there were no statistically significant differences for abundances of total meiofauna ($P = 0.6324$), nematodes ($P = 0.7800$), harpacticoids ($P = 0.3385$) and other taxa ($P = 0.8238$) among different core sizes. Thus, even though total abundance (adjusted for unit area) in the smallest core was about half that found in the three larger cores, it was not statistically different. Because each core yielded the same abundance estimate, total counts per core were used to choose the appropriate core size. For statistical purposes, it is imperative to obtain > 30 organisms per taxa per sample. Therefore, the 5.5 cm core was chosen for the benthic survey.

Nearly all meiofauna were found in surface sediments and no meiofauna were found below 13 cm sediment depth, so just the top 13 cm are plotted (Figure 8-88). Most organisms were found in the top 3 cm. A total of 87% of total meiofauna were in the top 3 cm, and 97% of the harpacticoid copepods. In addition, 77% of the harpacticoid copepods were found in the top 1 cm. Because the distribution is so skewed to the surface, it was decided to sample the top 3 cm only during the benthic community survey cruise. Because harpacticoid copepods were so restricted to the top 1 cm, the core was split into 2 sections: 0 - 1 cm and 1- 3 cm.

There were no statistically significant differences for abundances of total meiofauna ($P = 0.2281$), nematodes ($P = 0.0632$), harpacticoids ($P = 0.9999$) and other taxa ($P = 0.1988$) among different box core types. Because of convenience, the GoMEX boxcore (Boland and Rowe 1991) was used throughout the study.

8.8.3.1.2 General Results

A total of 586 samples from 51 stations in the study yielded 1.71×10^5 individuals from 21 meiofauna taxa. Samples were collected from a depth range of 200-3,700 meters in the northern Gulf of Mexico. Mean abundance (extrapolated to number of individuals per m^2, Nm^{-2}) per station was 2.63×10^5 Nm^{-2}, with standard deviation of 2.01×10^5 (calculated from Table 8-16). Maximum and minimum meiofauna abundances were found at stations MT1 and JSSD3 with values of 9.46×10^5 and 0.60×10^5 Nm^{-2}, respectively (Table 8-16). A strong linear relationship exists between log abundance ($R^2 = 0.658$, $P<0.0001$) and depth (Figure 8-89). Spatial variability in meiofauna abundance (bubble size representing relative abundance) indicates highest values in the shallow northeastern stations (Figure 8-90. Relatively lower abundance was observed in the western transects, but the general trend of decreasing abundance was consistent along western transects (RW & W), and in the west-central area (WC5, WC12, B1-B3, NB2-NB5). Exceptionally high abundance was found at stations MT1, MT3, S35, S36, S42 and C7, all located in the northeast region at depths ranging from approximately 450 – 1,900 m. Variation from the general pattern of decreasing abundance with depth was observed at these northeastern stations.The meiofauna community was composed of individuals from 21 taxonomic groups (Table 8-17). Nematoda and Harpacticoida (including nauplii) were the two dominant groups, accounting for 65.3 and 25.4% of individuals, respectively. Unknown fauna were the next most abundant, comprising 6.6% of individuals. The unknown group likely included representatives from various soft-bodied taxa including (but not limited to) various taxa within the Turbellaria and representatives of the Protista (e.g., Ciliophora). Soft-bodied taxa, such as these, often become unrecognizable during bulk fixation with buffered formaldehyde. The remaining 3.7% of the meiofauna community was composed of representatives from various taxa, including: Polychaeta, Kinorhyncha, Ostracoda, Cyclopoida, Tardigrada, Tanaidacea, Nemertinea, Acari, Isopoda, Bivalvia, Gastrotricha, Anthozoa, Priapulida, Gastropoda, Aplacophora, Rotifera, Sipuncula, and Loricifera (Table 8-17). The complete major taxa data set is accessible from the DGoMB data base.

The expected number of major taxa per 1,000 individuals [ES(1000)], followed a quadratic pattern, where major taxa diversity was maximized at stations just deeper than 1,000 meters, and then decreased with increasing depth (Figure 8-91A). This pattern was also observed when only non-dominant taxa are considered (Figure 8-91B). The ES(20) for non-dominant taxa (excluding nematodes, harpacticoids, nauplii, and polychaetes) followed a similar quadratic pattern, but major taxa diversity was highest at stations around 1,800 meters, decreasing thereafter.

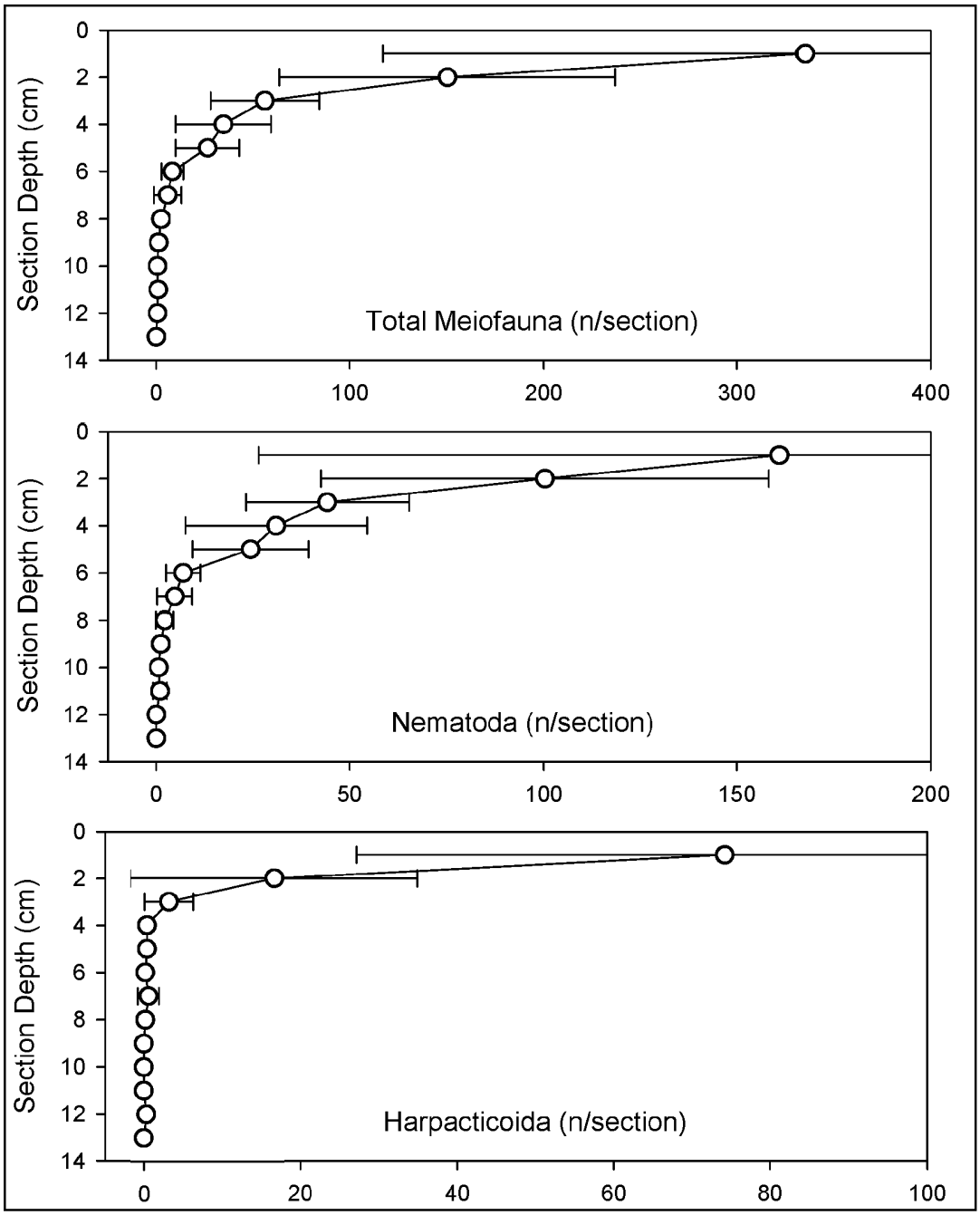

Figure 8-88. Vertical distribution of meiofauna taxa from sediment cores collected at station W2 during the shakedown cruise. Cores were sectioned in 1-cm increments, and fauna were enumerated from each 1-cm section. Plotted data is the average of five replicates (error bars = standard deviation).

Table 8-16

DGoMB station Locations, Depth, and Average Meiofaunal Abundance (Five Replicate Cores) for Pooled Taxonomic Groups

Station	Latitude	Longitude	Depth (m)	Abundance (N m^{-2})
AC1	26.393567	-94.573082	2440	129974
B1	27.202542	-91.405218	2253	157417
B2	26.550012	-92.215082	2635	139907
B3	26.164445	-91.735100	2600	155817
BH	27.780000	-91.500000	545	407852
C1	28.059838	-90.249917	336	369129
C12	26.379730	-89.240298	2924	138792
C14	26.938238	-89.572505	2495	146578
C4	27.453150	-89.763083	1463	273585
C7	27.730437	-89.982033	1066	542119
GKF	27.000000	-90.250000	2460	84348
HIPRO	28.550000	-88.580000	1565	343118
JSSD1	25.000000	-92.000000	3545	87547
JSSD2	23.500000	-92.000000	3725	87295
JSSD3	24.750000	-90.750000	3635	60441
JSSD4	24.250000	-85.500000	3400	63451
JSSD5	25.500000	-88.250000	3350	135698
MT1	28.541110	-89.825018	482	945657
MT2	28.447925	-89.671945	677	535216
MT3	28.221510	-89.494045	990	885995
MT4	27.827605	-89.166145	1401	246058
MT5	27.332838	-88.656065	2267	128964
MT6	27.001648	-87.999130	2743	155312
NB2	27.134833	-92.000068	1530	168276
NB3	26.558033	-91.822550	1875	165245
NB4	26.246750	-92.392287	2020	148409
NB5	26.245400	-91.209908	2065	117263
RW1	27.500142	-96.002847	212	411809
RW2	27.254027	-95.746807	950	219457
RW3	27.008356	-95.492362	1340	248752
RW4	26.751420	-95.250175	1575	232842
RW5	26.507527	-94.996722	1620	170633
RW6	25.997303	-94.495578	3000	144453
S35	29.335152	-87.046363	668	501629
S36	28.918513	-87.672150	1826	799963
S37	28.553627	-87.766848	2387	291179
S38	28.279947	-87.327592	2627	157164
S39	27.483675	-86.999815	3000	83170
S40	27.839477	-86.751415	2972	99501

Table 8-16 DGoMB Station Locations, Depth, and Average Meiofaunal Abundance (Five Replicate Cores) for Pooled Taxonomic Groups (continued)

Station	Latitude	Longitude	Depth (m)	Abundance (N m^{-2})
S41	28.013642	-86.573348	2974	181408
S42	28.251003	-86.419270	763	492537
S43	28.502943	-86.076790	362	276279
S44	28.749993	-85.747703	212	318516
W1	27.577165	-93.551005	420	387228
W2	27.413927	-93.340328	625	263315
W3	27.172397	-93.323293	875	262642
W4	26.730823	-93.319727	1460	187806
W5	26.267772	-93.332723	2750	104552
W6	26.002845	-93.320277	3150	124166
WC12	27.323242	-91.555810	1175	218447
WC5	27.775912	-91.765678	348	412061

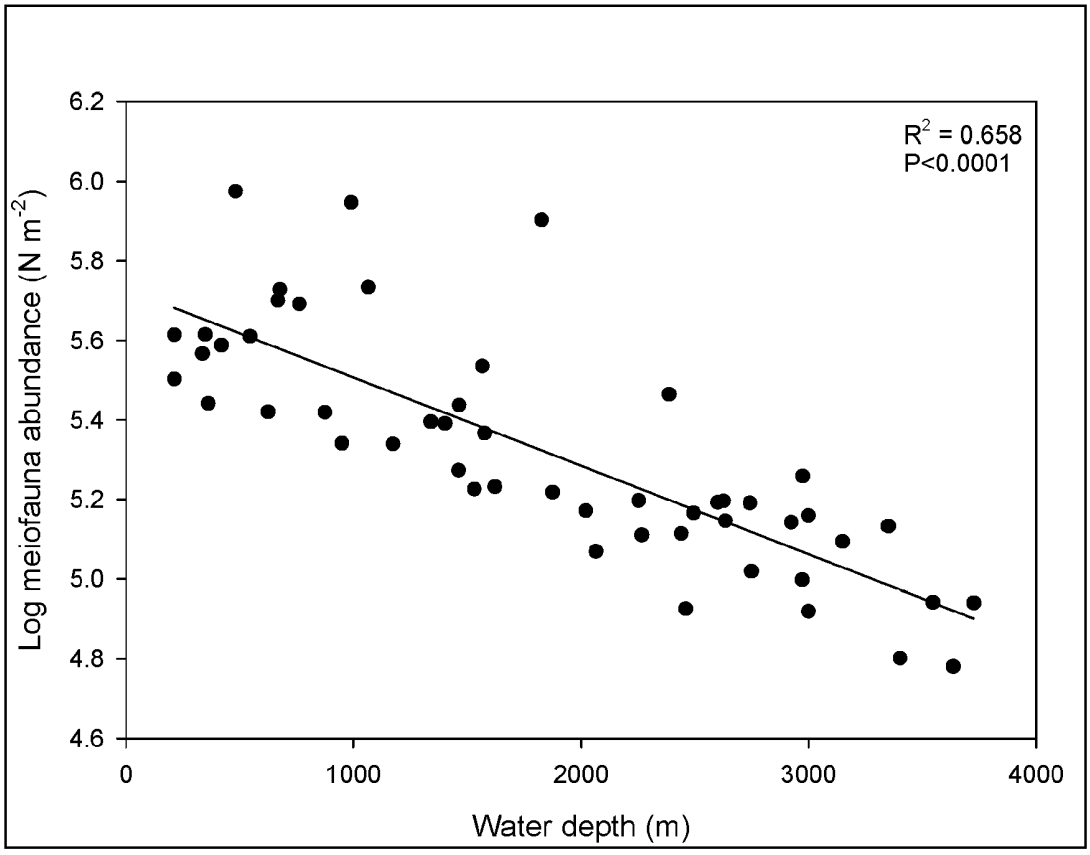

Figure 8-89. Log (x+1) transformed meiofauna abundance (N m^{-2}) versus water depth (m) for all stations sampled during DGoMB project.

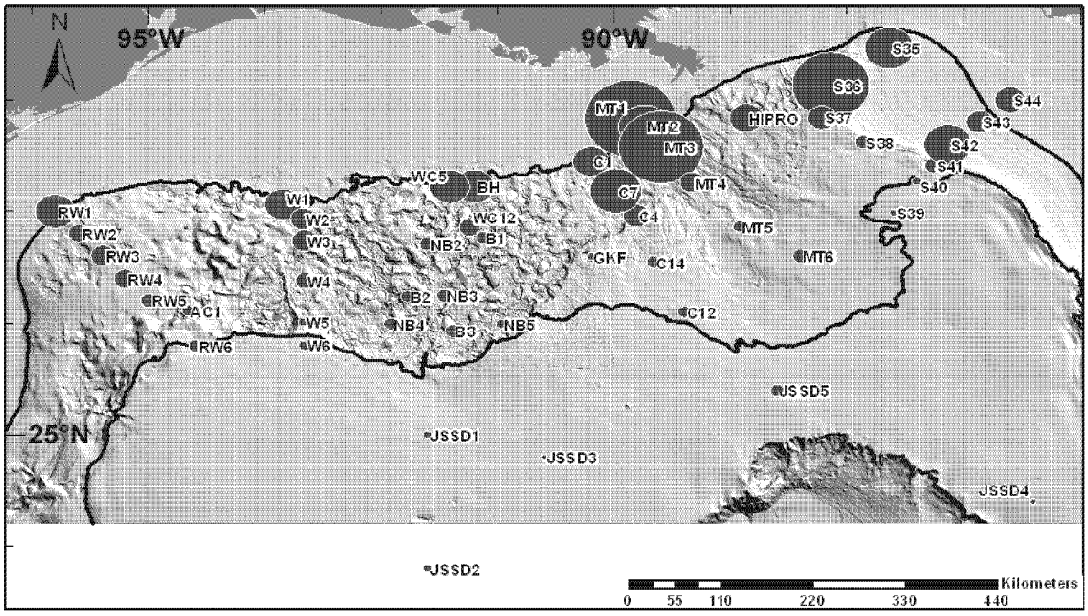

Figure 8-90. Spatial analysis of meiofauna abundance at all DGoMB stations. Buffer size equals relative meiofaunal abundance. Highlighted contours are 300 and 3,000 m from shallow to deep, respectively.

Table 8-17

Average Abundance (AA), Percent Contribution (Contrib.%), and Cumulative Percent Contribution (T%) of Meiofauna Major Taxa Per Core (5.5 cm i.d.) (Data summarized for all 51 stations (five replicates per station))

Taxa	AA	Contrib.%	T%
Nematoda	415.0	65.3	65.3
Nauplii	74.8	13.1	78.4
Harpacticoida	74.0	12.3	90.7
Unknown	37.3	6.6	97.3
Polychaeta	12.5	1.5	98.8
Kinorhyncha	2.7	0.3	99.1
Ostracoda	2.7	0.3	99.5
Cyclopoida	2.1	0.2	99.6
Tardigrada	1.0	0.1	99.8
Tanaidacea	0.8	0.1	99.9
Nemertinea	0.6	0.1	99.9
Acari	0.3	0.0	100.0
Isopoda	0.3	0.0	100.0
Bivalvia	0.2	0.0	100.0
Gastrotricha	0.1	0.0	100.0
Anthozoa	0.1	0.0	100.0
Priapulida	0.1	0.0	100.0
Gastropoda	0.0	0.0	100.0
Aplacophora	0.0	0.0	100.0
Rotifera	0.0	0.0	100.0
Sipuncula	0.1	0.0	100.0
Loricifera	0.0	0.0	100.0

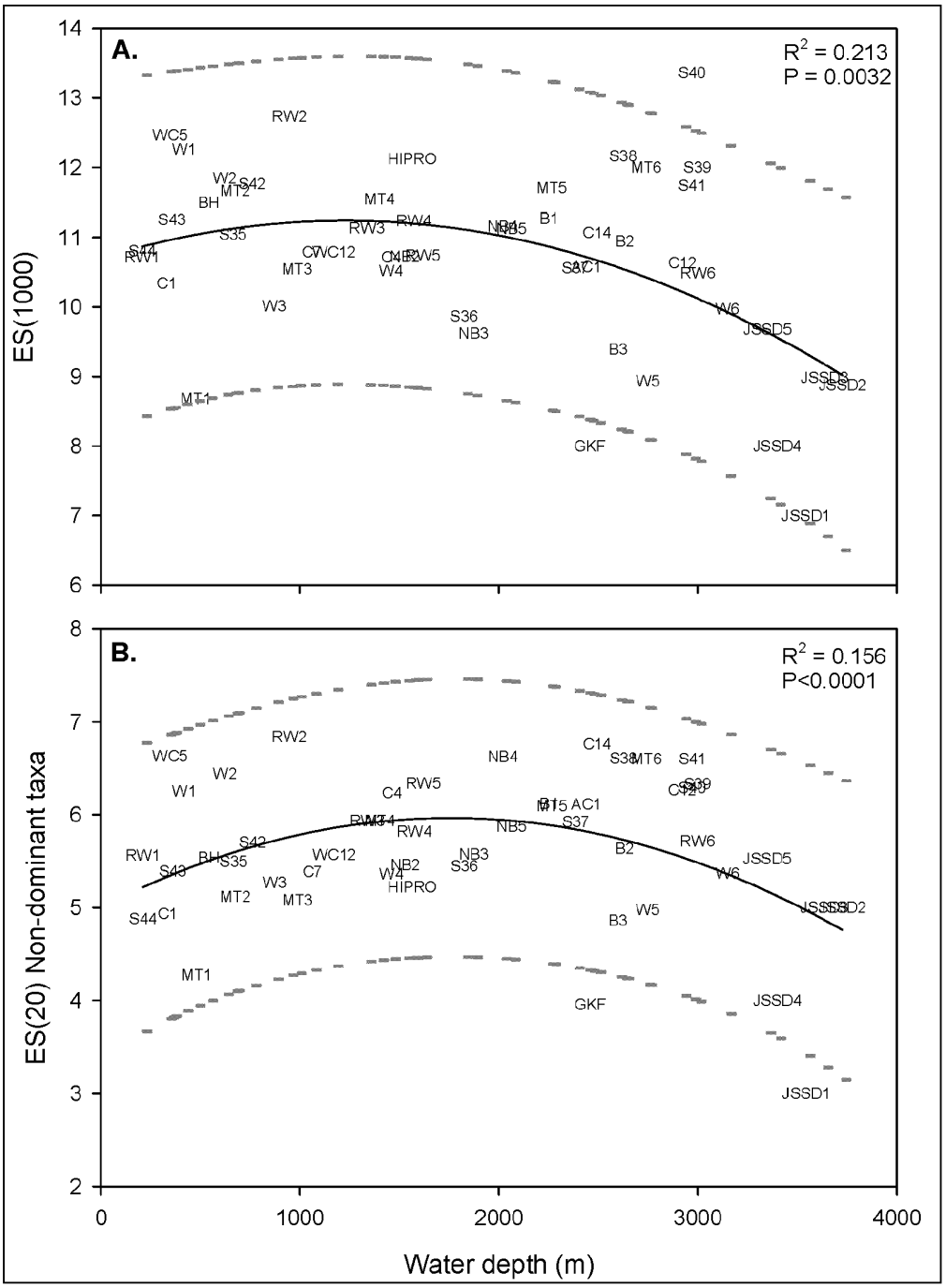

Figure 8-91. A) Expected number of taxa per 1,000 individuals [ES(1000)] as a function of depth. B) Expected number of taxa per 20 individuals [ES(20)] for non-dominant meiofauna taxa (excluding nematodes, harpacticoid copepods, harpacticoid nauplii, and unknowns). A quadratic regression was fit to the data (dashed lines = 95% confidence intervals).

8.8.3.1.3 Hypothesis Testing

In the test for differences over depth and longitude (H01 & H02), significant main effects for longitude and depth were observed (P<0.0001, Table 8-18), as well as a significant longitude by depth interaction term (P<0.0001). The two western transects (RW and W) had a gradual (very linear) decrease in abundance with depth (Figure 8-90). With increasing proximity to the Mississippi River, (transects C and MT) abundance increased greatly at stations between 300 and 1,000 meters (Figure 8-90). The Florida slope transect (S) had highest abundance at station S36 (ca. 2,000 meters), which was located in the DeSoto Canyon. Transects became more similar with increasing depth, with abundance being very similar at all stations > 2,500 meters water depth (Figure 8-90).

Table 8-18

ANOVA Results, Tests for Differences in Meiofauna Abundance
(Dependent variable = $\log_{10}(N+1)$. ANOVA abbreviations: DF = degrees of freedom, SS = sum of squares, MS = mean square, F = F-test value, P = Pr > F. Factor abbreviations: long. = longitude, basin = basin vs. non-basin stations, dfs = distance from shore, escarp. = escarpment vs. non-escarpment transects.)

Source		DF	SS	MS	F	P
H_{01} & H_{02}	Depth/Longitude					
	Long.	4	1.222	0.305	12.07	<.0001
	Depth	4	5.867	1.467	57.94	<.0001
	Long.*Depth	16	3.104	0.194	7.67	<.0001
	Error	100	2.531	0.025		
H_{03}	Basins					
	Basin	1	0.012	0.012	0.38	0.5421
	DFS	2	0.016	0.008	0.25	0.7773
	Basin*DFS	2	0.023	0.011	0.37	0.6980
	Error	56	1.708	0.031		
H_{04}	Canyons					
	Canyon	1	0.167	0.167	8.58	0.0059
	Depth	4	3.931	0.982	50.41	<.0001
	Canyon*Depth	4	0.338	0.085	4.34	0.0058
	Crror	36	0.702	0.019		
H_{05}	Escarpment					
	Escarp.	1	0.001	0.001	0.07	0.7906
	DFS	5	2.998	0.600	50.51	<.0001
	Escarp.*DFS	5	0.279	0.056	4.70	0.0015
	Error	46	0.546	0.012		

In the test for differences between basin and adjacent non-basin stations (H03), no significant difference was observed between main effects (P = 0.5421, and P = 0.7773, Table 8-18), and no significant interaction was observed (P = 0.6980, Table 8-18).

In the test for differences between canyon and adjacent non-canyon stations (H04), significant treatment (P = 0.0059) and depth zone (P<0.0001) effects were observed (Table 8-18), but a significant interaction term was also observed (P = 0.0058, Table 8-18). Abundance was elevated at the head of the canyon (MT1 & MT3) compared to stations of similar depth in the adjacent transect (C1 & C7; Figure 8-90). However, the two transects became increasingly

similar with depth, and showed no differences at stations greater than 1,500 meters (Figure 8-90).

In the test for differences in meiofauna abundance due to the presence of an escarpment (H05), no significant escarpment effect was observed in comparison to the reference transect ($P = 0.791$). However, a significant main effect was observed for distance from shore ($P<0.0001$, Table 8-18), and a significant interaction term was observed ($P = 0.002$, Table 8-18). Abundance was dramatically lower below the Florida Escarpment than above (Figure 8-90). Station S41 had nearly twice the abundance of stations S40 and S39, which are of similar depth, but further offshore. Comparison to the reference transect in the western gulf (stations W1-W6) illustrates deviation of the escarpment transect from an expected decrease in abundance along a relatively constant slope, with elevated abundance just above and below the escarpment (Figure 8-90).

The amount of chl-a biomass in the overlying water column that reaches the sea floor decreases in a log-log relationship with depth (Figure 8-92A). Meiofauna abundance increased with increasing chl-a in the water column (Figure 8-92B). Although considerable variability exists in the linear regression ($R^2 = 0.413$), the relationship was significant ($P<0.0001$). Accordingly, meiofauna had a moderate, and significant relationship with sediment POC concentration (Figure 8-93, $R^2 = 0.331$). Although null hypothesis six (H06) was not tested with ANOVA as above, detailed analysis of the meiofauna community with respect to food availability and sediment environmental variables was accomplish with multivariate procedures (Section 9).

8.8.3.2 Harpacticoida (Copepoda) Community Structure

Harpacticoid copepods were collected from 423 samples at 43 locations on the continental slope of the northern Gulf of Mexico. In total 12,480 individuals were collected, of which 3654 were identifiable adult harpacticoid copepod individuals, 696 species were identified from 22 families and 175 genera (see Appendices for complete species list, grouped by family). Nine families accounted for approximately 93% of all harpacticoida (Table 8-19), and two, Tisbidae and Ectinosomatidae, accounted for 46%. Only 182 of these species (27%) have been formally described in the literature.

Average abundance over all stations (from five pooled replicate cores = 118.8 cm^2) was 172 ± 94, with maximum and minimum values of 412 and 54, found at stations WC5 and MT6, respectively (Table 8-20). The average number of species was 52 ± 19 (from pooled replicate cores) with maximum and minimum values of 104 and 23, found at stations WC5 and MT6, respectively (Table 8-20). Total abundance (N) and species richness (S) decreased significantly ($R^2 = 0.466$ and 0.495, respectively) with increasing water depth (Figure 8-94A & B). The number of species was highly correlated to the number of individuals encountered ($r = 0.91$). However, rate of decrease with water depth was approximately five times greater for abundance than species richness (slope = -0.068 and -0.014, respectively).

Shannon-Wiener diversity (H') decreased in a strong relationship with depth ($R^2 = 0.501$, $P<0.0001$, Figure 8-95). H' had a mean of 3.73 and standard deviation of 0.32 (calculated from Table 8-20). Maximum values of H' were found at stations S35, WC5, MT2 and MT1, while minimum values were found at stations NB2, NB4, B1, B2 and MT6 (Table 8-20). The expected number of species per 30 harpacticoid individuals [ES(30)] formed a moderate non-linear, unimodal relationship with depth ($R^2 = 0.312$, $P = 0.0006$, Figure 8-96). Mean ES(30) was 22.24 with standard deviation of 2.08 (calculated from Table 8-20). Maximum

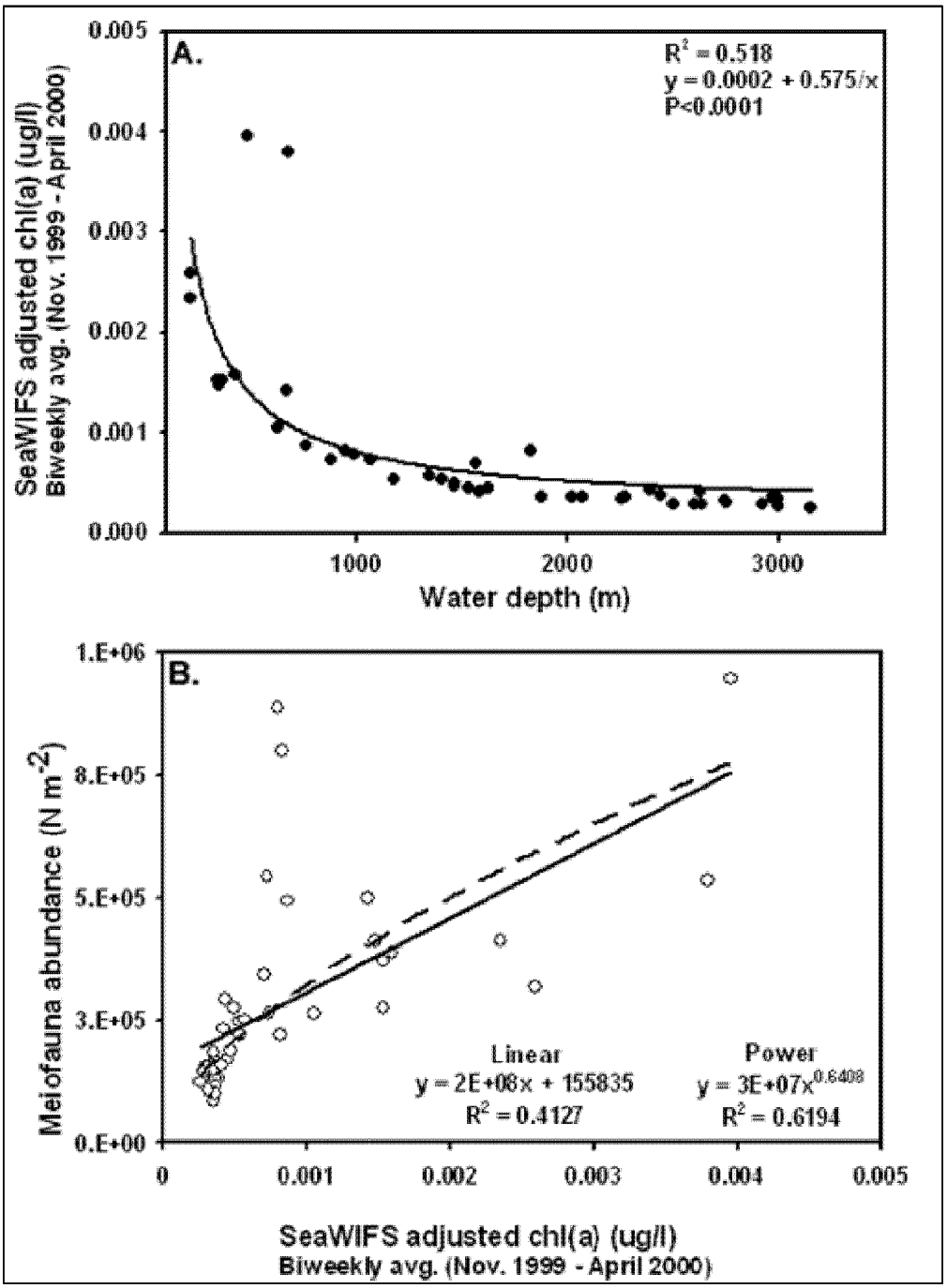

Figure 8-92. SeaWIFS chl-a (µg/L) biweekly average (November 1999 through April 2000). Chl-a concentration was adjusted for remineralization with depth. A) Inverse first-order relationship of adjusted chl-a with water depth. Chl-a concentration decreases with depth reflecting rapid remineralization in surface waters. B) Meiofauna abundance versus adjusted chl-a.

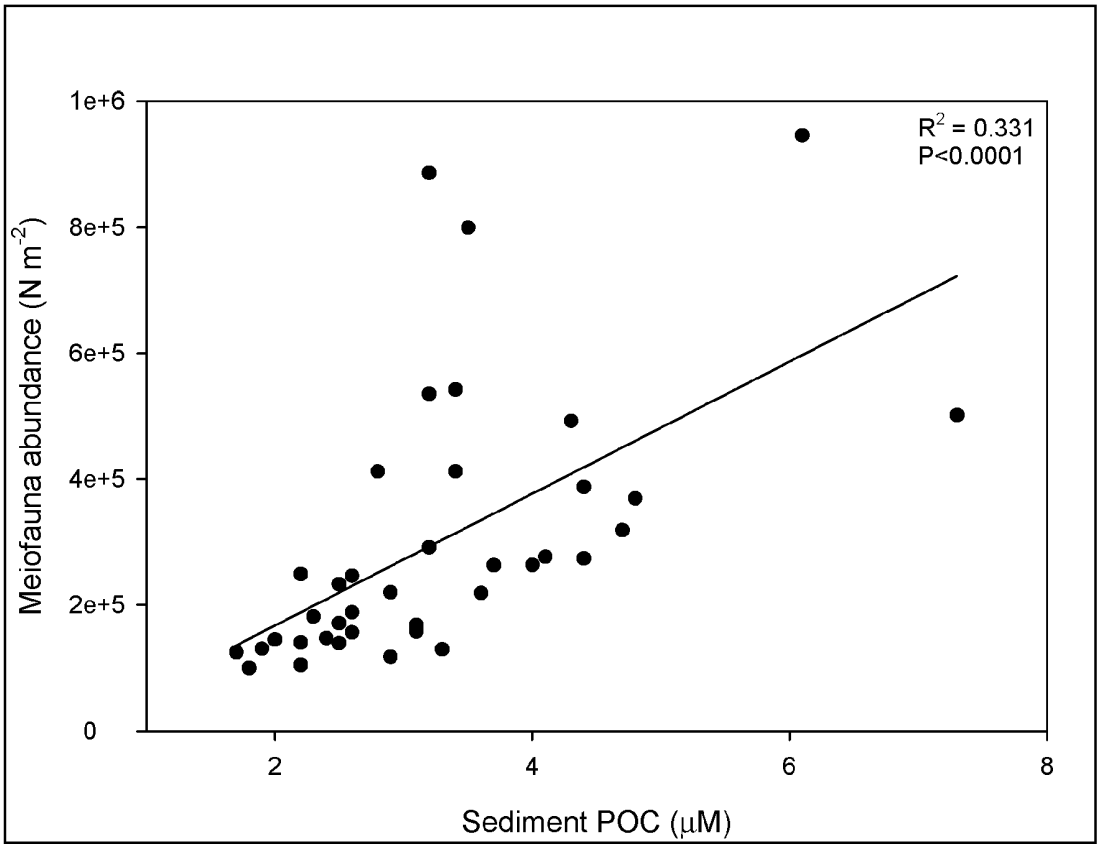

Figure 8-93. Meiofauna abundance (Nm^{-2}) as a function of sediment particulate organic carbon (POC).

Table 8-19

Results of SIMPER Analysis (Primer 5.0) Indicating Family Percent Contributions to Total Harpacticoid Abundance
(AA = Average abundance, Contrib.% = percent contribution of family, T% = cumulative percent contribution of families.)

Family	AA	Contrib.%	T%
Tisbidae	40.19	32.98	32.98
Ectinosomatidae	24.12	13.27	46.24
Diosaccidae	19.74	9.84	56.09
Ameiriidae	15.71	8.24	64.33
Argestidae	11.00	8.08	72.41
Paranannopidae	9.15	6.50	78.91
Canthocamptidae	12.38	6.03	84.95
Paramesochriidae	6.73	4.15	89.10
Cletodidae	6.62	3.42	92.52
Neobradyidae	2.73	1.39	93.91
Thalestridae	2.34	1.09	95.00
Normanellidae	2.41	1.09	96.08
Cerviniidae	2.55	1.05	97.13
Danielssenidae	3.55	0.93	98.06
Huntemannidae	1.70	0.93	98.99
Unid. family	1.79	0.61	99.60
Ancorabolidae	1.21	0.32	99.93
Laophontidae	0.42	0.03	99.96
Canuellidae	0.28	0.03	99.99
Darcythompsonidae	0.19	0.01	100.0
Longipedidae	0.16	0.00	100.0
Euterpinidae	0.05	0.00	100.0

Table 8-20

Total Species (S) and Total Individuals (N) Per Five Pooled Replicates Cores (= 118.8 cm^2) (Species diversity indices: expected species per 30 individuals [ES(30)], Shannon-Wiener diversity (H'), average taxonomic diversity (Δ), and average phylogenetic diversity (Φ^+) at each of the 43 stations where harpacticoid copepods were identified to species.)

Station	Depth	S	N	ES(30)	H'	Δ	Φ^+
AC1	2440	51	114	24.91	3.90	102.14	59.79
B1	2253	27	74	19.56	3.21	105.25	70.97
B2	2635	32	90	20.27	3.33	102.51	62.74
B3	2600	37	108	21.00	3.46	96.59	64.92
C1	336	51	195	19.70	3.73	96.85	58.63
C12	2924	34	125	17.34	3.31	95.37	70.14

Table 8-20 Total Species (S) and Total Individuals (N) Per Five Pooled Replicates Cores (= 118.8 cm^2) (Species diversity indices: expected species per 30 individuals [ES(30)], Shannon-Wiener diversity (H'), average taxonomic diversity (Δ), and average phylogenetic diversity (Φ^+) at each of the 43 stations where harpacticoid copepods were identified to species.)(continued)

Station	Depth	S	N	ES(30)	H'	Δ	Φ+
C14	2495	33	118	17.37	3.31	93.49	66.12
C4	1463	56	148	23.98	3.91	101.77	63.23
C7	1066	74	212	24.64	4.14	96.27	54.62
MT1	482	69	322	22.68	3.95	91.44	57.51
MT2	677	67	338	21.45	3.82	92.72	53.06
MT3	990	81	418	21.68	3.92	92.99	55.02
MT4	1401	53	144	23.80	3.87	101.76	63.93
MT5	2267	44	110	23.35	3.71	102.31	62.27
MT6	2743	23	54	18.92	3.04	111.88	79.92
NB2	1530	40	112	22.14	3.59	99.71	64.78
NB3	1875	50	120	24.02	3.83	101.57	63.81
NB4	2020	39	108	21.76	3.54	100.51	63.91
NB5	2065	36	94	21.90	3.50	101.88	65.86
RW1	212	66	240	23.54	3.99	95.83	57.38
RW2	950	57	178	23.41	3.89	97.50	59.27
RW3	1340	61	174	23.47	3.92	95.49	57.34
RW4	1575	57	148	24.28	3.94	101.27	65.85
RW5	1620	43	112	22.56	3.64	101.49	66.40
RW6	3000	49	130	22.99	3.74	96.16	61.75
S35	668	89	388	23.02	4.10	93.75	54.72
S36	1826	74	306	23.14	4.02	95.58	56.98
S37	2387	70	198	24.49	4.09	99.48	60.17
S38	2627	44	108	23.36	3.71	100.96	63.09
S39	3000	38	96	21.85	3.50	102.23	66.89
S40	2972	30	78	19.94	3.24	105.63	71.18
S41	2974	31	84	20.69	3.35	104.42	72.10
S42	763	58	178	23.33	3.89	98.33	57.55
S43	362	57	178	23.17	3.87	95.31	56.08
S44	212	41	133	20.14	3.64	99.64	64.76
W1	420	94	306	25.46	4.37	96.45	56.50
W2	625	65	214	23.12	3.93	97.02	56.36
W3	875	65	212	23.55	3.98	96.13	57.16
W4	1460	52	146	23.79	3.86	100.75	66.58
W5	2750	35	86	22.10	3.49	101.27	64.93
W6	3150	33	108	17.39	3.02	90.01	68.15
WC12	1175	52	180	21.75	3.71	98.55	62.62
WC5	348	104	412	25.26	4.42	96.28	55.24

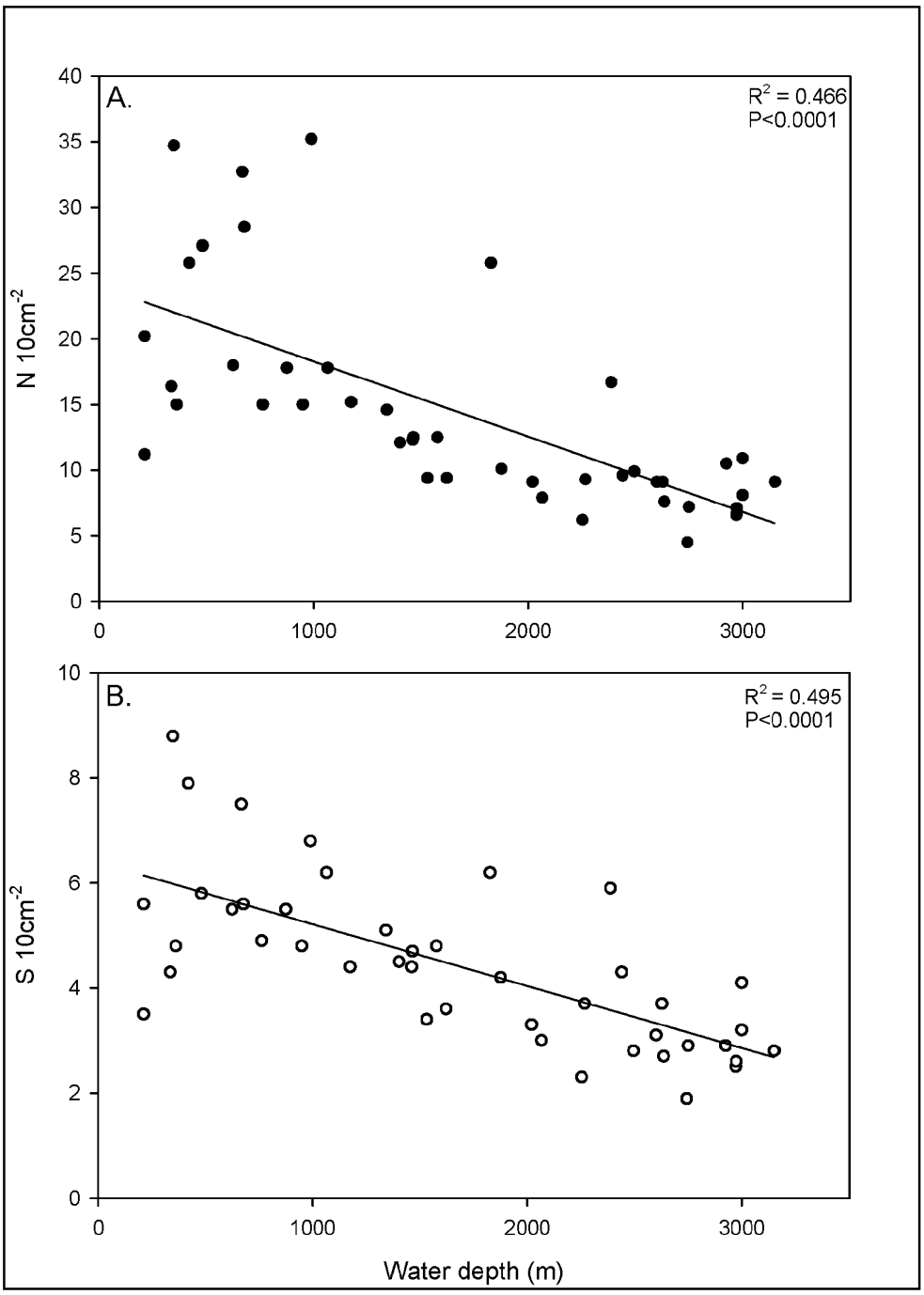

Figure 8-94. Harpacticoid copepod abundance (N) and species richness (S), adjusted to the number per 10 cm^2, as a function of depth. Abundance and richness are highly correlated (r = 0.91).

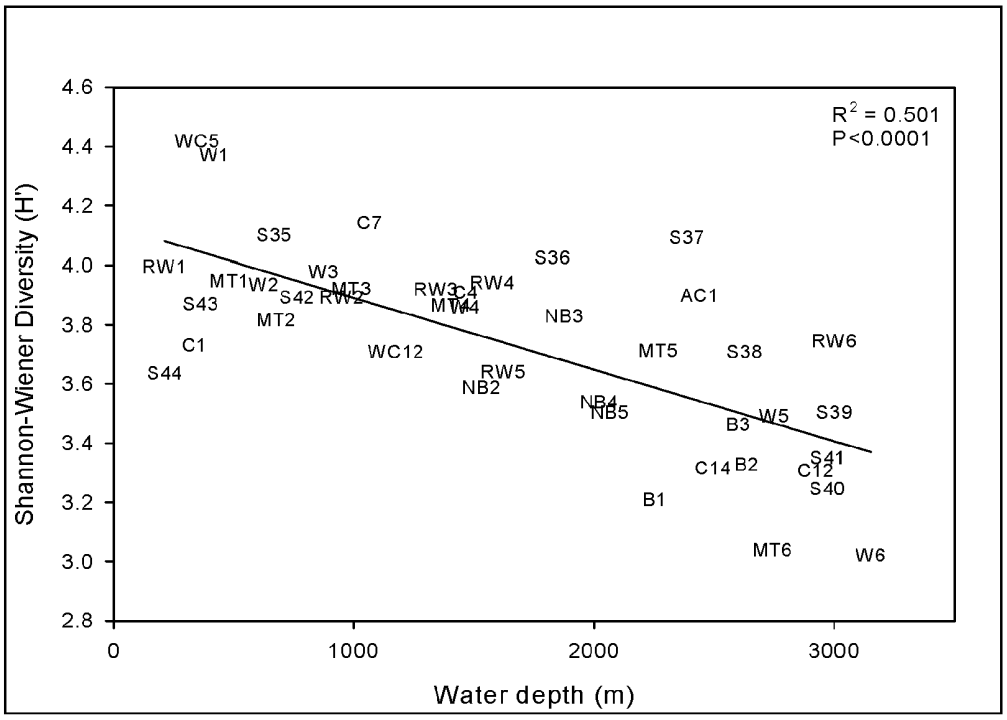

Figure 8-95. Shannon-Wiener diversity index (H') as a function of depth for pooled replicate core samples of harpacticoid copepods.

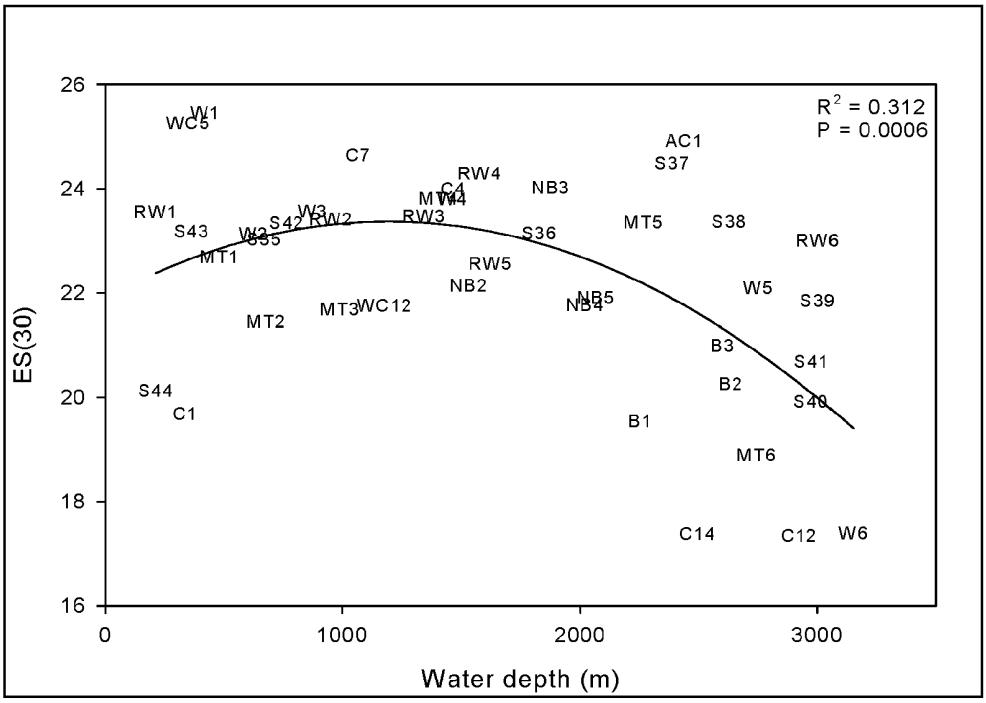

Figure 8-96. Expected number of harpacticoid species per 30 individuals [ES(30)], for pooled replicate core samples of harpacticoid copepods.

values of ES(30) were found at stations WC5 and W1, while minimum values were found at stations C12, C14, and W6. Although the relationship was moderately significant, ES(30) was highly variable at both shallow and deep stations (Figure 8-96).

Average taxonomic diversity (Δ), the average taxonomic distance apart of any two individuals chosen at random within a sample, increased with increasing water depth (R^2 = 0.185, P = 0.004, Figure 8-97A). Determination of average taxonomic diversity was based on a 4-level taxonomic scheme, from species to order. Δ had a mean value of 98.76 and standard deviation of 4.24 (calculated from Table 8-20). Highest average taxonomic diversity was found at station MT6 (111.88), with lowest values at station MT1 (91.44). Although the relationship is moderately significant, variance in Δ increased at deep stations (Figure 8-97A). Another index of taxonomic relatedness is average phylogenetic diversity (Φ^+), which is the cumulative branch length of the phylogenetic tree within each sample. As with average taxonomic diversity (above), average phylogenetic diversity was calculated with a 4-level taxonomic scheme, from species to order. Average phylogenetic diversity followed a strong, and highly signficant, increasing trend with depth (R^2 = 0.500, P<0.0001, Figure 8-97B). The mean value of average phylogenetic diversity was 62.33 with standard deviation of 5.73 (calculated from Table 8-20). Maximum average phylogenetic diversity of 79.92 was found at station MT6, while the minimum was 54.62 at station C7 (Table 8-20). Both Δ and Φ^+ suggest proportionally more higher order taxa (genera and families) per individual with increasing depth.

8.8.3.2.1 Hypothesis Testing

In the test for differences between depth and longitude (H_{01} and H_{02}), a highly significant depth main effect was observed (P<0.0001, Table 8-21), but a weak significant interaction was also observed (P = 0.0203). Overall, harpacticoid Φ^+ responded similarly over most of the transects with a small peak in Φ^+ at mid depths (approx.1,500 m) followed by relatively constant diversity until a second peak at depths greater than 3,000 meters. The eastern stations (S transect) had a decrease in Φ^+ at shallow depths (S44 to S35), but then a constant increase in Φ^+ with increasing depth.

In the test for differences in Φ^+ between basin and non-basin stations (H_{03}), no significant differences were observed for main effects, and no interaction was observed (Table 8-21). Similarly, in the test for canyon effects (H_{04}) no significant difference in Φ^+ was observed between canyon and non-canyon transects, but a significant depth effect was observed (P<0.0001, Table 8-21). No significant canyon by depth interaction was observed. In the test for escarpment effects on Φ^+, a weak transect main effect was observed (P = 0.035) but strongly significant interaction between transect and distance from first station was observed (P = 0.0003). There was a peak in diversity at the two deep stations below the Florida Escarpment (S40 and S41), and then a decrease in diversity moving away from the escarpment (S39). The western (W) transect had a peak in Φ^+ at approximately 1,500 meters (W4), and a second peak at the deepest station (W6).

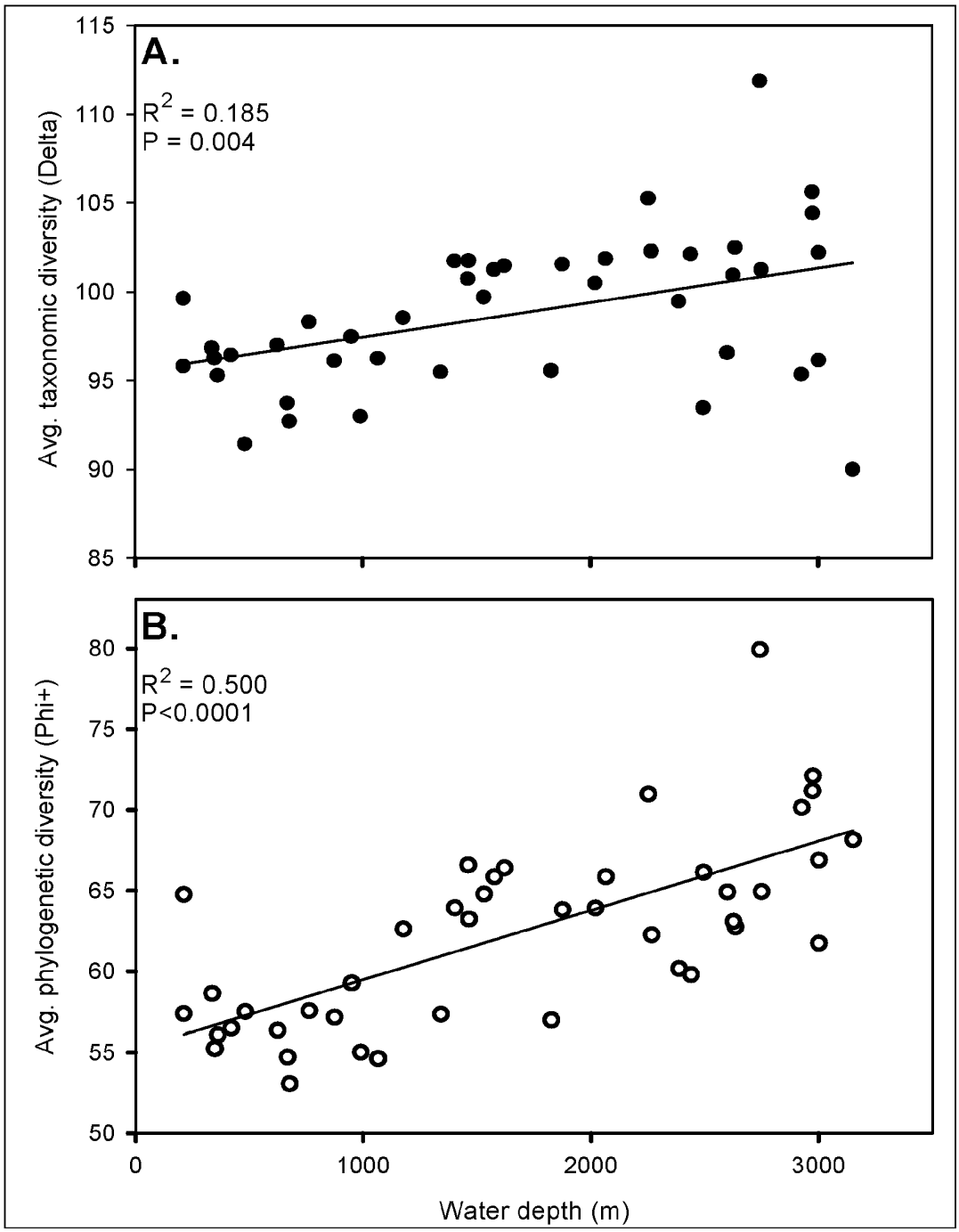

Figure 8-97. A) Average taxonomic diversity (Δ) and B) average phylogenetic diversity (Φ+) as a function of depth for the 43 original survey stations. Diversity indices were calculated based on the average species abundance from five replicate core samples.

Table 8-21

ANOVA Results of Test for Differences in Harpacticoida Diversity
(Dependent variable is average phylogenetic diversity (Φ+). DFS = distance from shore; DFFS = distance from first station.)

Source		DF	SS	MS	F Value	Pr > F
$H_{01\&02}$						
	Transect	4	110.02	27.51	0.50	0.7332
	Depth	4	2198.28	549.57	10.06	<.0001
	T*Depth	16	1749.36	109.34	2.00	0.0203
	Error	96	5243.96	54.62		
H_{03}						
	Treatment	1	16.45	16.45	0.18	0.6711
	DFS	2	109.87	54.93	0.62	0.5479
	T*DFS	2	57.33	28.67	0.32	0.7277
	Error	23	2045.74	88.95		
H_{04}						
	Transect	1	2.67	2.67	0.05	0.8312
	Depth	4	1870.96	467.74	8.08	<.0001
	T*Depth	4	302.41	75.60	1.31	0.2855
	Error		37	2141.06	57.87	
H_{05}						
	Transect	1	241.31	241.31	4.73	0.0347
	DFFS	5	56.15	11.23	0.22	0.9521
	T*DFFS	5	1450.89	290.18	5.69	0.0003
	Error	47	2396.81	50.99		

8.8.3.2.2 Spatial and Bathymetric Species Zonation

The concept of geographic or bathymetric zonation was analyzed using cluster and subsequent Geographical Information System (GIS) analysis (Figure 8-98). Cluster analysis was performed on the harpacticoid data set implementing Bray-Curtis similarity and group average linking (not shown, see Baguley 2004). Minimum Bray-Curtis similarity, i.e. the similarity of all 43 survey stations, was 8.4%. Groups, or "zones," were chosen on the basis of >20% similarity. A total of 17 zones were determined, with 1-7 stations per zone (Figure 8-98). Stations that did not group with at least one other station at the 20% level were designated as unique zones. Highest zone similarity was found for stations MT1, MT2 and MT3 (36.8%), and highest similarity between any two stations was 48.4%, for stations MT2 and MT3. All other zones, that included at least two stations, had similarity values between 20 and 36%.

8.8.3.2.3 Regional and Global Species Estimates

Two Gulf of Mexico data sets were analyzed in order to extrapolate to regional and global scales (Montagna and Harper 1996). Species accumulation curves (Figure 8-99) were constructed for each data set. The sigmoidal growth model parameters for the two data sets were as follows: NGoM (DGoMB data), a = -16.6, b = 541.1, c = 1739.7, and d = 0.72; NWGoM (Montagna and Harper 1996), a = -2.28, b = 166.08, c = 457.06, and d = 0.57. The models for

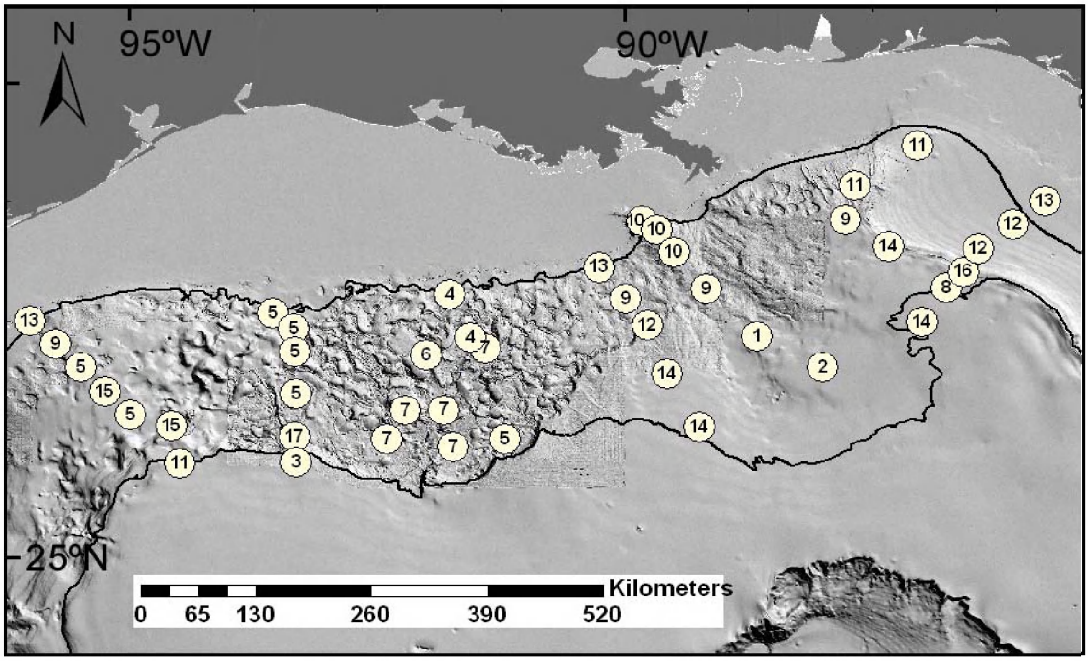

Figure 8-98. Geographic location of recurrent groups of harpacticoid copepods, based on percent similarity (see text). Highlighted contour lines are at 300 and 3,000 m water depth.

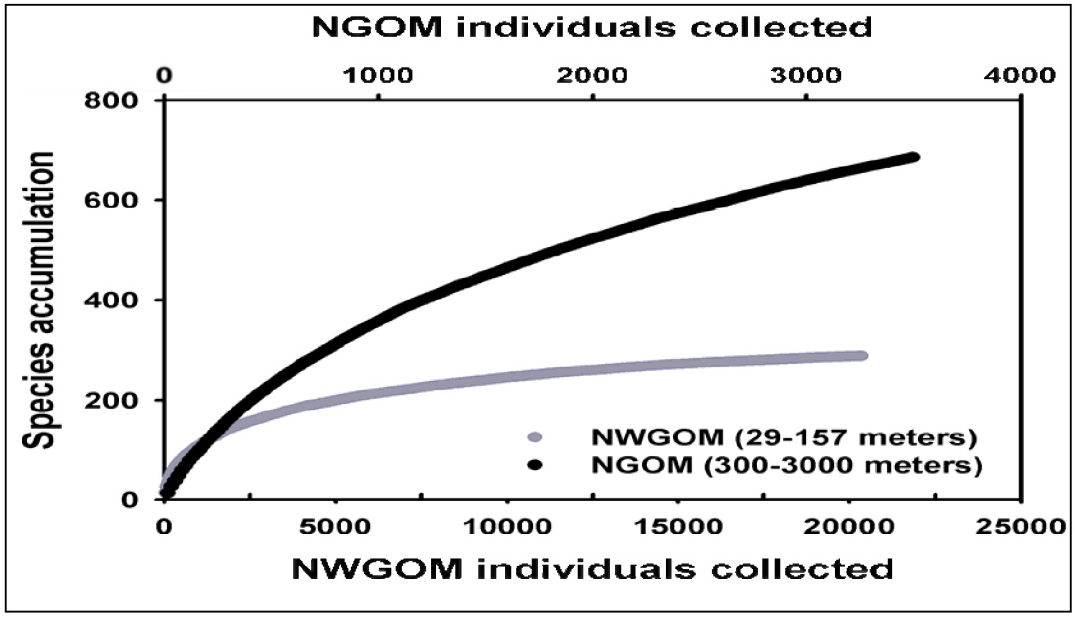

Figure 8-99. Species accumulation curves used to estimate regional Harpacticoida species abundance in the Gulf of Mexico by extrapolation.

both NGoM and NWGoM fitted the data very closely, R^2 = 0.99996 and 0.99980, respectively. The model interpolation indicates that asymptotes exist at 1740 and 457 species for deep-sea (NGoM) and shallow (NWGoM) regions of the Gulf of Mexico respectively.

Summing the shelf and deep-sea estimates yields the regional biodiversity of the entire Gulf of Mexico at approximately 2200 species, assuming there is no overlap between shallow shelf and deep-sea species. The approximate area of the Gulf of Mexico is $1.5x10^6$ km^2, which is about 0.4 % of the world's oceans. Assuming the rate of increase of new species with area remains constant then extrapolation suggests a global species richness of $5.5x10^5$ for the Harpacticoida.

8.8.3.3 Meiofauna Biomass

Meiofauna biomass is dominated by the two dominant taxa, Nematoda and Harpacticoida (Table 8-22). Mean biomass per station was 273 mg wet weight m^{-2} (43.3 mg C m^{-2}). Maximum and minimum biomass values of 157.1 and 3.5 mg C m^{-2} were found at stations S42 and JSSD3, respectively (Table 8-22). A strong linear relationship exists between log meiofauna biomass (R^2 = 0.726, P<0.0001) and water depth (Figure 8-100). A general trend of decreasing biomass per individual with increasing water depth was observed for Nematoda (R^2 = 0.125, P = 0.0202, Figure 8-101A), while Harpacticoida had a general increasing trend of biomass per individual with increasing water depth (R^2 = 0.167, P = 0.0066, Figure 8-101B). Spatial trends in meiofauna biomass (Figure 8-102) closely parallel those observed with abundance (See previous subsections). However, highest biomass was observed at station S42 (Table 8-21, Figure 8-102). High biomass at station S42 reflects proportionally larger nematode individuals at this location (Figure 8-101A).

The general relationship of decreasing meiofauna biomass with water depth was seen over the entire northern GoM continental margin. Variance from this pattern was observed primarily in the northeastern GoM (Figure 8-102), where highest biomass was often observed at mid-depth stations (S36, S42, MT3). Interpolated biomass estimates over the entire sampling region, and to the extent of the available bathymetry, illustrates the general pattern of decreasing biomass with depth, and also highlights biomass hot spots (Figure 8-102). Average biomass per 2.8 km^2 cell, as calculated by the model, was $2.7x10^5 \pm 1.6x10^5$ µg wet mass m^{-2}. A total of 83,844 cells (each 2.8 km^2) were created by the model, equaling a total area of $6.57x10^5$ km^2. Total meiofaunal biomass within the region was found to be $2.1x10^7 \pm 1.2x10^7$ kg Carbon (wet mass converted to carbon using conversion factors of 0.25 dry/wet mass, and 0.48 carbon/dry mass, Baguley et al. 2004).

8.8.3.4 Allometric Respiration Estimates and Community Carbon Transfer

The mean mass-dependent respiration rate of meiofauna was estimated using the average individual biomass at each DGoMB station (Table 8-22, Figure 8-103A). Mean respiration (d^{-1}) increased as a function of depth, in a weak, but significant linear relationship (Figure 8-103A, R^2 = 0.256, P<0.0001). Mean respiration (d^{-1}) increased with decreasing average biomass (Table 8-22). Meiofauna community respiration (mg C m^{-2} d^{-1}) decreased in a strong linear relationship with depth (Figure 8-103B, R^2 = 0.598, P<0.0001). Variance in community respiration was higher in shallower water (200-1,500 meters). Meiofaunal respiration ranged from a low of 0.3 mg C m^{-2} d^{-1} at stations JSSD2-4 to a high of 6.3 mg C m^{-2} d^{-1} at S36 and S42.

Table 8-22

Biomass Contribution of the Major Taxonomic Groups
to Total Meiofaunal Biomass (mg C m^{-2}) at Each DGoMB Station
(NEMA = Nematoda, HARP = Harpacticoida, NAUP = Harpacticoida nauplii, POLY = Polychaeta, OSTR = Ostracoda, CYCL = Cyclopoida, TANA = Tanaidacea, ISOP = Isopoda, KINO = Kinorhyncha.)

STA	NEMA	HARP	NAUP	POLY	OSTR	CYCL	TANA	ISOP	KINO
AC1	17.52	6.83	0.18	0.20	0.08	0.09	0.30	0.00	0.01
B1	23.97	8.60	0.36	0.22	0.31	0.05	0.10	0.07	0.02
B2	12.50	3.52	0.34	0.25	0.12	0.00	0.20	0.07	0.00
B3	11.88	5.41	0.55	0.28	0.04	0.00	0.22	0.00	0.01
BH	23.31	20.80	0.98	1.42	0.48	0.16	0.50	0.40	0.02
C1	89.37	8.04	0.64	1.27	0.24	0.24	0.38	0.00	0.04
C12	12.83	7.27	0.54	0.17	0.10	0.04	0.13	0.00	0.01
C14	14.30	7.45	0.32	0.17	0.12	0.02	0.38	0.00	0.01
C4	60.26	9.12	0.79	0.36	0.44	0.07	0.30	0.13	0.01
C7	69.86	10.97	0.68	0.81	0.33	0.09	0.45	0.00	0.02
GKF	3.20	2.87	0.13	0.10	0.00	0.00	0.00	0.00	0.01
HIPRO	9.24	8.88	0.44	1.71	0.25	0.37	0.30	0.07	0.00
JSSD1	1.76	2.32	0.30	0.13	0.00	0.00	0.00	0.00	0.00
JSSD2	1.90	1.57	0.26	0.14	0.02	0.00	0.00	0.13	0.00
JSSD3	1.51	1.54	0.13	0.13	0.06	0.00	0.00	0.07	0.00
JSSD4	1.28	1.87	0.22	0.13	0.07	0.00	0.00	0.00	0.00
JSSD5	3.51	2.71	0.25	0.13	0.15	0.00	0.20	0.00	0.00
MT1	110.02	6.44	0.56	1.32	0.74	0.40	0.29	0.05	0.02
MT2	45.12	8.22	0.82	3.07	0.33	0.94	1.70	0.20	0.05
MT3	87.39	15.57	0.76	1.43	0.75	0.34	0.60	0.20	0.04
MT4	33.69	9.46	0.51	0.75	0.21	0.16	0.60	0.07	0.01
MT5	24.92	4.38	0.33	0.42	0.23	0.09	0.50	0.00	0.01
MT6	9.99	1.37	0.18	0.17	0.03	0.04	0.05	0.03	0.00
NB2	15.55	6.24	0.43	0.36	0.17	0.02	0.20	0.35	0.01
NB3	17.31	8.12	0.91	0.42	0.04	0.00	0.20	0.00	0.01
NB4	10.23	6.51	0.46	0.21	0.04	0.02	0.30	0.07	0.00
NB5	10.63	9.68	0.35	0.15	0.15	0.02	0.30	0.07	0.01
RW1	66.47	9.47	1.06	1.04	0.50	0.39	0.10	0.20	0.03
RW2	23.33	7.96	0.56	0.53	0.30	0.24	0.56	0.07	0.02
RW3	36.20	7.45	0.53	0.59	0.38	0.10	0.45	0.00	0.01
RW4	37.36	7.74	0.53	0.61	0.02	0.19	0.70	0.00	0.03
RW5	24.12	8.61	0.35	0.29	0.12	0.05	0.10	0.13	0.01
RW6	16.95	10.46	0.28	0.25	0.06	0.02	0.20	0.00	0.01
S35	49.83	14.81	1.34	1.59	0.67	0.58	1.00	0.47	0.05

Table 8-22 Biomass Contribution of the Major Taxonomic Groups to Total Meiofaunal Biomass (mg C m^{-2}) at Each DGoMB Station (NEMA = Nematoda, HARP = Harpacticoida, NAUP = Harpacticoida nauplii, POLY = Polychaeta, OSTR = Ostracoda, CYCL = Cyclopoida, TANA = Tanaidacea, ISOP = Isopoda, KINO = Kinorhyncha (continued))

STA	NEMA	HARP	NAUP	POLY	OSTR	CYCL	TANA	ISOP	KINO
S36	98.41	11.48	0.89	0.83	0.43	0.09	0.70	0.20	0.02
S37	20.51	10.73	0.71	0.53	0.33	0.16	0.40	0.20	0.01
S38	9.70	6.46	0.48	0.38	0.15	0.11	0.20	0.00	0.01
S39	6.37	3.10	0.21	0.25	0.04	0.05	0.20	0.07	0.00
S40	9.82	5.95	0.31	0.35	0.15	0.19	0.30	0.07	0.00
S41	23.79	5.33	0.27	0.21	0.10	0.04	0.22	0.04	0.00
S42	141.54	12.92	0.68	0.72	0.17	0.22	0.30	0.13	0.02
S43	36.72	6.98	0.37	0.95	0.19	0.30	0.50	0.07	0.03
S44	29.38	7.48	0.69	1.83	0.38	0.60	0.50	0.00	0.02
W1	46.80	17.31	1.16	1.19	0.33	0.37	0.50	0.07	0.04
W2	41.97	10.77	0.62	0.62	0.13	0.32	1.00	0.07	0.01
W3	58.87	10.97	0.95	0.55	0.33	0.35	0.50	0.07	0.02
W4	16.81	8.73	0.56	0.55	0.15	0.18	0.40	0.00	0.00
W5	10.23	4.50	0.19	0.09	0.04	0.00	0.30	0.00	0.01
W6	15.95	5.94	0.27	0.28	0.02	0.05	0.10	0.07	0.01
WC12	61.48	14.56	0.57	0.53	0.37	0.02	0.80	0.07	0.00
WC5	81.55	13.25	1.04	1.00	0.15	0.41	0.80	0.20	0.03

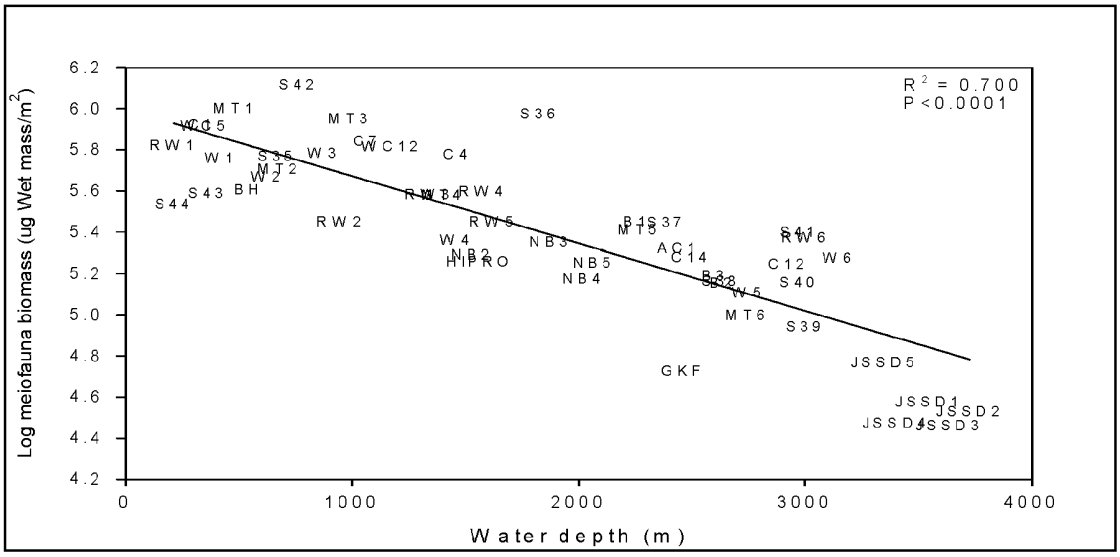

Figure 8-100. Meiofauna biomass (µg wet wt/m2) versus water depth at all DGoMB stations.

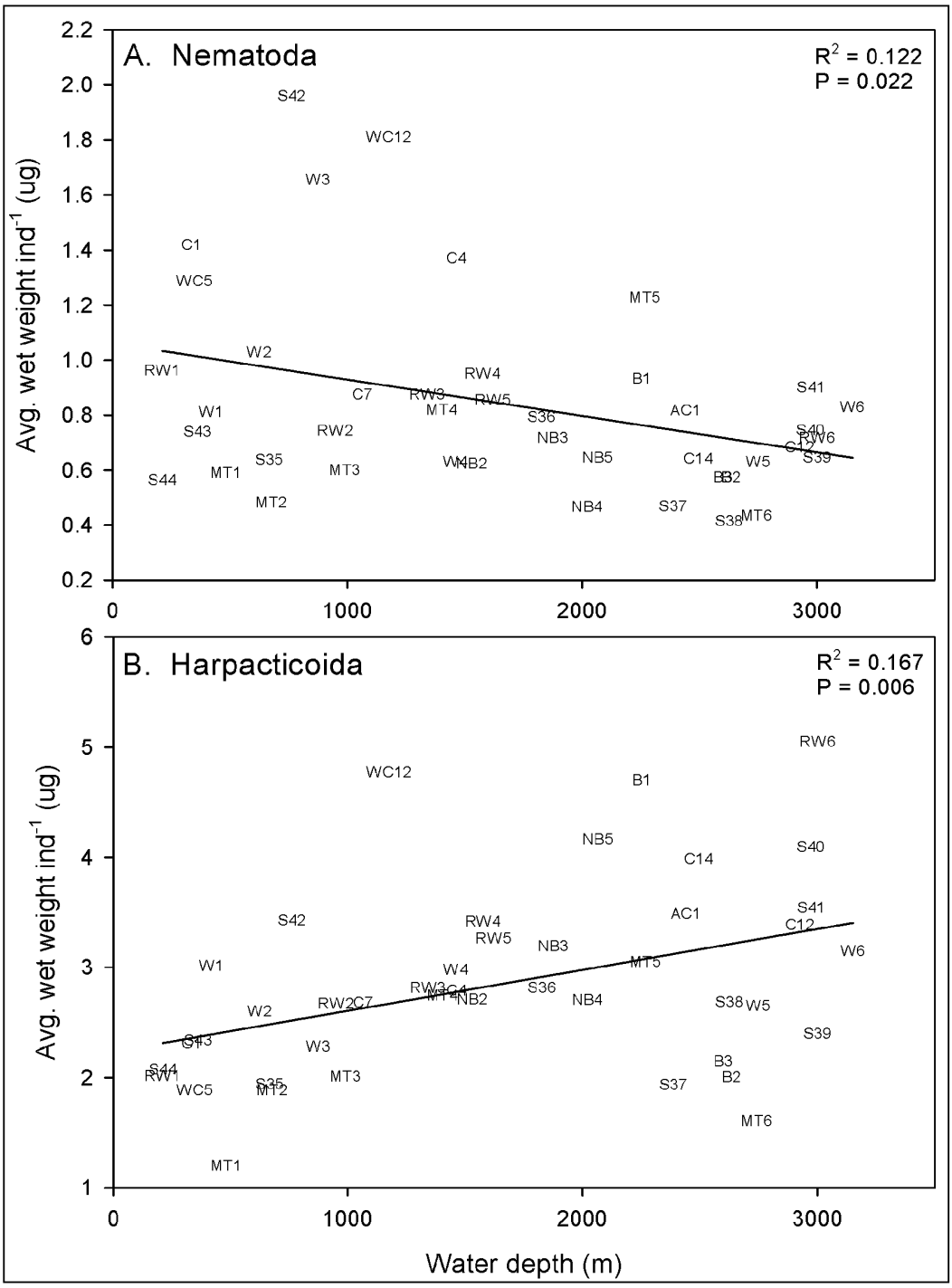

Figure 8-101. Average wet mass (mg) per individual A) Nematode, and B) Harpacticoid, as a function of depth. Data is for the 43 original survey stations, and based on biomass estimates from 12,288 nematode and 13,279 harpacticoid individuals.

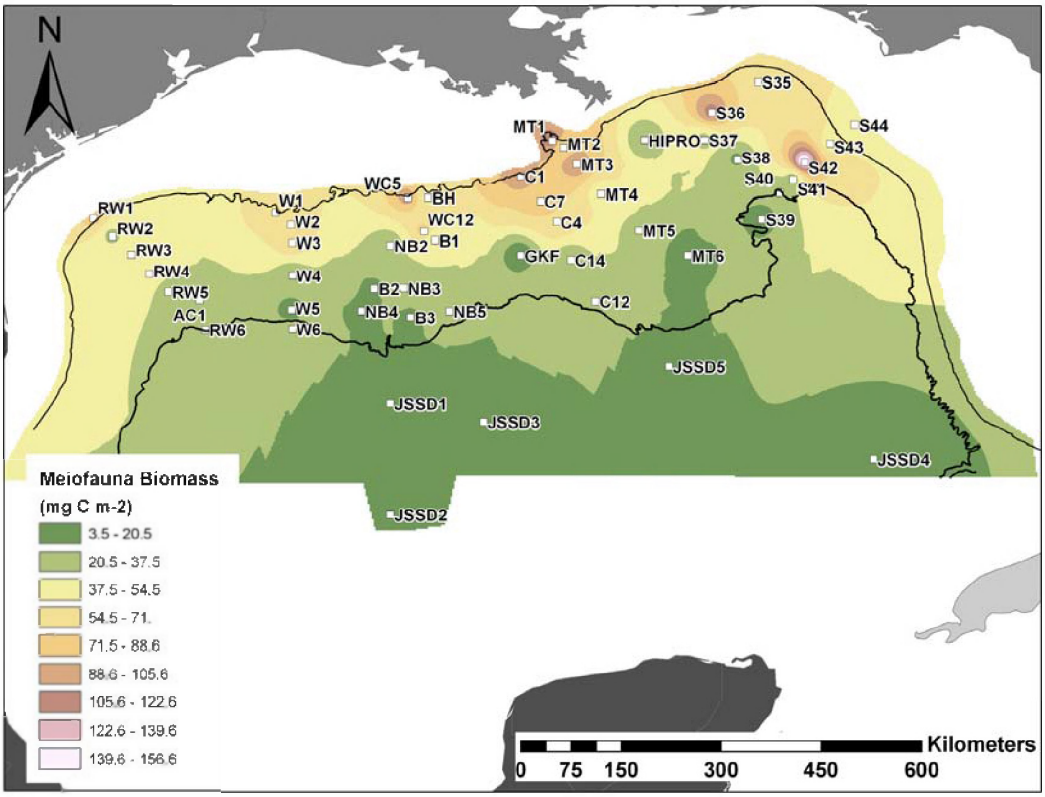

Figure 8-102. Spatial interpolation of meiofaunal biomass (mg C m^{-2}) in the northern Gulf of Mexico deep sea, using the inverse-distance weighted model. Highlighted contour lines are at 300 and 3,000 m from shallow to deep, respectively.

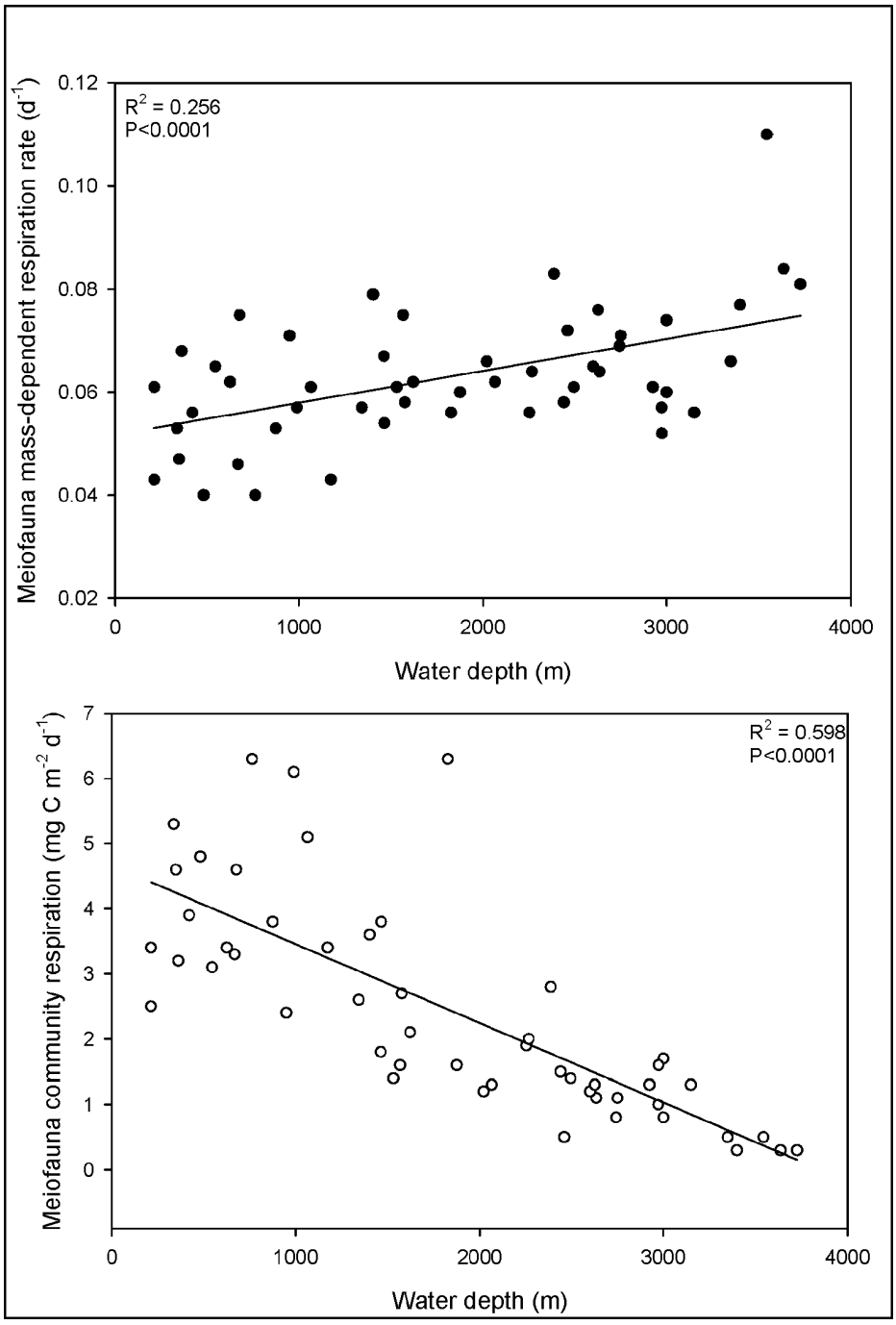

Figure 8-103. A) Meiofauna mass-dependent respiration rate (d^{-1}) and B) meiofauna community respiration (mg C m^{-2} d^{-1}) at each of the 51 DGoMB stations in the northern Gulf of Mexico deep-sea.

Geographic variation in community organic carbon requirement (assuming respiration = 80% of total metabolic requirement) was observed mainly at water depths less than 1,500 meters (Figure 8-104). Stations MT1 and MT3 in the Mississippi Trough, station S36 located in the De Soto Canyon, and station S42 directly above the Florida Escarpment, had the highest community organic carbon requirement. These four stations were located in the northeastern Gulf of Mexico and also had highest biomass. Stations in the western Gulf of Mexico had comparably lower community respiration and lower biomass (Figure 8-102 and 8-104). The theoretical organic carbon requirement over the northern GoM deep sea study area was estimated to be $1.5x10^{6}$ ($\pm$ $8.4x10^{5}$) mg C km^{-2} d^{-1}. The ratio of total estimated organic carbon requirement to total estimated

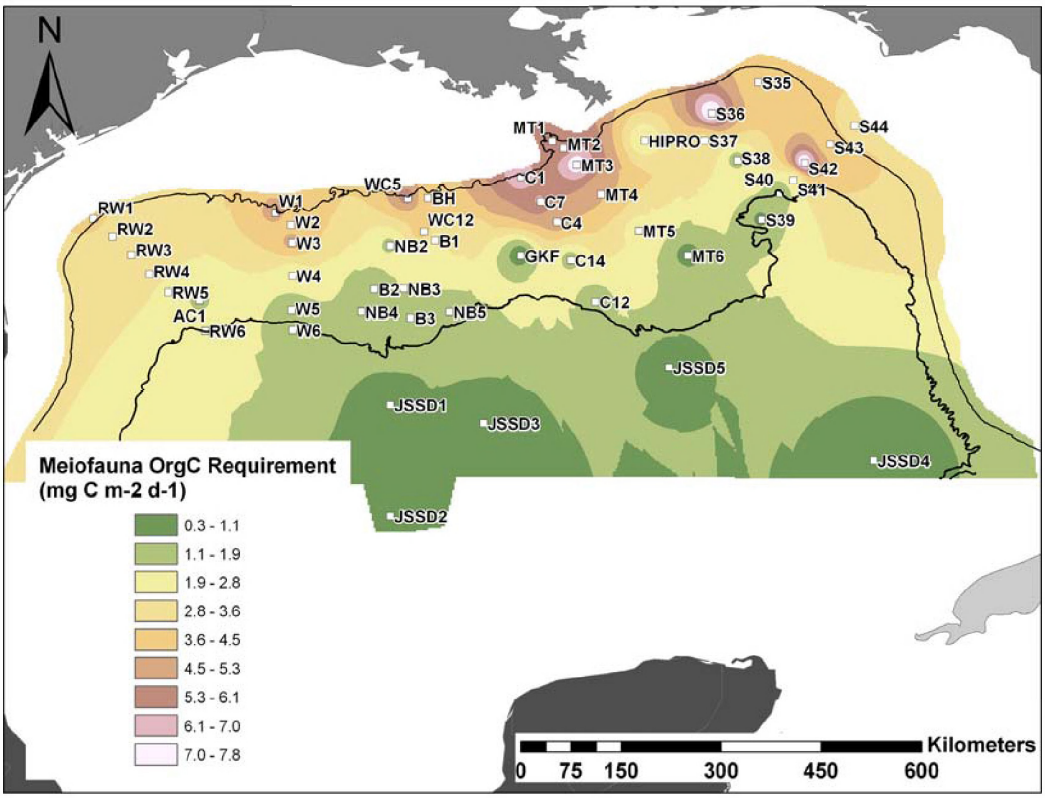

Figure 8-104. Spatial interpolation of the meiofaunal commun ity daily carbon requirement (mg C m^{-2} d^{-1}), based on allometric estimations of community respiration. Respiration is conservatively assumed to be 80% of total carbon consumption.

biomass was 0.07 ($1.5x10^{6}$ kg C d^{-1}/$2.1x10^{7}$ kg C) in units of d^{-1}; which equals 7% of the community biomass. Thus the turnover time of living carbon in the meiofauna fraction of the community was approximately 14 days, on average for the entire continental margin.

As a conservative estimate, respiration was assumed to account for 80% of the total metabolic budget. The mean meiofaunal respiration rate increased with increasing water depth, reflecting overall decrease in animal size with depth (Figure 8-103A), although harpacticoids displayed an opposing trend (Figure 8-101B). Meiofauna community respiration decreased with depth (Figure 8-103B), reflecting a decrease in overall biomass.

Geographic variation in community respiration, and therefore the overall metabolic budget, was greatest at depths less than 2,000 meters (Figures. 8-103B and 8-104). Highest respiration was found at stations near Mississippi River outflow, and where there is an interaction between the Loop Current and canyon (MT1-3, S36) and escarpment (S42) features. A comparison of experimentally measured consumption versus allometrically-derived requirements, indicates poor agreement by measured grazing, confirming poor results from the grazing study (Table 8-23). Alternatively, it is possible that there was a lack of trophic linkage between bacteria and meiofauna, and that deep-sea meiofauna depend heavily on surfaced-derived detritus. Compared to total bacterial biomass, meiofauna only require approximately 0.1 to 0.7% of the bacterial standing stock to meet their theoretical metabolic requirements (Table 8-24). But, grazing rates were, at most, 10% of the theoretical metabolic requirement.

In comparison to total benthic community respiration (CO_2, converted from sediment community oxygen consumption, Section 8.5), meiofauna are responsible for approximately 10-25 % of the total benthic community CO_2 flux (Table 8-25). Total global oxygen utilization in the deep sea has been estimated to be $1.2x10^{14}$ mol O_2 yr^{-1}, which equals approximately $1.22x10^{15}$ g C yr^{-1} (converted to units of carbon using a respiratory quotient of 0.85, and stoichometric conversion of 12g C per mole O_2). If meiofauna are responsible for 10 % of this flux (conservative), then they are responsible for processing $1.2x10^{14}$ g C yr^{-1}, and are therefore a globally significant component of the carbon cycle.

8.8.4 Macrofauna

8.8.4.1 Quantitative Distribution of Macrofauna

A total of 215 GoMEX boxcores were taken during DGoMB Cruise 1 in 2000, supplemented by replicate sampling at targeted sites on the two consecutive years, to provide detailed information about the macrofauna on the continental slope. The quantitative information on macrofauna from the boxcores was analyzed to test the eight hypotheses related to what controls the quantity and composition of life in the deep GoM. While more detailed sampling would be helpful, there is no reason to expect that the geographically broad patterns presented here will change as more data are accrued. Regressions of animal abundance as a function of depth for the entire data set indicate that mean density declines from about 10,000 down to about 3000 ind./m^2 at the base of the escarpment, with further declines out to less than 1,000 out on the abyssal plain (Figure 8-105a, top). The variability of these values is extremely high, however, from estimates of more than 30,000 down to less than a 1,000 ind./m^2. Variability seems to decline with depth. As the highest densities were found in eastern GoM at the S locations or in the MT sites (Mississippi Trough), it is worth noting that if these sites are excluded from the analysis, then the extreme highs are eliminated and the mean at the shallow sites goes down to just less than 8,000 ind./m^2 (Figure 8-105b, bottom). The Mississippi Trough (MT) sites plotted as a function of depth down the canyon (Figure 8-106) illustrate that the extreme highs nearshore were found at the canyon head. However, the tendency for the canyon to have higher values lessened with depth (MT5 and MT6). The mean at the shallow station was approximately 16,000 ind./m^2, or well above the average mean for the entire set of data. MT5 and 6 were both characterized by quantities of iron stone material mixed into the sediments. It was sampled with the box core and the trawl and it is visible in bottom photographs. It does not form a pavement, however, as has been observed in deeper waters, but appears as a bumpy, red-colored material in irregular patches at the sediment surface.

Table 8-23

Allometric Estimations of the Mass-Dependent Meiofauna Respiration Rate (R, in d^{-1} Units) and Meiofauna Community Respiration (CO_2, m^{-2} d^{-1}) and Total Organic Carbon Demand (OrgC, mg C m^{-2} d^{-1})
(Mass-dependent respiration was calculated using an allometric rate law which is dependent upon the ratio (W) of biomass (B, mg C m^{-2} d^{-1}) to abundance (A, N m^{-2}). Respiration (CO_2, mg C m^{-2} d^{-1}) is the product of the mass-dependent rate ® and the total biomass (B), and total carbon demand (OrgC) was calculated under the assumption that respiration equals 80% of the total metabolic budget (see discussion).)

Sta	Lat.	Long.	Depth	B	A	W	R	CO_2	OrgC
AC1	26.3936	-94.5731	2440	25.2	129974	1.9E-04	0.06	1.5	1.8
B1	27.2025	-91.4052	2253	33.8	157417	2.1E-04	0.06	1.9	2.4
B2	26.5500	-92.2151	2635	17.1	139907	1.2E-04	0.06	1.1	1.4
B3	26.1644	-91.7351	2600	18.5	155817	1.2E-04	0.06	1.2	1.5
BH	27.7800	-91.5000	545	48.4	407852	1.2E-04	0.06	3.1	3.9
C1	28.0598	-90.2499	336	100.4	369129	2.7E-04	0.05	5.3	6.7
C12	26.3797	-89.2403	2924	21.2	138792	1.5E-04	0.06	1.3	1.6
C14	26.9382	-89.5725	2495	22.8	146578	1.6E-04	0.06	1.4	1.7
C4	27.4532	-89.7631	1463	71.6	273585	2.6E-04	0.05	3.8	4.8
C7	27.7304	-89.9820	1066	83.3	542119	1.5E-04	0.06	5.1	6.3
GKF	27.0000	-90.2500	2460	6.4	84348	7.6E-05	0.07	0.5	0.6
HIPRO	28.5500	-88.5800	1565	21.8	343118	6.3E-05	0.08	1.6	2.0
JSSD1	25.0000	-92.0000	3545	4.5	87547	1.3E-05	0.11	0.5	0.6
JSSD2	23.5000	-92.0000	3725	4.1	87295	4.6E-05	0.08	0.3	0.4
JSSD3	24.7500	-90.7500	3635	3.5	60441	4.0E-05	0.08	0.3	0.4
JSSD4	24.2500	-85.5000	3400	3.6	63451	5.9E-05	0.08	0.3	0.3
JSSD5	25.5000	-88.2500	3350	7.0	135698	1.1E-04	0.07	0.5	0.6
MT1	28.5411	-89.8250	482	119.9	945657	8.8E-04	0.04	4.8	6.0
MT2	28.4479	-89.6719	677	60.9	535216	6.4E-05	0.08	4.6	5.7
MT3	28.2215	-89.4940	990	107.4	885995	2.0E-04	0.06	6.1	7.7
MT4	27.8276	-89.1661	1401	45.5	246058	5.1E-05	0.08	3.6	4.5
MT5	27.3328	-88.6561	2267	31.0	128964	1.3E-04	0.06	2.0	2.5
MT6	27.0016	-87.9991	2743	12.0	155312	9.3E-05	0.07	0.8	1.0
NB2	27.1348	-92.0001	1530	23.4	168276	1.5E-04	0.06	1.4	1.8
NB3	26.5580	-91.8226	1875	27.0	165245	1.6E-04	0.06	1.6	2.0
NB4	26.2468	-92.3923	2020	17.9	148409	1.1E-04	0.07	1.2	1.5
NB5	26.2454	-91.2099	2065	21.4	117263	1.4E-04	0.06	1.3	1.7
RW1	27.5001	-96.0028	212	79.6	411809	6.8E-04	0.04	3.4	4.2
RW2	27.2540	-95.7468	950	33.7	219457	8.2E-05	0.07	2.4	3.0
RW3	27.0084	-95.4924	1340	45.9	248752	2.1E-04	0.06	2.6	3.2
RW4	26.7514	-95.2502	1575	47.4	232842	1.9E-04	0.06	2.7	3.4
RW5	26.5075	-94.9967	1620	33.8	170633	1.5E-04	0.06	2.1	2.6
RW6	25.9973	-94.4956	3000	28.3	144453	1.7E-04	0.06	1.7	2.1

Table8-23 Allometric Estimations of the Mass-Dependent Meiofauna Respiration Rate (R, in d^{-1} Units) and Meiofauna Community Respiration (CO_2, m^{-2} d^{-1}) and Total Organic Carbon Demand (OrgC, mg C m^{-2} d^{-1}) (Mass-dependent respiration was calculated using an allometric rate law which is dependent upon the ratio (W) of biomass (B, mg C m^{-2} d^{-1}) to abundance (A, N m^{-2}). Respiration (CO_2, mg C m^{-2} d^{-1}) is the product of the mass-dependent rate ® and the total biomass (B), and total carbon demand (OrgC) was calculated under the assumption that respiration equals 80% of the total metabolic budget (see discussion).)(continued.)

Sta	Lat.	Long.	Depth	B	A	W	R	CO_2	OrgC
S35	29.3352	-87.0464	668	70.5	501629	4.9E-04	0.05	3.3	4.1
S36	28.9185	-87.6722	1826	113.2	799963	2.3E-04	0.06	6.3	7.9
S37	28.5536	-87.7668	2387	33.6	291179	4.2E-05	0.08	2.8	3.5
S38	28.2799	-87.3276	2627	17.5	157164	6.0E-05	0.08	1.3	1.7
S39	27.4837	-86.9998	3000	10.5	83170	6.7E-05	0.07	0.8	1.0
S40	27.8395	-86.7514	2972	17.3	99501	2.1E-04	0.06	1.0	1.2
S41	28.0136	-86.5733	2974	30.2	181408	3.0E-04	0.05	1.6	2.0
S42	28.2510	-86.4193	763	157.1	492537	8.7E-04	0.04	6.3	7.9
S43	28.5029	-86.0768	362	46.4	276279	9.4E-05	0.07	3.2	4.0
S44	28.7500	-85.7477	212	41.1	318516	1.5E-04	0.06	2.5	3.2
W1	27.5772	-93.5510	420	68.7	387228	2.2E-04	0.06	3.9	4.8
W2	27.4139	-93.3403	625	55.7	263315	1.4E-04	0.06	3.4	4.3
W3	27.1724	-93.3233	875	72.7	262642	2.8E-04	0.05	3.8	4.8
W4	26.7308	-93.3197	1460	27.5	187806	1.0E-04	0.07	1.8	2.3
W5	26.2678	-93.3327	2750	15.4	104552	8.2E-05	0.07	1.1	1.4
W6	26.0028	-93.3203	3150	22.7	124166	2.2E-04	0.06	1.3	1.6
WC12	27.3232	-91.5558	1175	78.5	218447	6.3E-04	0.04	3.4	4.3
WC5	27.7759	-91.7657	348	98.9	412061	4.5E-04	0.05	4.6	5.8

Table 8-24

Mean Meiofaunal (MB) and Bacterial (BB) Biomass for Pooled Replicates and Pooled Taxonomic Groups at Four of the Process Stations (Bacterial biomass from Section 8.8.1.)

Station	Depth (m)	Latitude (N)	Longitude (W)	MB (mg C m^{-2})	BB (mg C m^{-2})
S42	768	28.2565	86.4284	157	1180
MT3	985	28.2170	89.5106	107	2320
S36	1838	28.9118	87.6773	113	1680
MT6	2737	26.9956	88.0090	12	920

Table 8-25

Comparison Of Whole Community Respiration (CR, mg C m^{-2} d^{-1}) to Meiofauna Allometric Respiration Estimates (MR, mg C m^{-2} d^{-1}) (Meiofauna account for 10-25% of whole community respiration. Note: whole community respiration (mg C m^{-2} d^{-1}), converted from sediment community oxygen consumption (SCOC) as measured by the Benthic Lander (Section 8.5). SCOC (mmol O_2 m^{-2} d^{-1}) was converted to carbon using a respiratory quotient of 0.85 and stoichiometric conversion factor of 12 mg C/32 mg O_2.)

Station	Depth	CR	MR	%MR
S42	763	41	6.3	15.4
S36	1826	26	6.3	24.2
MT1	482	40	4.8	12.0
MT3	990	28	6.1	21.8
C7	1066	49	5.1	10.4
JSSD1	3545	4	0.5	12.5
JSSD4	3400	2.6	0.3	11.5

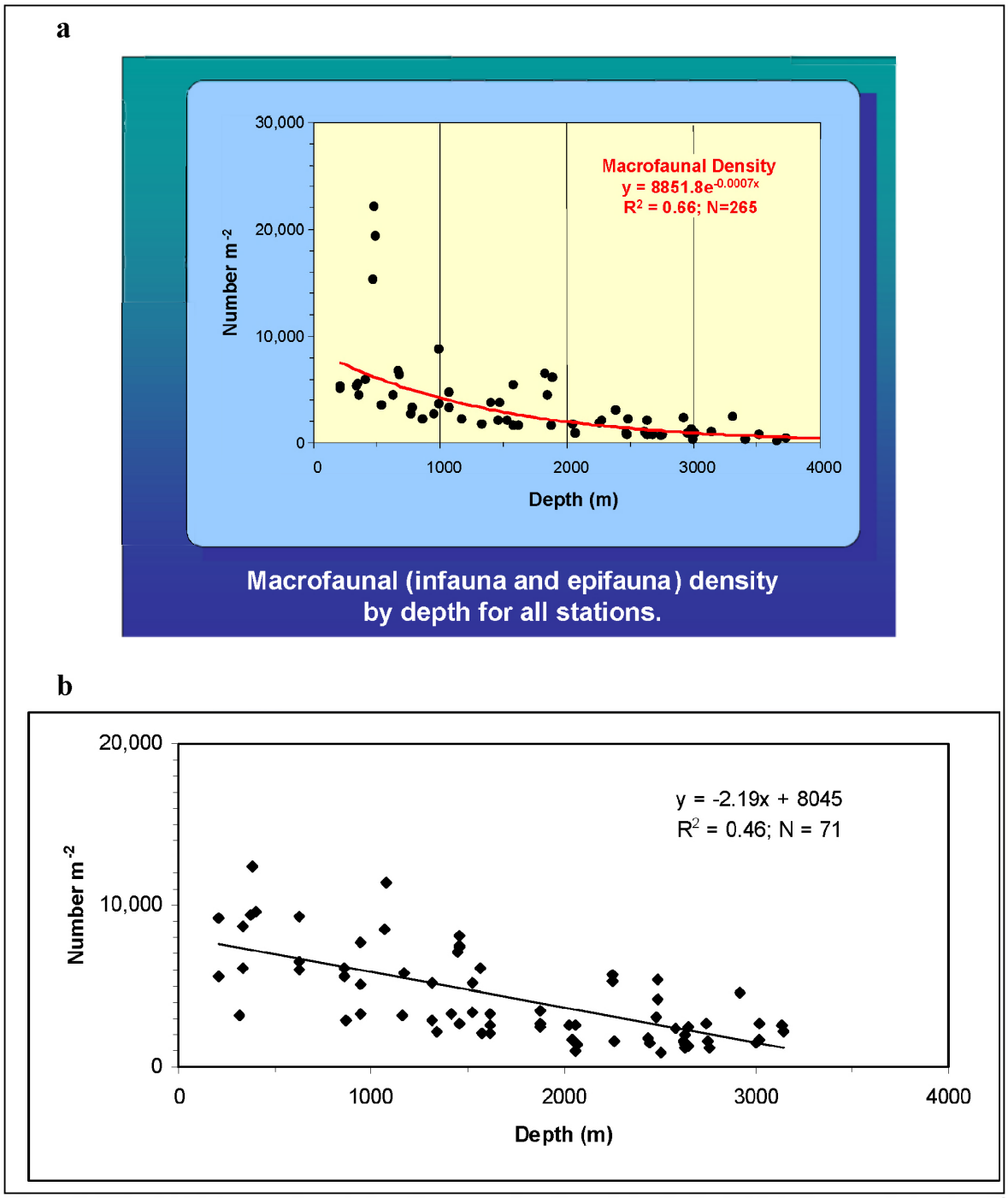

Figure 8-105. a) Total macrofaunal densities as a function of depth (top); b) bottom excludes 'east,' Mississippi Canyon and abyssal sites.

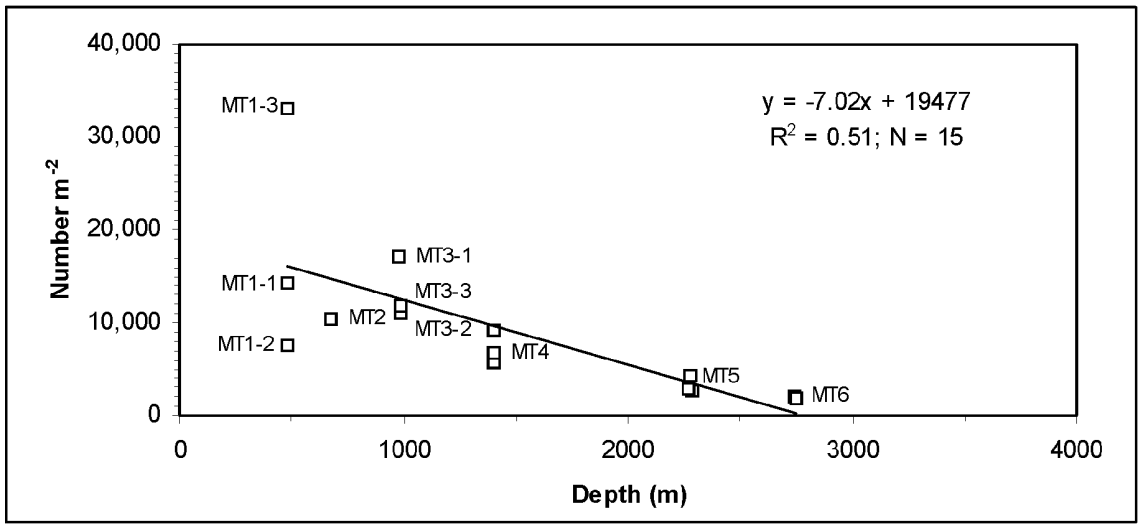

Figure 8-106. Total macrofaunal densities by depth plotting all sorted samples from the Mississippi Trough (MT).

The sites in the eastern GoM illustrate several features that were peculiar to that area (Figure 8-107). The samples have been partitioned between those lying east and those lying west of the DeSoto Canyon axis. Those to the east form a series of samples across the west Florida slope and steep escarpment. Those on the west side lie on the eastern margin of the Mississippi sediment cone. While the eastern samples formed a general pattern that declined in density with depth, with a mean trend line that more or less mimics that of the entire sample set, the macrofauna at sites west of the axis did not follow the typical pattern with depth. All of the macrofaunal abundance values were higher than their eastern counterparts and the highest values were at S36 at a depth of 1,850 meters. The high density of macrofauna at this intermediate depth suggests that the site was unique among the sites sampled. The geographic distribution of relative densities provides a clear picture of these relationships (Figure 8-108).

8.8.4.2 Dominant Macrofauna Taxa

Six major groups of macrofauna were distributed to taxonomists and identified to the lowest possible taxonomic level possible, and the species lists are available in the database. However, each taxon will not be presented in detail in this report. Three have been chosen for detailed description because each is representative of one of important categories of macrofauna: the Crustacea (Isopoda), the Mollusca (Bivalvia) and the Annelida (Polychaeta). The detailed descriptions of each of these taxons individually will be followed by a composite analysis in which all 973 species of macrofauna (from the groups in Figure 8-109) have been analyzed as a single unit. This gives the reader a comparison between the individual groups and how they compare to all the macrofauna groups lumped together. The principal variables of concern in all these analyses have been population densities, biodiversity and bathymetric zonation of recurrent groups.

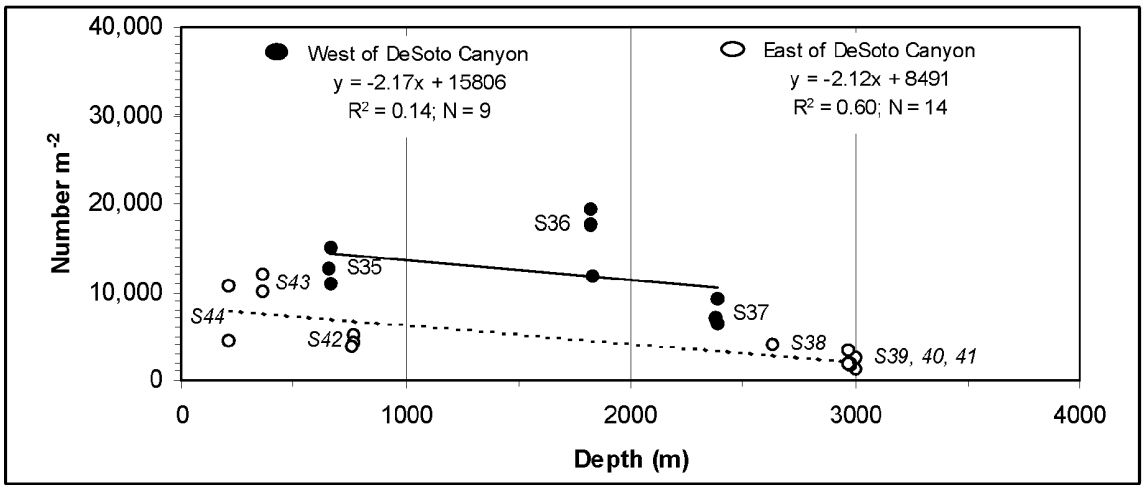

Figure 8-107. Total macrofaunal densities by depth plotting all sorted samples from the eastern Gulf of Mexico (S). Samples from the western side of DeSoto Canyon are indicated by the closed circles (●); those from east of DeSoto Canyon are indicated by open circles (○).

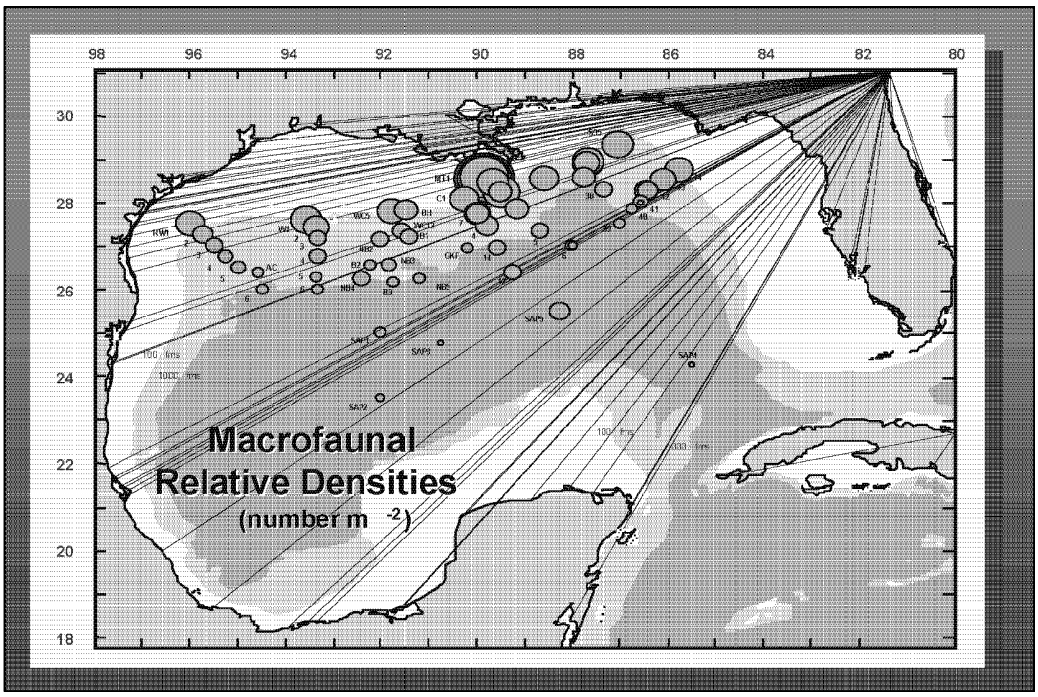

Figure 8-108. Densities of total macrofauna (all fauna >300 micron sieve) at NGoM sampling sites. Note decline with depth over the entire area, but with maximum values near the Mississippi Canyon. The abundance of the macrofauna has not been related to taxonomic composition, with one notable exception. While the macrofauna of the entire GoM was in general dominated by polychaete annelid worms and macrofaunal-sized nematode worms, the macrofauna in the shallow head of the Mississippi Trough (MT1) was dominated in all the replicates by tube-dwelling amphipod crustaceans. Circle size is proportional to total macrofauna density.

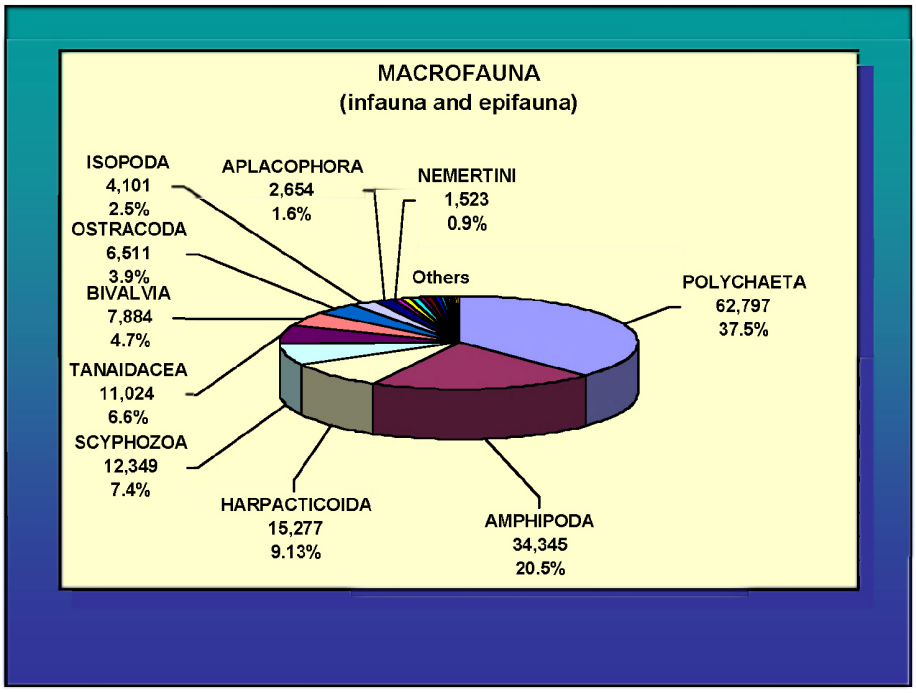

Figure 8-109. Distribution of macrofauna greater than >300 micron sieve size, excluding the large Nematoda (round worms usually lumped with the meiofauna; see previous section).

8.8.4.2.1 Isopod Crustaceans (Geo."Buz" Wilson, Aust. Nat. Mus.)

The isopods are a speciose order of crustaceans that are a common component of all deep-sea faunas. They are particularly important in this report because they are one of two groups of macrofauna which have been identified by the same taxonomist, Dr. George 'Buz' Wilson, in this study and in an earlier investigationn of the deep GoM. [The other is Dr. G. Fain Hubbard, who worked up the polychaetes.] The earlier work is referred to as the NGoMCSS (Northern Gulf of Mexico Continental Slope Study) or as the LGL study, since it was conducted by LGL Ecological Research Associate, Inc. (Figure 8-110). A comparison has been made of the two and it is presented in this report, thus allowing an assessment of the two approaches (Figure 8-111).

Species richness among the sites ranged from 52 species at the Mississippi Canyon site 3 (MT3) to 1 species at MT1. The low values are not representative of the overall diversity at these sites, but are related to low densities. Individuals and species in a sample were correlated, as expected, and both species and individuals from an individual core were related significantly: Species = $1.2124\text{inds}^{0.6652}$; $R^2 = 0.8215$ (Figure 8-112). Species richness was not distributed homogeneously across the GoM. Figure 8-113 estimates the distribution of $E(S_{15})$. As expected the shallowest samples were also the poorest in species, but so were the Sigsbee deep samples. Below the Mississippi River delta region, species richness seemed to peak around 2,000 meters, but had shallower peaks toward the West, particularly around the "Bush Hill" site. The deepest diversity hotspots seemed to occur in the vicinity of the saline basin regions between 2000 and 3,000 meters. The pattern seen in Figure 8-114, however, was highly sensitive to individually diverse samples, so less sensitive analyses are given below.

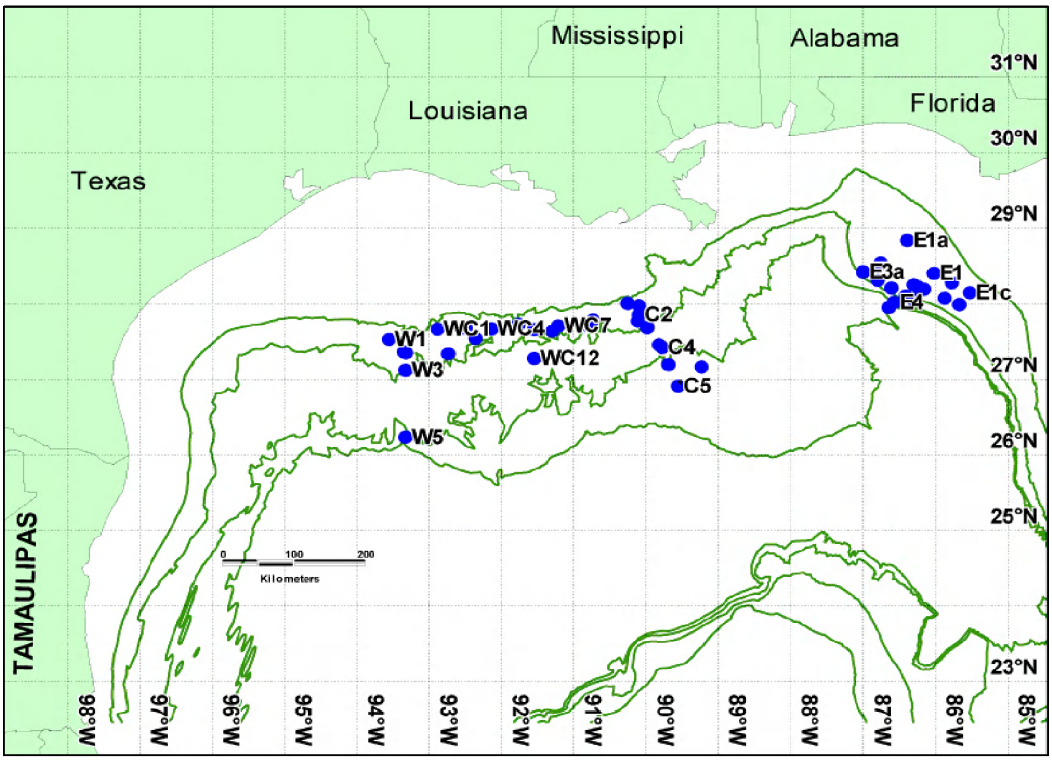

Figure 8-110. Sampling pattern of the LGL study (Pequegnat et al., 1990).

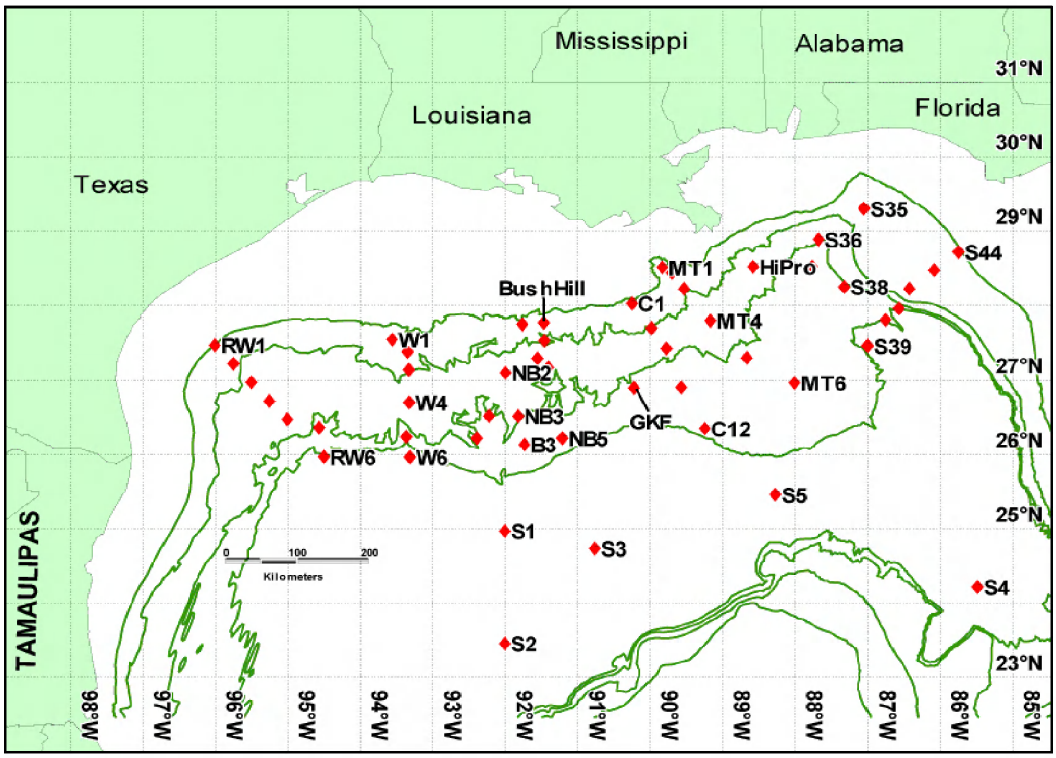

Figure 8-111. Sampling pattern of the DGoMB study.

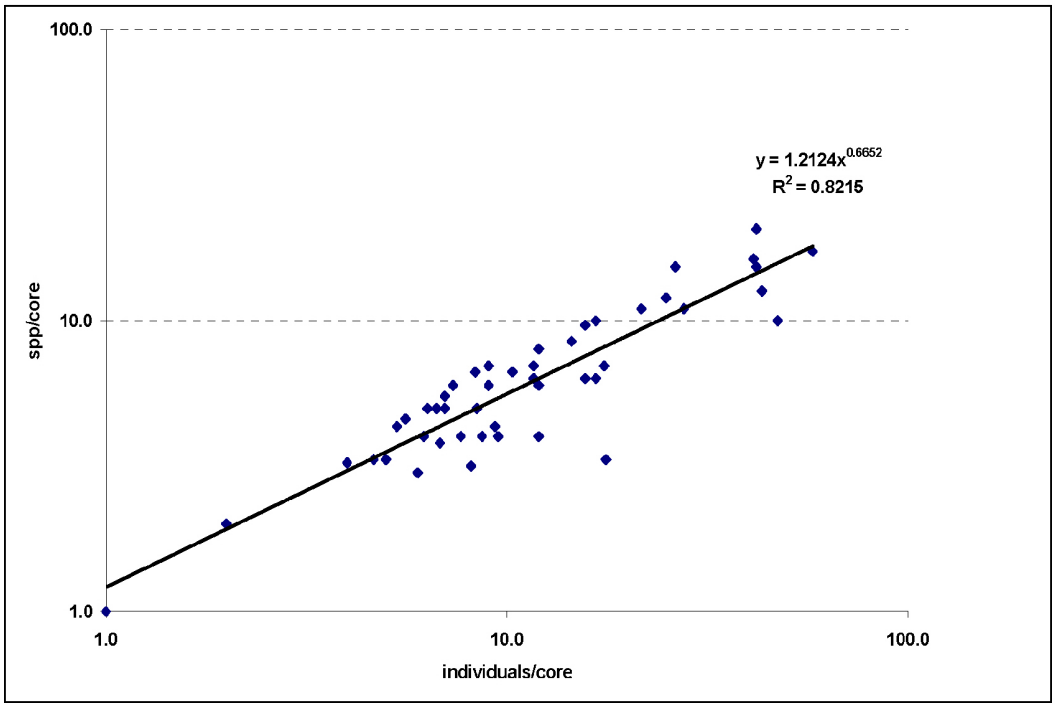

Figure 8-112. Relationship between isopod species and individuals in individual replicates.

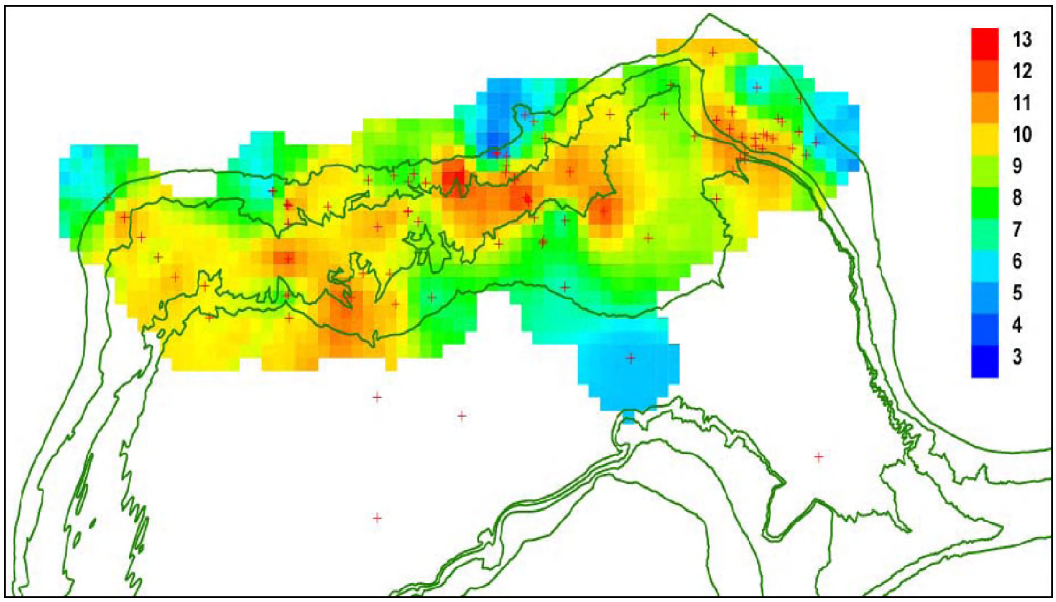

Figure 8-113. Patterns of species richness, using $E(S_{15})$, in the Gulf of Mexico. Isobaths from top to bottom are 200 m, 1,000 m, 2,000 m, 3,000 m. Red crosses indicate sample locations.

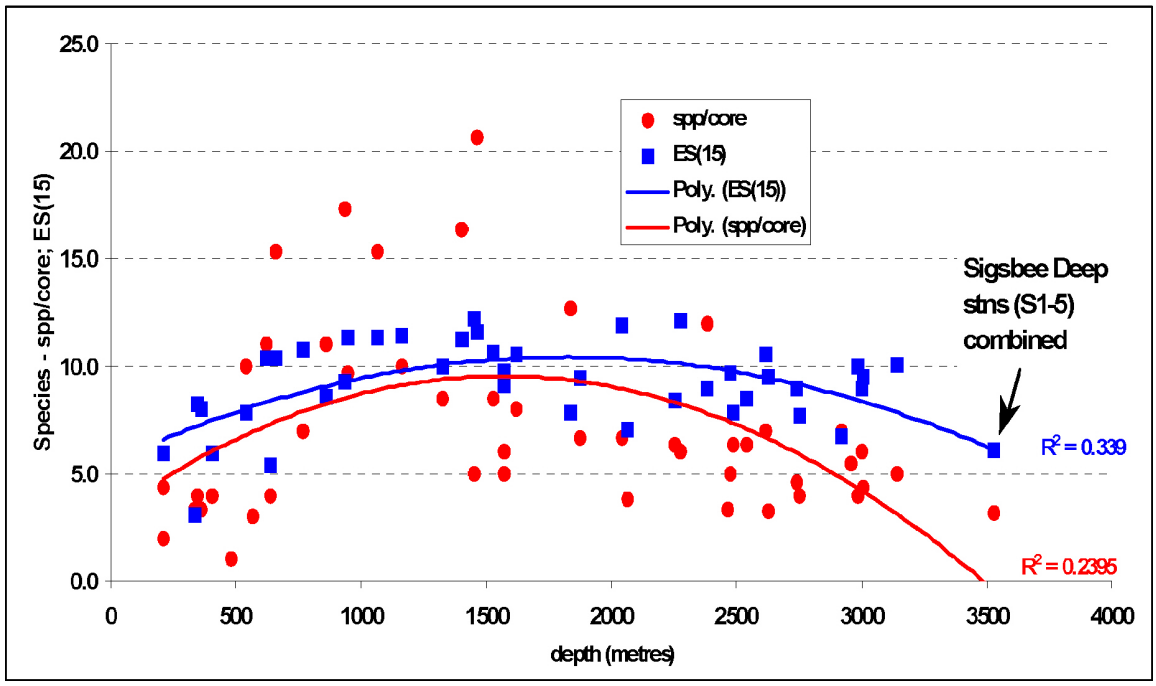

Figure 8-114. Species richness, using ES_{15}, and species density (species per core) by depth in the Gulf of Mexico. Because the Sigsbee Plain (S1-5) stations showed extremely low individual densities, they were combined for this analysis.

Both species density and species richness (Figure 8-114) show an expected peak at mid depths, although the polynomial curves are not well supported by the noisy data. The curves are also relatively flat, suggesting that overall site diversity did not change considerably with depth. Across the GoM longitudinal scale, species richness does not change significantly (Figure 8-115). Both of these relationships can be explained by broad depth and geographic ranges in GoM (Figure 8-116) for most of the species. Various ordinations and classifications of the identification data (analyses not shown) did not show any geographic coherence, suggesting that most species are found at most GoM sites. Therefore the GoM regional isopod fauna appears to be well mixed at large scales.

The LGL and the DGoMB studies, when compared using simple rarefaction curves (Figure 8-117), show a surprising difference that apparently contradicts the last statement. Although the two programs had similar numbers of identified individuals, the LGL curve falls distinctly below the DGoMB curve, thus highlighting the different species count (species richness) between the two programs (114 LGL species vs. 135 DGoMB species). This difference can be explained in a general way by comparing areas sampled. The DGoMB transects subsume a polygon of approximately 220,428 km^2, while the LGL transects lie within a smaller polygon of approximately 105,837 km^2. Therefore the often-observed species–area relationship appears in these data as well; larger areas find more species.

Most rare species, the "short range endemics," have small distributions, suggesting that larger numbers of samples may find more species. Certainly the Sigsbee Plain is substantially undersampled, given the density of the isopods in this region, and so higher numbers of samples are needed to adequately characterize this region. The GoM appears to have a well-mixed and

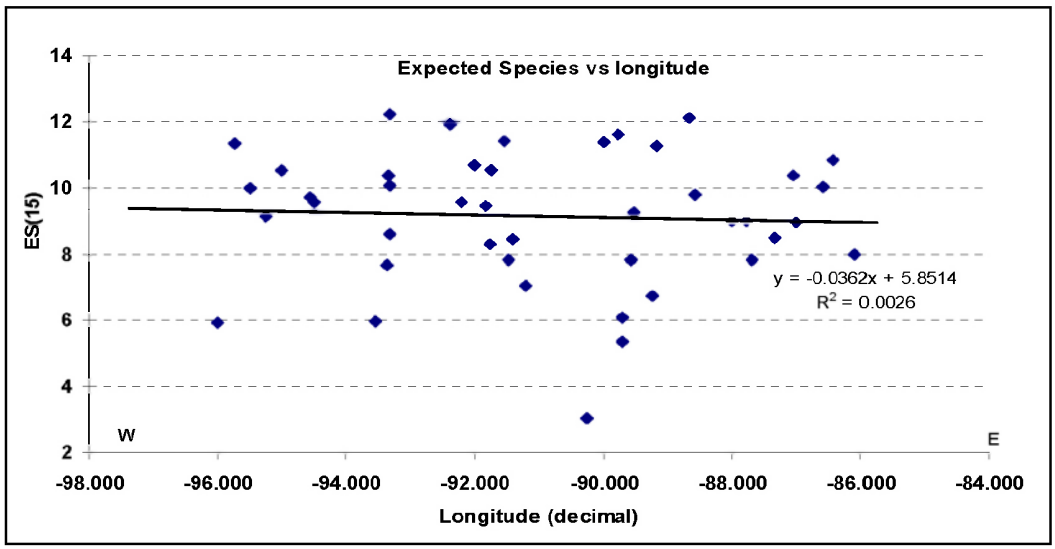

Figure 8-115. Species richness and longitude.

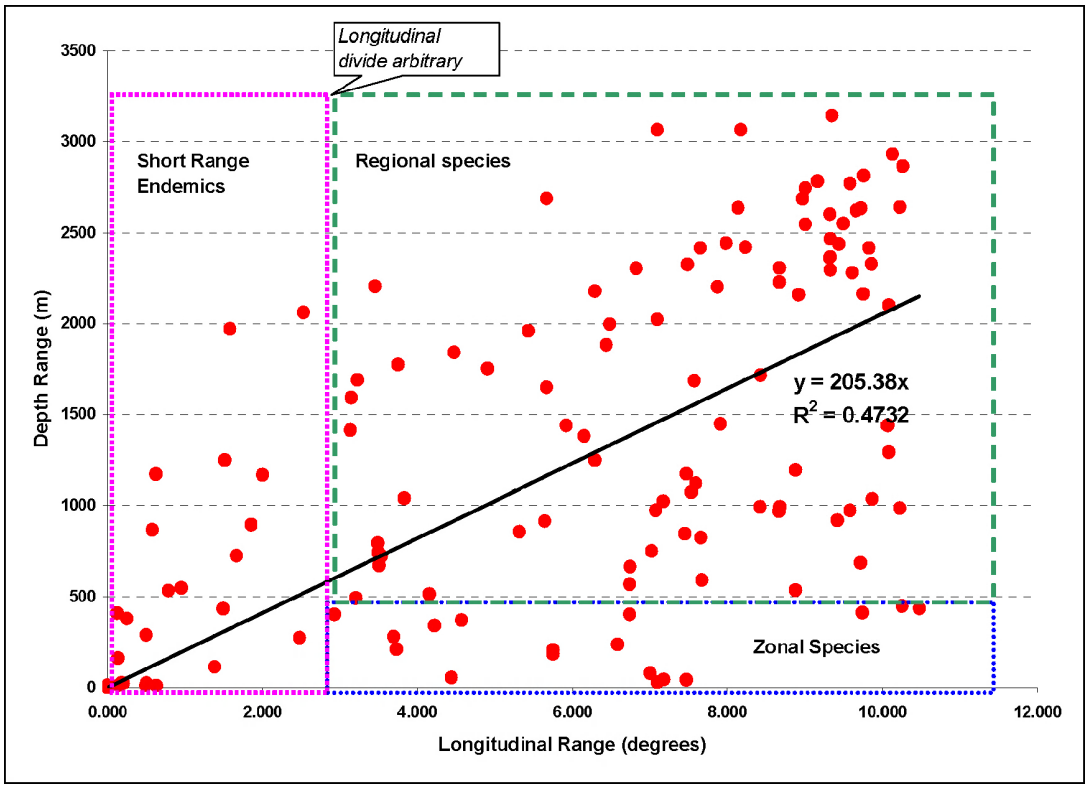

Figure 8-116. Depth ranges and longitudinal ranges of Isopoda in the Gulf of Mexico.

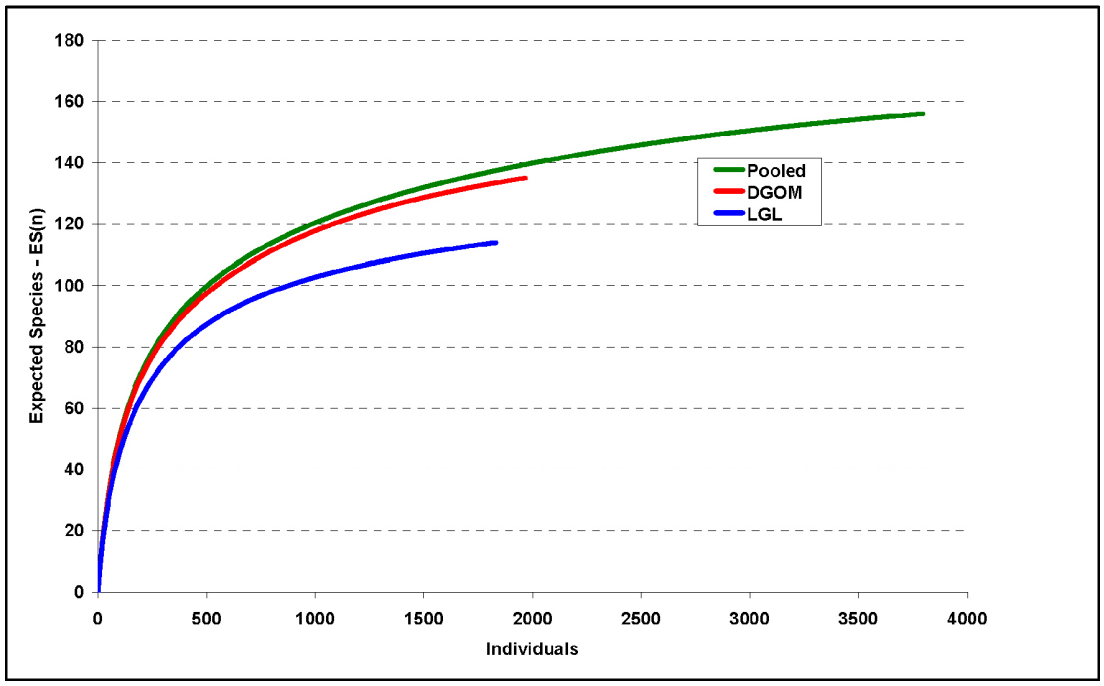

Figure 8-117. DGoMB and LGL isopod macrofauna species richness compared.

diverse regional isopod fauna that, with more than 60 new species, may be substantially distinct from adjacent regions in the North Atlantic or Caribbean. If further sampling programs are contemplated, the isopod data suggest that the deeper regions of the Sigsbee Abyssal Plain be targeted for detailed sampling to further understand how diversity varies with geography.

8.8.4.2.2 Bivalve Molluscs (Min Chen, Mary Wicksten and Roe Davenport, TAMU)

There were 144 samples collected at 48 sites in this study which yielded a total of 3615 individuals and 94 species of bivalves from the depths of 213 m to 3,732 m in the northern GoM (Table 8-26). The mean density was 147 bivalves m^{-2}, with a standard deviation of 104. The site MT3 had the maximum density of 439, and site S3 had the minimum density of 35 individuals m^{-2}.

8.8.4.2.2.1 Abundance

Bivalve abundance was highest at the shallow sites, with particularly high values in the Mississippi Canyon, and decreased with depth and distance from the shore (Figure 8-118). A linear relationship was found between $\log_{10}$ bivalve density and depth ($y = -0.17x + 2.40$, $R^2 = 0.41$, $p<0.01$; Figure 8-119). Site S5 had extraordinarily high density among the deep stations at which depths exceeded 3 km. Hypothesis 1a, there is no difference in benthic bivalve density with depth, and Hypothesis 2a, there is no difference in benthic bivalve density along an east to west gradient, were tested using a randomized complete block design analysis of variance where the depth was the main factor with 3 levels and transect was the blocking factor with 5 levels. The result indicated that the mean values for the bivalve density at different depths were not significantly different ($F_{2,8}=2.823$, $p=0.118$) and the mean values for

Table 8-26

Depth (m), Total Individuals Per Site, Number of Individuals m^{-2}, Total Number of Species, Species Richness, Pielou's Evenness (J'), Expected Number of Species (50), and Shannon-Wiener Species Index (H') for Bivalves
(The sample area per replicate was 0.1725 m^2 and three replicates were collected for each location.)

Site	Depth(m)	Total Individuals (N)	Number of Individuals (m^{-2})	Total Species (S)	Species Richness (d)	Pielou's Evenness (J')	Expected Number of Species (50)	Shannon-Wiener Species Index (H)
C1	335	67	129	23	5.23	0.82	20	2.58
C4	1457	107	207	34	7.06	0.91	24	3.19
C7	1072	112	216	27	5.51	0.88	20	2.91
C12	2922	91	176	25	5.32	0.83	19	2.68
C14	2490	89	172	22	4.68	0.81	17	2.50
NB2	1530	69	133	22	4.96	0.91	20	2.81
NB3	1875	45	87	22	5.52	0.93	22	2.87
NB4	2033	65	126	27	6.23	0.91	23	2.99
NB5	2063	27	52	17	4.85	0.93	17	2.64
RW1	213	104	201	23	4.74	0.85	17	2.66
RW2	950	112	216	33	6.78	0.86	22	3.02
RW3	1327	39	75	18	4.64	0.92	18	2.67
RW4	1575	70	135	21	4.71	0.91	18	2.77
RW5	1620	70	135	23	5.18	0.91	20	2.85
RW6	3010	33	64	14	3.72	0.91	14	2.41
WC5	356	90	174	24	5.11	0.85	18	2.69
WC12	1156	69	133	26	5.90	0.92	23	3.01
S35	664	159	307	28	5.33	0.68	16	2.26
S36	1828	142	274	28	5.45	0.72	15	2.40
S37	2386	79	153	13	2.75	0.89	12	2.29
S38	2635	45	87	11	2.63	0.82	11	1.97
S39	3002	29	56	15	4.16	0.94	15	2.55
S40	2974	27	52	13	3.64	0.93	13	2.38
S41	2974	30	58	15	4.12	0.90	15	2.44
S42	766	68	131	18	4.03	0.85	16	2.45
S43	363	121	234	18	3.54	0.74	12	2.15
S44	213	61	118	15	3.41	0.88	14	2.37

Table 8-26 Depth (m), Total Individuals Per Site, Number of Individuals m-2, Total Number of Species, Species Richness, Pielou's Evenness (J'), Expected Number of Species (50), and Shannon-Wiener Species Index (H') for Bivalves (The sample area per replicate was 0.1725 m2 and three replicates were collected for each location.) (continued)

Site	Depth(m)	Total Individuals (N)	Number of Individuals (m^{-2})	Total Species (S)	Species Richness (d)	Pielou's Evenness (J')	Expected Number of Species (50)	Shannon-Wiener Species Index (H)
B1	2256	29	56	15	4.16	0.89	15	2.42
B2	2629	44	85	12	2.91	0.83	12	2.07
B3	2620	79	153	23	5.03	0.77	17	2.40
AC1	2469	30	58	10	2.65	0.87	10	2.00
W1	396	124	240	19	3.73	0.81	14	2.39
W2	625	77	149	16	3.45	0.76	13	2.10
W3	865	46	89	25	6.27	0.91	25	2.93
W4	1447	45	87	22	5.52	0.93	22	2.88
W5	2748	24	46	9	2.52	0.85	9	1.86
W6	3145	55	106	11	2.50	0.78	11	1.88
S1	3525	22	43	4	0.97	0.83	4	1.16
S2	3732	24	46	8	2.20	0.96	8	2.00
S3	3670	18	35	5	1.38	0.97	5	1.56
S4	3410	33	64	11	2.86	0.96	11	2.29
S5	3314	160	309	15	2.76	0.72	11	1.95
MT1	481	226	437	13	2.21	0.23	5	0.59
MT2	677	226	437	21	3.69	0.47	10	1.44
MT3	987	227	439	27	4.79	0.76	15	2.51
MT4	1401	70	135	23	5.18	0.87	20	2.74
MT5	2277	42	81	18	4.55	0.92	18	2.65
MT6	2746	24	46	10	2.83	0.85	10	1.95

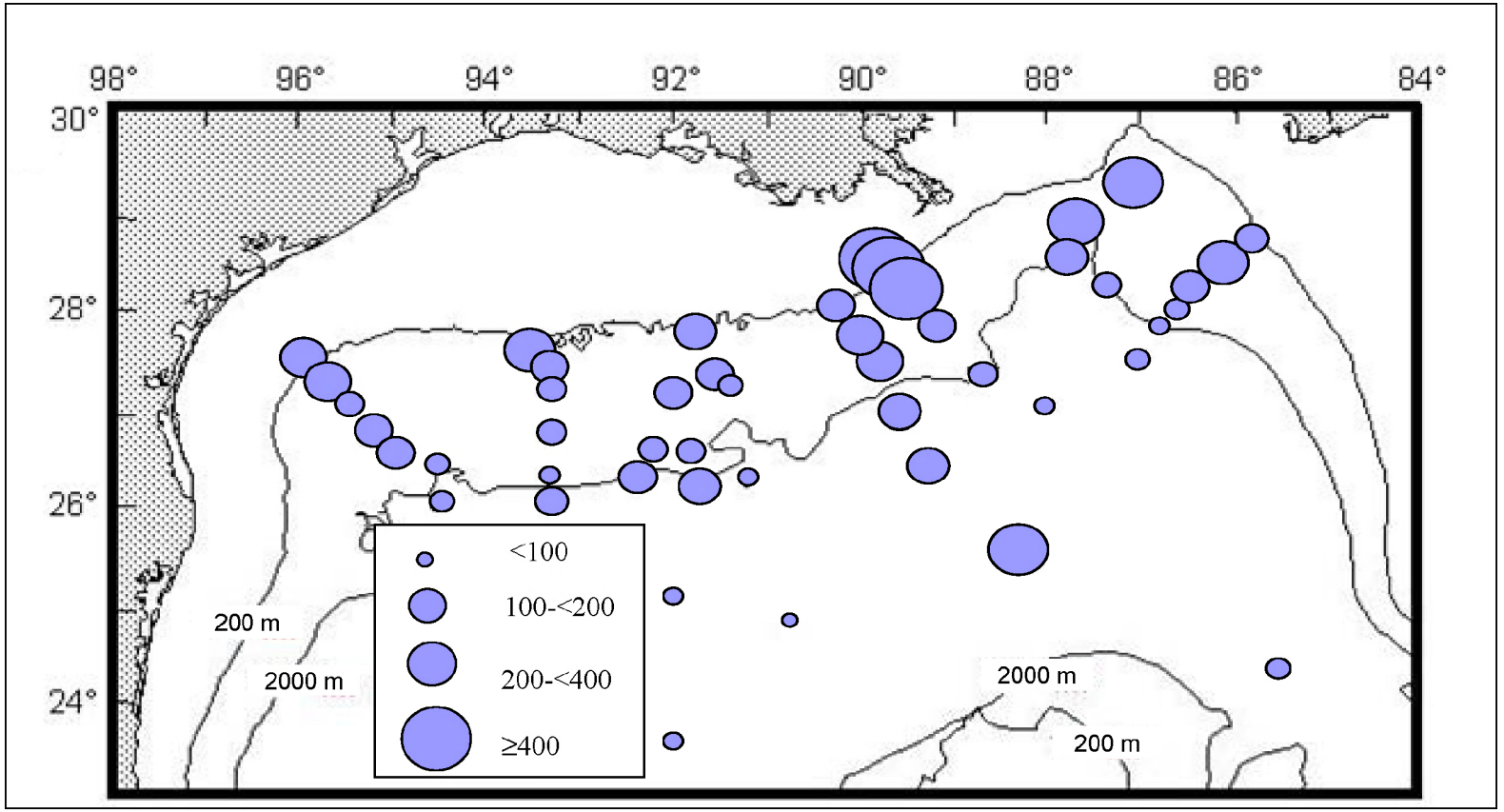

Figure 8-118. Map of density distribution of bivalves (ind. m^{-2}) in the GoM.

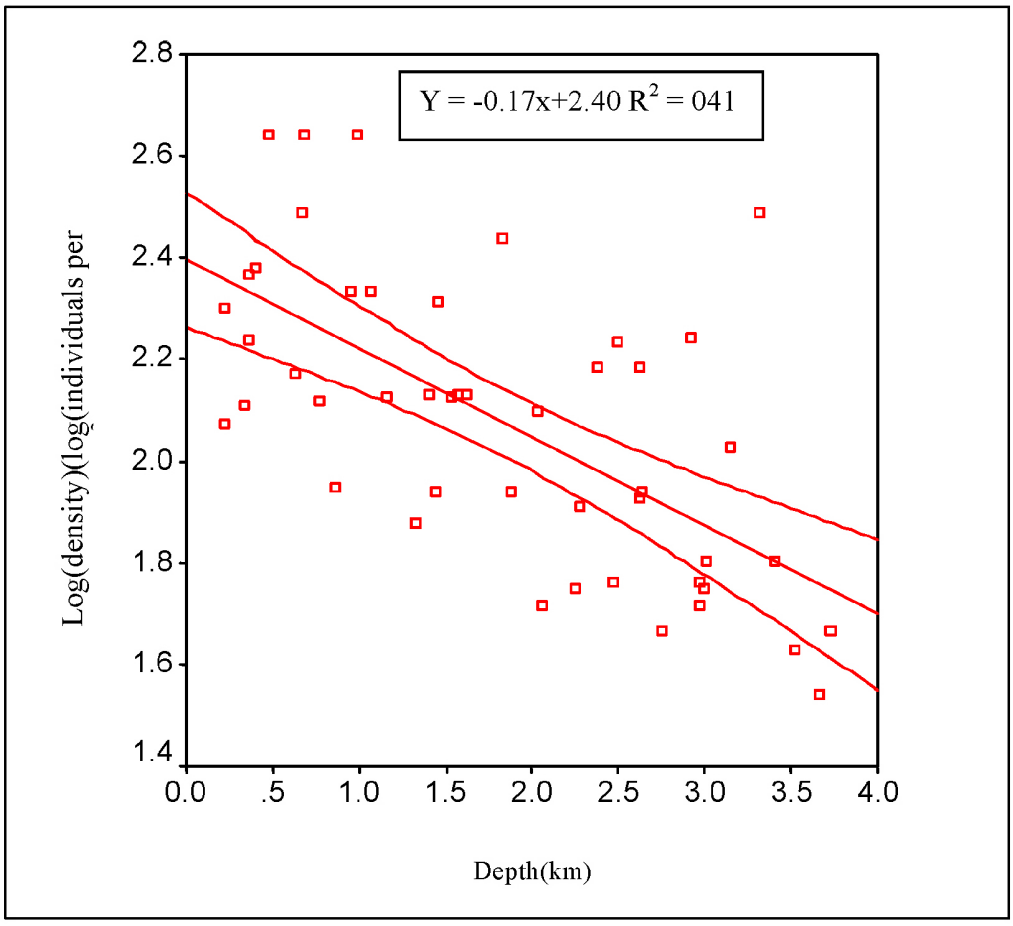

Figure 8-119. Linear regression plot of bivalve log density against depth.

the bivalve density in western, central and eastern transects were not significantly different ($F_{4,8}$=0.561, p=0.698), i.e., there was no difference in bivalve mollusc density among transects (Table 8-26). The mean value of bivalve density in 0.3km was 225±129 individuals m^{-2} whereas the mean value of bivalve density in 1.5km was 139±43 individuals m^{-2}. The mean value of bivalve density in 3 km is 90±53 individuals m^{-2}. The least squares regression analysis of density and depth illustrated a linear correlation between bivalve density and depth. Hypothesis 3a, there is no difference in benthic bivalve density between basin and non-basin, was tested using a single-factor analysis of variance, which indicated that the mean values for the basin bivalve density and non-basin bivalve density were not significantly different ($F_{1,5}$=.002, p=0.963). The mean value of bivalve density in basin stations was 98±50 individuals m^{-2} and 100±38 individuals m^{-2} at non-basin stations. Hypothesis 4a, there is no difference in benthic bivalve density between canyon and non-canyon, was tested using a single-factor analysis of variance which indicated that the mean values for the canyon and non-canyon bivalve density were significantly different ($F_{1,4}$=84.6, p=0.001. The mean value of bivalve density in canyon stations was 437±1 individuals m^{-2} while the mean value in non-canyon stations was 184±48 individuals m^{-2}.

8.8.4.2.2.2 Diversity

Diversity of bivalves increased slightly from the shallow stations, with especially low values in the Mississippi canyon, to a maximum at intermediate depths, and then decreased down to the deepest station (Figure 8-119). A parabolic (quadratic) relationship was found between diversity and depth. The Shannon-Wiener Species Index (Figure 8-120) displayed the same pattern. The three sites that had lowest diversity were MT1, MT2, and S1. Hypothesis 1b, there is no difference in benthic bivalve diversity with depth (Figure 8-121), and Hypothesis 2b, there is no difference in benthic bivalve diversity along an east to west gradient, were tested using a randomized complete block analysis of variance where the depth was the main factor with three (3) levels and transect was the blocking factor with five (5) levels. The result indicated that the mean values for bivalve diversity at different depths were not significantly different (F2, 8=2.709, p=0.126) and the mean values for bivalve diversity in western, central and eastern transects were not significantly different (F4, 8=2.010, p=0.186), i.e., there was no difference in bivalve mollusk diversity among transects. The least squares regression analysis of diversity and depth showed there was a quadratic correlation between bivalve diversity and depth. Hypothesis 3b, there is no difference in benthic bivalve diversity between basin and non-basin, was tested using a single-factor analysis of variance which indicated that the mean values for the basin bivalve diversity and non-basin bivalve diversity were significantly different (F1,5=17.137, p=0.009. The mean value of bivalve diversity in basin stations was 2.30±0.11. The mean value in non-basin stations was 2.83±0.07.

Hypothesis 4b, there is no difference in benthic bivalve diversity between canyon and non-canyon, was tested using a single-factor analysis of variance which indicated that the mean values for canyon bivalve diversity (H') and non-canyon bivalve diversity were not significantly different ($F_{1, 4}$=5.61, p=0.08). The mean value of bivalve diversity in canyon stations was 1.51±0.96, whereas the mean value in non-canyon stations was 2.89±0.31. Evenness of bivalves had no clear tendency in the Gulf of Mexico. However, the dominance in MT1 and MT2 were high with evenness of 0.23 and 0.47, respectively.The least squares regression analysis showed there was a quadratic relationship between diversity and depth. For linear term the p-value was 0.002 and the power was 0.906 (Table 8-27). For quadratic term the p-value was less than 0.01 and the power was 0.971. The diversity of bivalve mollusks increased from shallow continental slope depths, with especially low values in the Mississippi Canyon, to a maximum at intermediate depths (1-2km), followed by a decrease down to the deepest areas (3.7km) in the Gulf of Mexico. However, the ANOVA test showed no difference in diversity of bivalve mollusks for different depth.

A parabolic relationship was found between diversity (H'(S)) of bivalves and depth ($y = -0.24x^2 + 0.79x + 1.99$, $R^2 = 0.29$, p-value=0.0003), but the maximum documented was on the upper continental slope (1-2km), rather than the upper continental rise (3 km), where a maximum has been observed in the northwestern Atlantic (Rex, 1983).

To reduce the influence of the outlier diversity (H'(S)) of MT1 which had standardized residual –4.05, iteratively reweighted least squares was used by applying weights that varied inversely with the size of the residual. Outlying case diversity (H'(S)) of MT1 that had largest residual was thereby given smallest weight. The iteratively reweighted least squares robust regression for diversity (H'(S)) became $y = -0.22x^2 + 0.66x + 2.20$, $R^2 = 0.40$, p-value<0.01.

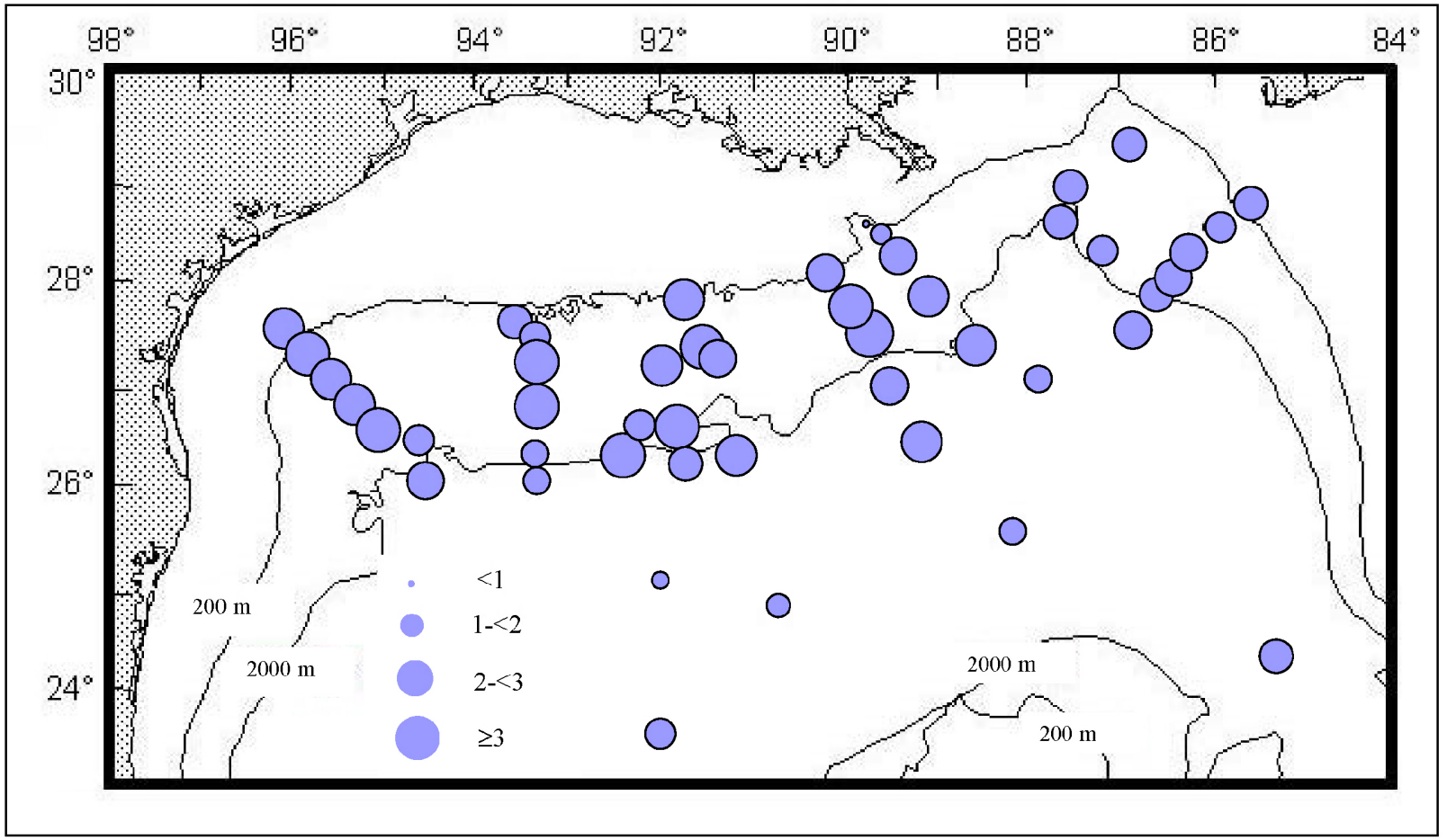

Figure 8-120. Map of diversity (Shannon-Wiener Species Index) distribution of bivalves in the GoM.

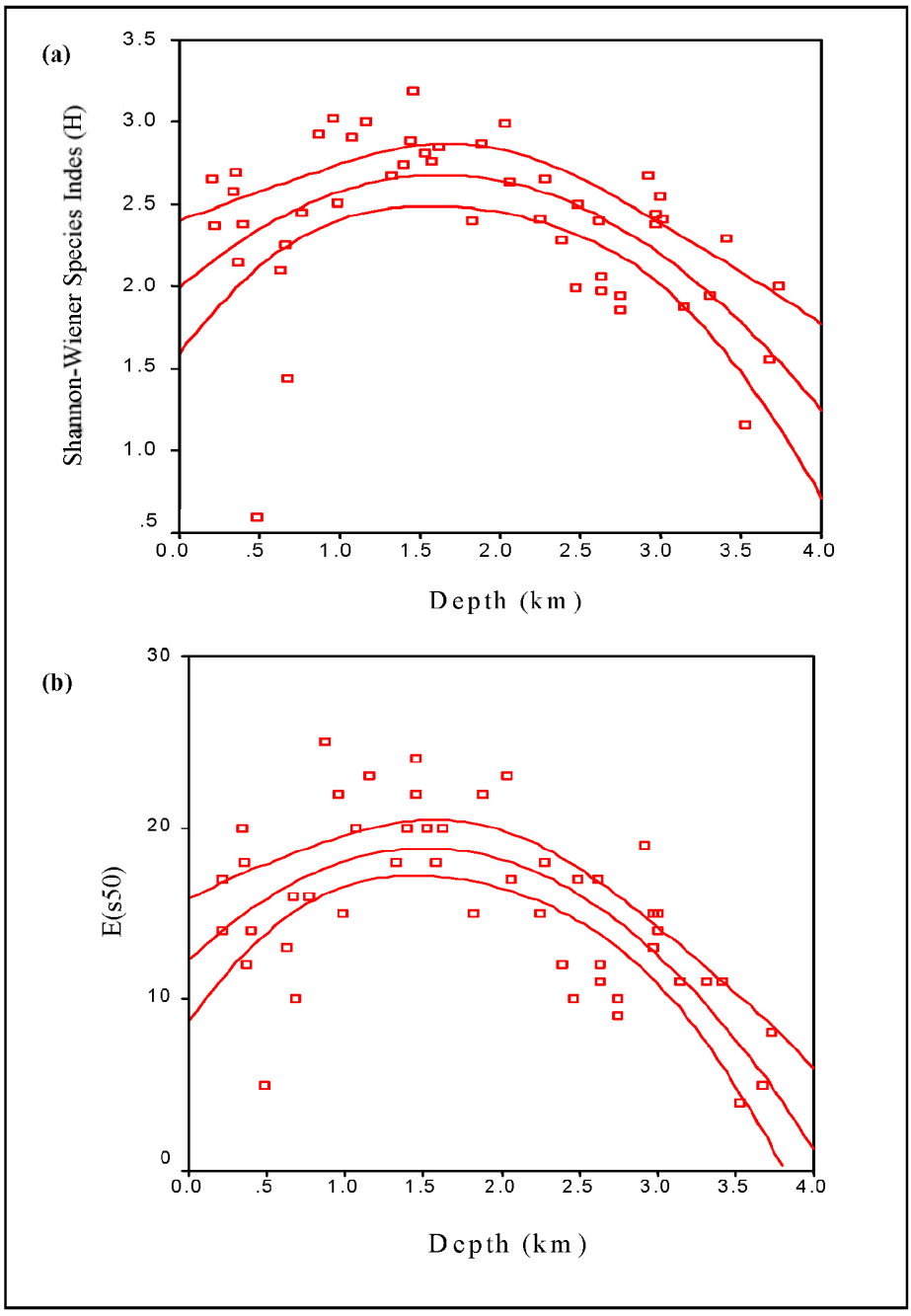

Figure 8-121. Curvilinear regression plot of bivalve diversity against depth. Reported are: curves created from Shannon-Wiener Species Index (H) ($y=-0.26x^2+0.84x+2.00$ $R^2=0.31$) (a) and for Expected Number of Species [ES(50)] ($y=-2.84x^2+8.62x+12.28$ $R^2=0.47$) (b).

Table 8-27

List of Station Groups Based on Percent Similarity with Respect to Species Composition

Group	Description	Stations	Depth(m)	Group	Description	Stations	Depth(m)
1	Shallow, Mississippi	MT1	481	6	Deep area	MT5	2277
	Canyon	MT2	677			RW5	1620
						NB4	2033
2	Shallow, non-canyon	RW1	213			NB5	2063
		WC5	356			B2	2629
						B1	2256
3	Mid-slope, eastern	MT3	987			AC1	2469
	and cental area	MT4	1401			W5	2748
		S36	1828			RW6	3010
4	Shallow, eastern and	S44	213	7	Deep area	S4	3410
	west-central area	S35	664			S2	3732
		S43	363			S41	2974
		W1	396			S3	3670
						MT6	2746
5	Mid-slope area, most	W2	625			S1	3525
	inclusive	RW2	950			S40	2974
		C7	1072			S39	3002
		W4	1447				
		NB3	1875	8	Shallow, central area	C1	335
		WC12	1156				
		S42	766	9	Deep area	S38	2635
		W3	865			S37	2386
		RW3	1327			S5	3314
		RW4	1575			W6	3145
		C4	1457			C14	2490
		NB2	1530			B3	2620
						C12	2922

8.8.4.2.2.3 Zonation

The stations were separated into nine groups according to percent similarity of species composition (Figure 8-122). Within each group, the stations shared at least 25% of the species, except group 4, which shared at least 20% of the species. The species composition appeared to change with depth. Group 1 included MT1and MT2, which ranged from 481 m to 677 m in the Mississippi Canyon. Group 2 included RW1 and WC5, which ranged from 213 m to 356 m in western GoM. Group 3 included MT3, MT4, and S36, which ranged from 987 m to 1,828 m, which is in the eastern and central GoM. Group 4 included S44, S35, S43, and W1, which ranged from 213m to 664m in eastern and western GoM. Group 5 included W2, RW2, C7, W4, NB3, WC12, S42, W3, RW3, RW4, C4, and NB2, which ranged from 625 m to 1,875 m. Group 6 included MT5, RW5, NB4, NB5, B2, B1, AC1, W5, and RW6, which ranged from 1,620 m to 3,010 m. Group 7 included S4, S2, S41, S3, MT6, S1, S40, and S39, which ranged from 2,746 m to 3,732 m. Group 8 included central site C1 which is 335m.Group 9 included S38, S37, S5, W6, C14, B3, and C12, which ranged from 2,386 m to 3,314 m (Figure 8-123).

The depth interval of 213 m to 677 m contained four groups: 1, 2, 4 and 8. From 625 m to 1,875 m, there were two groups: 3 and 5. Three groups occurred in the range of 1,620 m to 3,732 m. They were group 6, 7, and 9.

8.8.4.3 Polychaete Annelids (G. Fain Hubbard, TAMUG, and Yuning Wang, Texas Tech)

A total of 17,881 polychaete specimens from 96 replicate samples (with at least one replicate from each sampling station) were collected during the three annual cruises conducted between 2000–2002. These represent 543 taxonomic entities, including 53 families, 226 genera, and 410 species, many of which are undescribed (Tables 8-28 though 8-39). The extremely small size of most of the specimens (300μ lower cut-off in sorting) and their generally poor physical condition (many battered beyond recognition or broken into several fragments) result in many samples being identifiable only to family or genus level.

8.8.4.3.1 Polychaete Density

The abundance of polychaetes declined exponentially with depth (Figure 8-124), as expected from previous studies elsewhere. Highest densities were found on the upper slope (3,500 ind. m^{-2}); the lowest were on the abyssal plain. The densities in the central gulf were higher than those in the eastern or western extremities of the study area, including at those sites in deep water, similar to the total macrofauna. Polychaetes were the most abundant of all the macrofauna, sensu strictu, with the exception of the Amphipoda at the head of the Mississippi Trough.

8.8.4.3.2 Polychaete Species Richness and Diversity

The polychaete worms were the most speciose of all the macrofaunal groups (Table 8-29 through 8-39), with a total of 410. Shannon Weiner diversity (H'(s)) declined from a mean of almost 6 on the upper slope down to 3.5 on the abyssal plain (Figure 8-125). Expected species per individual declined from the upper slope down to the lower slope at approximately the same rate (Figure 8-126). Based on 50 individuals, the expected number of species was approximately 25 to 35, whereas based on 100 individuals, the expected number was 50 to 60 species. The low value on the abyssal plain was on the order of 10 to 15 species.

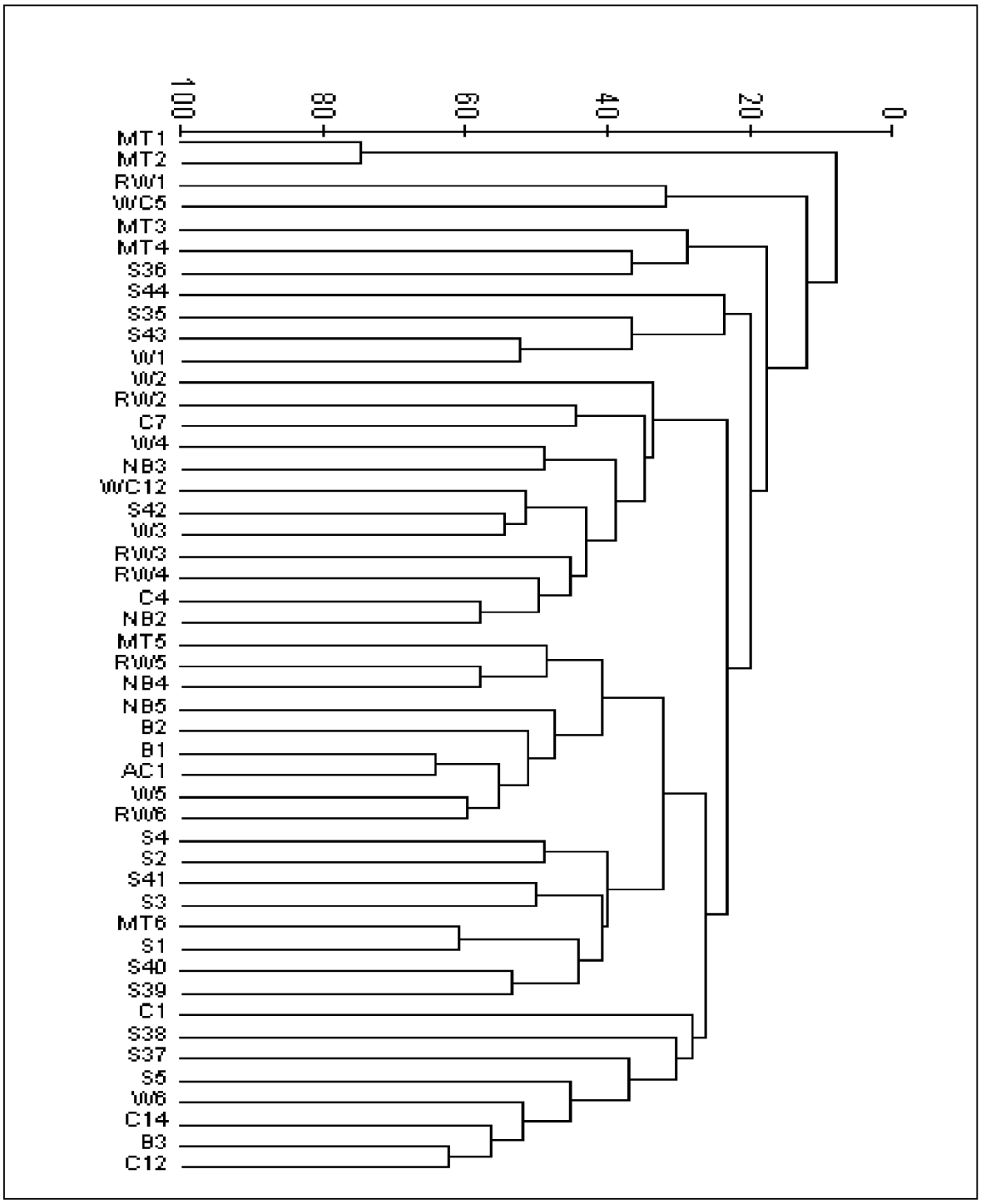

Figure 8-122. Dendrogram based on percent similarity of bivalve mollusk species

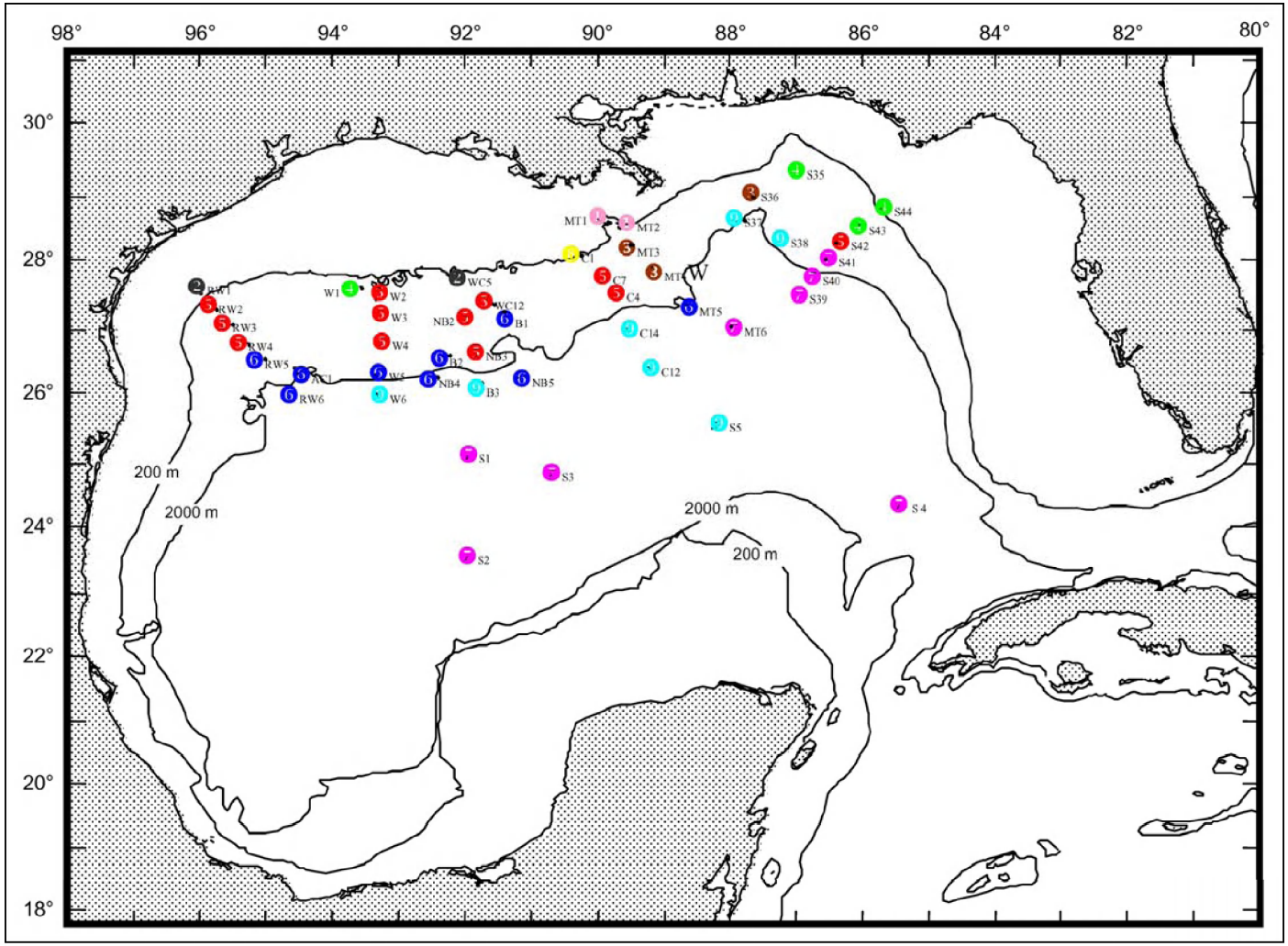

Figure 8-123. Bathymetric zonation of bivalves based on percent similarity.

Table 8-28

The 50 Most Abundant Polychaete Species by Number

Family	Genus Species	N	# Reps	N m^{-2}
Paraonidae	*Aricidea suecica*	535	58	32.31
Paraonidae	*Paraonella monilaris*	472	69	28.50
Spionidae	*Prionospio cirrifera*	471	22	28.44
Cirratulidae	*Tharyx marioni*	429	71	25.91
Paraonidae	*Aedicira* sp.	385	39	23.25
Spionidae	*Prionospio ehlersi*	382	20	23.07
Spionidae	*Spiophanes berkeleyorum*	369	49	22.28
Spionidae	*Prionospio cristata*	352	7	21.26
Pilargidae	*Litocorsa antennata*	343	8	20.71
Opheliidae	*Tachytrypane* sp. A	317	65	19.14
Nephtyidae	*Aglaophamus verrilli*	308	12	18.60
Paraonidae	*Aricidea simplex*	284	52	17.15
Paraonidae	*Levinsenia uncinata*	282	73	17.03
Paraonidae	*Aricidea mirifica*	267	15	16.12
Cossuridae	*Cossura delta*	243	28	14.67
Acrocirridae	*Macrochaeta clavicornis*	181	46	10.93
Syllidae	*Exogone* sp. A	177	43	10.69
Paraonidae	*Levinsenia oligobranchiata*	159	30	9.60
Trichobranchidae	*Terebellides distincta*	156	40	9.42
Paraonidae	*Levinsenia gracilis*	142	28	8.57
Cirratulidae	*Tharyx annulosus*	139	40	8.39
Maldanidae	*Micromaldane* sp.	136	21	8.21
Paraonidae	*Aricidea fragilis*	136	38	8.21
Syllidae	*Exogone longicirrus*	127	24	7.67
Fauveliopsidae	*Fauveliopsis* sp. A	126	38	7.61
Lumbrineridae	*Lumbrinerides dayi*	123	38	7.43
Spionidae	*Prionospio heterobranchia*	118	7	7.13
Paraonidae	*Sabidius cornatus*	116	27	7.00
Syllidae	*Exogone* sp. B	114	24	6.88
Paralacydoniidae	*Paralacydonia paradoxa*	108	33	6.52
Spionidae	Genus B	108	23	6.52
Lumbrineridae	*Lumbrineris verrilli*	98	23	5.92
Spionidae	*Prionospio cirrobranchiata*	94	9	5.68
Pilargidae	*Sigambra tentaculata*	93	35	5.62
Nereididae	*Ceratocephale oculata*	87	34	5.25
Syllidae	*Exogone dispar*	83	16	5.01
Amphinomidae	*Paramphinome jeffreysii*	82	26	4.95
Paraonidae	*Aricidea catherinae*	82	11	4.95
Longosomatidae	*Heterospio longissima*	81	20	4.89
Pilargidae	*Synelmis klatti*	81	36	4.89
Phyllodocidae	*Protomystides bidentata*	76	35	4.59
Spionidae	*Spiophanes* sp. D	74	22	4.47
Syllidae	*Exogone* sp. D	74	30	4.47
Ampharetidae	*Melinna maculata*	69	5	4.17
Onuphidae	*Sarsonuphis hartmanae*	69	30	4.17

Table 8-28 The 50 Most Abundant Polychaete Species by Number (continued)

Family	Genus Species	N	# Reps	N m^{-2}
Paraonidae	*Paraonella* sp. A	69	25	4.17
Paraonidae	*Aricidea lopezi lopezi*	66	17	3.99
Sigalionidae	*Sthenelais* sp. A	65	23	3.93
Ampharetidae	*Isolda pulchella*	63	4	3.80
Opheliidae	*Armandia maculata*	63	31	3.80

Table 8-29

Western Transects (W1-6, RW1-6, and AC1) Produced 2,141 Polychaetes
Representing 172 Taxa and 14 Replicates
(The most abundant species by numbers (≥ 20).)

FAMILY	GENUS SPECIES	N	N m^{-2}
Pilargidae	*Litocorsa antennata*	246	101.86
Cirratulidae	*Tharyx marioni*	77	31.88
Paraonidae	*Paraonella monilaris*	55	22.77
Paraonidae	*Levinsenia uncinata*	45	18.63
Opheliidae	*Tachytrypane* sp. A	42	17.39
Paraonidae	*Aricidea suecica*	40	16.56
Amphinomidae	*Paramphinome jeffreysii*	34	14.08
Acrocirridae	*Macrochaeta clavicornis*	30	12.42
Lumbrineridae	*Lumbrinerides dayi*	27	11.18
Spionidae	Genus B	27	11.18
Nephtyidae	*Aglaophamus verrilli*	26	10.77
Paraonidae	*Aedicira* sp.	24	9.94
Phyllodocidae	*Protomystides bidentata*	22	9.11
Paraonidae	*Aricidea fragilis*	20	8.28

Table 8-30

Characteristic Species of Western Transect Stations

FAMILY	GENUS SPECIES	N	N m^{-2}
Pilargidae	*Litocorsa antennata*	246	101.86
Cirratulidae	*Tharyx marioni*	77	31.88
Paraonidae	*Paraonella monilaris*	55	22.77
Paraonidae	*Levinsenia uncinata*	45	18.63

Table 8-31

B and NB Stations Intended to Test Basin Vs Non-Basin Communities [B1-3, NB2-5, Additionally Including WC5, WC12, and BH (Bush Hill)] Produced 1,930 Polychaetes Representing 150 Taxa and 15 Replicates.
(The most abundant species by numbers (≥ 20).)

FAMILY	GENUS SPECIES	N	N m^{-2}
Spionidae	*Prionospio cristata*	313	120.97
Cirratulidae	*Tharyx marioni*	64	24.73
Paraonidae	*Levinsenia uncinata*	51	19.71
Paraonidae	*Paraonella monilaris*	50	19.32
Paraonidae	*Aricidea suecica*	48	18.55
Opheliidae	*Ophelina* sp. A	41	15.85
Opheliidae	*Tachytrypane* sp. A	40	15.46
Trichobranchidae	*Terebellides distincta*	28	10.82
Paraonidae	*Aricidea simplex*	27	10.43
Spionidae	*Prionospio heterobranchia*	26	10.05
Paraonidae	*Levinsenia oligobranchiata*	25	9.66
Syllidae	*Exogone longicirrus*	24	9.28
Pilargidae	*Litocorsa antennata*	23	8.89

Table 8-32

Characteristic Species of the Basin/Non-Basin Transect Stations

FAMILY	GENUS SPECIES	N	N m^{-2}
Spionidae	*Prionospio cristata*	313	120.97
Paraonidae	*Levinsenia uncinata*	51	19.71

Table 8-33

Central Transect Stations [C1, C4, C7, C12, C14, GKF (Green Knoll Furrows) and S5 (Sigsbee Abyssal Plain)] Produced 2,445 Polychaetes Representing 185 Taxa and 17 Replicates (The most abundant species by numbers (≥ 20).

FAMILY	GENUS SPECIES	N	N m^{-2}
Paraonidae	*Paraonella monilaris*	140	54.11
Opheliidae	*Tachytrypane* sp. A	61	23.57
Paraonidae	*Levinsenia uncinata*	52	20.10
Cirratulidae	*Tharyx marioni*	48	18.55
Paraonidae	*Aricidea suecica*	45	17.39
Syllidae	*Exogone dispar*	40	15.46
Spionidae	*Spiophanes berkeleyorum*	38	14.69
Pilargidae	*Litocorsa antennata*	38	14.69
Fauveliopsidae	*Fauveliopsis* sp. A	37	14.30
Paraonidae	*Aedicira* sp.	36	13.91
Syllidae	*Exogone* sp. A	36	13.91
Spionidae	*Prionospio cirrifera*	35	13.53
Paraonidae	*Sabidius cornatus*	31	11.98
Paraonidae	*Aricidea simplex*	28	10.82
Syllidae	*Exogone longicirrus*	28	10.82
Amphinomidae	*Paramphinome jeffreysii*	25	9.66
Pilargidae	*Synelmis klatti*	20	7.73
Paraonidae	*Levinsenia brevibranchiata*	20	7.73

Table 8-34

Characteristic Species of the Central Transect Stations

FAMILY	GENUS SPECIES	N	N m^{-2}
Paraonidae	*Paraonella monilaris*	140	54.11
Syllidae	*Exogone dispar*	40	15.46
Fauveliopsidae	*Fauveliopsis* sp. A	37	14.30

Table 8-35

Mississippi Trough Transect Stations (MT1-6) Produced 6,868 Polychaetes
Representing 333 Taxa and 25 Replicates
(The most abundant species by numbers (≥ 20).)

FAMILY	GENUS SPECIES	N	N m^{-2}
Spionidae	*Prionospio cirrifera*	429	99.48
Spionidae	*Prionospio ehlersi*	356	82.55
Paraonidae	*Aricidea suecica*	301	69.80
Paraonidae	*Aedicira* sp.	284	65.86
Nephtyidae	*Aglaophamus verrilli*	275	63.77
Spionidae	*Spiophanes berkeleyorum*	236	54.72
Paraonidae	*Aricidea mirifica*	197	45.68
Cossuridae	*Cossura delta*	155	35.94
Paraonidae	*Aricidea simplex*	152	35.25
Opheliidae	*Tachytrypane* sp. A	116	26.90
Cirratulidae	*Tharyx marioni*	112	25.97
Paraonidae	*Levinsenia gracilis*	93	21.57
Maldanidae	*Micromaldane* sp.	88	20.41
Spionidae	*Prionospio heterobranchia*	88	20.41
Paraonidae	*Levinsenia oligobranchiata*	81	18.78
Spionidae	*Prionospio cirrobranchiata*	75	17.39
Trichobranchidae	*Terebellides distincta*	75	17.39
Lumbrineridae	*Lumbrineris verrilli*	71	16.46
Paraonidae	*Aricidea catherinae*	71	16.46
Paraonidae	*Levinsenia uncinata*	70	16.23
Ampharetidae	*Melinna maculata*	69	16.00
Paraonidae	*Paraonella monilaris*	69	16.00
Ampharetidae	*Isolda pulchella*	62	14.38
Longosomatidae	*Heterospio longissima*	58	13.45
Paraonidae	*Aricidea fragilis*	58	13.45
Paraonidae	*Aricidea lopezi lopezi*	53	12.29
Cirratulidae	*Tharyx annulosus*	52	12.06
Spionidae	*Prionospio steenstrupi*	52	12.06
Pilargidae	*Sigambra tentaculata*	50	11.59
Paraonidae	*Aedicira belgicae*	47	10.90
Paralacydoniidae	*Paralacydonia paradoxa*	40	9.28
Syllidae	*Exogone dispar*	40	9.28
Syllidae	*Exogone* sp. A	35	8.12
Fauveliopsidae	*Fauveliopsis* sp. A	32	7.42
Spionidae	*Laonice cirrata*	32	7.42
Paraonidae	*Paraonella sp. A*	31	7.19
Maldanidae	*Maldane glebifex*	29	6.72
Syllidae	*Exogone sp. B*	29	6.72
Capitellidae	*Genus AA*	28	6.49
Cossuridae	*Cossura soyeri*	28	6.49
Nephtyidae	*Micronephthys minuta*	27	6.26
Paraonidae	*Aricidea cerrutii*	24	5.57
Lumbrineridae	*Ninoe sp. A*	23	5.33
Paraonidae	*Sabidius cornatus*	23	5.33
Syllidae	*Exogone atlantica*	23	5.33
Dorvilleidae	*Schistomeringos rudolphi*	22	5.10
Oweniidae	*Myriowenia sp. A*	22	5.10

Table 8-35 Mississippi Trough Transect Stations (MT1-6) Produced 6,868 Polychaetes Representing 333 Taxa and 25 Replicates (The most abundant species by numbers (≥ 20).) (continued)

FAMILY	GENUS SPECIES	N	N m^{-2}
Pilargidae	*Synelmis klatti*	22	5.10
Spionidae	Genus B	22	5.10
Capitellidae	*Notomastus americanus*	21	4.87
Spionidae	*Spiophanes* sp. D	20	4.64
Dorvilleidae	*Schistomeringos* sp. B	20	4.64

Table 8-36

Characteristic Species of the Mississippi Trough Transect Stations (*Melinna maculata, Isolda pulchella and Nephtys* squamosa are essentially endemic to the Mississippi Trough Stations, while *Aricidea catherinae, Aricidea cerrutii, Aricidea lopezi lopezi, Aedicira belgicae, Capitellidae Genus AA, Ceratocephale loveni, Cossura soyeri, Exogone atlantica, Heterospio longissima, Laonice cirrata, Maldane glebifex, Notomastus americanus, Prionospio steenstrupi, Schistomeringos rudolphi, Schistomeringos sp. B, and Terebellides atlantis* all exhibit maximum numbers there.)

FAMILY	GENUS SPECIES	N	N m^{-2}
Spionidae	*Prionospio cirrifera*	429	99.48
Spionidae	*Prionospio ehlersi*	356	82.55
Paraonidae	*Aricidea suecica*	301	69.80
Paraonidae	*Aedicira* sp.	284	65.86
Nephtyidae	*Aglaophamus verrilli*	275	63.77
Spionidae	*Spiophanes berkeleyorum*	236	54.72
Paraonidae	*Aricidea mirifica*	197	45.68
Cossuridae	*Cossura delta*	155	35.94
Paraonidae	*Aricidea simplex*	152	35.25
Opheliidae	*Tachytrypane* sp. A	116	26.90
Cirratulidae	*Tharyx marioni*	112	25.97
Paraonidae	*Levinsenia gracilis*	93	21.57
Maldanidae	*Micromaldane* sp.	88	20.41
Spionidae	*Prionospio heterobranchia*	88	20.41
Paraonidae	*Levinsenia oligobranchiata*	81	18.78
Spionidae	*Prionospio cirrobranchiata*	75	17.39
Trichobranchidae	*Terebellides distincta*	75	17.39
Lumbrineridae	*Lumbrineris verrilli*	71	16.46
Paraonidae	*Aricidea catherinae*	71	16.46
Ampharetidae	*Melinna maculata*	69	16.00
Ampharetidae	*Isolda pulchella*	62	14.38
Longosomatidae	*Heterospio longissima*	58	13.45
Paraonidae	*Aricidea lopezi lopezi*	53	12.29
Spionidae	*Prionospio steenstrupi*	52	12.06
Pilargidae	*Sigambra tentaculata*	50	11.59
Paraonidae	*Aedicira belgicae*	47	10.90
Spionidae	*Laonice cirrata*	32	7.42
Maldanidae	*Maldane glebifex*	29	6.72
Capitellidae	Genus AA	28	6.49
Cossuridae	*Cossura soyeri*	28	6.49
Nephtyidae	*Micronephthys minuta*	27	6.26
Paraonidae	*Aricidea cerrutii*	24	5.57
Syllidae	*Exogone atlantica*	23	5.33

Table 8-36 Characteristic Species of the Mississippi Trough Transect Stations (*Melinna maculata, Isolda pulchella and Nephtys* squamosa are essentially endemic to the Mississippi Trough Stations, while *Aricidea catherinae, Aricidea cerrutii, Aricidea lopezi lopezi, Aedicira belgicae, Capitellidae Genus AA, Ceratocephale loveni, Cossura soyeri, Exogone atlantica, Heterospio longissima, Laonice cirrata, Maldane glebifex, Notomastus americanus, Prionospio steenstrupi, Schistomeringos rudolphi, Schistomeringos sp. B, and Terebellides atlantis* all exhibit maximum numbers there.) (continued)

FAMILY	*GENUS SPECIES*	N	N m-2
Dorvilleidae	*Schistomeringos rudolphi*	22	5.10
Capitellidae	*Notomastus americanus*	21	4.87
Dorvilleidae	*Schistomeringos* sp. B	20	4.64

Table 8-37

Eastern Transect Stations [S35-44 and HP (High Productivity)] Produced 4,337 Polychaetes Representing 207 Taxa from 21 Replicates
(The most abundant species by numbers (≥ 20).)

FAMILY	GENUS SPECIES	N	N m^{-2}
Paraonidae	*Paraonella monilaris*	125	34.51
Cirratulidae	*Tharyx marioni*	118	32.57
Acrocirridae	*Macrochaeta clavicornis*	102	28.16
Paraonidae	*Aricidea suecica*	101	27.88
Syllidae	*Exogone* sp. A	73	20.15
Paraonidae	*Aricidea mirifica*	67	18.50
Spionidae	*Spiophanes berkeleyorum*	66	18.22
Paraonidae	*Levinsenia uncinata*	64	17.67
Syllidae	*Exogone* sp. B	64	17.67
Paraonidae	*Aricidea simplex*	60	16.56
Lumbrineridae	*Lumbrinerides dayi*	58	16.01
Opheliidae	*Tachytrypane* sp. A	53	14.63
Cossuridae	*Cossura delta*	50	13.80
Syllidae	*Exogone longicirrus*	48	13.25
Nereididae	*Ceratocephale oculata*	44	12.15
Spionidae	Genus B	38	10.49
Paralacydoniidae	*Paralacydonia paradoxa*	36	9.94
Pilargidae	*Litocorsa antennata*	36	9.94
Cirratulidae	*Tharyx annulosus*	35	9.66
Oweniidae	*Myriochele* sp. A	35	9.66
Fauveliopsidae	*Fauveliopsis* sp. A	34	9.39
Paraonidae	*Aedicira* sp.	33	9.11
Paraonidae	*Cirrophorus lyra*	32	8.83
Paraonidae	*Aricidea fragilis*	31	8.56
Sigalionidae	*Sthenelais* sp. A	31	8.56
Phyllodocidae	*Protomystides bidentata*	29	8.01
Paraonidae	*Sabidius cornatus*	28	7.73
Paraonidae	*Levinsenia oligobranchiata*	27	7.45
Syllidae	*Exogone* sp. D	27	7.45
Trichobranchidae	*Terebellides distincta*	27	7.45
Flabelligeridae	*Diplocirrus* sp. A	26	7.18
Maldanidae	*Maldane* sp. A	25	6.90
Maldanidae	*Micromaldane* sp.	23	6.35

Table 8-37 Eastern Transect Stations [S35-44 and HP (High Productivity)] Produced 4,337 Polychaetes Representing 207 Taxa from 21 Replicates (The most abundant species by numbers (≥ 20).) (continued)

FAMILY	GENUS SPECIES	N	N m^{-2}
Opheliidae	*Armandia maculata*	23	6.35
Capitellidae	*Barantolla* sp. A	21	5.80
Lumbrineridae	*Ninoe* sp. A	21	5.80
Flabelligeridae	*Diplocirrus capensis*	20	5.52
Sigalionidae	*Pholoe* sp. B	20	5.52

Table 8-38

Characteristic Species of the Eastern Transect Stations

FAMILY	GENUS SPECIES	N	N m^{-2}
Paraonidae	*Paraonella monilaris*	125	34.51
Cirratulidae	*Tharyx marioni*	118	32.57
Acrocirridae	*Macrochaeta clavicornis*	102	28.16
Syllidae	*Exogone* sp. A	73	20.15
Lumbrineridae	*Lumbrinerides dayi*	58	16.01
Nereididae	*Ceratocephale oculata*	44	12.15
Spionidae	Genus B	38	10.49
Oweniidae	*Myriochele* sp. A	35	9.66
Sigalionidae	*Sthenelais* sp. A	31	8.56
Opheliidae	*Armandia maculata*	23	6.35
Lumbrineridae	*Ninoe* sp. A	21	5.80

Table 8-39

Sigsbee Abyssal Plain Stations (S1-5) Produced 267 Polychaetes Representing 48 Taxa and 6 Replicates
(The most abundant species by numbers (≥ 10). No species was found to occur at all five deep stations, although Paraonella monilaris and Sigambra tentaculata were found at four of the stations. Greater numbers of specimens and numbers of species were found at station S5 than at S1-S4.)

FAMILY	GENUS SPECIES	N	N m^{-2}
Paraonidae	*Paraonella monilaris*	33	31.86
Paraonidae	*Sabidius cornatus*	23	22.22
Pilargidae	*Synelmis klatti*	15	14.49
Cirratulidae	*Tharyx marioni*	10	9.66
Fauveliopsidae	*Fauveliopsis* sp. A	10	9.66
Pilargidae	*Sigambra tentaculata*	10	9.66

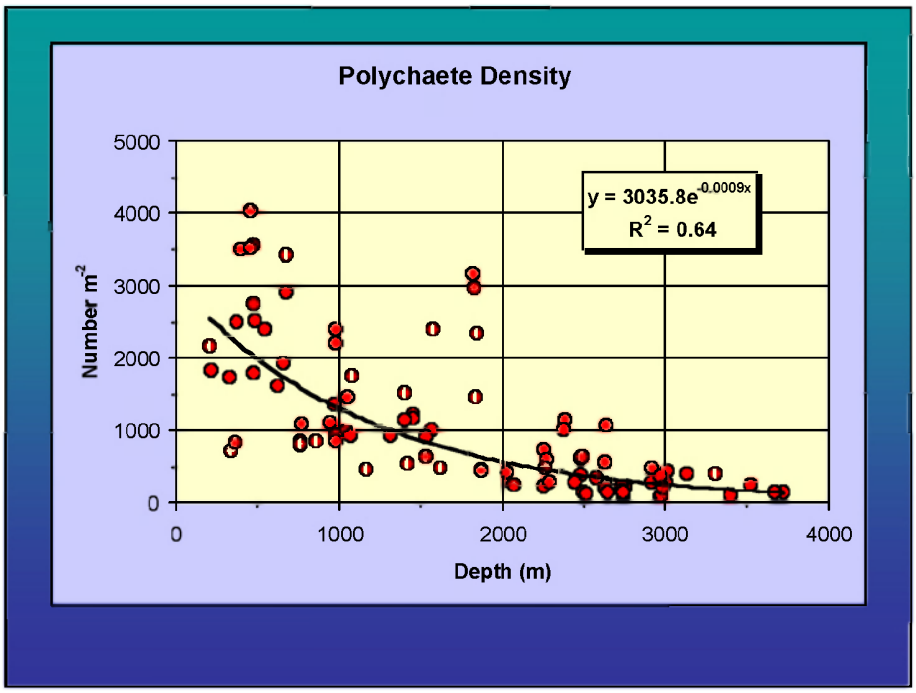

Figure 8-124. Abundance of polychaete annelid worms in the northern GoM.

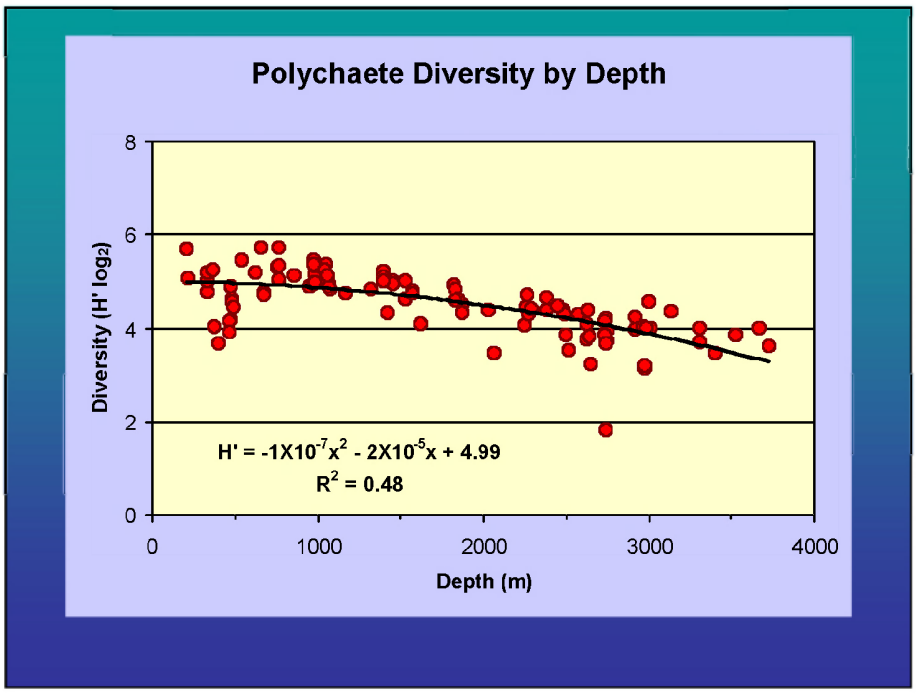

Figure 8-125. Diversity (H(s')) of polychaetes as a function of depth.

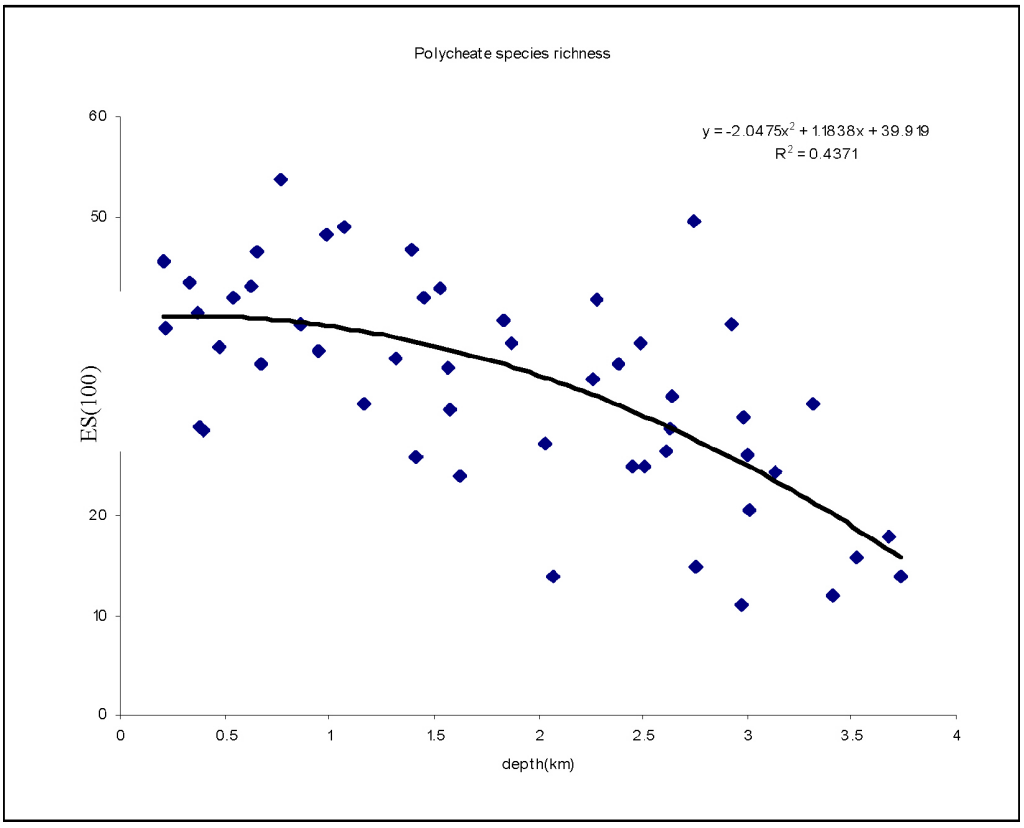

Figure 8-126. ES(50) of polychaetes as a function of depth. Note that the pattern is the same as in 8.125, but spread out.

The maximum diversity (H(s')) was found on the upper slope, at a depth of about 750 meters. Low values were encountered at 500 m depth in the central trough (MT1) due to a dominance of a few species. Evenness was high, but tended to increase gradually from shallow to deep water. The maximum 'evenness' possible (one) was approached in the deepest sites primarily because almost all individuals encountered were different species. Low values were observed in the Mississippi Trough at the 500 m site (MT1) due to dominance by a few species.

8.8.4.3.3 Bathymetric Zonation of Recurrent Groups of Polychaetes

Nine groups of species were defined on the basis of percent similarity of species composition (Figure 8-127, based on the dendrogram in Figure 8-128). In general the groups were confined to specific depth ranges, or to particular physiographic features within depth ranges, but with frequent exceptions to this generalization. The groups were 1) an abyssal plain group, 2) a central Mississippi Cone group, 3) a Mississippi Trough upper slope group, 4) a mid-slope group, 5) a lower slope group, and 6) a combination of upper slope and central groups that occur intermittently from east to west in seemingly no predictable manner.

The diversity declines monotonically as well (Figures 8-129 and 8-130), which makes it rather unusual compared to the other groups, in which parabolas exhibited maxima at 1,200 to 1,600 meters depth.

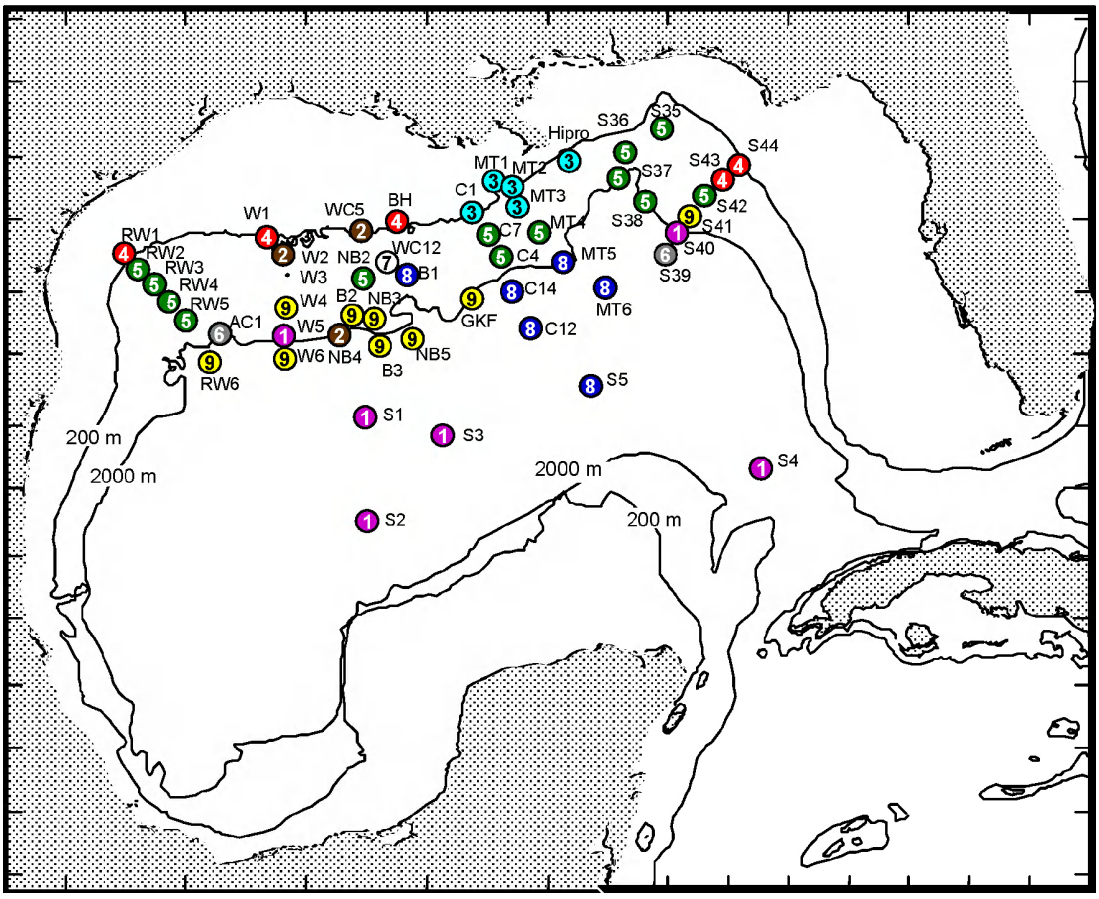

Figure 8-127. Map of nine recurrent groups based on percent similarity (polycheate).

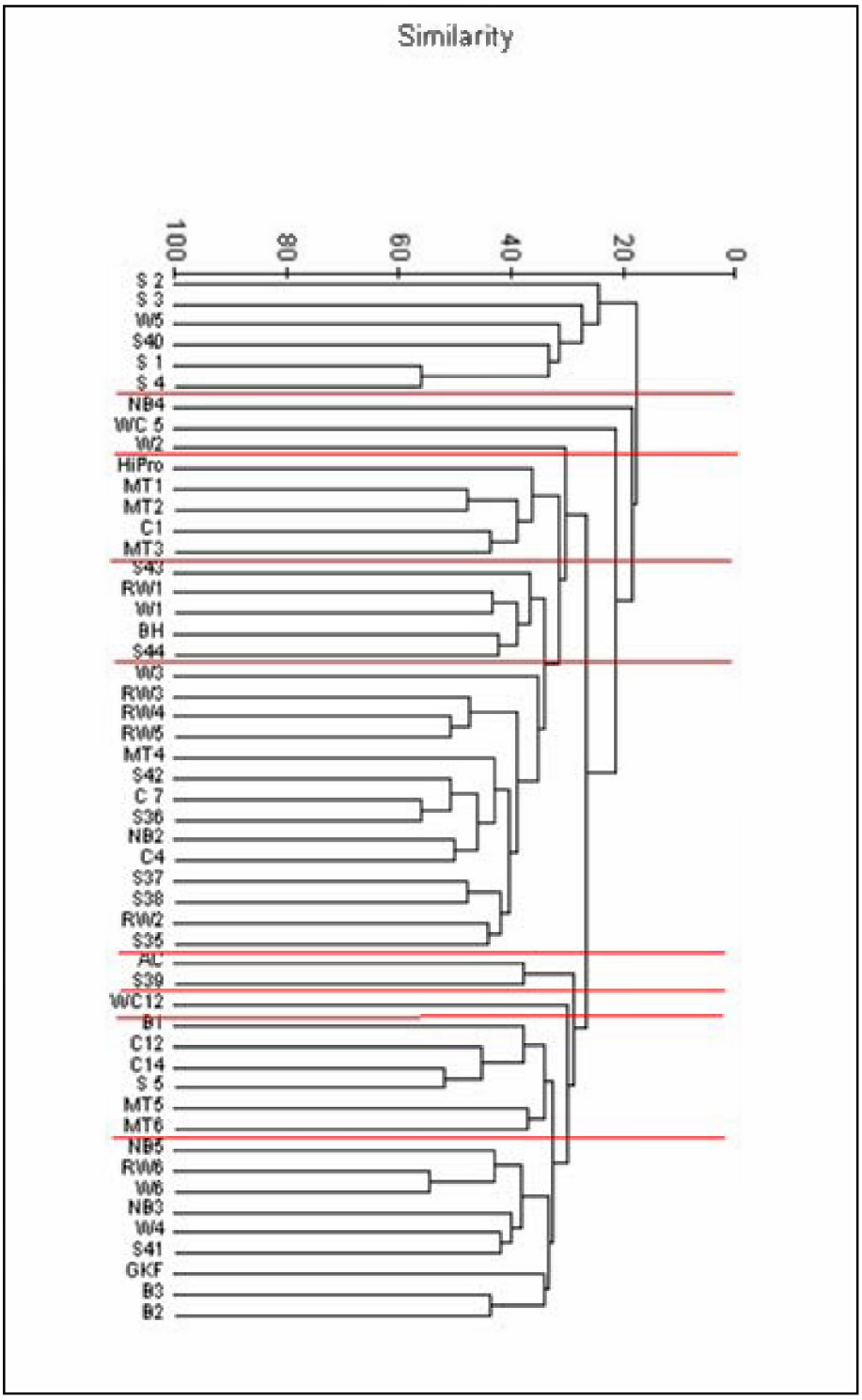

Figure 8-128. Dendrogram of percent similarities of polychaetes in the northern Gulf of Mexico. Nine groups are delimited at >20%.

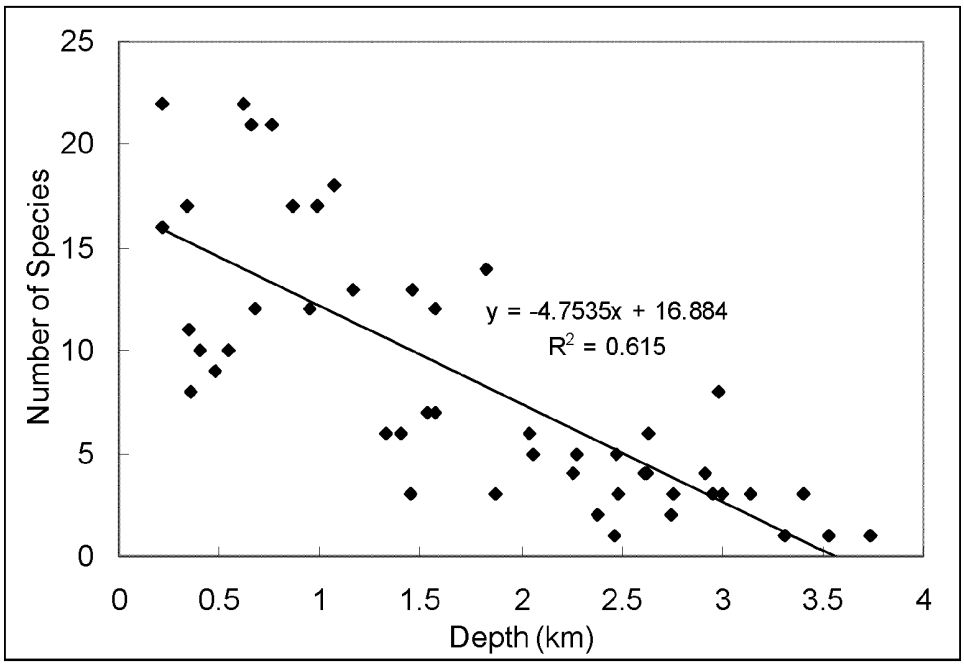

Figure 8-129. Species richness (γ diversity) of amphipods.

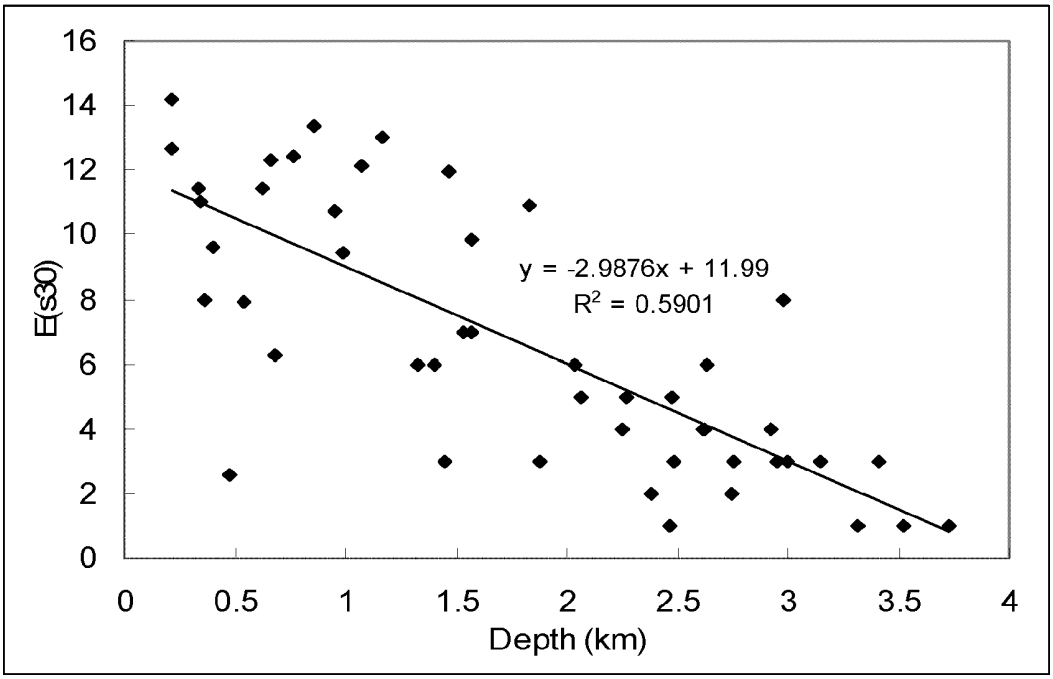

Figure 8-130. Species diversity [ES(30)] of amphipods.

8.8.4.4 Amphipod Crustaceans (John Foster, MSU, and Yousra Soliman, TAMU)

The amphipods fell into about 8 groups, based on % similarity of species in common between sites (Figure 8-131). However, only 3 (Zones 4, 5 and 6) of the groups spanned more than just a few locations. Four sites failed to be aligned with any group and oddly these outliers included both the shallow site dominated by the amphipod *Ampelisca* sp. nov. at MT1 with as many as 20,000 individuals per square meter and the deepest most southerly site, S2, with very few individuals and species. There was less coherence with depth among the amphipods than with the other groups analyzed above. For example, the amphipods at abyssal sites were in different groups whereas the previous taxa all had a distinct abyssal zone. Although 1 and 2 were always found in shallow water, Zones 3 and 6 spanned great depths. Zone 5 was isolated to the western transects at mid-slope depths. Zone 4 was just upslope and 6 was downslope from 5, but both extended over the complete east to west range of the sampling (Figure 8-132).

A multidimensional scaling analysis has been added for the amphipods to uncover why they were not as coherently grouped as the other taxa (Figure 8-133). The large groups (4 and 6) hang together fairly well, but with unpredictable outliers, e.g., MT6 and NB 3. The independent sites all lie outside the inner group. Nonetheless, this gives us little additional insight into why the relationship to depth is substantially less with the amphipods than the other groups. This pattern is more similar to the meiofaunal harpacticoid copepods than the other macrofauna.

8.8.4.5 "Total" Macrofauna Community Structure (Chihlin Wei and G. Rowe, TAMU and TAMUG)

The above groups were analyzed individually because they are numerically the most important macrofauna and are traditionally dealt with individually. As a summary of the macrofauna community structure, a total of 973 species have been analyzed together to determine overall biodiversity gradients and bathymetric zonation. In addition to the above groups, the cumacean crustaceans, the gastropod mollusks, the scaphopod mollusks, and spiney mollusks were included in the analyses. It does not include the nematode worms or harpacticoid copepods normally considered with the meiofauna component, even though they were large enough to be sampled with the macrofauna sieve (>300 microns).

The macrofauna displayed more or less the same patterns exhibited by the individual groups, as might be expected. Five recurrent groups could be identified (Figures 8-134, 8-135, 8-136), based on rates of change in composition as a function of depth and percent similarity > 20% between sites and groups of sites. The analysis in the 2nd figure of this section was attempted with the individual groups but is somewhat similar to that utilized by Menzies et al. (1973), which Pequegnat et al. (1990) used on the megafauna of the GoM. This analysis considers the number of species added and lost across the bathymetric gradient. The depths at which the greatest change occurs is defined as a boundary between bathymetric zones of groups of animals in which the change in composition is less, e.g., it is homogeneous. This approach can now be compared with the analysis of a site-by-site comparison of the relatedness of the fauna based on how similar each site is to another in species. This is more useful than the prior analysis because it does not presume a priori that depth is the controlling variable. In general the two approaches agree. Zones of related groups aligned themselves into 4 groups with depth but with a boundary between 2E and 2W bisecting the middle of the upper slope region. The 3th area dipped down into the abyssal plain (4), thus cutting group 4 into two areas. In terms of the hypotheses, one can thus say that the east and the west GoM are similar, with the exception of the boundary between 2E and 2W.

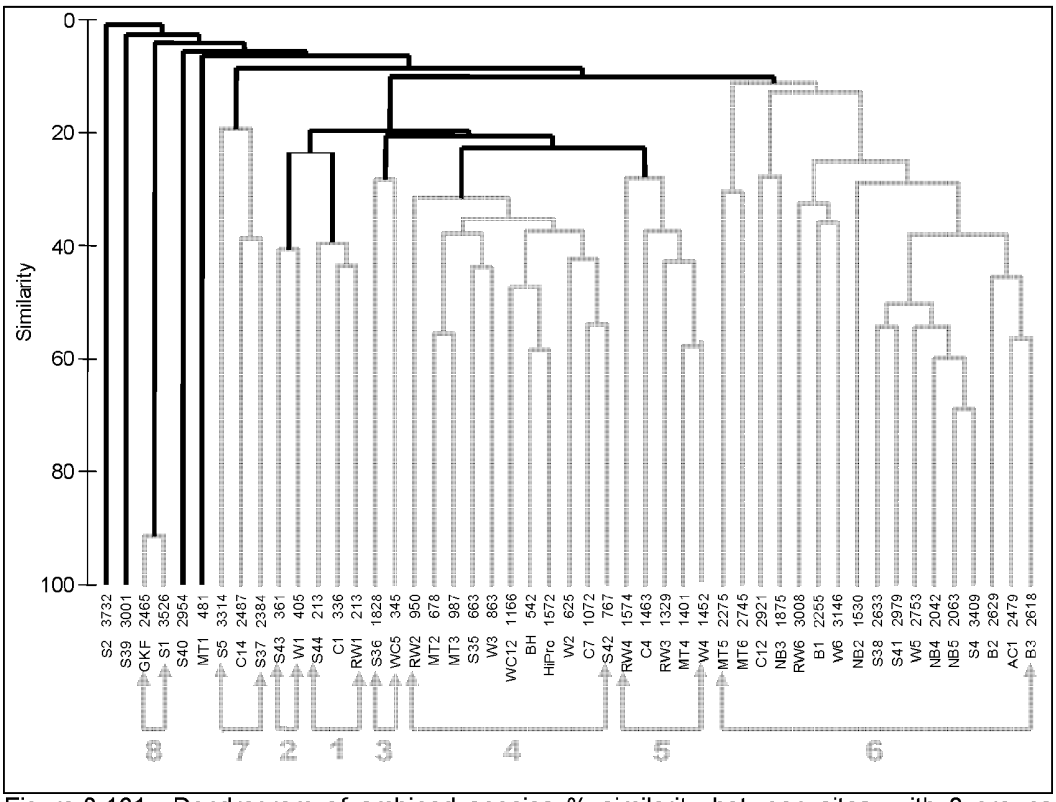

Figure 8-131. Dendrogram of amhipod species % similarity between sites, with 8 groups identified at greater than 20% similarity.

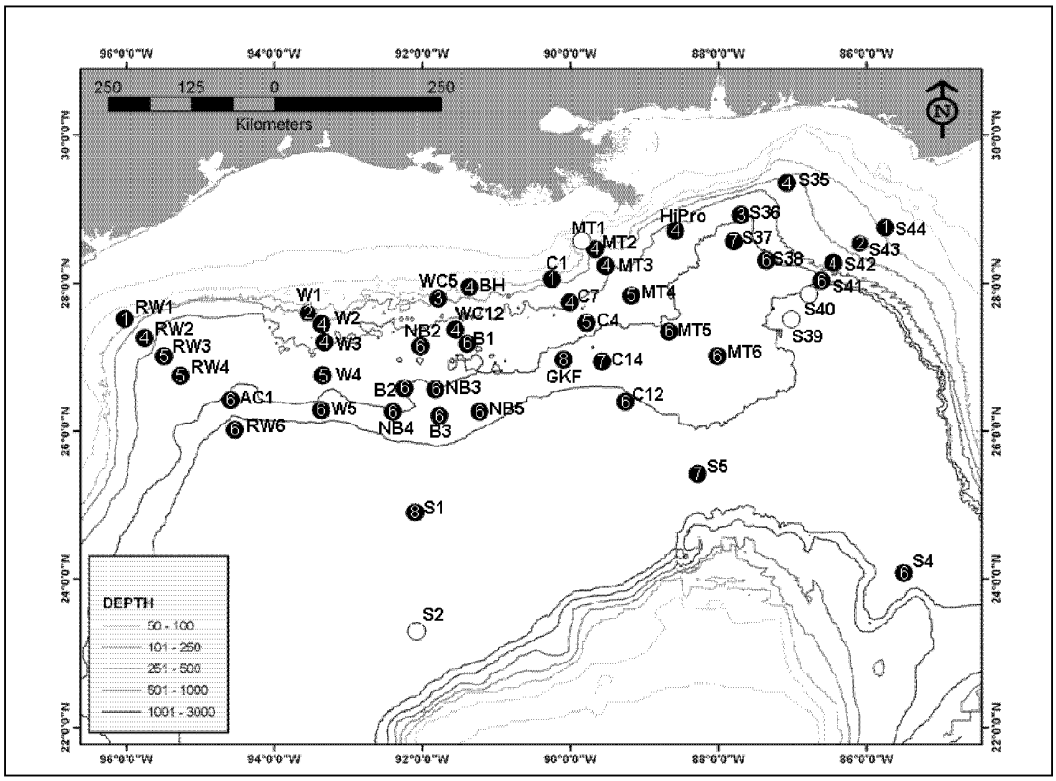

Figure 8-132. Bathymetric zonation of amphipods, based on the dendrogram in the previous Figure.

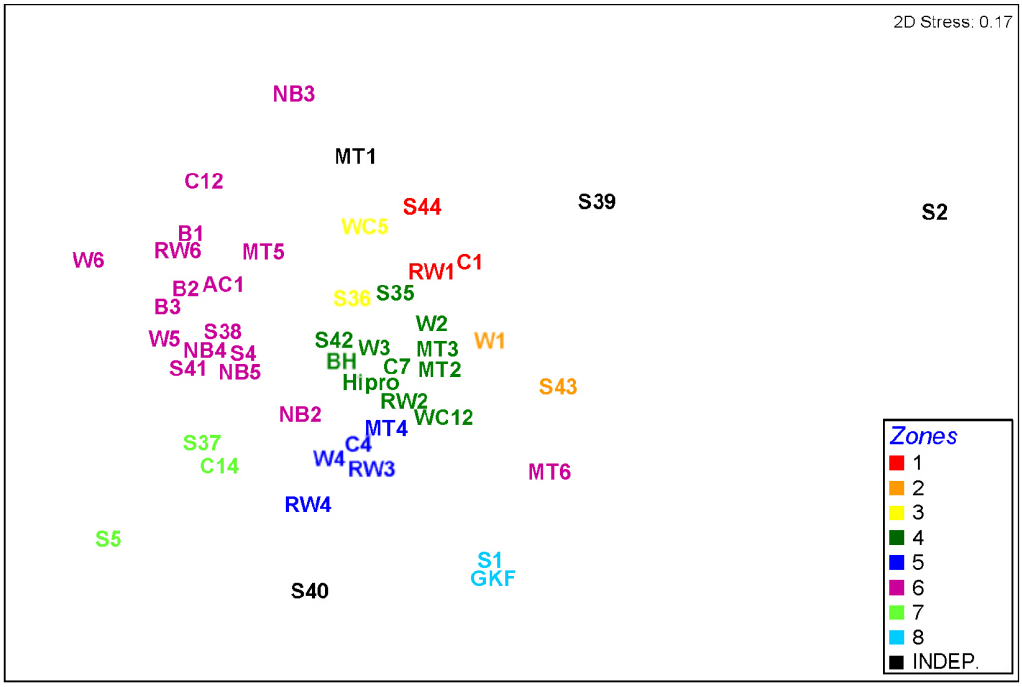

Figure 8-133. Multidimensional scaling analysis of zones of amphipods based on Bray Curtis % similarities between sites.

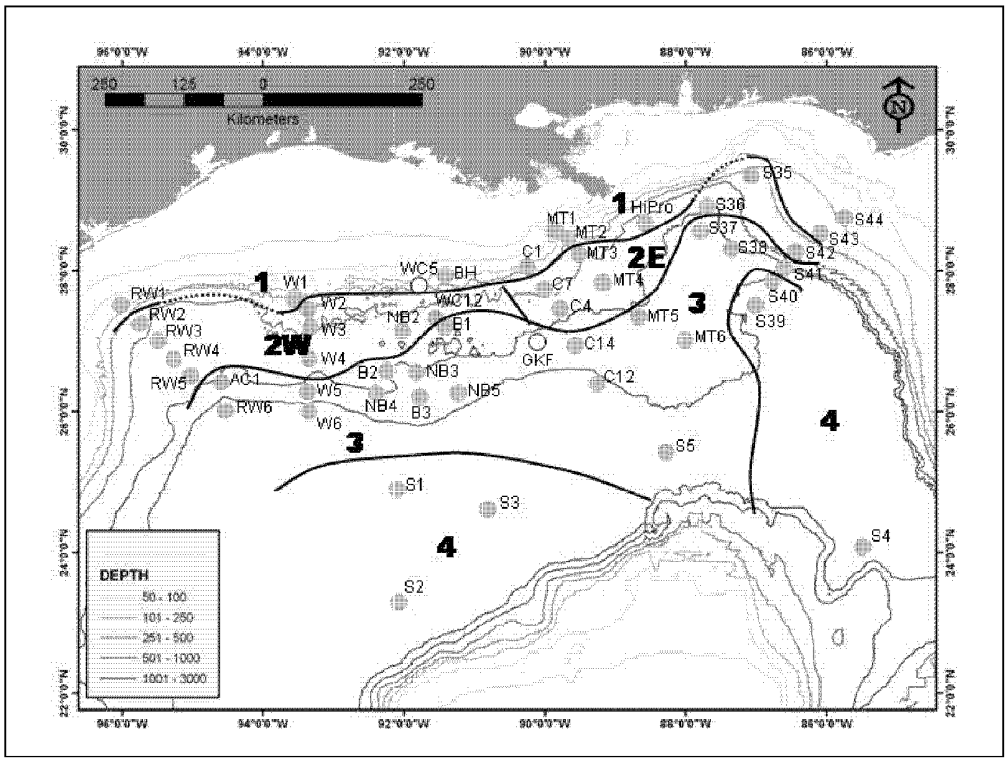

Figure 8-134. Macrofauna zonation based on 973 species. Groups determined as equal to or greater than 20% similar.

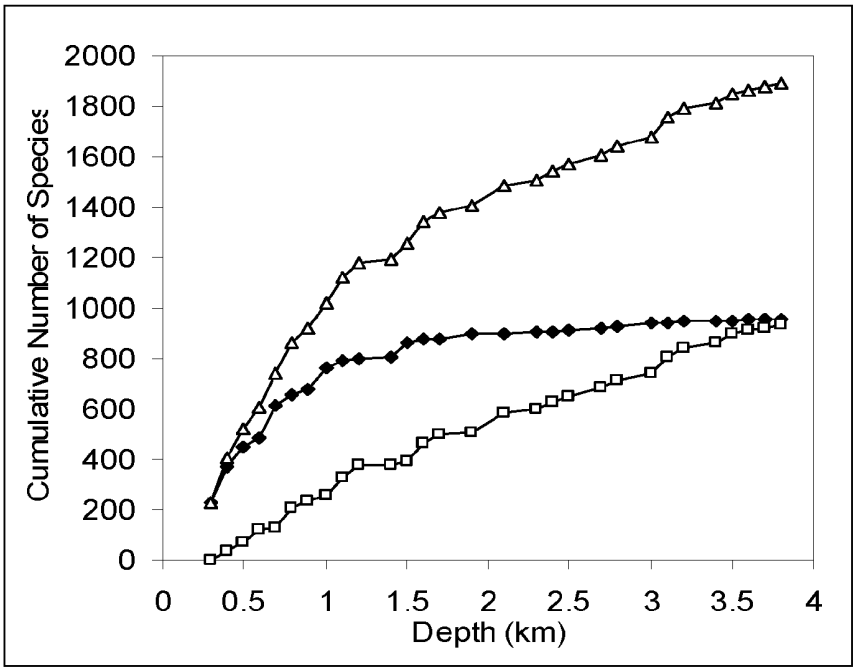

Figure 8-135. The cumulative number of species renewal (empty triangle), appearance (solid rectangular), and disappearance (empty square) plotted against depth.

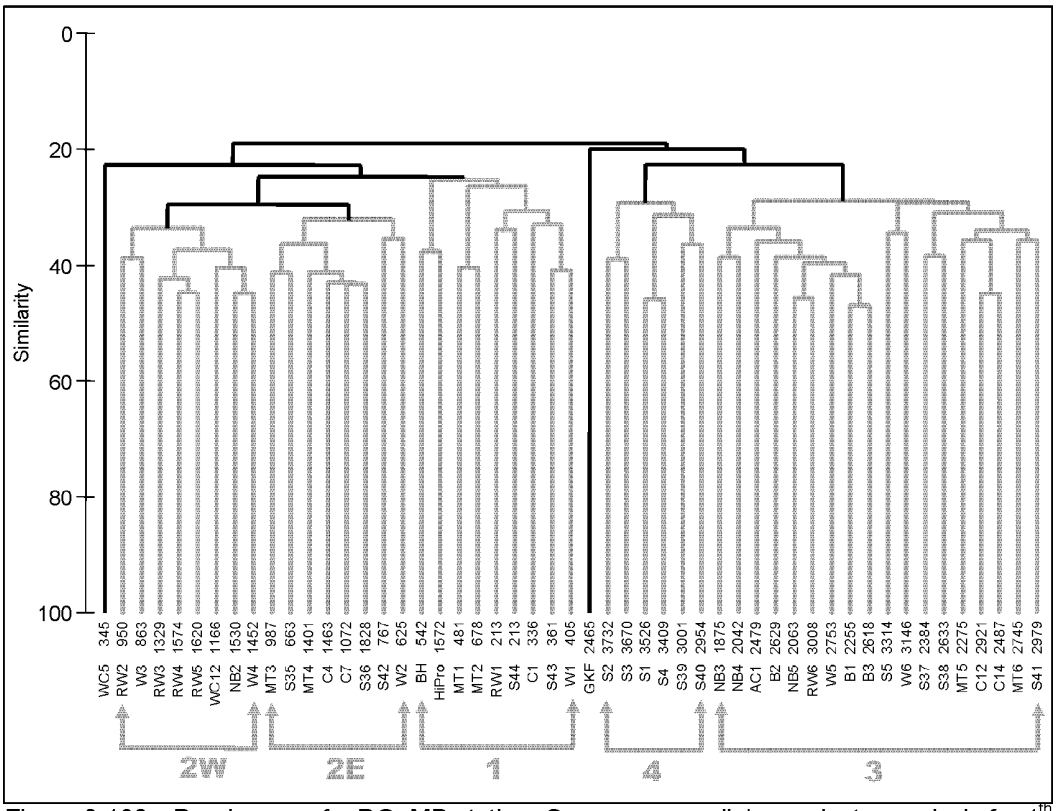

Figure 8-136. Dendrogram for DGoMB station. Group average-linkage cluster analysis for 4th root transformed species abundance data based on Bray-Curtis similarity coefficient. X axis is depth (m) followed by station names. Y axis is Bray-Curtis similarity (%). The solid line indicates significant evidence of structure (SIMPROF test, P<0.05, available on PRIMER v6). Dotted line indicates no evidence of structure (SIMPROF test, P>0.05). Five distinct zones and two independent stations (WC5, GKF) were identified by SIMPROF.

Diversity too reflects the patterns in the individual groups (Figure 8-135 and 8-137). The maximum was located on the upper continental slope (Figure 8-137). Lowest values were encountered at the head of the Mississippi Canyon in all groups. Diversity then declined slowly out to the abyssal plain. This pattern replicates that in all the four individual groups considered individually.

The mean size of macrofauna declined with depth (Figure 8-138), as had been suggested by earlier workers for the GoM macrofauna. The variance appears to decline as mean size declines.

In summary, one could suggest that four parameters of macrofauna community structure are all, in some way, a function of depth:

1) animal density declines sharply,
2) diversity follows a parabolic relationship, with a maximum on the upper slope,
3) species are added and replaced at an uneven rate such that they are grouped into distinct zones, and

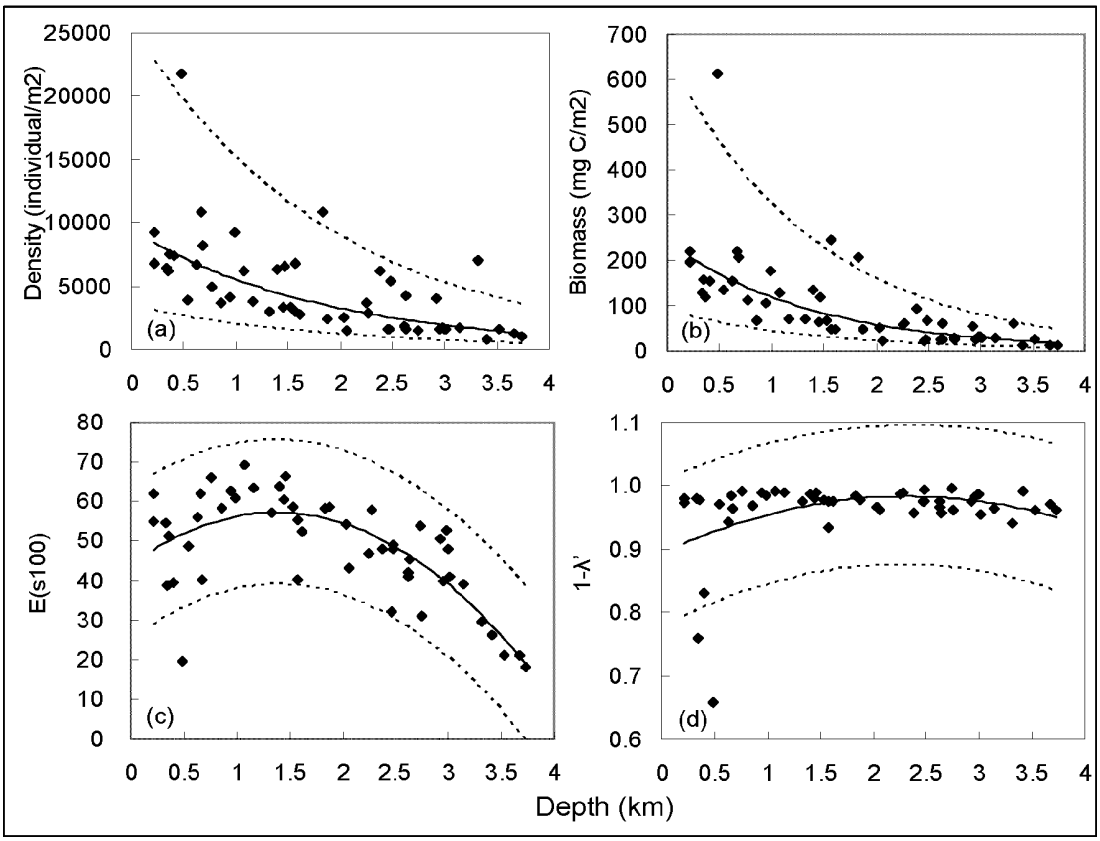

Figure 8-137. Mean density, biomass, and ES(100), and 1-λ' as a function of depth.

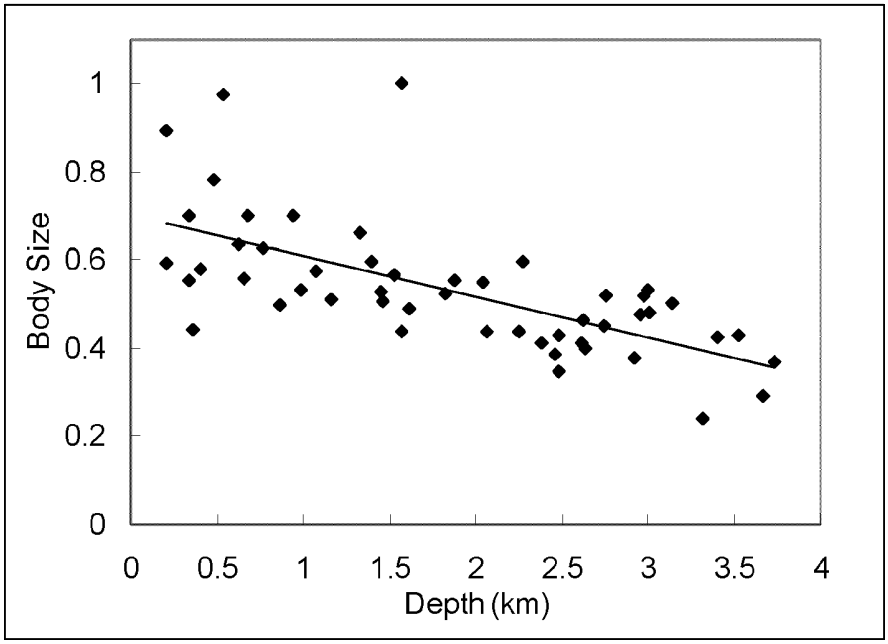

Figure 8-138. The standardized ratio of mean biomass to density as a function of depth.

4) the mean animal size declines.

The central area in close proximity to the Mississippi River had highest densities, whereas the far western transect had the lowest densities, at any given depth. The central axis of DeSoto Canyon also had high densities. The highest densities were located at the Mississippi Canyon head and these also had the lowest diversity values. In the DeSoto canyon, however, the high densities were accompanied by high rather than low diversity.

8.8.5 Benthic Megafaunal Invertebrates

A total of at least 185 species of megafaunal invertebrates (over 10 mm in greatest dimension, or attached to objects over 10 mm in size) were collected by trawl or trap during the DGoMB study in 2000-2002. The amphipod *Eurythenes gryllus* was taken only in traps. Species richness was greatest in the DeSoto Canyon at station S35, with 38 species. Other stations with more than 30 species were C4, MT5, S38 and S41, all in the eastern half of the basin. Stations on the Sigsbee Abyssal Plain (S1-5 and JSSD stations) had 20 or fewer species, as did stations of the Mississippi Trough (MT1, MT2, MT3 and MT4).

Species diversity calculated by the Shannon-Wiener Index (H) was highest at station MT6 (H=5.754). Station MT5 also had high diversity (H=4.425). Lowest diversity was at stations of the upper slope (MT1, S42, S43 and S44), basins (B1, B2 and B3) and dominated by small sponges (NB4 and S37). Most other stations, regardless of depth or geographic location, had diversity values between 3 and 4.

Biomass was highest at stations of the DeSoto Canyon (S35, S37, S38 and S41) and station MT3. Much of the biomass was due to wet weight of holothuroids. All samples with biomass greater than 6 kg were in the DeSoto Canyon or Mississippi Trough. The greatest number of individuals in any sample was taken was at S37, with 1,612 individuals, most of them small sponges. Stations MT1, MT5, MT6, NB5 and S38 had more than 300 individuals per station.

Many species of echinoderms, sea anemones and crustaceans were widespread in geographic distribution. The holothuroid *Molpadia blakei* was taken at the basin and central transects, but not in the canyons. The crab *Trichopeltarion nobile* and the mussel *Amygdalum politum* were more common in canyons than at other stations. Crustaceans were more diverse and abundant in the DeSoto Canyon than in the Mississippi Trough.

The most common group of invertebrates was the Crustacea, with 58 species. Three of these were collected and identified for the first time in the Gulf of Mexico. Thirty-three species of echinoderms were collected. Of these, an unidentified holothuroid, probably *Benthodytes* sp., was the most abundant and contributed significantly to the biomass of stations of the lower slope. An undescribed species of sea anemone living on shells of hermit crabs was collected.

In situ photographs, sediment samples and observations of newly-caught animals show that many species live on or buried in mud. Feeding types varied according to taxonomic group. The starfish *Dytaster insignis* was found to feed on fallen *Sargassum*. Small barnacles, zooanthids, and crabs were encountered associated with larger crustaceans, sponges and gorgonians. Parasitic crustaceans infected galatheid crabs.

8.8.5.1 Comparison of Catches by Type of Gear

There were no obvious differences between the faunal composition taken in beam trawls versus otter trawls. At the abyssal plain stations in the central Gulf of Mexico, no species was

taken both in trawls and traps, although *Munidopsis bermudezi*, taken in a trap at JSSD 3, was also trawled at S41 and S42.

Trawl net mesh size affected the catch. At the JSSD sites, small mollusks (families Nuculanidae, Cuspidariidae, etc.) were taken. These were not caught in previous trawls. The brachiopod *Chlidonophora incerta* was taken by trawl only once in 2000-2001, but was found in all JSSD stations. The epibenthic sled captured mostly small (less than 1 cm) invertebrates, mostly demersal or midwater species rather than benthic species. Isopods, amphipods, ostracods and other small crustaceans found in the sled samples were not collected in the trawls.

There were no apparent differences in the fauna taken by beam trawl at RW2 and RW1 with that collected elsewhere with an otter trawl. The lack of specimens in stations such as B2 on 12 May 2000 and RW2 may be due to problems in trawl operation. Both contained midwater species, suggesting that the net was off the bottom for at least part of its supposed bottom time. Station C7 was a failure because the trawl "fished water"—it was off the bottom for the entire tow. The scanty catch at other stations of the western transects may have been due to similar problems.

8.8.5.2 Species Richness, α Diversity, Biomass and Abundance

The greatest species richness at any station was at S35, with 38 species. Other stations with more than 30 species were C4, MT5, S38 and S41. Of the deep stations of the southern Gulf, JSSD5 had the greatest species richness, with 20 species. The least species richness (less than 10 species) was at stations B2 on 12 May 2000, C14, MT1 in 2001, RW2 and S42 in 2001. Stations MT2, 3 and 4 as well as JSSD 1, 2, 3, and 4 had less than 20 species per station. There were no apparent patterns of species richness in the other stations, which had between 10 and 20 species.

The location with the highest species diversity was MT6 (H=5.754). Most stations, regardless of depth or location, had an index between 3 and 4. Stations RW2 and B2 12 May 2000 had low indices, but this may have been a result of the trawl being off the bottom for part of the tow. The shallowest stations of the upper slope (MT1, S42, S43, S44) were less diverse than those at greater depths. Of stations taken on the middle slopes (1,000-2,500 m), the basin stations (B1, B2 and B3) had lower diversity on average than other stations at comparable depths. The diversity indices of non-basin stations (NB) were higher than those of the basin stations, except for NB4, where the fauna was dominated by small sponges. Station S37, which also had a low diversity index (H=1.256), was also dominated by numerous individuals of a small sponge, as well as two species of echinoderm. The highest mid-slope diversity was at MT5 (H=4.4). On the lower slope (2,500 m and deeper to the abyssal plains), all stations except MT6 had a diversity index between 3 and 4.

Five stations had wet weight samples weighing greater than 10 kg: MT3, S35, S37, S38 and S41. Much of this biomass was due to holothuroids, but not always the same species. At station S41, sea anemones contributed 5.3 kg; at MT3, 3.3 kg was due to six large crabs. Stations S36 and S42 also had biomass over 10 kg if one included a single large squid, *Pholidoteuthis adami* (Figure 8-139). Each squid weighed approximately 10 kg.

Figure 8-139. June 10, 2000. Dr. Mary Wicksten with the large squid, *Pholidoteuthis adami*, caught from the trawl at S42.

There were 13 stations with a sample weight exceeding 6 kg. Four were in the Mississippi Trough: MT1, MT3, MT5 and MT6. Five were located in or near the DeSoto Canyon: S35, S37, S38, S40 and S41. The other stations were B3, C4 and C12. Of the deep abyssal plain sites of the southern Gulf, the greatest sample mass was at station JSSD5, with 0.82 kg.

It was difficult to count the number of individuals at some sites because many sponges and sea cucumbers were broken or smashed. The greatest number of individuals was at station S37, with 1612 individuals. Of these, approximately 600 were small sponges (family Ancorinidae) and 650 were the large orange brittle star *Ophiocrates heros*. Stations MT1, MT5, MT6, NB5 and S38 had more than 300 individuals per station. Station JSSD5 had the most specimens, 414, of the southern stations. Of these, 207 were the white brittle star *Ophiosphalma planum*. It should be noted that JSSD5 was located in the central GoM offshore of the MT transect down the Mississippi Trough. The most northerly of the abyssal plain sites investigated in June and August, 2002, JSSD5 (=S5) had high abundances in all size categories of benthos compared to the other abyssal sites.

8.8.5.3 Comparisons by Transects

The fauna with the greatest species richness was taken in the two canyon transects, the Mississippi Trough stations (MT) and the DeSoto Canyon stations (S). In both, the crab *Trichopeltarion nobile* and the mussel *Amygdalum politum* were taken in quantity. However, various sea anemones, mussels and the flatback lobster *Stereomastis sculpta* were more abundant in the Mississippi Canyon. In the DeSoto Canyon, the burrowing shrimp *Glyphocrangon aculeata* and *G. alispina* were more abundant, as was the crustacean fauna in general.

Of the various transects, the RW and W stations had the least species and biomass. Sampling problems may have affected the results. The NB stations were dominated by echinoderms and small sponges. The B stations had a fauna characteristic of their depth, dominated by echinoderms. The C stations were intermediate in biomass and diversity. There were no obvious differences between eastern and western transects except for the holothuroid *Molpadia blakei*, taken at the B, C and NB transects but not farther east.

Throughout the study area, echinoderms were abundant and widespread, especially elasipodids and other holothuroids, and not apparently restricted to any single or set of transects. These occurred at depths of 2,000 m or more at almost all stations. Other widespread groups included the ophiuroids *Bathypectinura heros* and *Ophiopsalthma planum*, the barnacle *Arcoscalpellum antillarum*, the shrimp *Nematocarcinus rotundus* and *Glyphocrangon longirostris* and the flatback lobster *Stereomastis sculpta*.

8.8.5.4 Comparisons by Taxonomic Groups

The most speciose group in the megafauna was the Crustacea, with 58 species. Of these, nine were barnacles, two were isopods and the rest were decapods. The most speciose station for crustaceans was S42, with 17 species. Station S35 had the most individuals, 186, but of these, 82 were the large barnacles *Arcoscalpellum regina*, attached in clumps. The other 104 belonged to 12 other species. Other stations with more than 10 decapod species were C4, MT5, S36, S41, S42 and W1. Common and widespread species included *Benthesicymus bartletti*, *Glyphocrangon aculeata*, *Nematocarcinus rotundus*, *Penaeopsis serrata*, *Plesiopenaeus armatus* (Figure 8-140) and *Stereomastis sculpta*. The largest crustaceans were the golden crab *Chaceon fenneri* (80 g, MT5) and giant isopod *Bathynomus giganteus* (Figure 8-141, about 250 g, @ S42). *Sabinea*

Figure 8-140. June 13, 2000. Deep-sea shrimp, *Plesiopenaeus armatus*, collected from the trawl at S37.

Figure 8-141. June 10, 2000. Giant isopod, *Bathynomus giganteus*, collected with other trawl samples at S42.

hystrix (@ MT4), *Benthesicymus carinatus* (@ B2, 19 June 2000) and *Neoscalpellum debile* (@ S38 and S41) represent the first reports of these species in the Gulf of Mexico.

The next most speciose group was the Echinodermata, with approximately 33 species. By far the most abundant group was the Elasipodida, soft-bodied deep-sea holothuroids (sea cucumbers). "Elasipodid A" (Figure 8-142, Figure 8-143) contributed 14.0 kg to the biomass of station S37 alone. Other locations with over 1 kg of this species were B3, C12, MT5, MT6, S38, S40 and S41. These are all on the lower slope, at 2,000 m or deeper, and none was in the western half of the GoM basin. The species designation may involve more than one species. Often, elasipodids arrive at the surface smashed or entangled in nets. Distinctive features are lost during capture, or do not remain intact if the specimen is preserved in formalin. The majority of the specimens may be *Benthodytes lingua*, but specimens of *Psychropotes* sp. or other species of *Benthodytes* might be included. The large whitesea cucumber *Mesothuria lactea* was also abundant, especially at station MT3. Twenty-seven specimens of this species taken at MT3 had an estimated displacement of 13.0 kg.

Brittle stars (Ophiuroidea) were common inhabitants of the continental slope. Many small individuals remain unidentified. The two most abundant species were *Ophiocrates heros*, especially at S37, and *Ophiosphalma planum* at JSSD5. (In previous reports, *O. planum* was called *Ophiomusium planum*). The most common sea stars (Asteroidea) were *Dytaster insignis*, *Nymphaster arenatus* and *Litonotaster intermedius*. A few heart urchins (Echinoidea) (order Spatangoida, *Brissopsis* sp. and others) were taken, as well as the leathery sea urchin *Phormosoma placenta*. No crinoids were encountered.

Approximately 40 species of mollusks were collected. No more than six live species of mollusks was taken at any station, in the megafaunal fraction. Those with five or six species were C1, MT1, JSSD5, and S40. Empty shells were common, as were shells occupied by hermit crabs. These are not included in counts of individuals or biomass. The greatest displacement volume, estimated at 10 kg, was of a scaled squid, *Pholidoteuthis adami*, at station S36 and S42. The greatest biomass for a group of mollusks was 1.6 kg of the nesting mussel, *Amygdalum politum*, at MT1. At MT6, the *scaphopod Antalis occidentalis* contributed 90 g. of biomass. The most abundant mollusk per station was *Amygdalum politum*. There were 138 mussels at MT1, where they also dominated the biomass for mollusks. *Amygdalum politum* also was taken at MT2, MT4, and W1. Although many gastropods were collected, they were scattered in occurrence. Chitons (class Polyplacophora) were taken only at W3. Cephalopods included octopuses, squid, and fragments of the shells of *Argonauta* sp. Finned octopuses, family Stauroteuthidae, were taken at stations S35, MT2 and W6-RW6. Approximately 17 species of cnidarians were collected. Some of these were very small members of the order Zoanthidea, which cannot be identified to species. Others were very small sea anemones that could not be removed from the rocks to which they were attached. Of the identifiable species, the sea anemones were most abundant in terms of numbers and size. At MT5, the most individuals, 93 of the large sea anemone *Chondrophellia coronata*, were collected. These sea anemones had a displacement volume equivalent in wet weight to 3.4 kg. At station S41, four individuals of an unidentified sea anemone of the family Hormathiidae (Hormathiid "A") had a displacement volume equal to 5.3 kg.

Sea anemones tended to be the most common cnidarians. Specimens from at least one species, the "cloak anemone" covering the shells of hermit crabs is an undescribed species (D. Fautin, University of Kansas, pers. comm.) No more than five species of cnidarians was taken

Figure 8-142. June 15, 2000. Deep-sea holothuroid, Elasipodid A, collected from the trawl at S38.

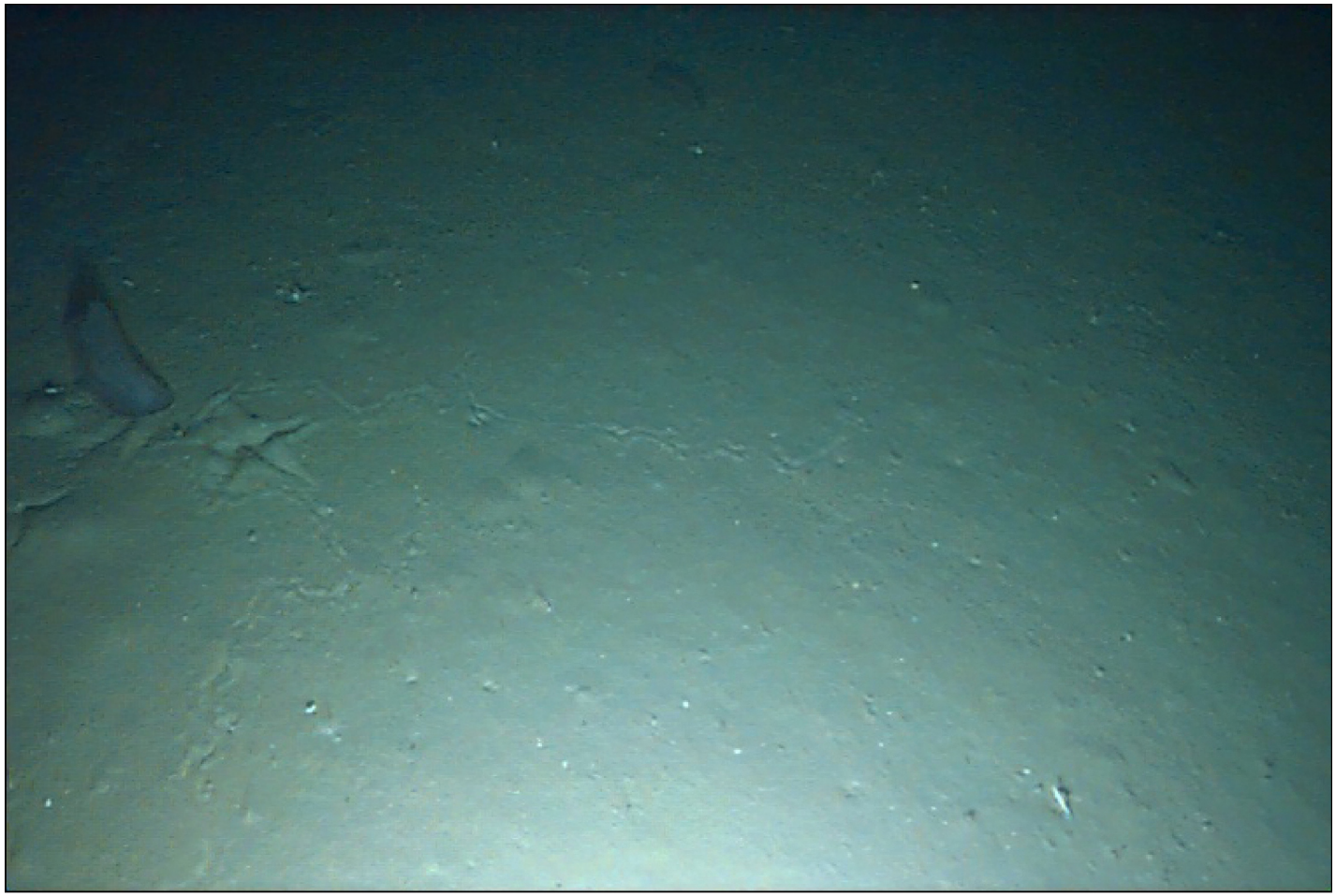

Figure 8-143. June 5, 2000. Deep-sea holothuroid, Elasipodid A present on the sea floor of Mississippi trough (MT6). Image was taken during the first cruise.

per station. Species-rich stations included C4, C12, MT5 and S42. Station C12 had the most individual cnidarians, 110, of which the majority were sea pens (Figure 8-144, *Umbellula* sp. and an unidentified pennatulacean). There were 67 cnidarians at station B1, 61 of them a small unidentified sea anemone. Most of the cnidarians seem to be widespread species in the Gulf of Mexico. One specimen of the flytrap anemone, *Actinoscyphia* sp., was collected at station B2, 19 June 2000. Flytrap anemones (Figure 8-145) have been photographed (but not collected) previously in the Gulf of Mexico (I. MacDonald, TAMU-Corpus Christi, pers. comm).

Eight species of sponges, at least, were collected. At present, the taxonomy of deep-sea sponges (classes Hexactinellida and Demospongiae) is in a state of confusion. By morphology alone, it is certain that at least five species were present. Five recognizable species were collected at S38, the most species-rich station for sponges. The greatest number of individuals, approximately 600, was collected at S37. Over 100 sponges also were taken at stations NB5 and JSSD5.

Vermiform (worm-shaped) animals appeared sporadically in trawls. Most were unidentified annelids of the class Polychaeta, including species of the family Onuphidae and Serpulidae. Of particular interest are the pogonophoran polychaetes taken at B2, 12 May 2000. These animals, once assigned to a separate phylum, now are included in the Annelida. They are noted for their association with chemosynthetic bacteria, located within the worm's body. Pogonophorans live near gas hydrate seeps. No such seep has been reported previously at or near B2. Station B2 was sampled again on 19 June 2000 in hopes of locating more pogonophorans, but none was taken.

The brachiopod *Chlidonophora incerta* was taken at S37 during 2000-2001. It was collected at all JSSD stations, at which the trawl was outfitted with a fine mesh at the cod end. A few ascidians were collected. All were attached to pieces of rock, wood or "clinkers" (coal residue from ships).

8.8.5.5 Diversity Gradients

Expected Species (E(s)) has been calculated for the composite megafauna (e.g., all groups combined together) based on 25, 50 and 100 individuals (Figure 8-146). There was little evidence for a depth gradient, although the highest values were located in the center of the distribution across the gradient. Low diversity was consistently encountered on the upper slope, including the head of the Mississippi Trough, but S42 on the upper Florida slope was particularly diverse. At the deep sites on the abyssal plain, the values were consistently low. The qualitative narratives above referred to gear type, taxa and transects with the highest species richness, and rarely were any sites in the western GoM mentioned. This may reflect a real difference between east and west or simply reflect a reduced sampling intensity in the west.

- Es25: N=19~1588, r^2=0.05, $F_{2,33}$=2.03, P= 0.15, $Y=11.88-2.76X+0.69X^2$
- E(s50): N= 25~1588, r^2= -0.06, $F_{2,32}$= 0.47, P= 0.95, $Y=13.65-0.51X+0.14X^2$
- E(s100): N=56~1588, r^2= -0.36, $F_{2,30}$= 0.44, P= 0.64, $Y= 15.77+1.87X-0.61\ X^2$

Figure 8-144. May 7, 2000.Sea pen, *Umbellula* sp., collected from the trawl at B1.

Figure 8-145. June 19, 2000. Flytrap anemones, *Actinoscyphia* sp., collected from the trawl at B2.

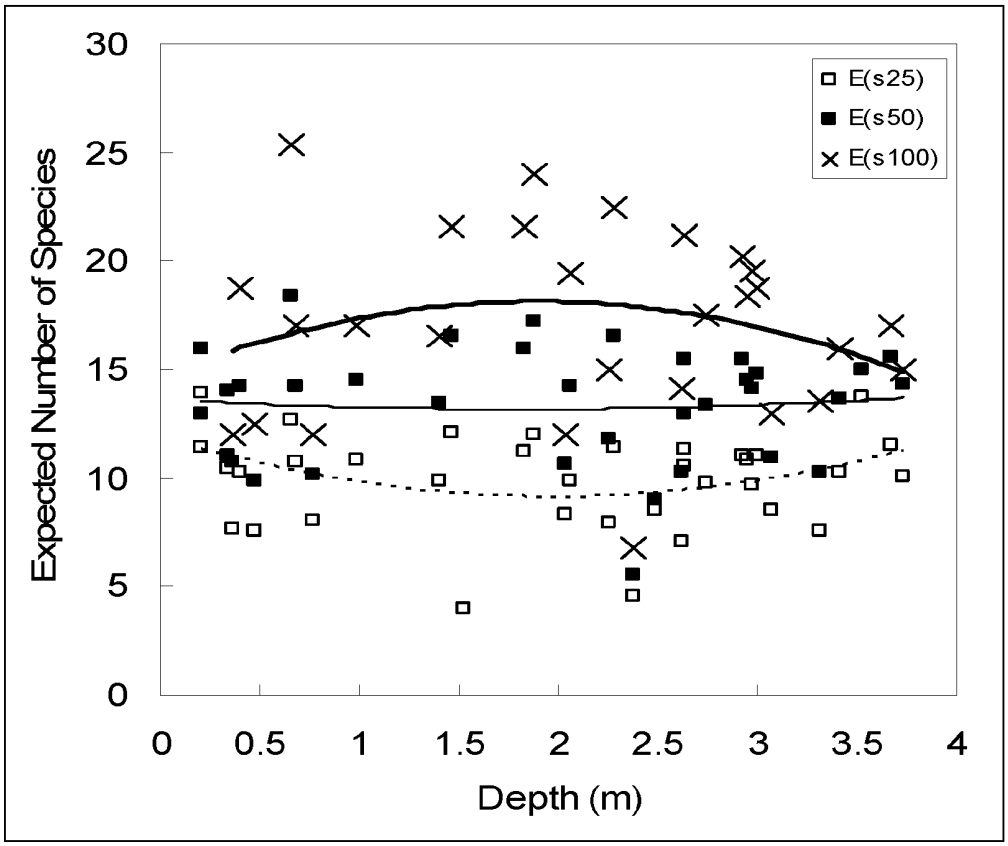

Figure 8-146. Comparison of diversity gradients (H(s)) at 100, 50 and 25 species of megafauna in the trawl samples at the sites sampled.

8.8.5.6 Zonation of the Megafaunal Invertebrates

The composite megafauna was subjected to a similarity analysis similar to that for the species lists of the meiofauna harpacticoid copepods (Section 8.8.3) and the composite macrofauna (Section 8.8.4). In this case, seven (7) different groups or bathymetric zones could be identified on the dendrogram (Figure 8-147) based on percent similarity in species between sites. A map of these zones reveals their affinities to specific areas of the GoM continental margin (Figure 8-148). Zone 1 on the upper slope was located at both the most extreme east and west sites, suggesting that little longitudinal difference existed at the shallow margins of the study. The abyssal plain had five sites also extending across the entire GoM that has so far been sampled. In this case, S5 in the central GoM retained its affinity to east and west, unlike the macrofauna which was penetrated at this central deep location by the next shallowest zone. Zone 7 was located at intermediate depths, both above and below the escarpments, as well as on the Mississippi Cone. Mapping the longitudinal extent of the zones along the middle slope was limited because of sparse sampling along the western transects, unfortunately. The canyons and the basins were not particularly unique in terms of their species composition. Zones 2, 3 and 6 occurred in both the Mississippi and DeSoto canyons, but they also occurred at a few locations at similar depths outside the canyon. Only Zones 6, 7 and 8 occurred at more than three sites, perhaps reflecting the poor sampling in the Western Gulf.

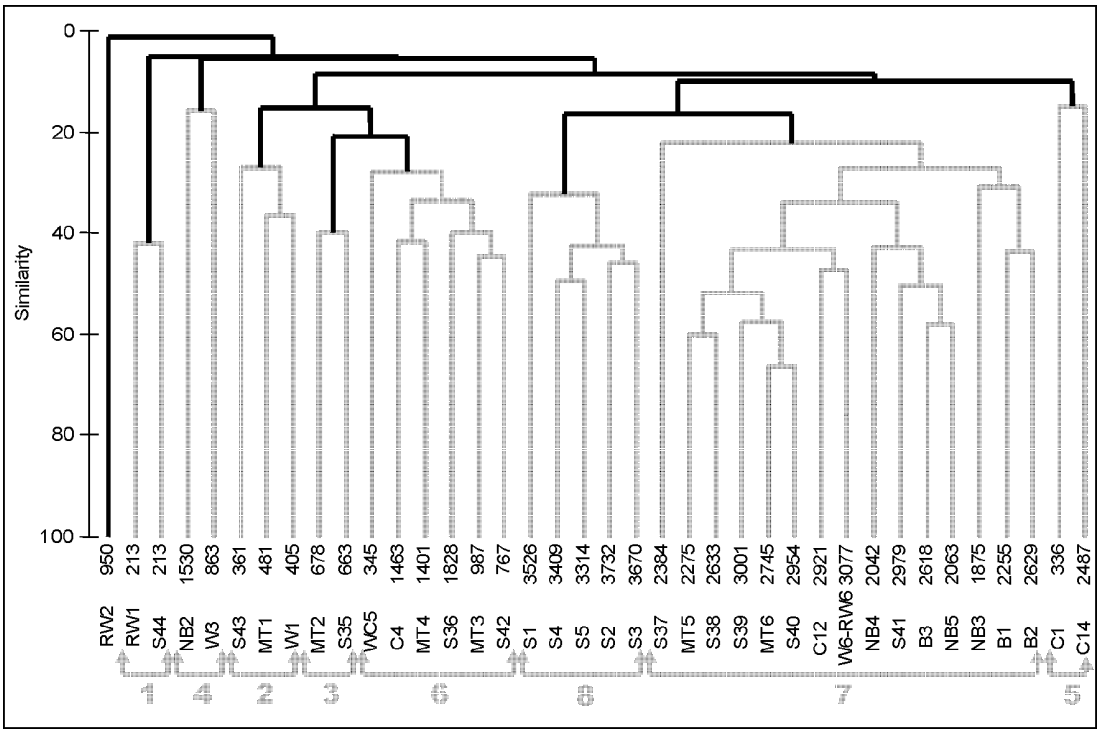

Figure 8-147. Dendrogram of megafaunal groups, based on Bray Curtis similarity of the 4th root transformed abundance of each species in the trawls samples at each site sampled.

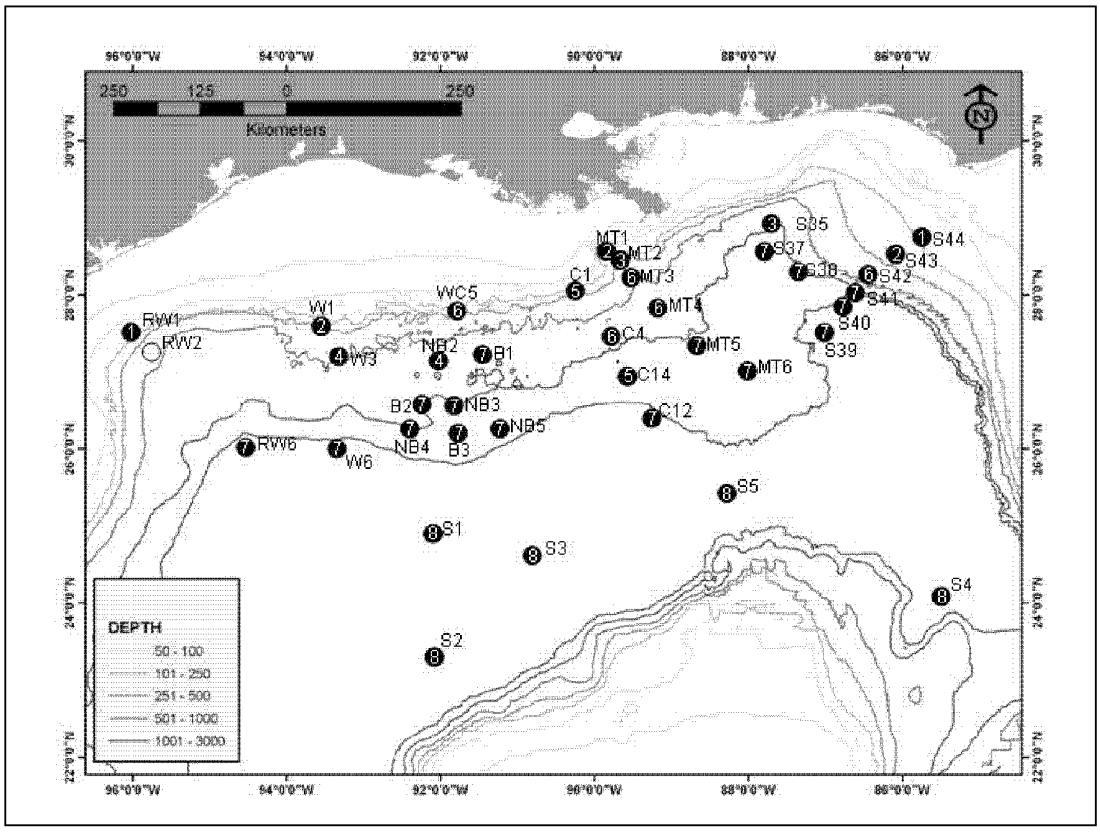

Figure 8-148. Distribution of megafaunal zones in the NW GoM.

8.8.5.7 Megafauna Assessment Using Seafloor Photography (Matthew Ziegler, UNM)

The epibenthic megafauna is the most widely studied size group in the deep ocean because they are visible to the naked eye. They are comprised of large bottom-dwelling organisms dominated by echinoderms, cnidarians (sessile sea anemones, pens and whips), decapod crustaceans, and demersal fish.

The objective of the bottom photography was to provide a general description of the northern GoM continental slope megafauna identified to the lowest possible taxonomic level. This included comparing DGoMB with NGoMCSS photographic density data to look at megafauna density variations with time, examining the relationship between megafaunal density and depth, and comparing megafaunal densities of contrasting regions both in and outside the GoM.

DGoMB images were analyzed for megafauna, area, bioturbation level, and general features – current markings, plant material, consolidated material, and water clarity. Area viewed was calculated by photographing a grid in water. This measurement was reinforced by comparison with the average size of the trawl-caught fauna. Based on this approach, area viewed was calculated at 2 m^2/image. Images obscured by clouds of resuspended sediment were overlain with the photographed grid and the visible area calculated. Only those animals that were readily identifiable in each image were counted. While macrofaunal features such as those exhibited by amphipods and polychaetes at site MT1 (Figure 8-149) can be numerous in many of the images, they were often too small to count accurately, but their presence was noted. Density of animals

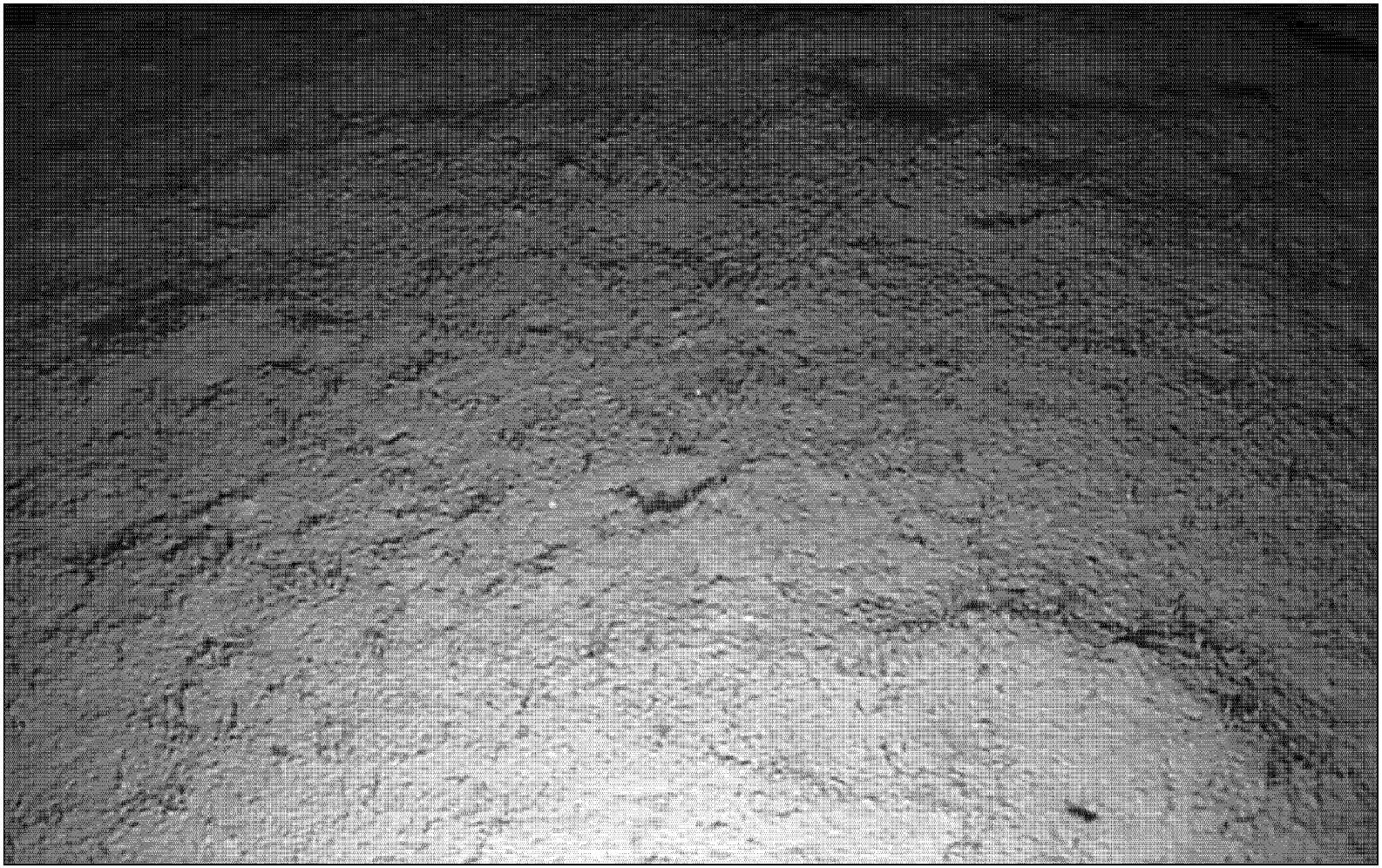

Figure 8-149. Amphipod tubes present in great numbers cover this site at the head of the Mississippi trough (MT1). This image was taken during the second visit to MT1 during the second DGoMB cruise.

per unit area was standardized to individuals/hectare (equivalent to 10,000 m^2). Trawl specimens, with the help of taxonomic experts, aided in identification of the animals in the photographs.

Photographs obtained during NGoMCCS were digitized as described by Gallaway et al. (1988a). Subsamples of 100 or 200 frames per site (of the total 800 frames) were analyzed for benthic megafauna, including demersal fishes, anthropogenic material, terrigenous material, consolidated materials, and lebenspurren. Animal density was standardized to individuals/ha.

Qualitative maps were made using ESRI ArcInfo software to illustrate large-scale distribution patterns of megafauna and other associated features. Two types of parametric tests were employed to examine megafauna distribution using the statistical software package SPSS. The first, linear regression analysis (p=0.05), considered the relationship between megafauna and depth down the slope. The second, analysis of variance (ANOVA; p=0.05), was used to compare DGoMB and NGoMCSS and associated regional variations.

Linear regression analyses (p=0.05) were carried out on animal population density for DGoMB and NGoMCSS individually, both studies combined by similar sites, both studies combined by all sites, and for individual taxa from both studies combined – alcyonarians, asteroideans, decapods, demersal fishes, echinoids, holothuroids, ophiuroids, polychaetes, scaphopods, and *Sargassum*. Megafaunal densities from each site were grouped into 100 m depth intervals, the dependent variable in the analyses. Linear regression analyses (p=0.05) were run by depth interval for all DGoMB sites, real west transect sites (RW1-RW4, RW6), west transect sites (W1-W5), central transect sites (C1, C4, C7, C12), Mississippi Trough transect sites (MT1-MT6), and east transect sites (S39-S44; Figure 8-150). Linear regression analyses (p=0.05) were done by depth interval for all NGoMCSS sites, west transect sites (W1-W5 cruise 2), central transect sites (C1-C5 cruise 2 & C1-C12 cruise 3), west-central transect sites (WC1-WC12 cruise 5), and east transect sites (all of cruise 4 sites; Figure 8-151). Using the density data from similar sites for both DGoMB and NGoMCSS – W1, W2, W3, & W5 (DGoMB cruise 1 and NGoMCSS cruise 2), C1, C4, C7, C12 (DGoMB cruise 1 and NGoMCSS cruise 3), S43/E1, S42/E3, S41/E5 (DGoMB cruise 1/NGoMCSS cruise 4), WC5, and WC12 (DGoMB cruise 1 and NGoMCSS cruise 5) – linear regression analyses (p=0.05) were performed by depth interval for all similar DGoMB and NGoMCSS sites, similar west transect sites, similar central transect sites, similar west-central transect sites, and similar east transect sites. Using the combined DGoMB and NGoMCSS densities, linear regression analyses were run by depth interval for all DGoMB and NGoMCSS sites combined, all west transect sites, all central transect sites, all west-central transect sites, and all east transect sites. Casewise diagnostics (±3 standardized residuals) in SPSS was used to identify outliers. A post analysis examination of standardized residuals was used to verify that they were independent, normally distributed, had constant variances, and means near zero.

ANOVA's (p=0.05) were run to compare megafaunal densities – grouped into 100 m depth intervals – by program (DGoMB and NGoMCSS) and site for both similar sites and all sites, by region (eastern and western GoM) for both DGoMB alone and combined with NGoMCSS data, and by feature (basins and non-basins or canyons and non-canyons) using only DGoMB densities. In the case of examining DGoMB megafaunal densities by region, ANOVA's were also performed on average depth and area viewed numbers. The test was further used to compare density numbers from the northern GoM continental slope, the slope off east Greenland, and Suruga Bay, Japan. The assumptions for ANOVA were verified using a K-S test for normality

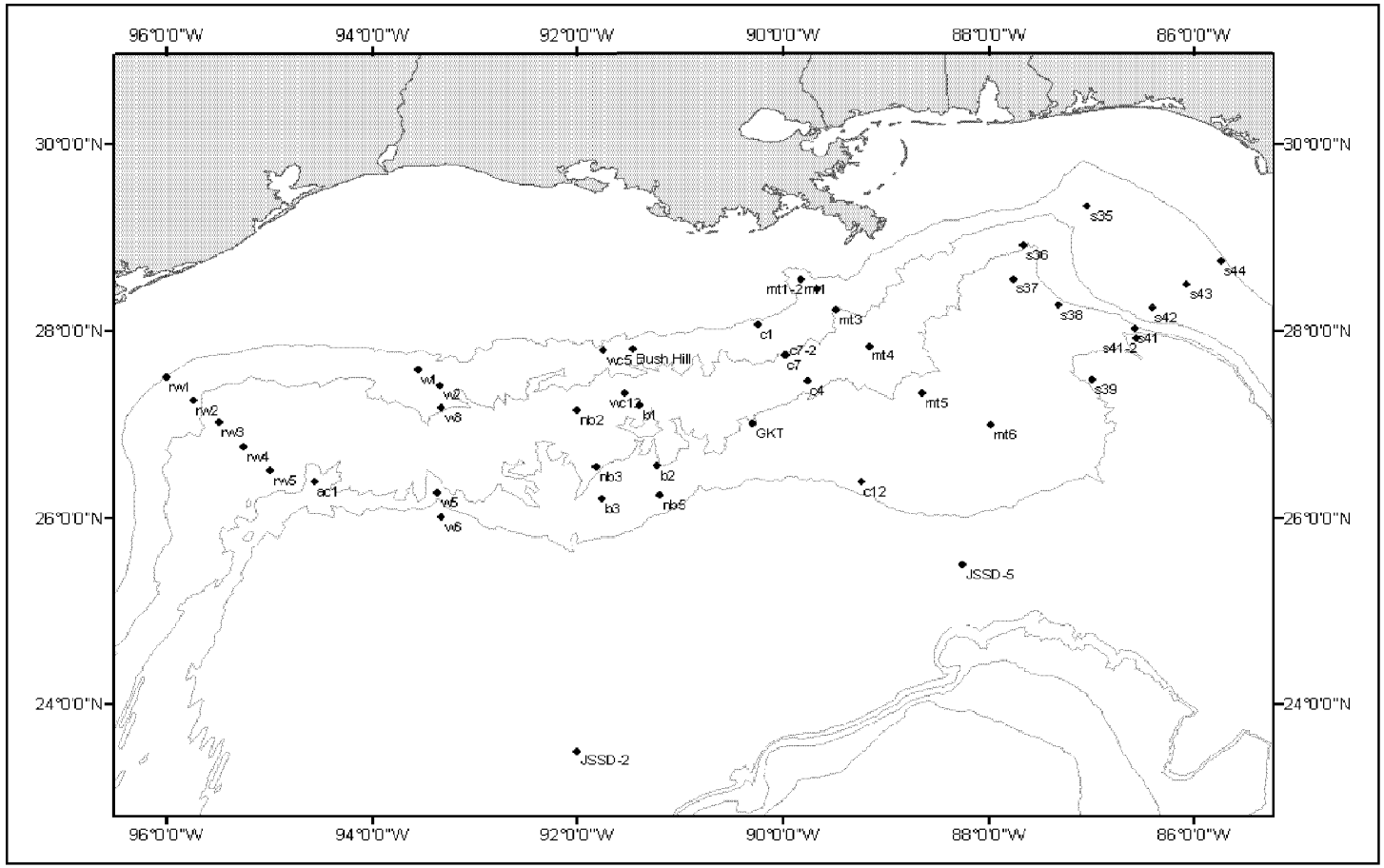

Figure 8-150. DGoMB photographic sites; rw-real west, ac-Alaminos Canyon, W-west, WC-west central, B-basin, NB-non basin, C-central, MT-Mississippi Trough, S-east, GKT-top of Green Knoll, JSSD-Joint Studies of the Sigsbee Deep. Lines represent the 200, 1,000, 2000, and 3000-meter isobaths.

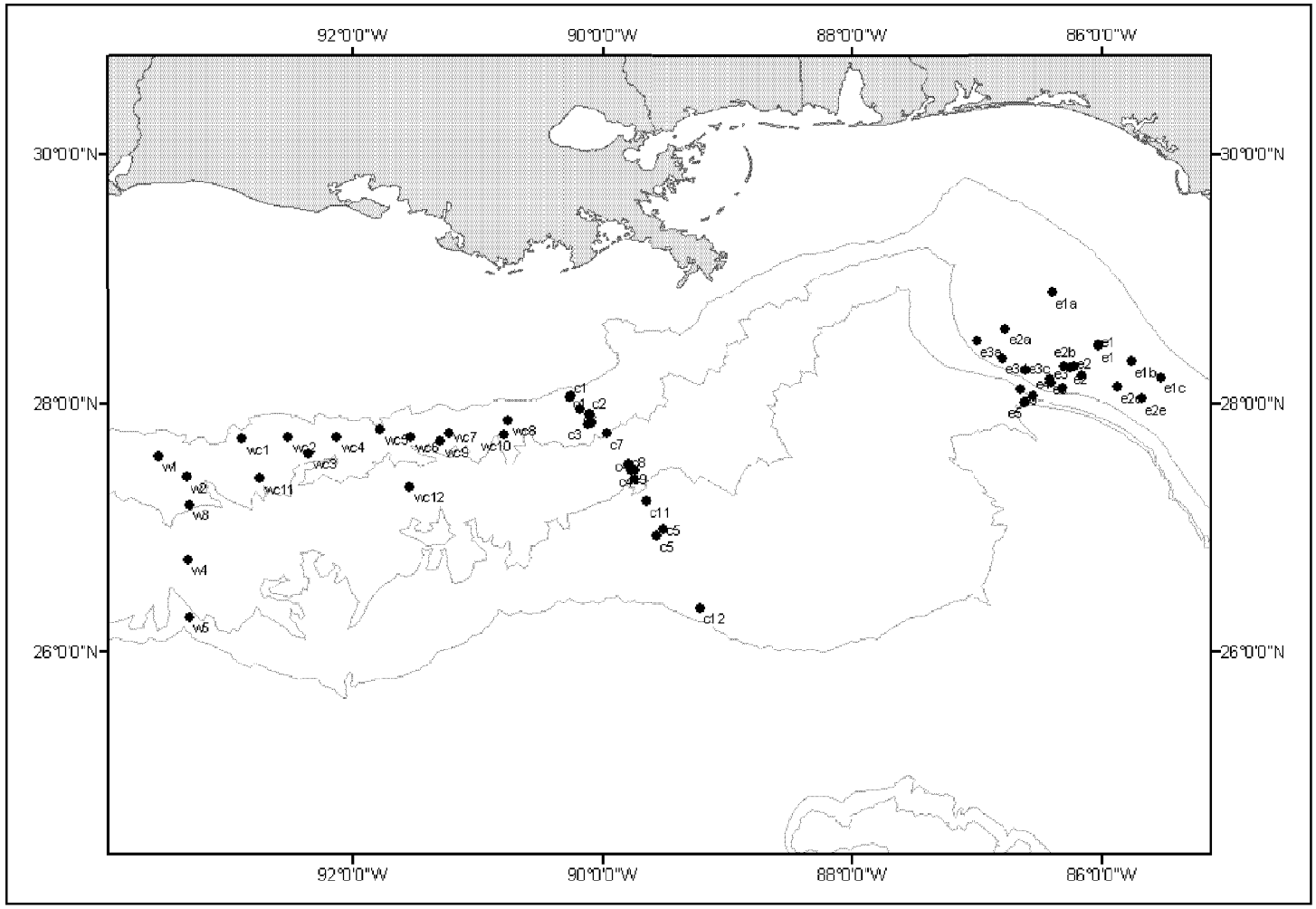

Figure 8-151. NGoMCSS photographic sites; W-west, WC-west central, C-central, E-east. Lines represent the 200, 1,000, 2000, and 3000-meter isobaths.

(p=0.05) and a Levene's test for homogeneity (p=0.05). Outliers were identified using boxplots in SPSS. Data that did not meet the assumptions for ANOVA were transformed. In cases where two-factor ANOVA's were performed, a model was chosen to look only at the main effects because a lack of replications prevented examination of interactions between factors.

During DGoMB, 1,421 images were taken at 45 sites and analyzed for megafauna, bioturbation level, current, and other features of interest (Table 8-40). These images encompass a total area of 2,559 m^2. A total of 273 megafaunal representatives were viewed, constituting a total density of 1,067 individuals/hectare (ha). The highest densities were 3,009 burrowing anemones/ha (Figure 8-152) at Bush Hill. Sites at the top of Green Knoll and in the west – W3, W5, and WC5 – had the lowest megafaunal densities with no individuals represented in photographs. The highest megafaunal densities were observed in the Mississippi Trough (MT) transect where a total of 54 individuals were seen over an area of 418 m^2 for a density of 1,290/ha (Figure 8-153). The next highest densities occurred on the western transect with 937 individuals/ha followed by the central transect with 900/ha and the real west (rw) transect with 895/ha. The transect with the lowest densities was the one in the east (s) where megafaunal densities reached 780/ha. A total of 15 major taxonomic groups were identified from photographs during DGoMB (Figure 8-154). The taxonomic group most well represented was the Holothuroidea (Sea Cucumbers) with densities approaching 189 individuals/ha, followed by demersal fish (199/ha), decapods (161/ha), and alcyonarians with 149 individuals/ha.

During NGoMCSS a total of 8,967 benthic photographs were analyzed from a total of 44,000 photographs taken at 55 sites (Gallaway et al. 1988b). These photographs contain an area equivalent to 24,132 m^2 in which a total of 17,094 animals were tabulated. Total megafaunal density for NGoMCSS was 7,084 individuals/ha. The numbers for total abundance and density included 11,156 representatives of the holothuroid *Peniagone* sp. that were encountered at six central transect stations during cruise 3. Without the influence of this species, the total was reduced to 5,938 individuals for a density of 2,461 individuals/ha. A total of 18 major taxonomic groups were identified during NGoMCSS (Figure 8-155). This included four taxa that were not viewed during DGoMB – Ascidiacea, Bivalvia, Scleractinia, and Isopoda. The densities of these four groups, Isopoda (0.4/ha), Scleractinia (4/ha), Ascidiacea (4.1/ha), and Bivalvia (7.8/ha), were among the lowest seen during NGoMCSS. The highest densities were found with the actiniarians (707/ha), the decapods (645/ha), and the sponges (404/ha).

Table 8-40

General Results by Site for DGoMB

Site	Average Depth	Total Area Viewed (m2)	Total Abundance	Total Density (#/hectare)
AC1	2550.0	43.2	7	1620
B1	2256.0	79.4	2	252
B2	2611.0	7.8	1	1282
B3	2649.0	27.6	1	362
NB2	1535.0	52.6	3	570
NB 3	1874.0	52.4	1	191
NB 5	2110.0	50.0	8	1600
RW1	207.0	87.0	15	1724
RW 2	945.0	84.0	7	833
RW 3	1317.5	51.4	1	195
RW 4	1570.0	65.6	5	762
RW 5	1628.5	69.4	4	576
W1	464.5	39.4	8	2030
W 2	619.5	22.6	1	442
W 3	875.0	10.8	0	0
W 5	2742.5	2.0	0	0
W 6	3125.0	64.0	4	625
WC5	328.0	2.4	0	0
WC12	1300.0	3.4	1	2941
C1	350.5	83.6	2	239
C4	1445.5	80.8	6	743
C7 2000	1022.0	80.0	5	625
C12	2922.0	89.0	17	1910
MT1 2000	474.0	69.6	13	1868
MT 2	679.5	54.0	2	370
MT 3	995.5	87.0	9	1034
MT 4	1403.0	84.0	13	1548
MT 5	2294.5	72.0	8	1111
MT 6	2757.5	52.0	9	1731
S35	663.5	88.0	9	1023
S36	1838.5	83.6	3	359
S37	2382.0	89.6	13	1451
S38	2647.0	63.4	10	1577
S39	2998.5	88.0	5	568
S41 2000	2963.0	78.0	14	1795
S42	766.0	89.0	2	225
S43	359.0	39.6	5	1263
S44	212.5	90.0	4	444
Bush Hill	530.5	43.2	13	3009
C7 2001	1083.0	79.4	13	1637
GKT	1897.5	7.8	0	0
MT 1 2001	475.5	27.6	8	2899
S41 2001	3039.5	52.6	14	2662
JSSD-2	3732.0	21.4	2	935
JSSD-5	3316.0	51.0	5	980

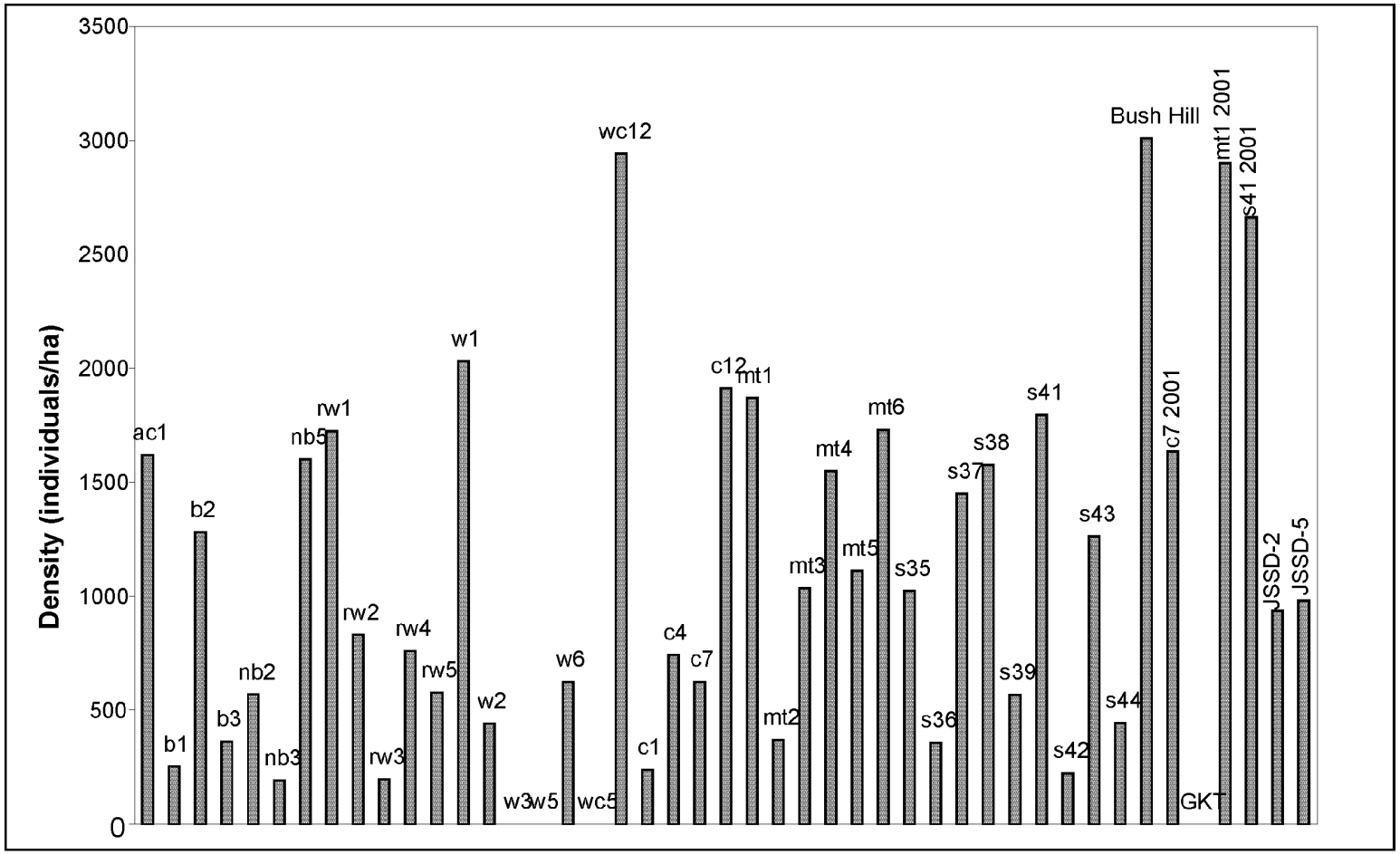

Figure 8-152. DGoMB total megafaunal density (individuals/ha) by site.

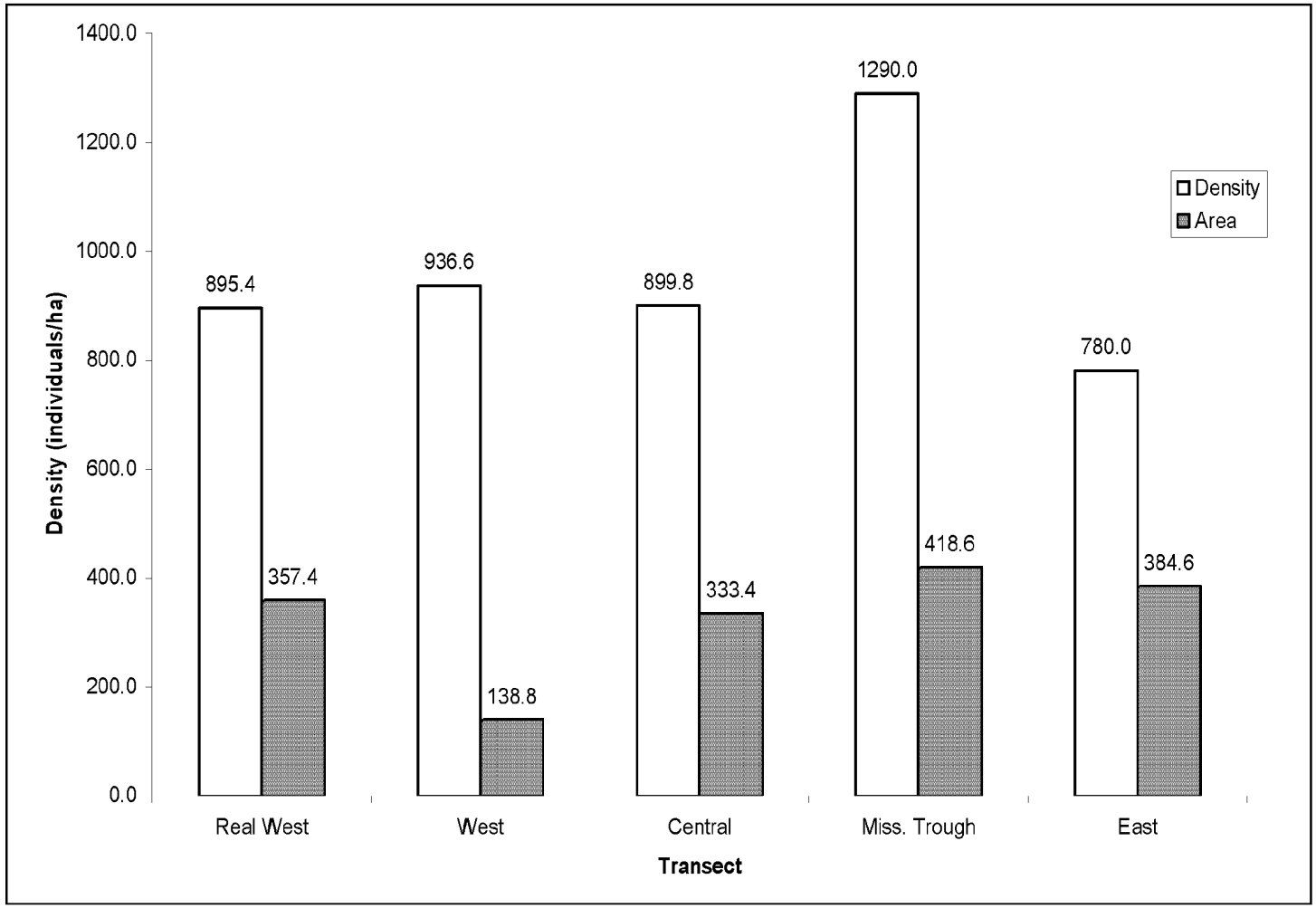

Figure 8-153. DGoMB total megafaunal density (individuals/ha) and total area (m^2) surveyed by transect.

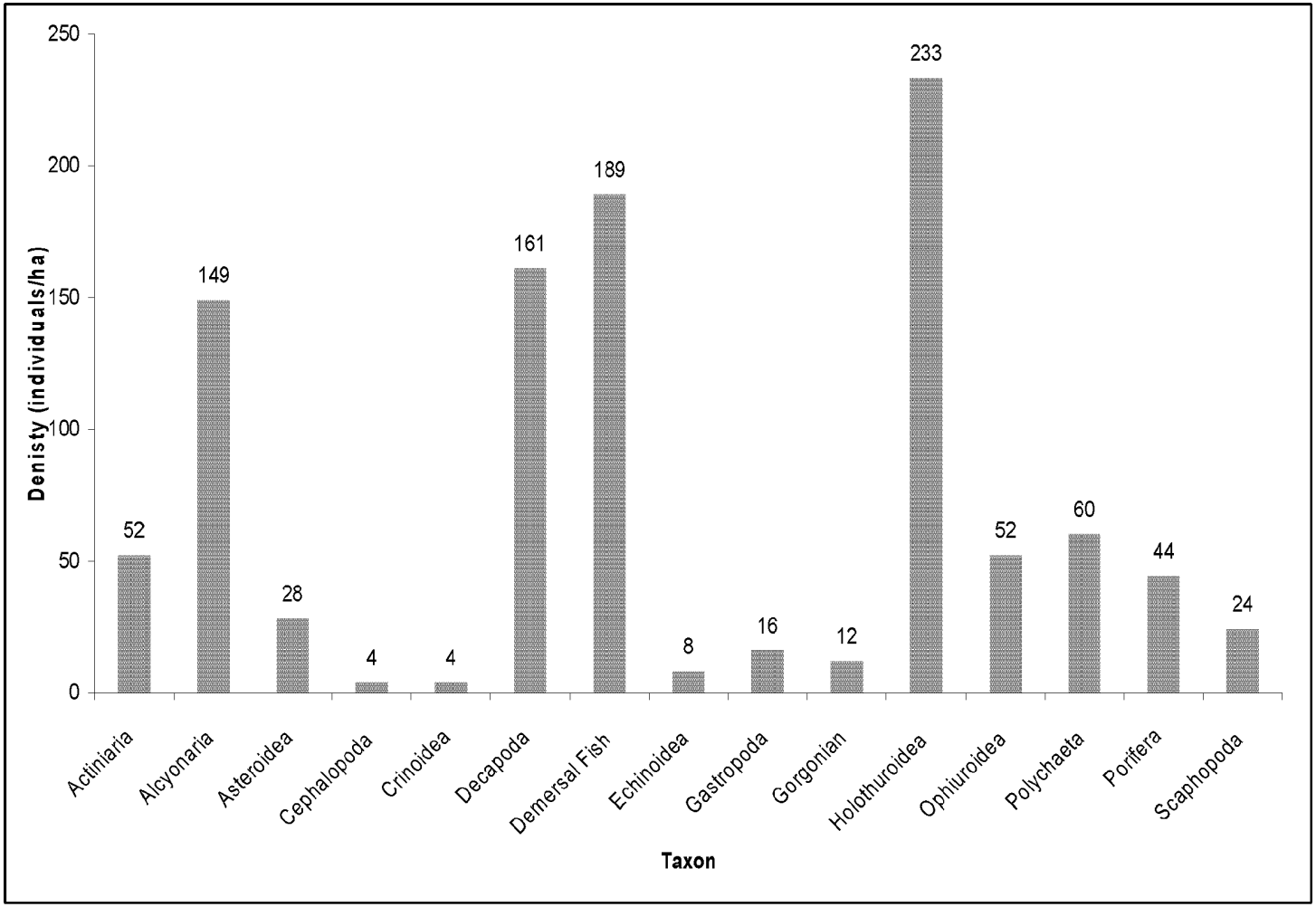

Figure 8-154. DGoMB total megafaunal density (individuals/ha) by taxon.

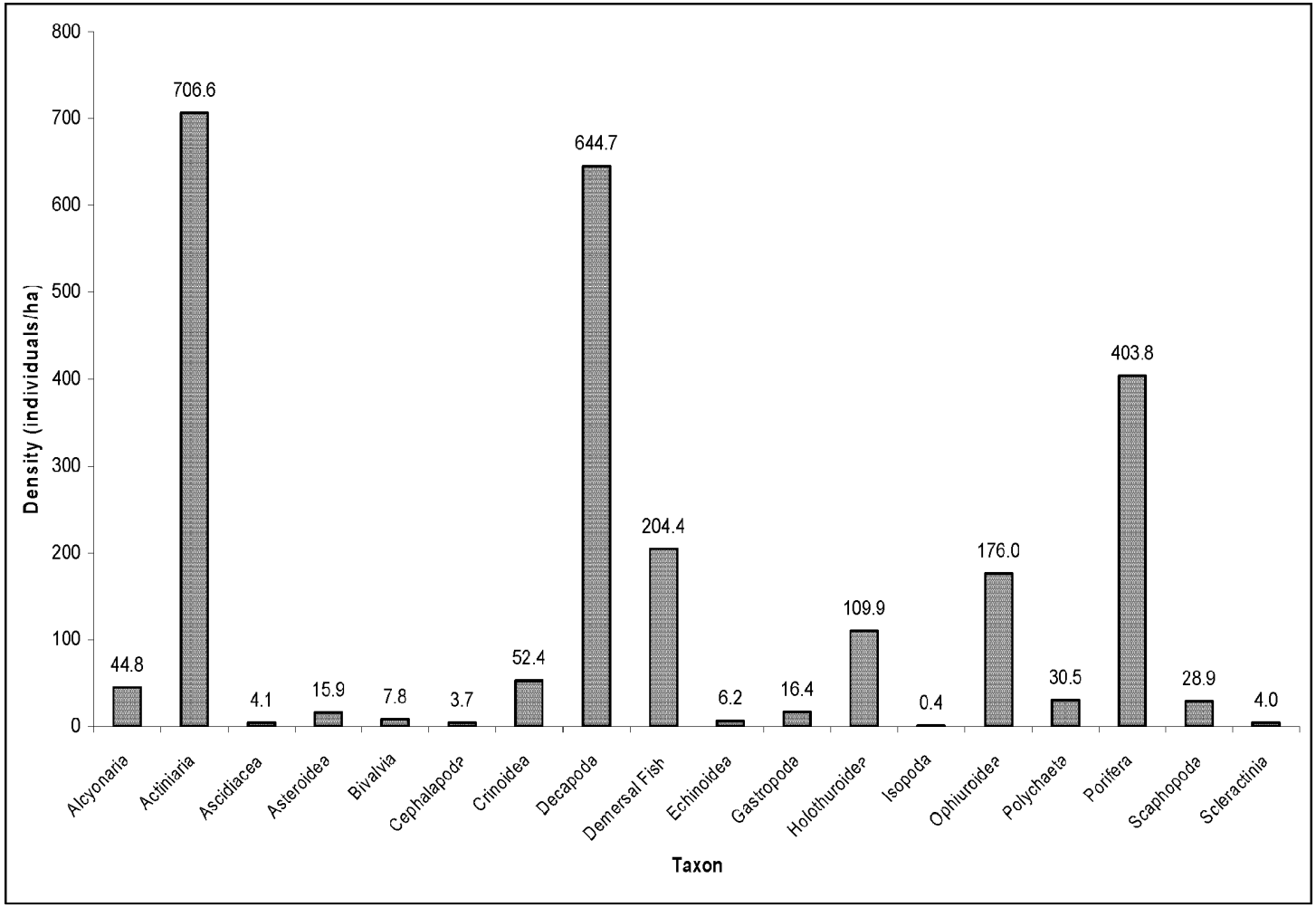

Figure 8-155. NGoMCSS total megafaunal density (individuals/ha) by taxon.

During Cruise 3 of NGoMCSS very high densities of the holothuroid *Peniagone* sp. were seen in the photographs at C3, C4, C7, C8, C9, and C10. *Peniagone* sp. was not viewed at any other sites during NGoMCSS or DGoMB. Further, no representatives of this holothurian were caught in any of the trawls. The grouping of *Peniagone* was centered on site C9 at 1,325 m depth where densities reached 154,669/ha (Figure 8-156). Around this central site there appears to be a gradient of the species both up and down the slope. The photographic depth range for this species is 864-1,611 m.

The Phaeophyceae plant *Sargassum* was commonly seen in photographs from both studies. The combined density distribution of *Sargassum* from photographs across the slope is shown in Figure 8-157. On the whole, DGoMB densities were higher than NGoMCSS densities (Figure 8-158). From Figure 8-159, it is interesting to note on the apparent lack of *Sargassum* between the far western GoM and the west-central GoM. Further, *Sargassum* was not seen in the Mississippi Trough, the DeSoto Canyon area and many eastern GoM sites. By combining both DGoMB and NGoMCSS *Sargassum* data by location, it becomes apparent that there was a gradient in *Sargassum* density between the western (296/ha) and the eastern GoM (41/ha; Figure 8-159).

When photographing the benthos there are often many features that commonly recur. During DGoMB the characteristics most commonly observed in benthic photographs were trash, pteropod tests, ironstone, and markings from current effects. Figure 8-160 shows that items of trash occurred at nine stations all centered on the Mississippi Trough with all but one below the 1,000-m isobath. Occurrences of pteropod tests were also centered around the Trough with shells littering the sediments at four sites, all but one of which were below the 2000-m isobath (Figure 8-161). Ironstone appeared on the bottom in slate-like layers and was primarily composed of an iron oxide precipitate (Morse, personal communication). Pequegnat first noted it in benthic skimmer samples in the 1960's. Generally, this "Ironstone" region is thought to be centered on the Mississippi Fan, or cone of sediments derived from the trough. The portion of this region that was sampled during DGoMB is seen in Figure 8-162 and Figure 8-163. Ironstone occurrences in this figure are from both photographs and trawls. Finally, the winnowing and erosion effects of currents were common. The DGoMB sites where current effects were visible are all below the 2000-m isobath. Further, these currents appear to be situated on and below the Sigsbee and Florida Escarpments.

DGoMB sediment cores from cruise 1 were analyzed for bioturbation levels – low, medium, and high. The distribution of core bioturbation levels across the slope is seen in Figure 8-164. In order to compare the bioturbation levels seen in the cores with what is seen in photographs, the bioturbation levels from DGoMB cruise 1 photographs were subjectively determined and are shown in Figure 8-165. Photographic bioturbation levels were defined in terms of the percent of an image covered by tubes, tracks, or burrows. Low levels had less than 10% coverage, medium levels had 10-50% coverage and high levels were greater than 50% coverage. Values based on core samples and those based on photographic samples were generally comparable. The cases where they were not may be due to the difference in spatial scales between the cores (cms) and the photos (meters). The cores are considering evidence within the sediments, whereas the photos pictured only the sediment – water interface. The two may not be directly related.

Two types of comparisons were performed to quantitatively examine the difference in megafaunal densities between DGoMB and NGoMCSS. The first compared only the sites that DGoMB and NGoMCSS had in common and the second compared all sites for both studies. Total megafaunal densities for similar sites (Figure 8-166) were evaluated with a two-way

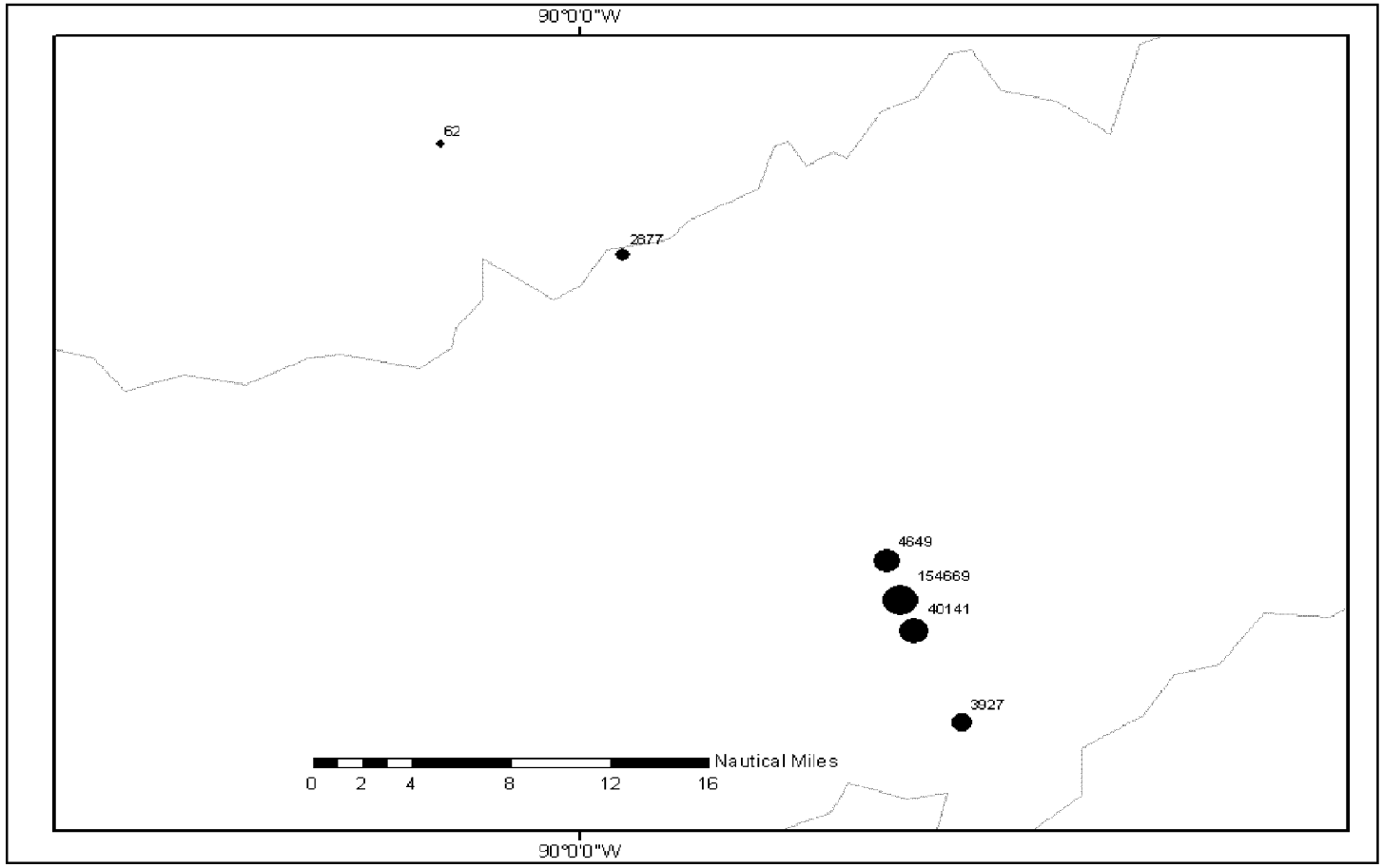

Figure 8-156. Density (individuals/ha) of the holothuroid *Peniagone* sp. seen in large numbers in the central GoM during NGoMCSS cruise 3. Sizes of the circles represent the density (individuals/ha) of *Peniagone* sp.. Lines represent the 1,000 and 2000-meter isobaths.

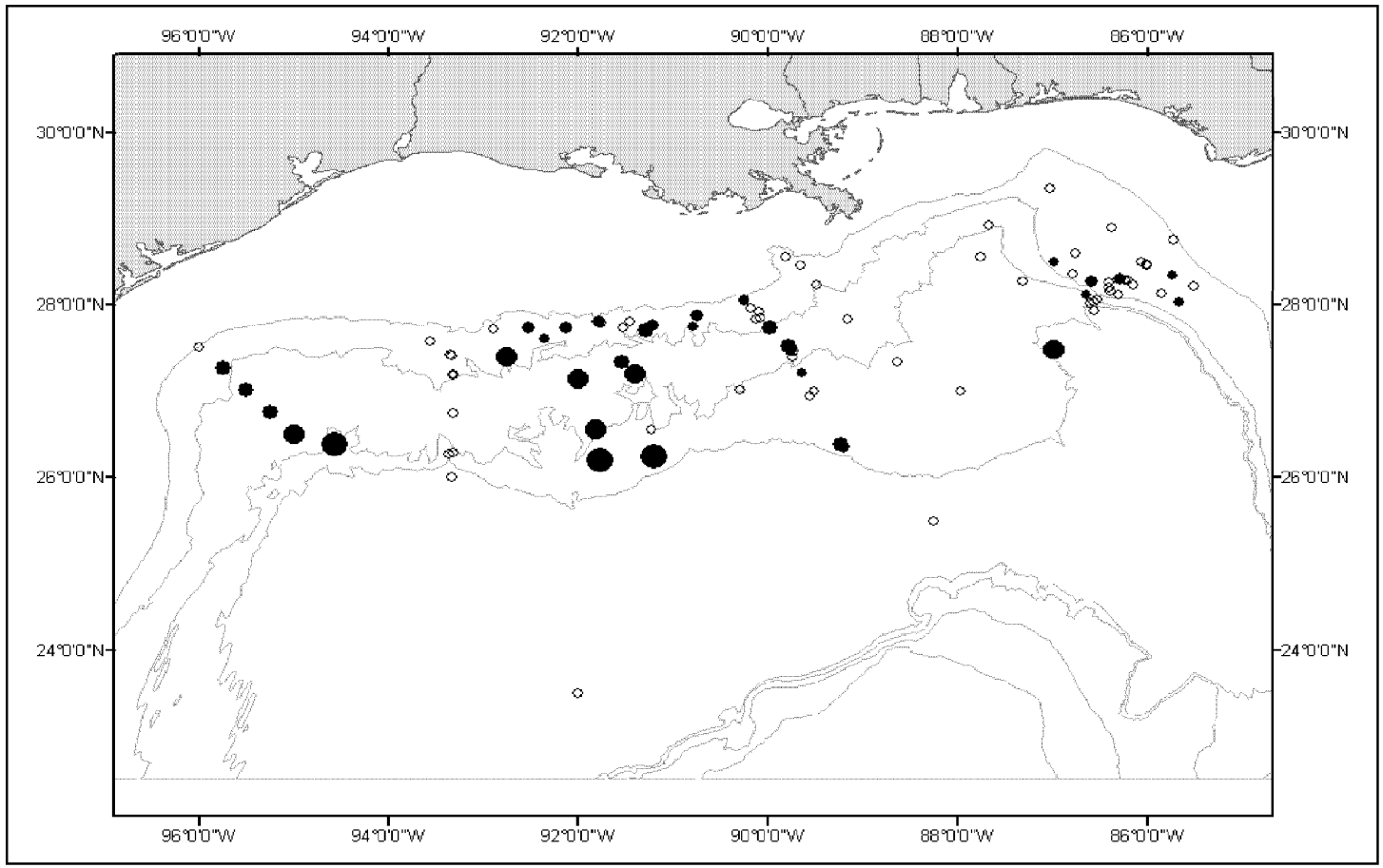

Figure 8-157. GoM photographic sites. Closed circles represent sites where *Sargassum* was visible in photographs. Size of the circle represents density (individual clumps/ha). Open circles represent sites where *Sargassum* was not present in photographs. Lines represent the 200, 1,000, 2000, and 3000-meter isobaths.

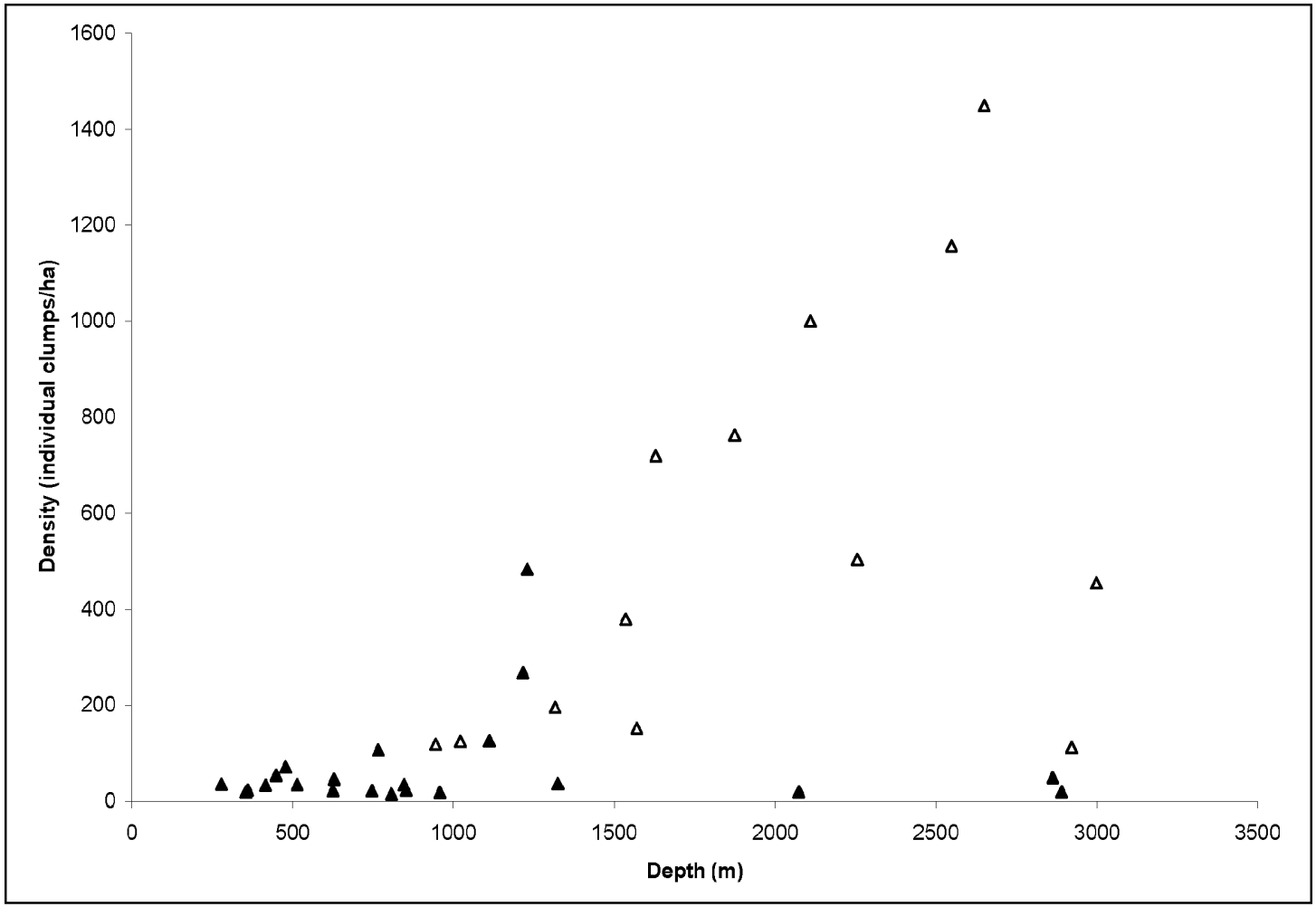

Figure 8-158. DGoMB (open triangles) and NGoMCSS (closed triangles) *Sargassum* density (individual clumps/ha) with depth.

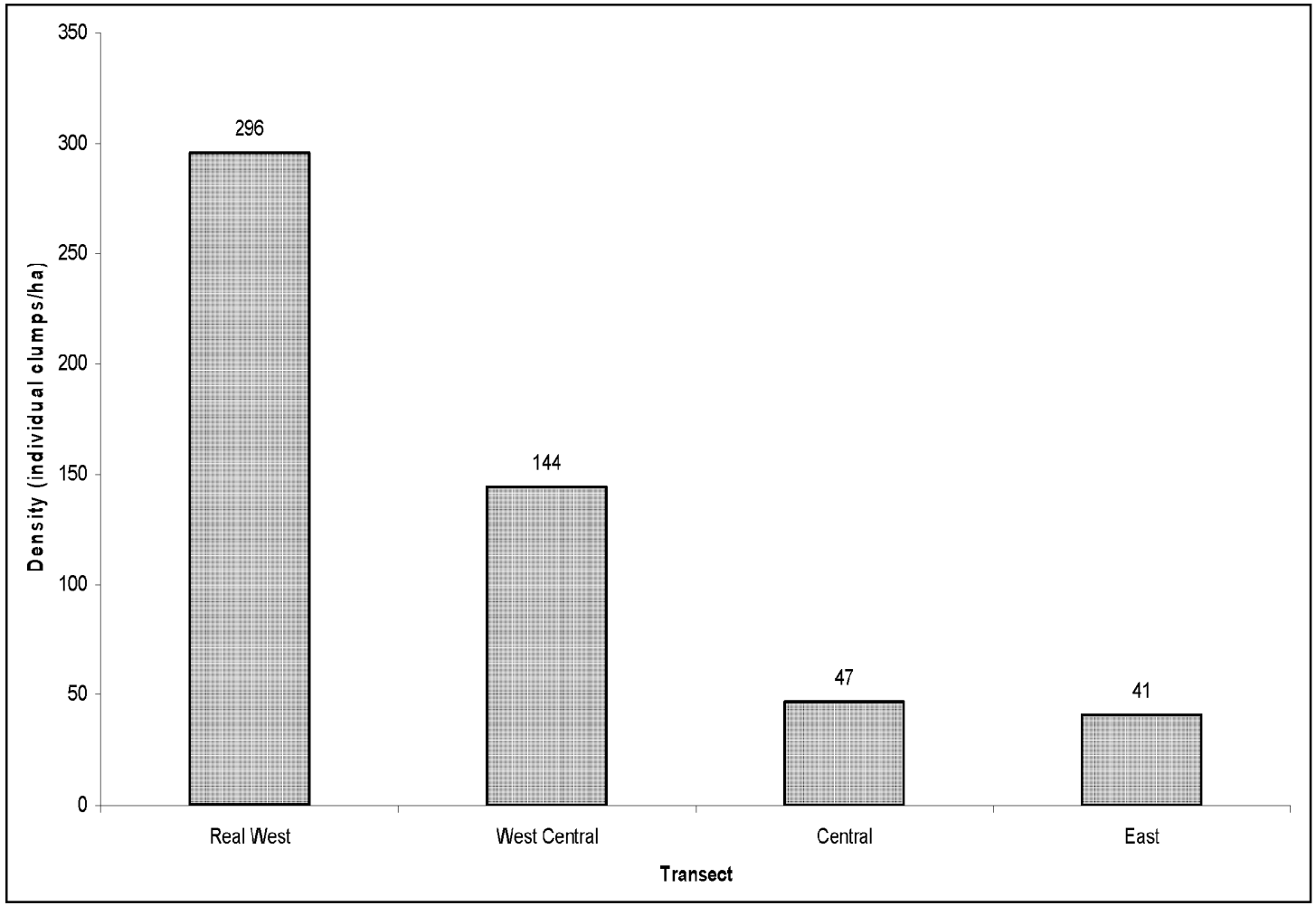

Figure 8-159. Total GoM *Sargassum* density (individual clumps/ha) by transect for all sites combined.

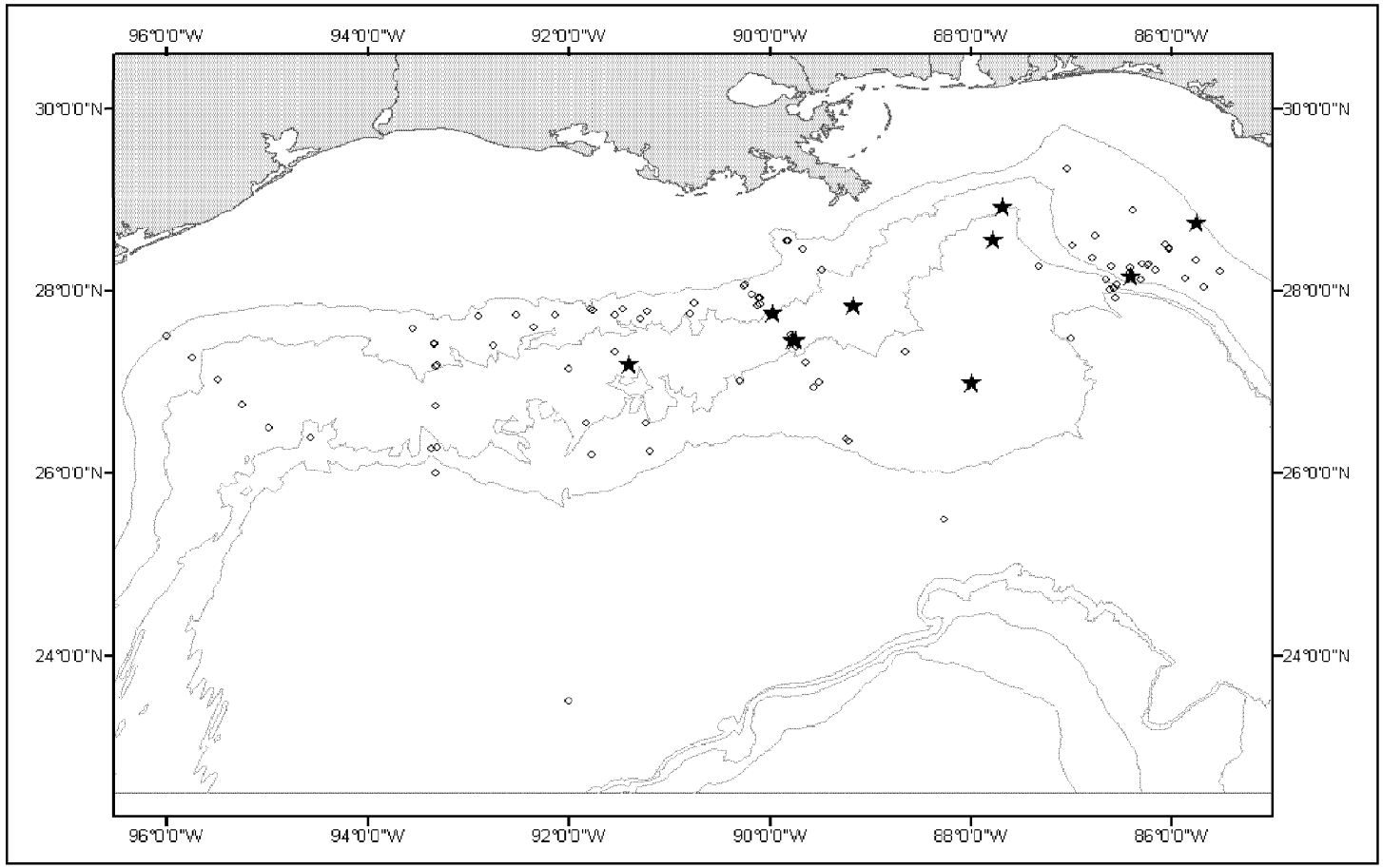

Figure 8-160. GoM photographic sites. Stars represent sites where trash was seen in the images. Open circles represent sites where trash was not seen. Lines represent the 200, 1,000, 2000, and 3000-m isobaths.

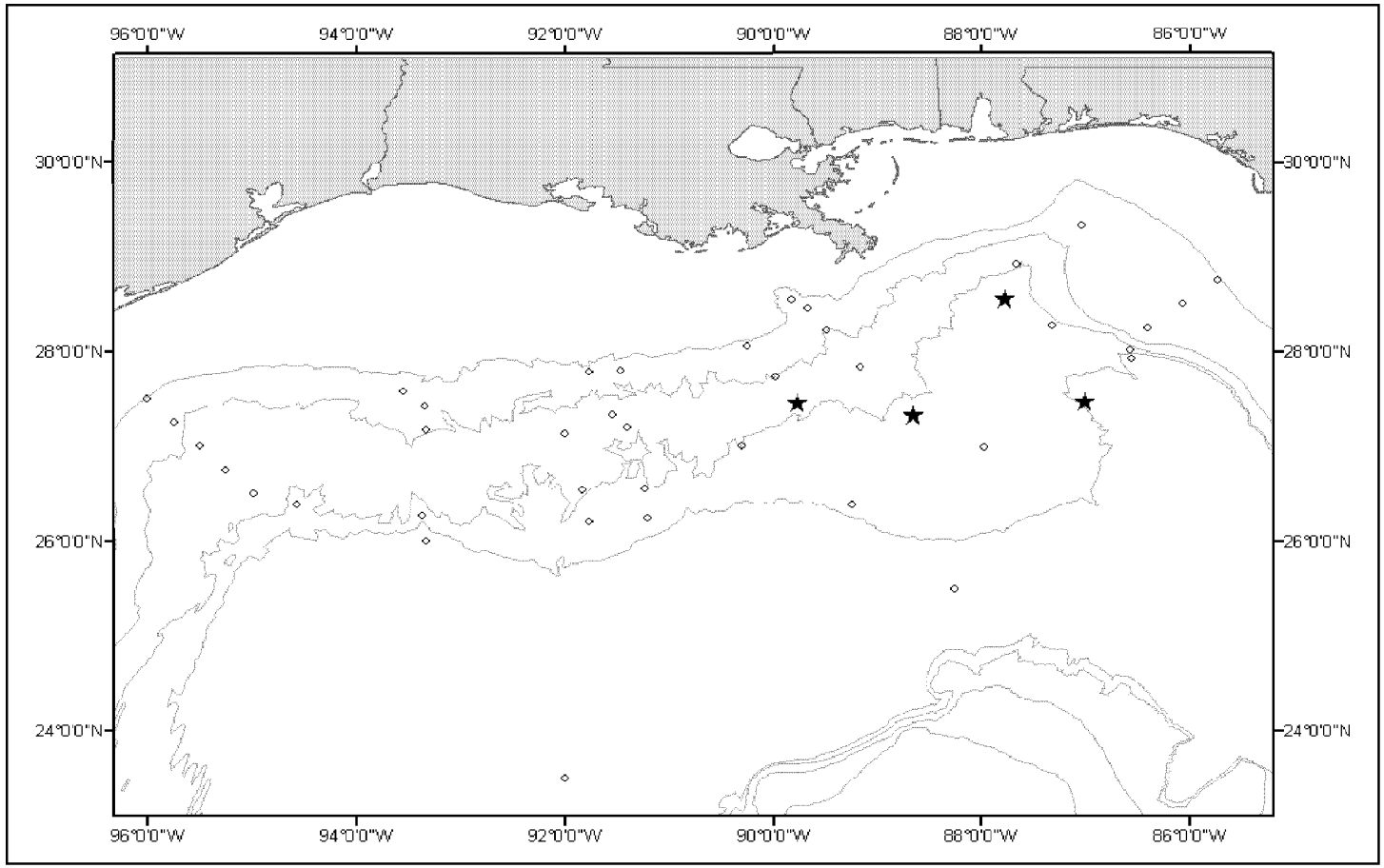

Figure 8-161. DGoMB photographic sites. Stars represent sites where pteropod tests were seen covering the sediment surface. Open circles represent sites where pteropod tests were not seen. Lines represent the 200, 1,000, 2000, and 3000-m isobaths.

Figure 8-162. June 5, 2000. Dr. Rowe sifted through iron stones for specimens. Image is taken at MT6.

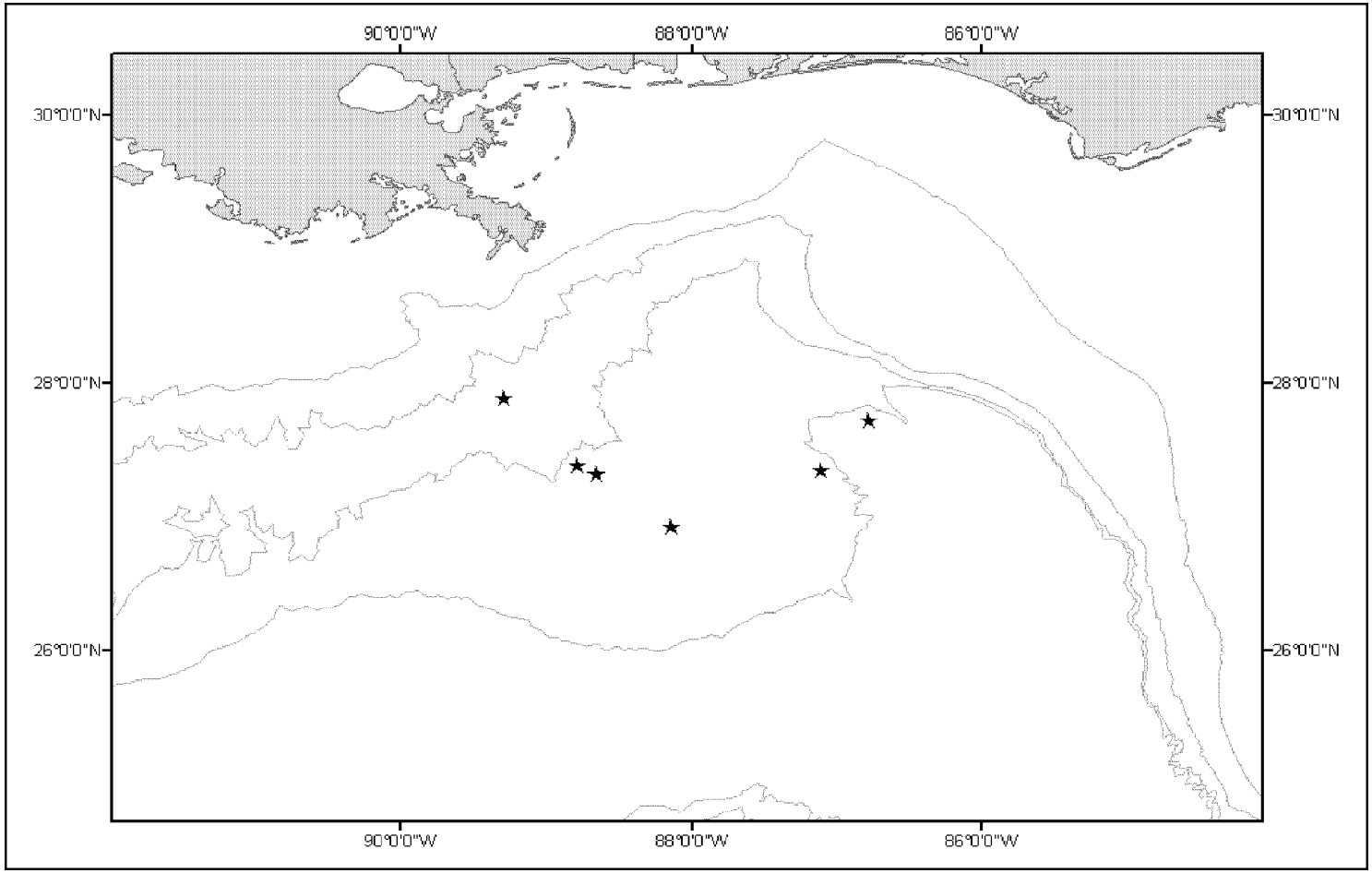

Figure 8-163. DGoMB trawl and photographic sites where Ironstone was sampled. Lines represent the 200, 1,000, 2000, and 3000-meter isobaths.

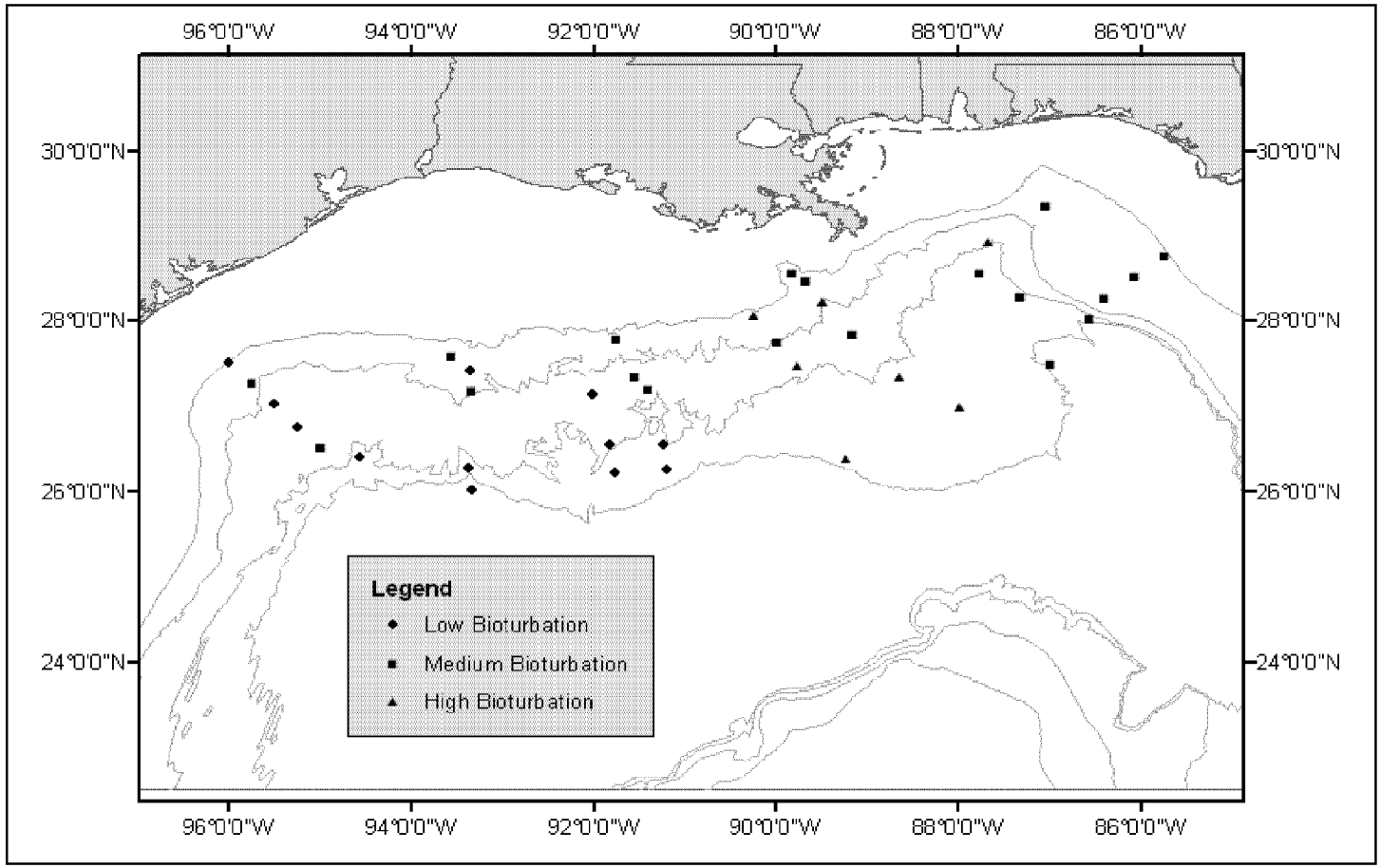

Figure 8-164. Bioturbation levels from DGoMB year 1 sediment cores. Lines represent the 200, 1,000, 2000, and 3000-m isobaths.

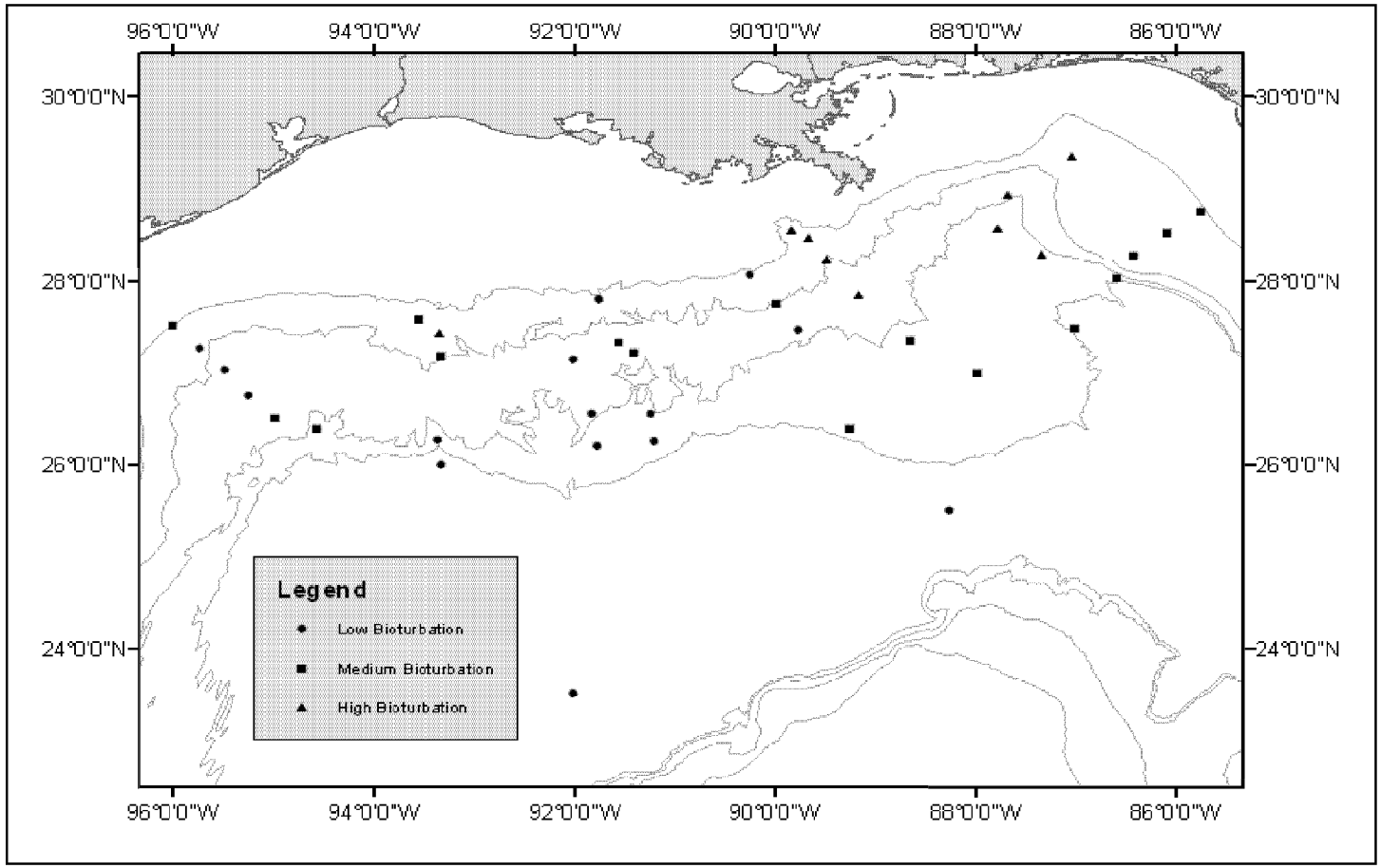

Figure 8-165. Bioturbation levels seen in photographs during DGoMB. Lines represent the 200, 1,000, 2000, and 3000-m isobaths.

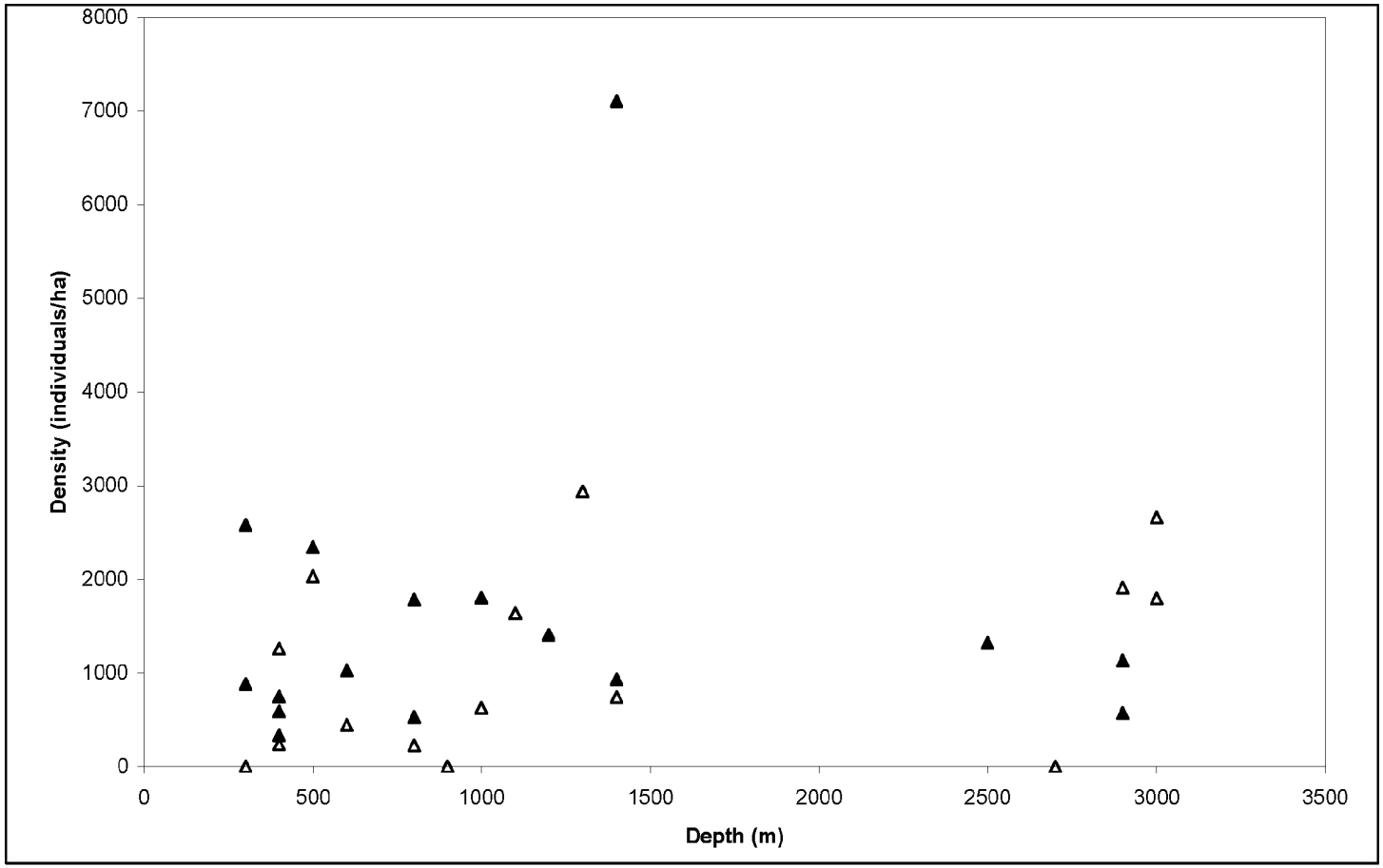

Figure 8-166. Megafaunal densities (individuals/ha) in photographs at similar depts in DGoMB (open triangles) and NGoMCSS (closed triangles).

ANOVA ($p=0.05$). The assumptions for this parametric test were verified for each program using a K-S test for normality ($p>0.05$) and a Levene's test for homogeneity ($p>0.05$). Assumptions for site could not be verified because of a lack of replication. Results of the analysis indicate that there was no significant difference in megafaunal densities ($p>0.05$) both between programs and between similar sites.

Total megafaunal densities from all sites in both DGoMB and NGoMCSS (Figure 8-167) were compared with a 2-way ANOVA ($p=0.05$). A total of 10 outliers and three extremes were identified using boxplots and removed. The assumptions for a two-way ANOVA were verified for each program using a K-S test for normality ($p>0.05$) and a Levene's test for homogeneity ($p>0.05$). An attempt was made to verify the assumptions for an ANOVA by Depth Interval, but again lack of replication made this difficult. The density within the 400, 500, 800, and 900 m depth intervals – the only intervals with adequate replication – were determined to be normally distributed ($p>0.05$) using a K-S test. The ANOVA indicated no significant difference in megafaunal densities between Program and Depth Interval for all sites ($p>0.05$).

DGoMB density and abundance numbers were examined by themselves to look at the significance of their relationship with depth. Linear regression analyses ($p=0.05$) were run for both density and abundance by depth for all DGoMB sites, "real west" transect sites, "west" transect sites, "central" transect sites, "Mississippi Trough" transect sites, and "east" transect sites. No outliers were identified. The analyses indicated that there was not a significant ($p>0.05$) relationship between depth and megafaunal abundance for all sites and by transect. Assumptions for the analyses were verified through a post analyses examination of standardized residual.

NGoMCSS density and abundance numbers were examined by themselves to look at the significance of depth. Linear regression analyses ($p=0.05$) were performed on density abundance by depth for all sites, "west" transect sites, "central" transect sites, "west-central" transect sites, and "east" transect sites. *Peniagone* and the unidentified sponge species found in large numbers at C10 were identified as outliers and they were removed from the analyses. The analyses indicated that there was not a significant ($p>0.05$) relationship between depth and megafaunal density and abundance for all sites and by transect. Post analyses verification of standardized residuals verified the assumptions of the regression.

DGoMB and NGoMCSS density and abundance numbers were examined to look at the significance of their relationship with depth. Linear regression analyses ($p=0.05$) was done for abundance by depth for all similar sites, similar "west" transect sites, similar "central" transect sites, similar "west-central" transect sites, and similar "east" transect sites. *Peniagone* and site c4 (NGoMCSS cruise 2) were identified as outliers and removed from the analyses. The analyses indicated that there was not a significant ($p>0.05$) relationship between depth and megafaunal density and abundance for all sites and by transect. Post analyses verification of standardized residuals indicated that they were independent, normally distributed, had constant variances, and means near zero. The analyses did indicate that there was a significant relationship ($p<0.05$, $R^2=0.065$) between WC-transect megafaunal densities and depth interval (Figure 8-168). Assumptions for the regression were verified through a post-analysis verification of standardized residuals.

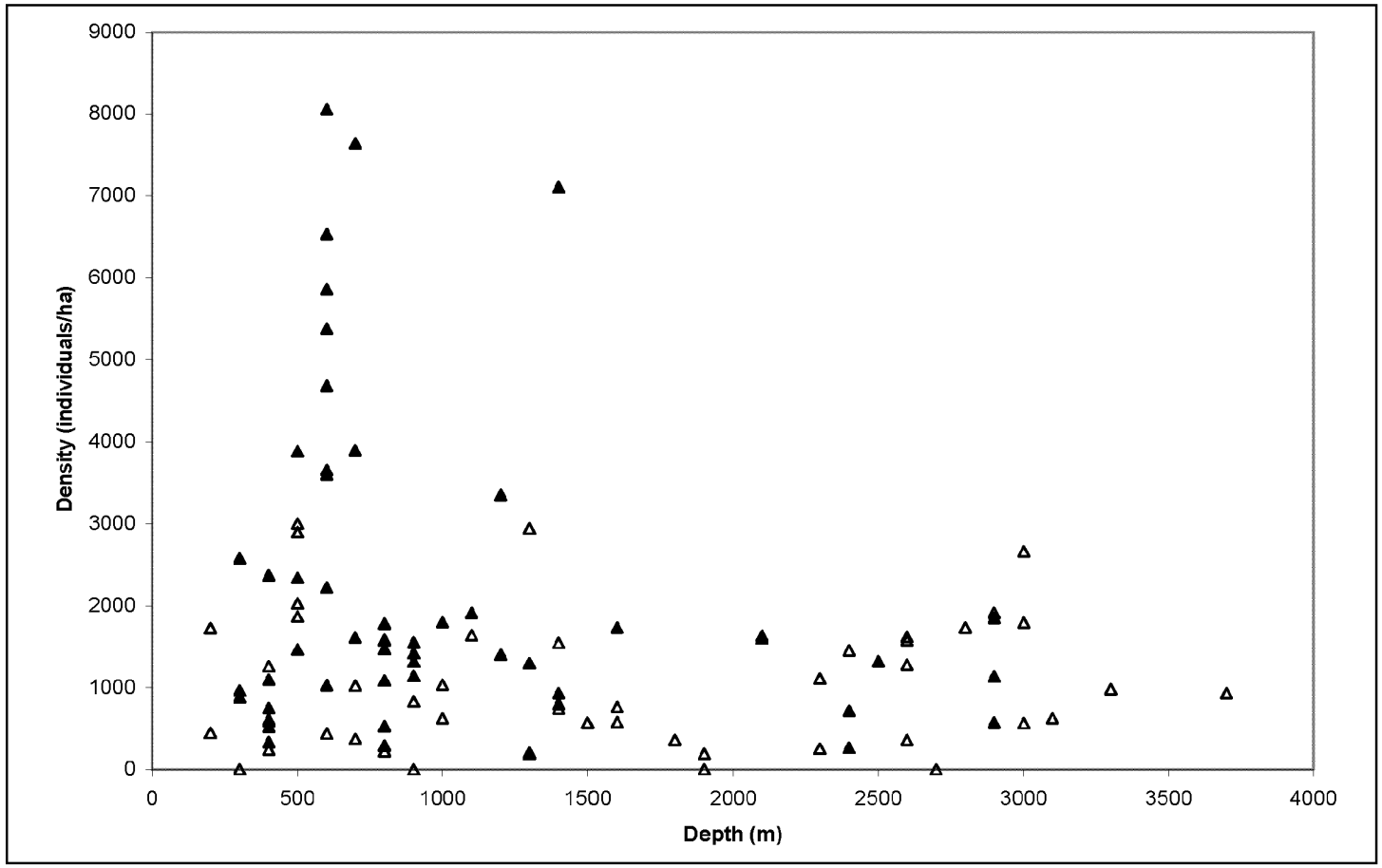

Figure 8-167. Megafaunal densities (individuals/ha) for all sites. The open triangles represent DGoMB data; the closed triangles represent NGoMCSS data.

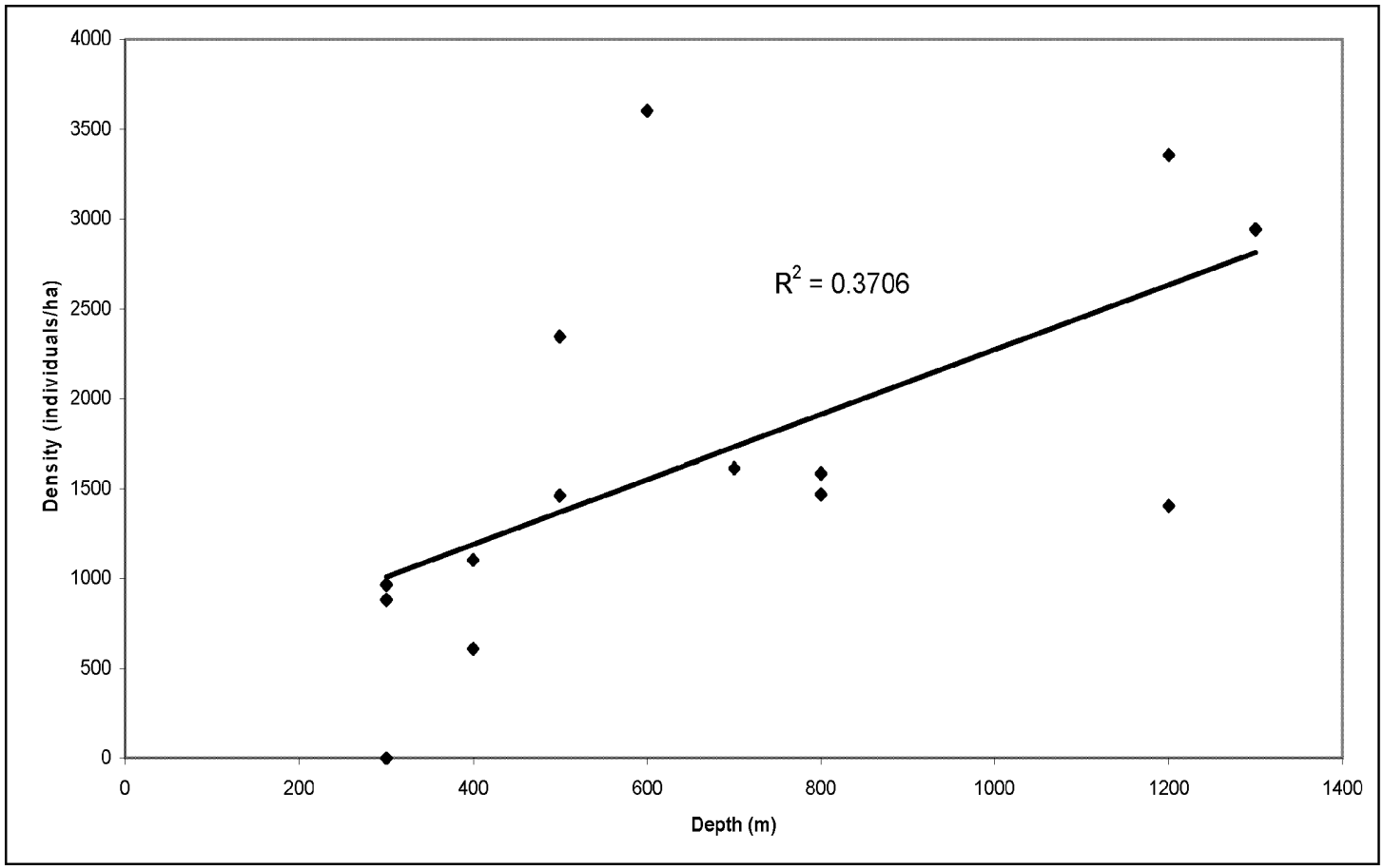

Figure 8-168. West-central transect megafauna density (individuals/ha) as a function of depth for both DGoMB and NGoMCSS sites.

One-way ANOVA's ($p=0.05$) for DGoMB density, area viewed (m^2), and average depth (m) were performed to examine the difference between eastern and western benthic populations,. Outliers were identified for the density data using boxplots and removed. To meet the assumptions of normality and equal variances the density data had to be square root +1 transformed. This allowed the east and west density data, along with the untransformed area viewed, and average depth numbers to meet the assumptions for an ANOVA – K-S test for normality ($p>0.05$), Levene's test for homogeneity ($p>0.05$). The population densities in the east were different from those in the west ($p<0.05$, $R^2=0.289$; Figure 8-169).

One-way ANOVA's ($p=0.05$) were performed on the density, area viewed, and average depth values for both basin and non-basin sites. Data were normally distributed (K-S test of normality $p>0.05$), and had equal variances (Levene's test for homogeneity $p>0.05$) for the variables listed. For the "area viewed" values, equal variances (Levene's test for homogeneity $p<0.05$) could not be assumed. Results of ANOVA ($p>0.05$) indicated that there was not a significant difference between basin and non-basin density, abundance, and area viewed values. Average depth however was shown to be significantly different ($p<0.05$, $R^2=0.718$) between basins and non-basins. Examination of the major megafaunal groups present at basin and non-basin sites show that while they only share one group—Holothuroidea—many more taxonomic groups were found at non-basin sites (Figure 8-170).

It has been shown previously that canyon fauna differs from non-canyon fauna at similar depths (Rowe 1971; Ohta 1983) with certain species serving as indicator species for the canyon fauna. The idea of canyons being different was examined in the GoM using DGoMB photographic data from transects down the Mississippi and DeSoto Canyons (Figure 8-171). Canyon transects were compared with transects from areas immediately adjacent to the canyons. A univariate ANOVA was performed on megafaunal density and abundance numbers for both canyon transects and adjacent transects. Based on boxplots, it appears that density at MT1 2001 (2,899/ha) along with density at MT2 (two individuals), were outliers and removed from the analysis. Levene's test for homogeneity ($p>0.05$) and the K-S test of normality ($p>0.05$) ensured that variances were equal and the density and abundance data were normally distributed. ANOVA indicated that there was not a discernable difference ($p>0.05$) in megafaunal densities between canyon and non-canyon transects. Examination by taxon at both canyon and non-canyon sites (Figure 8-172) indicates that the four transects shared 63-75% of the eight most abundant taxa.

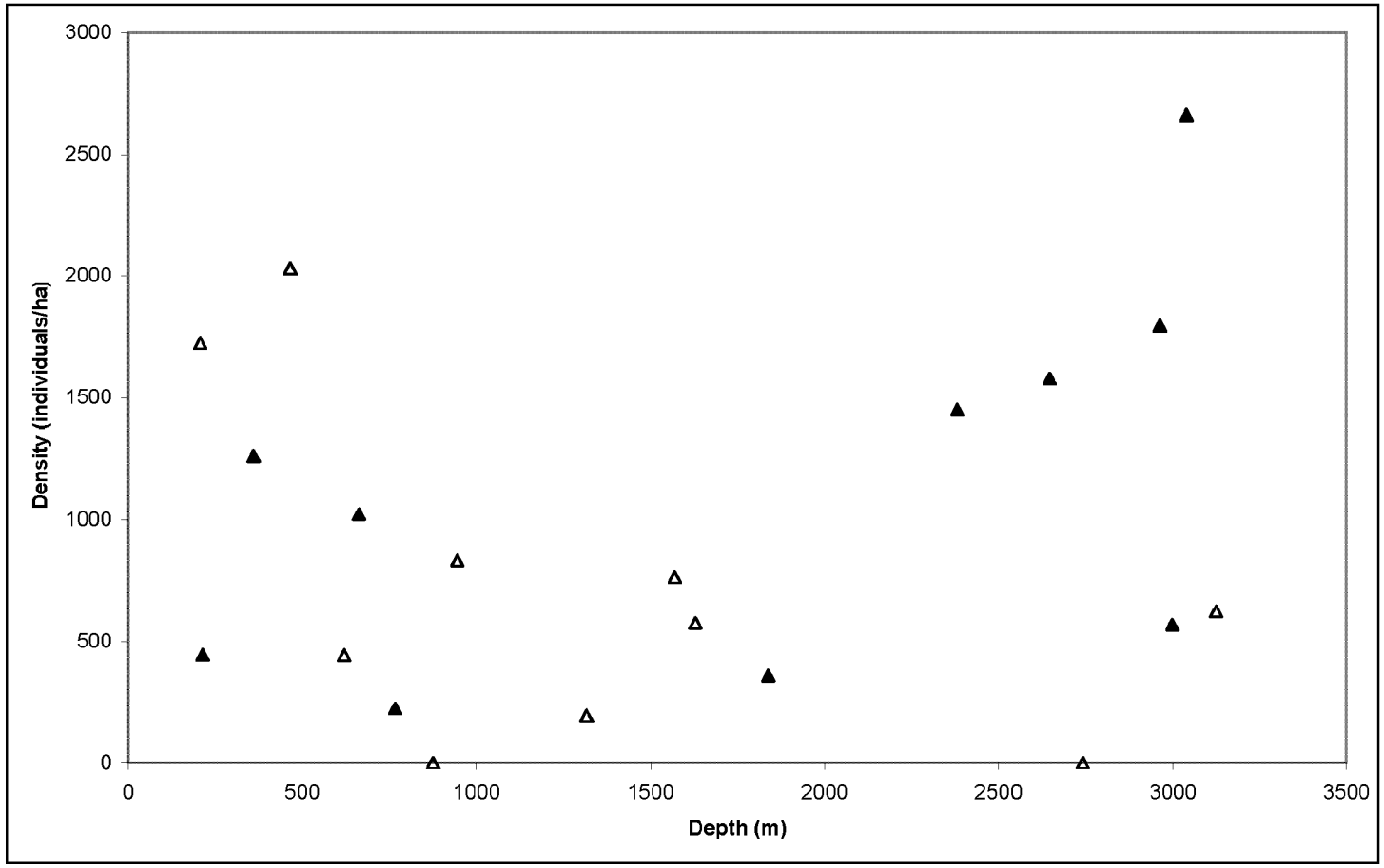

Figure 8-169. DGoMB western (open triangles) and eastern (closed triangles) megafaunal densities (individuals/ha) as functions of depth.

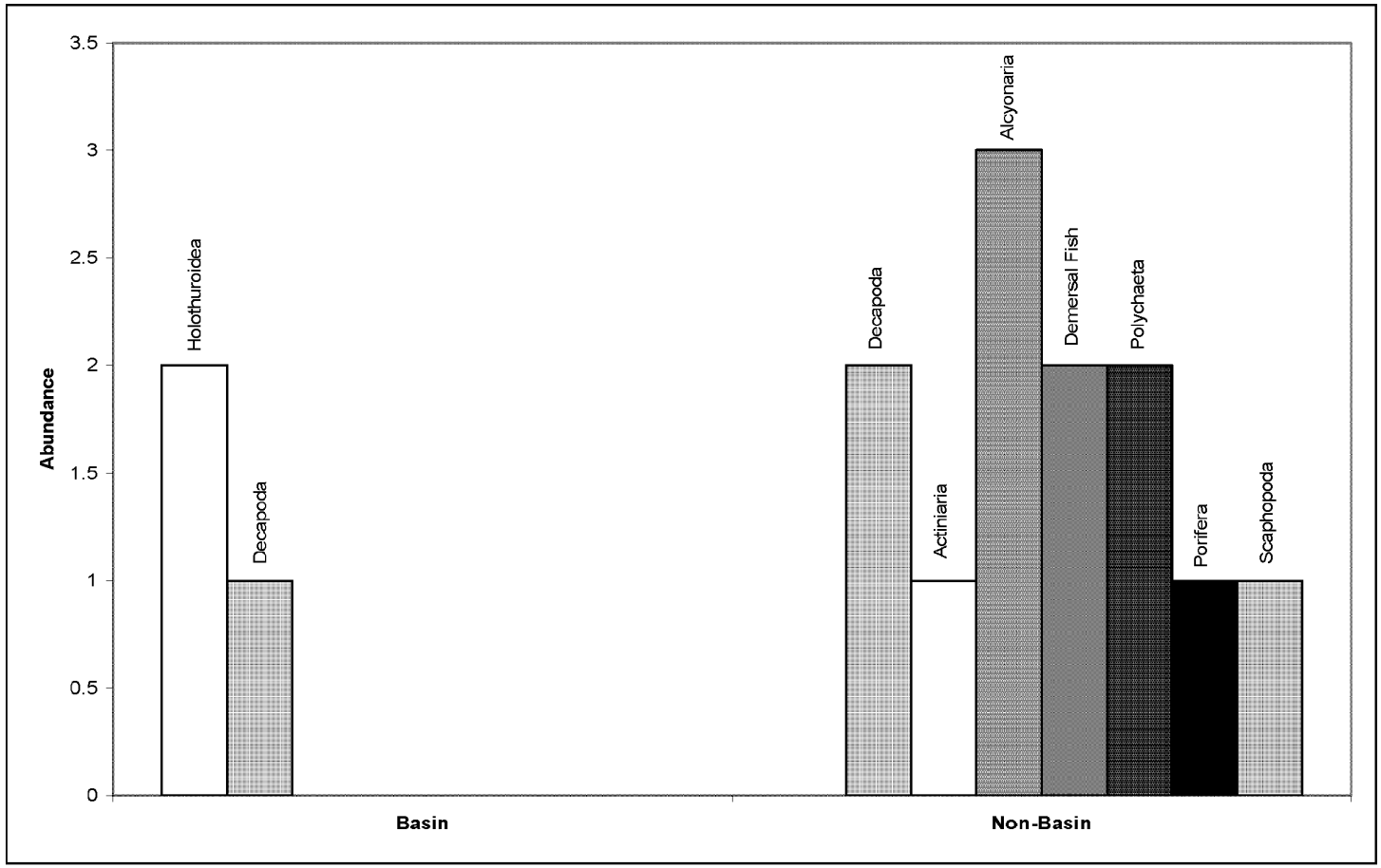

Figure 8-170. DGoMB total megafaunal abundances by taxon for both basin and non-basin sites.

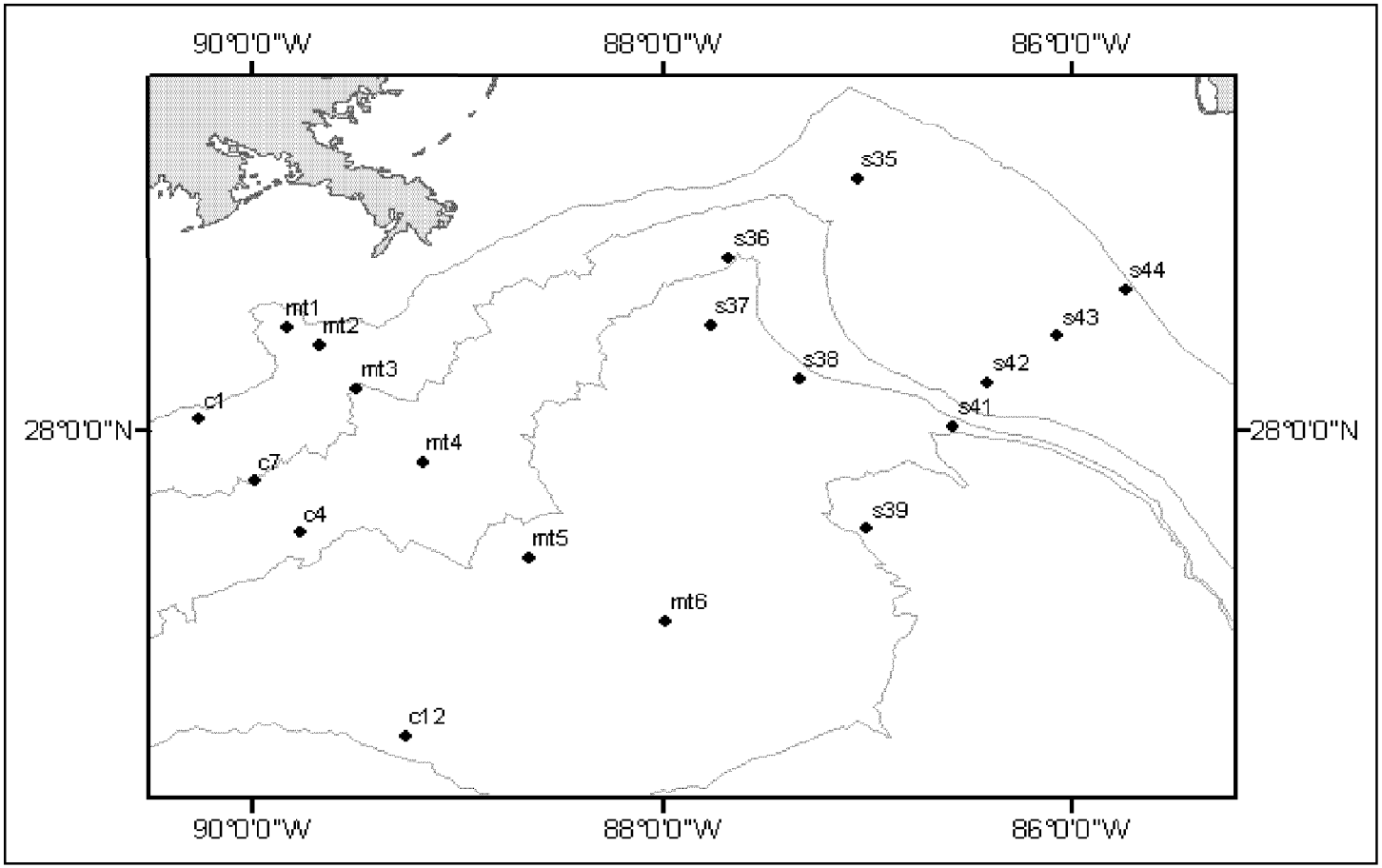

Figure 8-171. DGoMB Mississippi Canyon (MT1-MT6), Mississippi Canyon adjacent (C1, C4, C7, and C12), DeSoto Canyon (S35-S37), and DeSoto Canyon adjacent (S38-S44) sites. Lines represent the 200, 1,000, 2000, and 3000-meter isobaths.

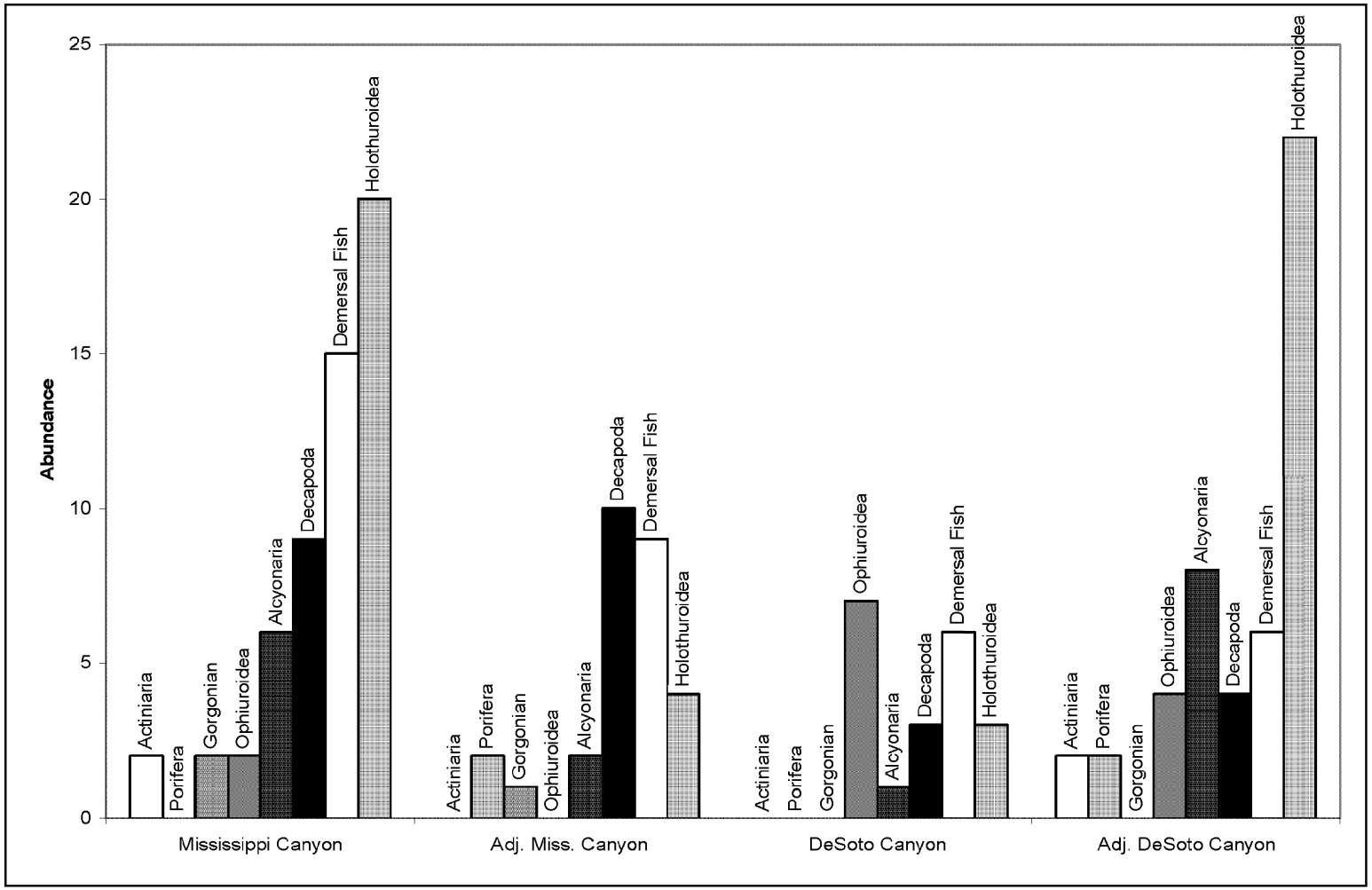

Figure 8-172. DGoMB total megafaunal abundances (number per hectare) of the eight most abundant taxa in the Mississippi and DeSoto Canyons and the areas adjacent to these canyons.

GoM photographic megafaunal density data were compared with density data from several other studies the relative to evaluate richness of the deep GoM. This included in Suruga Bay, Japan by Ohta (1983) and the continental slope off east Greenland by Mayer and Piepenburg (1996). ANOVA was performed by location after the data were ln+1 transformed. The data were normally distributed (K-S test of normality $p>0.05$), but variances were not equal (Levene's test for homogeneity $p<0.05$). However, ANOVA is robust with departures from homogeneity. Results of ANOVA indicate that megafaunal densities were significantly different ($p<0.05$) by location. Because equal variances could not be assumed Tamhane's was used for multiple comparisons. Results of multiple comparisons indicate that megafaunal density numbers were significantly different ($p<0.05$) between the GoM, Greenland, and Japan. Megafaunal densities were up to two orders of magnitude higher than the GoM on the continental slope off Greenland and up to an order of magnitude higher in Suruga Bay, Japan (Figure 8-173).

Megafaunal densities from photographs taken during DGoMB and NGoMCSS were compared with one another by site, transect, region, and program. ANOVA results indicate that megafaunal density was not statistically different from NGoMCSS for any of these cases. Furthermore, the studies share four out of the top six taxa by density. While NGoMCSS results list four more groups than DGoMB, these are all groups that are relatively rare with less than eight individuals/ha appearing study wide. Therefore, it would seem that the megafaunal populations of the northern GoM continental slope have not changed significantly in the past 15 years in terms of numbers and types of animals.

Food availability, it has been suggested, is the single most important factor affecting benthic megafaunal distribution (Sokolova 1959). This factor manifests itself in abundance and biomass, which both typically exhibit negative linear functions of depth and distance from shore. As depth increases, there is a greater chance for the remineralization and use of organic matter before reaching the benthos. For the megafauna, this means decreased biomass as food decreases with depth (Lampitt et al. 1986). As distance from shore increases, surface production decreases because of a decrease in primary producers, resulting in a commensurate decrease in both benthic abundance and biomass.

The low benthic biomass seen in equatorial regions is the result of both large nutrient-poor mid-oceanic gyres and high surface water temperatures that degrade organic matter at a higher rate. In contrast to these depauperate conditions, there are areas of upwelling – typically along western continental margins – where cold, nutrient rich waters increase surface production which in turn increases benthic abundance and biomass (Pfannkuche et al. 1983). In some instances too much surface production can lead to anoxia on the bottom (Thiel 1982).

Since food is the single most important factor in shaping the benthos (Sokolova 1959), it follows that in areas where food is concentrated, abundances will be as well. This is seen with chemosynthetic seep communities and might explain the intense concentration of *Peniagone* sp. seen in the central gulf during NGoMCSS cruise 3. In the case of the seep communities, the food source is presumed to be constant over some finite period of time, while for *Peniagone* sp., the food source may be more transient or intermittent in both time and space. Photography or trawls have not sampled this group on three subsequent visits to the area. Transient food resources are likely a forcing factor for many members of the benthic megafauna. Overall it appears that while megafauna numbers and composition change on the small scale in response to localized conditions, they still remain constant on the whole.

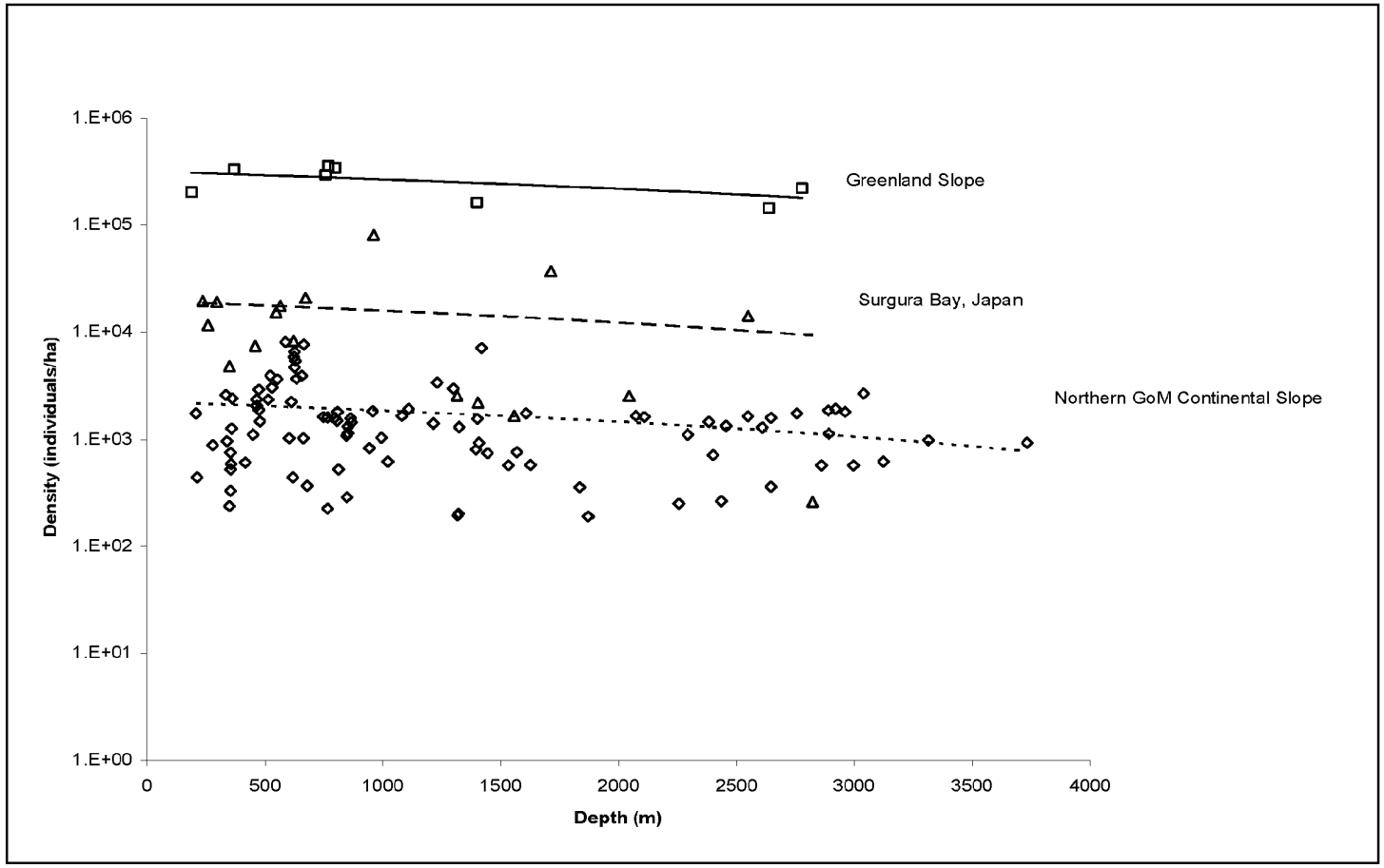

Figure 8-173. Total megafaunal densities (individuals/ha) from the northern GoM continental slope (open diamonds), the slope off east Greenland (open squares), and Suruga Bay, Japan (open triangles).

Aside from seeps and the *Peniagone* sp. grouping, there is statistically no significant trend for the accumulation of megafauna on a particular area of the northern GoM continental slope. ANOVA showed that megafaunal densities remained constant between the eastern and western gulf, between large basin features and the adjacent slope, and between canyons and non-canyon areas. While there was a statistically significant difference shown in DGoMB eastern and western GoM densities, this result might best be explained by sampling effort, an issue that will be discussed later. Furthermore, there does not appear to be any relationship between total megafauna density (individuals/ha) and depth. Examination of individual taxa relationships with depth indicates that some of the more common and widely distributed groups—the decapods and demersal fishes—exhibit a negative linear relationship with depth (Figures 8-174 and 8-175). Any general trend seen overall in the density data might be attributed to these two groups. The less common scaphopods exhibited a positive linear relationship with depth (Figure 8-176). Their small size and difficulty in identifying as dead or alive makes conclusions regarding this group difficult.

In general, most activity appears to be centered on the Mississippi Trough area where the highest densities for DGoMB were seen. The highest densities for NGoMCSS were seen just to the east of this area and the *Peniagone* sp. grouping was seen just to the west of it. Further, the distributions of nearly all other features of interest—the trash, pteropod tests, and ironstone (Figures 8-160 to 8-163)—were centered on the trough. Increased activity around the trough is evidence that it is an area of enhanced food resources.

Of all the items seen in the slope photographs, the distribution of *Sargassum* might hold the most interest. Thought to be an important source of energy to the benthos, *Sargassum* can have a long residence time on bottom (Schoener and Rowe 1970). Using combined data from both DGoMB and NGoMCSS, linear regression analysis showed that *Sargassum* exhibited a positive linear relationship with depth (Figure 8-177).

The distribution of *Sargassum* densities from photographs indicates that there were three general areas on the northern GoM continental slope where this plant material is accumulated: the eastern slope, the central slope, and the far western slope, supposedly with zones of no accumulation in between. Furthermore, there appears to be a gradient in density of *Sargassum*, with the lowest values being found in the east and the highest in the west. At first glance the distribution of *Sargassum* seems counterintuitive. It would appear however that *Sargassum* was accumulating in areas with decreased biological activity—the western and deep GoM. The lower densities of *Sargassum* seen in areas with more activity may reflect higher utilization of the plant material by the benthic fauna.

GoM megafauna in worldwide terms are depauperate when compared with similar photographic studies at higher latitudes. There appears to be a latitudinal gradient in megafaunal density with the highest values found in Greenland and the lowest values found closer to the equator in the GoM (Figure 8-178). Latitudinal gradients in the deep-sea benthos have been observed in terms of diversity before (Rex et al. 1993). Differences in surface production, habitat variability, and available substrate might all be reasons for the differences in densities observed.

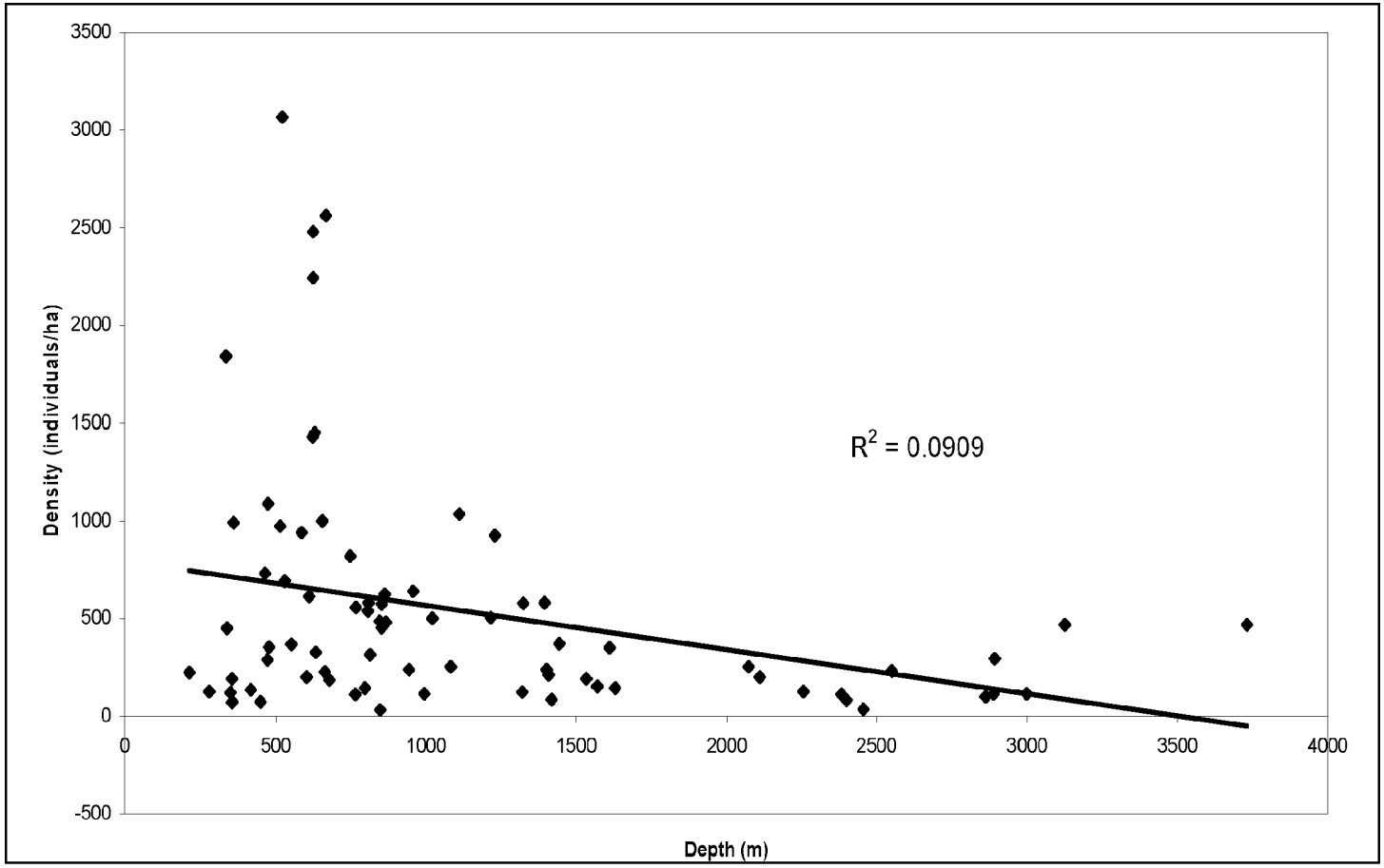

Figure 8-174. Decapoda density (individuals/ha) from both DGoMB and NGoMCSS photos as a function of depth.

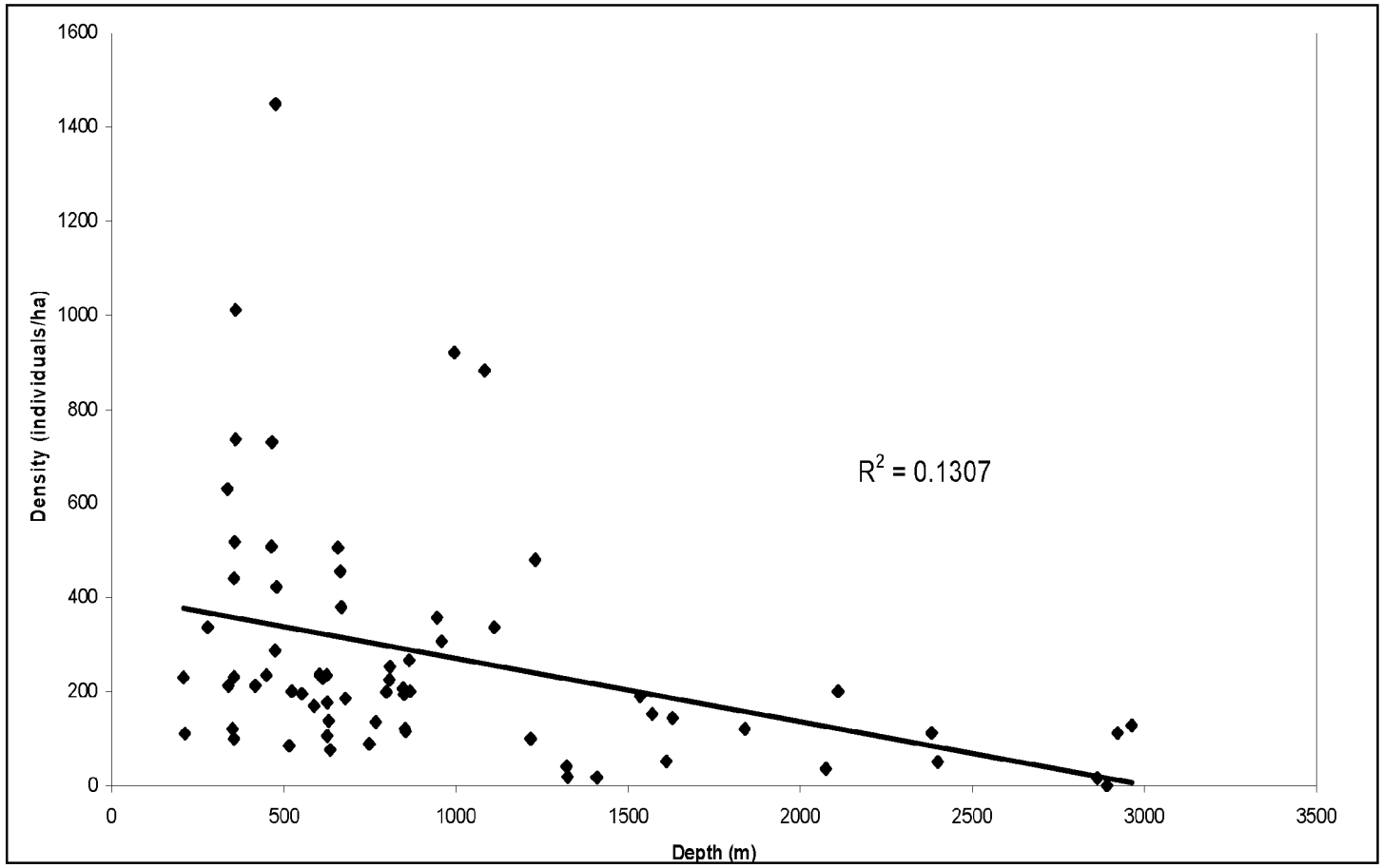

Figure 8-175. Demersal fish density (individuals/ha) from both DGoMB and NGoMCSS photos as a function of depth.

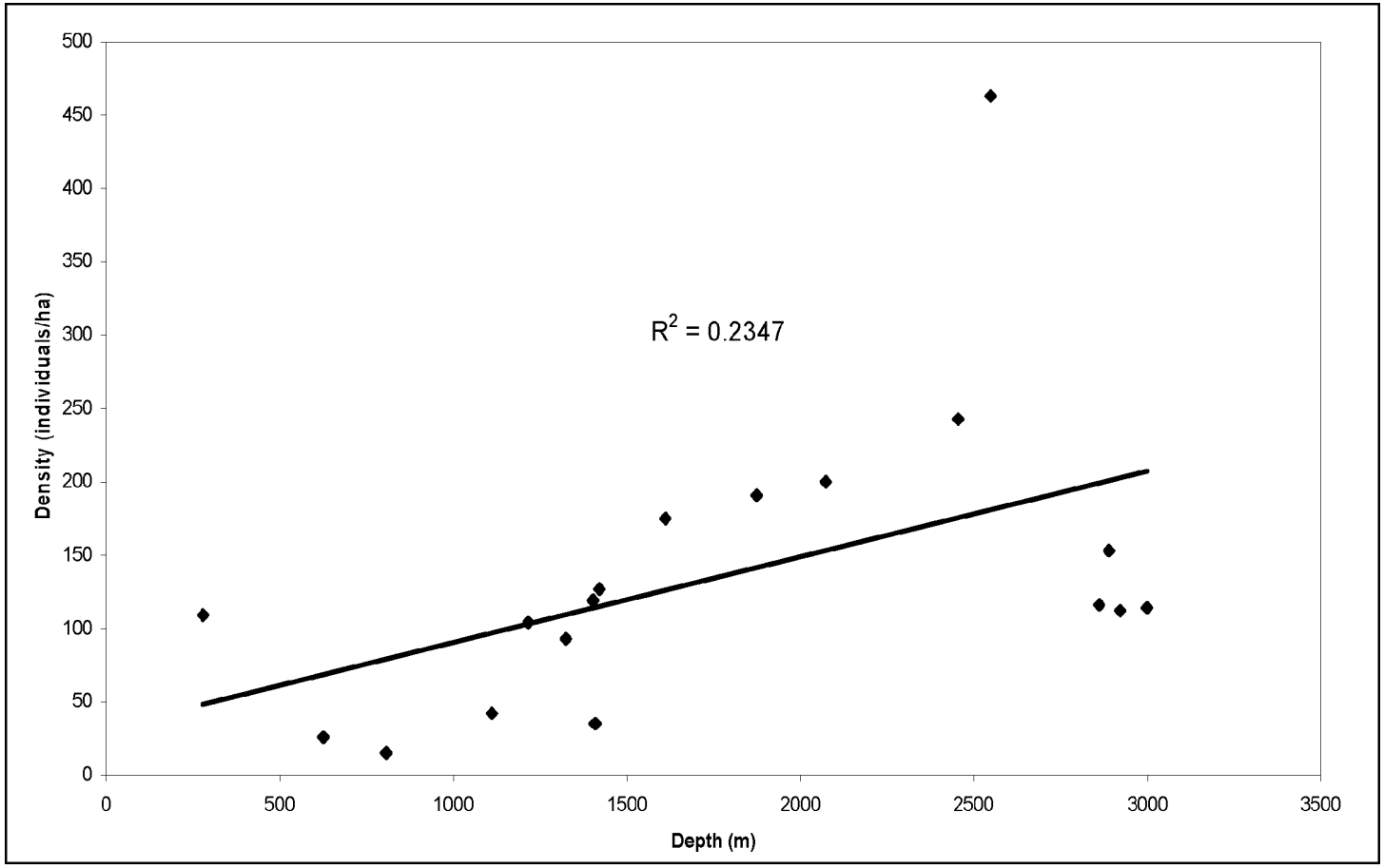

Figure 8-176. Scaphopoda density (individuals/ha) from both DGoMB and NGoMCSS photos as a function of depth.

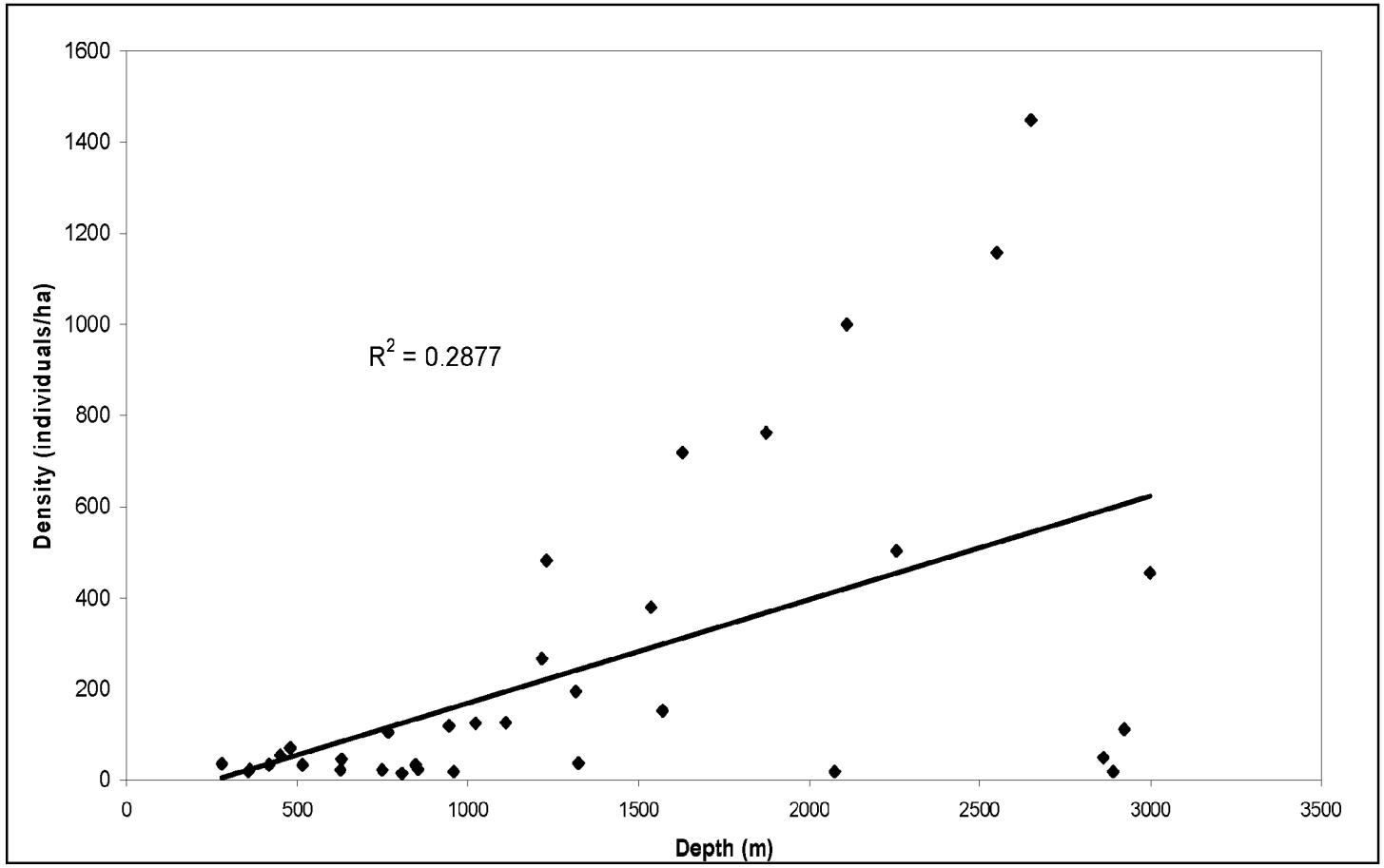

Figure 8-177. *Sargassum* density (individuals/ha) from both DGoMB and NGoMCSS photos as a function of depth.

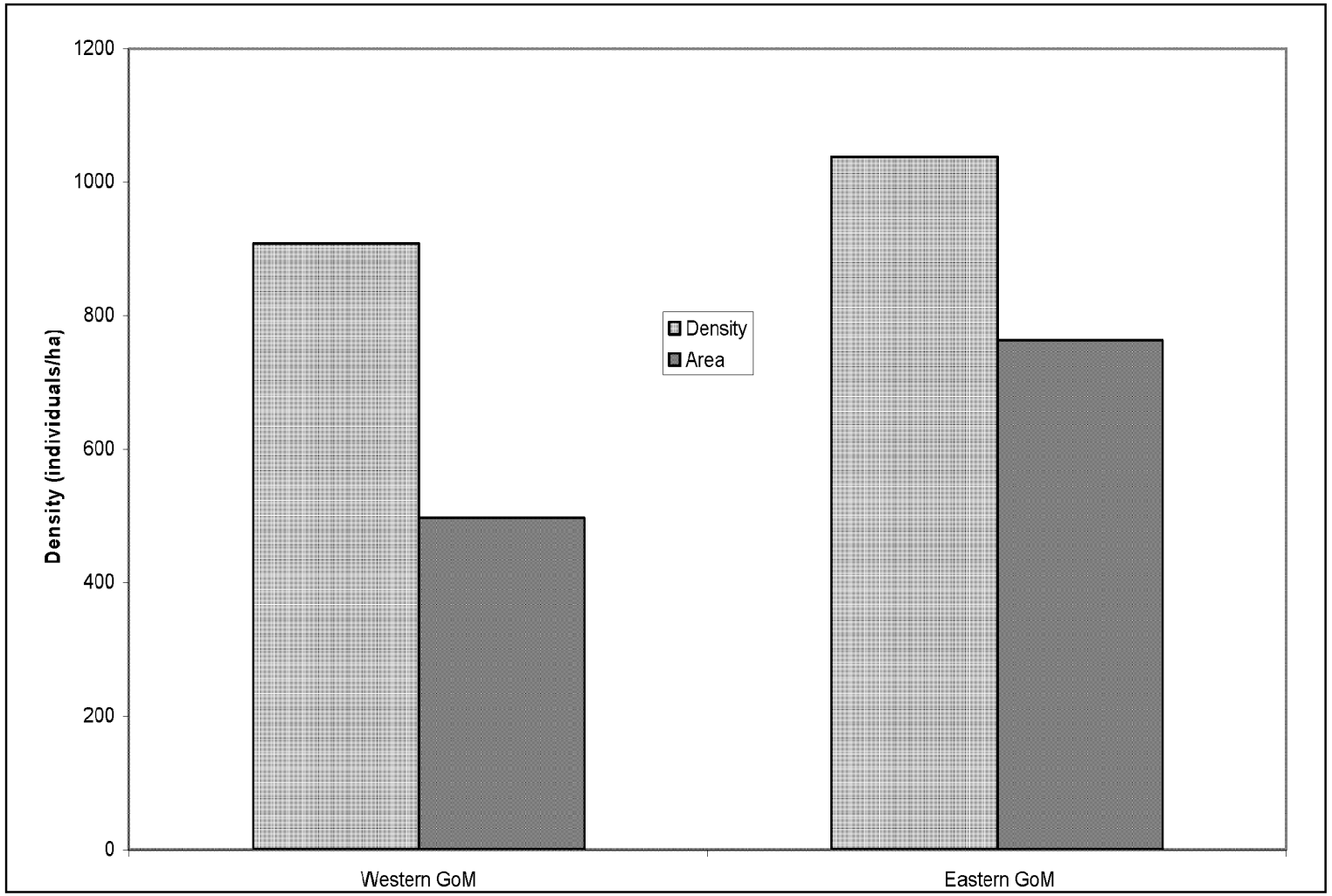

Figure 8-178. Eastern and western continental slope megafaunal densities (individuals/ha) and area surveyed (m^2).

8.8.6 Demersal Fishes (John McEachran, TAMU, and Richard Haedrich, MUN)

Trawling for demersal fishes was conducted during 2000, 2001, and 2003 surveys of the Deepwater Program: Northern Gulf of Mexico Study (DGoMB). However, the only comprehensive survey occurred in the 2000 survey. During the 2000 survey fishes were captured at 31 of the 43 stations representing all of the DGoMB transects (Figure 8-179). During the 2001 survey trawl collections were taken at only two of the stations (MT1 and S42). In 2003 trawling was conducted outside of the survey area. Because of the disparities in coverage among the surveys only the 2000 survey is included in this report. This report describes the species composition, distribution, relative abundance and diversity over the study area, and to test three hypotheses generated by the DGoMB project. A longer version of this report was previously published.

A total of 1065 individual demersal fishes, representing 119 species and 42 families, were collected in the 31 trawl collections conducted on the 2000 survey (Figure 8-180). The families Macrouridae (grenadiers or rattails), with 21 species; Ophidiidae (cuskeels), with 15 species; and Alepocephalidae (slickheads), with eight species, dominated the samples. Families of secondary importance were: Halosauridae (halosaurs), with four species, Ipnopidae (tripodfishes), with four species, Moridae (morid cods), with two or three species; and Trichiuridae (cutlassfishes) with two or three species. Discrepancies in number of species within families were due the inability, due to damage, to identify some fishes to species. A total of 34 specimens, representing 11 species and 10 families of demersal fishes, were captured at two stations (MT1 and S42) on 2001 survey. Three of the species and two of the families represented on the 2001 survey were not captured on the 2000 survey. For the two surveys a total of 121 demersal species representing 44 families were captured.

A cluster analysis (Bray-Curtis Dissimilarity Coefficient) was used to group stations by species composition and relative abundance. The analysis, based on 19 stations at which a minimum of five species were captured, grouped fishes into four nearly discrete depth assemblages (Figure 8-180). These assemblages consisted of: an outer continental shelf assemblage between 188 and 216 m, an upper slope assemblage between 315 and 785 m, a mid-slope assemblage between 686 and 1,369 m, and a deep assemblage between 1,533 and 3,075 m. The similarity analysis suggested that depth is the major factor determining species distributions and that the upper slope and mid-slope assemblages were more similar in species composition than either was to the deep assemblage and outer continental shelf assemblage. The outer continental shelf assemblage was most distinct.

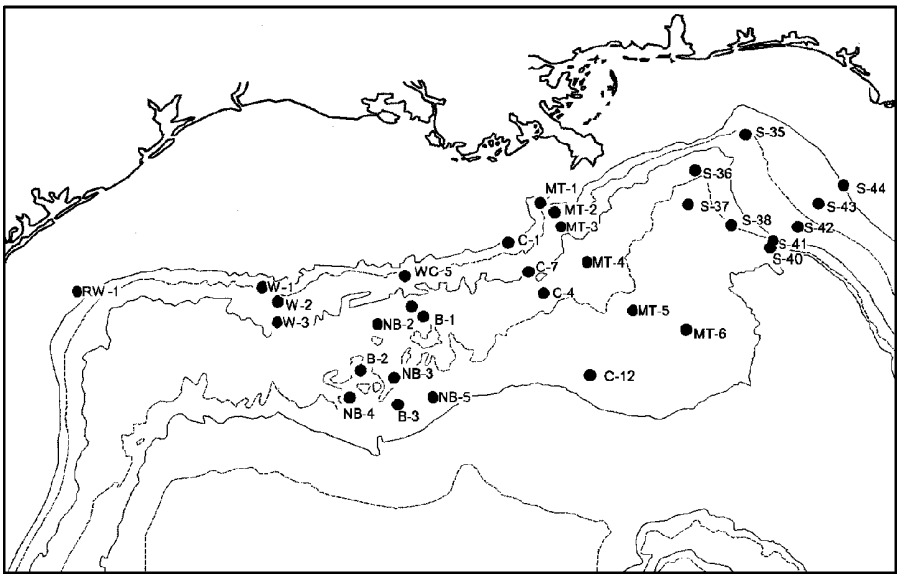

Figure 8-179. DGoMB stations in the northern Gulf of Mexico that yielded fish specimens on the 2000 survey. Depth contours are 200 m (solid line), 500 m (dashed line), 1,000 m (solid line), 2,000 m (dashed line), and 3,000 m (solid line). Outer Continental Shelf Stations: RW-1, S-44 (188-216 m); Upper Slope Stations: C-1, MT-1, S-42, S-43, W-1, W-2 (315-785 m); Mid-Slope Stations: C-4, C-7, MT-2, MT-3, MT-4, S-35, W-3, WC-5 (686-1,369 m); Deep Stations: B-1, B-2, B-3, C-12, MT-5, MT-6, NB-2, NB-3, NB-5, S-36, S-37, S-38, S-40, S-41, W-6 (1,533-3,075 m).

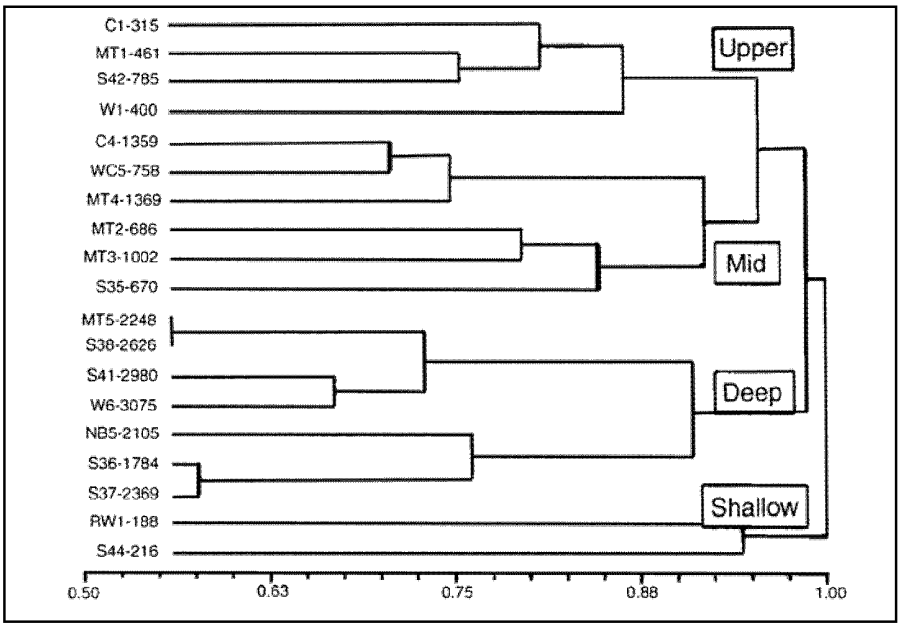

Figure 8-180. A cluster analysis of the DGoMB stations at which a minimum of five fish species were captured using the Bray-Curtis Dissimilarity Coefficient. The stations are indicated by their codes (Figure 8-179) and depth at the start of the trawl.

A total of 16 species representing 12 families were captured at the two outer continental shelf stations. The most species rich families were Paralichthyidae (summer flounders), with three species; and Bothidae (lefteyed flounders), with two species. The remaining families were represented by one species each. The most abundant species were *Antigonia capros* (Figure 8-181, Caproidae: boar fishes) and *Peristedion miniatum* (Figure 8-182, Peristediidae: armored searobins), making up 52% and 15% of the specimens, respectively.

Forty-seven species representing 27 families were captured at the six upper slope stations. The most species rich family was Macrouridae (grenadiers), with 14 species. The other 26 families were represented by one or two species each. The most abundant species were *Caelorinchus caribbaeus* (Figure 8-183, Macrouridae) making up 11.6%, *Steindachneria argentea* (Steindachneriidae: luminous hake) making up 8.3%, and *Yarella blackfordi* (Phosichthyidae: lightfishes) making up 7.8% of the specimens, respectively.

Forty-five species representing 22 families were capture at the eight mid-slope stations. The most species rich families were Macrouridae, with 14 species and Alepocephalidae (slickheads), with four species. The 20 other families were represented by one or two species each. The most abundant species were *Nezumia cyrano* (Macrouridae), *Coryphaenoides zaniophorus* (Macrouridae), and *N. aequalis* (Macrouridae) making up 15.8%, 13.8%, and 11.1% of the specimens, respectively.

A total of 32 species representing nine families were captured at the deep stations. The most species rich families were Ophidiidae (cuskeels), with 12 species; Alepocephalidae, with six species; and Ipnopidae (tripod fishes), with three species. The six other families were represented by one or two species each. The most abundant species were *Dicrelene kanazawai* (Ophidiidae) and *Bassozetus robustus* (Ophidiidae) making up 11.8% and 9.9% of the specimens, respectively.

The largest numbers of fishes per unit of effort were obtained from the upper slope and mid-slope stations (Figure 8-184). The deep stations produced the least number of fishes per unit effort. Across the station transects, the greatest numbers of fishes per unit effort were obtained from transects along the Mississippi Trough and the DeSoto Canyon (Figure 8-185). The lowest abundances occurred at the stations to the west the Mississippi.

The upper slope and mid-slope zones had the greatest and second greatest species richness, respectively, among the four depth zones, and the deep zone had considerably greater species richness than the outer continental shelf zone (Figure 8-186). Across the station transects the greatest species richness occurred along the Mississippi Trough and DeSoto Canyon transects (Figure 8-187). With one exception (W-2), stations to the west of the Mississippi had relatively low species richness.

The upper slope zone had the greatest H' diversity, followed closely by the deep and the mid-slope zones (Figure 8-188). The outer shelf zone had the lowest species diversity.

Figure 8-181. June 11, 2000. Boar fishes, Antigonia capros, collected from the trawl at S44.

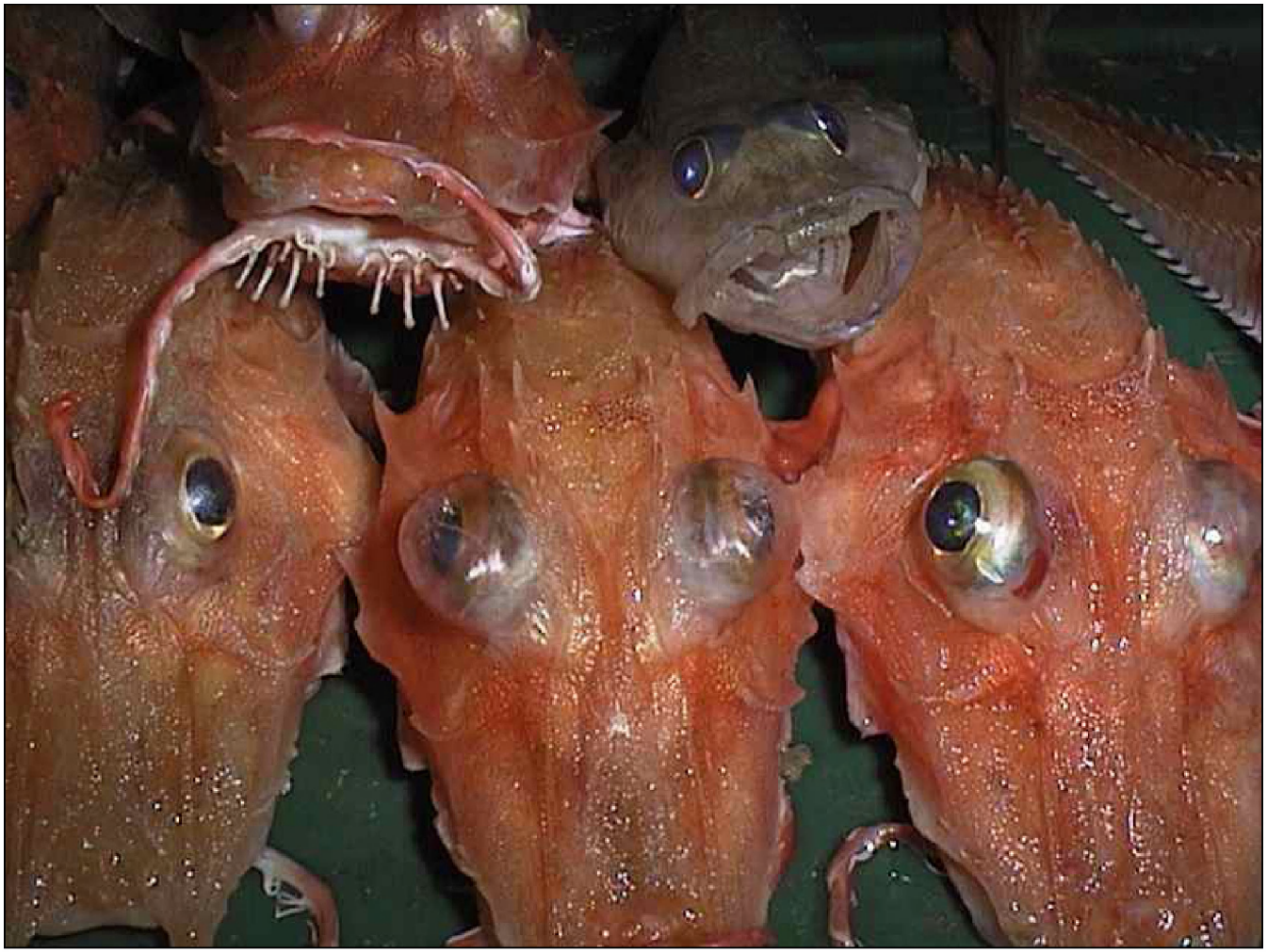

Figure 8-182. June 11, 2000. Armored searobins, *Peristedion miniatum*, collected from the trawl at S44.

Figure 8-183. June 17, 2000. *Caelorinchus caribbaeus* collected from the trawl at MT1.

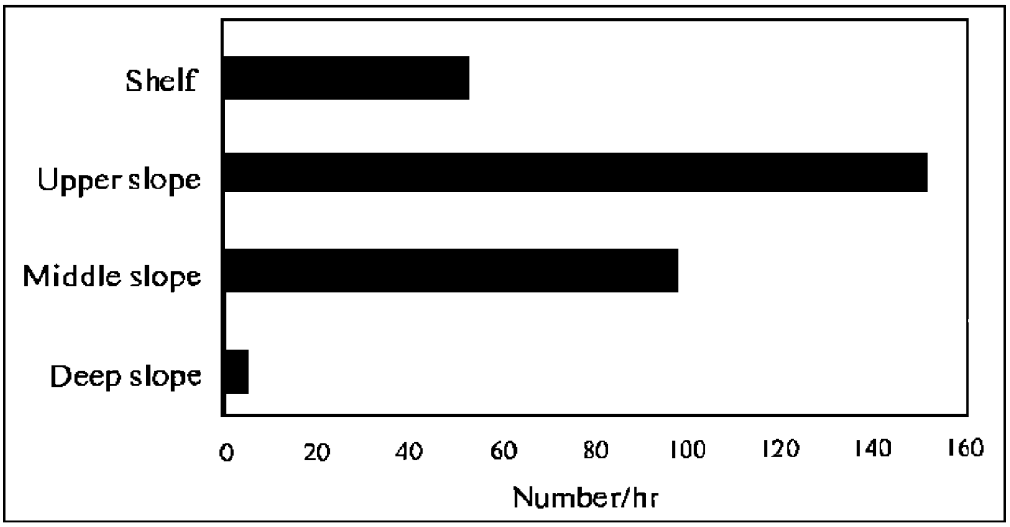

Figure 8-184. Abundance (catch per unit effort) of fishes at each of the four depth.

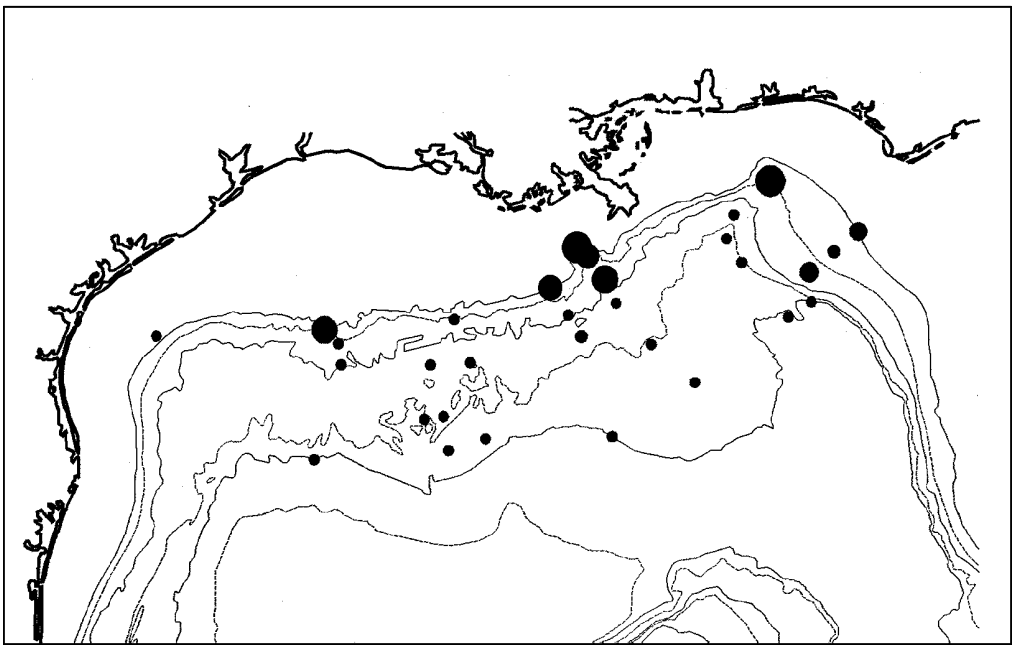

Figure 8-185. Abundance, scaled as the log of number/hour, of the fishes at each DGoMB trawl station. Largest symbol equals a catch per unit effort of 290 fishes/hour. Remaining symbols are scaled accordingly.

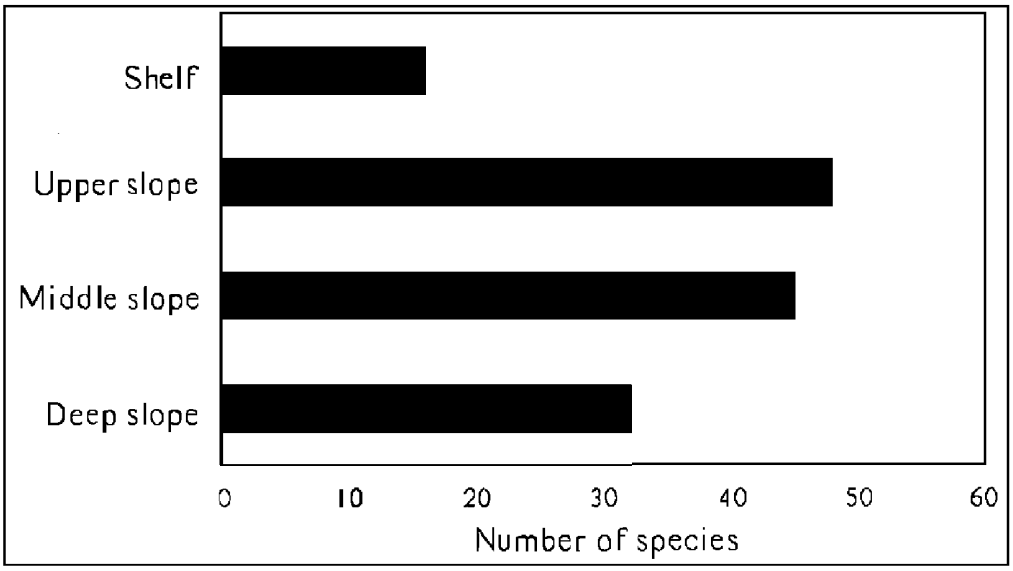

Figure 8-186. Species richness of the fishes represented as number of species at each of the four depth zones.

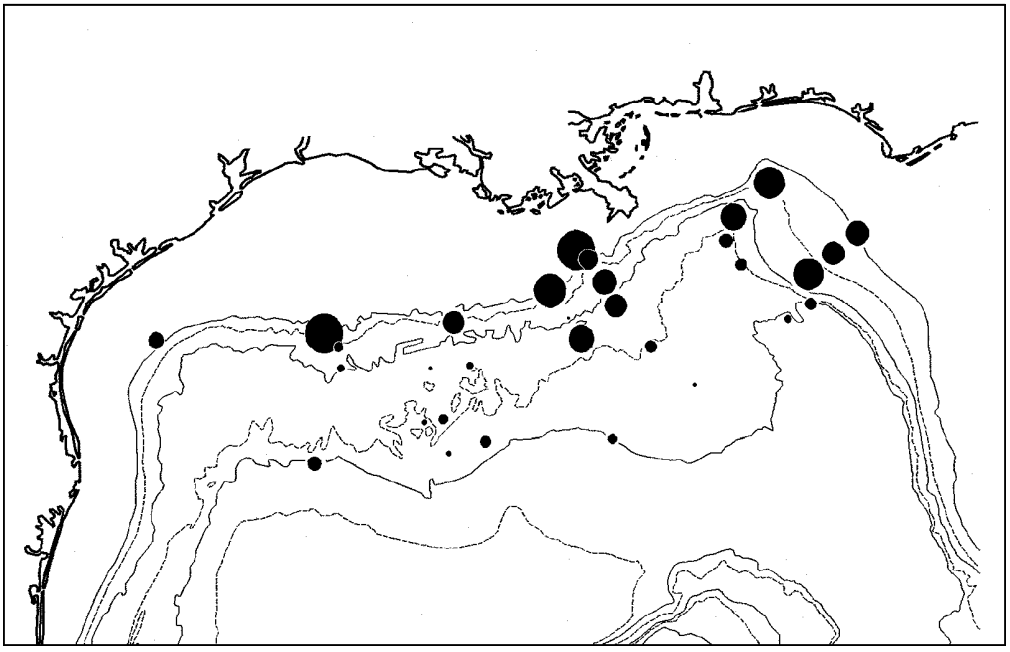

Figure 8-187. Species richness of fishes scaled as number of species at each DGoMB station. The largest symbol equals 18 species. The remaining symbols are scales accordingly.

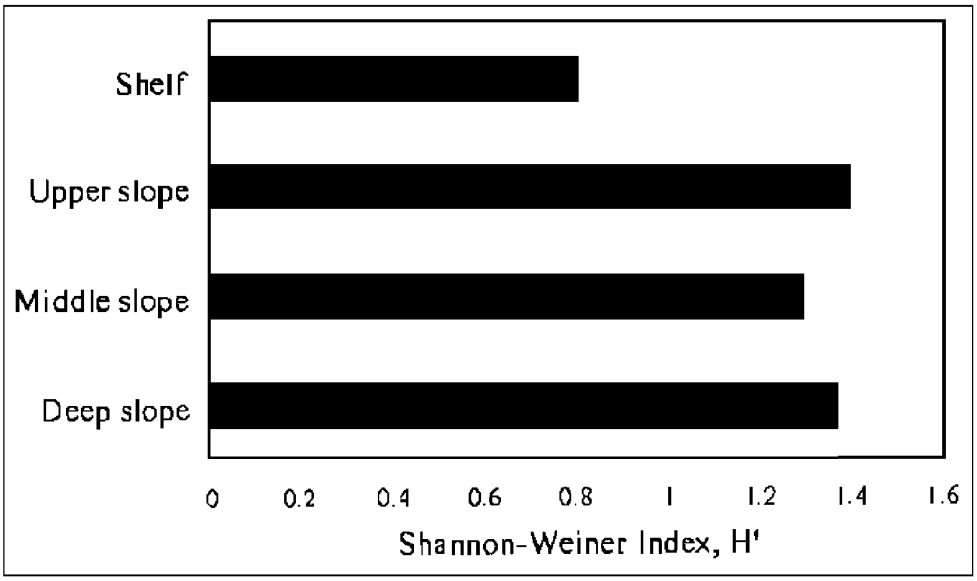

Figure 8-188. Species Diversity (H') of the fishes in each of the four depth zones.

The first hypothesis states that variation in demersal fauna is correlated with depth. The highest catch per unit effort (CPUE), greatest species richness, and highest species diversity are on the upper slope zone (Table 8-41). The next highest catch per unit effort and species richness are at the mid-slope zone. The deep zone had the second highest species diversity. The relatively low percent overlap among the zones suggests that they are well defined. With exception of the outer shelf zone fish species diversity appears to be strongly inversely correlated with depth. The data for the outer shelf zone are based on only two stations and the low values are probably due to sampling error.

Table 8-41

Fish Faunal Data for All 31 Stations by Depth Zones

Depth Zones	Shelf	Upper slope	Mid-slope	Deep
CPUE	52.8	152	98	5.2
Species	16	48	45	32
H' Diversity	0.80	1.39	1.29	1.36
% overlap	3.2	16.8	5.9	

The second hypothesis states that the fauna exhibit an east-to-west gradient. Comparisons lumping the outer shelf and upper slope zones revealed that the greatest abundance of fishes were obtained at the stations along the Mississippi Trough and the Central transects and the greatest species richness and H' diversity occurred at the stations along the West and East transects (Table 8-42). The stations along the Mississippi Trough had the greatest fish abundance and the stations along the West transects had greatest species richness and H' diversity. The percent overlap between the four areas varied from 9.9 to 22.8 suggesting that the regions are

rather distinct from one another. The Mississippi Trough was treated separately from the remainder of the Central Area transects because at shallow depths it is well defined feature of the bottom of the Central Area.

Table 8-42

Faunal Comparisons Among Four Groups
of Outer Continental Shelf and Upper Slope Stations
(The last % overlap value is between East and West transects.)

Shelf / Upper Slope (n=10)	West	Central	Trough	East
CPUE	65.3	196.0	234.0	103.0
Species	36	15	27	34
H' Diversity	1.28	0.81	1.14	1.22
% overlap	9.9	13.4	22.8	16.9

Comparisons lumping the mid-slope and deep zones revealed that the stations along the East transects had the highest abundance off fishes, and the greatest species richness and H' diversity (Table 8-43). The lowest abundance occurred at stations along the West transects, and the lowest species richness and H' diversity occurred at stations along the Central transects. The comparisons failed to reveal a consistent east-to-west gradient. The percent overlap among the three areas is considerably greater than the percent overlap between the two shallow zones and the greatest overlap is between the stations along the East and the West transects.

Table 8-43

Faunal Comparisons Among Three Groups
of Mid-Slope and Deep Stations
(The last % overlap value is between East and West transects.)

Lower Slope/Rise (n=15)	West	Central	East
CPUE	3.4	4.0	8.1
Species	17	10	21
H' Diversity	1.13	0.94	1.23
% overlap	24.1	30.8	51.1

The third hypothesis states that the basin faunas are distinct from the non-basin faunas. Comparisons lumping three stations from oceanographic basins and lumping the three stations from non-basin areas suggests that fish abundance, species richness, and H' diversity were higher in non-basins than in basins (Table 8-44). However, the differences are slight and the sample sizes are low. Percent overlap in species composition is rather low but again differences may reflect the small sample sizes.

Table 8-44

Faunal Comparisons between
Basins and Non-Basins

Lower slope (n=6)	Basin	Non-basin
CPUE	2.3	4.0
Species	6	8
H' Diversity	0.73	0.86
% overlap	31.3	

The DGoMB survey suggests that demersal fishes of the northern GoM are divided into four depth assemblages: outer continental shelf, upper slope, mid-slope, and deep slope. The outer continental shelf assemblage extends from 188 to 216 m. This zone yielded the third highest abundance and lowest species richness and lowest H' species diversity among the four depth zones. The upper slope assemblage extends from the 315 and 785 m. This zone yielded the highest abundance of fishes, the greatest species richness and highest H' species diversity. The mid-slope assemblage extends from the 686 and 1,369 m zone and thus partially overlaps the upper slope zone. This zone yielded the second highest abundance, second greatest species richness and the third highest H' diversity of fishes. The deep assemblage extends from the 1533 and 3,075 m depth zones. This zone yielded the lowest abundance, and second lowest species richness and second highest H' diversity of fishes. The greatest amount of overlap occurred between the upper and mid-slopes. The high overlap may partially be due to the fact that the two zones overlapped but also to the fact that there are distinct differences between the species and families occurring on the upper and mid-slope from those occurring on the upper slope and rise.

The 2000 DGoMB survey captured a total of 119 demersal fish species representing 42 families. Pequegnat (1983) captured 206 demersal fish species in the 10 year (1964-1973) survey of the northern GoM and the Texas Cooperative Wildlife Collection (TCWC) houses 208 demersal deep-sea fish species, representing 72 families from the northern GoM. Thus the 2000 DGoMB survey sampled about 57.2% of the species and 58.3% of the families of fishes thought to regularly occur in the northern GoM. McEachran and Fechhelm (1998 and in press), recorded 233 demersal deep-sea fishes, representing 72 families, from the northern GoM. Thus the DGoMB survey sampled 45.5% of the species and 48.6% of the families known from the northern GoM.

The families Macrouridae, with 21 species; Ophidiidae, with 15 species; and Alepocephalidae, with eight species, dominated the samples on the 2000 DGoMB survey, and the families Halosauridae, with four species, Ipnopidae, with four species, Moridae, with three species; and Trichiuridae, with three species were of secondary importance. Pequegnat (1983) also found Macrouridae, Ophidiidae, and Alepocephalidae to be the most specious families followed by Gadidae (=Phycidae, Merlucciidae, Steindachneriidae, and Moridae), Bothidae (=Bothidae, Parilichthydae), and Rajidae. Halosauridae and Trichiuridae were less species rich in Pequegnat (1983) than in the present survey and Rajidae (skates) was represented by more species in Pequegnat (1983) than in the present study. Ipnopidae was well represented in both surveys (listed as Bathypteroidae in Pequegnat 1983). Records of demersal deep-sea fishes in the TCWC and in McEachran and Fechhelm (1998 and in press) also suggest that the above families are some of the dominate components of the demersal deep-sea fauna of the northern GoM. There are 37 species of Macrouridae, 24 species of Ophidiidae, 14 species of Alepocephalidae,

four species of Halosauridae, eight species of Ipnopidae, four species of Moridae, and six species of Trichiuridae in the northern GoM (McEachran and Fechhelm, 1998 and in press). Thus the 2000 DGoMB survey sampled 56.8% of the Macrouridae, 62.5% of the Ophidiidae, 57.1% of the Alepocephalidae, 100% of the Halosauridae, 50% of the Ipnopidae, 75% of the Moridae, and 50% of the Trichiuridae in the northern GoM. Other families such as Rajidae, Dalatiidae (spiny sharks), and Peristediidae (armored searobins) that have relatively high species diversity in the northern GoM (McEachran and Fechhelm, 1998 and in press) were poorly represented in the present survey. Thus the DGoMB survey sampled the dominant demersal fish families according to their presumed relative diversity in the northern GoM.

The DGoMB survey included two stations on the outer continental shelf at which a total of 16 species representing 12 families were collected. The most species rich family was Paralichyidae and the most abundant species were *Antigonia capros* and *Peristedion miniatum*. Pequegnat (1983) listed *Poeciliopsetta beani* (Pleuronectidae), *Hymenocephalus italicus* (Macrouridae), and *Pontinus longispinus* (Scorpaenidae) as the most abundant species at this depth zone. According to the holdings of the TCWC about 139 demersal fish species in 50 families are normally encountered on the outer continental shelf of the northern GoM, and about half of these species also occur on the upper slope. Thus the outer continental shelf was not adequately surveyed in this study and the values given for this zone may not reflect the species assemblage.

The present survey found Macrouridae to be the most abundant family on the upper slope, with *Caelorinchus caribbaeus* the most abundant species. Pequegnat (1983) also found Macrouridae to be the most abundant family on the upper slope, with *Nezumia aequalis*, *Bathygadus melanobranchus*, and *Corphaenoides colon* being the most abundant species in the family. All of the macrourids captured on Pequegnat's study were captured on the present study, however, specimens classified as *C. colon* in Pequegnat (1983) are now identified as *C. zaniophorus*. *Caelorinchus caribbaeus* was abundant but not dominant in Pequegnat's study. *Dibranchus atlanticus* (Ogcocephalidae: batfishes) and *Symphurus marginatus* (Cynoglossidae: tonguefishes) were the first and fourth most abundant species on the upper slope in Pequegnat's study but neither was captured on the present study.

The DGoMB survey found Marcrouridae and Alepocephalidae to be the most specious families on the mid-slope, with *Nezumia cyrano*, *Coryphaenoides zaniophorus*, and *N. aequalis* the most abundant species. Pequegnat (1983) listed Macrouridae, Ophidiidae, and Alepocephalidae as the most abundant families in this depth zone, with *Gadomus longifilis*, *Dicrolene intronigra*, and *Synaphrobranchus oregoni/brevidorsalis* the most abundant species. All of these species were captured on the present study but *Coryphaenoides zaniophorus* was identified as *C. colon* in Pequegnat's survey.

The DGoMB survey found Ophidiidae, Alepocephalidae, and Ipnopidae to be the most specious families in the deep zone, with *Dicrelene kanazawai* and *Bassozetus robustus* (Ophidiidae) the most abundant species. Pequegnat (1983) listed Ophidiidae and Alepocephalidae as the most specious families in this depth zone, with *Dicrolene kanazawai*, *Lamprogramus*, *Bassozetus normalis*, and *Bathyonus pectoralis* as the most abundant species. *Lamprogramus* sp. and *Bathyonus pectoralis* were not captured on the present study.

Both the DGoMB survey and Pequegnat (1983) found that the demersal fish fauna of the northern GoM is subdivided into several depth assemblages. In the present study there are four assemblages: the outer continental shelf (188-216 m), the upper slope (315-785 m), the mid-slope (686-1,369 m), and the deep slope (1,533-3,075 m). The upper slope and mid-slope were

most similar in species composition and outer continental shelf had the most distinct species composition. Pequegnat (1983) described five depth assemblages: shelf/slope transition (150-450 m), archibenthal zone (475-950 m), upper abyssal zone (975-2,250 m), mesoabyssal zone (2,275-3,200 m), and lower abyssal zone (3,225-3,850 m). Similarity indices basally grouped the shelf/slope and archibenthal zones, and the abyssal zones, with the upper abyssal zone grouped with both the mesoabyssal and lower abyssal zones. Thus the present study found that outer shelf zone was distinct from the three slope zones while Pequegnat found greater similarity between zones either above or below 1,000 m than between zones above or below 200 m. Both studies agreed that the demersal fauna is strongly zoned by depths but not in how the four or five zones are linked by species composition. Part of the disparities may be due to sampling design and sampling intensity. The present study is based on a single year survey of 31 stations. Pequegnat was a seven year survey of 121 stations (86 skimmer dredge hauls, seven two meter dredge hauls, and 28 trawl hauls). Also Pequegnat sampled a greater number of stations on the outer continental shelf (10 versus 2 in the present study) and greater number of stations over a wider depth range in the deep slope zone (>1,533 m) (31 versus 15 in the present study). Thus the faunal composition of Pequegnat's study may better typify the outer shelf and deep slope zones than the present study.

Both the present study and Pequegnat (1983) corroborate the first hypothesis but not the second or third hypotheses of the DGoMB study. The first hypothesis states: Variation in demersal fauna is best correlated with depth. Similarity analyses based on species compositions grouped stations by depths in both studies. The faunal overlap between zones was relatively small suggesting that zones were distinct and the zones of the two studies showed a fair degree of overlap. However, affinities among the zones varied between studies. The present study suggested that the outer continental shelf zone was distinct from the three deeper slope zones while Pequegnat suggest that the two upper zones were distinct from the two or three deeper zones. Because of the differences in sampling intensity, the Pequegnat's. grouping may better present the affinities among the depth zones.

The second hypothesis states: Faunas exhibit an east-west gradient. Results of the present study demonstrate east-west differences in abundance, species richness, and H' diversity of demersal fishes. However, the differences do not suggest an east-west gradient. Comparisons among the two shallow zones indicated that the central transects had higher abundance and lower species richness and H' prime diversity values than either the west or east transects. Percent overlap was low among the transects but was higher between the east and the trough transects and lowest between the central and western transects. Comparisons among the two deeper zones indicated that the central transect had a higher abundance than the west transect but a lower abundance than the east transect. The central transects had a lower species richness and lower H' diversity than either the west or east transects. Percent overlap was relatively low among the transects but was highest between the east and west transects. Thus there is little indication of an east-west gradient of the demersal fishes.

The third hypothesis states: Basin faunas are different from non-basin faunas. Comparisons between the three basin and three non basin stations were not definitive possibly because of the small sample size.

8.8.7 Near-Bottom and Pelagic Fauna

8.8.7.1 ADCP Detection of Mobile Near-Bottom Fauna

Beginning in the second field year of the DGoMB study, a downward-looking RD Instruments Workhorse ADCP was deployed four times, for 27, 20, 55, and 26 hours at four stations in the northeastern GoM. In summer 2001 this ADCP looked down from 35 m above bottom at DGoMB process stations MT3, S42, S36, and MT6 so that near-bottom current velocity and near-bottom acoustic backscatter data could be collected concurrent with benthic lander deployments at these stations (Figure 8-189).

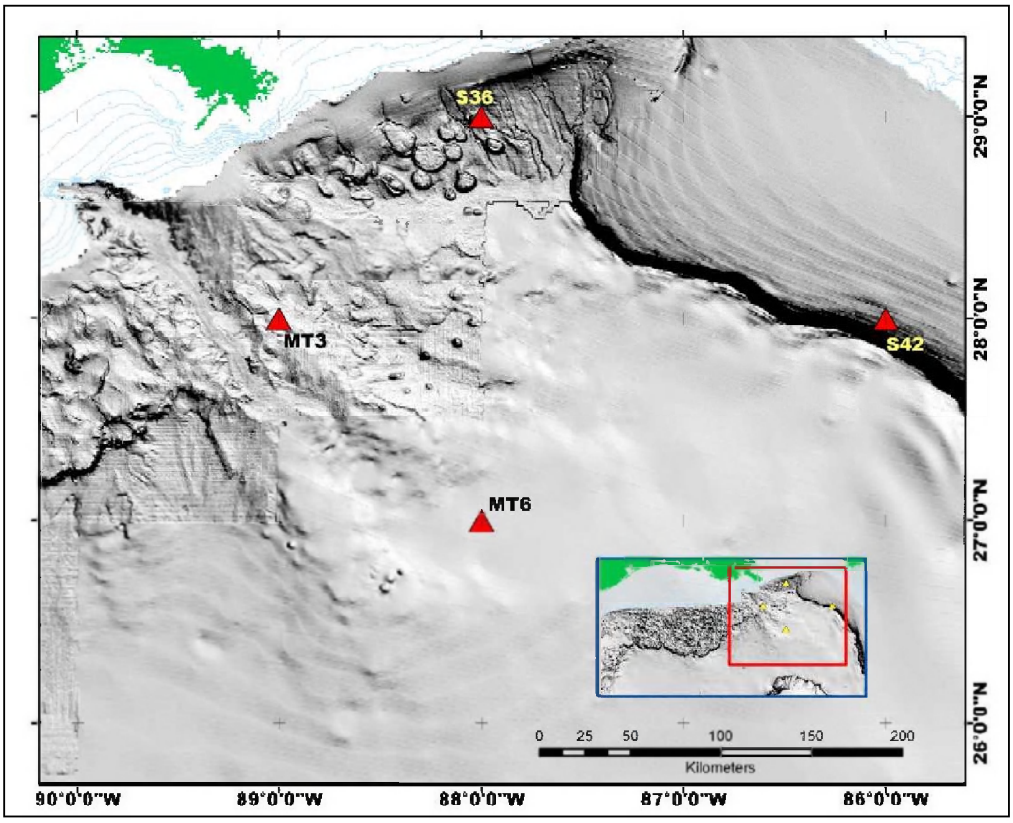

Figure 8-189. Process stations for the 2001 field year of DGoMB. The four ADCP deployment sites are marked with red triangles, and water depths for these deployments are indicated.

Additional Workhorse ADCP data were obtained from a deployment of 39 hours in April 2002 and from a deployment of four weeks duration in June-July 2002 (Figures 8-190 and 8-191). During the 2002 deployments, the Workhorse ADCP looked down from 60 m above bottom to give additional vertical information on how near-bottom current velocity and near-bottom backscatter intensity decreased with height into the water column immediately above the bottom.

It was intended that the ADCP backscatter data gained from these 2001 and 2002 near-bottom deployments would give comparative information about the mean biomass of small

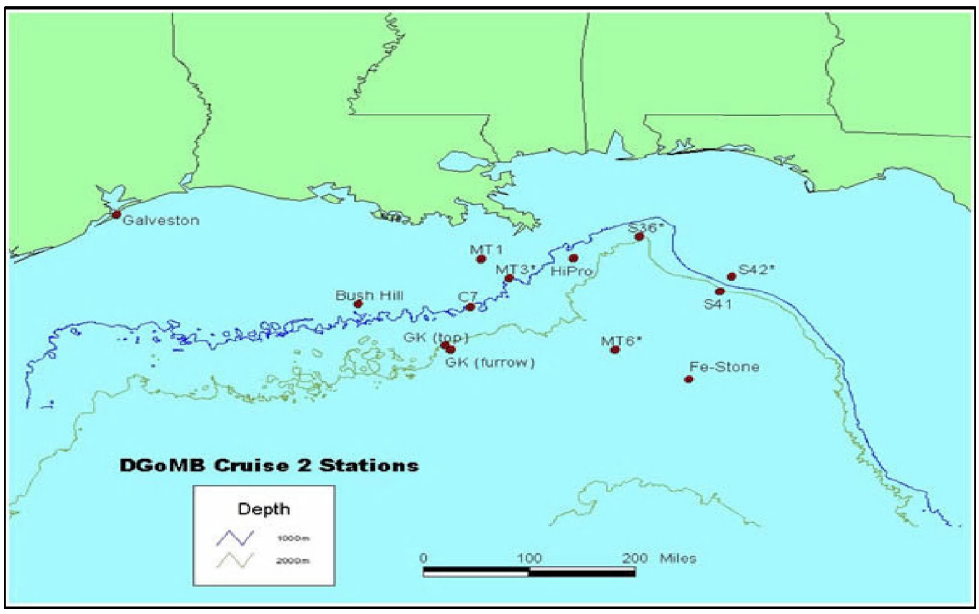

Figure 8-190.Sampling stations for the 2002 field year of DGoMB including station MT-1 (depth = 300 m) where the ADCP mooring was deployed for 39 hours in April 2002.

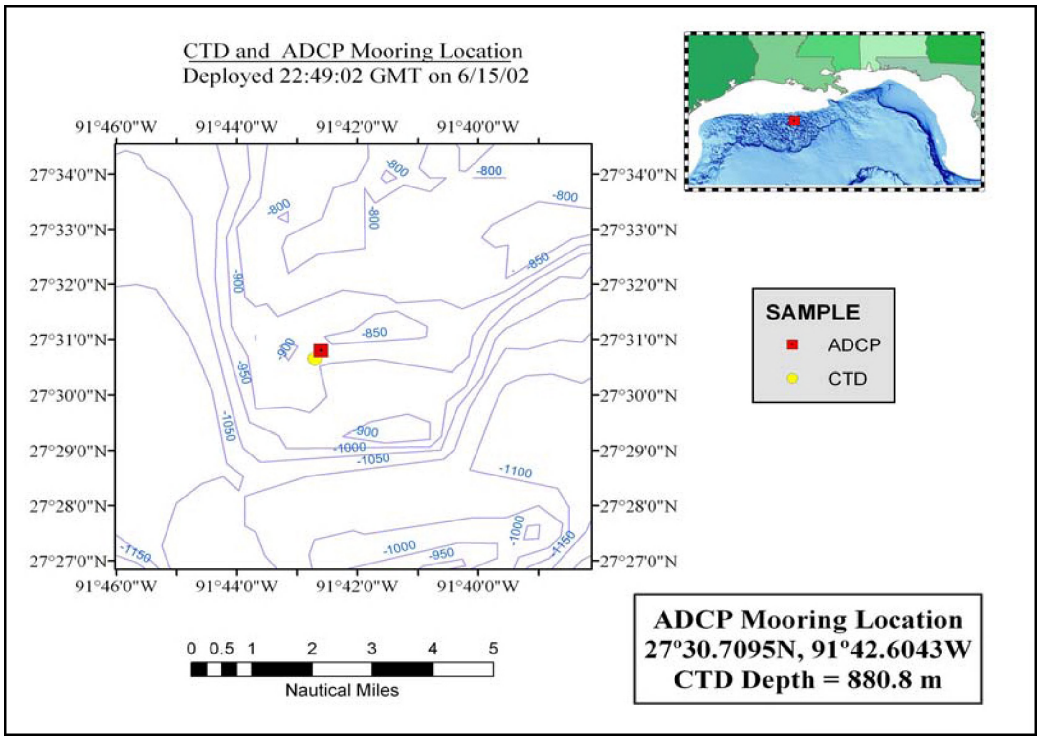

Figure 8-191. Location of the 14 June-12 July 2002 ADCP mooring in water depth of 880 m. Location of the CTD cast made 22:49 GMT on 14 June 2003 is also shown.

mobile near-bottom fauna that have previously been difficult to inventory, as well as whether

this backscatter would vary on a diel cycle. It was not possible to collect any of the organisms responsible for this near-bottom backscatter, however, because baited traps were not incorporated into the ADCP moorings.

To analyze the acoustic volume backscatter intensity signal (ABI) obtained by the Workhorse ADCP, we first converted the raw data from binary to ASCII format using the software program BBLIST (http://www.rdinstruments.com), along with the date and time that they were recorded. Programs written for the visual data analysis software program, PV-Wave, that were originally created by S.F. DiMarco and R.L. Scott for analysis of ADCP data collected during the DeSoto Canyon Eddy Intrusion Study, were used to correct the data for spherical spreading loss and to estimate the absolute backscatter coefficient, or S_v, in units of decibels. Table 8-45 summarizes the six deployment locations, details of data collection, and ABI averages.

The comparison of 4 deployments in different water depths in June 2001 showed that mean near-bottom backscatter intensity increased as the bottom was approached and was greatest at the stations with shallowest water depths (Figures 8-192a and b). The largest intensity and the most variability were seen in deployment two (S42), where the water depth was 755 m, and the smallest intensity and variability in deployment four (MT6), where the water depth was 2,740 m. There was also a higher mean and more vertically structured current velocity at deployment two (S42).

For each deployment, cross-correlation coefficients were calculated for each of the 12 depth bins investigated in this study. In general, correlation values decreased for each deployment as the vertical separation between the bins increased (Tables 8-46 and 8-47). There was no apparent phase change seen in the data collected during the four deployments to indicate diel vertical migration of scavengers or zooplankton. However, all stations with the possible exception of S42 (depth = 755 m) were below depths at which twilight should penetrate to give a day/night cue. Each of the deployments was less than 60 hours, so it was difficult to determine whether low frequency (multi-day) temporal variability in ABI was in fact present.

The data collected from the 39 h deployment at MT-1 at 300 m depth in April 2002 also showed that ABI increased near-bottom (Figure 8-193). When Bins 7 to 20 m above bottom were averaged, the mean ABI was –41 dB, whereas when only those bins 7 to 10 m off bottom were averaged, the mean ABI was 3 dB greater (–38 dB). This increase in mean backscatter as the bottom was approached was also evident in the four-week 14 June to 12 July 2002 record (Figure 8-194). The mean backscatter signal in bins averaged from 7 to 10 m above bottom (-74 dB) was again approximately 3 dB greater than in bins averaged from 7 to 20 m above bottom (-77 dB). As in the 2001 deployments, the correlation coefficients decreased with vertical distance between depth bins for both the 2002 records.

A signal with approximately one cycle per day (CPD) periodicity is present in the month-long, June-July 2002 record. This had not been seen in the April data or in the previous summer's ADCP deployments. This signal is surprising since, based on an average irradiance extinction coefficient of k = 0.05 for the deepwater northern GoM, the day/night light cue believed to initiate vertical migration in shallow water should not be present at 880 m. However, diurnal current oscillations present in this region may affect the abundance of scatterers at the deepwater mooring site. Between 3-4 July, there was a marked increase in the ABI measurements. This broad peak in ABI was seen throughout the ensonified column of water 10-60 m off bottom and represents a positive shift in ABI by about 7 dB (Figure 8-194). This event

Table 8-45

Summary Statistics for the Six Near-Bottom ADCP Deployments in 2001 and 2002

Station	Date/Time (local time)	Location	Water Depth	Average Backscatter (dB)
Deployment 1 Station MT-3	6/3/01 [noon] to 6/4/01 [3:00pm]	Lat 28°13.3N Lon 89°30.0W	935 m	-75.3 (7-29 m above bottom)
Deployment 2 Station S-42	6/6/01 [6:15pm] to 6/7/01 [2:00pm]	Lat 28°15.0N Lon 86°25.0W	755 m	-70.2 (7-29 m above bottom)
Deployment 3 Station S-36	6/9/01 [9:45am] to 6/11/01 [4:30pm]	Lat 28°55.2N Lon 87°40.1W	1,823 m	-78.3 (7-29 m above bottom)
Deployment 4 Station MT-6	6/12/01 [11:00pm]to 6/14/01 [00:30am]	Lat 27°00.0N Lon 88°00.0W	2,740 m	-82.0 (7-29 m above bottom)
Deployment 5 Station MT-1	4/7/02 [5:51am] to 4/8/02 [9:16pm]	Lat 28°54.0N Lon 89°83.0W	300 m	-42.0 (7-54 m above bottom)
Deployment 6 Louisiana slope	6/14/02 [4:30pm] to 7/12/02 [11:27am]	Lat 27°51.0N Lon 91°71.0W	880 m	-78.0 (7-55 m above bottom)

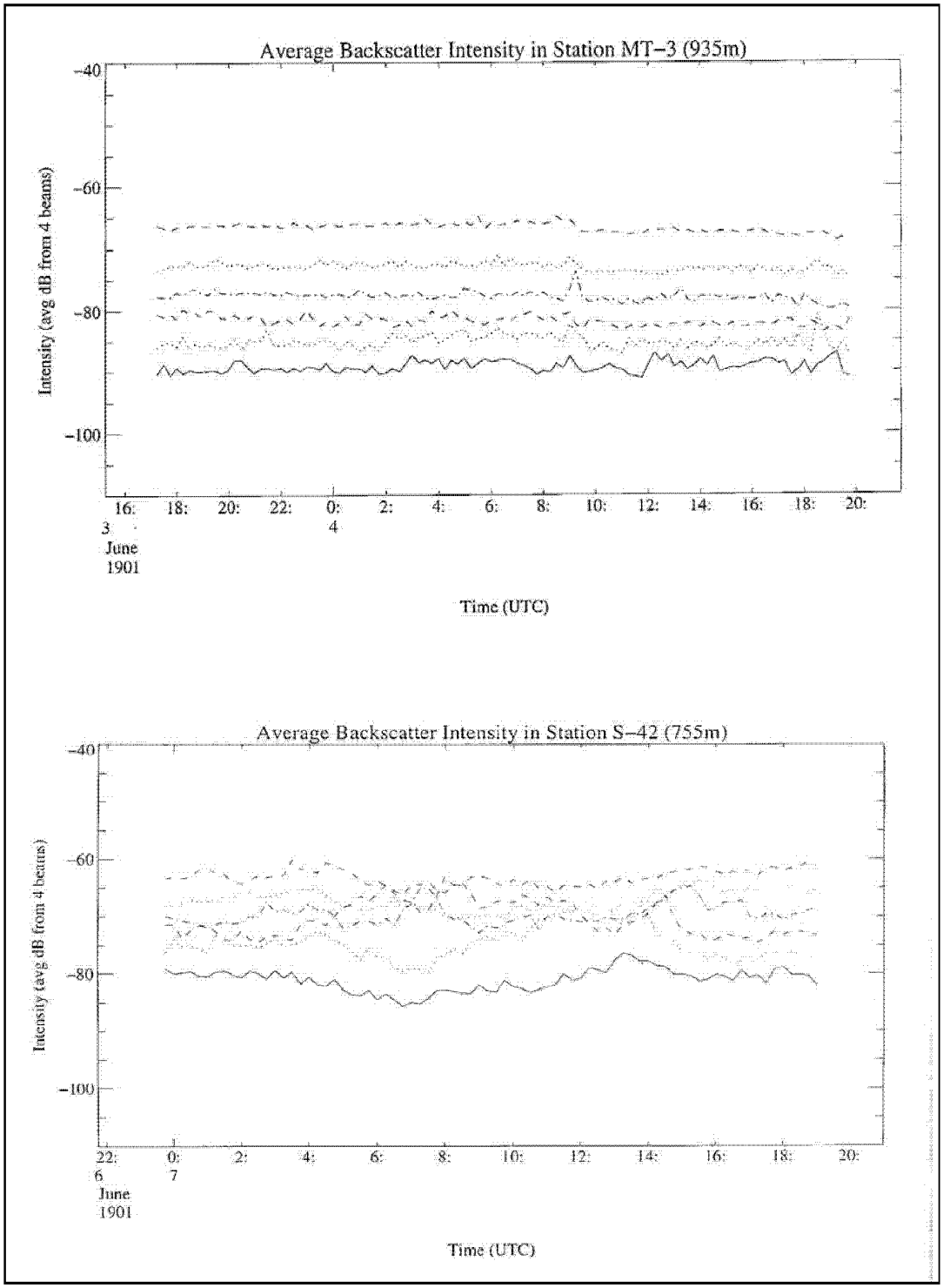

Figure 8-192a. Time series plots of acoustic backscatter intensity for summer 2001 stations 935 (top) and 755 (bottom) m deep. The ABI was averaged from the 4 beams of the ADCP, and backscatter intensity is plotted for every other depth bin 9-29 m off bottom.

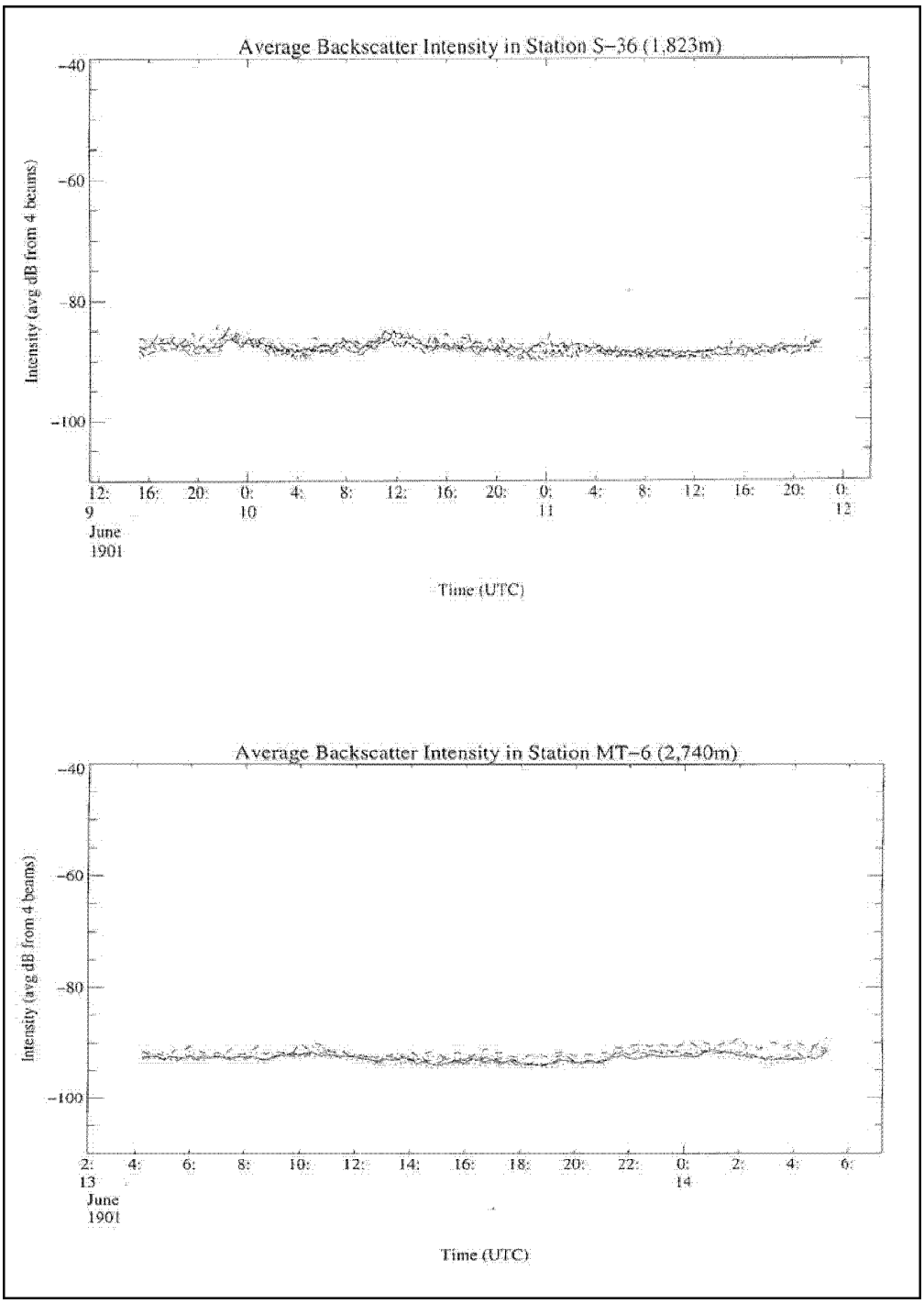

Figure 8-192b.Time series plots of acoustic backscatter intensity for summer 2001 stations 1,823 (top) and 2,740 (bottom) m deep. The ABI was averaged from the 4 beams of the ADCP, and backscatter intensity is plotted for every other depth bin 9-29 m off bottom.

Table 8-46

Correlation Coefficients (r Values) Calculated between Each Depth Bin
for the Two Shallowest Stations of the Summer 2001 ADCP Deployments
(Significant correlations (values ≥ 0.53 are significant at the p = 0.05 level) are highlighted.)

Station S-42 (bins given as depth off bottom)

	29m	27m	25m	23m	21m	19m	17m	15m	13m	11m	9m	7m
29m	1.00	0.81	0.71	0.62	0.21	-0.47	-0.61	-0.47	-0.25	0.001	0.32	0.44
27m	-	1.00	0.88	0.72	0.36	-0.34	-0.69	-0.62	-0.27	0.04	0.36	0.50
25m	-	-	1.00	0.86	0.46	-0.26	-0.66	-0.66	-0.34	0.01	0.36	0.48
23m	-	-	-	1.00	0.70	-0.12	-0.59	-0.59	-0.35	-0.05	0.29	0.45
21m	-	-	-	-	1.00	0.49	-0.18	-0.42	-0.31	-0.15	0.02	0.18
19m	-	-	-	-	-	1.00	0.64	0.12	-0.28	-0.45	-0.54	-0.44
17m	-	-	-	-	-	-	1.00	0.70	0.05	-0.36	-0.60	-0.63
15m	-	-	-	-	-	-	-	1.00	0.60	0.10	-0.23	-0.44
13m	-	-	-	-	-	-	-	-	1.00	0.79	0.46	0.16
11m	-	-	-	-	-	-	-	-	-	1.00	0.83	0.55
9m	-	-	-	-	-	-	-	-	-	-	1.00	0.83
7m	-	-	-	-	-	-	-	-	-	-	-	1.00

Station MT-3 (bins given as depth off bottom)

	29m	27m	25m	23m	21m	19m	17m	15m	13m	11m	9m	7m
29m	1.00	0.86	0.64	0.54	0.63	0.59	0.58	0.57	0.39	0.28	0.14	0.36
27m	-	1.00	0.69	0.53	0.59	0.61	0.52	0.53	0.41	0.27	0.09	0.36
25m	-	-	1.00	0.62	0.51	0.54	0.44	0.51	0.46	0.16	0.06	0.37
23m	-	-	-	1.00	0.51	0.38	0.39	0.28	0.13	0.02	0.03	0.35
21m	-	-	-	-	1.00	0.70	0.43	0.39	0.21	0.22	0.04	0.27
19m	-	-	-	-	-	1.00	0.60	0.51	0.29	0.27	0.02	0.22
17m	-	-	-	-	-	-	1.00	0.62	0.17	0.12	-0.09	0.23
15m	-	-	-	-	-	-	-	1.00	0.51	0.33	0.10	0.29
13m	-	-	-	-	-	-	-	-	1.00	0.49	0.26	0.27
11m	-	-	-	-	-	-	-	-	-	1.00	0.46	0.05
9m	-	-	-	-	-	-	-	-	-	-	1.00	0.36
7m	-	-	-	-	-	-	-	-	-	-	-	1.00

Table 8-47

Correlation Coefficients (r Values) Calculated between Each Depth Bin
for the Two Deepest Stations of the Summer 2001 ADCP Deployments
(Significant correlations (values ≥ 0.53 are significant at the p = 0.05 level) are highlighted.)

Station S-36 (bins given as depth off bottom)

	29m	27m	25m	23m	21m	19m	17m	15m	13m	11m	9m	7m
29m	1.00	0.89	0.79	0.72	0.68	0.65	0.62	0.58	0.60	0.55	0.60	0.59
27m	-	1.00	0.85	0.76	0.71	0.66	0.61	0.54	0.59	0.52	0.55	0.53
25m	-	-	1.00	0.89	0.80	0.75	0.71	0.65	0.66	0.60	0.60	0.58
23m	-	-	-	1.00	0.89	0.76	0.72	0.68	0.72	0.60	0.59	0.57
21m	-	-	-	-	1.00	0.83	0.76	0.72	0.75	0.66	0.64	0.62
19m	-	-	-	-	-	1.00	0.85	0.74	0.74	0.71	0.67	0.66
17m	-	-	-	-	-	-	1.00	0.86	0.78	0.78	0.72	0.71
15m	-	-	-	-	-	-	-	1.00	0.86	0.80	0.75	0.72
13m	-	-	-	-	-	-	-	-	1.00	0.86	0.76	0.72
11m	-	-	-	-	-	-	-	-	-	1.00	0.83	0.77
9m	-	-	-	-	-	-	-	-	-	-	1.00	0.83
7m	-	-	-	-	-	-	-	-	-	-	-	1.00

Station MT-6 (bins given as depth off bottom)

	29m	27m	25m	23m	21m	19m	17m	15m	13m	11m	9m	7m
29m	1.00	0.92	0.85	0.84	0.82	0.70	0.70	0.73	0.64	0.63	0.57	0.57
27m	-	1.00	0.93	0.91	0.89	0.77	0.75	0.75	0.65	0.65	0.61	0.60
25m	-	-	1.00	0.94	0.90	0.84	0.76	0.74	0.65	0.64	0.58	0.57
23m	-	-	-	1.00	0.93	0.85	0.80	0.77	0.68	0.65	0.61	0.61
21m	-	-	-	-	1.00	0.89	0.84	0.80	0.68	0.66	0.61	0.62
19m	-	-	-	-	-	1.00	0.84	0.77	0.60	0.59	0.58	0.58
17m	-	-	-	-	-	-	1.00	0.92	0.78	0.78	0.72	0.67
15m	-	-	-	-	-	-	-	1.00	0.85	0.82	0.75	0.69
13m	-	-	-	-	-	-	-	-	1.00	0.91	0.80	0.75
11m	-	-	-	-	-	-	-	-	-	1.00	0.83	0.70
9m	-	-	-	-	-	-	-	-	-	-	1.00	0.88
7m	-	-	-	-	-	-	-	-	-	-	-	1.00

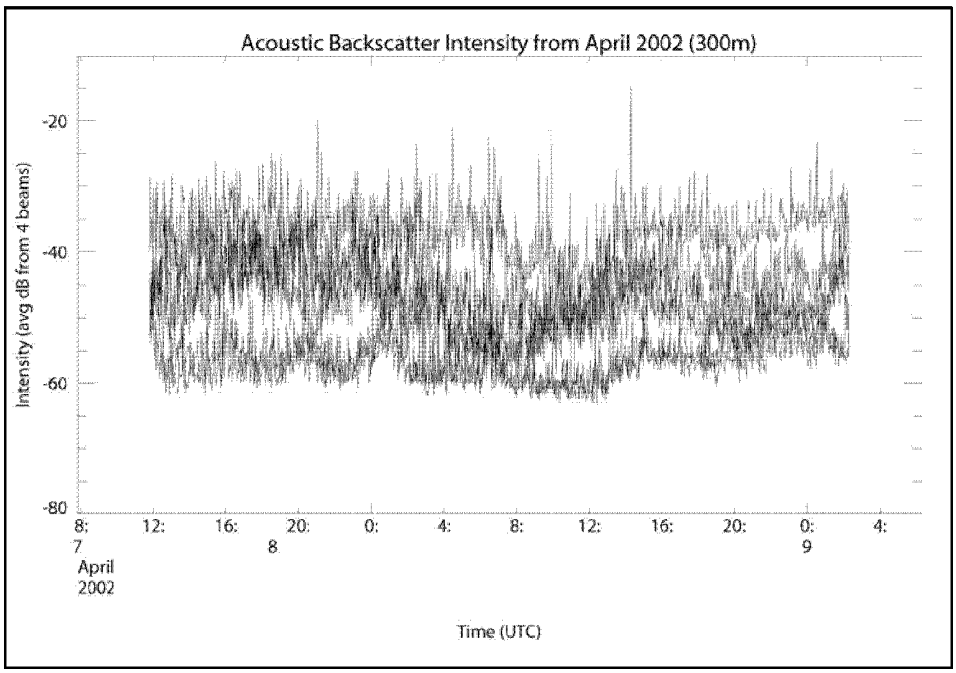

Figure 8-193. Time series plot of acoustic backscatter intensity from the April 2002 deployment in water depth 300 m. Labels on plot indicate distance above bottom.

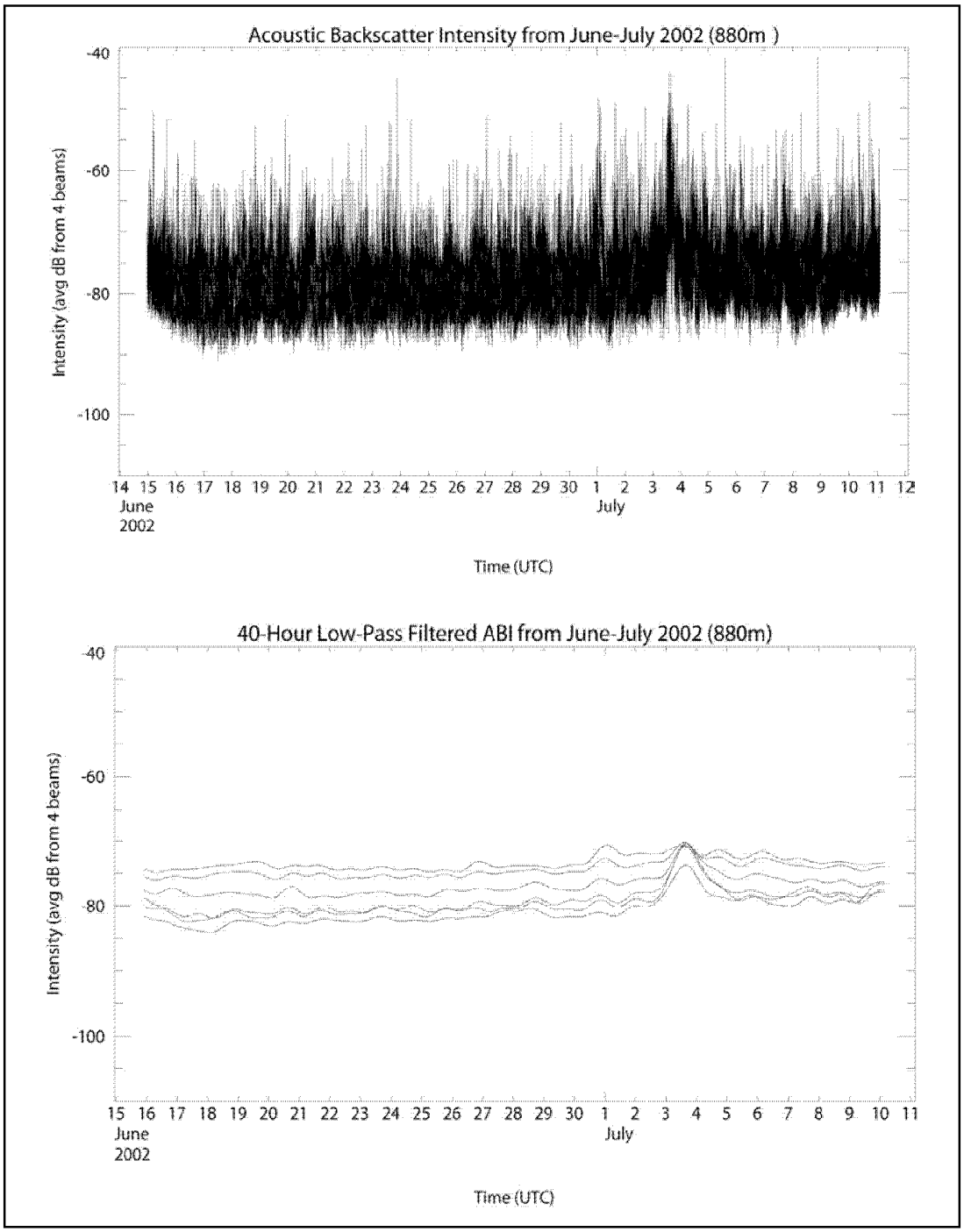

Figure 8-194. Time series plots of unfiltered (top) and 40-hour low-pass filtered (bottom) ABI from the June-July 2002 deployment in water depth 880 m. Labels on plots indicate distance above bottom. Time interval between samples is 5 minutes.

was likely due to increased near-bottom currents (Figure 8-22) which likely acted to resuspend flocculent "marine snow" or similar large-size particulate matter from a local topographic high situated NE of the mooring site and carry this material downcurrent into the area where the ADCP was moored.

The four-week deployment was long enough to allow spectral analysis to be performed. This analysis was conducted to determine what, if any, variability can be detected in the patterns of deepwater scatterers. The spectra show a peak in energy density centered at 0.9-1.2 cycles per day (Figures 8-195 and 8-196), although this peak is less evident in the spectra created for 7 m depth nearest bottom. Spectral analysis was also performed on the 14 June to 12 July ABI data after the application of a 40-hour low-pass filter to remove the noise at higher frequencies as well as the peak centered at 0.9-1.2 cycles per day. The spectra of the filtered data confirm that there was low frequency variability present in the deepwater data on weekly (0.07-0.14) time scales, as well as on 3-4 day (0.25-0.33) time scales.

Bernal (2001) reported that particulate matter concentrations in bottom nepheloid layers were greater during spring and summer than during fall in the northeastern GoM. She also reported interannual variability in particulate matter concentrations near bottom. Three casts with a CTD with transmissometer attached were taken during the course of the four-week deployment in summer 2002 to look for possible nepheloid layers or aggregations of marine snow near the deployment site. These CTDs were taken at the mooring site when the ADCP was deployed on 14 June, during an opportunity on 22 June, and at the mooring site when the ADCP was recovered on 12 July. No indication of markedly increased particulate matter near-bottom (nepheloid layer) was found in any of the transmissometer data (Figure 8-197), although percent transmittance generally decreased about 0.1% to 0.4% from mid-water minimum values as bottom was approached in all of these records.

In writing this chapter we have assumed that the acoustic backscatter intensity signal in the ADCP data is due to mobile near-bottom scavengers and/or to relatively large-size resuspended flocculent particles, rather than to small-size particles like resuspended silt-clay sediment, or to physical factors such as sharp salinity differences. This conjecture is warranted by the 300 kHz frequency of the sound emitted by the Workhorse ADCP. Acoustic waves can generally detect objects one quarter of their wavelength. If the speed of sound in seawater is approximately 1.5 km/s, then the wavelength of the emitted signal from the Workhorse ADCP is approximately 5 mm (1,500 m/s/300 kHz), and thus the size limit of detection of sound reflected directly from particles would be about 1.25 mm.

As a corollary, studies trying to measure suspended or resuspended sediments directly generally use frequencies in the mega Hz range, and such studies have optimum signal-to-noise returns when concentrations of suspended sediments exceed 10^4 ug/L. From the transmissometer data collected in June-July 2002, it is unlikely that suspended or resuspended sediments of these concentrations were present in what appears to be a very weak nepheloid layer.

Very little acoustic backscatter should reflect off a salinity gradient unless this exceeds 10 psu, at a frequency of 300 kHz. In fact, the companion CTD data show no indication of any near-bottom salinity gradient >0.1 psu at the deployment site. Rather, near-bottom salinity there varied from 34.9 - 35.0.

Due to the difficulty in collecting samples, very little research has been conducted to study zooplankton scatterers in the deep-sea. Deep-sea benthopelagic plankton were studied at depths of 1,000 to 4,700 m using an opening-closing net attached to a Deep Tow instrument. Horizontal transects were performed near-bottom at an average speed of 1.5 kt, but at this speed, net

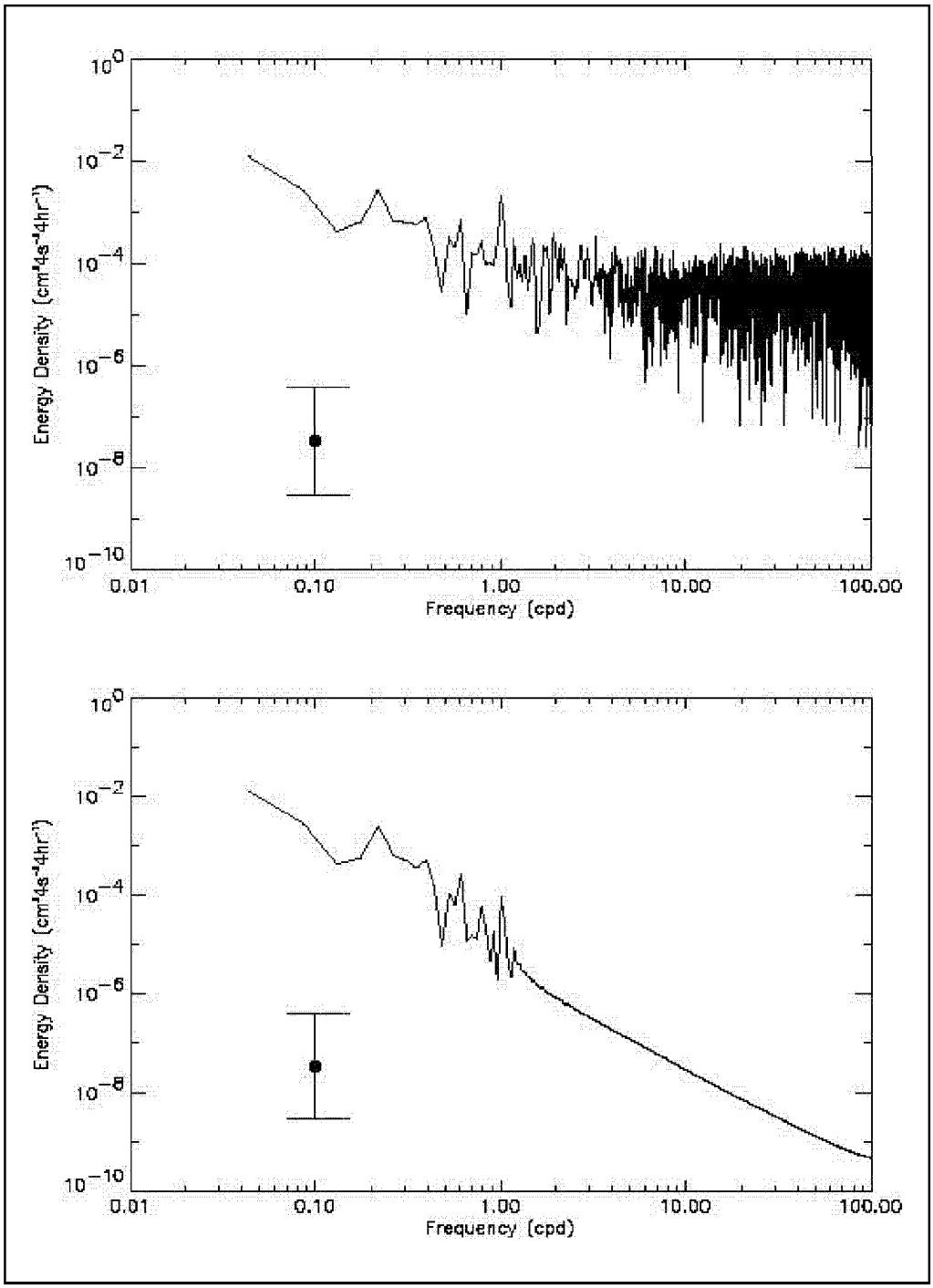

Figure 8-195. Variance spectra of raw (top) and 40-hour low-pass filtered (bottom) ABI data from 48 m above bottom in the June-July 2002 month-long deployment.

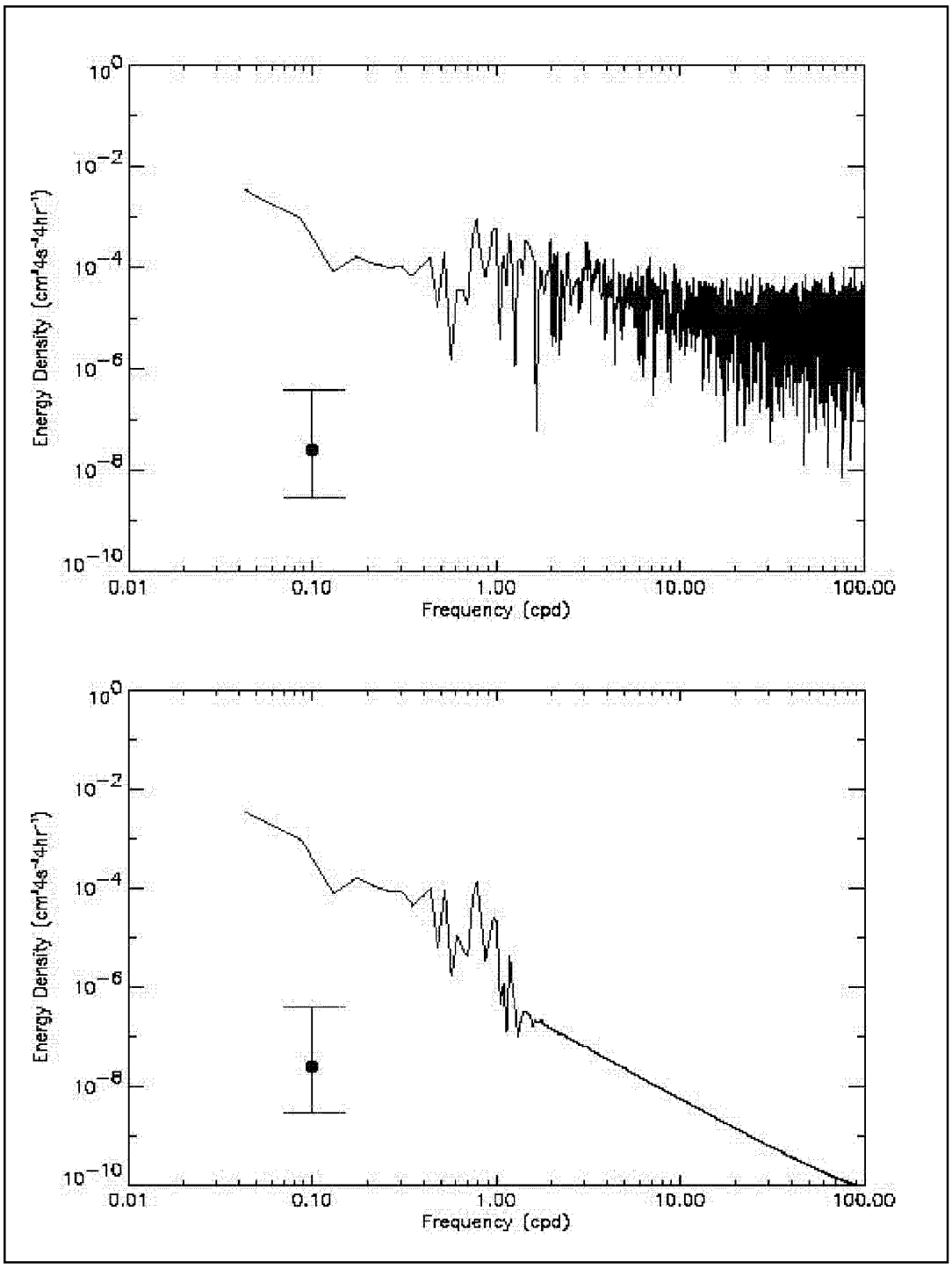

Figure 8-196. Variance spectra of raw (top) and 40-hour low-pass filtered (bottom) ABI data from 7 m above bottom in the June-July 2002 month-long deployment.

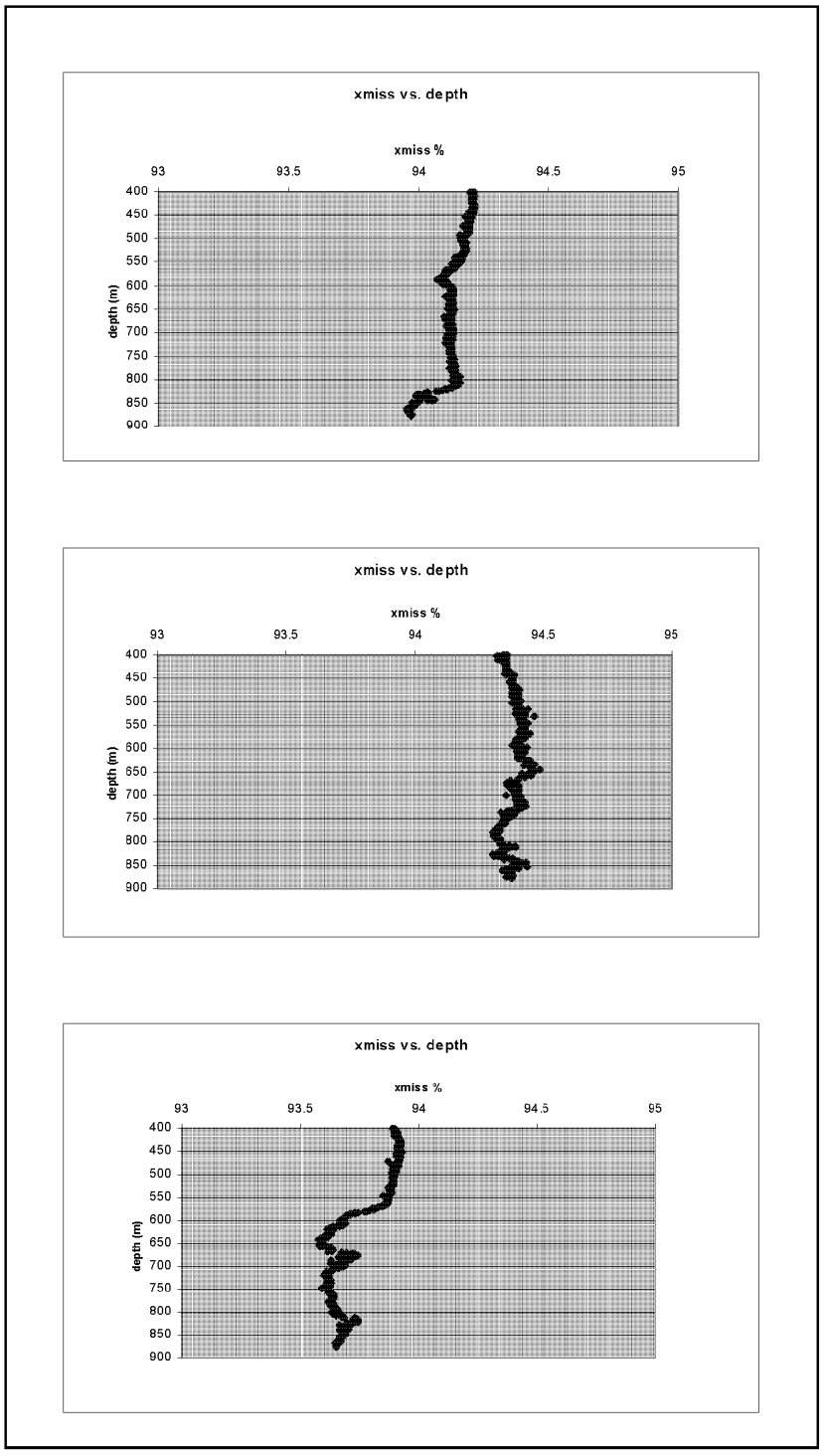

Figure 8-197. Percent light transmittance from CTD casts made during deployment (top), on 22 June (middle), and recovery (bottom) of the June-July 2002 near-bottom-moored ADCP.

avoidance is expected by the faster swimming organisms so that the collected biomass may be an underestimate. However, Wishner did find higher benthopelagic biomass in her net samples taken 10 m above bottom than in samples taken 100 m above bottom. The larger ABI measurements seen near-bottom in this study suggest that there are near-bottom scatterers associated with the sea floor. Regrettably, neither baited traps nor near-bottom net tows were undertaken in this study to "sea truth" the backscatter data, and so it is impossible to conclude if the increased bottom signal was due solely to benthopelagic organisms, or whether most of the ABI came from aggregates of marine snow and other large-size particulate matter suspended or resuspended near-bottom.

In conclusion, although this study has collected the first near-bottom ABI data in the deep GoM, the data that were collected can only allow us to speculate on the processes affecting the distribution and patchiness of deep-sea benthopelagic organisms. More deployments of ADCPs in the deep sea are needed to evaluate their ability to measure the abundance of small, mobile near-bottom fauna. If ADCP data could be made available from ADCP deployments that are done routinely by oil and gas exploration companies in conjunction with their development of lease blocks for oil and gas production, this would greatly increase the available ABI database.

Ressler (2001) has begun the process to match ABI with scatterer size and density, but it is still difficult to identify the specific types of scatterers that contribute to a backscatter signal measuring using ADCPs. Multi-frequency acoustic techniques offer a promising solution to these problems, but we still need to know more about how zooplankton and micronekton patches vary both spatially and temporally. Such information could help to better explain the distribution and foraging strategies of larger, apex predators.

8.8.7.2 Trap Caught Organisms

A total of 133 amphipods of the species *Eurythenes gryllus* were collected in the abyssal plain of the Gulf of Mexico using baited traps at three sites. The specimens were identified based on morphological criteria; schemes of diagnostic features were useful on the recognition of differences with schemes shown on the literature. The meristic data analysis revealed significant differences between Gulf of Mexico and north Atlantic populations (n= 147 individuals). The smallest size range recorded in specimens from the Gulf of Mexico (1.4 to 7.9 cm) in relation with ranges reported on the literature and with one found on the north Atlantic and was related with the oligotrophic condition in the deep Gulf of Mexico. The longitude – biomass allometric growth relationship obtained from specimens collected in the Gulf of Mexico was expressed by a power curve that fits the data with an equation $W = 0.0232L^{2.8674}$ (r^2 =0.98).

A total of 133 amphipods of the species *E. gryllus* were collected on the abyssal plain of the Gulf of Mexico using baited traps at three sites. The specimens were identified based on morphological criteria; schemes of diagnostic features were useful on the recognition of differences with schemes shown on the literature. The meristic data analysis revealed significant differences between Gulf of Mexico and north Atlantic populations. The normal size-frequency distribution and the late sexual maturity of the individuals suggest that strong predation is not acting over the smallest instars. The shorter size range (1.4 to 7.9 cm) in relation with ranges reported on the literature and with one found on the north Atlantic was related with deficient food conditions on the deep Gulf of Mexico. The longitude – biomass allometric growth relationship obtained from 94 individuals was expressed by a power curve that fits the data with an equation $W = 0.0232L^{2.8674}$ (r^2 =0.98). Microscope photography showed the presence of chemosensorial microstructures which are useful to the location of food. The C and N stable

isotope analysis shown that the amphipod is positioned on a high trophic level with a feeding based on detritus and degraded exported materials from the water column. The sequences of the 16S RNA mitochondrial gene obtained from two locations of the Gulf of Mexico *E. gryllus* were similar to sequences obtained of amphipods from the Atlantic and Pacific, nevertheless the difference percentage (3.6 to 9.5 %) between them revealed that the Gulf of Mexico has a an independent or isolated population.

Amphipods of the species *E. gryllus* were collected in three locations in the abyssal plain of the Gulf of Mexico using baited traps with the objective to test isolation of the scavenger amphipods in this peripheral sea. The sequences of the mitochondrial gene 16S RNA from *E. gryllus* obtained from two locations of the Gulf of Mexico showed small differences with sequences of other *Eurythenes* amphipods from the Atlantic ocean (3.6 to 3.9 %) and from the Pacific ocean (4.0 to 4.1 %). Larger differences (4.2 to 9.5 %) were recorded with specimens from shallower sites (<500m), e.g. in seamounts from the Pacific Ocean. The largest difference (18 %) was recorded in the region with *Eurythenes sp.* from the Tongue of the Ocean, sequences that suggest the existence of a different species. The differences with the external genus *Abyssorchomene* were of 25 % suggest that the abyssal scavenger amphipods of the *E. gryllus* species of the Gulf of Mexico still maintain a continuous genetic flow with the north Atlantic amphipod populations. Their predominant swimming behavior allows the populations to move horizontally along the abyssal water masses in the region.

8.8.8 Effects of Hydrocarbon Seep Sites

Cold seeps in the Gulf of Mexico provide an additional source of carbon to benthic fauna communities that are typified by high biomass and low diversity (Brooks et al. 1987, Agard et al 1993). The larger megafauna that inhabit cold hydrocarbon seeps (tube worms, clams and mussels) utilize endosymbiotic bacteria to mediate methane and petroleum (Ahraon 2000, Brooks et al., 1987, Sassen et al., 1993). This symbiotic relationship thus only occurs near seeping fluids and limits the spatial extent of the community (Aharon 2000, Hecker 1985). Bioenhancement however may not be limited to the megafauna and bacteria. The benthic infauna may also be affected by the additional food found at cold seeps.

Seep sites previously studied in 1993, 1995 and 2001 during the Shelf and Slope Experimental Taphonomy Initiative Experiment (SSETIE) were used as reference seep sites to compare macrofauna community structure and sediment community function with DGoMB sites (Figure 8-198). Sediment cores taken from Gulf of Mexico cold seeps were higher in abundance of macrofauna and exhibited lower diversity (Figure 8-199) (Nunnally, 2003). The mean abundance of macrofauna found at the cold seeps: Garden Banks 425 and Green Canyon 234, was 28,774 individuals per square meter (Table 8-48). The mean abundance of DGoMB sites within similar depth ranges (200-1,000 meters) was significantly less, at 8,883 individuals m^{-2} (Table 8-48). The diversity of taxonomic groups at these seeps was also lower than similar DGoMB stations, a mean of 10 groups at seeps compared to 21 groups. The mean Shannon-Weiner index of diversity (H') for cold seeps was 1.36, versus 1.79 for DGoMB stations, a significant difference. The only community attribute measured in which cold seeps and DGoMB stations did not differ significantly was Eveness, where cold seeps had a value of 0.64 and DGoMB stations had an average of 0.58 (Table 8-48).

An interesting comparison is with the other location at the same depth that also had extremely high standing stocks: MT1 at the head of the Mississippi Trough (see Section 8.5.4 on

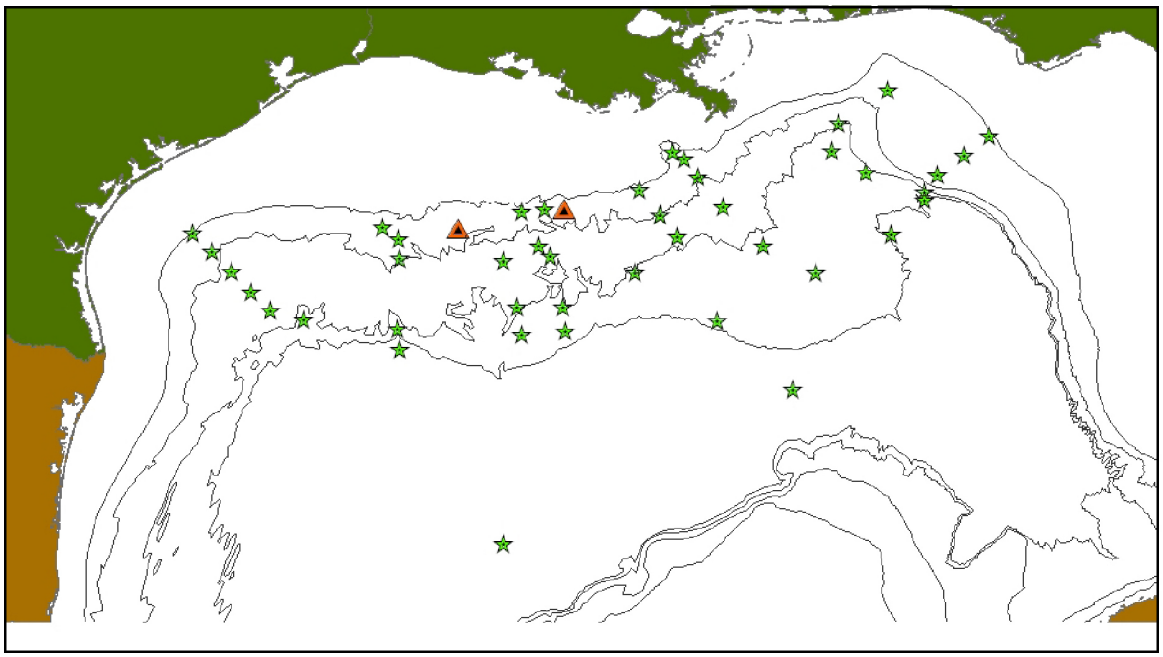

Figure 8-198. Northern GoM continental slope displaying DGoMB study sites with green stars and the two seep sites with orange triangles.

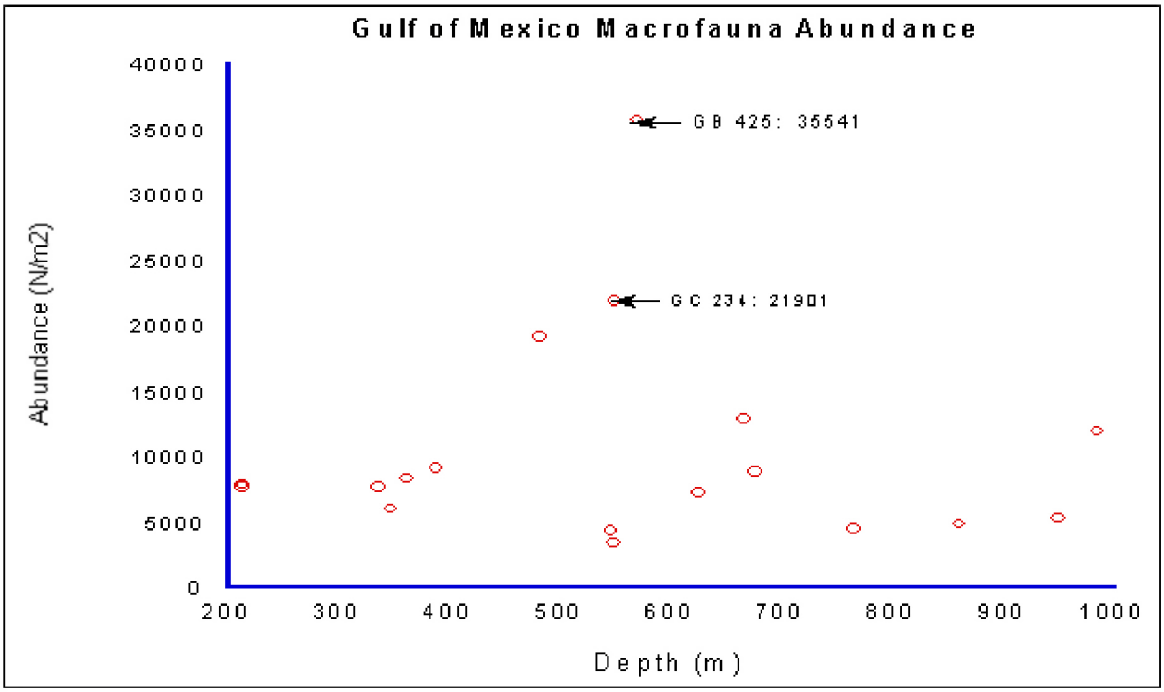

Figure 8-199. Macrofauna means for DGoMB and SSETIE sites in the Northen Gulf of Mexico are plotted against depth; the two seeps GB 425 and GC 234 are denoted by arrows with their mean macrofauna abundance in number m-2.

Table 8-48

Mean Values of Macrofauna Abundance, Higher Taxa, H'(s) (Shannon-Weiner), and Evenness for DGoMB Study Stations (Non-Seep) and SETTIE Stations (Seep)

	TYPE	Mean	Std. Deviation	N
Major Taxa	*non-seep*	21	4.2	92
	seep	10	0.5	4
Abundance (N/m^2)	*non-seep*	8883	5616	92
	seep	28774	9738	4
H'(s)	*non-seep*	1.80	.3054	92
	seep	1.35	.0354	4
Eveness	*non-seep*	.584	.0936	92
	seep	.635	.0071	4

macrofauna). Average density there was approximately 21,000 ind. m^{-2} and diversity was low, but the fauna was dominated by a single species of amphipod. In that location it was inferred that the high standing stock was a function of the input of particulate matter that was swept off the shelf into the canyon, rather than seep-derived hydrocarbons emanating up through the sediments. Both types of habitats illustrate the effects that enhanced organic supplies can have on community structure: enhance standing stocks but reduce alpha diversity.

Sampling site termed "Bush Hill" or BH on the map of stations was added during the field program to specifically test the hypothesis that organic input by cold seeps affects the fauna at some distance from the actual seep. This sampling was thus positioned two kilometers from the large cold seep known as Bush Hill, one of the original seeps discovered in the GoM. The macrofauna community at BH showed no differences in densities or diversity from the other sites tested. The community structure values were 4006 individuals m^{-2}, 19 higher taxonomic groups, an H'(s) of 1.89 and an Evenness of 0.64. Although these values do not differ significantly from the other DGoMB stations studied. The low abundance and high diversity of taxonomic groups indicated that at two kilometers distance from an active seep, the benthos exhibited no recognizable bioenhancement within the macrofauna.

Sediment community oxygen consumption was measured using incubation chambers at the two SETTIE locations above. The paired chambers are identical to those utilized with a remote lander (as described in Section 8.4), but they were set in place and recovered by the DSRV *Johnson Sea Link*, rather than being deployed by the lander. The rates have been plotted along the regression line which describes SCOC as a function of depth in the GoM, as presented in Section 8.4. In general, the SCOC rates from all the sites best fit a log-log or log-normal relationship with depth (Figure 8-200). Note, however, that the two seep site rates are well above the regression line as plotted, indicating that rates were enhanced above what one would expect at that depth. The mean of the two seep sites (ca. 110 mg C m^{-2} d^{-1} is about three times that encountered on the upper slope (see Section 8.4), but is only half the mean rate measured on the adjacent continental shelf. This suggests, by subtraction of the non-seep rates from the seep rates, that on the order of 70 to 80 mg C m^{-2} d^{-1} was being utilized by the community that is supplied by the seep alone, in addition to pelagic sources.

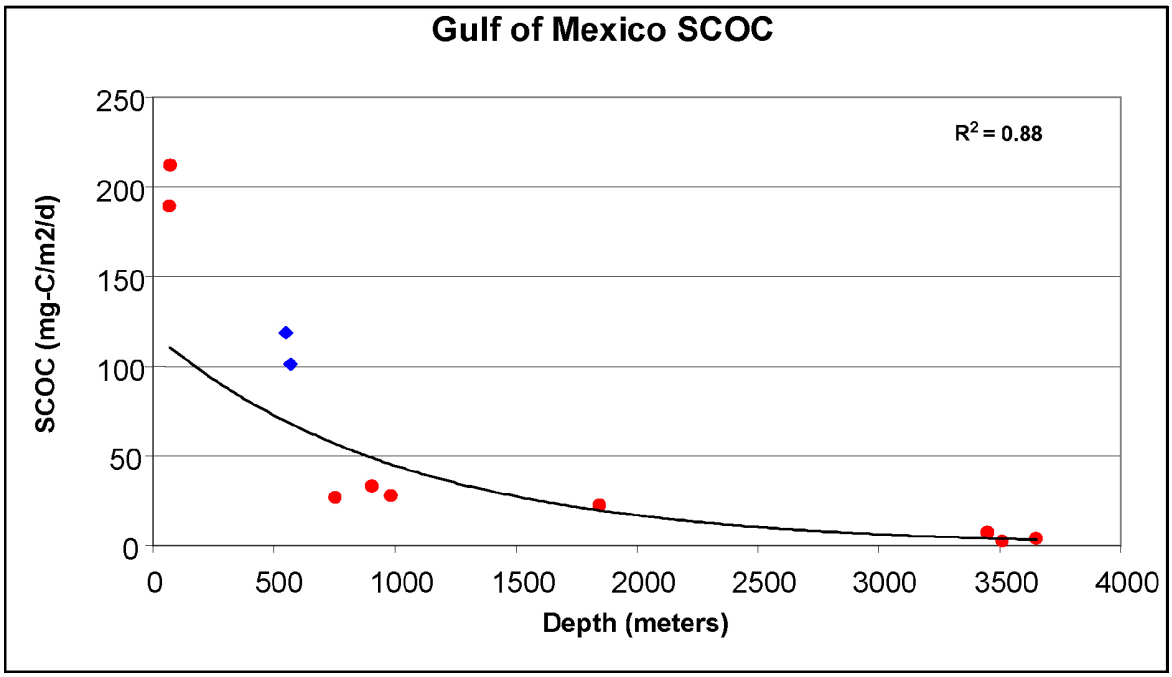

Figure 8-200. DGoMB and SSETIE sediment community oxygen consumption (SCOC) rates (mg-carbon m^{-2} d^{-1}) are plotted versus depth. Seep sites GB 425 and GC 234 are denoted by the blue diamonds.

Evidence of enhancement of food supplies for the benthos by cold hydrocarbon seeps in the Gulf of Mexico appears to be localized on a scale of 5 meters or less from the seepage of gas-carrying fluids. This conforms to the deep-sea oasis theory relating chemosynthetic communities to oases in the desert (Carney, 1994). Each are dependent on a 'below-ground' supply that is lacking from the background environment. This supply limits bioenhancement to within the periphery of the seeping fluids.

Cold seeps do concentrate a significantly large standing stock biomass reservoir in the midst of a low-biomass habitat. Diversity at such seep sites is diminished, due we presume to the competition for a type of resource that is not widely distributed in space. This competition for newly-introduced and peculiar form of food in a food-limited environment assures that little of the labile carbon ever leaves the vicinity of a cold seep. This reasoning however does not eliminate the possibility that carbon and energy are exported from the site as living biomass, either in the fishes or the vagile megafauna that feed within the seep-encompassed sediments and on the seep bacterial symbiont-supported sessile megafauna.

9. DISCUSSION AND SYNTHESIS

9.1 Animal Distributions and Community Structure

9.1.1 Mapping Distributions

For the first time in the study of life in the deep ocean, animal distributions can be mapped by species, groups of species or population abundances, over a broad geographic area. The species-level maps include most major taxonomic groups, from the harpacticoid copepods up through the fishes. In previous studies, single transects across depth gradients were used to investigate rates of change with depth (Carney 2005; Rex et al. 2005; Kendall and Haedrich 2006). Transects were then compared at different latitudes and longitudes to infer geographic differences. In the present study, a set of transects extending from the Mexican border to Florida now allows each size group, or some quantitative characteristic of the group (diversity, biomass, etc.), to be mapped. In those groups where taxonomic identifications were taken to the species level, individual species can be portrayed, as illustrated in Section 8, Results.

9.1.2 Standing Stocks and Biomass Implications

Densities of large taxonomic groups, such as the macrofauna, meiofauna, etc., can be contoured, as can recurrent assemblages that share species in common, within the large taxonomic groupings. The relationships between the groupings, whether based on quantitative or qualitative features, and large-scale taxonomic features, can thus be visualized. The large Mississippi Trough, a canyon-like feature in the central GoM, exhibits greater densities in all size groups, principally on the upper slope. While densities of organisms decline with depth in a systematic way, as seen in the contours or 'bubble' maps for each large size group, the MT sites in the trough on the upper continental slope were exceptionally high, suggesting that more organic matter is entrapped in the trough than elsewhere. Densities were also higher in the DeSoto Canyon, but not in the deep, western Alaminos Canyon, where remarkably low densities were sampled.

The decline in total biomass is a reflection of two parameters: individual animal size (Table 9-1) and total abundance (Table 9-2), both of which decline with depth. This is illustrated by measurements of the mean size of the macrofauna taken from the batch sediment community respiration deck-board incubations at the process sites (Figure 9-1). Previous studies have observed a marked decline in animal density and biomass as a function of depth on all continental margins (Rowe 1983), but the significance of a decline in individual size is, according to these data, an important component of this.

Table 9-1

Determination of the Mean Size of Macrofaunal Individuals (from Selected Samples)

Station	Depth(km)	Repl	N	Wet wt. (mg)	OC (mg)	Size (mg/ind)	Size (mgC/ind)
C7	1.07	3	189	85.71	3.01	0.453	0.0159
MT1	0.48	3	334	148.40	6.71	0.444	0.0201
MT3	0.99	3	266	109.91	4.48	0.413	0.0168
MT6	2.75	3	52	1.129	0.050	0.022	0.00096
S36	1.83	2	78	10.87	0.375	0.139	0.00482
S42	0.77	3	201	85.55	3.749	0.425	0.0187

Table 9-2

Process Station Macrofauna Biomass, Based on Densities and Individual Weight Estimates, in mg C/Individual

Station	Depth	Mean Size (mg-C/Indiv)	Density	Biomass (mg-C/m2)
MT1	0.481	0.0201	21801	438.6
MT3	0.987	0.0169	9219	155.5
S42	0.767	0.0187	4917	91.7
S36	1.828	0.0048	10859	52.3
MT6	2.745	0.00096	1485	1.43

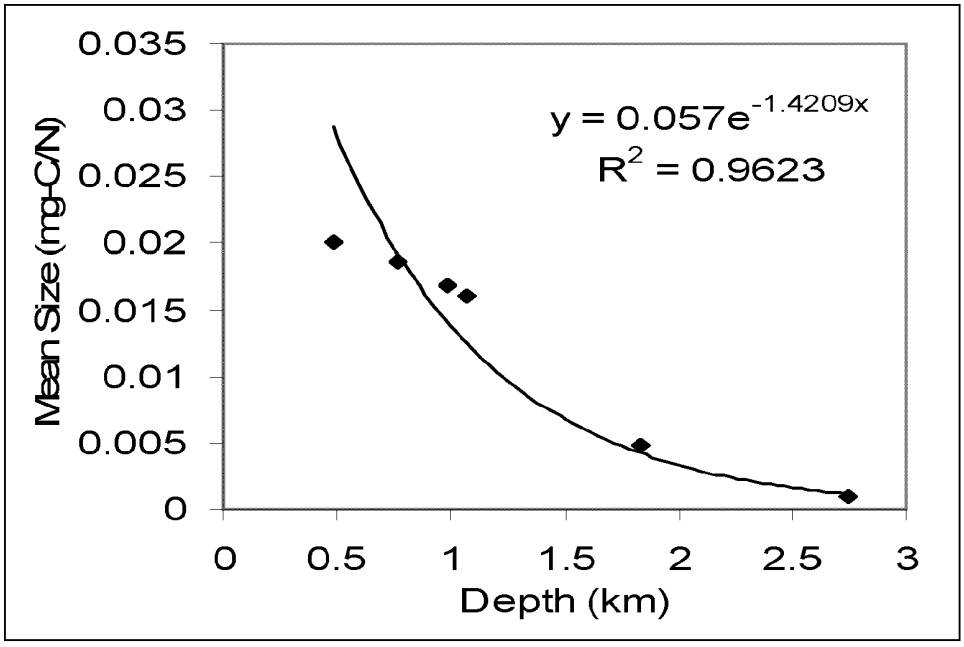

Figure 9-1. Mean macrofauna individual size (mg C per individual) as a function of depth.

9.1.3 Diversity and Species Richness Generalizations

The comprehensive taxonomic analyses in which individuals were identified to species, ranging from the meiofaunal harpacticoid copepods up to the fishes, allows comparisons to be made of the species richness and diversity between size groups (e.g., fishes, megafauna, macrofauna and meiofauna), between prevailing taxa within the different size groups (e.g., amphipod macrofauna vs. the polychaete macrofauna, etc.), and in contrasting geographic regions with presumably different conditions (canyon vs. non-canyon, etc.).

In most of the cross-slope representations of species diversity using E(s) as a measure, the maximum was encountered on the mid to upper continental slope (1.2 to 1.6 km depth). The form and statistical spread of the data varied by group, however. The polychaete worms, the most speciose of all the macrofauna, declined rather evenly with depth, without an abrupt mid-slope maximum, whereas the other major groups displayed pronounced parabolic shapes.

The lowest diversity values for the macrofauna were in the head of the Mississippi Trough (MT1). This low was the result of the dominance by a single amphipod *Ampelisca* sp. nov. (Soliman and Wicksten, submitted), which reached population densities of tens of thousands per square meter. This high density and low diversity is inferred to result from the extraordinary accumulation of silt and clay from the continental shelf in the pocket-like incision of the trough into the shelf in proximity to the Mississippi delta and the principal outflow of the river (Southwest Pass) onto the shelf. The trawls from the canyon head (MT1) contained fragments of large, aquatic vegetation. The substrate was so soft that all the weight had to be taken off the box corer to prevent "over penetration" and loss of material out the top of the corer. Comparisons of E(s) in the canyon with adjacent cross-slope transects illustrate that species diversity was generally lower in, as opposed to outside (the C line), the upper canyon (MT1through MT3), but species richness for the entire down-canyon transect (the MT sites) was higher than that outside the canyon. This, we suggest, is a function of greater structural complexity within the canyon.

The cause of the "intermediate depth species maximum" (IDSM) remains open to speculation. The increase in diversity with depth on the upper slope is presumed to be a relaxation of competitive exclusion up to the maximum at 1.2 to 1.6 km. But it is cause of the decline seaward of the upper slope maximum that is particularly equivocal. Recruitment into the GoM derives from the southern Yucatan Strait, with a sill depth between 1.5 and 2 km. Perhaps this restricts recruitment into the deeper aspects of the basin. The abyssal plain has been formed over geologic time by turbidity flows emanating from the Mississippi Cone or fan of sediments. A frequent submersion of the fauna under flows of fine organic-poor clay may retard recruitment. Evidence is mounting that the deep GoM is characterized by strong bottom boundary currents; this too, if true, could select for a community of low diversity. Note that species composition at GKF (Green Knoll Furrows) is different from that in the standard zones (Figure 9-2), reminiscent of the studies of communities in the Western Boundary Undercurrent of the NW Atlantic (ref. HEBBLE study).

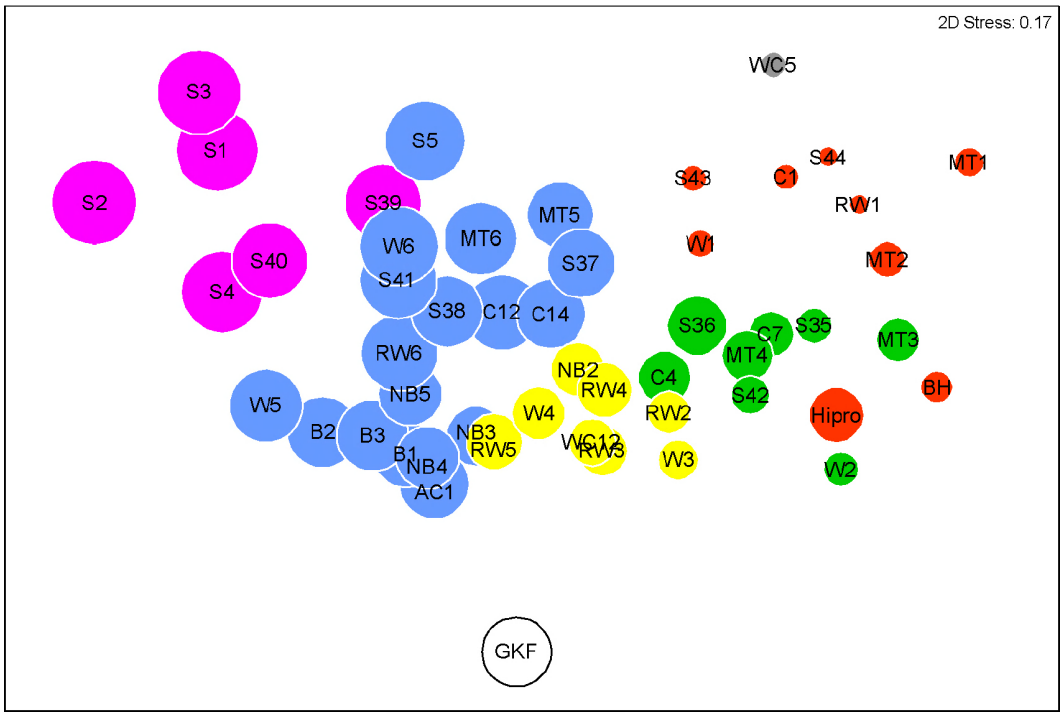

Figure 9-2. Non-metric MDS plots for 4th root species abundance data of all macrofauna, based on Bray-Curtis similarity. Bubble size is directly proportional to depth and colors represent different faunal zones. Note that "Green Knoll Furrows" (GKF) species composition is distinctly different.

9.1.4 Bathymetric Zonation—Variations and Putative Causes

The distribution of recurrent groups of species of macrofauna (Figure 9-2), megafauna, and fishes, leads to the conclusion that the entire fauna, by and large, is zoned with depth. In general the depth zones for all the macrofauna, megafauna and fishes, grouped together, appeared to be 1) upper slope, 2) mid-slope, 3) lower slope and 4) abyssal plain assemblages. Figure 9-2 illustrates how each depth zone of total macrofauna conforms to more or less similar depths, with some exceptions. "Hipro" for example is similar to the shallow sites, even though it is in rather deep water. We suggest that this submersion is related to high primary productivity in the surface water, hence the "Hipro" name. Sub-groupings were also related to physiographic features, such as the Mississippi canyon, east vs. west, etc. The macrofauna, the most speciose of the large size categories, was divided on the mid-slope into an east and a west sub-group (Figure 9-2 green and yellow bubbles), each having its own characteristic biomass and diversity (Figure 9-2). GKF was located at the base of Green Knoll in the area of giant "Aggie bus-sized" furrows (W. Bryant, personal observation), and the species composition was not similar to any of the other groups. Each zone has a characteristic biomass and diversity, as well as species composition. The correlation of zonal characters with depth suggests that the declining food supply with depth is a possible cause of the zonation. In particular, both organism density and biomass decline along the depth gradient and each zone occupies a distinct region along the gradient (Figure 9-3). Note that the two mid-slope east and west zones are separated on the basis of biomass and density, indicating that less organic matter is supplied to the west area than to the east. This supports the underlying hypothesis that food resources control zonation.

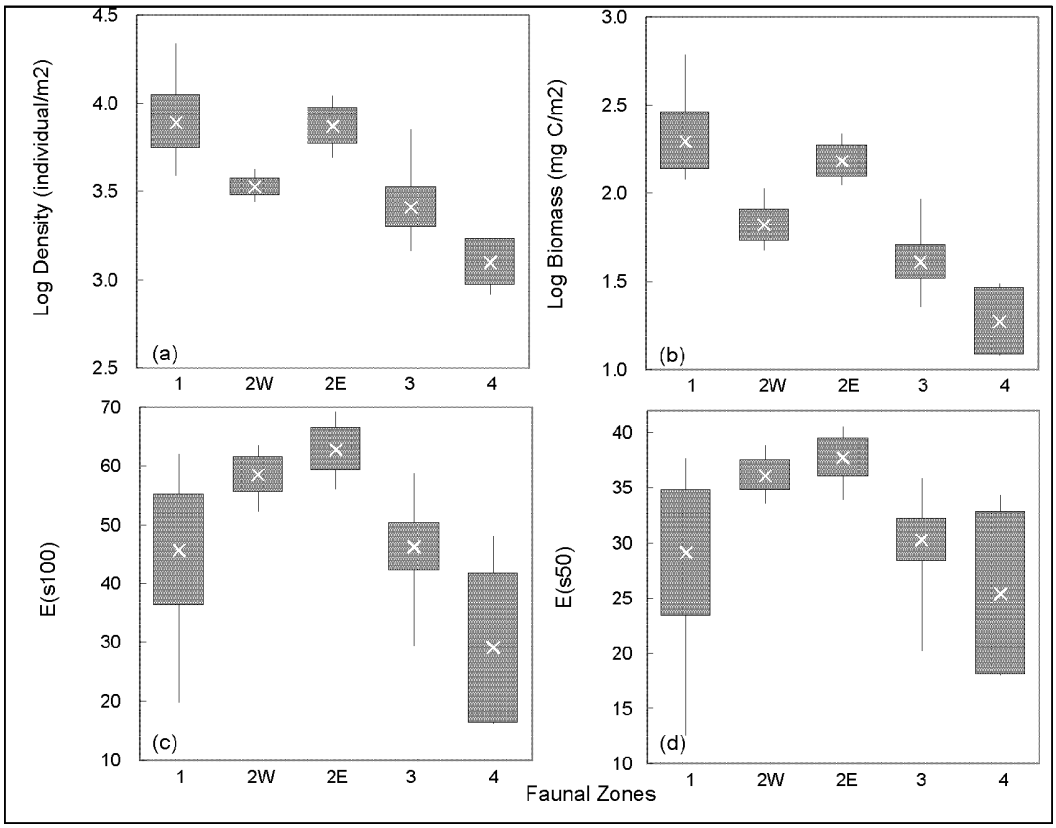

Figure 9-3. Mean density, biomass, $E(S_{100})$, and $E(S_{50})$ in each macrofaunal zone. Note white cross indicates the mean values, gray box indicates 95% confidence level, and vertical line indicates the range between maximum and minimum value.

Some individual taxa appeared to occur in more zones than others. The bivalve mollusks for example occupied nine depth-dominated zones, whereas the harpacticoid copepods were encountered in what appeared to be as many as 17 separate regional clumps, with diameters of 50 to 150 km, cutting across depth contours (Baguley et al. In press). Such differences may be due to larval dispersal in the bivalves versus brooding in the copepods.

A plot of the number of zones as a function of relative animal size (Figure 9-4) indicates that the smaller organisms occurred in more groups, and these appeared as clumps that, on the map, were less aligned with depth than the larger groups. We infer that this is a function of motility and larval dispersal: larger organisms that are motile tend to be zoned, whereas the smaller groups are restricted to small geographic areas and are thus isolated in particular regions. Among groups that are about the same general size, the brooders occurred in more groups (e.g., the amphipods) than those that do not brood their young (mollusks, polychaetes and isopods).

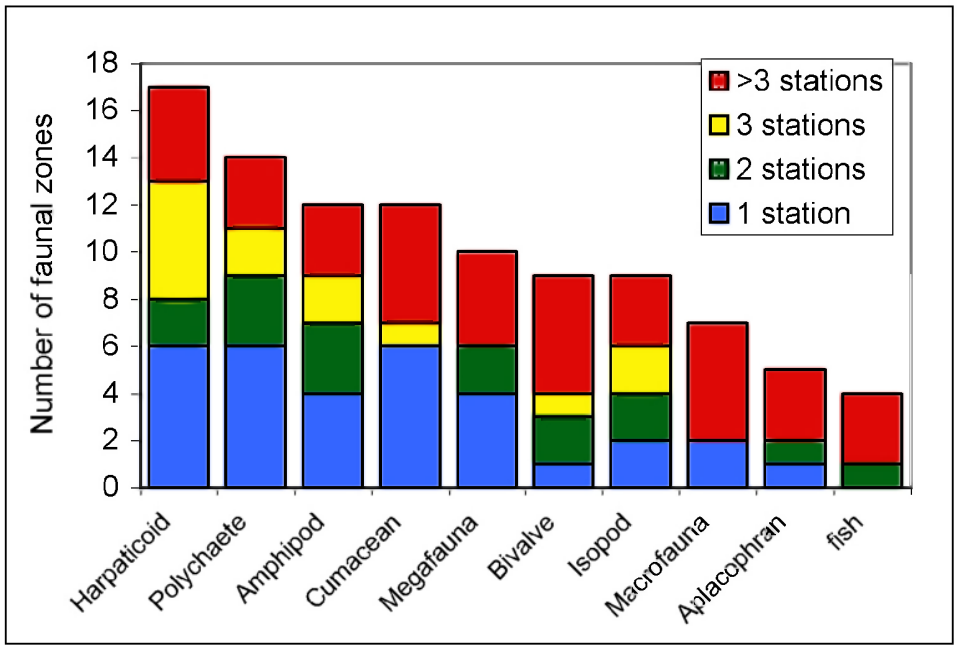

Figure 9-4. Number of 'zones' (recurrent groups of species) in each group. Colors indicate number of sites in each zone. For example, the Harpacticoids had six zones with only one site in a zone (blue), three zones with more than three sites in three zones, five zones with three sites and two zones with two sites. The blue indicate isolated sites that are not grouped with any other site, based on species composition.

9.1.5 Implications of and Conclusions Based on the Hypothesis Test Results

An underlying premise of all the hypotheses tested was that the input of food resources was the paramount controlling variable of the distribution of deep-ocean organisms. For example, the patterns of macrofaunal abundance can be used to infer the locations where the input of organic matter is accentuated within the study area. In general, the western GoM was characterized by lower densities than the eastern GoM, leading to the assumption that the organic matter available to the deep benthos is less in the west than in the eastern GoM. This was unexpected since the Mississippi River generally flows to the west and the eastern GoM is characterized by the warm relatively unproductive waters of the loop current. The high abundance values in the upper reaches of the Mississippi Trough reflect larger inputs of organic matter that can be assumed to be related to the Mississippi River. This could either be direct input from river-borne material or enhanced primary production that accumulates in the trough where it intersects the continental shelf just west of the delta. The differences in the densities on the two sides of the DeSoto Canyon suggest that in general Mississippi cone sediments are enriched in carbon compared to those off Florida. The cone sediments are primarily terrigenous and it might be assumed richer in organics than the predominantly carbonate sediments off west Florida. The high numbers at S36 near the canyon axis suggest that perhaps this is a location of organic matter accumulation. It is also worth noting that the surface water over and just inshore of S36 is thought to be characterized by unusually high productivity for the GoM, probably due to the incursion of high nitrate water onto the upper slope and continental rise (See Sections 8.1, 8.2 and 8.3).

The hypothesis tests discussed below reflect the degree to which the geographic or seafloor physiographic features control animal distributions because they affect the delivery of organics to the sea floor.

Standing Stocks Decline Sharply but Predictably with Increasing Depth

[HO1: Standing stocks are independent of depth]

The testing of null hypotheses was utilized in this study because it was recognized that a complete geographic coverage would be impossible (see Section 4, Table 4-1). Each null hypothesis, if properly tested, would allow the elimination or inclusion of particular environmental features in terms of their significance to animal distributions in the GoM, even though total geographic coverage would never be attainable.

Depth has long been recognized as a dominating independent variable that correlates strongly with deep-sea distributions, although the specific underlying mechanisms for the correlations are obscure and remain ill-defined. Because total stocks and rates of processes are known from numerous previous studies to decline sharply with depth, *it has been presumed that depth is inversely related to food supply.* Thus, depth was the primary variable to be considered in this study.

The principal statistical tool utilized for investigating the relationship of the standing stocks with depth was regression analysis. The statistical significance of a regression is tested by calculating the probability that the slope of the regression line is different from zero. The differences in the height of one regression line from another above the abscissa can be tested, as can the differences in the slopes of the lines. These tests have utilized extensively on the sediment characteristics and on each group of organism in Section 8.

Without doubt, many of the features did, as expected, correlate with depth. Animal densities and depth were inversely correlated, as has been demonstrated by countless studies, including earlier studies in the GoM (Rowe 1983). Among the different size groups, however, the smaller the organisms, the less profound was the decline with depth. The result was that the relative importance of the bacteria and the meiofauna increased with depth because their declines were less pronounced. The declines with depth, in all size categories, are thought to reflect a general overall decline in the input of organic matter – the lower the input of organic carbon, the lower the total biomass. This apparently affects the larger organisms to a greater degree than the smaller size groups. Pequegnat et al. (1990) had previously recognized the increase in the relative importance of the meiofauna.

An unexpected surprise was the relative increase in the bacterial densities on the abyssal plain relative to the slope. This is counter to all the conclusions about the metazoans. That this was a sampling or analytical artifact needs to be explored in future studies. There is no reasonable explanation, at this time, for an increase in bacterial densities on the abyssal plain when all other indicators show a continued decline in organic matter with increased depth and distance from land. *In conclusion, depth does affect organism densities, with the possible exception of the bacteria.*

Diversity too correlates with depth, but this varies with the group being studied. In general, an intermediate depth maximum is observed, but this was absent or reduced in some groups. In this pattern, diversity first increases with depth to a maximum at intermediate depths. Then it declines gradually to a low on the abyssal plain, regardless of the diversity index used. The increase is due, it is thought, to a relaxation in competitive exclusion, followed by a general decrease in organic matter with depth. There is no real evidence in support of this however; it is only conjecture. Nonetheless, it is a repeatable correlation with a characteristic shape. It is

repeatable with each group in which the taxonomy has been taken to lowest possible level (species).

There are several important exceptions to the general abundance-depth pattern. Highest densities in most groups were NOT found in the shallowest samples (200 to 300 m), but rather in the head of the Mississippi Trough (500 to 1,000 m). Likewise, densities on the abyssal plain were highest on the large sediment cone that extends south from the continental slope off the Mississippi River to the area where the Mississippi Trough appears to debouch onto the northern extremity of the Sigsbee Abyssal Plain (SAP), that is at Site S5. The species composition of the infauna at that site was more akin to shallower sites than to that at the slightly deeper SAP sites (S1 through S4). It can be inferred that both exceptions to the more general abundance-depth pattern are the result of the entrapment and channeling of organic detritus by the Mississippi Trough.

The Biota Associated with the Sea Floor in the Eastern GOM Has Some Demonstrable Differences from that in the Western GOM, but these Difference Are Limited.

[HO2: the eastern GoM fauna is not different from the western GoM fauna]

The transect with the lowest standing stocks was that in the far west (RW), whereas all the sites with the highest densities of all groups considered were located in the eastern half of the GoM, from the C line eastward. However, the zones of recurrent groups of macrofauna lined the basin from east to west, with the exception of the upper slope zone, which was divided down the middle (referred to as Zone 2E and 2W). This suggests that quantitatively the east and the west may differ, but qualitatively for the most part they are rather similar. The quantitative difference may be related to surface water primary production [see HO4 discussion below].

Canyons* Increase Standing Stocks, Lower Diversity and Increase Species Richness

[HO3: Submarine canyons have no discernable effect on standing stocks, species composition, diversity and zonation of the deep GoM benthos]

The second most convincing hypothesis to be accepted (as posed in Section 4, Table 4-1) was the significance of the Mississippi Trough on the biota. This canyon head between 500 and 1,000 m contained a fauna which grouped together, being dominated by a single species of amphipod crustacean. This dominance was most pronounced at the shallowest site. This reflects, again, the input from shallow water, of detrital material building up at a rapid rate. The material is thought to be a combination of surface productivity, shelf sediment export and fluvial plant detritus, based on the seasonal surveys of surface-water pigments, PAHs in the sediments, organic matter, and large plant material in the trawl samples. Stable isotopes suggest that pelagic *Sargassum* detritus may be important too. Animal densities were extremely high, but not of polychaete indicator species (e.g., capitellids) and nematodes expected adjacent to or impacted by eutrophication or oil contamination, but of amphipod crustaceans, supposedly quite sensitive to stressful conditions. The megafauna and the fish fauna were also encountered in high abundance

* Two other canyon-like features were sampled. The Alaminos Canyon, just to the east of the deep end of the RW transect, was characterized by some of the lowest animal densities sampled on the deep slope. It is assumed that it is no longer active but rather a remnant of the Holocene Transgression. The DeSoto Canyon, that area between the eastern Mississippi Cone and the Florida Escarpment, was characterized by high animal densities. However, it is not a typical submarine canyon formed as an incision in the continental slope but rather a geophysical feature. The high animal densities there are assumed to be a combination of high surface primary production, as reflected in the ocean color analyses (see Section 8.3), and detrital material trickling down the eastern flank of the slope off the Mississippi River mouth, eventually being focused and thus building up in the tight constraints of the canyon-like valley, as sampled at S35 to S39.

in the canyon head, which may reflect the widely-recognized preference of small crustaceans as prey items.

Standing Stocks are Directly Proportional to Surface Primary Production

[HO4: Geographic variation in rates of surface water primary production have no discernable effects on the standing stocks of the deep-living biota of the Gulf of Mexico]

Surface primary productivity was indirectly assessed by mapping surface water pigment concentrations seasonally over the entire DGoMB area (see Section 8.3). The effects of variations in surface-water primary production on the deep benthos is difficult to distinguish from other variables, especially depth. However, a comparison of animal densities along the upper slope suggests that proximity to the high surface pigment regions near and east of the Mississippi River clearly implicates surface primary productivity as at least a secondary control on bottom faunal densities. Noting that high densities were encountered in both the Mississippi and the DeSoto canyons, the program added a "HiPro" site at equivalent depths between the two, but out of canyon-like influences. The high densities at the "HiPro" site add credence to the importance of surface sources of organic matter as having an effect on animal densities. As noted above (Figure 9-2), the "HiPro" site is in relatively deep water (ca. 2 km) but has a species composition associated with the upper slope, suggesting that some process allows shallow species to exist in slightly deeper water than normal; it is tempting to suggest that this submersion is due to a higher than normal delivery of POC. This supports the strong link between surface water primary production and deep ocean biomass.

Earlier studies comparing the GoM with other regions suggested that the GoM was characterized by low benthic biomass because in general the productivity of surface water is low compared to the NWAtlantic or the coast of Peru, both of which are known to be characterized by primary productivity that far exceeds that in the GoM (Rowe 1983). The present study attempts to distinguish the effects within the GoM basin, not between geographically distant basins, a substantially more difficult task. There is little justification however for rejecting the idea that the higher biomasses that characterize the eastern GoM at all depths on the upper slope are not, at least in part, a function of the higher surface productivities there compared to the western margin of the basin.

How much phytoplankton production of these surface waters reaches the seabed? Figure 9-5 summarizes a 1980s paradigm that away from land only a slow vertical "rain" of primary production escapes the surface waters, although there are occasional foodfalls of animal carcasses that may also be important. While this may be what happens in the western and central deepwater GoM, the SeaWiFS ocean color climatology data indicate the paradigm should be revised to include the role of eddies and eddy-like features (see discussion of WSEs in 8.3) that entrain green water and transport it off the continental margin into deepwater in the easterm GoM.

In the western and central deepwater GoM, the standing stocks and biological productivity of the plant and animal communities living in the upper part of the water column are also, in general, those that might be expected in a nutrient-limited ecosystem. In the late 1960s, as part of a review of plankton productivity of the world ocean, Soviet scientists characterized the deepwater GoM as very low in standing plankton biomass, with mean productivity of just 100-150 mg C m^{-2} d^{-1} (Koblenz-Mishke et al. 1970). A few years later, extensive ship surveys of phytoplankton chlorophyll and primary production that span the period 1964-1971 were summarized by El-Sayed (1972) in atlas format, as averages within 2^{o} squares of latitude and longitude. These atlas maps showed that surface CHL generally ranges 0.06 - 0.32 mg m^{-3} in

deepwater central and western GoM. There is usually a subsurface "deep chlorophyll maximum" (DCM) within which concentrations are 2-3 fold higher, and the atlas reported that CHL in deepwater could reach 21 mg m^{-2} when integrated from the surface to the base of the photic zone. Most values for CHL, though, ranged 5-17 mg m^{-2} where water depth was > 2 km (El-Sayed 1972).

During an algal bloom, the C:CHL ratio for living phytoplankton cells ranges from 23 to 79 (Antia et al., 1963). From mesocosm experiments, Antia et al. (1963) reported that vigorously growing phytoplankton with measurable nitrate in the water had C:CHL ratios of about 25, while senescent phytoplankton in nitrate-depleted water had C:CHL ratios of 60 or more. Using a C:CHL ratio of 25, a CHL standing stock of 0.1 mg m^{-3} is equivalent to a POC concentration of about 2.5 mg m^{-3}. From ^{14}C uptake experiments conducted in the GoM, El-Sayed (1972) has shown that primary production at "blue water" locations increases the phytoplankton POC pool by on average 0.25 mg C m^{-3} h^{-1}, which is equivalent to an increase of about 10% per hour. Such low values of primary production are typical for surface waters at the majority of the oceanic stations in the El-Sayed (1972) atlas, equivalent to only about 10 mg C m^{-2} h^{-1} when integrated from the surface to the base of the photic zone. If there are on average 12 hours of sunlight per day, this rate is equivalent to 120 mg C m^{-2} d^{-1} and so is in good agreement with the characterization by Koblenz-Mishke et al. (1970). Allowing for primary production to proceed 365 days a year in the GoM because of its subtropical climate, this rate of primary productivity is about 44 g C m^{-2} y^{-1}. As a consequence, the deepwater GoM is usually placed at the low end of the estimated range of 50-160 g C m^{-2} y^{-1} that is generally accepted for the annual gross primary production in open-ocean ecosystems (Smith and Hollibaugh 1993).

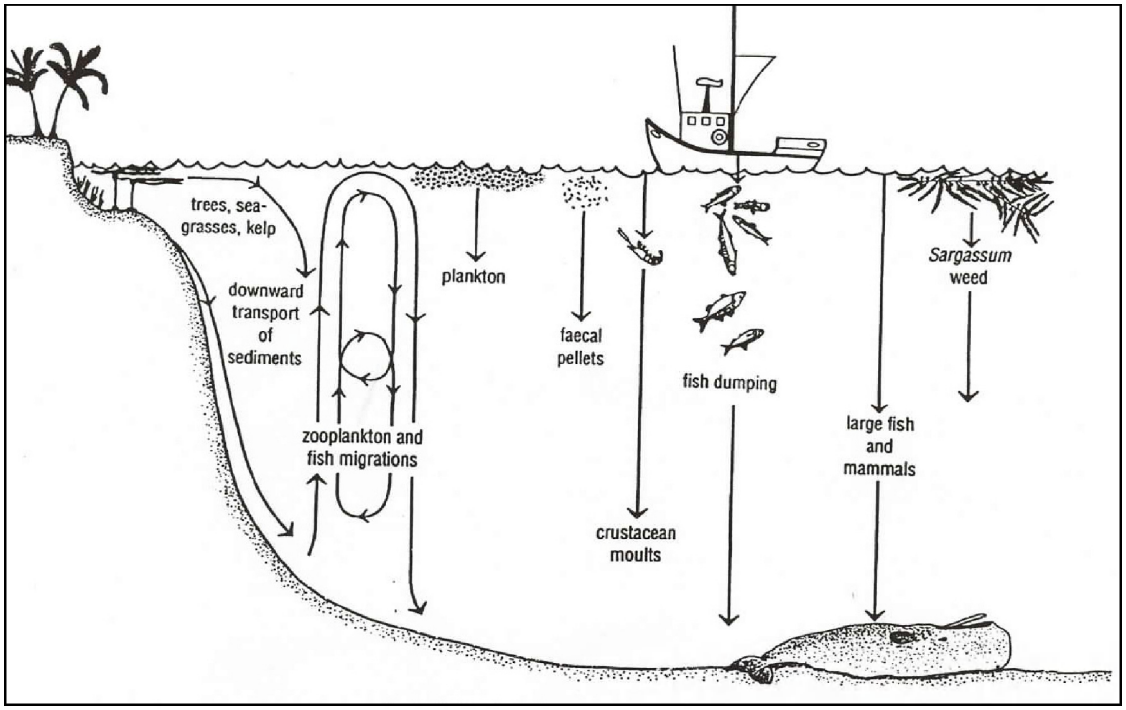

Figure 9-5. Schematic illustration of pathways by which POC is transferred from surface waters to the benthos. From Lalli and Parsons (1997) after Nybakken (1988).

If on average 10% of the primary production sinks out of the photic zone, and if 3-10% of this flux, in turn, reaches the seabed, then at a typical deepwater location just 100-360 mg C m^{-2} y^{-1} might reach the benthos. However, productivity in "hot spots" of locally higher nutrient concentrations over the continental slope can be more than an order of magnitude higher than the typical 100-150 mg C m^{-2} d^{-1} (Biggs and Ressler 2001). For example, Gonzalez-Rodas (1999) documented ^{14}C uptake of > 2 g C m^{-2} d^{-1} in the northern margins of two deepwater eddies interacting with the continental slope of the central GoM. When and where such eddy interactions with the slope are common, as they appear to be in the eastern GoM during summertime, we hypothesize that POC flux to the seabed is likely to be several times greater than the deepwater average of 100-360 mg C m^{-2} y^{-1}. Based on the difference between grand means for remotely-sensed CHL between the 22 DGoMB stations north of 26°N and west of 91°W in the western Gulf (0.19 mg CHL m^{-3}) and the 22 DGoMB stations north of 26°N and east of 91°W in the eastern Gulf (0.54 g CHL m^{-3}), we hypothesize that most of the stations along central and eastern DGoMB transects C, MT, and S receive at least 0.54/0.19 = 2.8 times greater annual POC input than do stations located west of 91°W.

These estimated rates of input to the seafloor (0.3 to1.0 mg C m^{-2} d^{-1}) are slightly less than those measured in situ using a remote benthic lander (see Section 8), in which rates ranged from ca. 2 to 7.5 mg C m^{-2} d^{-1}. Rates on the middle and upper continental slope were substantially higher, by more than a factor of 10 to 20, than those estimated above. The difference may be attributable to input from the margin, which could be accentuated in the GoM by the fluvial input of sediments, nutrients and organic matter.

Enhanced Standing Stocks and Accelerated Sediment Community Metabolism within Close Proximity to Methane Seep Sites

[HO5: Methane seeps have no effect on the biota of the deep Gulf of Mexico]

Methane seeps appear to have a profound effect of animal densities, possibly species composition and rates of sediment community oxygen consumption. However, there is little evidence so far that the effects go beyond the immediate proximity of a seep community.

Effects of Deep, Steep Escarpments Remain Unknown

[HO6: Steep escarpments have no effect on the biota]

The general decline in abundance as a function of water depth was slightly altered at the base of steep escarpments, giving some credence to the positive effects of proximity to escarpments. On transects W and S the densities at approximately 3 km depth just below the Sigsbee and the Florida Escarpments, respectively, were slightly above the general regression line, suggesting that material moving down the escarpment enhances organic input at the escarpment base. This is very meager evidence, however, and would need other evidence before it is accepted. The cause, if the increases are real, may be due to other processes, such as seep activity associated with the slope-rise junction or other local seep effects that are encountered along the steep escarpment.

Mesoscale Basins as Peculiar Habitats

[H07: Mesoscale basins on the continental slope have no effect on the biota]

Three of the numerous small basins dotting the continental slope were sampled in and adjacent to the basins. The basin, it was thought, could trap sediments that could enhance seafloor densities and rates of metabolic processes. There was no evidence that the basins differed in any way from non-basin environments. This hypothesis was thus accepted, based on the data to date, for the faunal groups, bacteria and sediment properties (Section 8). It should be

pointed out however that the basins visited, as far as can be determined, were not characterized by active methane seeps.

Potential Effects Associated with Seasonal or Inter-annual Variations were Not Discernable

[H08: Variations in the biota are independent of time over the periods in which the study has taken samples]

The study always sampled in May or June over a three-year period. Thus, no seasonal effects would be discerned. It was suggested initially that Site C7, a site repeated from earlier MMS-supported studies, might be characterized by seasonal variations in animal density or composition. However, further scrutiny of the earlier data indicated that that location was close to a methane seep and the intermittent high densities of macrofauna observed were more likely a result of input of organics from the seep than to seasonality. It should be noted that the macrofaunal densities encountered during the initial survey (2000) were almost all significantly higher than those encountered at the same sites the following year (2001) (See Section 8.4.4). An explanation for this eludes us to date.

9.1.6 Variations In and Between Size Categories

Within most shallow benthic communities, with normal levels of organic matter available for food and no obvious physiological stressors, the biomass is dominated by the larger categories of organisms (mega- and macrofauna), with lesser total biomass in smaller sized organisms (meiofauna, microfauna and bacteria). This distribution is accentuated at high latitudes. Under stressful conditions such as low oxygen, the reverse occurs: the smaller organisms dominate the biomass. It has been suggested that in the deep ocean, the upside-down biomass distribution also occurs, with domination by bacteria and the meiofauna (Rowe et al. 1991). In most locations in the deep GoM this appears to be the case as well: most of the biomass is contained in the smaller organisms – bacteria, forams and meiofauna – rather than in the larger forms (Table 9-3). The pattern for the meiofauna and macrofauna was suggested by earlier work in the GoM (Pequegnat et al. 1990), and the present study, which has included bacteria and foraminiferans in addition to metazoan meiofauna, confirms it. The largest size category, the megafauna, is far below densities of similar groups in other ocean basins, based on photography and bottom trawling. The most palatable explanation is that the overall productivity of the surface water is low compared to other basins where similar studies have been undertaken. Additionally, the warmer temperatures in the surface water column suggest that remineralization of sinking organic matter would be higher, resulting in proportionately less reaching the sea floor. This has long been an explanation for higher biomass at high latitudes (Rowe 1983). Also, the sea floor temperature (4° C) is higher in the GoM than at similar depths in both the Atlantic and Pacific basins, which would result in slightly higher metabolic rates per unit biomass, on average, which may also contribute to the general dominance of small organisms. Working under similar depth/temperature conditions in the Caribbean, Richardson and Young (1987) have suggested that the bacteria must function to remobilize refractory or relatively unreactive organic detritus, thus requiring them to maintain a relatively high concentration to support grazing meiofauna, principally nematodes. The relative distribution of biomass among the size groups in the deep GoM supports this contention as well.

The first step in understanding food web relationships is quantifying the standing stocks of the components. Each process site can be characterized by the biomass of organic carbon (per square meter, integrated down to a depth of 15 cm) of each size category (Table 9-3). This summary is constructed from information in Section 8, Results. This includes the detrital

Table 9-3

Inventories of Organic Matter (mg C m^{-2}-15 cm) in the Detrital and Living Fractions at the Process Sites

Depth	Site	Sed. Org.C	Bacteria	Meio fauna	Macro fauna	Mega fauna	Fishes	Total Living	Living /[OC]	Bacti/Living
500	MT1	760000	2350	208	816	30.6	35.9	3441	0.0045	0.68
1000	MT3	702000	2550	194	34	59.5	35.4	2873	0.0041	0.89
750	S42	375000	1300	197	47.3	7.9	24.7	1577	0.0042	0.82
1850	S36	672000	1850	272	19.6	9.43	7.4	2158	0.0032	0.86
2750	MT6	222000	1010	27	1.56	6.67	1.8	1047	0.0047	0.96
3450	S4	321000	1480	10.5	2.1	0.75	0	1493	0.0046	0.99
3600	S1	287000	1400	13.8	8.3	0.19	0.4	1423	0.005	0.98

organic carbon for comparison. Of the total organic matter, the living fraction appears to be only .03 to .05%, with no predictable pattern over this range. The highest detrital carbon and the highest living carbon are at the shallow sites (Figure 9-6), whereas the opposite is true – the lowest of both detritus and biota are at MT6. It is somewhat surprising however that the lowest values are at MT6 at 2,750 m depth rather than out on the abyssal plain much further offshore at about 1 km greater depth. The large size groups (macrofauna, megafauna and fishes) declined

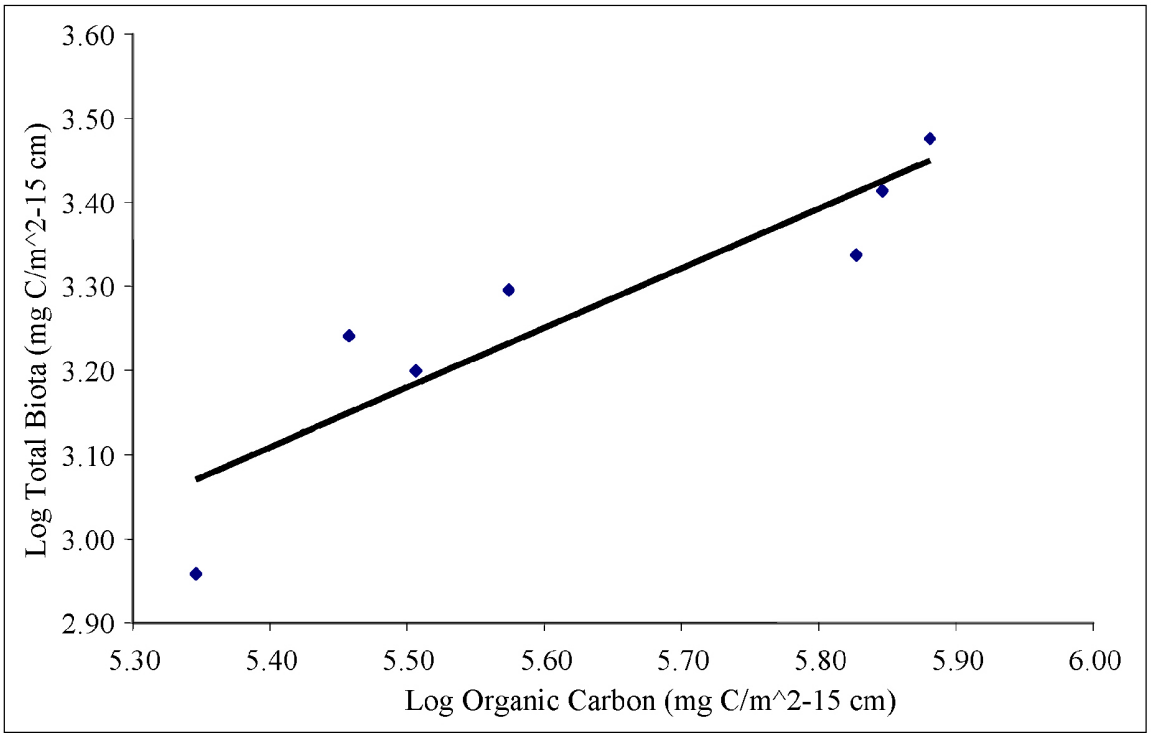

Figure 9-6. Log total community biomass as a function of log detrital organic carbon in the sediments, both integrated to a depth of 15 cm.

by about two orders of magnitude over the depth range of the process sites, whereas the meiofauna declined by a factor of 10 to 15 and the bacteria declined by a factor of 1.6 to 2.0 from the highest to the lowest biomass. This suggests that the smaller organisms are better adapted to surviving and maintaining their population densities at great depths than the larger organisms. Contemporary ecological theory would suggest that this could be related to declining organic energy available at the depths involved (Banaver 2002). If total detrital organics and total living carbon are a direct reflection of organic material delivery to a particular habitat, it is interesting that MT6, on the lower continental slope, is the lowest of the process sites in both criteria, but it is not located on the abyssal plain.

9.1.7 Comparison with Other Continental Margins

Biomass declines with depth, but its mean is lower and the slope is steeper than in most other basins, within the macrofauna and the megafauna; this is not true for the bacteria or the meiofauna – although they decline with depth in selective sets of data, the slope is less steep and well defined for the meiofauna than for larger forms. The regressions are not in general statistically significant for the bacteria in deeper water, principally because densities were greater on the abyssal plain than on the slope.

This suggests that GoM productivity is lower and material exported vertically to the sea floor is less reactive, making the smaller forms (the bacteria–nematode link) necessarily more important in the food web. The depauperate "typical" soft sediment fauna, interspersed by a mosaic of seeps with their luxuriant biota, suggests that rapid burial of relatively slowly reacting material is sequestered or "saved" by rapid burial for deeply-buried reactions that lead to oil and gas deposits. This differs from typical continental margins where OM is not buried rapidly but consumed by the biota almost completely on the sediment surface.

9.2 Principal Components Analysis

Principal Components Analysis (PCA) was used to search for groups of environmental variables, independent of the biotic analysis, which would add insight into the causes of the faunal distributions. In the PCA, the first three principal components accounted for 61.5 percent of the total variance in the data set (Table 9-4). However, four PCs out of 15 had eigenvalues greater than one, which means the first four were significant. The sign of variable loads (negative or positive) indicates gradients in concentrations. Variables that load negatively will have highest concentrations for negative PC loads with decreasing concentrations moving in the positive direction, and vice versa. PC1 accounted for 33.5% of the total variance, had high positive loadings by clay, total PAH's, tin, chromium, and high negative loadings by sand, strontium and calcium (Table 9-5; Figure 9-7). PC1 is interpreted as the sediment properties, with high silt, clay, organic (PAH) and metal (Cr and Sn) contaminants near the Mississippi River, and higher sand and natural background metals (Ca and Sr) with increasing distance from the Mississippi River.

PC2 accounted for 16.7% of the total variance and highly positive loadings by chl-a and POC, weak positive loadings by OrgN and NH_4, and weak negative loadings by NO3- and urea (Table 9-5, Figure 9-7A). PC2 is interpreted as particulate organic matter (POM) flux. PC3 accounted for 11.3% of the total variance and had highly positive loadings by DOC, and highly negative loadings by urea (Figure 9-7B). PC4 accounted for 10.2 % of the total variance and had moderate positive loadings by silt, NH_4, NO_3, and PAH. However, PC3 and PC4 did not have

Table 9-4

Eigenvalues of the Correlation Matrix for the Environmental PCA, Proportion of Variance Explained by Each Principal Component, and Cumulative Variance

	Eigenvalue	Difference	Proportion	Cumulative
1	5.019	2.504	0.335	0.335
2	2.515	0.818	0.168	0.502
3	1.697	0.162	0.113	0.615
4	1.535	0.606	0.102	0.718
5	0.929	0.077	0.062	0.780
6	0.851	0.217	0.057	0.837
7	0.635	0.044	0.042	0.879
8	0.591	0.060	0.039	0.918
9	0.530	0.218	0.035	0.954
10	0.312	0.111	0.021	0.974
11	0.201	0.066	0.013	0.988
12	0.135	0.105	0.009	0.997
13	0.030	0.017	0.002	0.999
14	0.014	0.008	0.001	1.000
15	0.005	0.000	1.000	1.000

Table 9-5

Variable Loads for the Rotated (Varimax) Factor Pattern of the Environmental PCA

	Factor1	Factor2	Factor3	Factor4	Factor5
Chla	0.11096	0.90356	-0.00047	0.08619	0.03993
Sand	-0.76437	0.21025	0.20489	-0.19623	-0.48221
Silt	0.43118	-0.03573	0.05246	0.65701	0.25268
Clay	0.65541	-0.28278	-0.27347	-0.09372	0.52084
NH4	-0.26511	0.35890	0.18627	0.66324	0.12841
POC	-0.04478	0.81893	0.06908	0.05581	0.08796
UREA	0.01605	-0.14464	-0.80871	-0.09793	0.09566
NO3	-0.19939	-0.49356	-0.21657	0.53803	-0.07637
DOC	-0.09904	-0.03622	0.87375	-0.00081	-0.06273
OrgN	-0.00531	0.27374	-0.10288	0.11126	0.88406
TPAHWP	0.55797	0.14311	0.14306	0.55440	-0.19339
Ca	-0.87212	-0.30214	0.09420	-0.23840	0.02223
Sr	-0.85733	-0.25022	0.14018	-0.20549	0.05741
Cr	0.86572	-0.12582	-0.06502	-0.16531	0.09411
Sn	0.83863	-0.00196	0.14965	-0.17825	-0.01304

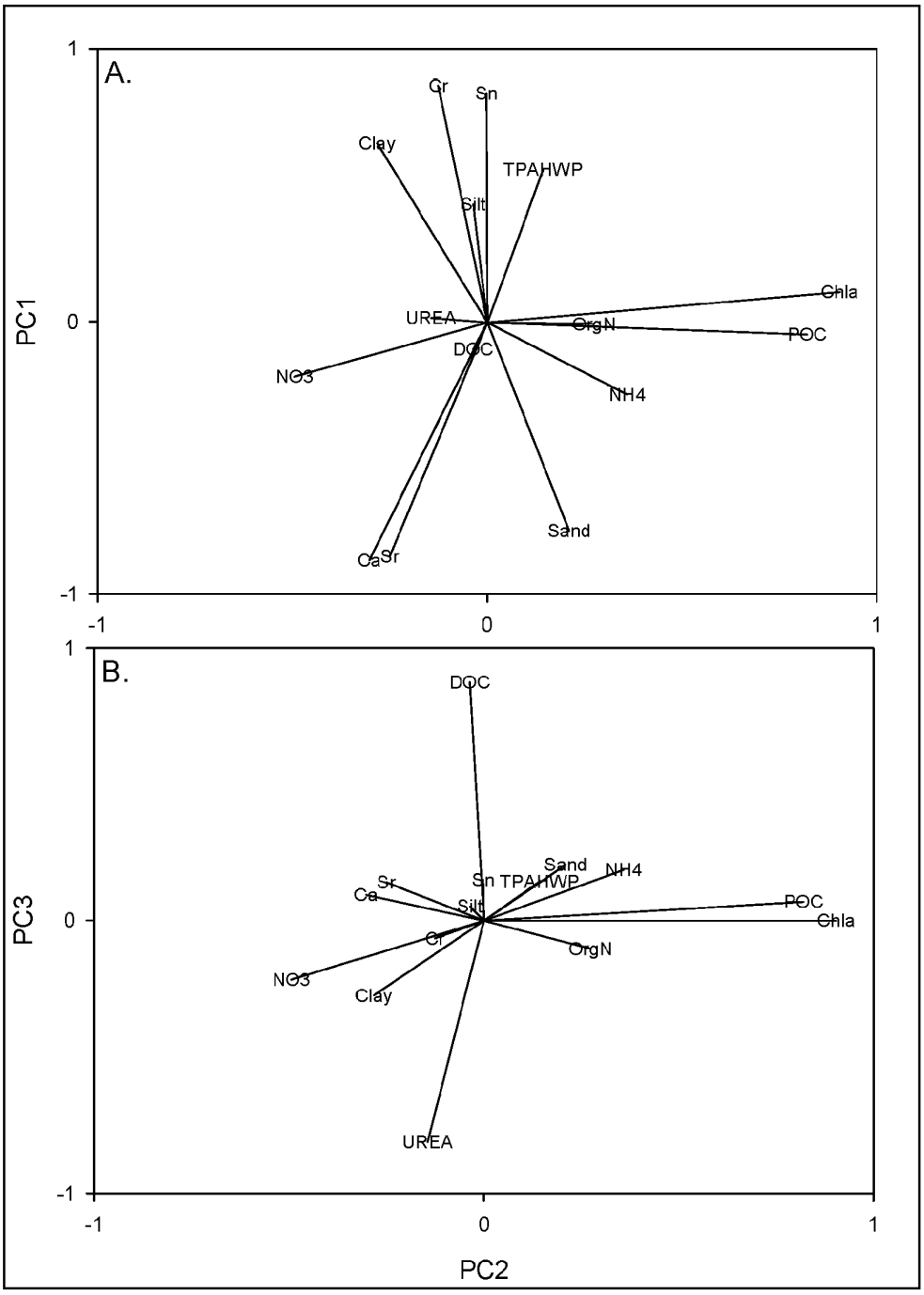

Figure 9-7. Principal components analysis of environmental variables, A) variable loading scores for PC1 versus PC2, B) variable loading scores for PC2 versus PC3.

obvious interpretations. PCs 1-4 were regressed against abundance to determine if they were significantly related to the biotic community. PC1 had a weak, but significant, positive relationship with meiofauna abundance, but accounted for only 22% of the variance in the biotic data set (Figure 9-7A, R^2 = 0.215). PC2 had a moderate, and significant, relationship with meiofauna abundance (Figure 9-7B, R^2 = 0.303). PC3 and PC4 did not have significant relationships with abundance. The ranges of values in deep water are remarkably narrow compared to shallow water environments, which probably accounts for the limited number of relationships that the PCA was able to identify with obvious interpretations. In this data set for example organic carbon, which normally is thought to control biochemical reactions, was above 1% at only a couple of sites. Oxygen, temperature and salinity were essentially invariable below 1 km depth (Figure 9-8).

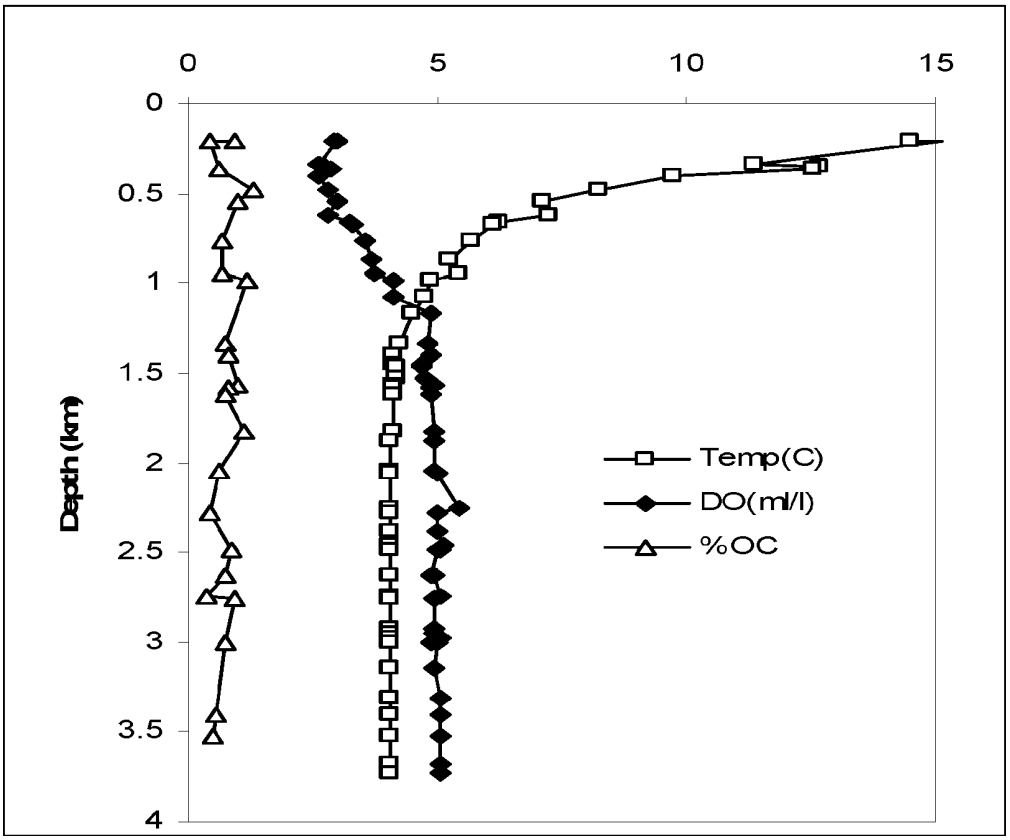

Figure 9-8. Composite profiles of temperature, dissolved oxygen and percent organic carbon in the sediments in the northern Gulf of Mexico.

9.3 Biogeochemical Processes—Community Function

9.3.1 Comparison of Methods

Four approaches have been utilized to estimate benthic community heterotrophic metabolism (= organic matter remineralization):

1) the food-web organic carbon model,

2) the organic carbon gradient/sediment accumulation rate model derived from radionuclide accumulation and age dating,

3) the vertical pore water profiles of the oxidation states of metabolites (O_2, Mn, NO_3, Fe and S), and

4) benthic chamber incubations conducted in situ with a benthic lander or in the laboratory with chambers recovered from box cores.

These can be ranked in the following order of descending rates of total carbon turnover: food-web model > chamber incubations > pore water profiles of metabolites > organic carbon gradient model. Resolving the disparities between these approaches is difficult, but some important issues are readily evident. The food-web model is based on information from the literature for estimating respiration rates as a function of animal size and temperature, with only limited direct measurements in the laboratory during this study. That this would lead to overestimation of rates, rather than simple stochastic inaccuracies, is not known. The pore water profiles and the organic carbon profiles may underestimate rates because they do not incorporate highly reactive material being reworked right at the sediment – water interface. A similar distinction has been observed over large areas of the deep Atlantic by, who refer to the chamber incubation-based rate the 'total flux' (of oxygen) and the rate based on the oxygen gradient as the 'diffusive flux', but they did not elaborate on the theoretical explanation of the differences.

9.3.2 Comparison of Total Community Metabolism with Other Ocean Margins

There is little reason based on the results of this study to suggest that the sea floor community metabolism differs appreciably from that measured at similar depths in other ocean basins. The abyssal plain sites had by far the lowest values in terms of carbon respiration rates (2.6 to 7.5 mg C $m^{-2}d^{-1}$), but these are not different, based on the data so far, from Pacific and Atlantic measurements on the middle continental rise at equivalent depths. The upper continental slope values also are somewhat less than what has been measured in the NW Atlantic continental margin organic carbon "depocenter" (Anderson et al. 1994). At similar depths in the Pacific such comparisons are difficult because at those depths the intense oxygen minimum impinges on the bottom and aerobic metabolism is inhibited (Devol and Christensen 1993).

An abrupt decline of known values of SCOC from the continental shelf adjacent to the slope sites was also observed. The highest values on the shelf have been measured near the Mississippi Delta in the area that becomes hypoxic or anoxic during stratified periods. The maximum rates there are on the order of 500 mg C m^{-2} d^{-1}, but that includes the high sulfate reduction that is known to occur near the delta but which is not incorporated into the oxygen uptake rates during low oxygen periods. In general, average shelf rates, according to the above authors, is on the order of 100 to 250 mg C m^{-2} d^{-1}, plus or minus 50%, over an annual cycle. Thus, the rates on the upper slope are on the order of ½ to 1/10 of the average shelf rates, but decline with depth to the abyssal plain by a factor of 10. This decline is typical of most continental margins.

9.4 Community Function and Structure Relationships

9.4.1 Carbon Budgets for Process Sites

The rate at which the carbon stock turns over can be calculated by dividing the stock at each site by the SCOC, both from Section 8, Results (Table 9-6). The biota turns over on the order of months at the upper to middle continental slope sites but this goes up to nearly a year on the abyssal plain.

Table 9-6

Relationship Between Site, Depth, Total Living and Total Detrital Carbon, Sediment Community Oxygen Consumption (SCOC, mg C m^{-2}-day) and Carbon Turnover Time in Days (Living Carbon) and Years (Detrital Carbon), Where 'Time' Equals the Stock Divided by the Rate

Depth	Site	Sed.Org.C	Total Living	SCOC	Biota (t=d)	[OC] (t=y)
500	MT1	7.60E+05	3441	35.7	96.4	58.3
1000	MT3	7.02E+05	2873	28	102.6	68.7
750	S42	3.75E+05	1577	56	28.2	18.3
1850	S36	6.72E+05	2158	22.4	96.3	82.2
2750	MT6	2.22E+05	1047			
3450	S4	3.21E+05	1493	4.8	311	183.2
3600	S1	2.87E+05	1423	4	356	196.6

On the other hand, the detrital carbon turns over much more slowly, but the general trend is the same as that for the biota. At the shallower sites, the turnover time is on the order of tens of years, whereas on the abyssal plain the turn over approaches 200 years. A comparison of similar calculations for the western North Atlantic suggests that the turnover time in the Gulf of Mexico at similar depths is somewhat longer for the living and the detrital carbon (Rowe et al. 1991). This possibly reflects the low concentrations of organic matter, and its diminished reactivity, in the Gulf compared to the N. Atlantic. It might have been suspected that the opposite would be the case because the temperature at depth in the GoM is higher than that in either the Atlantic or Pacific. The continental shelf off Louisiana has much faster carbon recycling time, which indicates that the delivery of organic matter to continental shelf benthos is much higher than the adjacent deep sea.

9.4.2 Metabolism as a Function of Biomass

SCOC declines as a function of total biomass, when all the infaunal organism biomass is summed up (Figure 9-9). It has been suggested that bacterial biomass is a function of POC input, rather than depth (Deming and Baross 1993), and SCOC is regarded as a the best surrogate for POC delivery to the sediment-water interface; thus it is logical that biomass of all the sediment organisms correlates with SCOC. Likewise, as the food-web model illustrates, the respiration of each group is parameterized as a function of the biomass of that group. Summing up those rates for those organisms living within the sediments is thus equivalent to the measured SCOC. As indicated in the introduction, a basic assumption of the approach used has been that THE underlying cause of variations in both structure and function is the amount and quality of organic matter entering the benthic boundary layer ecosystem.

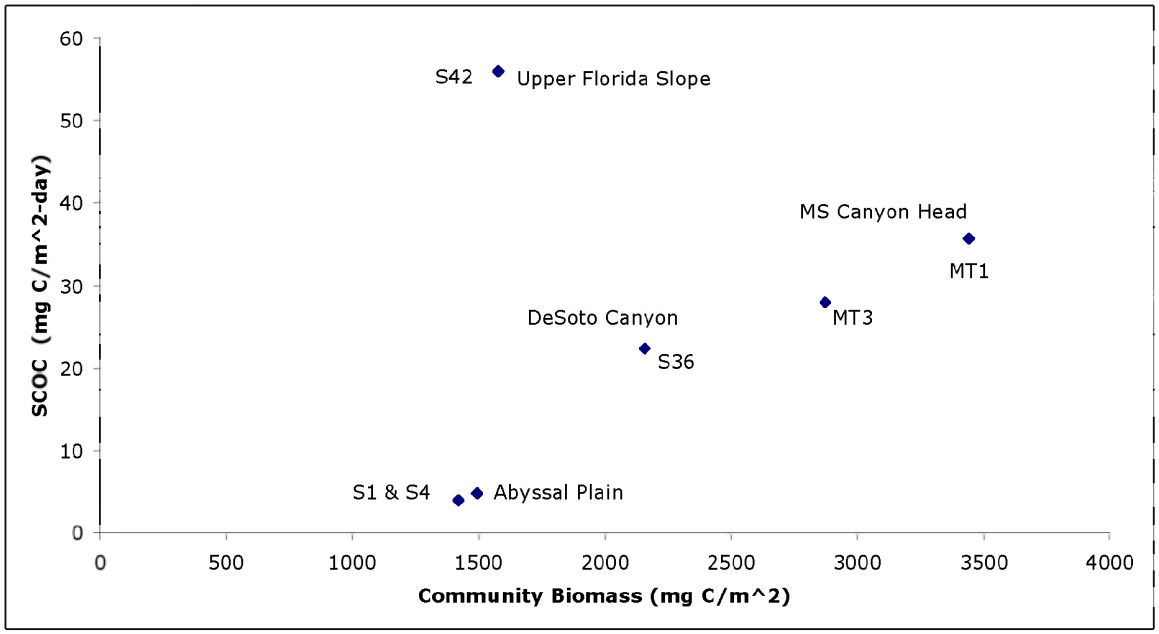

Figure 9-9. Relationship between sediment community oxygen consumption (SCOC) and total community biomass at the process sites, as indicated. Data from Section 8 – Results.

9.4.3 Total Metabolism and Its Relation to Species Composition

The species composition of the macrofauna, megafauna and fish groups (and meiofauna?) differed at the "process sites," reflecting, it is suspected, substantial differences in the intensity, and to some degree the quality, of organic matter input. For example, MT1, characterized by intense deposition of material originating from within the Mississippi River plume, was dominated by the amphipod *Ampelisca* sp. nov. and the megafauna, dominated by organisms that feed on suspended particulate matter (the anemone *Actinauge longicornis* and the bivalve mollusk *Amygdalum politum*). The dominance by crustaceans at the other sites on the upper continental slope changes to a dominance by echinoderms at depths greater than 1.5 km. This "echinoderm boundary" has been observed elsewhere, but never adequately explained (Rowe and Menzies 1969; Pequegnat et al. 1990). Bottom-dwelling demersal fish have all but disappeared by the abyssal plain. The boundaries between the "zones" of recurrent species of macrofauna, we contend, reflect regions of similar POC input and sediment type. Because these zones are each characterized by different densities of organisms, aligned along isobaths, we infer that each is characterized by different rates of POC input that decline downslope. Thus there is an upper and lower boundary of POC input rates which govern the distribution of each zone. Unfortunately, we have yet to quantify these controlling rates using conventional methods.

It is possible to define these boundaries indirectly however. By plotting the upper and lower depth boundaries of each zone over the SCOC – depth plot, the "net POC input" can be estimated for the presumptive upper and lower POC boundaries for each zone (Figure 9-10), making the assumption that SCOC is a good reflection of POC input. The weakness of this approach with this data is that the SCOC was measured at a limited number of sites, and defining this relationship was not the intention of the study. Note that this does not include sites in the western GoM. To generate a similar relationship for the western transects, the SCOC has been

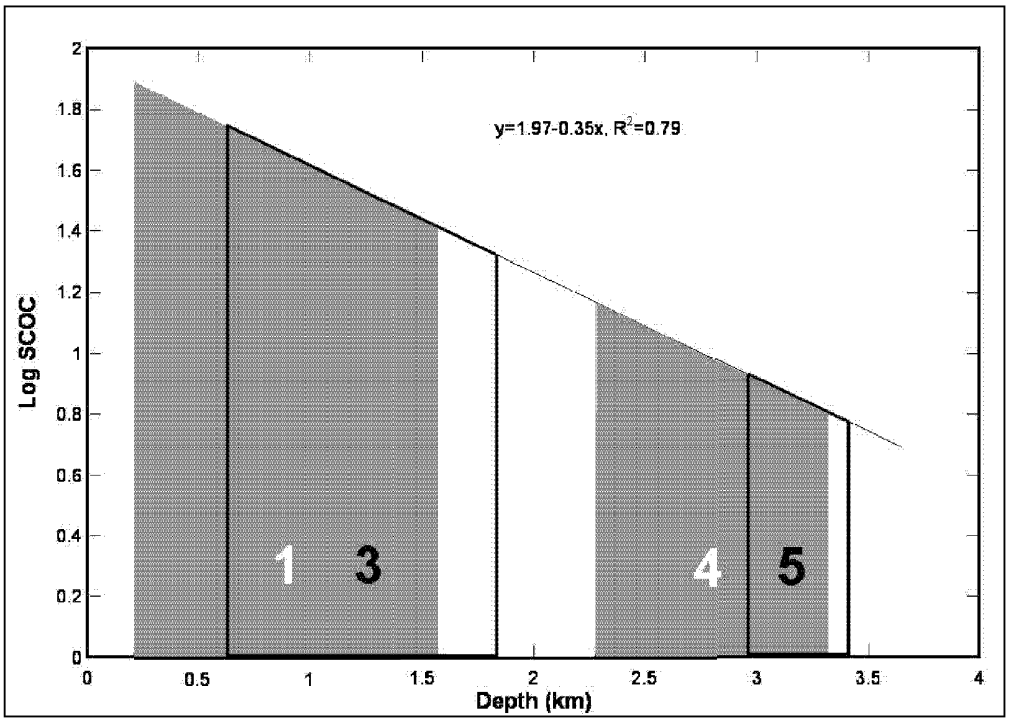

Figure 9-10. Log SCOC (sediment community oxygen consumption) (mg C/m^2 day) as a function of water depth (km) for process stations.

estimated from the macrofauna biomass (Figure 9-11). Note that the mid-slope zone (Zone 2) is bounded by a rate that is below the rate in the zone at the same depth interval (Zone 3), more inferential evidence that it is the input of POC that controls the zones.

9.4.4 Food Web Carbon Budget

The standing stocks, in terms of organic carbon (mg C m^{-2}-15 cm), have been assembled for each of the process sites (Table 9-3) for comparison. A summary of measured carbon fluxes would also include the total measured sediment community oxygen consumption (SCOC, Table 9-6) and the rate at which organic matter is buried (OMB), the latter calculated from percent organic carbon profiles and mean rate of sediment accumulation at each site estimated by the rates of the fluxes are in units of mg C m^{-2} d^{-1}. The variation in stocks along the rows (Table 9-3) allows a comparison of the carbon stocks at each site, as mean organism size increases, whereas the variation in the columns provides a comparison of differences in stock size at the different experimental sites, from shallow to deep water. The last three columns and rows in Table 9-6 allow comparison of net measured rates with the total stocks, either by site or across the depth gradient. The sum of the burial and the community respiration rates can be assumed to be more or less equal to net organic carbon flux to the sea floor at that site. In general, the net accumulation is so small relative to the respiration (Rowe et al. 1991) that many investigators ignore it in food web carbon budgets (Smith and Hinga 1983, Smith 1992). In general, however, there is considerably more detrital organic matter than living material at all the sites, which is not unusual. There is universally more organic matter, both living and detrital, at the shallow sites compared to the deep ones; that too is typical of most continental-margin depth gradients. At all

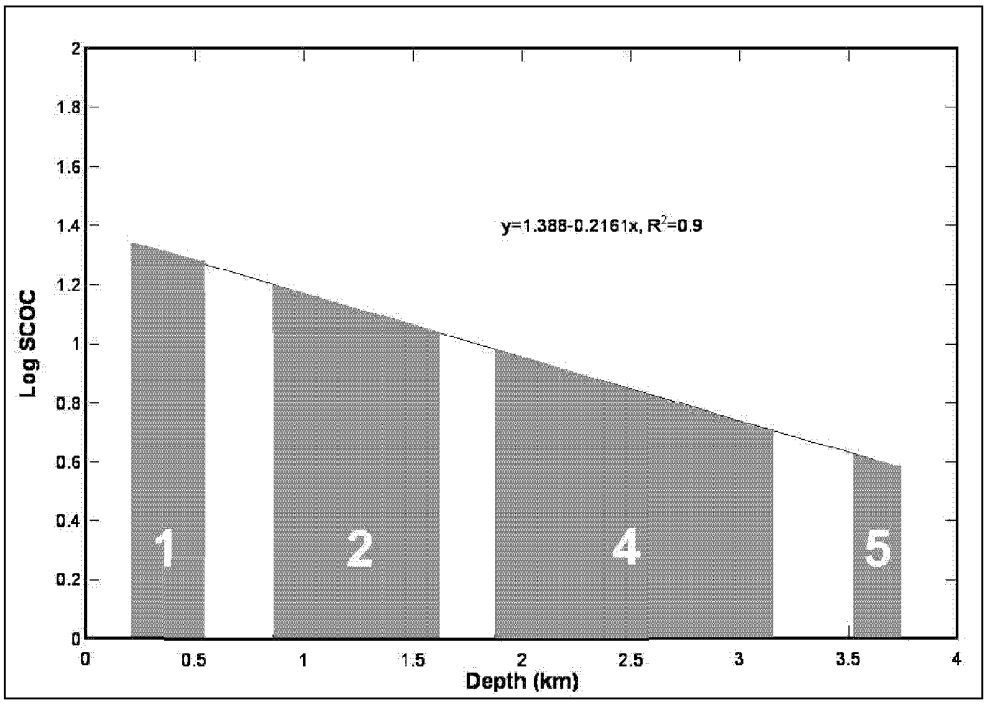

Figure 9-11. Log SCOC (mg C/m^2 day) as a function of water depth (km) for western transects, with SCOC estimated from macrofauna biomass.

sites, regardless of depth, most of the organic matter was found in the smaller size groups. The relative decline in total biomass from small- to large-sized organisms was greater in deep than in shallow water, which is counter to the "bigger – deeper" rule, which simply illustrates that for the GoM the larger organisms are of less significance in deep water. The organic detritus and the bacteria declined by factors of two or less with depth, whereas the larger organisms declined by one to two orders of magnitude over the same depth interval. This implies that the quality of the organic matter in the sediments and the portion of the total bacteria that are active are both declining with depth.

The standing stock and rate data from two sites have been put into two, oversimplified, contrasting food-web carbon budgets to illustrate how the shallow, upper-slope sites with relatively high biomass differ from the deep, abyssal plain sites with low biomass, meager input of organic matter and low SCOC. The shallow budget is based on MT1 at the head of the Mississippi Trough at a depth of 500 m (Figure 9-12), whereas the deep site is JSSD 1 on the Sigsbee Abyssal Plain at a depth of 3,650 m (Figure 9-13). The boxes represent each stock, whereas the arrows represent fluxes between the stocks. Each living stock is represented by a loss to respiration. This was estimated from the literature, based on animal size and temperature, for the animals. The bacteria respiration stock was estimated by subtracting the sum of the meiofauna and macrofauna respiration rate estimates from the chamber-determined "whole" sediment community rate, SCOC, in Table 9-6.

Steady state has been assumed and therefore the sum of the fluxes into each stock must equal to the sum of the negative fluxes out of each box. The fluxes between the stocks, mostly predator-prey relationships, have been based on presumed secondary production (growth) and

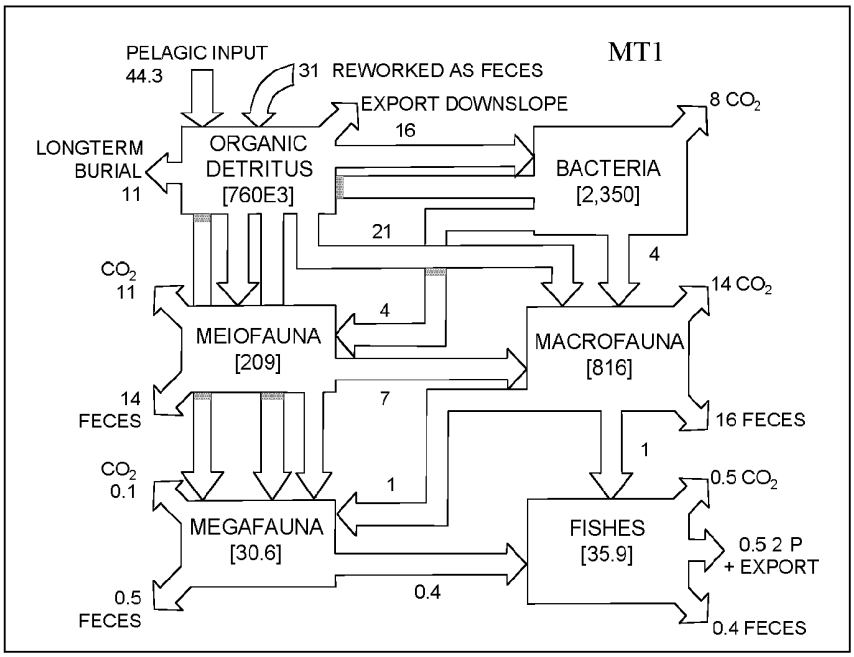

Figure 9-12. Carbon budget in the food web at MT1, at the Head of the Mississippi Canyon. Stocks (boxes) are mg C/m^2-15 cm and fluxes (arrows) are mg C/m^2-day. Data from Section 8, calculated as indicated in text or by algebraic substitution, at steady state.

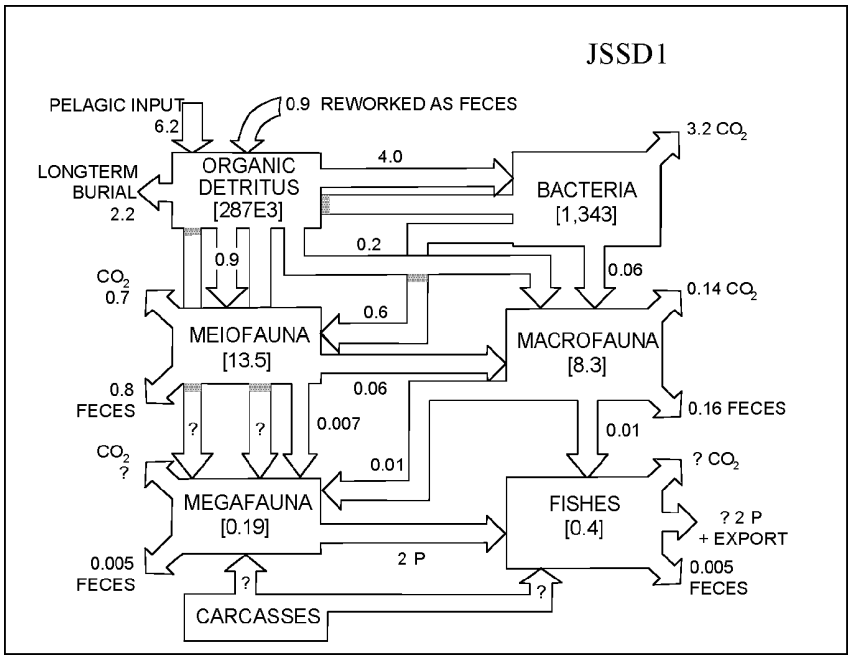

Figure 9-13. Carbon budget in the food web at steady state for the Sigsbee Abyssal Plain. Units are mg C/m^2-15 cm for the stocks (boxes) and mg C/m^2-day for the fluxes (arrows). Data from Section 8, calculated as indicated in the text, or calculated by algebraic substitution.

assimilation efficiencies. The growth to respiration efficiency for the bacteria is assumed to be 50%. The respiration to growth ratio of the megafauna and the fishes was assumed to be 10%. Growth rates for the fishes were derived from growth-curve constants available in "FishBase," but were transformed into first-order (linear) rates for simplicity. Fluxes between stocks have been rounded off to one significant digit. Assimilation efficiency (assimilated food/total food ingested x 100) has been assumed to be 50% for invertebrates and 75% for the fishes.

Each of the two budgets or stock/flux models is represented by the same six stocks in a similar order, with organic detritus on the upper left, terminating with the fishes on the lower right. The input terms in both extremes are defined as a rain of sedimenting particulate matter (POC) as the principal supply of carbon to the system, but the deep site also includes an input from carcasses in the lower left, the value of which is unknown. At both sites, the bacteria feed only on organic detritus, the meiofauna feed on both the bacteria and the organic detritus, the macrofauna feed on the latter three components, the megafauna feed on the latter four components, but the fishes feed only on the megafauna and the macrofauna. Although the relative proportions of the food sources to each feeding stock are unknown, it is presumed that each stock will prefer to feed on the largest size available because this is the most energetically efficient pathway. The secondary production of each stock at steady state is divided up to meet the needs of the next level of the food web. The production to biomass ratio for the macrofauna is assumed to be one (P/B=1) and the meiofauna are assumed to produce a cohort every month.

The carbon-based food web budgets, calculated on the basis of biomass per individual, total biomass and temperature for each experimental site, provide an integrated picture of how carbon is cycled within a food web. By summing up all the respiration values, one can estimate total community oxygen consumption (SCOC). At a site in the deep NW GoM investigated the rate calculated by the model was several times that measured with a single benthic chamber in situ on the lander. Nonetheless, the general trends between the two are in agreement: directly measured rates with chambers and indirectly estimated rates based on biomass follow parallel, linear patterns that also correspond to depth or unique location, e.g., the head of the Mississippi Trough. The pore water profiles followed the same pattern too, but with some exceptions on the upper slope. Biomass, we can conclude, is a better determinant of SCOC than is depth (Figure 9-14), a relationship pointed out previously.

Several generalizations can be stated about these two budgets, both in terms of how they are similar and how they differ. Most of the carbon is in the detritus box, followed by the bacteria, at both the shallow and the deep sites. The "dead" carbon is several orders of magnitude higher than the living bacteria. The animal stocks are also orders of magnitude lower than the detritus and bacteria components, but the ratio between the dead and small to the larger boxes ((bacteria+detritus carbon) / (meiofauna+ macrofauna+megafauna+fishes)) is much larger at the deep site. At both sites, a large fraction of the detritus is recycled back into the detritus box as feces, but the ratio of the recycled POC to the "fresh" POC is greater at the deep site. This transit of "mud" through the guts of animals results in mixing of surface material and results in the bioturbation redistribution of radionuclide tracers investigated [See Section 8.5]. The food-web carbon budgets confirm the radionuclide profiles that suggest that the mixing is proportional to how many animals are present. That is, the total turned over or recycled through the guts of organisms is considerably greater in shallow water than out on the abyssal plain. At both sites, most of the cycling occurs within the three small components living in and on the sediments, rather than through the larger organisms (megafauna and fishes).

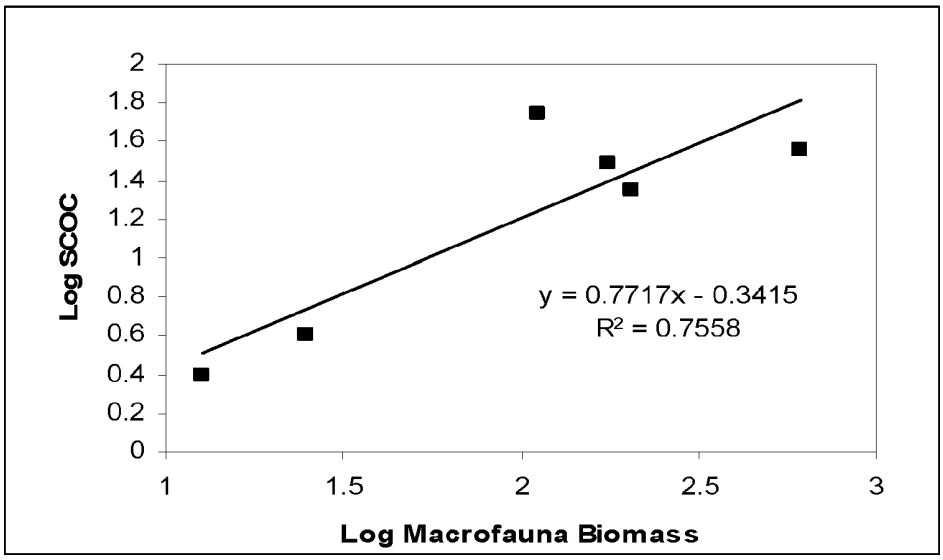

Figure 9-14. Sediment Community Oxygen Consumption (mg C/m^2-day) as a function of the macrofauna biomass at the process sites. The high SCOC is S42 on the west Florida upper slope (740 m depth), whereas the high biomass is MT1 at the head of the Mississippi Canyon. The two low values are on the Sigsbee Abyssal Plain.

The relative contributions of each category of biomass contribute to the total suggest that as input declines the larger forms are eliminated first, as suggested previously (Thiel 1975). Species composition may also be important at this "reductionist" level of analysis. In some cases "keystone species" are seemingly important at some process sites. Can we possibly characterize each site by these species? For example, S42 (on the upper Florida escarpment; 750 m) shares dominance with two big crustaceans and about 10 other large crustaceans (decapods), but not a single species that is functionally dominant at structuring the assemblage of smaller organisms. This may simply be a function of S42 being some sort of faunal transition zone, as suggested in the literature (Menzies et al. 1973).

The clear dominance of the bacteria at the abyssal plain and lower slope sites (JSSD1, JSSD4 and MT6) suggests that bacteria have greater importance in deep water and support the idea that they are necessary for the remobilization of organics. But new thoughts on bacterial role below The sharing of total biomass between the mid-sized and larger metazoans at upper slope sites with the highest biomass values suggests, it follows, that they are not dependent on the bacteria and size groups more or less share newly arrived detritus that is energy-rich and reactive. In essence, the different size categories not only share this material, but compete for it. All these forms support the limited numbers of predators that, from the top down, affect community structure.

In general, the megafaunal invertebrates collected during the current study followed much the same pattern of depth distribution reported previously by Pequegnat (1983) and Pequegnat et al. (1990), who reported that overall species diversity decreased with depth. However, in this study, diversity tended to be lowest at the shallowest stations, in basins, and in areas dominated by small sponges. The greatest species diversity was at the deepest stations of the Mississippi Trough. On the upper and middle slopes, diversity tended to be slightly more variable from station to station than on the lower slopes and abyssal plain, where, except for the high value at

station MT6, diversity indices were comparable throughout the sampling area. At the deepest stations, echinoderms tended to dominate the megafauna.

Soto et al. (1999) concluded that diversity and biomass of decapod crustaceans in the southwestern Gulf of Mexico were associated with substrate heterogeneity and seasonal pulses of organic material from rivers. The abundance and species diversity of megafaunal invertebrates in the Mississippi Trough and DeSoto Canyon would seem to support this relationship in the northern Gulf as well. The great biomass of echinoderms at depths of 2,500 m or more may be misleading, because much of this wet weight is due to fluid in the coelomic cavities of the animals.

On the upper slopes (1,000 m or less), many animals were associated with soft, silty bottoms. The crabs *Acanthocarpus alexandri*, *Lyreidus bairdii*, and *Bathyplax typhla* were characteristic of such areas. Live specimens of the first two species burrowed into mud when kept in aquaria. Species of *Nephropsis* have been photographed in burrows in the mud (Pequegnat, 1983). Studies on the related *Nephrops norvegicus* indicate that groups of lobsters build tunnels in mud. On the other hand, Soto (1985) reported that the crab *Rochinia hystrix* favored hard substrates.

The nested mussel *Amygdalum politum* was particularly common in the area of the Mississippi Trough. This mussel is able to attach to conspecifics, forming a mass that will not sink into loose sediment. Its abundance in the Mississippi Trough may be related to the flow of organic food particles in the area. Stalked barnacles (*Arcoscalpellum* and *Neoscalpellum* spp.) did not show any relationship to any large-scale environmental feature, but often were attached to "clinkers" or sponge spicules. The sponges *Hyalonema* sp. and *Euplectella* sp. possess anchor spicules that raise the feeding parts of the sponge above the substrate. These sponges usually were collected in clay.

The data and the model of the small-size categories suggest that we might re-consider the role of bacteria in the food webs of the deep GoM. POC rains down from surface waters to support metabolic processes and growth of all the organisms. It contains with it an ill-defined fraction of bacteria on the particulate matter but it can probably be presumed that these have been inactivated by the cold and pressure of the environment – the attached surface bacteria too have become inert POC particles while sinking into an environment alien to them. Once on the sea floor they contribute to the total organic matter at a level that is proportional to detrital organic matter and the inorganic clay particles, including siliceous or calcarious biogenic material. These inert cells are introduced into a living bacterial assemblage composed of psychrophilic, barotolerant (or barophilic) populations that are presumed to be consuming detrital organics in proportion to that available to them.

Within shallow environments it is presumed that most of the bacterial activity is supported by DOM rather than POM. This would imply that the sinking POM must be remobilized into DOM before it is available to potentially active bacterial populations, either through "messy feeding" or released with the feces. In this scenario, much of the POM would be consumed first by invertebrates who would digest some fraction of it and release a companion fraction in the form of DOM to be consumed by the bacteria (Jumars et al. ref.). The model for these pathways is implied for the food-web models representing our composite "process sites" but we make no distinction in the detritus box between DOM and POM. Our model does include fecal production that re-enters the detrital pool (Figure 9-10 and 9-11), but again no distinction is made between POC and DOC. A model in which a distinction between POC and DOC illustrates that bacteria consume DOC primarily and this repackaging conserves carbon and energy; it suggests that the bacteria are dependent on the invertebrates but diminishes the role of the bacteria energetically as

an intermediary between organic detritus (POC) and the invertebrates. Such a configuration takes DOM and re-packages it into living organisms that can then be consumed by the invertebrates in a food web reminiscent of the "microbial loop" hypothesized for surface waters. The two budgets illustrate that the relative roles of the different size groups within the sediment are about equal, and implies that the bacteria, for the most part, are not actively growing. The relative proportion of them that are inactive increases with increasing depth, probably due to the hostile environment of low temperature, high pressure and meager amounts of reactive organic matter available.

9.4.5 Sequestration of Conservative Chemical Properties (Bioturbational Mixing)

The evidence suggests that biological reworking and mixing carries non-conservative chemicals, including contaminants, one might presume, to depth in the sediment, thus isolating them from further interaction with the biota of the Benthic Boundary Layer (BBL). This phenomenon has previously been noted for the continental shelf of the NW Atlantic, again using ^{210}Pb as a tracer. In the case of GoM slope sediments, it might be suggested that the grain size gradient, from sand-sized foraminiferal ooze down to clay-sized material, with depth as the $CaCO_3$ material dissolves, enhances sediment binding capacities.

10. UNKNOWNS AND RECOMMENDATIONS

10.1 Community Structure

It is presumed in contemporary literature [See the works of Gray in the references for a summary of these issues in the marine environment.] that community structure (the diversity of assemblages) is controlled by a suite of ecological parameters in concert with the given biogeographical history of a habitat within an ecosystem. For example,

Species Evenness = f(food input, variability, stress, competition, predation)

Species diversity, defined either as the alpha (relationship of numbers of species to individuals or area), beta (turnover or change in species composition along a gradient), or gamma diversity (total number of species), are each controlled, to a greater or lesser extent, by the following parameters: E(s) = f(controls of evenness, plus historical contributions), Gamma (species richness) = f(geological history, sources of species available for recruitment, structural complexity, all the other parameters listed above that affect evenness and alpha diversity measures). These processes work together, on each taxonomic group in question in a different way and at different rates, toward success (survival) or failure (extinction) of each species.

While considerable information on each of these measures of structure has been developed, NONE of the variables listed has been measured directly. In fact, these variables cannot be measured directly without applying the scientific method to direct experiments that test hypotheses. This study has been based on the correlations accrued from the extensive sampling grid, accompanied by considerable sampling replication. The conclusions drawn are based on correlations, and thus are no more than that. They are not based on experiments that manipulate the fauna and the conditions directly.

We are left with a set of statistical models that are purported to describe how structure of communities is related to variables in the deep ocean. However, that is all they are: statistical models. They have not been validated experimentally.

We are left, therefore, with a set of questions related to community structure:

- How do physical variables in concert affect community structure, if at all?
- Is structure a function of OM input alone, or to what degree is it just OM or a set of physico-chemical constraints? Can this be tested experimentally?
- How long does it take a set of community structural traits to be established?
- Is this a function of ocean basin age (10^x years) or ecological conditions (months to years)? and;
- What biological variables, which are characteristic of particular species and larger taxa, are important in this (growth rate, mode of reproduction, mean and maximum age, feeding strategies, dispersal vs brooding of eggs and juveniles, etc.)?

The present study attempted to be sequential, moving from a survey, relating community structure to the environment, into an experimental mode at a select set of "process" sites. What actually happened was that the suite of information at the process sites was enlarged to include some rates of processes, but no experiments were conducted in the classic sense. The result was that we know in better detail what is happening at the process sites, but the relationships between

the environment and community structure were not studied using experiments to test hypotheses, in the classic sense. We must conclude therefore that this study added evidence to what we believe controls structure, but simply allowed the investigators to revise their hypotheses without actually conducting experiments.

In the context of the responsibilities of the Minerals Management Service, this study has provided considerable information on what organisms might be affected by a broad suite of impacts from O&G activities, but it does not give definitive insights into what the responses might be.

This leads to one major conclusion concerning continued studies: direct experimentation should be designed and conducted to test hypotheses related to effects of oil and gas (O&G) activity on the deep ocean.

10.2 Community Function

An underlying theme throughout this study was that organic matter supplies are the ultimate control of both community structure (see above) and function, the latter defined as rates of biological and biogeochemical processes. The broad geographic sampling pattern comparing different habitats, followed by intensive rate measurements at a small set of contrasting habitats with characteristic communities, has allowed food web models to be constructed that contrast extremes encountered. The models implicate food supplies directly as the underlying or supporting component on which the food web relies. These appear to be very convincing, even though it is conceded that the specific estimates of the individual fluxes may be subject to large variations.

It must be conceded that most of the individual predator-prey transfers between the stocks in the food web have not been validated. The boundary conditions are subject to validation by direct sampling: more and better community respiration measurements, sediment trap measurements, and better, more extensive geochemical dating. However, these approaches will refine the boundaries, not the internal workings within the system. Attempts to measure some of these were tried, but their success is questionable because the rates derived do not match indirect measurements or predicted values of rates based on known shallow water work or deep-sea studies conducted elsewhere.

The next step in understanding biological community function ought to include direct measurement of rates of processes on the sea floor using a second generation of instruments capable of conducting experiments associated with the bottom boundary layer and the community of organisms living there. This would allow the validation of the models that have been developed from the present study. Without this validation, the results of this study will remain only hypothetical models.

A specific set of additional questions would include the following:

1) What fraction of the OM delivered to the sea floor from the water column is refractory and what is reactive?
2) Are there processes, within the food web, that transform refractory matter into reactive?
3) Are the bacteria inactive and just accumulating with the sediments, sort of like a conservative chemical parameter?

4) Even if bacteria are not active, are they eaten by the deposit feeders?

5) What happens when organic matter is added to the system? Does this confirm the model predictions?

The next step in understanding the deep ocean's responses to O&G activity is direct experimentation on the sea floor to test hypotheses related to potential O&G activity. For example, what is the effect of added hard substrate associated with exploratory drilling, processing on the sea floor, production and transport of product from site to site along the sea floor? What is the effect of added materials that are lost from or are byproducts of the processes and additions related to O&G activity. Reasonable hypotheses could be proposed for many of the most salient effects, and these need to be tested. Drilling mud for example has many different compositions. Each may have a different specific effect. However, the degree to which each contributes reactive organic matter may be rather general, and determining this might be very important for predicting the effects of O&G activity. These issues could and should be approached using hypothesis-based experiments in situ with state-of-the-art instrumentation available in the O&G service industry and government.

In summary, the next step in making progress toward rational decision-making in the environmental effects of O&G activity in the deep ocean would be to initiate experimental studies to test hypotheses that are related directly to O&G activity.

10.3 Taxonomy

The taxonomy of the larger forms sampled in this study is fairly well known, with few undescribed or poorly-described species encountered (the fishes and megafauna), but this is not true for the macrofauna and the meiofauna. On the order of 50% or more of all the groups of macrofauna studied were considered species that are either new to science (undescribed in the taxonomic literature) or so poorly described that their specific designation could not be determined. In these cases the individuals of specific morpho-types were lumped into single "species" categories and designated in the data base as "species a, b. ..., etc." or "species 1, 2, ..., etc." throughout. While this does no harm to the analyses of community structure in this report, the limited descriptions in the literature will remain a serious impediment to the usefulness of future work. Without good descriptions, an investigator will need to see the actual preserved "type" organisms themselves to which each designation refers in order to determine if a particular species observed in DGoMB is the same as that in both previous and future investigations. The reason for this problem is the serious lack of trained, committed taxonomists working on the invertebrate groups composing the bulk of the macrofauna and the meiofauna.

10.4 Relationships between Function and Structure

The goal of correlating structure and function met with considerable success. The broad sampling pattern allowed the degree to which zonation (beta diversity) extends continuously along isobaths to be tested and, ultimately, to be mapped for each size group and for taxonomically separate groups. The zonation's correlations with biomass and SCOC implicate the decline in the input of organic matter as a function of depth as a principal control of beta diversity or zonation. However, no direct experimental evidence is available to confirm these revised hypotheses. A direct step in such a question would deploy a set of sediment traps across and down the depth gradient. In this study, SCOC has been used as a surrogate for POC input (net). As each so-called zone has a characteristic biomass and species composition, it is

reasonable to presume that the input of supporting organic matter also controls those biological variables. However, as above, this has not been tested with direct experiments.

10.5 The Unknowns and the Unknowable

Following the general philosophical approach of the Census of Marine Life (CoML), deep ocean ecology must recognize that a distinction ought to be made between the "unknown," which can be understood, quantified, described, etc., through continued and improved observations and experiments, and those things that are, for one reason or another, categorized as the "unknowable." A goal of CoML in a variety of marine ecosystems at all depths is the tabulation of every known species, accompanied by the locations at which each has been observed. It is recognized however that descriptions of "all" species in the deep ocean will, for all practical purposes, never be accomplished. While much can and will be gained by future work that iinvolves more sampling from the surface with conventional gear and hypotheses concerning structure and function can be tested using direct experiments, some parts of the models and a complete listing of species for any given location will never be realized. The unknowns are listed in this Section, but the unknowables are not.

10.6 Summary of Unknowns and Recommendations for Further Study

This section is a list of specific unanswered questions which derive from the individual subsections in Section 8 and 9 of the final report.

Relationships between Physical Processes (Deep Bottom Currents) and the Biota

The fauna at the base of Green Knoll was not similar to any of the 5 zones described. This suggests that the fauna may be controlled by the conditions at that site, perhaps a deep, bottom-following current. The area is characterized by large bus-sized channels and it is presumed that these were or are caused by currents flowing around the base of the knoll. This is all conjecture, however. It is not known what caused this community to differ from others in the study.

Time-Dependent Variations in the Biota and Rates of Biological Processes

The study was conducted over a 3 year period, but always in the May or June, with the exception of two weeks in August, 2002. This sampling did not allow any variations in time on the scale of seasons to be determined. It has been observed elsewhere that the production of phytoplankton on the surface varies seasonally and this results in a seasonal pulse of organic to the sea floor. The fauna may respond to this pulse, but further study will require seasonal sampling at specified sites to determine this.

Direct Responses of the Biota in Terms of Species Composition and Rates to Pulsed Inputs of Organic Matter to the Sea Floor

While the premise behind the hypotheses tested was that the input of organics controls much of what is observed in the biota, this has not been tested directly. Experiments should be conducted to determine the effects of organic pulses on the sea floor. This issue is particularly important to MMS because loss of product or drilling mud onto the sea floor could, from a theoretical point of view, increase total biomass and amplify rates of processes on the sea floor measurably.

Distributions of Standing Stocks

While the standing stocks of all the major size groups represented in the bottom boundary layer food web conformed to more or less predictable declines with increasing depth, the bacteria densities did not. The bacteria declined in a smooth regression down to the base of the continental slope, but then increased out on the abyssal plain. This needs to be investigated further.

Rates of Metabolic Processes and Organic Carbon Turnover

The cycling of organic matter on and in the sea floor was estimated by a number of methods. The general trends in these rates were fairly well correlated from site to site, but the absolute values did not agree. It is recommended that a small number (2 to 3) of easily accessible, contrasting locations be chosen to conduct controlled sampling and experiments on rates of processes in order to resolve the disagreements. The most secure approach would be to conduct experiments in situ with a Remotely Operated Vehicle or a manned research submersible to eliminate issues that arise from decompression and temperature changes.

LITERATURE CITED

Agard, J.B.R., J. Gobin, and R.M. Warwick. 1993. Analysis of marine macrobenthic community structure in relation to pollution, natural oil seepage and seasonal disturbance in a tropical environment (Trinidad, West Indies). Marine Ecology Progress Series 92:233-243.

Agassiz, A. 1888. Three cruises of the *Blake*. New York, NY: Houghton Mifflin. 314 pp.

Aharon, P. 2000. Microbial processes and products fueled by hydrocarbons at submarine seeps. In: Riding, R.E. and S.M. Awaramik, eds. Microbial sediments. Berlin, Germany: Springer-Verlag. Pp. 270-281.

Aller, J.Y. 1989. Quantifying sediment disturbances bottom currents and its effect on benthic communities in a deep-sea western boundary zone. Deep-Sea Research 36A:901-34.

Alongi, D.M. 1990. Bacterial growth rates, production and estimates of detrital carbon utilization in deep-sea sediments of the Solomon and Coral Seas. Deep-Sea Research 37:731-746.

Alperin, M.J., C.S. Martens, D.B. Albert, I.B. Suayan, L.K. Benninger, N.E. Blair, and R.A. Jahnke. 1999. Benthic fluxes and porewater profiles of dissolved organic carbon in sediments from the North Carolina continental slope. Geochimica et Cosmochimica Acta 63:427-448.

Anderson, R.F., G.T. Rowe, P.F. Kemp, S. Trumbore, and P.E. Biscaye. 1994. Carbon budget for the mid-slope depocenter of the Middle Atlantic Bight. Deep-Sea Research II 41(2/3):669-703.

Antia, N.J., C.D. McAllister, T.R. Parsons, K. Stephens, and J.D.H. Strickland. 1963. Further measurements of primary production using a large-volume plastic sphere. Limnology and Oceanography 8:166-183.

Bell, S.S. 1980. Meiofauna macrofauna interactions in a high salt marsh habitat. Ecological Monographs 50:487-505.

Bernal, C.E. 2001. Spatial and temporal distributions of particulate matter and particulate organic carbon, northeast Gulf of Mexico. M.S. Thesis. Texas A&M University, Department of Oceanography, College Station, TX. 99 pp.

Berner, R.A. 1980. Early diagenesis: A theoretical approach. Princeton, NJ: Princeton University Press. 241 pp.

Bernhard, J.M. 1989. The Distribution of benthic foraminifera with respect to oxygen concentration and organic carbon levels in shallow-water antarctic sediments. Limnology and Oceanography 34:1131-1141.

Bianchi, T.S., S. Mitra, and B.A. McKee. 2002. Sources of terrestrially-derived organic carbon in lower Mississippi River and Lousiana shelf sediments: Implications for differential sedimentation and transport at the coastal margin. Marine Chemistry 77:211-223.

Biggs, D.C. and P.H. Ressler. 2001. Distribution and abundance of phytoplankton, zooplankton, ichthyoplankton, and micronekton in the deepwater Gulf of Mexico. Gulf of Mexico Science 19:7-35.

Bjornsen, P.K. and J. Kuparinen. 1991. Determination of bacterioplankton biomass, net production and growth efficiency in the Southern Ocean. Marine Ecology Progress Series 71:185-194.

Boland, G. and G.T. Rowe. 1991. Deep-sea benthic sampling with the GoMEX box corer. Limnology and Oceanography 35(5):1015-1020.

Boothe, P.N. and W.D. James. 1985. Neutron activation analysis of barium in marine sediments from the north central Gulf of Mexico. Journal of Trace and Microprobe Techniques 3(4):377-399.

Boothe, P.N. and B.J. Presley. 1985. Distribution and behavior of drilling fluids and cuttings around Gulf of Mexico drilling sites. American Petroleum Institute Draft Final Report. Washington, DC: American Petroleum Institute. API Project No 243. 140 pp.

Boothe, P.N. and B.J. Presley. 1989. Trends in sediment trace element concentrations around six petroleum drilling platforms in the northwestern Gulf of Mexico. In: Engelhardt, F.R., J.P. Ray, and A.H. Gillam, eds. Proceedings of the 1988 international conference on drilling wastes, Calgary, Canada, 5-8 April. New York, NY: Elsevier Applied Science. Pp. 3-21.

Boschker, H.T.S., J.F.C. De Brower, and T.E. Cappenber. 1999. The contribution of marcophyte-derived oganic matter to microbial biomass in salt-marsh sediments: Stable carbon isotope analysis of microbial biomarkers. Limnology and Oceanography 44:309-319.

Boudreau, B. 1996. Diagenetic models and their implementation. Springer-Verlag. Berlin. 414 pp.

Bright, T. 1968. A survey of the deep-sea bottom fishes of the Gulf of Mexico below 350 meter. Ph.D. dissertation. Texas A&M University, Department of Oceanography, College Station, TX.

Brooks, J.M., M.C. Kennicutt, II, C.R. Fisher, S.A. Macko, K. Cole, J.J. Childress, R.R. Bidigare and R.D. Vetter. 1987. Deep-sea hydrocarbon seep communities: evidence for energy and nutritional carbon sources. Science 238:1138-1142.

Capurro, L.R.A. and J.L. Reid, eds. 1972. Contributions on the physical oceanography of the Gulf of Mexico: Volume 2. Texas A&M University Oceanographic Studies. Houston, TX: Gulf Publishing. 288 pp.

Carney, R.S. 1971. Some aspects of the ecology of mesothuria lactea theel, a common bathyal holothurian in the Gulf of Mexico. M.S. Thesis. Texas A&M University, Department of Oceanography, College Station, TX.

Carney, R.S. 1994. Consideration of the oasis analogy for chemosynthetic communities at Gulf of Mexico hydrocarbon vents. Geo-Marine Letters 14:149-159.

Carney, R.S. 1998. Workshop on environmental issues surrounding deepwater oil and gas development: Final report. U.S. Dept. of the Interior, Minerals Management Service, Gulf of Mexico OCS Region, New Orleans, LA. OCS Study MMS 98-0022. 163 pp.

Charney, J.G. and G.R. Flierl. 1981. Oceanic analogues of atmospheric motions. In: Warren, B.A. and C. Wunsch, eds. Evolution of physical oceanography. MIT Press. Boston, MA. Pp. 504-548.

Cifuentes, L.A., J.H. Sharp and M.L. Fogel. 1988. Stable carbon and nitrogen isotope biogeochemistry in the Delaware estuary. Limnology and Oceanography 33:1102-1115.

Cooper, C.A., G.Z. Forristall and T.M. Joyce. 1990. Velocity and hydrographic structure of two Gulf of Mexico warm-core rings. Journal of Geophysical Research 95:1663-1679.

Coull, B.C. and S.S. Bell. 1979. Perspectives of marine meiofauna ecology. In: Livingston, R.J., eds. Ecological processes in coastal and marine systems. New York, NY: Plenum Publishing. Pp. 189-216.

Coull, B.C. and M.A. Palmer. 1984. Field experimentation in meiofaunal ecology. Hydrobiologia 118:1-19.

Coull, B.C., R.L. Ellison, J.W. Fleeger, R.P. Higgins, W.D. Hope, W.D. Hummon, R.M. Rieger, W.E. Sterrer, J. Thiel and J.H. Tietjen. 1977. Quantitative estimates of the meiofauna from the deep-sea off North Carolina, USA. Marine Biology 39:233-240.

deJonge, V.N. and L.A. Bouwman. 1977. a simple density separation technique for quantitative isolation of meiobenthos using the colloidal silica Ludox TM. Marine Biology 42:43-148.

Deming, J.W. 1985. Bacterial growth in deep-sea sediment trap and boxcore samples. Marine Ecology Progress Series 25:305-312.

Deming, J.W. and J.A. Baross. 1993. The early diagenesis of organic matter: Bacterial activity. In: Engel, M. H. and S. A. Macko, eds. Organic Geochemistry, Vol 6, Topics in Geobiology. New York, NY: Plenum Publishing. Pp. 119-144.

Deming, J.W. and P.L. Yager. 1992. Natural bacterial assemblages in deep-sea sediments: Towards a global view. In: Rowe, G.T. and V. Pariente, eds. Deep-sea food chains and the global carbon cycle. Boston, MA: Kluwer Academic Publishers. Pp. 11–27.

Denoux, G., P. Gardinali and T.L. Wade. 1998. Quantitative determination of polynuclear aromatic hydrocarbons by gas chromatography/mass spectrometry—selected ion monitoring (sim) mode. In: Lauenstein, G.G. and A.Y. Cantillo. Sampling and analytical methods of the national status and trends program, mussel watch project: 1993-1996 update. U.S. Dept. of Commerce, National Oceanographic and Atmospheric Administration, Seattle, WA. NOAA Technical Memorandum NOS ORCA 130. Pp.129-139.

Deuser, W.G. and E.H. Ross. 1980. Seasonal change in the flux of organic carbon to the deep Sargasso Sea. Nature 283:364-365.

Devol, A.H. and J.P. Christensen. 1993. Benthic fluxes and nitrogen cycling in sediments of the continental margin of the eastern North Pacific. Journal of Marine Research 51:345-372.

DiMego, G.J., L.F. Bosart, and G.W. Endersen. 1976. An examination of the frequency and mean conditions surrounding frontal incursions into the Gulf of Mexico and Caribbean Sea. Monthly Weather Review 104:709-718.

Duplisea, D.E. and B.T. Hargrave. 1996. Response of meiobenthic size-structure, biomass and respiration to sediment organic enrichment. Hydrobiologia 339:161-170.

Eckman, J.E. and D. Thistle. 1988. Small-scale spatial pattern in meiobenthos in the San Diego trough. Deep-Sea Research 35:1565-1578.

Eldridge, P. and G. Jackson. 1991. Benthic food web flows in the Santa Monica basin estimated using inverse methods. In: Rowe, G.T. and V. Pariente, eds. Deep-sea food chains and the global carbon cycle. Boston, MA: Kluwer Academic Publishers. Pp. 255-276.

Elliott, B.A. 1982. Anticyclonic rings in the Gulf of Mexico. Journal of Physical Oceanography 12:1292-1308.

El-Sayed, S.Z. 1972. Primary productivity and standing crop of phytoplankton. In: Bushnell, V. C., eds. Chemistry, primary productivity, and benthic algae of the Gulf of Mexico. New York, NY: American Geographical Society. Pp. 8-13.

Escobar-Briones, E.G., M. Signoret and D. Hernandez. 1999. Variacion de la densidad de la infauna macrobentica en un gradiente batimetrico: Oeste Del Gulfo de Mexico. Ciencias Marinas 25:1-20.

Firth, R. 1971. A study of the deep-sea lobsters of the families polychelidae and nephropidae (crustacea, decapoda). Ph.D. dissertation. Texas A&M University, Department of Oceanography, College Station, TX.

Florida A&M University. 1988. Meteorological databases and synthesis for the Gulf of Mexico. U.S. Dept. of the Interior, Mineral Management Service, Gulf of Mexico OCS Region, New Orleans, LA. OCS Study MMS 83-0064. 486 pp.

Frithsen, J.B., D.T. Rudnick, and P.H. Doering. 1986. The Determination of fresh organic carbon weight from formaldehyde-preserved macrofaunal samples. Hydrobiologia 133:203-208.

Gage, J.D. and P.A. Tyler. 1991. Deep-sea biology. Cambridge, MA: Cambridge University Press. 504 pp.

Gallaway, B.J., L.R. Martin, and R.L. Howard. 1988a. Northern Gulf of Mexico continental slope study, annual report: Year 3. Volume II: Technical report. U.S. Dept. of the Interior, Minerals Management Service, Gulf of Mexico OCS Region, New Orleans, LA. OCS Study MMS 87-0060. 586 pp.

Gallaway, B.J., L.R. Martin, and R.L. Howard. 1988b. Northern Gulf of Mexico continental slope study, annual report: Year 3. Volume III: Appendices. U.S. Dept. of the Interior, Minerals Management Service, Gulf of Mexico OCS Region, New Orleans, LA. OCS Study MMS 87-0061. 774 pp.

Giere, O. 1993. Meiobenthology. Berlin, Germany: Springer-Verlag. 328 pp.

Gonzalez-Rodas, G.E. 1999. Physical forcing of primary productivity in the northwestern Gulf of Mexico. Ph.D. dissertation. Texas A&M University, Department of Oceanography, College Station, TX. 149 pp.

Gooday, A.J. 1986. Meiofaunal foraminiferans from the bathyal porcupine seabight (northeast Atlantic): Size, structure, standing stock, taxonomic composition, species diversity and vertical distribution in the sediments. Deep-Sea Research 33:1345-1373.

Gordon, E.S. and M.A. Goni. 2003. Sources and distribution of terrigenous organic matter delivered by the Atchafalaya river to sediments in the northern Gulf of Mexico. Geochimica et Cosmochimica Acta 67:2359-2375.

Grassle, J.F., H.L. Sanders, R.R. Hessler, G.T. Rowe, and T. McLellan. 1975. Pattern and zonation: A study of the bathyal megafauna using the research submersible Alvin. Deep-Sea Research 22:457-481.

Haedrich, R.L. and J.E. Maunder. 1985. The echinoderm fauna of the Newfoundland continental slope. In: Keegan, B.F. and B.D.S. O'Connor, eds. Proceedings of the 5th International Echinoderm Conference. Galway, Ireland. September 1984. A.A. Balkema. Rotterdam, The Netherlands. Pp. 37-46.

Haedrich, R.L. and N.R. Merrett. 1988. Summary atlas of deep-living demersal fishes in the North Atlantic. Journal of Natural History 22:1325-1362.

Haedrich, R. and N. Merrett. 1991. Production/biomass rations, size frequencies, and biomass spectra in deep-sea demersal fishes. In: Rowe, G.T. and V. Pariente, eds. Deep-sea food chains and the global carbon cycle. Boston, MA: Kluwer Academic Publishers. Pp. 157-182.

Haedrich, R.L. and G.T. Rowe. 1977. Megafaunal biomass in the deep sea. Nature 269:141-142.

Haedrich, R.L., G.T. Rowe, and P.T. Polloni. 1975. Zonation and faunal composition of epibenthic populations on the continental slope south of New England. Journal of Marine Research 33:191-212.

Haedrich, R.L., G.T. Rowe, and P.T. Polloni. 1980. The megabenthic fauna in the deep-sea south of New England. Marine Biology 57:165-179.

Hamilton, P. 1990. Deep currents in the Gulf of Mexico. Journal of Physical Oceanography 20:1087-1104.

Hecker, B. 1985. Fauna from a cold sulfur-seep in the Gulf of Mexico: Comparison with hydrothermal vent communities and evolutionary implications. Biological Society of Washington 6:465-473.

Hecker, B. 1990. Variation in megafaunal assemblages on the continental margin south of New England. Deep-Sea Research 37:37-57.

Heezen, B.C. and C.D. Hollister. 1971. The face of the deep. New York, NY: Oxford University Press. 175 pp.

Henry, W.K. 1979. Some aspects of the fate of cold fronts in the Gulf of Mexico. Monthly Weather Review 107:1078-1082.
Hessler, R. 1981. Oasis under the sea-where sulphur is the staff of life. New Scientist 92:741-747.
Hessler, R. and H. Sanders. 1967. Faunal diversity in the deep-sea. Deep-Sea Research 14:65-78.
Hessler, R.R., C.L. Ingram, A.A. Yayanos, and B.R. Burnett. 1978. Scavenging amphipods from the floor of the Philippine trench. Deep-Sea Research 25:1029-1047.
Hu, C., F.E. Muller-Karger, D.C. Biggs, K.L. Carder, B. Nababan, D. Nadeau, and J. Vanderbloemen. 2003. Comparison of ship and satellite bio-optical measurements on the continental margin of the NE Gulf of Mexico. International Journal of Remote Sensing 24:2597-2612.
Hubbard, F. 1995. Benthic polychaetes from the northern Gulf of Mexico continental slope. Ph.D. dissertation. Texas A&M University, Department of Oceanography, College Station, TX.
Hulings, N.C. and J.S. Gray. 1971. A manual for the study of meiofauna. Smithsonian Contribut. to Zoology 78:1-84.
Ishihi Y., T.A.Y. Yamada, and H. Yokoyama. 2001. Distribution of Stable Carbon Isotope Ratio in Sargassum Plants. Fisheries Science 67:367-369.
Jahnke, R.A. 1990. Ocean flux studies: A status report. Reviews of Geophysics 28:381-398.
Jahnke, R., C. Reimers, and D. Craven. 1996. Intensification of recycling of organic matter at the sea floor near ocean margins. Nature 348:50-54.
James, B. 1972. Systematics and biology of the deep-water palaeotaxodonata (Mollusca: Bivalvia) from the Gulf of Mexico. Ph.D. dissertation. Texas A&M University, Department of Oceanography, College Station, TX.
Jochens, A.E. and D.C. Biggs. 2003. Sperm whale seismic study in the Gulf of Mexico; annual report: Year 1. U.S. Dept. of the Interior, Minerals Management Service, Gulf of Mexico OCS Region, New Orleans, LA. OCS Study MMS 2003-069. 139 pp.
Jochens, A.E. and W.D. Nowlin, Jr. 1998. Northeastern Gulf of Mexico chemical oceanography and hydrography study between the Mississippi delta and Tampa Bay, annual report: Year 1. U.S. Dept. of the Interior, Minerals Management Service, Gulf of Mexico OCS Region, New Orleans, LA. OCS Study MMS 98-0060. 126 pp.
Jochens, A.E., S.F. DiMarco, W.D. Nowlin, Jr., R.O. Reid, and M.C. Kennicutt, II. 2002. Northeastern Gulf of Mexico chemical oceanography and hydrography study: Synthesis report. U.S. Dept. of the Interior, Minerals Management Service, Gulf of Mexico OCS Region, New Orleans, LA. OCS Study MMS 2002-055. 586 pp.
Jones, W.B., L.A. Cifuentes, and J.E. Kaldy. 2003. Stable carbon isotope evidence for coupling between sedimentary bacteria and seagrasses in a sub-tropical lagoon. Marine Ecology Progress Series 255:15-25.
Kendall, V. and R.L. Haedrich. 2006. Species richness in Atlantic deep-sea fishes assessed in terms of the mid-domain effect and Rappaport's rule. Deep-Sea Research I 53(3):506-515.
Kennedy, E.A., Jr. 1976. A distribution study of deep-sea macrobenthos collected from the western Gulf of Mexico. Ph.D. dissertation. Texas A&M University, Department of Oceanography, College Station, TX.
Kennicutt, M.C., J.M. Brooks, R.R. Bidigare, R.R. Fay, T.L. Wade, and T.J. McDonald. 1985. Vent-type taxa in a hydrocarbon seep region on the Louisiana slope. Nature 317:351-353.
Kennicutt, M.C., II, P. Boothe, T. Wade, S. Sweet, R. Rezak, J. Brooks, B. Presley, and D. Wiesenburg. 1996a. Geochemical patterns in sediments near offshore production platforms. Canadian Journal of Fisheries and Aquatic Sciences 53:2554-2566.

Kennicutt, M.C., II, R. Green, P. Montagna, and P. Roscigno. 1996b. Gulf of Mexico offshore operations monitoring experiment (GOOMEX), phase I: Sublethal responses to contaminant exposure-introduction and overview. Canadian Journal of Fisheries and Aquatic Sciences 53:2540-2553.

Kirk, R.E. 1982. Experimental design: Procedures for the behavioral sciences. Belmont, CA: Brooks/Cole Publishing. 911 pp.

Koblenz-Mishke, O.J., V.K. Volkovinsky and J.C. Kabanova. 1970. Plankton primary production of the world ocean. In: Wooster, W. W., eds. Scientific exploration of the South Pacific. Washington, DC: National Academy of Science. Pp. 183-193.

Kuwae, T. and Y. Hosokawa. 1999. Determination of abundance and biovolume of bacteria in sediments by dual staining with 4',6-diamidino-2-phenylindole and acridine orange: Relationship to dispersion treatment and sediment characteristics. Applied and Environmental Microbiology 65(8):3407-3412.

Lalli, C.M. and T.R. Parsons. 1997. Biological oceanography: An introduction. Oxford, UK: Butterworth-Heinemann. 314 pp.

Lampitt, R.S., D.S.M. Billett, and A.L. Rice. 1986. Biomass of the invertebrate megabenthos from 500-4100m in the northeast Atlantic Ocean. Marine Biology 93:69-81.

Lauenstein, G.G. and A.Y. Cantillo. 1998. Sampling and analytical methods of the national status and trends program, mussel watch project: 1993-1996 update. U.S. Dept. of Commerce, National Oceanographic and Atmospheric Administration, Seattle, WA. NOAA Technical Memorandum NOS ORCA 130. 233 pp.

Leben, R.R., G.H. Born, and B.R. Engebreth. 2002. Operational altimeter data processing for mesoscale monitoring. Marine Geodesy 25:3-18.

Lee, S.H. and J.A. Fuhrman. 1987. Relationships between bivolume and biomass of naturally derived marine bacterioplankton. Applied and Environmental Microbiology 53:1298-1303.

Levin, L.A. and J.D. Gage. 1998. Relationship between oxygen, organic matter, and the diversity of bathyal macrofauna. Deep-Sea Research II 45:129-163.

LGL Ecological Associates Inc. (LGL) and Texas A&M University (TAMU). 1988. Northern Gulf of Mexico continental slope study. Final report: Year 4. Volume I: Executive summary; Volume II: Synthesis report; and Volume III: Appendices. U.S. Dept. of the Interior, Minerals Management Service, Gulf of Mexico OCS Region, New Orleans, LA. OCS Study MMS 88-0052, 88-0053, and 88-0054. 62, 701, and 265 pp., respectively.

Lillibridge, J., R. Leben and F. Vossepoel. 1997. Real-time processing from ERS-2. Proc. Third ERS Symp., Vol. 3. European Space Agency, Florence, Italy. SP414. Pp. 1449-1453.

Lin, S. and J.W. Morse. 1991. Sulfate reduction and iron sulfide mineral formation in Gulf of Mexico anoxic sediments. American Journal of Science 291:55-89.

Linke, P. 1992. Metabolic adaptations of deep sea benthic foraminifera to seasonally varying food input. Marine Ecology Progress Series 81:51-63.

Lochte, K. and C.M. Turley. 1988. Bacteria and cyanobacteria associated with phytodetritus in the deep sea. Nature 333:67-69.

Long, E.R. and L.G. Morgan. 1990. The potential for biological effects of sediment-sorbed contaminants tested in the national status and trends program. U.S. Dept. of Commerce, National Oceanographic and Atmospheric Administration, Seattle, WA. NOAA Technical Memorandum NOS ORCA 52.

Luther, G.W., III, P.J. Brendel, B.L. Lewis, B. Sundby, L. Lefrancois, N. Silverberg, and D.B. Nuzzio. 1998. Simultaneous measurement of O_2, Mn. Fe, I-, and S(-Ii) in marine pore water with a solid-state voltametric microelectrode. Limnology and Oceanography 43:325-333.

MacDonald, I.R. 1998. Stability and change in Gulf of Mexico chemosynthetic communities. interim report. U.S. Dept. of the Interior, Minerals Management Service, Gulf of Mexico OCS Region, New Orleans, LA. OCS Study MMS 98-0034. 96 pp.

MacDonald, I.R., W.W. Schroeder, and J.M. Brooks. 1996. Chemosynthetic ecosystem study. Final report. U.S. Dept. of the Interior, Minerals Management Service, Gulf of Mexico OCS Region, New Orleans, LA. OCS Study MMS 95-0021. 360 pp.

Mare, M.F. 1942. A study of marine benthic community with special reference to the micro-organisms. Journal of the Marine Biological Association of the United Kingdom 25:517-554.

Martin, W.R. and D.C. McCorkle. 1993. Dissolved organic carbon concentrations in marine pore waters determined by high-temperature combustion. Limnology and Oceanography 38:973-981.

Mayer, M. and D. Piepenburg. 1996. Epibenthic community patterns on the continental slope off east Greenland at 75°N. Marine Ecology Progress Series 143:151-164.

McEachran, J.D. and J.D. Fechhelm. 1998. Fishes of the Gulf of Mexico. Vol. 1. Myxiniformes to gasterosteiformes. Austin, TX : University of Texas Press. 1112 pp.

McEachran, J.D. and J.D. Fechhelm. 2005. Fishes of the Gulf of Mexico. Vol. 2. Scorpaeniformes to tetraodontiiformes. Austin, TX : University of Texas Press. 1014 pp.

Melo-Gonzalez, N., F.E. Muller-Karger, S.Cerdeira-Estrada, R. Perez de los Reyes, I. Victoria del Rio, P. Cardenas-Perez, and I. Mitrani-Arenal. 2000. Near-surface phytoplankton distribution in the western intra-Americas sea: The influence of El Nino and weather events. Journal of Geophysical Research 105:14029-14043.

Menzies, R.J., R.Y. George, and G.T. Rowe. 1973. Abyssal environment and ecology of the world oceans. New York, NY: John Wiley & Sons. 488 pp.

Merrett, N.R. and R.L. Haedrich. 1997. Deep-sea demersal fish and fisheries. London, UK: Chapman & Hall. 282 pp.

Miller-Way, T., G. Boland, G. Rowe, and R. Twilley. 1994. Sediment oxygen consumption and benthic nutrient fluxes on the Louisiana continental shelf: A methodological comparison. Estuaries 17:809-815.

Montagna, P.A. 1984. In situ measurement of meiobenthic grazing rates on sediment bacteria and edaphic diatoms. Marine Ecology Progress Series 18:119-130.

Montagna, P.A. 1991. Meiobenthic communities of the santa maria basin on the California continental shelf. Continental Shelf Research 11:1355-1378.

Montagna, P.A. 1993. Radioisotope technique to quantify in situ microbivory by meiofauna in sediments. In: Kemp, P.F., B.F. Sherr, E.B. Sherr, and J.J. Cole, eds. Handbook of methods in aquatic microbial ecology. Boca Raton, FL: Lewis Publishers. Pp. 745-753.

Montagna, P.A. 1995. Rates of meiofaunal microbivory: A Review. Vie et Milieu 45:1-10.

Montagna, P.A. and D.E. Harper, Jr. 1996. Benthic infaunal long term response to offshore production platforms. Canadian Journal of Fisheries and Aquatic Sciences 53:2567-2588.

Montagna, P.A. and J. Li. 1997. Modeling contaminant effects on deposit feeding nematodes near Gulf of Mexico production platforms. Ecological Modelling 98:151-162.

Montagna P.A, J.E. Bauer, D. Hardin, and R.B. Spies. 1989. Vertical distribution of microbial and meiofaunal populations in sediments of a natural coastal hydrocarbon seep. Journal of Marine Research 47:657-680.

Morrison, J.M. and W.D. Nowlin, Jr. 1977. Repeated nutrient, oxygen, and density sections through the loop current. Journal of Marine Research 35(1):105-128.

Morrison, J.M. and W.D. Nowlin, Jr. 1982. General distribution of water masses within the eastern Caribbean sea during the winter of 1972 and fall of 1973. Journal of Geophysical Research 87(C6):4207-4227.

Morrison, J.M., W.J. Merrell, Jr., R.M. Key, and T.C. Key. 1983. Property distributions and deep chemical measurements within the western Gulf of Mexico. Journal of Geophysical Research 88(C4):2601-2608.

Morse, J.W. and K.-C. Emeis. 1992. Carbon/sulfur/iron relationships in upwelling sediments. In: Summerhayes, C.P., W.L. Prell, and K.C. Emeis, eds. Evolution of upwelling systems since the early miocene. House, London: Geological Society Publishing. Pp. 247-256.

Morse, J.W. and G.T. Rowe. 1999. Benthic biogeochemistry beneath the Mississippi River plume. Estuaries 22:206-214.

Morse, J.W. and K.C. Emeis. 1990. Controls on c/s ratios in hemipelagic sediments. American Journal of Science 290:1117-1135.

Mucci, A. 1988. Manganese uptake during calcite precipitation from seawater: Conditions leading to the formation of pseudokuntnahorite. Geochimica et Cosmochimica Acta 52:1859-1868.

Muller-Karger, F.E., J.J. Walsh, R.H. Evans, and M.B. Meyers. 1991. On the seasonal phytoplankton concentration and sea surface temperature cycles of the Gulf of Mexico as determined by satellites. Journal of Geophysical Research 96:12645-12665.

Nardin, T.R., F.J Hein, D.S. Gorsline, and B.D. Edwards. 1979. A review of mass movement processes, sediment and acoustic characteristics, and contrasts in slope and base-of-slope systems versus canyon-fan-basin floor systems. Special Publications of the Society of Economic Paleontologists and Mineralogist. 27:61-73.

Neff, J.M., R.J. Breteler, and S.R. Carr. 1989. Bioaccumulation, food chain transfer and biological effects of barium and chromium from drilling muds by flounder (*Pseudopleuronectes americanus*) and lobster (*Komarus americanus*). In: Engelhardt, F.R., J.P. Ray, and A.H. Gillam, eds. Drilling Wastes. Elsevier. London. Pp. 439-459.

Norland, S. 1993. The relationship between biomass and volume of bacteria. In: Kemp, P.F., B.F. Sherr, E.B. Sherr, and J.J. Cole, eds. Handbook of methods in aquatic microbial ecology. Boca Raton, FL: Lewis Publishers. Pp. 303-307.

Nowlin, W.D., Jr. 1972. Winter circulation patterns and property distribution. In: Capurro, L.R.A. and J.L. Reid, eds. Contributions on the physical oceanography of the Gulf of Mexico. Texas a & M University Oceanography Study. Vol. 2. Houston, TX: Gulf Publishing. Pp. 3-53.

Nowlin, W.D.J., A.E. Jochens, R.O. Reid, and S.F. DiMarco. 1998. Texas-Louisiana shelf circulation and transport processes study: Synthesis report, Volumes I and II: Technical report and appendices. U.S. Dept. of the Interior, Minerals Management Service, Gulf of Mexico OCS Region, New Orleans, LA. OCS Study MMS 98-0035 and 98-0036. 502 and 288 pp., respectively.

Nowlin, W.D.J., A.E. Jochens, S.F. DiMarco, and R.O. Reid. 2000. Physical oceanography. In: Continental Shelf Associates, Inc. Deepwater Gulf of Mexico environmental and

socioeconomic data search and literature synthesis. Volume I: Narrative report. U.S. Dept. of the Interior, Minerals Management Service, Gulf of Mexico OCS Region, New Orleans, LA. OCS Study MMS 2000-049. Pp. 61-121.

Nowlin, W.D.J., A.E. Jochens, S.F. DiMarco, R.O. Reid, and M.K. Howard. 2001. Deepwater physical oceanography reanalysis and synthesis of historical data: Synthesis report. U.S. Dept. of the Interior, Minerals Management Service, Gulf of Mexico OCS Region, New Orleans, LA. OCS Study MMS 2001-064. 528 pp.

Nunnally, C.C. 2003. Macrobenthic community structure and total sediment respiration at cold hydrocarbon seeps in the northern Gulf of Mexico. Master Thesis. Texas A&M University, Department of Oceanography, College Station, TX.

Nybakken, J.W. 1988. Marine biology: An ecological approach. New York, NY: Harper & Row. 481 pp.

Ohta, S. 1983. Photographic census of large-sized benthic organisms in the bathyal zone of Suruga Bay, central Japan. Bulletin of the Ocean Research Institute, University of Tokyo 15:1-244.

Paull, C., B. Hecker, R. Commeau, R. Freeman-Lynde, C. Newumann, W. Corse, S. Golubic, J. Hook, E. Sikes, and J. Curray. 1984. Biological communities at the Florida escarpment resemble hydrothermal vent taxa. Science 226:965-967.

Pawson, D.L. 1982. Deep-sea echinoderms in the tongue of the ocean, Bahama Islands: A survey, using the research submersible *Alvin*. Australian Museum Memoir 16:129-145.

Pearre, S., Jr. 1980. The copepod width-weight relation and its utility in food chain research. Canadian Journal of Zoology 58:1884-1891.

Pequegnat, L. 1970. A study of deep-sea caridean shrimps (crustacea: decapoda: natantia) of the Gulf of Mexico. Ph.D. dissertation. Texas A&M University, Department of Oceanography, College Station, TX.

Pequegnat, W.E. 1972. A deep bottom current on the Mississippi cone. In: Capurro, L.R.A. and J.L. Reid, eds. Contributions on the physical oceanography of the Gulf of Mexico. Vol. 2. Houston, TX: Gulf Publishing. Pp. 65-87.

Pequegnat, W. 1983. The ecological communities of the continental slope and adjacent regimes of the northern Gulf of Mexico. Prepared by Tereco Corporation. U.S. Dept. of the Interior, Minerals Management Service, Gulf of Mexico OCS Region, New Orleans, LA. Contract No. AA851-CT-1-12. 398 pp.

Pequegnat, W.E., B.J. Gallaway, and L.H. Pequegnat. 1990. Aspects of the ecology of the deep-water fauna of the Gulf of Mexico. American Zoologist 30:45-64.

Pfannkuche, O., R. Theeg, and H. Thiel. 1983. Benthos activity, abundance and biomass under an area of low upwelling off Morocco, Northwest Africa. Meteor Forschungsergebnisse 36:85-96.

Pomeroy, L., W. Wiebe, D. Deibel, R. Thompson, G. Rowe, and J.D. Pakulski. 1991. Bacterial responses to temperature and substrate concentration during the Newfoundland spring bloom. Marine Ecology Progress Series 75:143-159.

Powell, S.M., R.L. Haedrich, and J.D. McEachran. 2003. The deep-sea demersal fish fauna of the northern Gulf of Mexico. Journal of Northwest Atlantic Fishery Science 31:19-33.

Presley, B.J., R.J. Taylor, and P.N. Boothe. 1992. Trace metal concentrations in sediments of the eastern Mississippi bight. Marine Environmental Research 33:267-282.

Qian, Y., J.L. Sericano, and T.L. Wade. 1998. Extraction and clean-up of sediments for trace organic analysis. In: Lauenstein, G.G. and A.Y. Cantillo. Sampling and analytical methods

of the national status and trends program, Mussel Watch Project: 1993-1996 update. U.S. Dept. of Commerce, National Oceanographic and Atmospheric Administration, Seattle, WA. NOAA Technical Memorandum NOS ORCA 130. Pp. 94-97.

Qian, Y., A.E. Jochens, M.C. Kennicutt II, and D.C. Biggs. 2003. Spatial and temporal variability of phytoplankton blooms and community structure over the continental margin of the northeast Gulf of Mexico based on pigment analysis. Continental Shelf Research 23:1-17.

Rapport, D.J. and W.G. Whitford. 1999. How ecosystems respond to stress. BioScience 49(3):193-203.

Rapport, D.J., R. Constanza, and A.J. McMichael. 1998. Assessing ecosystem health. Trends in Ecology & Evolution 13(10):397-402.

Relexans, J.C., J.W. Deming, A. Dinet, J.-F. Gaillard, and M. Sibuet. 1996. Sedimentary organic matter and micro-meiobenthos with relation to trophic conditions in the northeast tropical Atlantic. Deep-Sea Research 43(8):343-1368.

Ressler, P.H. 2001. Acoustic estimates of zooplankton and micronekton biomass in cyclones and anticyclones of the northeastern Gulf of Mexico. Ph.D. Dissertation. Texas A&M University, Department of Oceanography, College Station, TX. 145 pp.

Rex, M. 1983. Geographic patterns of species diversity in the deep-sea benthos. In: Rowe, G. T., eds. The sea. Volume 8. New York, NY: Wiley-Interscience. Pp. 435-472.

Rex, M.A., C.T. Stuart, R.R. Hessler, J.A. Allen, H.L. Sanders, and G.D.F Wilson. 1993. Global-scale latitudinal patterns of species diversity in the deep-sea benthos. Nature 365:636-639.

Rex, M., C. McClain, N. Johnson, R. Etter, J. Allen, P. Bouchet, and A. Waren. 2005. A source-sink hypothesis for abyssal biodiversity. The American Naturalist 165:163-178.

Richardson, M. and D.K. Young. 1987. Abyssal benthos of the Venezuela Basin, Caribbean Sea: Standing stock consideraitons. Deep-Sea Research 34:145-164.

Robinson, A.F. 1984. Comparison of five methods for measuring nematode volume. Journal of Nematology 16:343-347.

Rowe, G.T. 1966. A study of the deep water benthos of the northwestern Gulf of Mexico. Master Thesis. Texas A&M University, Department of Oceanography, College Station, TX.

Rowe, G.T. 1971. Benthic biomass and surface productivity. In: Costlow, J., eds. Fertility of the sea. Fertility of the sea, Volume 2. New York, NY: Gordon and Breach. Pp. 441-454.

Rowe, G.T. 1981. The deep-sea ecosystem. In: Longhurst, A., eds. Analysis of marine ecosystem. New York, NY: Academic Press. Pp. 235-267.

Rowe, G.T. 1983. Biomass and production of the deep-sea macrobenthos. In: Rowe, G.T., eds. The sea. Volume 8. New York, NY: Wiley-Interscience. Pp. 97-121.

Rowe, G.T. 1998. Organic carbon cycling in abyssal benthic food chains: Numerical simulations of bioenhancement by sewage sludge. Journal of Marine Systems 14:337-354.

Rowe, G.T. and J.W. Deming. 1985. The role of bacteria in the turnover of organic carbon in deep-sea sediments. Journal of Marine Research 43:925-950.

Rowe, G.T. and W. Gardner. 1979. Sedimentation rates in the slope water of the northwest Atlantic Ocean measured directly with sediment traps. Journal of Marine Research 37:581-60.

Rowe, G.T. and R.L. Haedrich. 1979. The biota and biological processes on the continental slope. In: Doyle, R. and O. Pilkey, eds. The continental slope. Tulsa, OK: American Association of Petroleum Geologists. Pp. 49-59.

Rowe, G.T. and M.C. Kennicutt, II. 2002. Deepwater program: Northern Gulf of Mexico continental slope habitats and benthic ecology study. Year 2: Interim report. U.S. Dept. of the Interior, Minerals Management Service, Gulf of Mexico OCS Region, New Orleans, LA. OCS Study MMS 2002-063. 158 pp.

Rowe, G.T. and D. Menzel. 1971. Quantitative benthic samples from the deep Gulf of Mexico with some comments on the measurement of deep-sea biomass. Bulleting of Marine Science 21:556-566.

Rowe, G.T. and R.J. Menzies. 1969. Zonation of large benthic invertebrates in the deep-sea off the Carolinas. Deep-Sea Research 16:531-537.

Rowe, G.T. and N. Staresinic. 1979. Sources of organic matter to the deep-sea benthos. Ambio Special Report 6:19-24.

Rowe, G.T., P. Polloni, and S. Hornor. 1974. Benthic biomass estimates from the NW Atlantic Ocean and the northern Gulf of Mexico. Deep-Sea Research 21:641-650.

Rowe, G.T., M. Sibuet, J. Deming, A. Khripounoff, J. Tietjen, and R. Theroux. 1990. Organic carbon turnover time in the deep-sea benthos. Progress in Oceanography 24:141-160.

Rowe, G.T., M. Sibuet, J. Deming, A. Khripounoff, J. Tietjen, S. Macko, and R. Theroux. 1991. "Total" sediment biomass and preliminary estimates of organic carbon residence time in deep-sea benthos. Marine Ecology Progress Series 79:99-114.

Rowe, G.T., G.S. Boland, W. Phoel, R. Anderson, and P. Biscaye. 1994. Deep seafloor respiration as an indication of lateral input of biogenic detritus from continental margins. Deep-Sea Research II 41:657-668.

Rowe, G.T., G.S Boland, E.G. Escobar, M.E. Cruz-Kaegli, A. Newton, D. Piepenburg, I.D. Walsh, and J.W. Deming. 1997. Sediment community biomass and respiration in the northeast water Polynya, Greenland: A numerical simulation of benthic lander and spade core data. Journal of Marine Systems 10:497-515.

Rowe, G.T., A. Lohse, G.S. Boland, E. Escobar Briones, G.F. Hubbard, and J. Deming. 2003. Preliminary trophodynamic carbon budget for the Sigsbee deep benthos, northern Gulf of Mexico. American Fisheries Society Symposium 36:225-238.

Salata, G.G. 1999. Stable carbon isotopes as tracers of microbial degradation. Ph.D. Dissertation. Texas A&M University, Department of Oceanography, College Station, TX. 123 pp.

Salata, G.G., L.A. Roelke, and L.A. Cifuentes. 1996. A rapid and precise method for the determination of dissolved inorganic carbon stable isotopes. In: B.J. Spargo, ed. In situ bioremediation and efficacy monitoring. Washington, DC: Naval Research Laboratory. NRL/PU/6115-96-317. Pp. 79-85.

Santschi, P.H., Y.H. Li, J. Bell, R.M. Trier, and K. Kawtaluk. 1980. Plutonium in the coastal marine environment. Earth and Planetary Science Letters 51:248-265.

Santschi, P.H., M. Allison, S. Asbill, A.B. Perlet, S. Cappellino, C. Dobbs, and L. McShea. 1999. Sediment transport and Hg recovery in lavaca bay, as evaluated from radionuclide and Hg distributions. Environmental Science & Technology 33:378-391.

Santschi, P.H., L. Guo, S. Asbill, M. Allison, A.B. Kepple, and L.S. Wen. 2001. Accumulation rates and sources of sediments and organic carbon on the palos verdes shelf based on radioisotopic tracers (^{137}Cs, ^{239,240}Pu, ^{210}Pb, ^{234}Th, ^{238}U, ^{14}C). Journal of Marine Chemistry 73:125-152.

Sassen, R., H.H. Roberts, P. Aharon, J. Larkin, E.W. Chinn, and R.S. Carney. 1993. Chemosynthetic bacterial mats at cold hydrocarbon seeps, Gulf of Mexico continental slope. Organic Geochemistry 20:77-89.

Schmidt, J.L., J.W. Deming, P.A. Jumars, and R.G. Keil. 1998. Constancy of bacterial abundance in surficial marine sediments. Limnology and Oceanography 43:976-982.
Schoener, A. and G.T. Rowe. 1970. Pelagic sargassum and its presence among the deep-sea benthos. Deep-Sea Research 17:923-925.
Science Applications International Corporation (SAIC). 1989. Gulf of Mexico physical oceanography program, final report: Year 5. Volume II: Technical Report. U.S. Dept. of the Interior, Minerals Management Service, Gulf of Mexico OCS Region, New Orleans, LA. OCS Study MMS 89-0068. 333 pp.
Smith, D.C. 1986a. Nekton falls, low-intensity disturbance and community structure of infaunal benthos in the deep-sea. Journal of Marine Research 44:567-600.
Smith, D.C. 1986b. A numerical study of loop current eddy interaction with topography in the western Gulf of Mexico. Journal of Physical Oceanography 16:1260-1272.
Smith, K.L., Jr. and K.R. Hinga. 1983. Sediment community respiration in the deep sea. In: Rowe, G.T., ed. The sea, Volume 8. New York, NY: Wiley-Interscience. Pp. 331-372.
Smith, K.L. and J.M. Teal. 1973. Deep-sea benthic community respiration: An in situ study at 1850 meter. Science 179:282-283.
Smith, K.L., Jr. 1992. Benthic boundary layer communities and carbon cycling at abyssal depths in the central north Pacific. Limnology and Oceanography 37:1034-1056.
Smith, K.L., Jr. and R. Kaufmann. 1999. Long-term discrepancy between food supply and demand in the deep eastern Pacific. Science 284:1174-1177.
Smith, S. and J.T. Hollibaugh. 1993. Coastal metabolism and the oceanic organic carbon balance. Reviews of Geophysics 31:75-89.
Snelgrove, P.V.R. and R.L. Haedrich. 1985. Structure of the deep demersal fish fauna off newfoundland. Marine Ecology Progress Series 27:99-107.
Snelgrove, P., J. Grassle, and R. Petrecca. 1996. Experimental evidence for aging food patches as a factor contributing to high deep-sea macrofaunal diversity. Limnology and Oceanography 4:605-614.
Snider, L.J., B.R. Burnett, and R.R. Hessler. 1984. The composition and distribution of meiofauna and nanobiota in a central North Pacific deep sea area. Deep-Sea Research 31:1225-1249.
Sokolova, M.N. 1959. On the distribution of deep-water bottom animals in relation to their feeding habits and the character of sedimentation. Deep-Sea Research 6:1-4.
Somayajulu, B.L.K., R. Rhushan, A. Sarkar, G.S. Burr, and A.J.T. Jull. 1999. Sediment deposition rates on the continental margins of the eastern Arabian sea using 210pb, 137cs and 14c. Science of the Total Environment 237/238:429-439.
Soto, L. 1985. Distributional patterns of deep-water brachyuran crabs in the straits of Florida. Journal of Crustacean Biology 5:480-499.
Soto, L. and E. Escobar. 1995. Coupling mechanisms related to benthic production in the southwestern Gulf of Mexico. In: Eleftheriou, A., A. Ansell, and C. Smith, eds. Proceedings of the 28th European marine biology symposium. Olsen and Olsen. Fredensborg, Denmark. Pp. 233-242.
Soto, L., S. Manickhand-Heileman, E. Flores, and S. Licea. 1999. Processes that promote decapod diversity and abundance on the upper continental slope of the southwestern Gulf of Mexico. In: von Vaupel Klen, J. and F. Schram, eds. The biodiversity crisis and Crustacea. Proceedings of the Fourth International Congress. Amsterdam, The Netherlands. July 20-24, 1998. Pp. 385-400.

Stull, J.K., D.J.P. Swift, and A.W. Niedoroda. 1996. Contaminant dispersal on the palos verdes continental margin: I. Sediment and biota near a major California wastewater discharge. Science of the Total Environment 179:73-90.

Stumm, W. and J.J. Morgan. 1996. Aquatic geochemistry: Chemical equilibria and rates in natural waters. New York, NY: Wiley-Interscience. 1022 pp.

Sturges, W. 1993. The annual cycle of the western boundary current in the Gulf of Mexico. Journal of Geophysical Research 98:18,053-18,068.

Sturges, W. and R. Leben. 2000. Frequency of ring separations from the loop current in the Gulf of Mexico: A revised estimate. Journal of Physical Oceanography 30:1814-1819.

Taylor, B.J. and B.J. Presley. 1998. Terl trace element quantification techniques. In: Sampling and analytical methods of the national status and trends program, Mussel Watch Project: 1993-1996 update. U.S. Dept. of Commerce, National Oceanographic and Atmospheric Administration. Seattle, WA. NOAA Technical Memorandum NOS ORCA 130. Pp. 32-92.

TerEco Corporation. 1976. Ecological aspects of the upper continental slope of the Gulf of Mexico. U.S. Dept. of the Interior, Minerals Management Service, Gulf of Mexico OCS Region, New Orleans, LA. Contract No. 08550-CT4-12. 560 pp.

TerEco Corporation. 1983. The Ecological Communities of the Continental Slope and Adjacent Regions. U.S. Dept. of the Interior, Minerals Management Service, Gulf of Mexico OCS Region, New Orleans, LA. Contract No. AA851-CT1-12. 675 pp.

Thiel, H. 1975. The size structure of the deep sea benthos. Internationale Revue Gesamptin der Hydrobiology 60:575-606.

Thiel, H. 1982. Zoobenthos of the cineca area and other upwelling regions. Rapport Et Procès-Verbaux Des Reunions. Conseil permanent internationale pour l'exploration de la mer 180:323-334.

Thistle, D., S.C. Ertman, and K. Fauchald. 1991. The fauna of the hebble site: Patterns in standing stock and sediment-dynamic effects. Marine Geology 99:413-422.

Trefry, J.H. and B.J. Presley. 1982. Manganese fluxes from Mississippi delta sediments. Geochimica et Cosmochimica Acta 46:1715-1726.

Tunnicliffe, V., A. McArthur, and D. McHugh. 1998. A biogeographical perspective of the deep-sea hydrothermal vent fauna. Advances in Marine Biology 34:353-442.

Turner, R.D. 1973. Wood-boring bivalves: Opportunistic species in the deep sea. Science 180:1377-1379.

Vázquez de la Cerda, A.M. 1993. Bay of Campeche Cyclone. Ph.D. Dissertation. Texas A&M University, Department of Oceanography, College Station, TX. 91 pp.

Vázquez de al Cerda, A.M., R.O. Reid, S.F. DiMarco, and A.E. Jochens. 2005. Bay of Campeche circulation: An update. In: Sturges, W. and A. Lugo-Fernandez, eds. Circulation in the Gulf of Mexico: Observations and models, Geophysical Monograph Series, Volume 161. American Geophysical Union. 279-293 pp.

Vukovich, F.M. 1988. Loop current boundary variations. Journal of Geophysical Research 93(C12):585-591.

Vukovich, F.M. 1995. An updated evaluation of the loop current's eddy shedding frequency. Journal of Geophysical Research 100:8655-8660.

Vukovich, F.M. and B.W. Crissman. 1986. Aspects of warm rings in the Gulf of Mexico. Journal of Geophysical Research 91:2645-2660.

Walsh, J.J., D.A. Dieterle, M.B. Meyers, and F.E. Müller-Karger. 1989. Nitrogen exchange at the continental margin: A numerical study of the Gulf of Mexico. Progress in Oceanography 23:248-301.

Wolff, T. 1979. Macrofaunal utilization of plant remains in the deep sea. Sarsia 64:127-147.

Woodruff, S.D., R.J. Slutz, R.L. Jenne, and P.M Steurer. 1987. A comprehensive ocean-atmosphere data set. Bulletin of the American Meteorological Society 68:1239-1250.

Zuo, Z., D. Eisma, R. Gieles, and J. Beks. 1997. Accumulation rates and sediment deposition in the northwestern Mediterranean. Deep-Sea Research II 44 (3-4):597-609.

Appendices

The Appendices to this document are available as a collection of online files. To view these files on the Internet, go to http://www.gomr.mms.gov/PDFs/2009/2009-039/Appendices/Appendices.htm.
To view these files from the CD version of this document, click here.

The Department of the Interior Mission

As the Nation's principal conservation agency, the Department of the Interior has responsibility for most of our nationally owned public lands and natural resources. This includes fostering sound use of our land and water resources; protecting our fish, wildlife, and biological diversity; preserving the environmental and cultural values of our national parks and historical places; and providing for the enjoyment of life through outdoor recreation. The Department assesses our energy and mineral resources and works to ensure that their development is in the best interests of all our people by encouraging stewardship and citizen participation in their care. The Department also has a major responsibility for American Indian reservation communities and for people who live in island territories under U.S. administration.

The Minerals Management Service Mission

As a bureau of the Department of the Interior, the Minerals Management Service's (MMS) primary responsibilities are to manage the mineral resources located on the Nation's Outer Continental Shelf (OCS), collect revenue from the Federal OCS and onshore Federal and Indian lands, and distribute those revenues.

Moreover, in working to meet its responsibilities, the **Offshore Minerals Management Program** administers the OCS competitive leasing program and oversees the safe and environmentally sound exploration and production of our Nation's offshore natural gas, oil and other mineral resources. The MMS **Minerals Revenue Management** meets its responsibilities by ensuring the efficient, timely and accurate collection and disbursement of revenue from mineral leasing and production due to Indian tribes and allottees, States and the U.S. Treasury.

The MMS strives to fulfill its responsibilities through the general guiding principles of: (1) being responsive to the public's concerns and interests by maintaining a dialogue with all potentially affected parties and (2) carrying out its programs with an emphasis on working to enhance the quality of life for all Americans by lending MMS assistance and expertise to economic development and environmental protection.